OCS Study
BOEM 2021-051

Atlantic Marine Assessment Program for Protected Species: FY15 – FY19

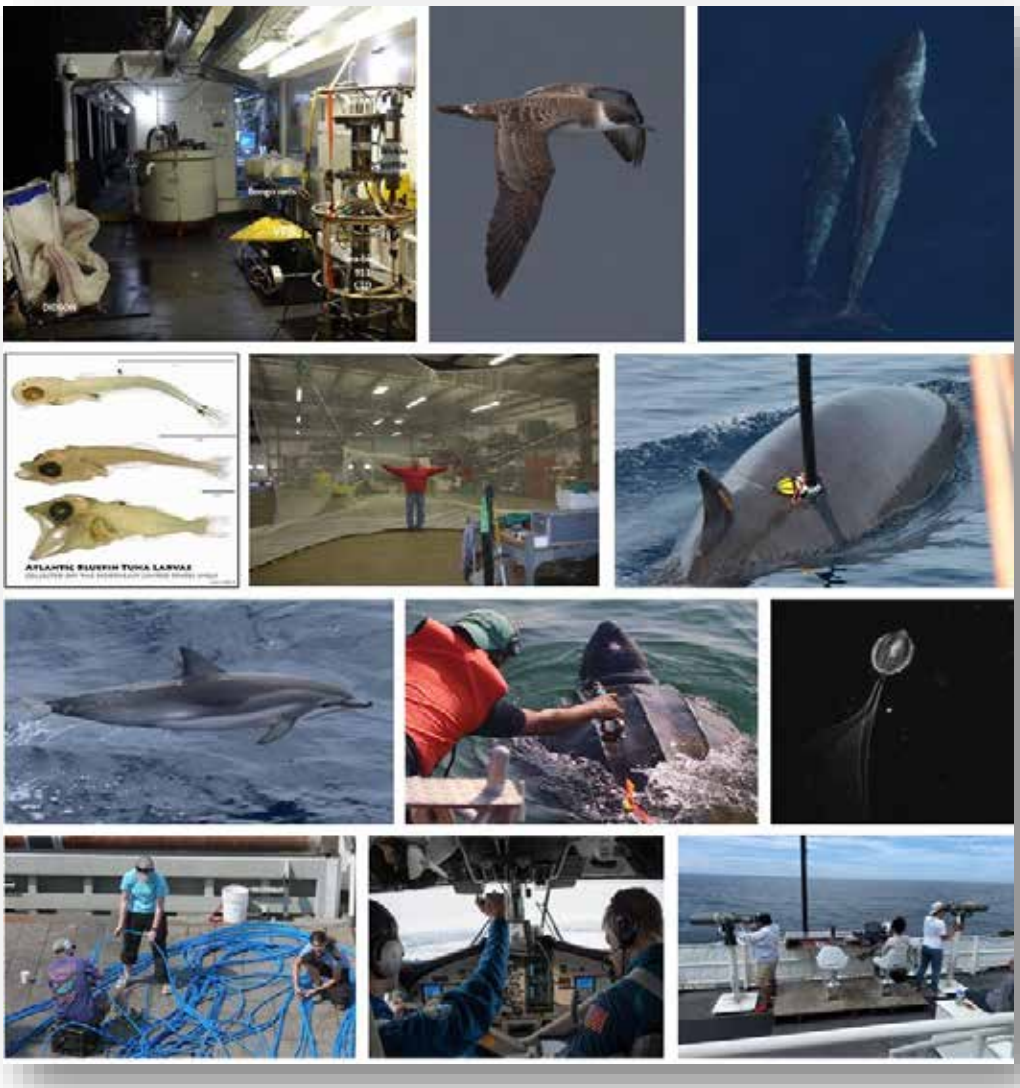

US Department of the Interior
Bureau of Ocean Energy Management
Headquarters
July 2021

OCS Study
BOEM 2021-051

Atlantic Marine Assessment Program for Protected Species: FY15 – FY19

July / 2021

Palka, Aichinger Dias, Broughton, Chavez-Rosales, Cholewiak, Davis, DeAngelis, Garrison, Haas, Hatch, Hyde, Jech, Josephson, Mueller-Brennan, Orphanides, Pegg, Sasso, Sigourney, Soldevilla, Walsh

Prepared under M14PG00005
By

National Oceanic Atmospheric Administration
National Marine Fisheries Service
Northeast Fisheries Science Center
166 Water Street
Woods Hole, MA 01543-1026

National Oceanic Atmospheric Administration
National Marine Fisheries Service
Southeast Fisheries Science Center
75 Virginia Beach Dr.
Key Biscayne, FL 33149

US Department of the Interior
Bureau of Ocean Energy Management
Headquarters
July 2021

DISCLAIMER

This study was funded, in part, by the U.S. Department of the Interior, Bureau of Ocean Energy Management (BOEM), Environmental Studies Program, Washington, DC, through Interagency Agreement Number M14PG00005 with the U.S. Department of Commerce, National Oceanic and Atmospheric Administration. This report has been technically reviewed by BOEM, and it has been approved for publication. The views and conclusions contained in this document are those of the authors and should not be interpreted as representing the opinions or policies of the U.S. Government, nor does mention of trade names or commercial products constitute endorsement or recommendation for use.

REPORT AVAILABILITY

To download a PDF file of this report, go to the U.S. Department of the Interior, Bureau of Ocean Energy Management Data and Information Systems webpage (http://www.boem.gov/Environmental-Studies-EnvData/), click on the link for the Environmental Studies Program Information System (ESPIS), and search on 2021-051. The report is also available at the National Technical Reports Library at https://ntrl.ntis.gov/NTRL/.

CITATION

Palka D, Aichinger Dias L, Broughton E, Chavez-Rosales S, Cholewiak D, Davis G, DeAngelis A, Garrison L, Haas H, Hatch J, Hyde K, Jech M, Josephson E, Mueller-Brennan L, Orphanides C, Pegg N, Sasso C, Sigourney D, Soldevilla M, Walsh H. 2021. Atlantic Marine Assessment Program for Protected Species: FY15 – FY19. Washington DC: US Department of the Interior, Bureau of Ocean Energy Management. OCS Study BOEM 2021-051. 330 p.

ABOUT THE COVER

The cover is a compilation of various work conducted as part of the AMAPPS II project including surveys of cetaceans, sea turtles, seals, seabirds, and general ecosystem conditions. The photos are courtesy of Dr. Debra Palka of the National Marine Fisheries Service. We conducted our surveys and collected pictures under U.S. Marine Mammmal Protection Act permit numbers 17355, and 21371 issued to the Northeast Fisheries Science Center and Marine Mammmal Protection Act permit numbers 779-1633, 14450-11, and 21938 issued to the Southeast Fisheries Science Center.

ACKNOWLEDGMENTS

This study was funded in part by two Interagency Agreements with the U.S. Department of the Commerce, National Oceanic and Atmospheric Administration (NOAA), National Marine Fisheries Service (NMFS), Northeast Fisheries Science Center (NEFSC): Interagency Agreements M10PG0075, M14G00005, and M19PG00007 with the U.S. Department of the Interior, Bureau of Ocean Energy Management, and Interagency Agreements NEC 11-009, NEC 15-004, and NEC-16-011-01 with the Department of Defense, U.S. Navy.

Contents

List of Figures

List of Tables

List of Abbreviations and Acronyms

ABC	Area backscattering coefficient
AIC	Akaike Information Criterion
AICc	Akaike Information Criterion corrected for small sample sizes
AMAPPS	Atlantic marine assessment program for protected species
AMO	Atlantic multidecadal oscillation
BOEM	Bureau of Ocean Energy Management
BOF	Bay of Fundy
CFL	Central Florida stock
CFF	Coonamessett Farm Foundation
CI	Confidence interval
CTD	Conductivity, temperature and depth sampling device
CMAST	Center for Marine Sciences and Technology
CV	Coefficient of variation
CvM	Cramer-von Mises goodness-of-fit test
DASBR	Drifting autonomous spar buoy recorder
DFO	Department of Fisheries and Oceans Canada
DOI	United States Department of the Interior
DS	Distance sampling
DTAG	Digital acoustic recording tag
EcoMon	Ecosystem Monitoring Program
EDF	Effective degrees of freedom
eDNA	Environmental deoxyribonucleic acid
ESA	Endangered Species Act
ESP	Environmental Studies Program
ESPIS	Environmental Studies Program Information System
EEZ	Exclusive Economic Zone
%FO	Percent frequency of occurrence
GAM	Generalized additive statistical model
GOM	Gulf of Maine
GOMMAPPS	Gulf of Mexico marine assessment for protected species
GPS	Global positioning system
HARPs	High-frequency recording packages
HYCOM	Hybrid Coordinate Ocean Model
HZ	Heezen Canyon
IFAW	International Fund for Animal Welfare
ITS.DEEP	Integrated Technologies for Deep Diving Cetaceans Program
kts	Knots, unit of speed equal to 1 nautical mile per hour
MAE	Mean absolute error goodness-of-fit test
MAPE	Mean absolute percentage error goodness-of-fit test
MARSS	Multivariate autoregressive state-space models
MARUs	Marine autonomous recording units
MIT	Massachusetts Institute of Technology

MmMe	True’s beaked whale or Gervais’ beaked whale
MMPA	Marine Mammal Protection Act
MODIS	Moderate Resolution Imaging Spectroradiometer
MR	Mark-recapture
MRDS	Mark-recapture distance sampling
NAO	North Atlantic Oscillation index
NASA	National Aeronautics and Space Administration
NC	Nantucket Canyon
NE	Northeast
NEFSC	Northeast Fisheries Science Center
NEPA	National Environmental Policy Act
NEUS Shelf	Northeast Atlantic U.S. shelf
NFL	Northern Florida stock
NM	Northern Migratory stock
NMFS	National Marine Fisheries Service
NOAA	National Oceanic and Atmospheric Administration
NYSERDA	New York State Energy Research and Development Authority
OBIS-SEAMAP	Ocean Biodiversity Information System - Spatial Ecological Analysis of Megavertebrate Populations
OC	Oceanographer Canyon
PBR	Potential biological removal
RHO	Spearman’s rank correlation goodness-of-fit test
ROVs	Remotely operated vehicles
SE	Southeast
SEFSC	Southeast Fisheries Science Center
SEUS Shelf	Southeast Atlantic U.S. shelf
SM	Southern migratory stock
spp.	Species
SST	Sea surface temperature
U.S.	United States
USFWS	US Fish and Wildlife Service
VIAME	Video and Image Analytics for a Marine Environment
VPR	Video Plankton Recorder
WHOI	Woods Hole Oceanographic Institution
XBT	Expendable bathythermograph

1 Executive Summary

The Atlantic Marine Assessment Program for Protected Species (AMAPPS) is a comprehensive multi-agency research program on the U.S. Atlantic outer continental shelf, from Maine to the Florida Keys, covering waters from the coast to beyond the U.S. Exclusive Economic Zone (EEZ). The overarching goal of AMAPPS is to assess the abundance, distribution, ecology, and behavior of marine mammals, sea turtles, and seabirds throughout the U.S. Atlantic outer continental shelf and to evaluate these data within an ecosystem context where the results are accessible to managers, scientists and the public. Because marine ecosystems are complex and involve dynamic assemblages of many coexisting species, to understand these marine ecosystem processes and achieve the AMAPPS objectives, our research integrates cross-taxonomic groups across multiple trophic levels and uses a suite of data collection and analytical techniques.

The main agencies involved are the National Marine Fisheries Service (NMFS), U.S. Fish and Wildlife Service, Bureau of Ocean Energy Management (BOEM), and the U.S. Navy. We have also built collaborations with numerous other national and international organizations.

During AMAPPS I (1 October 2010 to 30 September 2014), we focused on conducting broad scale aerial and shipboard surveys, developing spatially explicit contemporaneous density-habitat models, estimating abundance and describing distribution patterns of marine mammals, sea turtles and seabirds using visual, acoustic and telemetry data. We also collected ecosystem habitat and animal behavior data (Palka et al. 2017). AMAPPS I was the initial step in providing us with the data needed to develop a baseline that would allow us to evaluate future trends.

During AMAPPS II (1 October 2014 to 30 September 2019) we continued core field survey work, as these surveys were particularly important given the inter-annual differences evident in the observed oceanographic data during the AMAPPS I timeframe. We conducted 31 projects led by researchers associated with AMAPPS and other collaborators (Table 1-1). These projects resulted in 47 published or in-review papers, 47 talks and posters presented at meetings and conferences, and an additional 19 papers are currently in preparation (Table 1-2). The continued collection of data (Chapter 11) allowed us to accomplish the AMAPPS objectives. These data included visual detections from aerial and shipboards surveys, passive acoustic detections, animal-borne tag locations, dive pattern data, and direct and indirect samples of the physical and biological oceanic ecosystem. With these data, we updated cetacean abundance estimates (Chapter 5). We also updated and expanded our knowledge of the spatiotemporal distributions, ecology, behavior and ecosystem interactions of cetaceans (Chapters 6 and 7), turtles (Chapter 8), seabirds (Chapter 9), and lower trophic levels, such as tuna larvae, plankton, and fish (Chapter 10). In addition, we are documenting the co-occurrence of cetacean species and anthropogenic noise along the shelfbreak ecosystem of the east coast (Chapter 7).

Understanding the physical and biological characteristics associated with the protected species occurrence, and the potential influence on their distribution is critical for the proper management of the protected species, especially as they face increasing natural and anthropogenic impacts. To help us place protected species within an environmental context, we evaluated spatiotemporal patterns in the distribution and abundance of protected species using data collected during AMAPPS I and II. The broad scale components of AMAPPS, such as determining the overall distribution of protected species in the U.S. east coast, help us evaluate risk of potential exposure to human stressors such as areas of energy development and fisheries interactions, for example. The finer scale analyses we performed by looking at the physical parameters that may influence their distribution, in addition to the behavioral studies we

conducted, help us better understand and potentially predict their occurrence, which will inform marine spatial planning efforts, as well as inform the development of strategies to mitigate potential negative impacts of human activities.

The continued collection of visual and passive acoustic data during AMAPPS II allowed us to learn more about the distribution, abundance, and habitat usage of protected species. During the 5 years in AMAPPS II, we surveyed over 148,000 km of track lines during aerial and shipboard surveys, where we visually recorded nearly 12,000 marine mammals (Chapters 5 and 6), about 6,500 sea turtles (Chapter 8), and nearly 170,000 seabirds (Chapter 9). We collected passive acoustic data from towed hydrophone arrays associated with over 19,000 km of shipboard effort, as well as from 32 sonobuoys and 5 drifting autonomous spar buoy recorders (Chapter 7). We also collected passive acoustic data from bottom-mounted recorders at nearly 40 sites that spanned offshore the eastern seaboard from Massachusetts to Florida from 2015 to 2019 (Chapter 7). We collected 41 samples of environmental DNA near beaked whales, tagged the first True's beaked whale (*Mesoplodon mirus*) to learn about their diving patterns and habitat usage, and published the first acoustic description of this species' echolocation. We collected time-depth-temperature data from 49 animal-borne tags on loggerhead turtles (*Caretta caretta*) and 31 on leatherback turtles (*Dermochelys coriacea*; Chapter 8) to learn about their diving patterns and habitat usage. In addition, during the AMAPPS II timeframe, we gained access to data from 55 tags deployed by collaborators on other loggerhead turtles (Chapter 8). We collected data on water characteristics from over 400 conductivity-temperature-depth (CTD) sampling stations to learn more about the ecosystem these protected species inhabit (Chapter 10). In addition, we collected 18,700 temperature-depth profiles from the loggerhead turtle tags (Chapter 8). We also collected plankton data from 170 bongo tows, 38 deployments of a visual plankton recorder, 59 midwater trawl tows, and about 100 samples from other devices (Go-Pro camera, frame-net, and DIDSON) to learn more about the trophic ecology of these protected species and the planktonic environment itself (Chapter 10).

In addition to the suite of standard analytical methods that we used to analyze the newly and previously collected AMAPPS data, we are developing or using new statistical approaches. We are still in the process of developing a novel statistical framework to estimate the abundance of deep-diving cetaceans and obtain better estimates of availability bias using visual and passive acoustic data combined (Chapter 5). We are estimating long-term abundance trends using state-space models (Chapter 5). We are developing a new Bayesian hierarchical framework to estimate density surface models, as well as density surface models that incorporate potential prey data in addition to standard environmental data (Chapter 6). We developed a method to estimate the dive depths of deep-diving cetaceans from towed hydrophone passive acoustic data (Chapter 7). We have also implemented new methods for visualizing the spectral-temporal overlap between protected species' acoustic signals and anthropogenic sources (Chapter 7). In addition, we made a methodology contribution to the process of estimating space utilization distributions from satellite telemetry data by using geostatistical mixed effects models that explicitly account for spatial and/or temporal correlations (Chapter 8).

We also explored the use of several new technologies. We explored an emerging technique called environmental DNA (eDNA; genetic signatures from the environment of the animal, rather than directly sampling animal tissue). The goal was to determine if we could effectively document the presence and identify of cetacean species using water samples collected near animal dive positions, as well as to explore the use of the methodology to inform stock structure questions (Chapter 7). We also collaborated with researchers who used remotely operated vehicles to video-record turtle behavior and we, along with collaborators developed a tag and tagging procedure that is cost effective for studying leatherback turtles (Chapter 8).

We have improved and updated our knowledge on the distribution and abundance of protected species along the U.S. Atlantic Ocean thanks to the additional data collected and analyzed during AMAPPS II. We updated the stock assessments of 25 cetacean species using the abundance estimates derived from the AMAPPS II data (Chapter 5). We developed seasonal spatial density distribution models for 18 cetacean species or species groups (Chapter 6) that illustrated how the species use the AMAPPS study area including the wind energy areas. We documented recent declines in the abundance of some of the coastal bottlenose dolphins (*Tursiops truncatus*; Chapter 5). We documented shifts in the distribution and abundance of many cetaceans in U.S. waters, including declines in abundance of sei whales (*Balaenoptera borealis*) and harbor porpoises (*Phocoena phocoena*) since 2014 and increases in abundance of long-finned pilot whales (*Globicephala melas*; Chapters 5 and 6) since 2015. For other species, we documented spatial shifts correlated to changes in values of environmental covariates (Chapters 5 and 6). These species included humpback whales (*Megaptera novaeangliae*; associated with chlorophyll front strength), fin whales (*Balaenoptera physalus*; associated with the location of the north wall of the Gulf Stream), Atlantic white-sided dolphins (*Lagenorhynchus acutus*; associated with the location of the south wall of the Gulf Stream), and common bottlenose dolphins (*Tursiops truncatus*; associated with sea surface temperature). We used passive acoustic and visual data to better document the spatiotemporal distributions of cryptic deep divers like beaked (Ziphiidae), pygmy and dwarf sperm whales (*Kogia* spp.) and sperm whales (*Physeter macrocephalus*; Chapter 7). We documented the seasonal distribution of 5 baleen whale species along the U.S. eastern seaboard, including the winter distribution of pelagic baleen whales along the shelfbreak down through the Blake Plateau off Florida. We developed monthly relative abundance maps of tagged loggerhead turtles (Chapter 8). From the tagged loggerhead and leatherback turtles we observed broad dispersal throughout the AMAPPS study area, with extensive coverage on the shelf including the wind energy areas, and with overall coverage ranging from the Gulf of Mexico to the Mid-Atlantic Ridge (30°W; Chapter 8). We also collected seabird distribution data that showed there were spatial and seasonal changes in species composition and abundance on the Northeast U.S. shelf and adjacent offshore waters throughout the AMAPPS study area and period (Chapter 9).

The use of innovative technologies during AMAPPS II helped to improve our knowledge of the ecology and behavior of several protected species. We deployed the first ever DTAG (digital acoustic recording tag) on a True's beaked whale (*Mesoplodon mirus*), providing new insights into this species' dive and foraging behavior (Chapter 7). In addition, we learned about this species' acoustic detection rates, stock structure, and population dynamics through passive acoustic sampling, genetic sampling, photo-identifications, and focal follows (Chapter 7). Through AMAPPS and its collaborative efforts, we deployed over 300+ satellite tags on loggerhead turtles that collected data on location, surface availability, and behavior throughout the water column (Chapter 8) and we documented turtle behavior on video. The analysis of the loggerhead tag locations suggests there may be more loggerheads in the Mid-Atlantic than we previously estimated. In addition, loggerheads appear to frequently dive into cold, highly stratified portions of the water column, colder than we previously assumed (Chapter 8). We also collected data on the distribution and abundance of plankton and other trophic levels from the under-sampled waters that are deeper than the continental shelf using a variety of sampling devices (Chapter 10). Data on different trophic levels are assisting us in putting the distribution and abundance of cetaceans into an ecosystem context and explaining some of the variability we documented in the distribution and abundance patterns during AMAPPS II (Chapters 5 and 6) and previously during AMAPPS I (Palka et al. 2017).

End users, such as managers from NMFS and BOEM, ocean users from wind energy developers and the U.S. Navy, along with other scientists and the public in general, are interested in using the raw data we collected as well as the finished products resulting from the data we collected, processed, and analyzed.

To accommodate the sharing of the data and finished products, we described what data we collected, how the data were processed, and where the data and finished products are available to the public (Chapter 11). The raw data are available on websites allowing for easy downloading and subsequent usage in other research projects. Basic visual line-transect are available at OBIS-SEAMAP. Additional more detailed visual line-transect data are archived in a NEFSC Oracle database and are available upon request. Seabird strip transect data are available at the Northwest Atlantic Seabird Catalog. Temperature depth profiles collected from tagged loggerhead turtles are also available online.

In addition to raw data, we made various finished products readily available for access and use by managers, scientists and the public. We published papers and presented results at meetings and scientific conferences (Table 1-2). We provided cetacean abundance estimates and distribution maps at various spatial scales, ranging from the entire Atlantic Outer Continental Shelf off the coasts of the U.S. and Canada (Chapter 5, Appendices I and II, and Stock Assessment Reports) to smaller areas proposed for wind energy development off the Atlantic coast of the U.S. (Chapter 6 and Appendix III). In addition, we provided the cetacean abundance estimates and trends at various temporal scales. Abundance estimates ranged from species-specific estimates for the summer of 2016 (Chapter 5), to seasonal estimates averaged over 2010 to 2017 (Chapter 6), and to estimated abundance trends during 1992 to 2016 (Chapter 5). The species-specific spatiotemporal density map data from Chapter 6 and Appendix I will be available from the AMAPPS Marine Mammal Model Viewer, where we are currently hosting the 2010 to 2013 density maps. The shape files of estimated monthly distribution of tagged loggerheads are also available. In addition, the acoustically-detected daily presence results for 5 baleen whale species, beaked whales, and sperm whales are on a Passive Acoustic Cetacean Map (website will become public shortly).

Table 1-1 List of projects conducted by AMAPPS II researchers and collaborators
More information on each project is in the listed chapter and appendices within this document and in other references (including papers, talks, and online sources as itemized in Table 1-2).

Category	Project*	Current Target Species	Chapters	Product References
Abundance	Estimate abundance using visual line transect data	Cetaceans	5	1-6, 11-16, 48, 51, 53
Stock assessment	Assess status of stock using abundance, bycatch, etc data	Cetaceans, seals	5	5, 7-10, 18-19
Abundance	Estimate abundance using photographs	Harbor seal	AMAPPS I report	17, 48
Abundance	Estimate abundance using visual and passive acoustic data	Sperm whales	5	60 – 61
Abundance, Trends	Estimate abundance trends using state-space models	Cetaceans	5	
Abundance-supporting	Develop correction factors to account for availability bias of visual survey data using tag data from other studies	Cetaceans	5	48, 57
Abundance, Distribution, Ecosystem	Distribution and abundance using visual data in a 2-stage generalized additive model framework	Cetaceans	6, 7 Appendix I & III	1, 12 – 16, 38, 48, 51 – 52
Distribution, Ecosystem	Habitat suitability of cetaceans	Cetaceans	6	1, 38, 48 – 51

Abundance, Distribution, Ecosystem	Distribution and abundance using visual data in Bayesian hierarchical model framework	Cetaceans	6	15, 48, 58 – 59
Abundance, Distribution, Ecosystem	Distribution and abundance using visual and other trophic level data	Cetaceans	6, 10	38, 40, 62 – 64, 90 – 92
Abundance and distribution - supporting	Extract static and dynamic habitat values from satellite-based and model-based online sources	Cetaceans, turtles, birds, seals	6, 11	88, 95
Distribution, Ecology	Distribution using visual, passive acoustic, and eDNA data	Beaked whales, pygmy and dwarf sperm whales	7	65, 94
Abundance, Distribution, Ecology	Dive patterns and distribution using DTAG and focal follow data	Beaked whales	7	
Distribution	Distribution using fixed passive acoustic monitoring	Large whales	7	22-23, 27, 48, 66, 73 – 76
Ecology	Distribution of ambient noise using passive acoustic monitoring	NA	7	21, 27, 48, 66, 74, 75
Abundance and distribution - supporting	Effects of echosounders on beaked whales	Beaked whales	7	20, 48, 67 – 68, 71
Behavior and Abundance-supporting	Estimate dive depth from acoustic localizations of deep-diving species	Beaked whales	7	25, 48, 70
Ecology and Distribution - supporting	Characterize acoustic repertoire, vocal behavior, and anthropogenic noise	Whales	7	24, 26, 48, 69, 72
Behavior, Distribution	* Within water column distribution of turtles using tag data	Loggerhead and leatherback turtles	8	28 – 29, 48
Behavior, Distribution	* Within water column distribution of turtles using underwater remote vehicles	Loggerhead turtles	8	30
Abundance, Distribution	Estimate density distribution of turtles using tags and visual line transect data	Loggerhead turtles	8	32, 48, 78, 79
Life history	* Collect biological and life history characteristics	Loggerhead and leatherback turtles	8	33, 48, 77, 80, 81
Management	* Evaluate population monitoring metrics to assess impacts	Loggerhead turtles	8	31

Distribution	Distribution of seabirds	Seabirds	9	34, 48
Abundance	* Distribution and relative abundance of seabirds	Seabirds	9	34
Ecosystem-supporting	Distribution of ocean physical and biological (plankton, fish and other trophic levels) characteristics	Other trophic levels	10, 11	36, 39, 48, 89, 90
Ecosystem-supporting	Explore alternative sampling devices to document distribution of other trophic levels	Other trophic levels	10	30, 48
Ecosystem, Biology	*Salp ecology and species identification	Salps	10	35, 37, 82 – 84
Ecosystem, Biology	*Distribution and species identification of bluefin tuna larvae	Bluefin tuna	10	41 – 46, 48, 85 – 87, 93
Ecosystem, Biology	*Adapt the image analytics for Video Plankton Recorder data	Other trophic levels	10	
Outreach	Disseminate maps and abundance estimates to the public	Cetaceans, turtles	5, 6, 7, 8, 11	54 – 56, 100, 105
Outreach	Make field data available to the public	Cetaceans, turtles, seabirds, other trophic levels	5 – 11	88, 95 – 108
Outreach	Update on AMAPPS projects	Cetaceans, turtles, seabirds, other trophic levels	5 – 11	51, 54 – 56, 76, 99, 109 – 122

* A collaborator is the primary lead of these projects.

Table 1-2 List of products resulting from data collected under AMAPPS II
List of published and in review papers (A), conference and meeting presentations (B), databases (C), and web presence for data (D), web presence of newsletters, blogs, and news articles (E), and papers in preparation (F). Authors directly working on AMAPPS II projects are in bold.

A. PUBLISHED AND IN-REVIEW REFEREED/TECHNICAL PAPERS

Abundance and distribution

1) **Chavez-Rosales S, Palka DL, Garrison L, Josephson E.** 2019. Environmental predictors of habitat suitability and occurrence of cetaceans in the western North Atlantic Ocean. Sci Rep 9:5833.
2) **Garrison LP.** 2020. Abundance of marine mammals in waters of the U.S. east coast during summer 2016. Southeast Fisheries Science Center, Protected Resources and Biodiversity Division, 75 Virginia Beach Dr., Miami, FL 33140. PRBD Contribution #PRBD-2020-04; 17 pp.
3) **Garrison LP**. 2016. Abundance of marine mammals in waters of the U.S. east coast during summer 2011. Southeast Fisheries Science Center, Protected Resources and Biodiversity Division, 75 Virginia Beach Dr., Miami, FL 33140. PRBD Contribution # PRBD-2016-08; 21 pp.
4) **Garrison LP**, Barry K, Hoggard W. 2017. The abundance of coastal morphotype bottlenose dolphins on the U.S. east coast: 2002-2016. Southeast Fisheries Science Center, Protected Resources and Biodiversity Division, 75 Virginia Beach Dr., Miami, FL 33140. PRBD Contribution # PRBD-2017-01; 37 pp.
5) **Garrison LP**, Rosel PE. 2017. Partitioning short-finned and long-finned pilot whale bycatch estimates using habitat and genetic information. Southeast Fisheries Science Center, Protected Resources and Biodiversity Division, 75 Virginia Beach Dr., Miami, FL 33140. PRBD Contribution # PRBD-2016-17; 24 pp.
6) **Garrison LP, Palka D.** 2018. Abundance of short-finned pilot whales along the U.S. east coast from summer 2016 vessel surveys. Southeast Fisheries Science Center, Protected Resources and Biodiversity Division, 75 Virginia Beach Dr., Miami, FL 33140. PRBD Contribution # PRBD-2018-07; 18p.
7) Hayes SA, **Josephson E**, Maze-Foley K, Rosel P. eds. 2020. U.S. Atlantic and Gulf of Mexico marine mammal stock assessments - 2019. NOAA Tech Memo NMFS NE-264; 479 pp.
8) Hayes SA, **Josephson E**, Maze-Foley K, Rosel PE. 2019. US Atlantic and Gulf of Mexico marine mammal stock assessments - 2018. NOAA Tech Memo NMFS NE-258; 291 pp.
9) Hayes SA, **Josephson E**, Maze-Foley K, Rosel PE, Byrd B, **Chavez-Rosales S**, Col TVN, Engleby L, **Garrison LP**, Hatch J, Henry A, Horstman SC, Litz J, Lyssikatos MC, Mullin KD, **Orphanides C**, Pace RM, **Palka DL**, **Soldevilla M**, Wenzel FW. 2018. TM 245 US Atlantic and Gulf of Mexico marine mammal stock assessments - 2017. NOAA Tech Memo NMFS NE-245; 371 pp.
10) Hayes SA, **Josephson E**, Maze-Foley K, Rosel PE, editors. 2017. US Atlantic and Gulf of Mexico marine mammal stock assessments - 2016. NOAA Tech Memo NMFS-NEFSC-241; 274 pp.
11) **Palka D**. 2020. Cetacean abundance in the US Northwestern Atlantic Ocean summer 2016. US Dept Commer, Northeast Fish Sci Cent Ref Doc. 20-05; 60 pp.
12) Roberts JJ, Best BD, Mannocci L, Fujioka E, Halpin PN, **Palka DL**, **Garrison LP**, Mullin KD, Cole TVN, Khan CB, McLellan WA, Pabst DA, Lockhart GG. 2016. Habitat-based cetacean density models for the US Atlantic and Gulf of Mexico. Sci Rep 6:22615.

13) Roberts JJ, Mannocci L, Halpin PN. 2017. Final project report: Marine species density data gap assessments and update for the AFTT study area, 2016-2017 (Opt. Year 1), Document Version 1.4. Duke University Marine Geospatial Ecology Lab, Durham, NC; 87 pp.

14) Roberts JJ, Mannocci L, Schick RS, Halpin PN. 2018. Final project report: Marine species density data gap assessments and update for the AFTT Study Area, 2017-2018 (Opt. Year 2), Document Version 1.2. Report prepared for Naval Facilities Engineering Command, Atlantic by the Duke University Marine Geospatial Ecology Lab, Durham, NC; 114 pp.

15) **Sigourney DB**, **Chavez-Rosales S**, Conn PB, **Garrison L, Josephson E**, **Palka D**. 2020. Developing and assessing a density surface model in a Bayesian hierarchical framework with a focus on uncertainity: Insights from simulations and an application to fin whales (*Balaenoptera physlus*). PeerJ 8:e8226.

16) Virgili A, Authier M, Boisseau O, Canadas A, Claridge D, Cole T, Corkeron P, Doremus G, David L, DiMeglio N, Dunn C, Dunn TE, Garcia Baron I, Laran S, Lewis M, Louzao M, Mannocci L, Martinez-Dedeira J, **Palka D**, Panigada S, Pettex E, Roberts J, Ruiz Sancho L, Santos MB, VanCannery O, Vazquez Bonales JA, Monestiez P, Ridoux V. 2018. Combining multiple visual surveys to model habitats of deep diving cetaceans at the basin level. Glob. Ecol. Biogeogr. 28(3):300-314.

17) **Waring GT**, DiGiovanni RA Jr**, Josephson E**, Wood S, Gilbert JR. 2015. 2012 population estimate for the harbor seal (*Phoca vitulina concolor*) in New England waters. NOAA Tech Memo NMFS NE-235; 15 p.

18) **Waring GT**, **Josephson E**, Maze-Foley K, Rosel, PE, editors. 2016. U.S. Atlantic and Gulf of Mexico marine mammal stock assessments – 2015. NOAA Tech Memo NMFS NE 238; 464 pp.

19) **Waring GT**, **Josephson E**, Maze-Foley K, Rosel, PE, editors. 2015. US Atlantic and Gulf of Mexico marine mammal stock assessments - 2014. NOAA Tech Memo NMFS NE 231; 361 pp.

Passive acoustics

20) **Cholewiak D**, **DeAngelis AI**, **Palka D**, Corkeron P, **Van Parijs SM** 2017. Beaked whales demonstrate a marked acoustic response to the use of shipboard echosounders. R. Soc. Open Sci.:170940.

21) **Cholewiak D**, Clark CW, Ponirakis D. Frankel A, Hatch LT, **Risch D**, **Stanistreet JE**, Thompson M, **Vu E**, **Van Parijs SM.** 2018. Communicating amidst the noise: modeling the aggregate influence of ambient and vessel noise on baleen whale communication space in a national marine sanctuary. Endang Species Res 36:59-75.

22) **Davis GE**, Baumgartner MF, Bonnell JM, Bell J, Berchok C, Bort Thorntom J, Brault S, Buchanan G, Charif RA, **Cholewiak D**, Clark CW, Corkeron P, Delarue J, Dudzinski K, **Hatch L**, Hildebrand J, Hodge L, Klinck H, Kraus S, Martin B, Mellinger DK, Moors-Murphy H, Nieukirk S, Nowacek DP, Parks S, Read AJ, Rice AN, **Risch D**

the western North Atlantic using a decade of passive acoustic data. Glob. Change Biol. 26(9):4812-4840.

24) **DeAngelis A,** Stanistreet J, Baumann-Pickering S**, Cholewiak D**. 2018. A description of echolocation clicks recorded in the presence of True's beaked whale (*Mesoplodon mirus*). J. Acoust. Soc. Am. 144(5):2691-2700.

25) **DeAngelis A**, Valtierra R, **Van Parijs S**, **Cholewiak D**. 2017. Using multipath reflections to obtain dive depths of beaked whales from a towed hydrophone array. J. Acoust. Soc. Am. 142(2):1078-1087.

26) **Soldevilla MS**, Baumann-Pickering S, **Cholewiak D**, Hodge LE, Oleson EM, Rankin S. 2017. Geographic variation in Risso's dolphin echolocation click spectra. J. Acoust. Soc. Am. 142(2):599-617.

27) Weiss S, Baumann-Pickering S, Frasier K, Hildebrand J, Trickey J, **Van Parijs SM, Cholewiak D**. (*in review*). Monitoring the acoustic ecology of the shelf break of Georges Bank, northwestern Atlantic Ocean – new approaches to visualizing complex data. Submitted to Marine Policy.

Sea turtles

28) Patel SH, Barco SG, **Crowe LM**, Manning JP, **Matzen E**, Smolowitz RJ, **Haas HL**. 2018. Loggerhead turtles are good ocean-observers in stratified mid-latitude regions. Estuar. Coast. Shelf Sci. 213:128-136.

29) Patel SH, Dodge KL, **Haas HL**, Smolowitz RJ. 2016. Videography reveals in-water behavior of loggerhead turtles (*Caretta caretta*) at a foraging ground. Front. Mar. Sci. 3:254.

30) Smolowitz RJ, Patel SH, **Haas HL**, Miller S. 2015. Using a remotely operated vehicle (ROV) to observe loggerhead sea turtle (*Caretta caretta*) behavior on foraging grounds off the mid-Atlantic United States. J. Exp. Mar. Biol. Ecol. 471:84–91.

31) **Warden ML**, **Haas HL**, Richards PM, Rose KA, **Hatch JM**. 2017. Monitoring trends in sea turtle populations: walk or fly? Endang Species Res 34:323-337.

32) **Winton MV**, Fay G, **Haas HL**, Arendt M, Barco S, James M, **Sasso C**, Smolowitz R. 2018. Estimating the distribution and relative density of tagged loggerhead sea turtles in the western North Atlantic from satellite telemetry data using geostatistical mixed effects models. Mar. Ecol. Prog. Ser. 586:217-232.

33) Yang T, **Haas HL**, Patel S, Smolowitz R, James MC, Williard A. 2019. Blood biochemistry and hematology of migrating loggerhead turtles (*Caretta caretta*) in the Northwest Atlantic: reference intervals and intrapopulation comparisons. Conserv. Physiol. 7(1):coy079.

Seabirds

34) Winship AJ, Kinlan BP, White TP, Leirness JB, Christensen J. 2018. Modeling at-sea density of marine birds to support Atlantic marine renewable energy planning: Final report. U.S. Department of the Interior, Bureau of Ocean Energy Management, Office of Renewable Energy Programs, Sterling, VA. OCS Study BOEM 2018-010; 67 pp.

Ecosystem

35) Batta-Lona PG, Maas A, O'Neill R, Wiebe PH, Bucklin A. 2016. Transcriptomic profiles of spring and summer populations of the Southern Ocean salp, *Salpa thompsoni*, in the Western Antarctic Peninsula region. Polar Biol. 40:1261-1276.

36) Fratantoni PS, Holzwarth-Davis T, Melrose DC, Taylor MH. 2019. Description of oceanographic conditions on the Northeast US Continental Shelf during 2016. US Dept Commer, Northeast Fish Sci Cent Ref Doc. 19-07; 39 pp.

37) Jue N, Batta-Lona PG, Trusiak S, Obergfell C, Bucklin A, O'Neill MJ, O'Neill RJ. 2016. Rapid evolutionary rates and unique genomic signatures discovered in the first reference genome for the Southern Ocean salp, *Salpa thompsoni* (Urochordata, Thaliacea). Genome Biol. Evol. 8:3171-3186.

38) **LaBrecque E**. 2016. Spatial Relationships among Hydroacoustic, Hydrographic and Top Predator Patterns: Cetacean Distributions in the Mid-Atlantic Bight. PhD thesis. Duke University, Durham, NC.

39) NEFSC (Northeast Fisheries Science Center). 2010 – 2019. Hydrographic conditions of the Northeast continental shelf summaries for each year 2010 - 2018.

40) **Orphanides CD**. 2019. Relating marine mammal distribution to prey abundance. Ph.D. Dissertation. Graduate School of Oceanography, University of Rhode Island, Kingston, RI.

41) Richardson DE, Marancik KE, Guyon JR, Lutcavage ME, Galuardi B, Lam CH, **Walsh HJ**, Wildes S, Yates DA, and Hare JA. 2016a. Discovery of a spawning ground reveals diverse migration strategies in Atlantic bluefin tuna (*Thunnus thynnus*). Proc. Natl. Acad. Sci. U.S.A. 113(12):3299-3304.

42) Richardson DE, Marancik KE, Guyon JR, Lutcavage ME, Galuardi B, Lam CH, **Walsh HJ**, Wildes S, Yates DA, Hare JA. 2016b. Reply to Safina and Walter et al.: Multiple lines of evidence for size-structured spawning migrations in western Atlantic bluefin tuna. Proc. Natl. Acad. Sci. U.S.A. 113 (30):E4262-4263.

43) Rodríguez-Ezpeleta N, Díaz-Arce N, Walter Iii JF, Richardson DE, Rooker JR, Nøttestad L, Hanke AR, Franks JS, Deguara S, Lauretta MV, Addis P, Varela JL, Fraile I, Goñi N, Abid N, Alemany F, Oray IK, Quattro JM, Sow FN, Itoh T, Karakulak FS, Pascual-Alayón PJ, Santos MN, Tsukahara Y, Lutcavage M, Fromentin J-M, Arrizabalaga H. 2019. Determining natal origin for improved management of Atlantic bluefin tuna. Front. Ecol. Environ. 17:439-444.

44) Rypina II, Chen K, Hernández CM, Pratt LJ, Llopiz JK. 2019. Investigating the suitability of the Slope Sea for Atlantic bluefin tuna spawning using a high-resolution ocean circulation model. ICES J. Mar. Sci.:fsz079.

45) Safina C. 2016. Data do not support new claims about bluefin tuna spawning or abundance. Proc. Natl. Acad. Sci. U.S.A. 113(30):E4126.

46) Walter JF, Porch CE, Lauretta MV, Cass-Calay SL, Brown CA. 2016. Implications of alternative spawning for bluefin tuna remain unclear. Proc. Natl. Acad. Sci. U.S.A. 113(30):E4259-E4260.

Other

47) NEFSC and SEFSC (Northeast Fisheries Science Center and Southeast Fisheries Science Center). 2011-2019. Annual reports of work conducted under AMAPPS for each year 2010 to 2019. AMAPPS reports.

48) Palka DL, Chavez-Rosales S, Josephson E, Cholewiak D, Haas HL, Garrison L, Jones M, Sigourney D, Waring G (retired), Jech M, Broughton E, Soldevilla M, Davis G, DeAngelis A, Sasso CR, Winton MV, Smolowitz RJ, Fay G, LaBrecque E, Leiness JB, Dettlof M, Warden M, Murray K, Orphanides C. 2017. Atlantic Marine Assessment Program for Protected Species: 2010- 2014. US Dept. of the Interior, Bureau of Ocean Energy Management, Atlantic OCS Region, Washington, DC. OCS Study BOEM 2017-071; 211 pp.

B. CONFERENCE AND MEETINGS PRESENTATIONS:

Abundance and Distribution

49) **Chavez-Rosales S**, **Palka D**, **Garrison L**, **Josephson E**, **Sigourney D.** 2019. Habitat suitability as a tool to detect spatial and temporal distribution changes of marine mammals. Poster at the World Marine Mammal Conference. Barcelona, Spain. December 2019.

50) **Chavez-Rosales S**, **Palka D**, **Garrison L**, **Josephson E**. 2017. Environmental predictors of habitat suitability and cetacean occurrence in the western North Atlantic Ocean. Poster at Biennial Conference on the Biology of Marine Mammals. Halifax, Nova Scotia. October 2017.

51) **Chavez-Rosales S.** 2017. Atlantic Marine Assessment Program for Protected Species. Presentation at "Oceanos : Woods Hole Oceanographic Institution en Español e Português". Woods Hole, MA. September 2017.

52) **Chavez-Rosales S, Sigourney D.** 2017. Habitat density models for cetaceans in the Atlantic: A Brief overview of the AMAPPS modeling efforts. Presentation at the Density Modeling (DenMod) workshop. Halifax, Nova Scotia. October 2017.

53) **Dias LA**, **Ortega-Ortiz J**, Rappucci G, Litz J, **Garrison L**, **Soldevilla M**, Martinez A, Mullin K. 2019. Can you see me now? Evaluating the detectability of cetaceans during line-transect surveys in the SE US. Poster at the Gulf of Mexico Oil Spill and Ecosystem Science Conference. New Orleans, LA. 4 to 7 February 2019.

54) **Palka DL**. 2016. Atlantic Marine Assessment Program for Protected Species. Presentation at the Proceedings to the Atlantic Ocean Energy and Mineral Science Forum. Sterling, VA. 16 to 17 November 2016.

55) **Palka DL**. 2017. Atlantic Marine Assessment Program for Protected Species. Presentation at the "Best Management Practices Workshop for Atlantic Offshore Wind Facilities and Marine Protected Species". Silver Spring, MD. March 2017.

56) **Palka DL**, **VanParijs S**. 2018. Update on AMAPPS with focus on work in New York area. Presentation at the First Annual New York Bight Whale Monitoring Workshop. East Setauket, NY. 13 June 2018.

57) **Palka DL**, **Warden M. 2017**. Accounting for availability bias in line transect abundance estimates. Poster at Biennial Conference Biology of Marine Mammals. Halifax, Nova Scotia. October 2017.

58) **Sigourney DB**, **Palka D**, **Chavez S.** 2015. Developing species distribution models for large whales to inform marine spatial planning. Invited presentation to the University of Massachusetts - Dartmouth. School of Marine Science and Technology Fall Lecture Series. September 2015.

59) **Sigourney D**, **Chavez-Rosales S**, **Palka D**, **Garrison L**, **Josephson E**. 2017. Fitting a species distribution model to line transect data of humpback whales (*Megaptera novaeangliae*) in the western Atlantic using a Bayesian hierarchical framework: Implications for uncertainty. Presentation at the Biennial Conference on the Biology of Marine Mammals. Halifax, Nova Scotia. October 2017.

60) **Sigourney DB**, **Cholewiak D**, **Palka D**. 2018. Integrating passive acoustic data with visual line transect surveys to refine population estimates and estimate availability bias for sperm whales (*Physeter macrocephalus*). Presentation at the S&T Protected Species Toolbox mini-symposium. San Diego, CA. 1 March 2018.

61) **Sigourney D**, **DeAngelis A**, **Cholewiak D**, **Palka D**. 2019. Integrating passive acoustic data with visual line transect surveys to refine population estimates and estimate availability bias for sperm and beaked whales. Presentation at the Second Protected Species Assessment Workshop. San Diego, CA. 12 to 14 February 2019.

62) Stepanuk J, Chong-Montenegro C, Nye JA, Roberts JJ, Halpin PN, **Palka DL**, Past A, McLellan WA, Barco SG, Thorne LH. 2019. Developing short-term forecasts of marine mammal distributions in the Northeast United States. Presentation at the AAAS Ecological Forecasting Initiative Conference. Washington, DC. 13 to 15 May 2019.

63) Stepanuk J, Chong-Montenegro C, Nye JA, Roberts JJ, Halpin PN, **Palka DL**, Past A, McLellan WA, Barco SG, Thorne LH,. 2019. Developing short-term forecasts of marine mammal distributions in the Northeast United States. Poster at the World Marine Mammal Conference. Barcelona, Spain. December 2019.

64) Virgili AV, Authier M, Cadeira J, Canadas A, Cole T, Corkeron P, Doremus LD, Di-Meglio N, Dunn C, Dunn T, Hammond P, **Josephson E**, Laran S, Lewis M, Louzao M, Luiz L, Mannocci L, Moscrop A, **Palka D**, Panigada S, Pettex E, Roberts J, Santo MB, VanCanneyt O, Vazquez Bonales A, Monestiez P, Ridoux V. 2017. Basin-wide approach, combined datasets and gap analyses: Options to overcome the lack of sightings data on rare cetacean species. Focus is on deep divers (beaked and sperm whales). Presentation at the European Cetacean Society meeting. Denmark. 29 April to 3 May 2017.

Passive Acoustics

65) **Cholewiak D**, Baker CS, Cerchio S, Conger L, **DeAngelis A**, Hickmott L, Metheny N, Pitman R, **Stanistreet J**, Steel D, **Tremblay C**, Trickey J. 2019. True's beaked whale: a cryptic species revealed. Presentation at World Marine Mammal Conference. Barcelona, Spain. December 2019.

66) **Cholewiak D**, **Van Parijs SM**. 2019. Shelfbreak cetacean acoustic ecology and anthropogenic noise. Presentation at US Navy Marine Species Monitoring Program Atlantic Technical Review Meeting. Virginia Beach, NC. 12 to 13 March 2019.

67) **Cholewiak D**, **DeAngelis A**, **Palka D**, Corkeron P, **Van Parijs SM**. 2017. Beaked whales demonstrate a marked response to the use of shipboard echosounders. Presentation at the Biennial Conference on the Biology of Marine Mammals. Halifax, Nova Scotia. October 2017.

68) **Cholewiak D**, **DeAngelis AI**, Corkeron PJ, **Van Parijs SM**. 2017. Shipboard echosounders negatively affect acoustic detection rates of beaked whales. Presentation at the Joint Meeting of the Acoustical Society of America and the European Acoustics Association. Boston, MA. June 2017.

69) **DeAngelis AI**, **VanParijs S**, **Palka D**, **Cholewiak D**. 2017. Is it truly Trues? First description of True's beaked whale clicks. Presentation at the Biennial Conference on the Biology of Marine Mammals. Halifax, Nova Scotia. October 2017.

70) **Izzi A**, Valtierra R, **Van Parijs SM**, **Cholewiak D**. 2015. Using multipath arrivals to obtain three-dimensional localizations for beaked whales on acoustic line transect surveys. Presentation at the Biennial Conference on the Biology of Marine Mammals. San Diego, CA. 13 to 18 December 2015.

71) **Izzi A**, **VanParijs SM**, **Cholewiak D**. 2015. Understanding the effects of echosounders on detection rates of beaked whales from shipboard surveys. Presentation at the Watkins Memorial Marine Mammal Bioacoustics Symposium. New Bedford, MA. March 2015.

72) Rankin S, Sakai T, Archer E, Barlow J, **Cholewiak D**, **DeAngelis A**, Keating J, Oleson E, Simonis A, **Soldevilla M**. 2019. A machine learning approach to acoustic classification of beaked whales. Poster at World Marine Mammal Conference. Barcelona, Spain. December 2019.

73) **Van Parijs SM**. 2016. Migratory movements of marine mammals from historic acoustic measurements. Presentation at the Proceedings to the Atlantic Ocean Energy and Mineral Science Forum. Sterling, VA. 16 to 17 November 2016.

74) **VanParijs SM**. 2017. Atlantic passive acoustic monitoring of soundscapes. Presentation at the Best Management Practices Workshop for Atlantic Offshore Wind Facilities and Marine Protected Species. Silver Spring, MD. March 2017.

75) **Van Parijs S**, **Cholewiak D**, Davis G, **DeAngelis A**, Weiss S, Gurnee J. 2018. Atlantic species ecology and effects of anthropogenic noise. Presentation at the US Navy Marine Species Monitoring Technical Review Meeting. San Diego, CA. March 2018.

76) **Van Parijs SM**. 2019. Update on AMAPPS. Presentation at the New York Bight Whale Monitoring Workshop. Setauket-East Setuaket, NY. 6 June 2019.

Sea Turtles

77) Allen CD, **Haas HL**, Smolowitz RJ, Patel SH, Seminoff JA. 2018. Corticosterone concentrations in migratory loggerhead sea turtles. Presentation at Annual Symposium on Sea Turtle Biology and Conservation. Japan.

78) **Haas H**. 2018. Collaborative turtle research in the Greater Atlantic Region. Presentation at the New York Bight Sea Turtle Workshop. New York. 30 January 2018.

79) **Winton M**, Fay G, **Haas H**, Arendt M, Barco S, James M, **Sasso C**, Smolowitz R. 2017. Estimating loggerhead sea turtle densities from satellite telemetry data using geostatistical mixed models. Presentation at the Southern New England Chapter of the American Fisheries Society.

80) Yang T, **Haas HL**, Smolowitz R, Patel S, James M, Williard A. 2016. Baseline blood biochemical values for the Northwest Atlantic population of loggerhead sea turtles. Poster at the International Sea Turtle Symposium.

81) Yang T, **Haas HL**, Smolowitz RJ, Patel SH, James MC, Williard A. 2018. Blood biochemistry and hematological reference intervals for migrating loggerhead turtles (*Caretta caretta*) in the Northwest Atlantic. Presentation at the Southeast Regional Sea Turtle Meeting. Myrtle Beach, South Carolina.

Ecosystem

82) Batta-Lona PG, Llopiz JK, Govindarajan A, Bucklin A. 2019. Metabarcoding analysis of salp diets and trophic relationships in mesopelagic food webs. Poster at the ICES Annual Science Conference. Gothenburg, Sweden. 9 to 12 September 2019.

83) Batta-Lona PG, Llopiz JK, Govindarajan A, Bucklin A. 2019. Metabarcoding analysis of salp diets and trophic relationships in mesopelagic food webs. Presentation at SCOR MetaZooGene Symposium: Rediscovering pelagic biodiversity: Progress, promise, and challenges of metabarcoding of microbes to mammals. Gothenburg, Sweden. 13 September 2019.

84) Bucklin A, Llopiz JK, Thorrold SR, Batta-Lona PG, Glancy S, Wojcicki M, Frenzel A. 2019. Integrative analysis of the mesopelagic food web: metabarcoding, morphological taxonomy, and stable isotope analysis of the diets of fishes and salps in the ocean twilight zone. Presentation at the ICES Annual Science Conference. Gothenburg, Sweden.9 to 12 September 2019.

85) Hernandez C, Richardson D, Rypina, I, Chen K, Pratt L, Llopiz, J. 2018. Larval habitat suitability for Atlantic bluefin tuna spawned in the Slope Sea. Poster at the Ocean Sciences Meeting. Portland, Oregon. 12 to 16 February 2018.

86) Hernandez C, Richardson D, Rypina I, Chen K, Pratt L, Llopiz J. 2018. Larval habitat suitability for Atlantic bluefin tuna spawned in the Slope Sea. Presentation at the Annual Tuna Conference. Lake Arrowhead, California. 21 to 24 May 2018.

87) Hernandez C, Richardson D, Rypina I, Chen K, Pratt L, Llopez J. 2018. Larval habitat suitability for Atlantic bluefin tuna spawned in the Slope Sea. Presentation at the summer meeting of the Southern NE Chapter of the American Fisheries Society. 28 June 2018.

88) Hyde K. 2019. Applications of ocean color and SST data in fisheries science and management. Poster at the International Operational Satellite Oceanography Symposium. College Park, MD. 18 to 20 June 2019.

89) **Jech** M, Lavery A, Wiebe P, Stanton T. 2019. Comparison of net catches and acoustic abundance estimates of the deep-scattering layers. Presentation at the ICES WGFAST meeting. Galway, Ireland. 29 April to 2 May 2019.

90) **LaBrecque E**, Lawson G, Halpin P. 2016. Fronts and fine scale distributions of three cetacean species within the dynamic Mid-Atlantic Bight Shelf break system. Presentation at the Ocean Sciences Meeting. 21 to 26 February 2016.

91) **LaBrecque E**, **Palka D**, Lawson G, Halpin P. 2015. Cetaceans at the shelf break: fine scale habitat analysis of three cetacean species in the Mid-Atlantic Bight. Poster at the Biennial Conference on the Biology of Marine Mammals. 13 to 18 December 2015.

92) **LaBrecque E, Jech JM.** 2019. Spatial distribution of fish-like and fluidlike zooplankton acoustic categories across the Mid-Atlantic Bight shelf break, USA. Presentation at the ICES WGFAST. Galway, Ireland. 29 April to 2 May 2019.

93) Richardson D, Marancik K, Hernandez C, **Broughton E**, Walsh H. 2018. Atlantic tuna spawning off the Northeast US. 2018. Presentation at the summer meeting of the Southern NE Chapter of the American Fisheries Society. 28 June 2018.

Other

94) Baker SC, Baird RW, **Cholewiak D**, Constantine R, Fedutin ID, Filatova OA, Jacobsen L, Notarbartolo di Sciara G, Oleson E, Panigada S, Schorr GS, Klink H, Steel D. 2019. Species identification of cetaceans by environmental (e)DNA metabarcoding - a new tool for surveys of the high seas. Poster at the World Marine Mammal Conference. Barcelona, Spain. December 2019.

C. DATABASES

95) *Oracle database* (housed at NEFSC) holds the marine mammal, turtle, seal, seabird, plankton, oceanography, environmental, and passive acoustic data collected during the NEFSC and SEFSC AMAPPS fieldwork.

96) *Atlantic Offshore Seabird Dataset Catalog* originally developed by US Fish and Wildlife Service and currently housed at USGS hold seabird data collected by AMAPPS surveys among other surveys.

97) *OBIS-SEAMAP database* holds the marine mammal, turtle, and seal visual sightings detected during the shipboard and aerial abundance surveys.

98) A bar code library of the northwestern Atlantic salp species (*Thaliacea*) is being developed by the University of Connecticut utilizing salp specimens taken during AMAPPS shipboard surveys (Batta-Lona et al. 2016; Jue et al. 2018).

D. WEB PRESENCE – DATA

99) General information on AMAPPS.

100) AMAPPS marine mammal model viewer displays average seasonal species-specific density maps resulting from the AMAPPS habitat models output. Site is interactive to allow user to highlight a

boxed area of interest and then display and download the area's estimated density and abundance along with the individual density estimates for each cell in the area of interest.

101) NEFSC passive acoustic research, papers and updates
102) Locations of satellite-tagged Northeast Atlantic loggerhead turtles.
103) Locations of satellite-tagged Southeast Atlantic loggerhead turtles.
104) Temperature-depth profiles collected on tagged loggerhead turtles.
105) Shape files of estimated relative abundance of tagged loggerheads.
106) Locations of gray seal tags and general information on the tagging fieldwork.
107) Oceanography CTD/bongo data.
108) NOAA National Centers for Environmental Information water column sonar data portal.

E. WEB PRESENCE – NEWSLETTERS/BLOGS/NEWS ARTICLES

109) BOEM (Bureau of Ocean Energy Management). 2014. AMAPPS findings close critical data gaps. BOEM Ocean Science 11(2).
110) BOEM (Bureau of Ocean Energy Management). 2018. Findings from Atlantic Marine Assessment Program for Protected Species. BOEM Science Notes June 2018.
111) Ten News press articles on various NEFSC AMAPPS field work 2011 - 2018 https://www.nefsc.noaa.gov/press_release/pr2018/features/cetacean-survey-gunter-2018/.
112) AMAPPS in a web feature article: East Coast Marine Life Survey Renewed for Five More Years
113) NEFSC Highlights AMAPPS model mapper and a rare bird seen by an AMAPPS observer on an Ecomon survey (01 August 2019)
114) WCAI (NPR) reports on seabirds sighted during Offshore Cetacean Ecology survey (21 August 2019)
115) WCAI (NPR) reports on marine mammal acoustic work and the True's beaked whale tagging success from the offshore cetacean ecology project (14 March 2019)
116) NMFS Highlight reports on successful tagging of 9 leatherback turtles in Cape Cod Bay (01 October 2019)
117) NOAA Feature Story reports on record number of leatherback turtles tagged in North Carolina record number of leatherback turtles tagged in North Carolina (18 June 2019)
118) NOAA Feature Story using passive acoustic monitoring via towed arrays to estimate the dive depths of beaked whales (10 October 2017)
119) NOAA Feature Story on the offshore cetacean ecology project and how technology is helping to unlock the world of beaked whales (08 May 2020)
120) ecoRI news True's beaked whales found during AMAPPS surveys reports on True's beaked whales found during AMAPPS surveys (19 September 2018)
121) Cape Cod Times article highlighting the offshore cetacean ecology project and the True's beaked whale discoveries (09 September 2018)
122) Teacher at Sea: Postcard from the Atlantic by R. Kannan. Indian Birds Vol. 15 No. 5 (Publ. 16 January 2020)

F. PAPERS IN PREPARATION:

123) Carroll EL, McGowen M, Baker CS, Berrow S, **Cholewiak D**, Constantine R, Dalebout M, Gatesy J, van Helden A, Marx F, Morin P, Onoufriou A, Springer M, Steel D, Olsen MT. Deep genetic division in a deep diving mammal: True's beaked whale.

124) **Chavez-Rosales S**, **Palka D**, **Garrison L**, **Josephson E**, **Sigourney D**. Spatial and temporal changes of marine mammal habitat suitability from 2010 to 2017.

125) **Cholewiak D**, Miller D, Brady S, **Davis G**, Corkeron P, **Van Parijs SM**. Calculating calling density of North Atlantic right whales using passive acoustics: A case study.

126) **Cholewiak D**. Fine-scale habitat use and dive behavior of True's beaked whales off Georges Bank.

127) **Cholewiak D**, Cerchio S, Steele D, Baker S. Visual and acoustic identification of True's beaked whales (Mesoplodon mirus) confirmed by eDNA barcoding.

128) **Crowe LM**, **Hatch JM**, Patel SH, Smolowitz RJ, **Haas HL**. Riders on the storm: loggerhead sea turtles detect and respond to a major hurricane in the Northwest Atlantic Ocean

129) **DeAngelis A**, Heisenberg N, Scott A, Stokoe A, Valtierra R, **Van Parijs S**, **Soldevilla M**, **Cholewiak D**. Beaked whale and *Kogia* species distributions along the US eastern seaboard using passive acoustic monitoring.

130) **Hatch JM**, **Haas HL**, **Sasso CR**, Patel SH, Smolowitz RJ. Estimating the complex patterns of survey availability for a highly mobile marine animal.

131) Hernandez, C, **Richardson D**, Llopiz J, **Marancik K**, Shulzitski K, Rypina I, Chen K. Support for the Slope Sea as a major spawning ground for Atlantic bluefin tuna: evidence from larval abundance, growth rates, and backtracking simulations

132) **LaBrecque E**, Hench J, **Jech JM**, Lawson G, Halpin P. Patterns and spatial scales of biological scattering in the Mid-Atlantic Bight shelf break region.

133) **LaBrecque E**, Lawson G, **Palka D**, Halpin P. Cetaceans at the Mid-Atlantic Bight Shelf Beak: Fine scale habitat partitioning in a dynamic ecosystem.

134) Nicholas A, Farmer, Garrison LP, Horn C, Miller M, Gowan T, Kenney RD, Rappucci G, Aichinger Dias L, Vukovich M, Willmott JR, Pate J, Webb HD, Hickerson E, Stewart J, Bassos-Hull K, Jones D, Adams D, Carlson J, Kaijura S, Waldron J, Marshall A. The distribution of manta rays in the northwestern Atlantic Ocean and Gulf of Mexico.

135) **Orphanides C**. Examining marine mammal distribution relative to acoustic classification of prey in the water column.

136) **Orphanides C**. Opportunistically assessing right whale prey availability in southern New England wind energy areas.

137) **Palka D**. Warden M**.** Estimates of availability of cetaceans to visual abundance survey observers.

138) **Palka D.** Abundance and distribution trends of cetaceans from 1992 to 2016 using visual line transect survey data and state-space modeling techniques.

139) Patel SH, Smolowitz R, **Winton M**, Fay G, **Haas H**, **Hatch J**, Saba V. Using climate change scenarios to project loggerhead turtle distributions in the U.S. Mid-Atlantic.

140) **Sigourney D**, **DeAngelis A**, **Cholewiak D**, **Palka D**. Methods for integrating towed array passive acoustic data with visual line transect data: a case study with sperm whales (*Physeter macrocephalus*).

141) **Sigourney D.** et al. Application of a Bayesian density surface model to five species of large whales in the western Atlantic.

142) Stokoe A, **Cholewiak D**, **DeAngelis A**. A short note on the increased frequency range of True's beaked whale (*Mesoplodon mirus*) clicks using a higher sampling rate.

2 Introduction

The overarching goal of the Atlantic Marine Assessment Program for Protected Species (AMAPPS) is to assess the abundance, distribution, ecology, and behavior of marine mammals, sea turtles, and seabirds throughout the U.S. Atlantic state and outer continental shelf waters, and place them in an ecosystem context. We want to make these results in formats that are easily accessible and user-friendly for decision makers and others. AMAPPS is a collaborative program involving the National Marine Fisheries Service (NMFS) of the National Oceanic and Atmospheric Administration, Department of Commerce, Bureau of Ocean Energy Management (BOEM) of the Department of the Interior, U.S. Navy, and U.S. Fish and Wildlife Service (USFWS) of the Department of the Interior.

All 4 of the agencies involved in AMAPPS require information on protected species (marine mammals, sea turtles, and seabirds) to implement and support compliance with federal mandates. This includes the Marine Mammal Protection Act (MMPA; NOAA Fisheries 2021a), Endangered Species Act (ESA; NOAA Fisheries 2021b), National Environmental Policy Act (NEPA; NOAA Fisheries 2021c), Migratory Bird Treaty Act, and Executive Order 13186: Responsibilities of Federal Agencies to Protect Migratory Birds (USFWS 2021). In addition, up-to-date information on protected species enhances public outreach and education.

BOEM regulates energy and mineral resources associated with the Atlantic OCS, which includes all submerged lands lying seaward of state coastal waters (which extend to 3 miles offshore) to the Exclusive Economic Zone (EEZ) boundary approximately 200 nm from the coast (BOEM 2021). Areas of particular interest to BOEM relevant to AMAPPS include the areas related to development of offshore wind energy (Figure 2-1) and marine minerals, for example beach replenishment activities. In addition, the U.S. Navy requires this scientific information to support their environmental compliance documentation for their activities in the Atlantic and Gulf of Mexico that include at-sea training and testing, low-, medium-, and high-frequency sonar and explosives, and in-water construction projects involving pile driving at Navy installations. Areas of particular interest to the Navy are all waters within the U.S. EEZ and beyond. Furthermore, NMFS requires this information to develop Stock Assessment Reports, monitor and evaluate Take Reduction Plans, develop section 7 consultations (Biological Opinions), and section 10 incidental take permits. Areas of particular interest to NMFS are waters within the U.S. Atlantic EEZ.

AMAPPS II was in place during Fiscal Years (FY) 2015 to FY2019 (October 2014 through September 2019). It was an extension of AMAPPS I (FY2010 to FY2014; October 2010 through September 2014) and is being followed by AMAPPS III (FY2019 to FY2023; October 2019 through September 2023). USFWS and BOEM developed its own inter-agency agreement in FY17, so in this document we will only report on results from data collected by NMFS.

The products resulting from AMAPPS II update the available marine ecosystem data for marine mammals, sea turtles, and seabirds, and address critical information gaps in their assessments. Because marine ecosystems are complex and involve dynamic assemblages of many co-existing species, research under AMAPPS has integrated research across taxonomic groups and among trophic levels and uses a suite of data collection and analysis techniques. The primary spatial scope of the program includes the waters within the U.S. Atlantic EEZ, including waters of major estuarine systems (e.g., Delaware Bay, Chesapeake Bay, and Pamlico Sound). The primary researchers reporting results in this document are from the Northeast Fisheries Science Center (NEFSC) in Woods Hole, MA, and the Southeast Fisheries Science Center (SEFSC) in Miami, FL. However, nearly all of the projects are collaborative in nature; thus, a number of other organizations not involved in the inter-agency agreements also participated in the collection and analyses, in addition to funding the research results reported in Chapters 5 – 11.

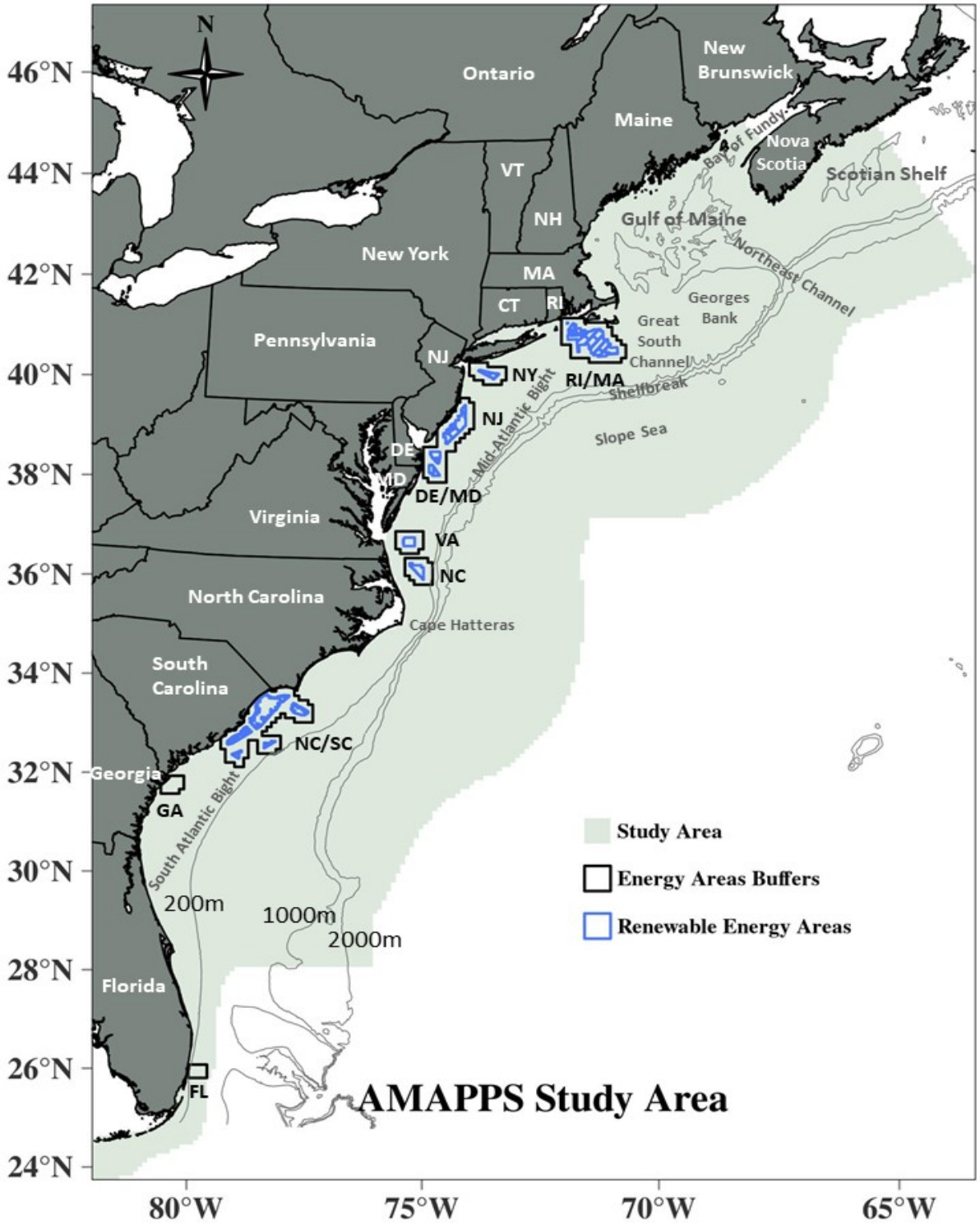

Figure 2-1 AMAPPS study area and wind-energy study areas
We identified the offshore wind-energy areas (blue lines) along with their associated 10 km buffer (black lines), together they encompass the wind-energy study areas (see section 6.2.1 for more details). The AMAPPS study area is shaded in green.

References Cited

[BOEM] Bureau of Ocean Energy Management. 2021. Outer Continental Shelf (accessed 10 April 2021).

[NOAA Fisheries] National Oceanic and Atmospheric Administration Fisheries. 2021a. Marine Mammal Protection Act (MMPA) polices, guidance, and regulations. (Accessed 10 April 2021).

[NOAA Fisheries] National Oceanic and Atmospheric Administration Fisheries. 2021b. Endangered Species Act (ESA). (Accessed 10 April 2021).

[NOAA Fisheries] National Oceanic and Atmospheric Administration Fisheries. 2021c. National Environmental Policy Act (NEPA). (Accessed 10 April 2021).

[USFWS] US Fish and Wildlife Service. 2021. Executive Order 13186, Responsibilities of Federal Agencies to Protect Migratory Birds (accessed 10 April 2021).

3 Background and Objectives

3.1 Background

Human activities are increasing in our oceans and exerting increasing pressures on the ocean's ecosystem. Activities such as maritime traffic, tourism, fisheries and aquaculture, hydrocarbon exploration, marine renewable energy development and naval activities are having impacts on marine ecosystems worldwide (Azzellino et al. 2012). There is an increasing concern over the effects on marine wildlife of human activities. Examples of human activities effecting protected species include sonar (e.g. DeRuiter et al. 2013; Parsons et al. 2008), noise (e.g. Cholewiak et al. 2018), seismic surveys (e.g. Gordon et al. 2003), ship strikes (e.g. Jensen and Silber 2003), fisheries interactions (e.g. Read et al. 2006), and construction impacts such as pile driving (Brandt et al. 2011). To assess the level of concern and mitigate potential negative impacts, the need to understand and predict the distribution, abundance, and habitat usage of marine wildlife has become an important marine conservation challenge. This challenge involves understanding interactions not only between humans and wildlife but also between wildlife and the abiotic and biotic factors in the ecosystem. Managers need species distribution information to develop management actions to manage biodiversity, conserve rare species, anticipate problematic invasions, identify hotspots, delimit valued habitat types, and inform wildlife action plans (Franklin 2010; Fontaine 2011). Managers and scientists have used species distribution information, along with other types of information, to evaluate potential effects from proposed land-use actions, assess spatially explicit threats, identify critical habitat, and direct recovery efforts to areas with optimal conditions for species persistence (Guisan et al. 2013). Over the last decades in an attempt to improve conservation and protection efforts, these needs have become widely recognized by national legislation of many countries and international organizations as they have developed legal obligations to gather knowledge of cetacean species and their habitats. Some examples include the MMPA, ESA, the Convention for the Protection of the Marine Environment in the Northeast Atlantic (OSPAR 2008), and the European Union's Habitats Directive (EU-COM 1992). Results for AMAPPS contribute to addressing this challenge with respect to protected species in the US Atlantic waters.

3.2 Objectives

Ideally, results from studies that are gathering this needed knowledge could discriminate between changes in wildlife populations due to natural environmental variability and changes due to anthropogenic impacts, but that is a difficult task. Wiebe et al. (2009) concluded that to understand the effects of anthropogenic activities on wildlife populations within the complexities of their ecosystem, scientists need to use a range of study tools on a range of taxonomic trophic levels. The objectives of AMAPPS follow this strategy. The specific objectives of AMAPPS II were to:

1) Collect broad-scale data over multiple years on the seasonal distribution and abundance of marine mammals (cetaceans and pinnipeds), marine turtles, and seabirds using fixed passive acoustic monitoring and direct aerial and shipboard surveys of coastal U.S. Atlantic Ocean waters;
2) Collect similar data at finer scales at several sites of particular interest to BOEM, NMFS, and partners using visual and acoustic survey techniques;
3) Conduct tag telemetry studies of protected species to develop corrections for availability bias in the abundance survey data and to investigate behavior and ecology of species in areas of interest;
4) Collect additional data on life-history and ecology, including habitat use, residence time, frequency of use, and behavior;
5) Identify currently used, viable technologies and explore alternative platforms and technologies to improve population assessment studies, if necessary;

6) Assess the population size of surveyed species at regional scales; and develop models and associated tools to translate these survey data into seasonal, spatially-explicit density estimates incorporating habitat characteristics; and
7) Collect long-term ambient noise data in U.S. Atlantic Ocean waters.

The primary species we targeted under AMAPPS II were protected species (marine mammals, sea turtles, and seabirds). However to fully understand these species, we also needed to investigated other parts of the ecosystem ranging from the physical attributes of the ocean's waters to plankton and fish species. Some consider these protected species populations are a proxy for ecosystem health (Sergio et al. 2006). That is, they act as an indicator species since they are typically long-lived, move over broad ranges and feed at a variety of trophic levels. The logic is, since they are responsive to ecosystem changes they are a good proxy for ecosystem health (Hooker and Gerber 2004). This implies that protecting and conserving them and their habitats have direct benefits for other species.

To study the various parts of the ecosystem, in AMAPPS II we used a range of tools including collecting visual, acoustic, and telemetry data of the protected species, along with direct (e.g. trawl and active acoustics) and indirect (photographic and satellite imagery) sampling of other trophic levels. Each of the study tools we used has inherent strengths and weaknesses, so we used a complimentary suite of data collection and analysis methods to address the AMAPPS objectives. For example, the aerial and shipboard visual data provided species-specific estimates of surface abundance, spatiotemporal information about distribution, and limited information on behavior and demographics. However, the collection of visual data was dependent on and constrained by wind and visibility conditions. On the other hand, the passive acoustic data provided detailed information on the spatiotemporal presence of vocalizing species and were not subject to the visual survey constraints. However, passive acoustic data on its own had a limited ability to provide assessments of abundance, behavior, or demographics. The animal-borne tag data provided individual-specific detailed information about distribution, behavior, and demographics. However, tag data on its own had limited ability to provide assessments of abundance. Nevertheless, utilizing all of these types of data together provided the best chance to understand the abundance, distribution, ecology, and behavior of these animals within an ecosystem context.

To address objectives 1, 2, 3, 5 and 6, we investigated seasonal and annual distribution patterns and abundance estimates by using various data sources. These sources include marine mammal/sea turtle visual aerial and shipboard surveys (Chapters 5 – 6), passive acoustic towed arrays and bottom mounted passive acoustic recorders (Chapter 7), satellite tags of sea turtles (Chapter 8), seabird shipboard surveys (Chapter 9) and data on physical oceanographic features and other trophic levels (Chapter 10). To address objective 4, we collected additional data to investigate life history and ecology, including habitat use, residence time, frequency of use, and behavior by using passive acoustic data (Chapter 7) and animal-borne tag data (Chapters 7 and 8). To address objective 7, we collected long-term ambient noise data in U.S. Atlantic Ocean waters using passive acoustic monitoring (Chapter 7). Chapter 11 summarizes all of the data types collected under AMAPPS, briefly describes how we processed the data and where the public can access the data.

The chapters in this report document research field and analytical efforts during AMAPPS II (2015 to 2019) that address 1 or more of the AMAPPS objectives. In addition to the collection of new data, many analyses utilized data collected during both AMAPPS I and AMAPPS II (2010 to 2019). Because NMFS and BOEM have renewed their inter-agency agreement with similar objectives, many of the research projects reported here are ongoing (AMAPPS III). Thus, in addition to reporting results completed during AMAPPS II, this report also identifies data gaps and discusses ongoing and future research.

3.3 References Cited

Azzellino A, Panigada S, Lanfredi C, Zanardelli M, Airoldi S, Notarbartolo di Sciara G. 2012. Predictive habitat models for managing marine areas: Spatial and temporal distribution of marine mammals within the Pelagos Sanctuary (Northwestern Mediterranean sea). Ocean Coastal Manag. 67: 63-74.

Brandt MJ, Diederichs A, Betke K, Nehls G. 2011. Responses of harbour porpoises to pile driving at the Horns Rev II offshore wind farm in the Danish North Sea. Mar. Ecol. Prog. Ser. 421:205-216.

Cholewiak D**,** Clark CW, Ponirakis D, Frankel A, Hatch LT, Risch D**,** Stanistreet JE, Thompson M, Vu E, Van Parijs SM. 2018. Communicating amidst the noise: modeling the aggregate influence of ambient and vessel noise on baleen whale communication space in a national marine sanctuary. Endang Species Res 36: 59-75.

DeRuiter SL, Southall BL, Calambokidis J, Zimmer WMX, Sadykova D, Falcone EA, Friedlaender AS, Joseph JE, Moretti D, Schorr GS, Thomas L, Tyack PL. 2013. First direct measurements of behavioural responses by Cuvier's beaked whales to mid-frequency active sonar. Biol. Lett. 9: 20130223.

EU-COM. 1992. Council Directive 92/43/EEC of 21 May 1992 on the conservation of natural habitats and of wild fauna and flora.

Franklin J. 2010. Mapping species distribution: Spatial inference and prediction. Cambridge University Press, Cambridge.

Fontaine C, Guimarães Jr PR, Kéfi S, Loeuille N, Memmott J, van der Putten WH, van Veen FJF, Thébult E. 2011. The ecological and evolutionary implications of merging different types of networks. Ecol. Lett. 14: 11-70-1181.

Gordon J, Gillespie D, Potter J, Alexandros F, Simmonds M, Swift R, Thompson D. 2003. A review of the effects of seismic surveys on marine mammals. Mar. Technol. Soc. J. 34(4): 16-34.

Guisan A, Reid T, Baumgartner JB, Naujokaitis-Lewis I, Sutcliffe PR, Tulloch AIT, Regan TJ, Brotons L, McDonald-Madden E, Mantyka-Pringle C, Martin TG, Rhodes JR, Maggini R, Setterfield SA, Elith J, Schwartz MW, Wintle BA, Broennimann O, Austin M, Ferrier S, Kearney MR, Possingham HP, Buckley YM. 2013. Predicting species distributions for conservation decisions. Ecol. Lett. 16: 1424-1435.

Hooker SK, Gerber LR. 2004. Marine reserves as a tool for ecosystem-based management: the potential importance of megafauna. Bioscience 54 (1): 27-39.

Jensen AS, Silber GK. 2003. Large whale ship strike database. U.S. Department of Commerce, NOAA Technical Memorandum NMFS-F/OPR 25. 37 pp

OSPAR. 2008. Convention for the Protection of the Marine Environment of the North-East Atlantic (the 'OSPAR Convention').

Parsons ECM, Dolman SJ, Wright AJ, Rose NA, Burns WCG. 2008. Navy sonar and cetaceans: Just how much does the gun need to smoke before we act? Mar. Pollut. Bull 56: 1248-1257.

Read AJ, Drinker P, Northridge S. 2006. Bycatch of marine mammals in US and global fisheries. Conserv. Biol. 20(1): 163–169.

Sergio F, Newton I, Marches L, Dedrini P. 2006. Ecologically justified charisma: preservation of top predators delivers biodiversity conservation. J. Appl. Ecol. 43: 1049-1055.

Wiebe PH, Harris RP, Werner FE, Young BD. 2009. BASIN: Basin-scale analysis, synthesis, and integration. Science plan and implementation strategy. GLOBEC Report 27. Plymouth, UK.

4 Organization of Report

In each chapter in this report we focused on either a data collection procedure applied to multiple species types or a species type that we investigated by using multiple data collection procedures. We also highlighted the key findings, data gaps, and future work within each chapter.

In Chapter 5, we focused on cetacean abundance estimates. We updated population abundance estimates of cetacean species that focused on the 2016 AMAPPS aerial and shipboard visual sightings line transect data (sections 5.2 to 5.3). We needed to conduct specialized analyzes to derive the abundance estimates of the coastal bottlenose dolphin stocks (*Tursiops truncatus*; section 5.4) and short-finned pilot whales (*Globicephala melas*; section 5.5). We also reported on 3 ongoing AMAPPS projects related to abundance estimates that are still under development. One project is the development of a novel methodology to combine sperm whale acoustic detections and the usual visual line transect data to improve the abundance estimate of deep diving vocalizing species (section 5.6). Another ongoing project is estimating the long-term abundance trends from 1992 to 2016 by using species-specific multivariate autoregressive state-space models that explicitly account for environmental factors that affect the distribution and abundance of species within the US Atlantic waters (section 5.7). We are also collating animal-borne tag data to document their dive patterns and estimate an availability bias correction factor (section 5.8). In addition, we provided brief summaries of several studies led by other researchers that incorporated the AMAPPS visual abundance data (section 5.9).

In Chapter 6, we focused on spatiotemporal species-specific density maps and abundance estimates of cetaceans. We developed these using the 2-stage generalized additive model framework based on the abundance data described in Chapter 5, along with static and contemporaneous dynamic habitat covariates (section 6.2). The results provided insights into the distribution and abundance patterns on the large-scale (the whole AMAPPS study area) and smaller-scale (the wind energy areas). We also reported on 2 ongoing related AMAPPS projects. One ongoing project is the development of a Bayesian hierarchical framework that estimates the spatiotemporal density and abundance estimates but also propagates more sources of uncertainty into the results (section 6.3). The other ongoing project is the development of spatiotemporal density-habitat models based on abundance data and *in situ* measurements of potential prey groups of species as measured from active acoustic backscatter data collected during the AMAPPS abundance shipboard surveys (section 6.4 and Chapter 10). Lastly, in this chapter, we provided brief descriptions of completed and ongoing research conducted by other investigators that involve cetacean density models using AMAPPS and other sources of data (section 6.5).

In Chapter 7, we focused on studies that have a large passive acoustic component. One ongoing study (section 7.2) is exploring the distribution, habitat use, and ecology of offshore deep-diving species, particularly beaked whales (Ziphiidae), pygmy sperm whales (*Kogia breviceps*) and dwarf sperm whales (*Kogia sima*). This study involved data collected from visual and passive acoustic detections, along with tagging, focal follows, genetic sampling and oceanographic sampling. These data contributed to new insights into the spatial distribution and diving patterns of some of these deep-diving species. Another ongoing study is exploring the distribution of cetacean and anthropogenic activities by using passive acoustic monitoring along the U.S. Atlantic coast (section 7.3).

In Chapter 8, we focused on studies that improved our understanding of the distribution, habitat usage, and biology of sea turtles, in particular loggerhead (*Caretta caretta*) and leatherback sea turtles (*Dermochelys coriacea*). To do so, collaborators and AMAPPS researchers developed an efficient tagging program for leatherbacks, in addition to the previously established tagging program for loggerheads. These studies involved extensive collaborations with other organizations and funding avenues (section 8.2.1). The studies collected distribution and dive data from tagged individuals, foraging behaviors from

videotaping by remote operated vehicles, and biological samples from tagged individuals. This is in addition to the visual sightings collected during surveys discussed in other chapters. These data contributed to insights into the spatiotemporal distribution, diverse diving patterns as related to water column characteristics, foraging behaviors, and blood biochemistry profiles.

In Chapter 9, we focused on studies targeting seabirds with the goal to improve our understanding of the spatiotemporal distribution of seabirds and relationships with other trophic levels within the changing marine ecosystem. Since 2017, we have conducted comprehensive visual surveys of seabirds, marine mammals, turtles, large pelagic fish, and marine debris on NEFSC EcoMon (Ecosystem Monitoring Program) research cruises that conducted oceanographic and plankton sampling on full-shelf surveys, with measurements focused on the chemical, physical, and biological properties of the water column. In this chapter, we describe the distribution of seabird data collected during 2017 to 2019. We also highlight the efforts of other researchers to map the modeled distribution of seabirds and understand their habitat usage by using data collected by AMAPPS and others.

In Chapter 10, we focused on the hydrography of the water column and the spatiotemporal distributions of lower trophic level organisms such as mesopelagic fish and plankton collected under AMAPPS II. The ultimate goal is to compare these data with distributional patterns of protected species. We collected these data from a variety of sampling devices. We used Simrad EK60's to collect acoustic backscatter data. We used several imaging devices to collect plankton images: video plankton recorders, go-pro camera systems, and an imaging sonar. We also used net samplers to collect live samples of plankton and fish: bongo nets, frame-nets, and midwater trawls. In addition, we used conductivity, temperature and depth (CTD) sampler casts and ship-mounted and flow-through systems to document physical oceanographic features. In this chapter, we also highlight some of the species studies that other researchers are conducting using samples that they requested us to collect.

In Chapter 11, we focused on documenting the large quantities of data collected under AMAPPS. We provided summaries of the many types of data that we collected, brief descriptions of how we processed the data, and where the public can access the data and analysis results. The general categories of data include visual sightings (section 11.1), environmental covariates (section 11.2), telemetry (section 11.3), passive acoustic (section 11.4), oceanographic (section 11.5), and biological data (section 11.6).

5 Cetacean Abundance Estimates

Primary authors: Debra Palka, Lance Garrison, Laura Aichinger Dias, Doug Sigourney, Sam Chavez-Rosales, and Elizabeth Josephson

5.1 Introduction

Assessing the level of concern over the effects on marine wildlife of the increasing levels of human activities in the oceans is a major conservation challenge. To do so, scientists and managers need to understand and predict the distribution, abundance, and habitat use of the marine wildlife. The objectives of AMAPPS address this challenge with respect to protected species. In this chapter, we updated abundance estimates of cetaceans, which address 4 of the 7 AMAPPS objectives (taken from the complete list of objectives in Chapter 3):

1) Collect broad-scale data over multiple years on the seasonal distribution and abundance of marine mammals (cetaceans and pinnipeds), marine turtles, and seabirds using fixed passive acoustic monitoring and direct aerial and shipboard surveys of coastal U.S. Atlantic Ocean waters;
2) Collect similar data at finer scales at several sites of particular interest to BOEM, NOAA, and partners using visual and acoustic survey techniques;
5) Identify currently used, viable technologies and explore alternative platforms and technologies to improve population assessment studies, if necessary; and
6) Assess the population size of surveyed species at regional scales; and develop models and associated tools to translate these survey data into seasonal, spatially explicit density estimates incorporating habitat characteristics.

We estimated abundance (objective 6) by using shipboard and aerial survey line transect abundance data (objectives 1 and 2) that we collected in 2010 to 2019 using the same protocols as reported in the AMAPPS I final report (Palka et al. 2017). We contributed to addressing objective 5 by exploring novel methods to 1) estimate the abundance of deep diving species by combining visual shipboard line transect data with towed hydrophone array recordings of acoustic detections of animals and 2) estimate population abundance trends by using multivariate autoregressive state-space models.

At the beginning of this chapter (section 5.2), we briefly describe the data that the Northeast and Southeast Fisheries Science Centers (NEFSC and SEFSC) collected during AMAPPS and the foundational analytical methods we used to estimate abundance from these data. We consider the analytical methods foundational because they are part of a variety of analyses described in this and the next chapter. The remainder of the chapter documents a series of focused projects that use or modify the foundational analysis methods. 3 projects are completed and 2 are under development. The last section in this chapter briefly describes analyses conducted by other researchers that have requested the use of the AMAPPS abundance data. The projects highlighted in this chapter are:

Estimate the population abundance of 25 species (or species groups) resulting from the summer Atlantic coastwise 2016 shipboard and aerial surveys (section 5.3).

Estimate the abundance and trends of coastal bottlenose dolphin (*Tursiops truncatus*) stocks accounting for the overlap of coastal and offshore bottlenose dolphins (section 5.4).

Estimate the abundance of short-finned pilot whales (*Globicephala macrorhynchus*) accounting for the spatial overlap in offshore northern waters of short-finned and long-finned (*Globicephala melas*) pilot whales (section 5.5).

Develop a methodology to estimate the abundance of sperm whales (*Physeter macrocephalus*) by using simultaneously collected visual transect and passive acoustic data (section 5.6).

Develop a methodology to estimate abundance trends of cetacean populations during 1992 to 2016 by using multivariate autoregressive state-space models (section 5.7).
Develop availability bias correction factors using newly acquired DTAG data from short-finned pilot whales and Cuvier's beaked whales (*Ziphius cavirostris*; section 5.8)
Summarize other projects that used AMAPPS sightings data (section 5.9).

For more information on the sea turtle and seabird data collected on these surveys, refer to Chapters 8 and 9, respectively.

5.2 Materials and Foundational Analysis Methods

5.2.1 Overview

We designed the data collection procedures and analysis methods to estimate abundance accounting for 2 types of visibility bias that are related to visual line transect data collected from ships and planes (McLaren 1961): availability and perception bias. Availability bias is due to observers missing animals because animals were submerged and thus not available for detection at the time the shipboard or aerial sighting survey platform traveled near the animals. Perception bias is due to observers missing animals that were available because, for example, the animals were too far from the platform or the sighting conditions, such as sun glare or sea state, were poor.

In brief, the foundational analysis is to estimate the number of animals of a species within the entire water column that comprises of the product of a surface abundance estimate derived from aerial and shipboard line transect visual sightings data (section 5.2.5) and a species-specific availability bias correction factor derived from diving pattern data (section 5.2.6). We used mark-recapture distance sampling (MRDS) analysis methods (Laake and Borchers 2004; Laake et al. 2020) to estimate the surface abundance accounting for perception bias. We used a 2-state continuous Markov process (Laake et al. 1997) to estimate the species-specific availability bias correction factor accounting for availability bias.

The general workflow of data collection and foundational analyses was as follows:

1. Collect aerial (section 5.2.2) and shipboard (section 5.2.3) data. There were 4 platforms (northeast (NE) ship, NE plane, southeast (SE) ship, and SE plane), where the NEFSC conducted the NE surveys, and the SEFSC conducted the SE surveys.
2. Conduct quality control checks, process, then collate all input data into a common database. Chapter 11 provides more details on this step.
3. Define the study area and divide the data into the appropriate spatial-temporal strata.
4. Estimate species- and platform-specific ocean surface density (and abundance) accounting for perception bias for each species (or species guild) within each spatial-temporal stratum using distance analysis techniques (section 5.2.5).
5. Estimate a species-platform specific availability bias correction factor using information on the average surface and dive times, group sizes, and viewing area from the platform (section 5.2.6).
6. Estimate the density (and abundance) that account for availability and perception bias for each spatial-temporal stratum by applying the species-platform specific availability bias correction factor to the species-platform ocean surface density estimate that accounted for perception bias.

We applied these foundational analyses to the 2016 shipboard and aerial survey data where we stratified the data into large ecosystem units with the goal to update population abundance estimates and thus update the status of the populations as reported in the Atlantic Stock Assessment Reports (section 5.3). We applied modifications of these foundational analyses to accommodate special cases so that we can

estimate the abundance of coastal bottlenose dolphins (section 5.4) and short-finned pilot whales (section 5.5). We also modified these foundational analyses to develop a new analysis method that integrates visual and passive acoustic data to estimate the abundance of deep diving species (section 5.6). In addition, we modified these foundational analyses to develop spatiotemporal density maps and abundances estimates (Chapter 6). Lastly, in section 5.7, we used abundance estimates from 1992 to 2016 (derived using these foundational analyses) to investigate long-term abundance trends.

5.2.2 Aerial Survey Data

The NEFSC and SEFSC conducted aerial line transect surveys aboard DeHavilland Twin Otter DHC-6 aircraft that flew at about 183 m (600 ft) above the water surface at about 185 km/h (100 kts). Timing of and other specifications of all surveys are described in Chapter 11. Surveys were typically flown during favorable sighting conditions at Beaufort sea states less than or equal to 4 (surface winds <12 kts). We designed the track lines to be parallel to each other at an angle that is approximately perpendicular to the coastline, when possible.

In addition to the 2 pilots on board the plane, 6 scientists operated as 2 independent observation teams that did not communicate with each other while actively surveying. Laake and Borchers (2004) describe how the 2-team configuration can account for perception bias. The forward team consisted of 2 observers stationed in forward bubble windows, 1 on each side of the plane. The back team consisted of 2 observers, 1 stationed in a bubble window located at the rear right-hand side of the plane and the other observer laying down and looking through a belly window. Each team had its own recorder. Upon observation of a marine mammal sighting, the forward observers would allow the plane to pass over the group allowing the back team the opportunity to see the group. Once the group passed the rear of the plane, the observers could notify the pilots to circle the group to verify species identification and group size. Sighting groups consisted of 1 or more marine mammals or sea turtles observed in the same general location and at the same time, where individuals are only a couple body lengths apart at the most. Note, the terms “sightings” and “groups” are interchangibly used throught the text because sightings are of groups of animals. The SE surveys circled on most cetacean groups but not turtle groups. The NE surveys circled only groups where the species identification was questionable. Conducting too many circles in regions with high local densities will cause a biased encounter rate. Cetacean density in the NE is relatively high and turtle density in the SE is high. To illustrate this potential bias, consider the situation when the plane circles the first group in a cluster of sightings. It is then possible the observers miss the other groups in the local high-density region or detect them while off-effort. In both cases, this results in a biased low encounter rate. Thus, to reduce biased results the NE circled only when necessary.

For each sighting, it was determined if it had been seen by the forward team only, the back team only, or both teams. This last step was achieved either at the time of data entry in the plane or afterwards during the survey analysis process.

To assist in understanding why groups were missed due to perception bias, we recorded weather (such as Beaufort sea state, visibility, glare, and water turbidity) and effort data (such as time of events, and position of all pilots and scientists) at the beginning of each leg or when conditions changed. In addition, we automatically recorded the ship’s location every few seconds (2 to 10 sec). Observers searched for marine mammals and sea turtles from directly beneath the aircraft out to the horizon, though they focused on the region approximately 1000 m on either side of the track line. Upon sighting an animal group (Table 5-1), the observer measured the angle from the vertical to the animal (or center of group) using a digital inclinometer or estimated the angle based upon markings on the windows indicating 10° intervals. More details of data collection methods are in the AMAPPS annual reports and in Chapter 11.

Table 5-1 List of species detected during at least 1 aerial or shipboard survey

Common Name	Species
Atlantic spotted dolphin	*Stenella fontalis*
Atlantic white-sided dolphin	*Lagenorhynchus acutus*
Basking shark	*Cetorhinus maximus*
Blainville's beaked whale	*Mesoplodon densirostris*
Blue whale	*Balaenoptera musculus*
Bottlenose whale	*Hyperoodon ampullatus*
Common bottlenose dolphin	*Tursiops truncatus*
Common dolphin	*Delphinus delphis*
Cuvier's beaked whale	*Ziphius cavirostris*
Dwarf sperm whale	*Kogia sima*
False killer whale	*Pseudorca crassidens*
Fin or sei whale	*Balaenoptera physalus* or *B. borealis*
Fin whale	*Balaenoptera physalus*
Gervais' beaked whale	*Mesoplodon europaeus*
Gray seal	*Halichoerus grypus*
Harbor porpoise	*Phocoena phocoena*
Humpback whale	*Megaptera novaeangliae*
Harbor seal	*Phoca vitulina*
Kemp’s ridley turtle	*Lepidochelys kempii*
Killer whale	*Orcinus orca*
Leatherback turtle	*Dermochelys coriacea*
Loggerhead turtle	*Caretta caretta*
Long- or short-finned pilot whale	*Globicephala* spp.
Long-finned pilot whale	*Globicephala melas*
Minke whale	*Balaenoptera acutorostrata*
Ocean sunfish	*Mola mola*
Pantropical spotted dolphin	*Stenella attenuate*
Pygmy killer whale	*Feresa attenuate*
Pygmy sperm whale	*Kogia breviceps*
Right whale	*Eubalaena glacialis*
Risso's dolphin	*Grampus griseus*
Rough-toothed dolphin	*Steno bredanensis*
Sei whale	*Balaenoptera borealis*
Short-finned pilot whale	*Globicephala macrorhynchus*
Sowerby's beaked whale	*Mesoplodon bidens*
Sperm whale	*Physeter microcephalus*
Striped dolphin	*Stenella coeruleoalba*
True’s beaked whale	*Mesoplodon mirus*
Unidentified beaked whale	*Mesoplodon* or *Ziphius*
Unidentified common/white-sided dolphin	*D. delphis* or *Lagenorhynchus acutus*
Unidentified seal	Phocidae
Unidentified pygmy/dwarf sperm whale	*Kogia* spp.
White-beaked dolphin	*Lagenorhynchus albirostris*

5.2.3 Shipboard Survey Data

Shipboard sighting line-transect surveys conducted by both the NEFSC and SEFSC were aboard NOAA research vessels, traveling at about 17 - 19 km/h (9 - 10 kts). Timing of and other specifications of all surveys are described in Chapter 11. Surveys were typically conducted during favorable sighting conditions at Beaufort sea states less than or equal to 5 (surface winds <12 kts). We designed the track lines in a zigzag pattern with the angle approximately perpendicular to the coastline or across depth contours, when possible. We stratified the survey effort into geographic strata reflecting regional differences in hydrographic and bathymetric structure and spatial variation in the density and occurrence of different cetacean species.

As with the aerial surveys, to account for perception bias 2 teams of shipboard observers independently visually searched for cetaceans, seals, turtles and some fish species. Each shipboard team consisted of 2 observers using high powered binoculars (25x150) that searched to the horizon in the arc from about 10° on the other side of the ship's bow to abeam (90°) on the side the observer was located at. In addition, at least 1 person recorded data into a computerized data entry system linked with a GPS (global positioning system) and the ship's environmental recording system. The recorder also searched for animals using naked eye when not recording data with a focus close to the ship where observers using high-powered binoculars could miss animals.

Each team recorded time, position, bearing, and reticle (a measure of radial distance) of the sighting, species, group size, behavior, bottom depth, and sea surface temperature for each sighting detected. Survey effort data were automatically recorded every minute or more often and included the ship's position and heading, effort status, observer positions, and environmental conditions that could affect the observers' ability to detect animals (e.g., Beaufort sea state, track line glare, etc.).

In addition, on most of the shipboard surveys, an independent team of 1 to 2 people were dedicated to conducting a 300 m strip transect survey for birds, which is described in more detail in Chapters 9 and 11.

Also, during the shipboard and aerial surveys conducted during 2010 to 2019, about 200 seals, 5500 turtles from 5 species or species guilds, 800 ocean sun fish (*Mola mola*) and 200 basking sharks (*Cetorhinus maximus*) sightings were recorded. Locations of these sightings are in Appendix II, though we did not discuss them in this report.

5.2.4 Availability Bias Data

We accounted for availability bias in the density estimate by incorporating an availability correction factor as defined by Laake et al. (1997) equation 7. To estimate this correction factor we needed the following species-specific data:

(1) Average time a group was at the surface where observers could detect the group (group was available);
(2) Average time a group was below the surface where observers could not detect the group (group was unavailable); and
(3) Average time a group remained in view of the observers, which depended on the speed of the observation platform, the species' behavior, and the size of the group.

The population abundance estimates in section 5.3 and density surface models in Chapter 6 used the tag data and resulting availability bias correction factors described in the AMAPPS I analyses (Palka et al. 2017).

To initiate additional work we started expanding the surface and dive time data. We obtained additional digital recording tags (DTAG) data from short-finned pilot whale, Cuvier's beaked whale, and True's beaked whale (Table 5-2). In section 5.8, we provide preliminary estimates of the amount of time an animal group remained in view of the observer during the aerial and shipboard surveys using the analysis methods described in section 5.2.6 for the short-finned pilot whales and Cuvier's beaked whales. In Chapter 7, we provide a preliminary examination of the True's beaked whale tag data, though we have not yet estimated an availability bias correction factor from these data.

Table 5-2 General information about new tag data used to estimate surface and dive times

Species	Number of Tags	Average Daytime Hours per Animal	Average Nighttime Hours per Animal	Total Daytime (Hrs)	Total Nighttime (Hrs)	Location Time	Source
Cuvier's beaked whale	2	5.8	-	11.7	-	Cape Hatteras, NC 2017, 2019	A. Read Duke Univ.
Short-finned pilot whales	52	3.4	6.2	178.8	56.0	Cape Hatteras, NC 2008 - 2018	A. Read Duke Univ.
True's beaked whales	1	2.5	10.7	2.5	10.7	Georges Bank 2018	Chapter 7 this document

5.2.5 Surface Abundance Estimation Analysis

Because it is harder to detect animals from a plane than from a ship, especially smaller animals, aerial data collected under Beaufort sea states of 4 or less were used to estimate abundance for all species except harbor porpoises, which used data collected under Beaufort sea states of 2 or less. In contrast, shipboard data collected under Beaufort sea states of 5 and less were used to estimate the shipboard abundance estimates, though only 3% of the shipboard track lines were surveyed in Beaufort 5 conditions.

We estimated abundance accounting for perception bias based on the independent observer approach assuming point independence of the mark-recapture distance sampling (MRDS) methods that are based on Horvitz-Thompson like estimators. Laake and Borchers (2004) provide the details on the derivation, assumptions, and implementation of this estimation approach. Briefly, this approach is an extension of standard line-transect distance analysis that includes direct estimation of sighting probability on the track line. The probability of sighting a particular group of animals is the product of 2 probability components. The first probability component is the distance sampling (DS) component that corresponds to the distance sampling sighting function such that the probability of detection declines with increasing distance from the track line following a known functional form (typically the half-normal or hazard function). The second probability component is the mark-recapture (MR) component where the likelihood of detection on the track line is modeled using a logistic regression approach and the "capture histories" of each sighting (i.e. seen by 1 or both teams). Both components can include covariate factors that affect the probabilities. We chose the most appropriate form of the sighting function (hazard vs. half-normal) and the inclusion of covariates (such as observer platform, group size, sea state, glare, swell height, wind speed, etc., including possible use of interactions such as platform and another covariate) in the DS and MR components using a variety of model selection techniques. These techniques included the Akaike

Information Criterion (AIC, Laake and Borchers 2004), Cramer-von Mises test, quantile-quantile plot fits, and visual inspection of the fitted models (Marques and Buckland 2003). The level of left and right truncation of the perpendicular distances was species-specific and used as needed.

Due to the physical limitations within the plane, the front and back teams could not search the exact same patch of water. The front team had full viewing coverage: from the horizon on the right side of the plane (90°) down to directly under the plane (on the track line; 0°) then over to the horizon on the left side of the plane (90°). The back team had limited viewing coverage: from the horizon on the right side of the plane down under the plane through the track line then over to about 30 – 35° from the track line on the left side of the plane. To account for this asymmetry we used a 2-step procedure to estimate the perception bias-corrected density for the aerial data. The first step was to estimate the probability of the primary team detecting a group at the track line, given the perpendicular distances and covariates (*p(0)*) in a 2-team MRDS analysis using only data collected from the area both teams could see. The second step used data only from the primary team in a standard single team multiple covariate distance sampling (MCDS) analysis to estimate densities that were then expanded by the estimate of *p(0)* for the primary team (as estimated in the first step). The primary team was the team that collected data resulting in the typically shaped detection function declining monotonically from the track line, which usually was the front team.

5.2.6 Availability Bias Correction Factor Analysis

We estimated the number of animals of a species within the entire water column ($\widehat{N_a}$) as the product of a surface abundance estimate of a species ($\hat{N}$; section 5.2.5) and a species-specific availability bias correction factor ($\hat{a}$):

$$\hat{N}_a = \frac{\hat{N}}{\hat{a}} \quad \text{(Eqn 5-1)}$$

The definition of the correction factor ($\hat{a}(S,x)$) is the probability that an animal, *S*, that is at a particular perpendicular distance (*x*) from the track line was at the surface and within the observer's field of view. The correction factor is large for species that perform long dives (such as sperm whales and beaked whales) because long divers spend less time at the surface and therefore there is a lower chance an observer can detected the animal at the surface. The correction factor is larger for species detected from an aerial platform, in contrast to the factor for the same species detected from a shipboard platform. This is because planes travel faster than ships, and therefore an aerial observer has less time to study the available field of view of the water, as compared to a shipboard observer. Thus, the probability of detecting an animal at the surface is lower for an aerial observer than for a shipboard observer.

Laake et al. (1997; equation 7) modeled the availability bias correction factor of a detected animal as a 2-stage continuous-time Markov process:

$$\hat{a}(S,x) = \frac{E(sf)}{E(sf)+E(d)} + \frac{\hat{w}(x)\text{-}\hat{w}(x)^2 E(d)^{-1} 0.5}{E(sf)+E(d)} \qquad (Eqn\ 5-2)$$

E(sf) is the expected (average) time at the surface where it is available to be detected. *E*(*d*) is the expected (average) time below the surface where it is unavailable to be detected; and $\hat{w}(x)$ is the amount of time an animal at perpendicular distance *x* from the track line remains in view of the observers, which depends on the speed of the observation vessel. The first stage of this model (left hand side of + in Eqn 5-2) represents the instantaneous proportion of time spent at the surface, which we estimated using the dive time patterns of individually tagged animals. The

second stage (right side of +) adjusts the instantaneous proportion for the amount of time an animal is within the viewing area, which we estimated using the observed times groups were within view. The second stage takes into account, for example, the situation where an animal was in a dive when entering the viewing area and it then surfaced while in the viewing area.

The correction factor as defined above represents a correction for an individual animal. However, we analyzed the line transect data based on groups of animals. Therefore, we expanded the individual correction factor to that for a group by using the power of the group size:

$$\widehat{a_g}(S,x) = 1 - \left(1 - \hat{a}(S,x)\right)^{GroupSize} \qquad (Eqn\ 5-3)$$

Because individuals within a group rarely surface exactly in a synchronized manner, this expansion takes into account the idea that the probability of at least 1 individual of a large group is at the surface and within the field of view. We estimated the overall availability correction factor, â (in Eq. 5-1), as the average of $\widehat{a_g}(S,x)$ for each observed group.

To estimate the average surface time, *E(sf)*, and average dive time, *E*(*d*), from the tag data, we first calculated the duration of each dive and surface interval for each dive cycle of each tagged animal. Then for each species, we fit a random effects model with normally distributed errors, where the surface (or dive) durations were the response variable and the animal identification numbers were the random effects variable. The use of random effects provides a more accurate average duration estimate because it controls for the fact that the duration of a surface (or dive) from an individual is correlated to the durations of other surfacings (or dives) recorded from the same individual.

The population abundance estimates in section 5.3 and density surface models in Chapter 6 used the tag data and resulting availability bias correction factors described in the AMAPPS I analyses (Palka et al. 2017). Section 5.8 provides updated estimated correction factors calculated from the newly acquired tag data.

5.3 2016 Population Abundance

5.3.1 Introduction

The objective of this analysis was to estimate abundance of as many cetacean populations as possible by using data from the 2016 shipboard and aerial line-transect surveys. To meet the mandates of the U.S. MMPA, NOAA Fisheries Service periodically updates the abundance estimates in the U.S. Marine Mammal Stock Assessments. To accomplish this the NEFSC and SEFSC conduct line transect sighting surveys that span the entire U.S. Atlantic waters plus some nearby Canadian waters. In the summer of 2016, the NEFSC and SEFSC coordinated with the Canadian Department of Fisheries and Oceans to conduct aerial and shipboard line-transect abundance surveys of marine mammals and sea turtles in the northwestern Atlantic from Labrador, Canada to Florida, U.S. The resulting abundance estimates from these surveys updated the species assessments reported in the U.S. Marine Mammal Stock Assessments (for example, Hayes et al. 2020). The previous assessments for most species used abundance data collected during summer 2011 in waters from Halifax, Nova Scotia to Florida, U.S. (Palka 2012; Waring et al. 2014; Garrison 2016). The updated abundance estimates are also now being used in various management related activities, such as by Take Reduction Teams, and environmental assessments of ocean activities. The U.S. portions of the 2011 and 2016 surveys were part of AMAPPS.

5.3.2 Methods

We derived the U.S. abundance estimates incorporated into the Stock Assessment Reports from the summer 2016 AMAPPS aerial and shipboard data that we collected and analyzed as described in section 5.2. See Palka (2020) for more details on the NEFSC surveys and Garrison (202) for more details on the SEFSC surveys.

For some species whose habitat extends into Canadian waters, the abundance estimate reported in the Stock Assessment Reports included estimates resulting from a Canadian surveys (Lawson and Gosselin 2018). In August and September 2016, a Canadian survey covered waters on the Atlantic Canadian shelf and shelfbreak, extending from the northern tip of Labrador to the U.S. border off southern Nova Scotia. The survey over the Gulf of St. Lawrence/Bay of Fundy/Scotian Shelf waters used 2 Cessna Skymaster 337 airplanes, while the survey over the Newfound/Labrador waters used a DeHavilland Twin Otter, similar to that used in the U.S. surveys. To estimate the surface abundance, the Canadians analyzed the Skymaster data using single team multi-covariate distance sampling analysis methods with left truncation to accommodate the obscured area under the plane. The Canadians analyzed the Twin Otter data using double platform mark-recapture distance sampling analysis methods that provided estimates of perception bias, similar to that described in section 5.2.5. They applied the Twin Otter derived perception bias correction factor to the single team Skymaster data. In addition, to account for availability bias, they applied to all of the surface abundance estimates, a species-specific availability bias correction factor based on published records of the cetaceans' surfacing intervals.

5.3.3 Results

For the U.S. surveys, we based the abundance estimates on a total of 33,360 km of track lines surveyed on-effort in 2016 (Figure 5-1; Table 5-3) where there were about 2,140 marine mammal sightings of animal groups from 32 species. A sighting can be of a single animal or a group of closely located animals, where we considered those animals within a few body lengths of each other as a sighting of 1 group. The Canadians based their abundance estimates on a total of 50,160 km where there were 1,876 marine mammal groups from 23 species.

Table 5-3 Summary of 2016 summer abundance surveys

Region	Platform	Area (km^2)	Track length (km)	Mammal Groups	Mammal species
U.S. Northeast	Ship	263,681	4,352	1,094	30
U.S. Northeast	Plane	176,598	11,783	354	12
U.S. Southeast	Ship	415,373	5,818	509	17
U.S. Southeast	Plane	11,356	11,406	183	14
Canadian Bay of Fundy to Gulf of St. Lawrence	Plane	547,677	29,123	1,035	23
Canadian Labrador/Newfoundland	Plane	741,699	21,037	841	23
TOTAL in U.S. WATERS		867,008	33,360	2,140	32
TOTAL in CANADIAN WATERS		1,289,376	50,160	1,876	23
GRAND TOTAL		2,156,384	83,519	4,016	32

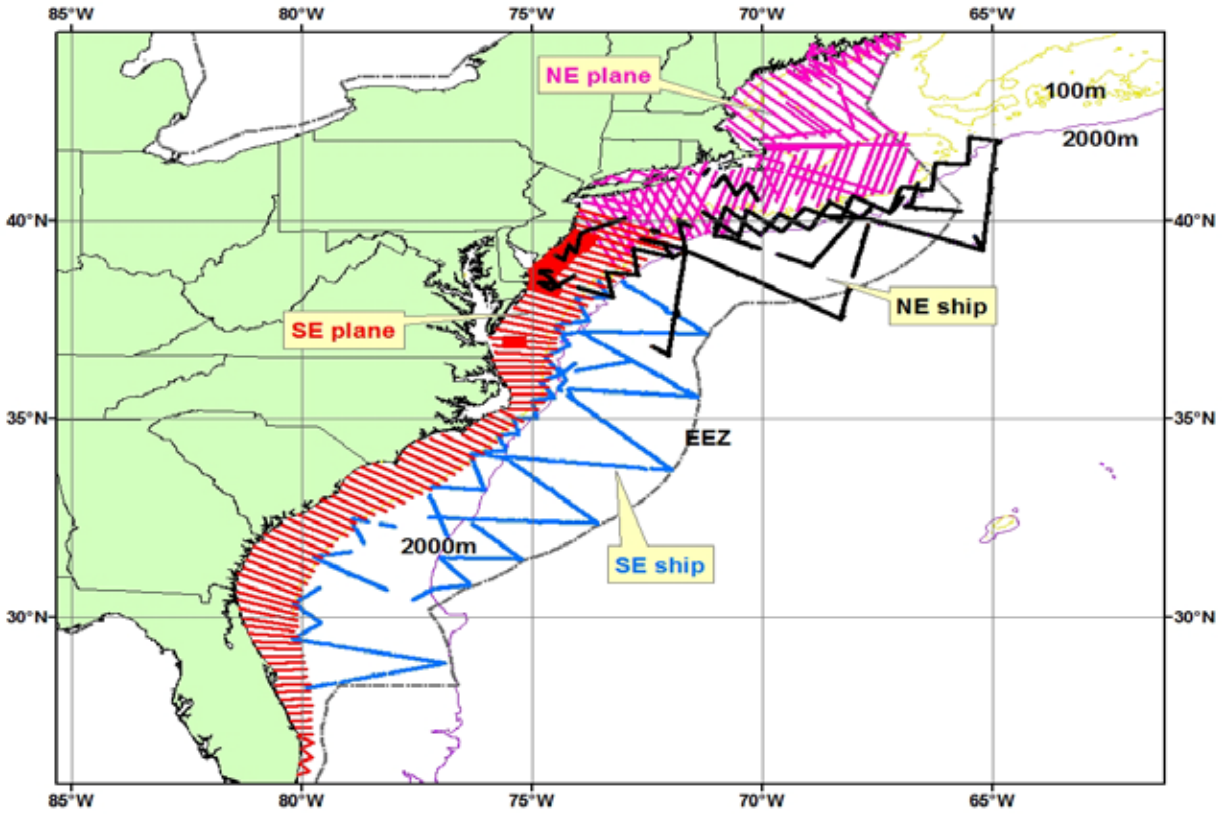

Figure 5-1 Completed track lines during U.S. shipboard and aerial 2016 abundance survey

From all of these surveys we estimated over 1.2 million cetaceans in U.S. and Canadian waters. Of these, nearly 500,000 were in U.S. waters (Table 5-4). These represent the most recent estimates used in the stock assessments for many of the species.

5.3.4 Key Findings

For many of the species that inhabit Atlantic waters off the coasts of the U.S. and Canada, these abundance estimates are the most current and they reflect more of their habitat than previous estimates. These estimates are also the least biased because the analyses accounted for perception bias (by using the 2 independent team data collection and analysis methods) and availability bias (by using data on animal dive patterns and survey platform characteristics).

5.3.5 Data Gaps and Future Work

The estimates discussed in this section were from data collected during the summer 2016 covering waters from Labrador, Canada to Florida, U.S. To more fully understand the changes in abundance patterns, we would require such large-scale surveys during seasons other than the summer. AMAPPS aerial survey effort provides such year-round coverage along the U.S. shelf out to about the 200 or 2000 m depth contour (depending on the location). However, since many of the species that inhabit U.S. waters also travel to Canadian waters, the ideal situation would be to conduct simultaneous surveys in seasons other than summer over both the U.S. and Canadian shelf waters, at least covering Canadian waters west and south of Nova Scotia. Results from such large scale surveys are becoming more important as climatic changes alter the physical and biological oceanic ecosystem and some cetacean species appear to be

responding to these changes by leaving U.S. waters (see section 6.6.2). Documenting the shifts in species abundance and distribution could be instrumental in understanding the trends in abundance in U.S. waters. Documenting the current shifts could also assist in understanding future distribution patterns around anthropogenic activities in U.S. waters (such as wind energy installations or commercial fisheries). To more fully understand the distribution shifts it is desirable to understand the reasons why the animals are shifting. At the least, it would be desirable to discover what physical and biological factors are also shifting as the cetaceans are shifting their distribution. The physical and biological covariates used in the multivariate autoregressive state-space (MARSS) trends analyses (section 5.7) and density-habitat models (Chapter 6) are an attempt to discover the physical and biological factors that associate with the distribution shifts. However, we still need future surveys to confirm future predictions that result from these types of analyses.

The value of the availability bias correction factor highly influences the resulting abundance estimate. Thus, it is important that we use appropriate correction factors to ensure the resulting abundance estimate is accurate. We currently only have 1 average value of the correction factor per species, and thus are applying this value to that species' sightings detected in all habitats and at all times of the year. However, we expect the amount of time an animal is at the surface (and therefore the value of the availability correction factor) will vary due to different animal behaviors. Examples of behaviors include fast swimming during transits, socializing at the surface, performing shallow dives in 1 habitat or time of the year, and performing deep dives in other type of habitat or time of the year (Quick et al. 2017; Shearer et al. 2019; Adamczak et al. 2020). The questions are how representative are our species-specific average correction values, and should we be applying different values of the correction factor to animals detected during different behaviors or in different habitats. To address these questions and data gaps, we need more dive profile data, where we look for spatiotemporal patterns, patterns associated with biotic and abiotic characteristics, and the time budget associated with different dive behaviors. To obtain more dive profile data, because we are not collecting cetacean tag data ourselves, we are reaching out to other researchers that are tagging cetaceans in an attempt to collaborate with them. Another possible way to approach this problem is to further expand the methods that we are developing to use both shipboard visual and passive acoustic data to simultaneously estimate abundance and surface availability (section 5.6). However, this applies only to shipboard surveys and to species that we can easily identify and track acoustically.

Another factor that could influence the distribution and abundance of cetaceans is human activities. Commercial and recreational fishing is 1 example of an anthropogenic activity that can adversely affect cetaceans. Fishing can adversely affect cetaceans directly through bycatch or indirectly through removing or competing for the cetacean's prey that is the target of a fishery. Other human activity examples that directly affect cetaceans include vessel ship strikes and the use of some types of sonars that can kill or injure cetaceans. Other indirect activities such as whale watching, constructing physical structures (such as wind turbines and oil drilling platforms), or modifying the physical habitat (such as dredging, trawling and mining) can change the localized behavior of individuals by interrupting feeding, mating, or migration patterns. However, it is difficult to measure these effects, especially from the indirect sources. Thus, a data gap is the quantification of these direct and indirect effects. In addition, future work would be to include the effects of these anthropogenic activities, along with abundance estimate trends, in an assessement framework.

Analytical issues that we would like to investigate in the future includes ways to more fully utilize data from sightings that we ambigously identified while in the field, such as sightings we identified as either a pygmy or dwarf sperm whales, or as 1 of the Mesoplodont beaked whale species. To address this project, once the passive acoustic analyses for these species are complete, we will attempt to match up passive acoustic events of positively identified animals to the visual ambiguous sightings to assign species

identification to the ambiguous sightings. Another technique we could explore to address this issue is to first develop habitat models that relate the presence of the positively identified passive acoustic events to physical and biological covariates. Then we could apply these models to the locations of the visual ambiguous sightings to assign it a species identification.

An issue that we are starting to consider is how we should design future broad scale abundance surveys over areas of water containing wind turbines. Currently we fly aerial surveys at 600 ft above the water's surface to insure we can positively identify the animals, especially the smaller sized animals, like turtles, porpoises, and dolphins. However, some turbines stand at a greater height than our low-flying altitude of 600 ft. To address this challenge, we are starting to investigate the use of cameras to assist in species identification when we are flying from higher, safer altitudes.

Table 5-4 Abundance estimates from summer 2016 U.S. and Canadian surveys

The abundance (N) and associated coefficient of variation [CV(N)] from the 4 surveys off the coasts of the U.S. northeast (US NE), U.S. southeast (US SE), from the Bay of Fundy to Gulf of St. Lawrence (BOF/Gulf), and off the coasts of Newfoundland and Labrador (Newf/Lab).

Species	US NE N	US NE CV(N)	US SE N	US SE CV(N)	BOF/GulfN	BOF/Gulf CV(N)	Newf/Lab N	Newf/Lab CV(N)	Total N	Total CV(N)
Harbor porpoise	75,079	0.38	0	0	20,464	0.39	0	0	95,543	0.31
Atlantic white-sided dolphin	31,912	0.61	0	0	0	0	0	0	31,912	0.61
Fin whale	2,390	0.38	0	0	2,235	0.41	2,177	0.47	6,802	0.24
Sei whale	52	0.53	0	0	0	0	0	0	52	0.53
Minke whale	2,802	0.81	0	0	6,158	0.4	13,008	0.46	21,968	0.31
Blue whale	39	0.64	0	0	0	0	0	0	39	0.64
Humpback whale	2,368	0.48	0	0	1,854	0.4	8,439	0.48	12,661	0.38
Sperm whale	3,321	0.35	1,028	0.35	0	0	0	0	4,349	0.28
Offshore bottlenose dolphin	16,995	0.35	44,893	0.29	0	0	0	0	61,888	0.23
Common dolphin	80,227	0.31	900	0.57	43,124	0.28	48,723	0.48	172,974	0.21
Atlantic spotted dolphin	8,247	0.24	31,674	0.33	0	0	0	0	39,921	0.27
Spinner dolphin	160	0	3,942	1.03	0	0	0	0	4,102	0.99
Clymene dolphin	0	0	4,237	1.03	0	0	0	0	4,237	1.03
Pantropical spotted dolphin	0	0	6,593	0.52	0	0	0	0	6,593	0.52
Risso's dolphin	21,897	0.23	7,245	0.44	6,073	0.45	0	0	35,215	0.19
Long-finned pilot whale	9,972	0.55	0	0	0	0	28,218	0.36	38,190	0.3
Short-finned pilot whale	3,811	0.42	25,115	0.273	0	0	0	0	28,926	0.24
False killer whale	1,182	0.63	609	1.08	0	0	0	0	1,791	0.56
Striped dolphin	42,873	0.25	24,163	0.66	0	0	0	0	67,036	0.29
White-beaked dolphin	0	0	0	00	5,478	0.495	530,538	0.31	536,016	0.31
All beaked whales	14,412	0.19	7,406	0.22	0	0	0	0	21,818	0.15
Cuvier's beaked whale	3,897	0.47	1,847	0.49	0	0	0	0	5,744	0.36
Unidentified Ziphiidae	3,755	0.42	2,212	0.43	0	0	0	0	5,967	0.43
All Mesoplodonts	6,760	0.37	3,347	0.29	0	0	0	0	10,107	0.27
All *Kogia* spp.	4,548	0.49	3,202	0.59	0	0	0	0	7,750	0.38
TOTAL	322,287		161,007		85,386		631,103		1,199,783	

5.4 Coastal Bottlenose Dolphin Abundance and Trends

5.4.1 Introduction

The objective of this analysis was to estimate the abundance and trends of the 5 defined stocks of coastal morphotypes of the common bottlenose dolphin (*Tursiops truncatus*) along the U.S. east coast during summer months (July to August) in 2002, 2004, 2010, 2011, and 2016. Surveys conducted under AMAPPS were the 2010 to 2016 data. A full description of this analysis is in Garrison et al. (2017).

The coastal stocks of the western North Atlantic common bottlenose dolphin have been the focus of assessment efforts during the last 2 decades due to the relatively high rate of observed interactions with several U.S. gillnet fisheries (Palka and Rossman 2001; Lyssikatos and Garrison 2018). Consequently, these coastal stocks have been the focus of efforts to reduce mortality and serious injury by the Coastal bottlenose dolphin Take Reduction Team since 2001 (Hogarth 2001).

The common bottlenose dolphin occurs in a complex mosaic of population stocks along the U.S. east coast including animals occupying estuaries, nearshore coastal habitats, the continental shelf, and oceanic waters. The stock structure is further complicated by the presence of 2 genetically distinct morphotypes of bottlenose dolphins, particularly over the continental shelf south of Cape Hatteras, NC where the more nearshore “coastal” morphotype overlaps spatially with the larger, more robust “offshore” morphotype that primarily occurs in oceanic waters (>200 m depth). Accurate and precise abundance estimates for each defined stock are a required component of adequate stock assessments for marine mammal stocks. Uncertainties in stock structure and the potential spatial overlap of stocks within a given survey stratum complicate the process of estimating abundance.

In waters of the U.S. continental shelf, there are 5 defined stocks of coastal morphotype bottlenose dolphins: Northern Migratory (NM), Southern Migratory (SM), South Carolina/Georgia (SC/GA), Northern Florida (NFL), and Central Florida (CFL; Figure 5-2). At least 2 of these stocks (Northern Migratory and Southern Migratory) undertake large-scale seasonal migrations and overlap spatially with other coastal and estuarine stocks during certain months of the year. Current knowledge indicates that during summer months, the stocks largely separate from each other and occupy discrete spatial ranges. However, there are significant uncertainties in the defined stock boundaries.

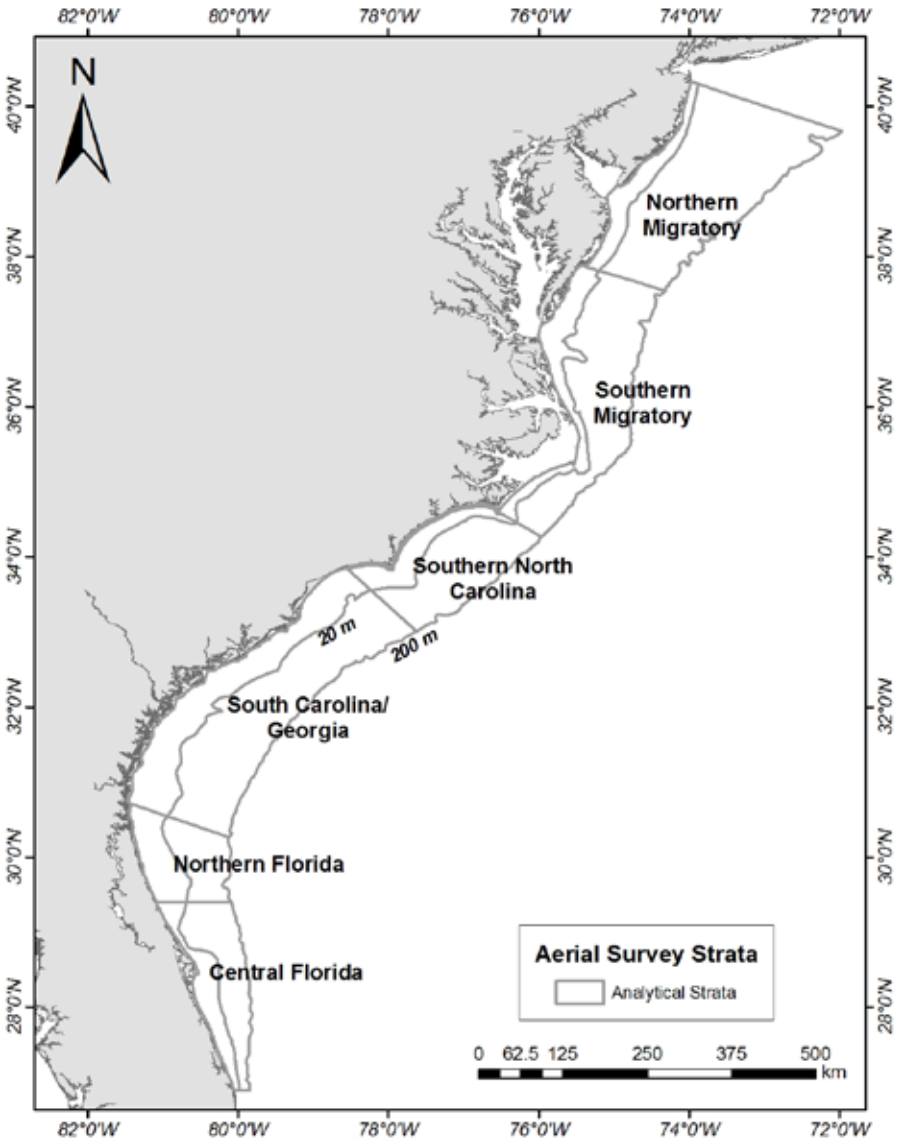

Figure 5-2 Strata used based on Atlantic coastal bottlenose dolphin stock boundaries

5.4.2 Methods

This analysis involved 2 steps. First, due to the spatial overlap between the coastal and offshore morphotypes south of Cape Hatteras, NC we used genetic identifications of skin biopsy samples collected during 1998 to 2015 to model the probability that a particular bottlenose dolphin is the coastal morphotype as a function of depth and latitude. We analyzed tissue samples for mitochondrial genetic markers that are unique to each morphotype and can positively classify individual animals (Torres et al. 2003; Rosel et al. 2009). Then we used logistic regression within a generalized linear model to evaluate the relationship between continuous explanatory variables and a binary response of either coastal or offshore morphotype (McCullagh and Nelder 1989). Explanatory factors (bottom depth, latitude, and their interaction) were included in a stepwise selection fashion, and we evaluated model fit based on analysis of deviance and evaluation of residuals (McCullagh and Nelder 1989). Following the selection of the best model, we evaluated the predictive capability by testing the classification error on a random sample of

30% of the data and re-fitting the model on the remaining 70%. We used this refit model to test the prediction of morphotype on the withheld data to develop a confusion matrix. The resulting confusion matrix provides an estimate of the predictive accuracy of the selected model.

Second, we analyzed the line transect aerial survey data following a stratified distance analysis framework accounting for imperfect detection on the trackline as outlined in section 5.2.5. The strata represented the locations of the 5 coastal stocks. Within the abundance estimation procedure, we accounted for the probability that observed bottlenose dolphins were of the coastal morphotype by multiplying the probability of the morphotype, as derived from biopsy data, by the estimated stratified abundance. Survey data were post-stratified to estimate the abundance of the different stocks.

We used a bootstrap procedure to estimate the uncertainty in the abundance estimates that arose from three sources: 1) uncertainty in the detection probability model, 2) sampling variability amongst the line transects, and 3) uncertainty in the assignment of coastal vs. offshore morphotype associated with uncertainty in the logistic regression model.

5.4.3 Results and Discussion

During 1998 to 2015, 1,275 biopsy samples were available for inclusion in the analysis. North of Cape Hatteras, NC there was a perfect segregation of coastal versus offshore morphotype biopsy samples, with no coastal samples collected in waters deeper than 20 m (Figure 5-3). On the other hand, south of Cape Hatteras, NC there was an apparent spatial overlap between coastal and offshore morphotype animals, where coastal morphotype animals occurred on the outer continental shelf and offshore morphotype animals occurred in relatively shallow water. However, the large majority of samples collected in waters <20m depth were of the coastal morphotype. Applying the logistic regression model to samples collected south of Cape Hatteras, NC and excluding samples collected in waters >200m, the resulting model predicted that in waters <13m in depth, greater than 90% of the observed bottlenose dolphins were expected to be of the coastal morphotype. There was a transition zone between 13 - 33 m depth and in waters >33m depth, less than 10% of observed dolphins were of the coastal morphotype. There were 2 “outlier” samples where coastal morphotype animals were at depths of 68.6 and 97.2m (Figure 5-3). These samples occurred in a region with a very low sample size, and where the model predicts a near-zero probability of coastal animals occurring. Therefore, it is uncertain whether these are outliers or are instead an indicator of aggregations of coastal morphotype animals occurring in deeper offshore waters.

In the 5 aerial surveys combined, we covered more than 39,000 km of survey effort and observed about 9,005 bottlenose dolphins. Effort and spatial coverage varied greatly between the 5 surveys as they had different survey designs (Figure 5-4). Still, there was a noticeable southern shift in sightings from 2002 to 2004 with fewer sightings in the Northern Migratory and the South Carolina/Georgia stock strata. We did not observe similar distribution shifts during the 2010, 2011, and 2016 surveys. This suggested that some other factor or factors (perhaps the underlying environmental variability) may have driven the interannual changes in spatial distribution and that the defined stock boundaries are not spatially stationary.

In terms of abundance estimation, inter-annual variation in stock abundance estimates may reflect changes in animal distribution rather than changes in population size over short periods. Due to this inter-annual variability between successive years, we performed an assessment of trends based upon averages across pairs of surveys: 2002 – 2004, 2010 – 2011 and 2016 to reduce the influence of variability related to both sampling variation and changes in spatial distribution. Comparisons of means between survey periods suggested statistically significant declines in abundance estimates for the Northern Migratory, Northern Florida and Central Florida stocks between 2010 – 2011 and 2016 (Figure 5-5). We observed a general decline over time for the South Carolina/Geogia and Southern Migratory stocks. For the Southern

Migratory stock, we noted a significant decline between 2002 – 2004 and 2010 – 2011 and the population estimate remained low for 2016.

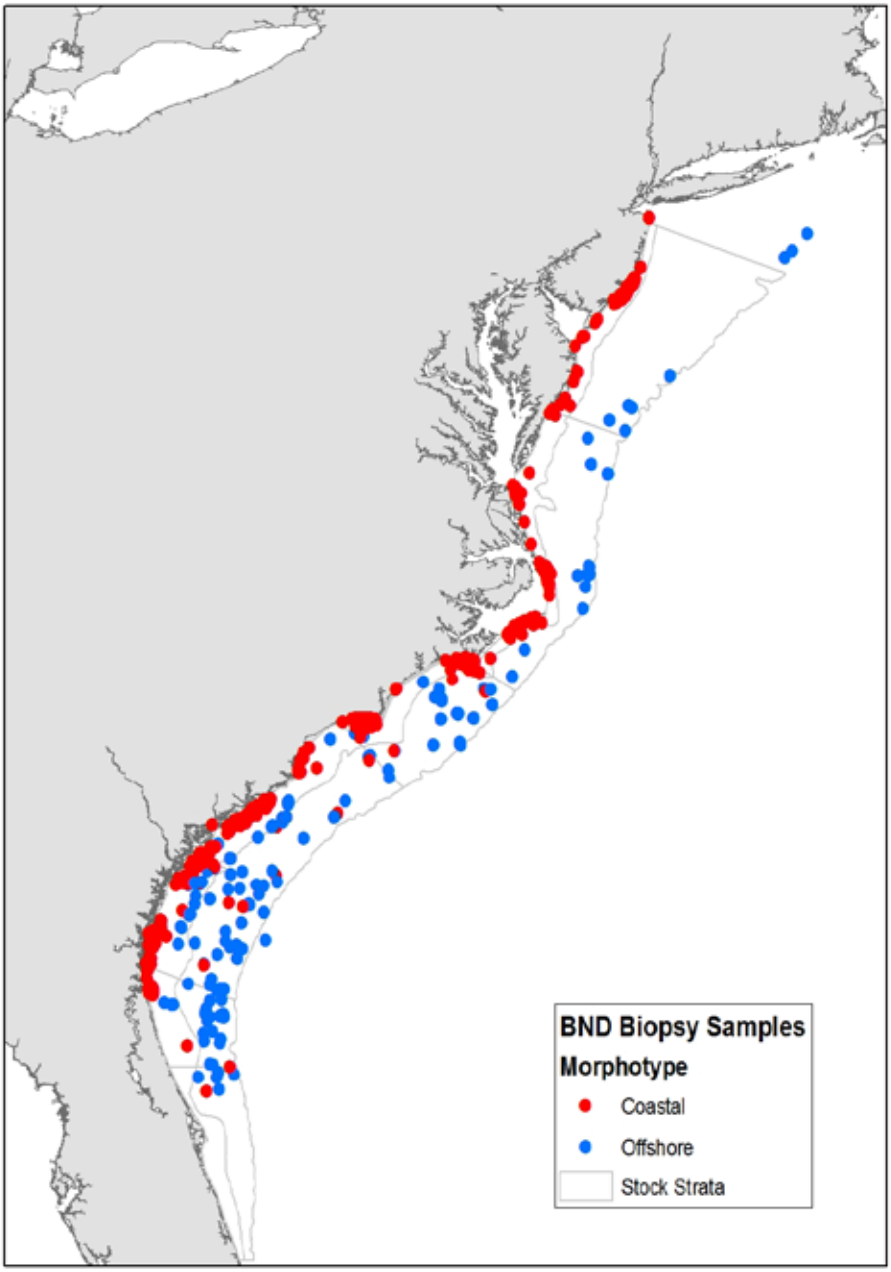

Figure 5-3 Biopsy sampling locations of coastal and offshore bottlenose dolphin morphotypes

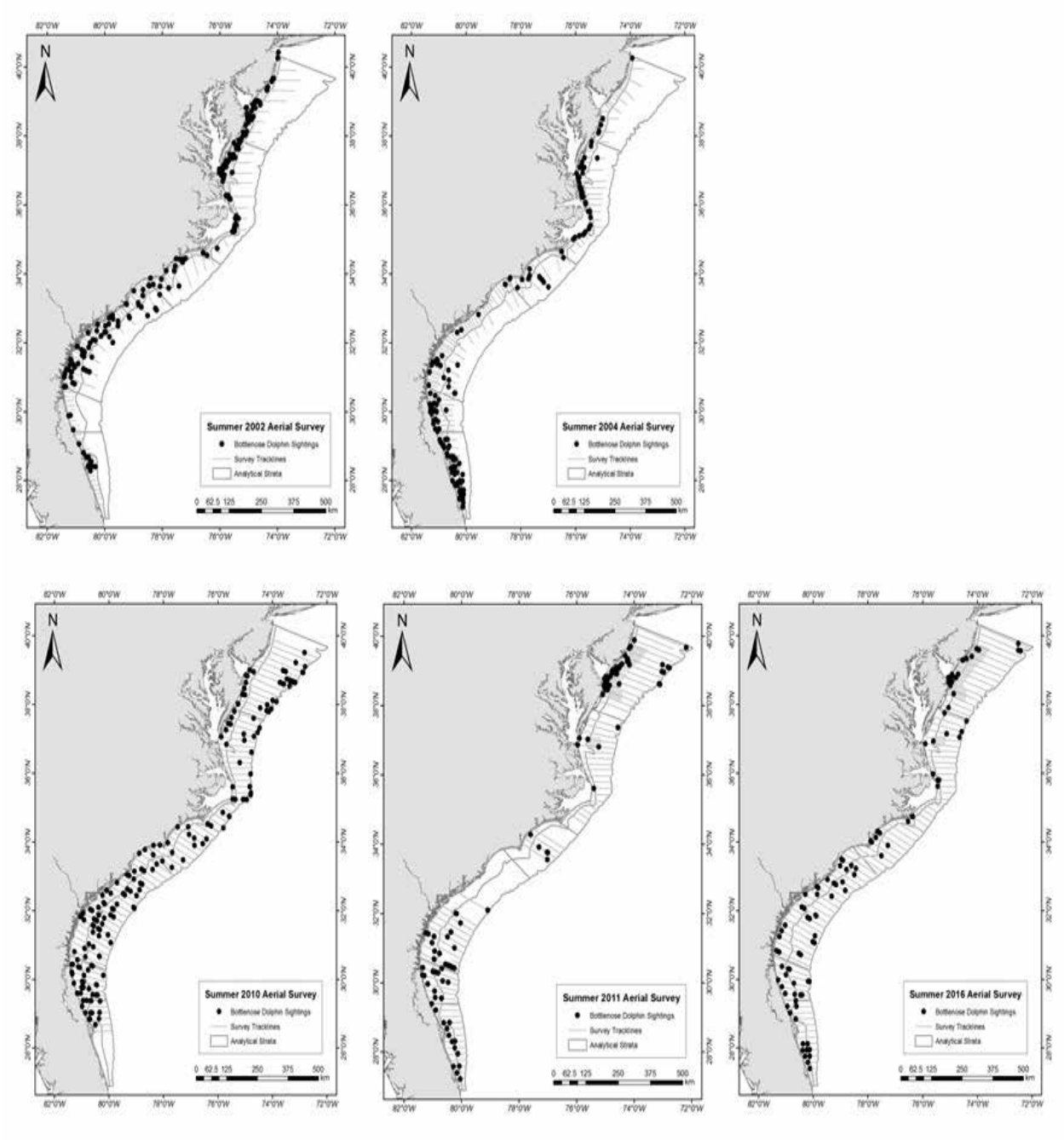

Figure 5-4 Distribution of effort and sightings for each aerial survey

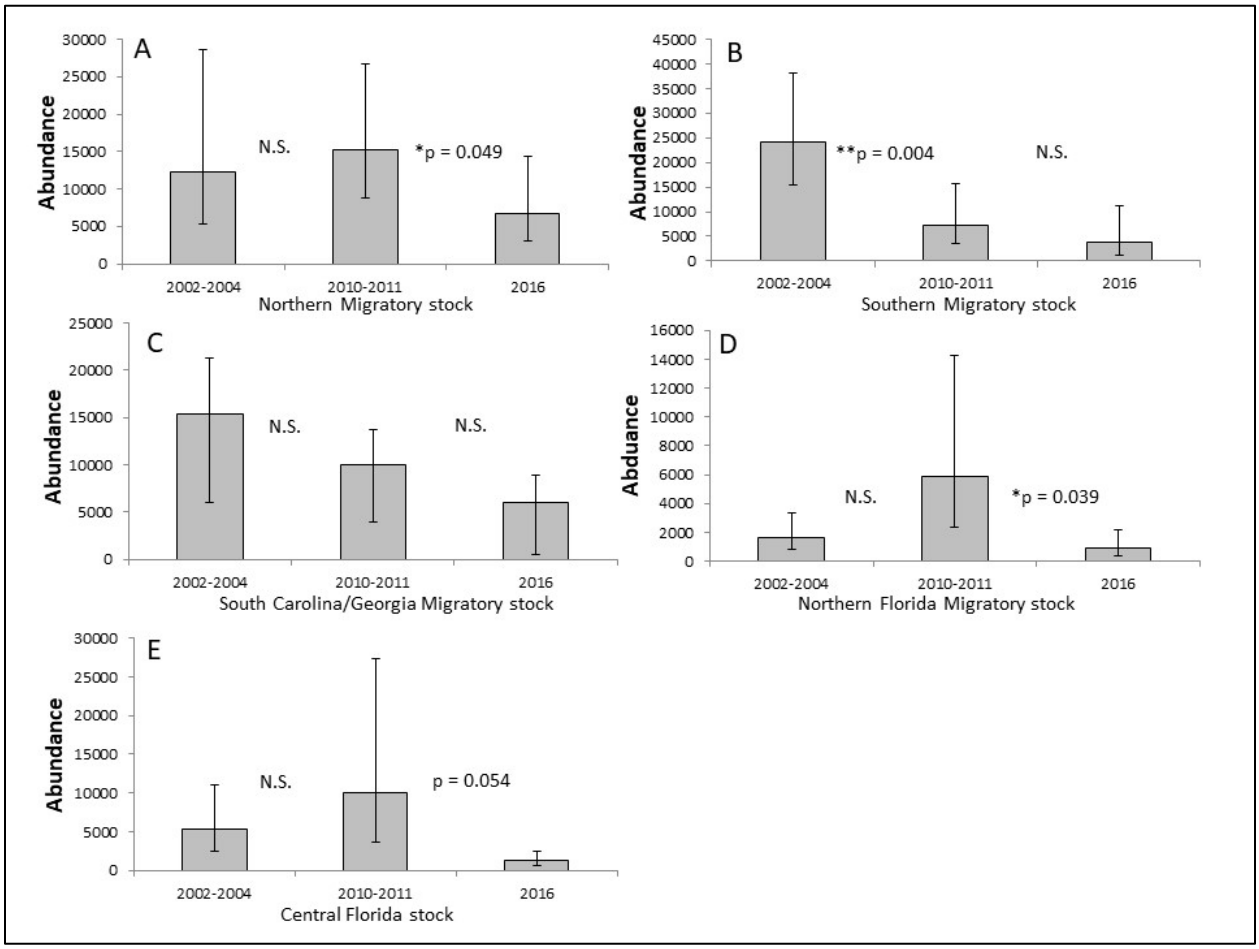

Figure 5-5 Mean abundance estimates for coastal bottlenose dolphin stocks
Results of z-test for difference of means indicated between successive years. Error bars indicate 95% confidence limits from the bootstrap distribution of estimates.

The coast wide estimate of population size (Figure 5-6) showed no significant decline between the 2002 to 2004 period (n = 57,203 [95% confidence interval (CI): 40,506-80,675]) and the 2010 to 2011 period (n = 49,039 [95% CI: 31,562 – 76,194]). However, there was a significant (p = 0.007) decline in the coast wide population size between 2010 to 2011 and 2016 (n = 19,470 [95%CI: 12,574 – 30,149]). This overall population decline is consistent with the large-scale mortality event that occurred in 2013 to 2015 associated with a morbillivirus outbreak and elevated strandings of bottlenose dolphins along the east coast.

We based the best estimate of population size for each stock (Table 5-5) solely on the summer 2016 survey since the apparent changes in population size from 2010 – 2011 to 2016 make it inappropriate to average population size across these years.

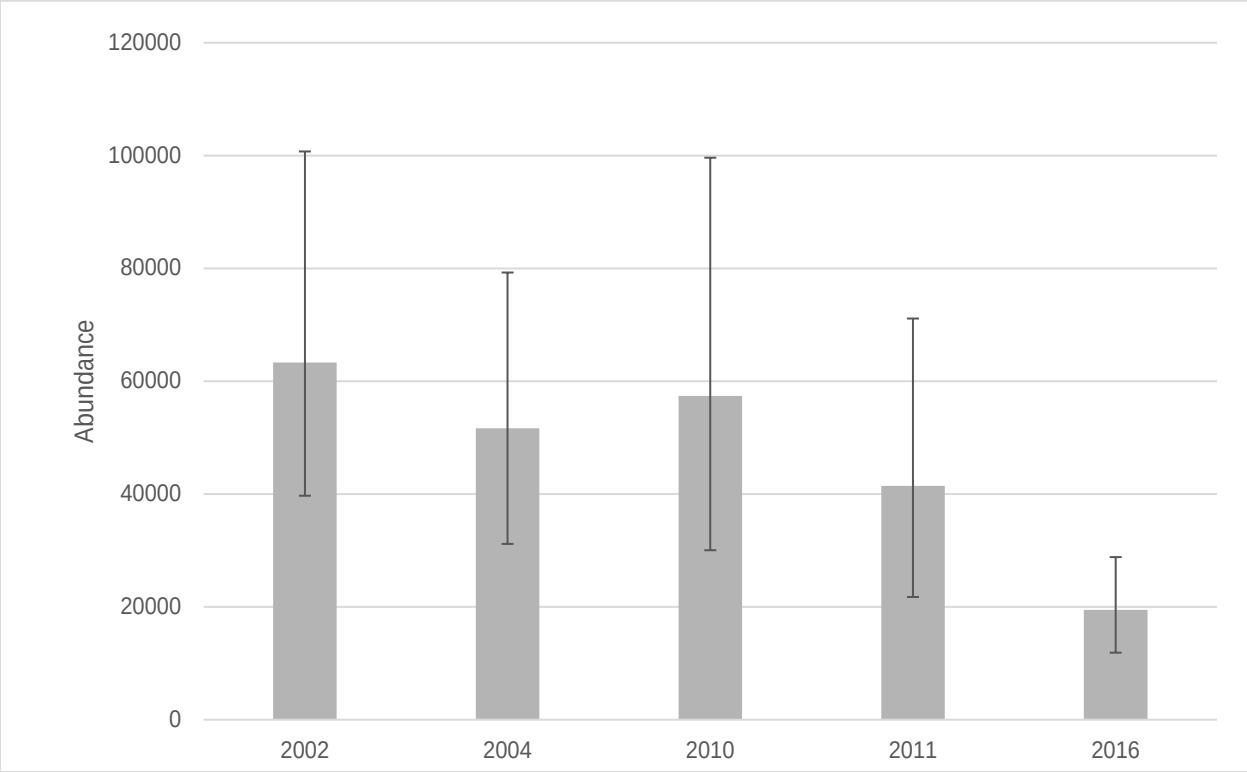

Figure 5-6 Coast wide estimates of coastal bottlenose dolphin abundance
Error bars indicate 95% confidence limits

Table 5-5 Best abundance estimates (N_{best}) for each coastal bottlenose dolphin stock
Other information provided includes minimum abundance estimates (N_{min}) and potential biological removal (PBR) for each stock. All estimated derived from the summer 2016 abundance estimates. For PBR calculations, we assumed maximum rate of increase, R_{max} was 0.04 and the recovery factor, F_r was 0.5 for all stocks (except the Southern Migratory stock where F_r was 0.48 because of a high bycatch coefficient of varation).

Stock	N_{best}	CV	N_{min}	PBR
Northern Migratory	6,639	0.41	4,759	47.6
Southern Migratory	3,751	0.60	2,353	22.6
South Carolina/Georgia	6,027	0.34	4,569	45.7
Northern Florida	877	0.49	595	6.0
Central Florida	1,218	0.35	913	91.3

5.4.4 Key Findings

We found that integrating distribution and abundance data from aerial surveys with samples collected during shipboard surveys allowed the development of abundance estimates for the coast versus offshore morphotypes of bottlenose dolphins along the U.S. east coast. North of Cape Hatteras, NC we found a perfect segregation of coastal and offshore dolphins in the biopsy samples, with no coastal samples collected in waters deeper than 20 m and all offshore samples over the outer continental shelf. South of Cape Hatteras, NC however, there is apparent overlap between coastal and offshore dolphins, with coastal samples occurring on the outer continental shelf and offshore samples occurring in relatively shallow water. Further, our logistic regression model predicted that in waters less than 13 m, we expected greater than 90% of the dolphins to be of the coastal morphotype. Despite having different effort and spatial coverage, we noticed a marked shift in the distribution of sightings between 2002 and 2004 that we did not detect in 2010, 2011, and 2016. Based on that, we suggest that the underlying environmental

variability may drive inter-annual changes in the spatial distribution and the stock boundaries are spatially flexible. In terms of abundance, we suggest that the inter-annual variation may reflect changes in animal distribution and movement instead of changes in population size, especially over a short period, like between 2002 and 2004. To assess trends in variation, we performed an analysis on pairs of surveys and found statically significant declines in abundance for the Northern Migratory, Northern Florida and Central Florida stocks between 2010 – 2011 and 2016, for the SM stock for 2002 – 2004 and 2010 – 2011 and a general decline overtime for the Southern Migratory and South Carolina/Georgia stocks. We also combined all stocks into a coast wide estimate of population size and found no significant decline between the pair of surveys of 2002 – 2004 and 2010 – 2011; however, we found a significant decline between the pair of surveys of 2010 – 2011 and 2016. This overall population decline is consistent with the large-scale mortality event of 2013 – 2015 associated with a large-scale mortality event associated with *Morbillivirus*.

5.4.5 Data Gaps and Future Work

There was a transition zone for coastal versus offshore samples between 13 and 33m water depth and in waters deeper than 33 m, less than 10% of dolphins were of the coastal morphotype. However, we detected 2 coastal samples in waters deeper than 68 m in the Central Florida strata, which had very low sample size and where the model predicted a near-zero chance of coastal animals occurring. We conclude that these 2 genetically distinct bottlenose dolphin morphotypes are sympatric over portions of the continental shelf south of Cape Hatteras. We require additional biopsy samples and genetic analyses to futher elucidate the habitat use and genetic characterization of these 2 morphotypes.

Surveys conducted during 2002 and 2004 covered primarily nearshore waters and the effort did not extend offshore to the 200 m isobath as the surveys conducted between 2010 and 2016. This limits the ability to evaluate trends between the older and newer surveys. However, survey effort was consistent since 2010. For coastal dolphins, we detected a noticeable shift in spatial distribution for some survey years but not for others. We hypothesize that underlying environmental variability may be driving inter-annual changes in distribution. To test this hypothesis we could overlay contemporaneous environmental remote-sensed data with variables collected *in-situ* at the time of the survey to help us understand why these variations may have occurred; help us understand animal movement; and help describe potential interannual changes in the spatial distribution of individual stocks.

At the level of individual stocks, there is a high degree of uncertainty in the abundance estimates, where the variability in abundance may relate to either changes in population size or shifts in spatial distribution. Therefore, understanding animal movement in these regions in association with analysis of environmental variability may help us elucidate true changes in abundance and better define the boundaries for each stock.

When we combined survey data across stocks, there was sufficient statistical power to detect a likely change in population size in coastal morphotype bottlenose dolphins between 2010 – 2011 and 2016. This decline in abundance is consistent with elevated mortality rates observed during 2013 – 2015. To better understand this trend, we should conduct similar surveys on an annual basis to assess true changes in population size and to determine if the stocks will recover from this mortality event. Furthermore, we need to take extraordinary events, such as *Morbillivirus* outbreaks, into account when assessing population shifts as they are a significant cause of mortality for bottlenose dolphin populations and may affect multiple stocks differently as animals move along the coast and across stock boundaries.

In addition to a better understanding of animal movement and of real changes in population size, we need certainty in stock identifications and variability in stock boundaries. This is important to assess, manage

and mitigate bycatch of bottlenose dolphins in gillnet fisheries in the U.S. Atlantic coast in respect to Potential Biological Removal levels.

5.5 Short-finned Pilot Whale Abundance

5.5.1 Introduction

The objective of this analysis was to estimate the abundance of western North Atlantic short-finned pilot whale stock (*Globicephala macrorhyncus*) from the shipboard and aerial survey data collected in 2016 by the SEFSC and NEFSC. A full description is in Garrison and Palka (2018). We incorporated these numbers into the Atlantic Stock Assessment Report (Hayes et al. 2020). In addition, the Pelagic Longline Take Reduction Team used these numbers.

The western North Atlantic short-finned pilot whale stock has been the focus of assessment efforts during the last 2 decades due to the relatively high rate of observed interactions with the U.S. Atlantic and Gulf of Mexico Pelagic Longline Fishery. Fisheries observers frequently document interactions between this species and longline gear. Mortalities and serious injuries are primarily due to hooks in the mouth of these animals (Garrison and Stokes 2020). The stock has been the focus of efforts to reduce mortality and serious injury by the Pelagic Longline Take Reduction Team since 2004.

Assessment of this stock is complicated by the fact that the short-finned and long-finned (*G. melas*) pilot whale species overlap spatially off the U.S. east coast between Virginia and New York during portions of the year. Detailed photographic data collections characterize distinctive coloration patterns between the 2 species. However, this requires both close approaches and light conditions that allow collection of high quality photographs (Rone and Pace 2012). Thus, this detailed data collection procedure cannot be a routine procedure during visual surveys for abundance estimation or during at-sea observations of pilot whales incidentally taken in commercial fisheries. Therefore, Garrison and Rosel (2017) used a habitat-based model to predict the probability that any given sighting was a short-finned pilot whale as a function of latitude, month of the year, and sea surface temperature. Tissue biopsy samples collected from pilot whales at sea allowed the identification of sampled animals to species. They detected an area of overlap between the 2 species during the summer months that was primarily along the shelfbreak off the coast of New Jersey (between 38°N and 40°N latitude). In addition, they determined that sightings in offshore waters near the Gulf Stream were predominantly short-finned pilot whales.

5.5.2 Methods

During the 2016 surveys, we detected pilot whales on the SEFSC shipboard survey and on the NEFSC aerial and shipboard surveys. Based upon sea surface temperature (SST) and location and this model, all of the sightings from the SEFSC shipboard survey had a greater than 95% probability of being from short-finned pilot whales, while the all the sightings during the NEFSC aerial survey were predicted to be long-finned pilot whales. Therefore, we applied the partitioning between the 2 species only to data collected from the NEFSC shipboard survey (Figure 5-7).

We described the straightforward data collection and analysis procedures of the 2016 SEFSC shipboard and NEFSC aerial surveys in sections 5.2 and 5.3 and in Garrison (2020) and Palka (2020). For the 2016 NEFSC shipboard survey, where there were overlapping pilot whale species, we used the SST value, latitude, and month of the pilot whale sightings to predict the probability that a sighting was short-finned pilot whales using the Garrison and Rosel (2017) logistic regression model discussed above. We then integrated this probability into the equations for estimating abundance (Garrison and Palka 2018). Variance for the estimates from the NEFSC survey included uncertainty in both the detection probability and logistic regression models using a bootstrapping approach.

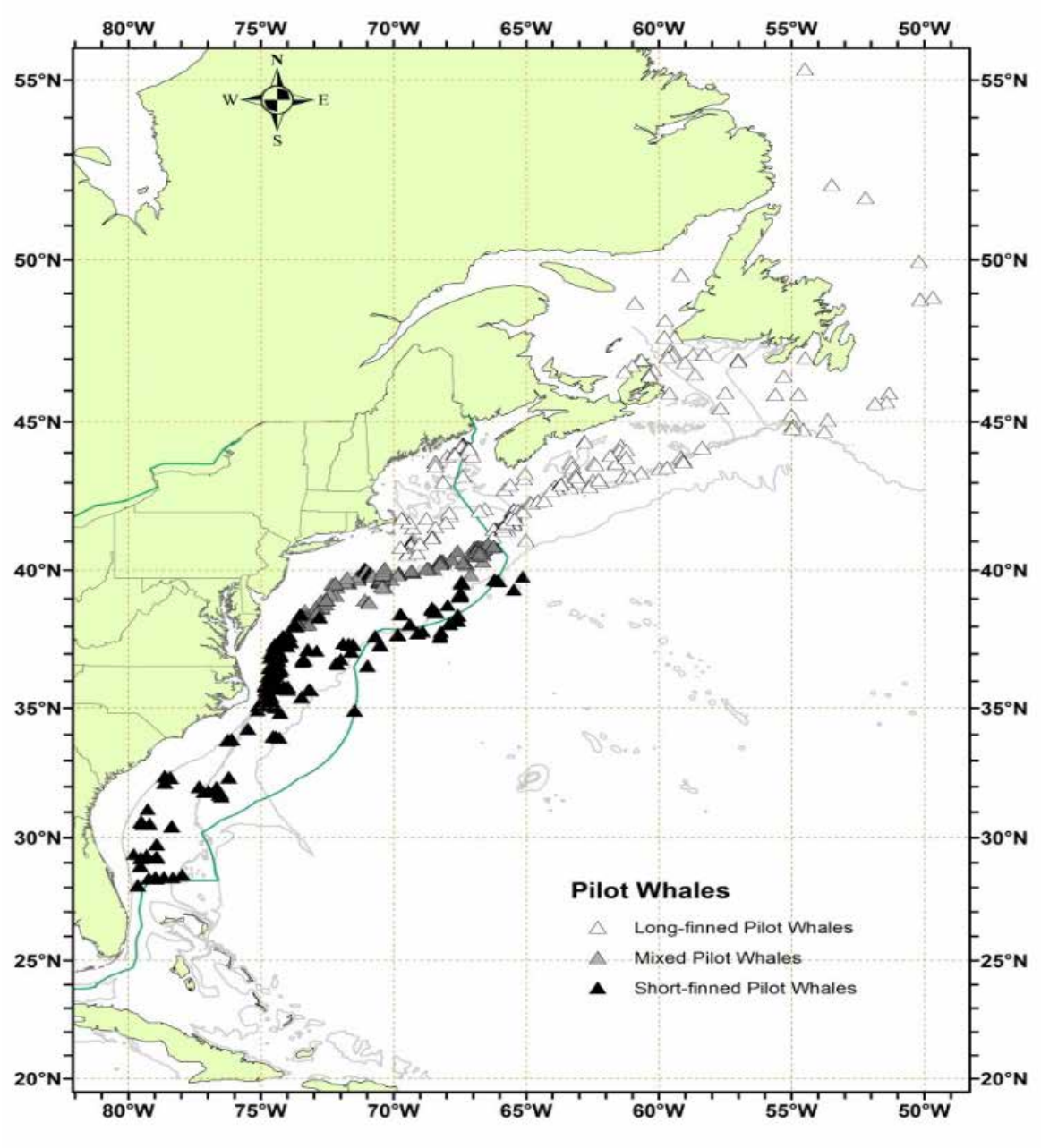

Figure 5-7 Distribution of pilot whales by species
Long-finned (open symbols), short-finned (black symbols), and possibly mixed (gray symbols; could be either species) pilot whale sightings from NEFSC and SEFSC shipboard and aerial surveys during the summers of 1998, 1999, 2002, 2004, 2006, 2007, 2011, and 2016 and Canada's 2007 and 2016 abundance surveys. The inferred distribution of the 2 species is preliminary and is valid for June-August only. Isobaths are the 100-m and 3,000-m depth contours. The U.S. EEZ is a green line.

In summary, we derived the short-finned pilot whale abundance from the southern surveys: all of the 2016 SEFSC shipboard survey and some of the 2016 NEFSC shipboard survey (Garrison and Palka 2018). The long-finned pilot whale abundance was derived from the northern surveys: some of the 2016 NEFSC shipboard survey (Garrison and Palka 2018), all of the NEFSC aerial survey (Palka 2020), and all of the Canadian aerial surveys (Lawson and Gosselin 2018).

5.5.3 Results and Discussion

The SEFSC vessel survey included 4,400 km of track line on effort and observed 64 groups of pilot whales totaling 944 animals. The minimum water temperature was 21.5ºC, and the majority of pilot whale sightings occurred in water temperatures of 23ºC or higher. The highest density and number of animals occurred in the shelf-break stratum north of Cape Hatteras, NC, but we also observed pilot whales in deeper waters throughout the survey range. Of all the pilot whale groups seen during the SEFSC survey, the upper team saw 22, the lower team 24, and both teams combined saw 18. In the area of short-finned and long-finned pilot whale overlap, the NEFSC shipboard survey included 3,738 km of track line on effort and observed 117 groups of pilot whales totaling 904 animals. The pilot whale sightings occurred along the southern flank of Georges Bank in 2 notable clusters, 2 off New York and the other at the tip of Georges Bank in Canadian waters (Figure 5-8). Sightings also occurred in deeper waters over the continental slope. The upper team saw 37 groups of pilot whales, the lower team saw 35, and both teams combined saw 45.

Pilot whale sightings detected during the 2016 NEFSC shipboard survey occurred across a range of water temperatures with distinct clusters of sightings at temperatures between 17.4ºC and 22ºC and 22ºC and 28ºC (Figure 5-9). The predicted probability of being a short-finned pilot whale was generally highest in the southern and offshore portions of the survey, and the lowest probability was in the northernmost area at the tip of Georges Bank. Interestingly, 1 large cluster of sightings at approximately 40ºN latitude was predicted to have a high probably of being short-finned pilot whales while another at approximately the same latitude had a very low probability of being short-finned (Figure 5-8). We observed the former cluster in mid- to late-August at water temperatures from 23ºC to 26ºC, while the latter was in late June at water temperatures from 17ºC to 19ºC.

Using the probability of each sighting being a short-finned pilot whale plus standard mark-recapture distance sampling analysis of all the short-finned pilot whale sightings (diagnostics and detail results in Garrison and Palka 2018), the resulting estimated abundance of short-finned pilots whales in the 2016 summer NEFSC shipboard survey was 3,811 individuals (CV = 0.42). The remaining pilot whales detected on the NEFSC shipboard survey were long-finned pilot whales (9,972; CV = 0.55). The total abundance estimate from the SEFSC survey was 25,114 short-finned pilot whales. We then used these estimates in the abundance estimates described in section 5.3 and Table 5-4 and in the Atlantic Stock Assessment Report.

In conclusion, analysis of accurate species distribution patterns and density models incorporating environmental conditions, namely sea surface temperature, can help us predict times and locations of high risk of bycatch. Thorne et al. (2019) predicted strong correlations between temperature and other oceanographic features in short-finned pilot whale occurrence and risk of bycatch in the pelagic longline fishery of the eastern U.S. Furthermore, they proposed that combining species distribution models with near real-time or forecasted environmental conditions can provide managers with a tool to mitigate bycatch of pilot whales in the North Atlantic.

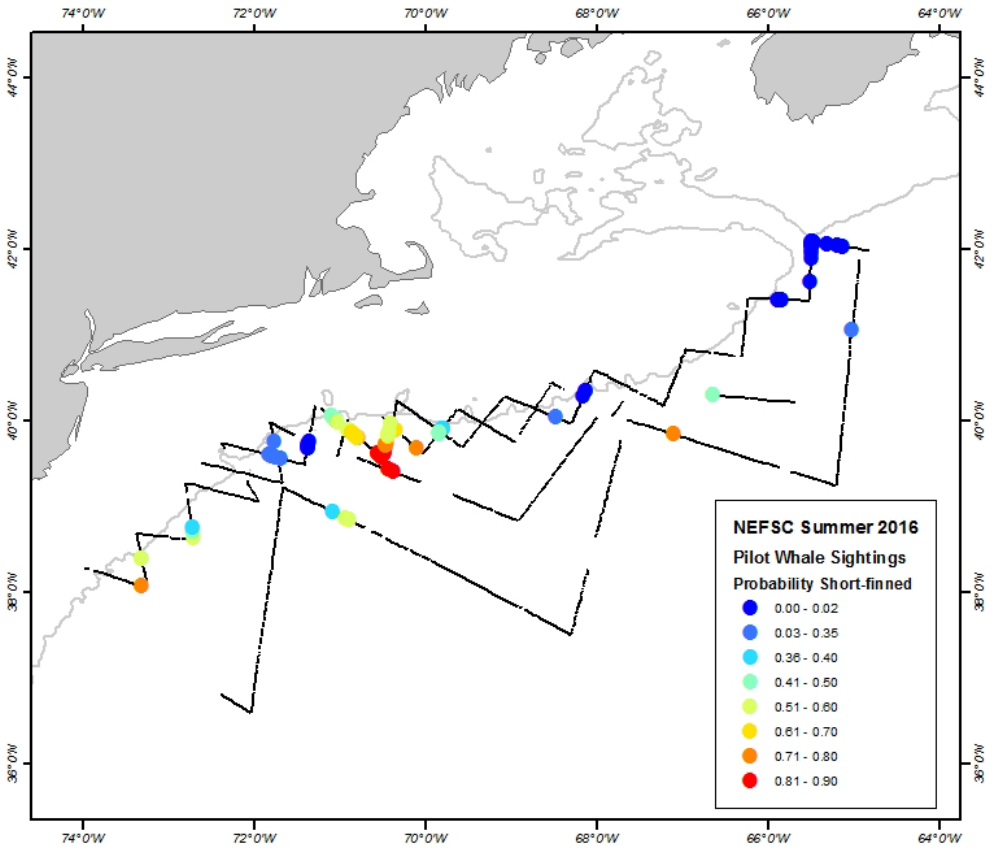

Figure 5-8 Probability of each sighting from NEFSC survey being of short-finned pilot whales

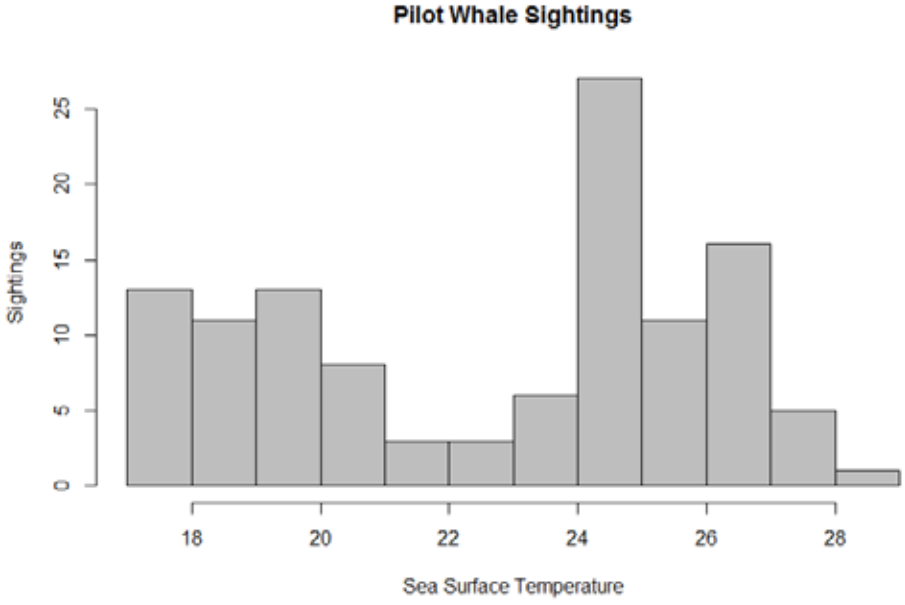

Figure 5-9 Sea surface temperature at locations of pilot whale sightings during the NEFSC survey
Temperatures (°C) based upon remote MODIS (Moderate Resolution Imaging Spectroradiometer) satellite data.

5.5.4 Key Findings

We found that based upon SST and location, all of the pilot whale sightings during the SEFSC survey had a greater than 95% probability of being from short-finned pilot whales. The minimum water temperature in which we recorded the SEFSC sightings was 21.5ºC, and the majority of sightings occurred in water temperatures of 23ºC or higher. We detected the highest density and number of animals in the shelf-break stratum north of Cape Hatteras, NC and calculated a total abundance estimate of 25,114 individuals.

During the NEFSC summer survey, we detected 2 notable clusters of pilot whale sightings along the shelfbreak of the southern flank of Georges Bank: 1 off New York, and the other at the tip of Georges Bank in Canadian waters. We recorded sightings across a range of water temperatures with 2 distinct clusters: 1 ranging at temperatures between 17.4ºC and 22ºC and the other cluster ranging from 22ºC and 28ºC. We predicted the highest probability of being a short-finned pilot whale in the southern and offshore portions of the survey area, and the lowest probability was in the northernmost area at the tip of Georges Bank. The total abundance of short-finned pilot whales we estimated was 3,811 individuals. Therefore, the total abundance of short-finned pilot whales along the U.S. Atlantic coast from central Florida to Georges Bank is the sum of the estimates from the NEFSC and SEFCS vessel surveys and that is 28,924 individuals. Compared to other abundance estimates from similar surveys and analysis methods, the generalized linear model indicated no significant trend in the estimates.

5.5.5 Data Gaps and Future Work

The Western North Atlantic short-finned pilot whale has a high incidence of interaction with the Pelagic Longline Fishery, which causes mortalities and serious injuries by primarily hooking the animals in the mouth. The fact that the short-finned and long-finned pilot whale species overlap spatially between Virginia and New York during portions of the year and differentiating both species at sea is difficult complicates the assessment of the effect of bycatch incidence to these stocks. We have already demonstrated that location and water temperature are reliable predictors that we could use to assign previous sightings and fishery interactions to species. However, it is unknown whether these environmental relationships vary across years. This question is particularly relevant as temperatures across the Atlantic seaboard are warming and there are associated shifts in fish distributions. An additional question is how the prey species of pilot whales change under these changing conditions. To address these questions, we need additional information on the prey species consumed by pilot whales and on the distributions of those prey species and other environmental conditions. In addition, we need to reliably identifying the species of the pilot whale when encountered. Additional biopsy sampling effort in areas where the 2 species overlap could start to address these questions since the samples can provide pilot whale species identifications and prey information via stable isotope analyses of the biopsy samples (or similar analysis methods). Together we could use the results to verify the species-environment relationships. Ideally, species identifications could be made reliably during survey effort, and we should explore acoustic methods or eDNA tools to directly assess the distribution of the 2 species. Finally, the spatial models developed during this project will improve our ability to predict times and locations of high risk of commercial fisheries bycatch.

5.6 Development of Integration of Visual and Passive Acoustic Data

5.6.1 Introduction

The objective of this analysis was to develop a statistical framework to directly integrate passive acoustic line transect data with visual line transect data to estimate abundance accounting for perception and availability bias simultaneously. As we did in section 5.3, we used visual line transect data to estimate

abundance accounting for perception bias, but in those analyses we had to use externally collected DTAG time-depth data to estimate a correction factor for availability bias (section 5.2.5). Unfortunately, deploying DTAGs is expensive, challenging to attach to an animal, and is usually only available for a limited number of animals in a limited number of habitats. The advent of passive acoustic technology to detect and track diving animals offers an opportunity to estimate abundance that accounts for availability bias using the animals encountered during a survey and to investigate changes in surface availability among habitats encountered during the survey. However, methods for estimating density and abundance from passive acoustic data are still in their infancy.

Scientists have been collecting passive acoustic data from towed hydrophone arrays on a cable towed behind the ship for decades. Historically, one approach used to estimate density and abundance was to apply standard distance sampling analysis methods to the passive acoustic detections; however, several challenging assumptions require further work (Marques et al. 2013). Another approach was to combine an abundance estimate from a passive acoustic survey with an abundance estimate from a visual survey to obtain an overall estimate of abundance. For example, Gerrodette et al. (2011) estimated the abundance of vaquitas (*Phocoena sinus*) by adding the abundance estimate resulting from an acoustic array survey in deep waters with the abundance estimate resulting from a visual survey in a totally separate shallow water area. In another example, Barlow and Taylor (2005) used visual data mostly to correct for cluster size, but designed their study to keep the 2 platforms independent such that they could estimate 2 separate abundance estimates from each platform for comparison.

Another approach scientists have used is to deploy towed hydrophone arrays simultaneously with visual observer surveys (such as what we have done in the AMAPPS shipboard abundance surveys; Chapters 7 and 10). The advantage of this survey design is it would directly account for availability bias using all the animals detected by the independent passive acoustic array. By combining passive acoustic data with visual data our method offers an opportunity to greatly increase the number of detections from the passive acoustic monitoring while still taking advantage of the visual line transect data to derive precise estimates of abundance. Our approach also offers advantages to estimating surface availability. By taking advantage of both the acoustic and visual data, we were able to use more information then what is typically collected from DTAG studies, which target an even smaller subset of the population than line transect surveys do. As a result, this approach has the potential to achieve more precise estimates than estimates derived from DTAG data. A further advantage of this approach is that we can calculate spatially or temporally explicit estimates of surface availability that would require more DTAGs than are commonly available. The challenge is accounting for animals detected both acoustically and visually. Stated in a statistical fashion, the challenge is to estimate the probability that an animal transitions between the acoustically detectable state and the visually detectable state (Flemming et al. 2018).

In this section we outline a preliminary novel statistical framework to estimate abundance accounting for availability bias by directly integrating passive acoustic line transect data with visual line transect data when visual and passive acoustic data are collected simultaneously. We developed 2 methods to adjust for duplicate detections when using passive acoustic data that we post-processed in 2 ways. In addition to estimates of density accounting for availability bias, our method explicitly produced estimates of surface availability. We used sperm whales as a case study because they are easy to identify visually and acoustically, they are acoustically very active, and their diving behavior is well studied. This approach provides a flexible framework that may be applicable to other species.

5.6.2 Methods

5.6.2.1 Visual Data

We used visual data on sperm whales that we collected during the 2013 NEFSC shipboard line-transect survey (Palka et al. 2017). We used the data from the 2 independent teams to estimate the detection probability on the track line to account for perception bias. Section 5.2 in this chapter provides a description of the data collection protocols. Chapter 11 provides more details on the data processing steps.

5.6.2.2 Passive Acoustic Data

During the 2013 NEFSC shipboard line-transect survey we deployed an 8-hydrophone array to record passive acoustic detections of diving sperm whales (and other species) simultaneously with the 2-team visual surveys who were collecting visual sightings. The array, towed 300 m behind the ship, was comprised of 2 oil-filled, modular sections, separated by 30 m of cable (see DeAngelis et al. 2017). Chapter 7 provides more information on how we collected and used the data from towed hydrophone arrays. Chapter 11 provides more details on the data processing steps.

In this analysis, we primarily used the data from hydrophones 6 and 8. We organized and analyzed the data using the software PAMGUARD (Gillespie et al. 2008), which hosts a built-in click detector of the sounds sperm whales produce while foraging at depth. We defined an "event" to be a series of received clicks with regular inter-click-intervals that were along similar bearings and thus, could represent an individual sperm whale. We archived the received bearings of each detected click, along with the event identifier and timestamp (Figure 5-10). With these archived data, we localized each event using PAMGUARD's Target Motion Analysis module, which is 2-dimensional Simplex Optimisation algorithm. The 2-dimensional localization algorithm is sufficient for sperm whales because they have a long detection range from the ship (>5 km; Madsen et al. 2002) relative to their deepest recorded dive (1,494 m; Wahlberg 2002). In essence, this flattens the 3-dimensional space into 2 dimensions. After we localized an event, at any click, we could estimate the radial distance between the whale and vessel by subtracting the latitude and longitude of the whale's position from the vessel's position at the time of the click (DeAngelis et al. 2017). This method is appropriate because the vessel is travelling faster than the whale; thus, the whale appears to be "static" during the detection timeframe.

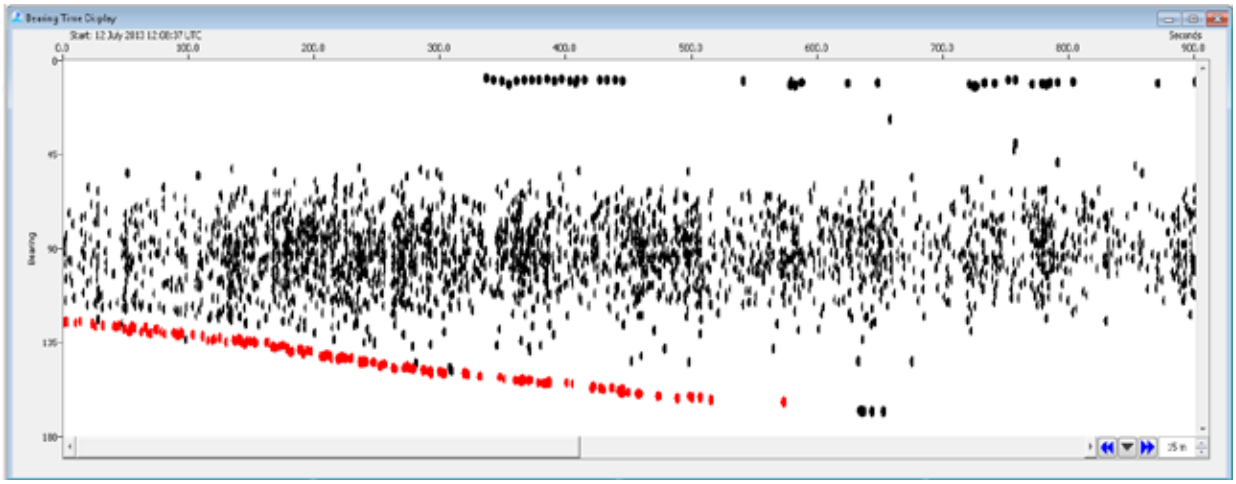

Figure 5-10 Example of sperm whale clicks following a similar change in bearings (red)
This is a display from PAMGUARD's click detector, with time on the x-axis and bearing on the y-axis. Bearings of 0° to 90° represent detections ahead of the array. Bearings of 90° to 180° represent detections behind the array. Clicks that are an "event" are in red. They have a steady change in received bearing angles over time and contain acoustic

properties that denote sperm whale clicks. The black dots from 45° to 120° represent impulsive noise detected by the towed array that is most likely from surface wave action. The black dots around 10° is the start of another individual sperm whale that PAMGUARD may identify as a separate event after more data are available.

5.6.2.3 Primary Analysis Method

The goal of our method was to estimate the unbiased total abundance of animals ( ), accounting for perception and availability bias. We accomplished this by combining capture mark-recapture (CMR) analysis methods with traditional distance sampling (DS) analysis methods (Eqn 5-4). This equation combines an abundance estimate for animals that are above the surface derived from visual data ( ) and an abundance estimate for animals below the surface derived from passive acoustic data ( ), then subtracts an abundance of duplicate whales that were included in both the above and below estimates ( ).

A consequence of this method is we can also derive an estimate of surface availability, such as that produced in section 5.2.6. We refer to this method as the *CMR-DS Method* and note that it requires that we identify all clicks from all events. In the rest of this section, we more fully describe this method, outline several challenges in implementing the method, and offer an alternative method to address some of the challenges.

We estimated the surface abundance ( ) in the traditional way: by using visual sightings data and standard mark-recapture distance sampling analysis methods, as described in section 5.2.5.

Because the passive acoustic array continuously tracks the position of a clicking subsurface whale, we can treat these data as capture mark-recapture data. Traditionally, we divide capture mark-recapture data into a time series, where an animal is marked in a time step, then in following time steps, it is either recaptured (1) or not (0). In our case, we divided the passive acoustic click data into distance intervals, which correspond to the traditional time steps. We defined the distance intervals for an event by dividing the forward distance locations (y in Figure 5-11) of all of the event's recorded clicks into a series of equally spaced distance intervals. The first interval was the maximum distance ahead that we could detect a whale by the acoustic array (similar to the truncation distance in a traditional distance sampling analyses). If an event (assumed whale) was detected clicking in a given distance interval, then we assigned a value of 1 to that distance interval. If we did not detect a click from that event (whale) in a distance interval, then we assigned a value of 0 to that distance interval (see Figure 5-11 for a conceptual diagram).

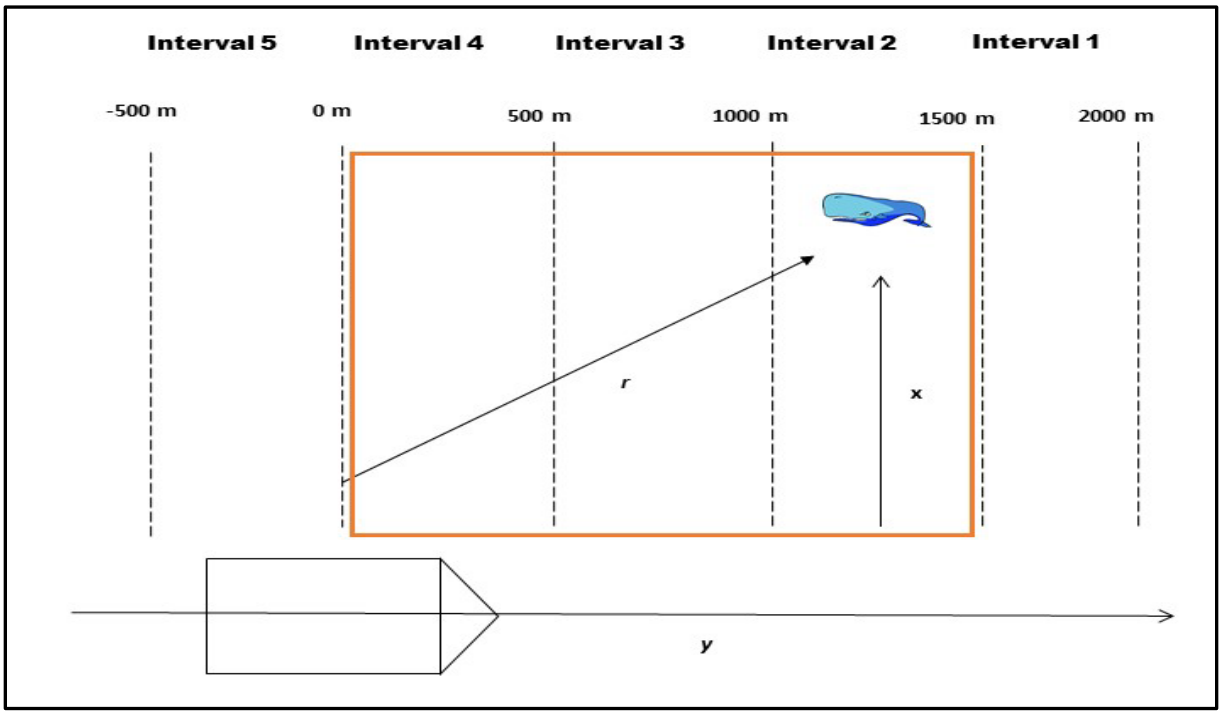

Figure 5-11 Conceptual diagram of a click train from an event (a submerged whale)

To analyze these data we adopted a state-space formulation of the Jolly-Seber model using data augmentation (Royle and Dorazio 2008). Traditionally this statistical method, when applied to capture mark-recapture data, produces estimates of population level statistics for an open population including estimates of recruitment into the population, estimates of survival (or mortality) between sampling occasions, and estimates of the population size. In addition, the method produces an estimate of the "super population" that represents the total number of individuals that were alive in the population at 1 time or another within the period of sampling. These traditional population level statistics are directly analogous to the statistics of interest in the *CMR-DS method*. That is, recruitment in the traditional method translates in our case to the probability of an animal transitioning from above the surface to below the surface (i.e., entering the diving phase). The traditional survival parameter translates in our case to the probability of an animal remaining below the surface. Thus, the traditional mortality parameter (which equals 1 minus the probability of survival) translates in our case to the probability of an animal transitioning to the surface. The traditional "super population" parameter translates in our case to the total number of animals that were below the surface at 1 time or another during the period of time we were passing by the animals; that is, the estimate of the total number of animals below the surface ( ).

Next we need to estimate the number of duplicate animals ( ) that is, the number of animals that were both above and below the surface during the period we were passing by. In other words, we need the number of animals that transitioned from below the surface to above the surface, in addition to the number of animals that transitioned in the opposite direction, from above the surface to below the surface. We derive these numbers from the estimated probability of entering the dive state, and the probability of leaving the dive state (to enter the surface state) while in the zone of overlap between the region where a whale is detectable by the visual team and region where a whale is detectable by the acoustic team. Subsequently, we can estimate the surface availability as ——— .

5.6.2.4 Challenges

An implicit assumption of the *CMR-DS Method* is that we can assign all clicks detected by the acoustic array to an individual whale (which we are assuming is 1 event). Because the passive acoustic data requires a considerable amount of effort to process, the nature of sperm whale data presents several challenges that complicate implementing the *CMR-DS Method*. These challenges include:

Ambiguous click trains – Sperm whales often dive and click within acoustic proximity of each other; thus, the towed array will pick up clicks from multiple individuals simultaneously. Depending on the location of the clicking whales relative to the ship, these bearings can often be only a few degrees apart, causing click trains from separate individuals to overlap in bearing and become ambiguous. In this case, it is impossible to distinguish between individuals (Figure 5-12). Thus, practically we are only able to assign some of the recorded clicks to an individual event.

Blind spots – The hull of the ship creates a blind spot for the passive acoustic array where we cannot detect any whale clicking directly forward of the array. In our case, the blind spot was 9° to either side of the track line. Consequently, vocalizing animals that are close to the trackline and those animals that are close to the surface, such as those animals at the start of their dive, are more likely to be in the blind spot.

Annotating clicks – Vocalizing sperm whales can produce large numbers of clicks; about 1,000 to 3,000 clicks (Madsen et al. 2002; Wahlberg 2002) during 1 dive, where the intervals between clicks can be as short as 0.33 sec. Consequently, the ability of an analyst to annotate every click is limited. This, coupled with the presence of ambiguous click trains, limited us to only annotating a portion of most whale events.

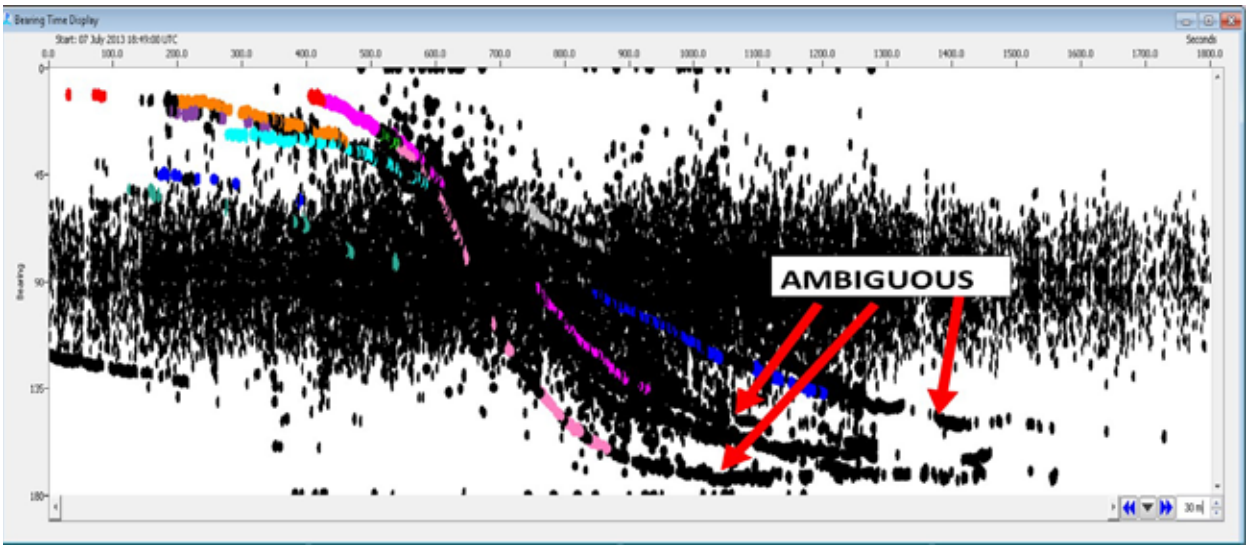

Figure 5-12 Example of ambiguous click trains from several vocalizing sperm whales
The color-coded regions indicate click trains (events) that we were able to assign to individuals. The black trains around 90° bearing (on the y-axis) and 700 secs (on the x-axis) merge and are masked by noise (the black vertical dashs). This then makes it impossible to tease apart which train after the 900 sec mark (indicated by red arrows) belongs to the trains detected earlier at 200 to 500 secs marks. We assigned the unmarked clicks at the smaller bearing angles to individuals in the analysis, even though we did not annotate them in this figure due to the sheer number of clicks in the events (highlighting the limitation of annotating clicks).

5.6.2.5 Hybrid Analysis Method

Because of the challenges listed above, we were not able to use all passive acoustic detections to estimate the abundance using the *CMR-DS Method*. However, we could still use Equation 1 to estimate abundance in an alternative hybrid analysis method. These challenges do not preclude us from localizing all events and calculating a perpendicular distance from the trackline for each event. Thus, we estimated using standard one-team distance sampling analytical methods. Despite the challenges, we still had a representative subset of events where we had high confidence of detecting and annotating all clicks during the whale's foraging dive where we could estimate the transition probabilities among states using the capture mark-recapture methods described above. Thus, we estimated by using a subset of completely annotated click trains to estimate the proportion of animals that transition within the zone of overlap ( ) by . We refer to this method as the *Hybrid Method*.

5.6.2.6 Simulation Testing

To test the applicability of these methods we designed a simulation framework with the intention of replicating sperm whale diving behavior as closely as possible. We based our simulation on data from Watwood et al. (2006) who used data collected from DTAGs to characterize the dive cycle and vocalizing behavior of sperm whales. Our simulations included individual variation in diving depth and dive cycles as well as periods of non-clicking while submerged. We used half-normal detection functions to simulate the detection process for both the visual and acoustic data. We simulated 100 scenarios of diving whales and visual and passive acoustic teams collecting data. Then we applied both the *CMR-DS* and *Hybrid Methods* to each simulated dataset to estimate abundance and surface availability as well as the coefficients of variation (CV) for each estimate. For comparison, we also applied a naive analysis method that simply applies standard distance sampling methods separately to the visual and acoustic data and then adds the 2 estimates together to produce an overall abundance estimate, but does not attempt to adjust for the probability of duplicates (referred to as the *DS-DS Method*). We calculated relative bias as ($_{ESTIMATE}$ - $_{TRUE}$)/ $_{TRUE}$ where $_{TRUE}$ represents the true abundance or surface availability and $_{ESTIMATE}$ represents the estimate from the 3 analysis methods.

5.6.3 Results

Simulations demonstrated that the relative bias of the estimates of abundance and surface availability were on average close to zero for both the *CMR-DS Method* and *Hybrid Method* (Figure 5-13). However, as expected the abundance estimate from the *DS-DS Method* was positively biased and the surface availability estimate was negatively biased.

Also as expected, the magnitude of the relative bias of the results from both the *CMR-DS Method* and *Hybrid Method* was less than that from the *DS-DS Method* (Figure 5-13). For the abundance estimates, the decrease in relative bias relative to the *DS-DS Method* was about 86% and 81% for the *CMR-DS Method* and *Hybrid Method*, respectively. For the surface availability estimates, the decrease in relative bias relative to the *DS-DS Method* was approximately 81% and 75% for the *CMR-DS Method* and *Hybrid Method*, respectively.

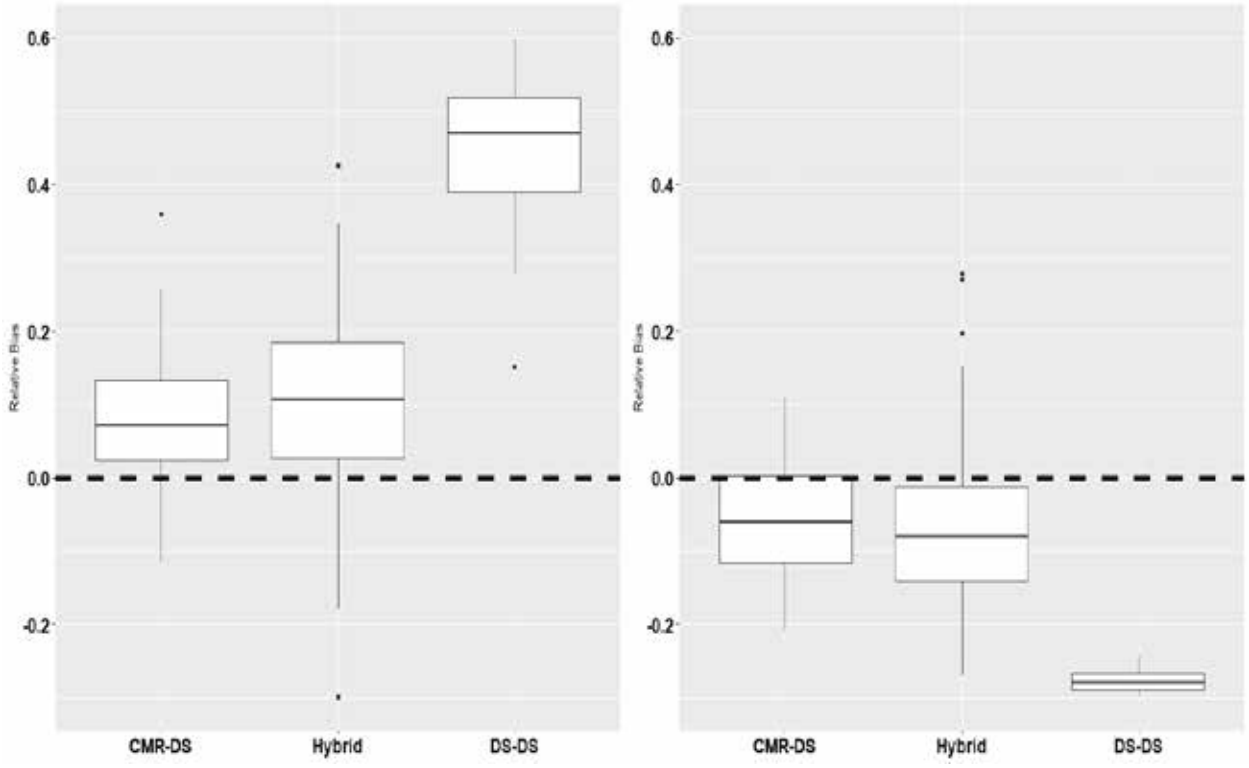

Figure 5-13 Comparison of relative bias from the Primary, Hybrid and Naive methods
We derived the relative bias of the abundance (A) and surface availability (B) from simulations of diving sperm whales where visual and passive acoustic teams are surveying.

5.6.4 Key Findings

In this section, we explored methods to integrate passive acoustic towed array data with visual line transect data when both sources of data are collected simultaneously. Our work highlights several challenges to integrating these 2 sources of data. We developed a general framework for estimating abundance and surface availability that carefully considers these challenges. To increase adaptability to data limited scenarios, we formulated 2 methods tailored to different ways of processing the passive acoustic data. Simulation testing demonstrated that the proposed methods achieve accurate estimates of abundance and availability bias, suggesting this framework has merit. We have identified several limitations of the current modeling framework but also offer possible solutions that could be incorporated in future iterations of the proposed modeling framework. Future work should be capable of reducing remaining biases and producing robust estimates that can improve demographic parameters of marine mammal populations.

5.6.5 Data Gaps and Future Work

We are currently applying the *Hybrid Method* to the visual and passive acoustic sperm whale data collected during the 2013 AMAPPS surveys. In addition, we are summarizing the methods, simulation results, and application to real data in a detailed report. Our plan is to have the detailed report reviewed by line transect experts via an online meeting. After responding to the review, we are planning to submit a paper to a peer reviewed journal. In addition, we will submit the resulting tool to NOAA's National Protected Species Toolbox Initiative repository and make an R package so the tool is accessible to the public.

Longer-term goals of this project include applying this approach to other species of cetaceans such as beaked whales. This step will involve additional simulation testing designed to replicate the diving behaviors of the species of interest. We also will use this method to explore spatial and temporal variability in availability bias. Finally, we will explore approaches for integrating this method into density surface models to enhance our spatially explicit estimates of density for deep-diving cetaceans in the AMAPPS study area.

5.7 Development of Trends Analyses

5.7.1 Introduction

The objective of this project was to explore multivariate autoregressive state-space modeling techniques to estimate long-term abundance trends of species in the AMAPPS area. We hoped to account for inter-annual variability by exploring the incorporation of process and observation errors, and to explore biotic and abiotic covariates that could influence the abundance trends. Since this project is a work in progress, in this section we have explored the technique using data from only a couple species.

Effective management measures that respond to observed wildlife abundance trends often leads to healthier wildlife stocks (Lindenmayer and Likens 2009; Hilborn et al. 2020). These types of management measures necessitate accurate estimates of population parameters and understanding of processes that drive them. However, temporal variation in climate and other aspects of the environment can have effects on population growth rates and spatial distributions of individuals. This variability complicates extracting accurate inferences from monitoring data. State space modeling is 1 technique that we can use to investigate abundance trends and potential drivers that cause variability in the trends. In general, the objective of state space modeling is to compute the optimal estimate of a hidden biological state derived from a time series of observed data. In our case, we want the optimal estimate of the abundance trend derived from a time series of abundance estimates. To do so, we account for 2 issues that lead to 2 equations: the process and observation error.

A state equation represents the hidden true process (in this case the true abundance), which is termed a state process. The state process depends on the state at a previous time modified by effects of covariates and by noise (i.e., natural variability), which is termed state process error.

An observation equation represents an estimate of the state process (in this case, an estimate of the abundance). The observation is a transformation of the hidden state modified by effects of covariates and by variability in the observations or measurements, which is termed observation error.

The state process error can represent temporal variability in the abundance due to environmental and demographic stochasticity (Ward et al. 2010). The observation error can represent variability in the sampling error, such as temporal changes in detectability or sampling changes resulting in only a sub-sample of the population counted.

Another complicating issue that is pertinent to trends in abundance and distribution patterns is not all animals within a single species act alike. That is, spatially distinct subgroups of animals may react in synchrony, or exhibit different behaviors due to subtle differences in local intrinsic and extrinsic factors. The existence of subgroups of animals within a population does not imply genetically separate parts of the population. It does imply that parts of the population may act differently than other parts of the population. On 1 hand, external drivers of temporal distribution changes (such as increasing water temperature) may occur across spatially distant subgroups, so the subgroups then react in synchrony to produce synchronized highs and lows of abundance. Conversely, the external drivers or perhaps intrinsic population traits may be locally different to each spatially distinct subgroup, hence resulting in spatially asynchronous population responses. These spatial subgroup patterns can occur within a species.

Alternatively, these patterns can also occur when looking across different species that share the same habitat. Both of these situations could be playing a role in the U.S. North Atlantic cetacean populations. Gaining an understanding of this is of practical importance for managing populations facing environmental and human-induced changes and for managing multiple species that share a common region.

The Northeast and Southeast Fisheries Science Centers (NEFSC and SEFSC) have been conducting abundance surveys since the early 1990's in Northwest Atlantic waters offshore of the coasts of the U.S. and Nova Scotia, Canada. When interpreting the abundance trend patterns resulting from these surveys, there are several complicating factors at play. One complicating issue is the areas surveyed and data collection methods changed slightly over time (observation error). Another complicating issue for many species is the species' normal habitat is larger than the study area where we conducted the abundance surveys. This could result in truly different numbers of animals within the study area that is solely due to localized emigration and immigration (process error).

Classical approaches to trend analyses often do not account explicitly for both process and observation errors. In this analysis, we applied multivariate autoregressive state-space (MARSS) models that explicitly account for process and observation errors to a time series of estimates of annual abundance. As a simple example, we investigated the abundance trends of the Gulf of Maine/Bay of Fundy harbor porpoise (*Phocoena phocoena*). During the summer, they inhabit the U.S. and Canadian Gulf of Maine, which is within our study area. However, they also inhabit Canadian Scotian shelf waters, which is outside our study area. As a more complicated example, we explored the abundance trends of common dolphins (*Delphinus delphis*). During summer, they inhabit waters throughout our entire study area, which ranges over 4 ecosystems that encompass the colder Gulf of Maine waters to the warmer southern and offshore waters near the Gulf Stream. However, they also inhabit Canadian Scotian shelf waters, outside of our study area.

To investigate the changes in abundance and distribution of these 2 species, we investigated the effects of climatic and other drivers that could potentially operate asynchronously in different ecosystem regions. It is important to note that, the estimated rate of change in abundance could be due to not only the natural biological growth rate involving the numbers of deaths and births, but also due to the effects of emigration and immigration between surveyed and unsurveyed waters.

5.7.2 Methods

To estimate the rate of change in abundance, we assumed a density-independent, stochastic Gompertz exponential growth model in log space that potentially could estimate process and observation error and incorporate covariates that could influence either the state space or observation space. This framework allows us to test the density-independent assumption. We implemented the abundance trends using the MARSS package in R (Holmes et al. 2020). The model consisted of a state equation (Eqn. 5-5) and an observation equation (Eqn. 5-6). Formally, the state equation represents a vector of unobserved first-order autocorrelated process over time and when written in log-space (Holmes et al. 2012) is:

Here x_t represents the unobserved value of the true log annual abundance state(s) at time t influenced by the abundance at time t-1 (x_{t-1}); B represents the autocorrelation in the state(s) estimating density dependence; c_t represents potential covariates that explain the autocorrelated state(s) and their respective coefficients, C; and u represents the rate of change. The process error (w_t) follows a multivariate normal distribution centered on zero with a covariance matrix Q.

The observation equation related the states (x) to observations (y) by:

Here the vector of observations of estimated annual log abundance at time t (y_t) was a linear combination of the autocorrelated state(s) x_{t-1} and the structural loading (Z) of each state(s) x_t on the observations (y_t), as well as any covariates (d_t) and their associated coefficients (D). The observation error (v_t) follows a multivariate normal distribution with covariance matrix R. Data were entered into the model as y's and x's were estimated. We standardized the covariates by subtracting the mean and dividing by the standard deviation (z-scored) to allow direct comparisons between covariates.

Over the years, we estimated the annual abundance of cetacean species using the 1992 to 2016 shipboard and aerial line transect data collected during summer. Earlier in this chapter, we described the collection procedures and analysis methods (sections 5.2 and 5.3). The estimated abundance time series for all species are in Appendix IV of the annual Atlantic Marine Mammal Stock Assessment Reports (the most recent is Hayes et al. 2020). For this analysis, we standardized the time series using the following adjustments:

1) All abundance estimates were for the same study area that included the U.S. Atlantic waters from Florida to Maine and the Canadian waters in the Gulf of Maine (Figure 5-14). In most survey years, we covered this region or nearly so. For the years that had slightly lower coverage, we estimated the density in the regions not surveyed using the density from appropriate surveyed strata. In other years, when we surveyed farther into Canadian waters, we truncated the estimate from the Canadian waters outside of the study area.
2) All abundance estimates included adjustments for perception and availability bias. In the very early years, we did not adjust for the aerial perception bias. In most years before 2016, we did not adjust for availability bias. Thus, to standardize the time series, for all years we applied appropriate adjustments for perception and availability bias.

Originally, we designed the line-transect surveys spatial strata to represent different large marine ecosystem units. That is, we divided the US Atlantic waters into shelf waters (< 100 m deep), shelfbreak waters (100 – 2000 m depth), and offshore waters (>2000 m depth; Figure 5-14). We surveyed the spatial strata using different platforms. We surveyed the Gulf of Maine (GOM) shelf stratum recently by planes, but before the year 2000, we surveyed it with both ships and planes. We used planes to survey the south coastal shelf stratum. We usually used ships to survey the shelfbreak, southern offshore and northern offshore strata. In conclusion, since the spatial strata are representative of different ecosystems and we used different survey platforms, we standardized the abundance estimates on a stratum basis.

At this time, we explored covariates affecting the state process of the true abundance trend. We explored 3 types of habitat covariates to represent ecosystem conditions that might affect the true cetacean population trends (Table 5-6):

1) Large-scale climate indices – North Atlantic Oscillation (NAO) and Atlantic Multidecadal Oscillation (AMO)
2) Physical conditions – sea surface temperature (SST), Gulf Stream location index, and bottom temperature
3) Biological conditions – zooplankton (Table 5-7) densities (numbers per $100m^3$)[1]

[1] The Ecosystem Monitoring Program (EcoMon) collected the zooplankton data from shelf-wide surveys using paired 61-cm bongo samplers equipped with 333-µm mesh nets. They sorted and identified plankton taxa. Then they

The values of the SST, bottom temperature, and the zooplankton covariates were available as spatially explicit grids covering much or all of the study area (examples are in Figure 5-15). The zooplankton and bottom temperature covariates represented conditions during only the spring and fall for each year and did not cover our offshore waters (example in Figure 5-15B). The SST was available as month-year averages for spatiotemporal strata covering our entire study area. To compare these contemporaneous spatially gridded covariates to the cetacean stratified abundance trends, we summarized the gridded covariate values for each of abundance survey strata by the mean of the gridded values within in each survey strata (Figure 5-15). This then created a time series for each covariate, month and year (examples in Figures 5-16 and 5-17).

The values of the NAO, AMO, and Gulf Stream location indices were available as a single value per index that represented the entire North Atlantic Ocean for each month of each year (Table 5-6 and Figure 5-18).

Because there are so many candidate covariates, we first limited the list of covariates to a handful of covariates that were the most highly correlated to the time series of standardized abundance estimates for each species. Then prior to fitting the models, we tested the limited set of predictor covariates for multicollinearity. When selecting a model with significant habitat covariates, we did not allow both covariates in a highly correlated set. Then within the MARSS model, we used a forward stepwise selection method to select the best fitting model. As measures of goodness-of-fit, we used the Akaike information criterion corrected for small sample sizes (AICc), visual inspection of the distribution of residuals and fit between the actual and predicted abundance time series, and the R^2 of the linear relationship between the predicted model abundance estiamtes and the actual standardized abundance estimate.

Because the harbor porpoises inhabited only 1 of the ecosystem strata within the study area (the Gulf of Maine strata), we used a univariate version of Eqns. 5-5 and 5-6.

In the case of common dolphins that inhabited 4 of the ecosystem strata, we used the multivariate versions of Eqns. 5-5 and 5-6, 1 state for each ecosystem strata, where we could interpret each state as a separate subgroup. We used model selection and AICc model weights to explore the data support for different spatial patterns of the temporal correlation between abundance trends and habitat covariates by exploring various pooling combinations of the ecosystem strata through different definitions of Z in Eqn. 5-6. We also tested for temporal independence between the ecosystem strata by comparing “diagonal” versus “non-diagonal” Q matrices in Eqn. 5-5.

calculated the density (number per $100m^3$) for the 18 most abundant taxonomic categories and an overall biomass indicator, settled bio-volume (Friedland et al. 2020).

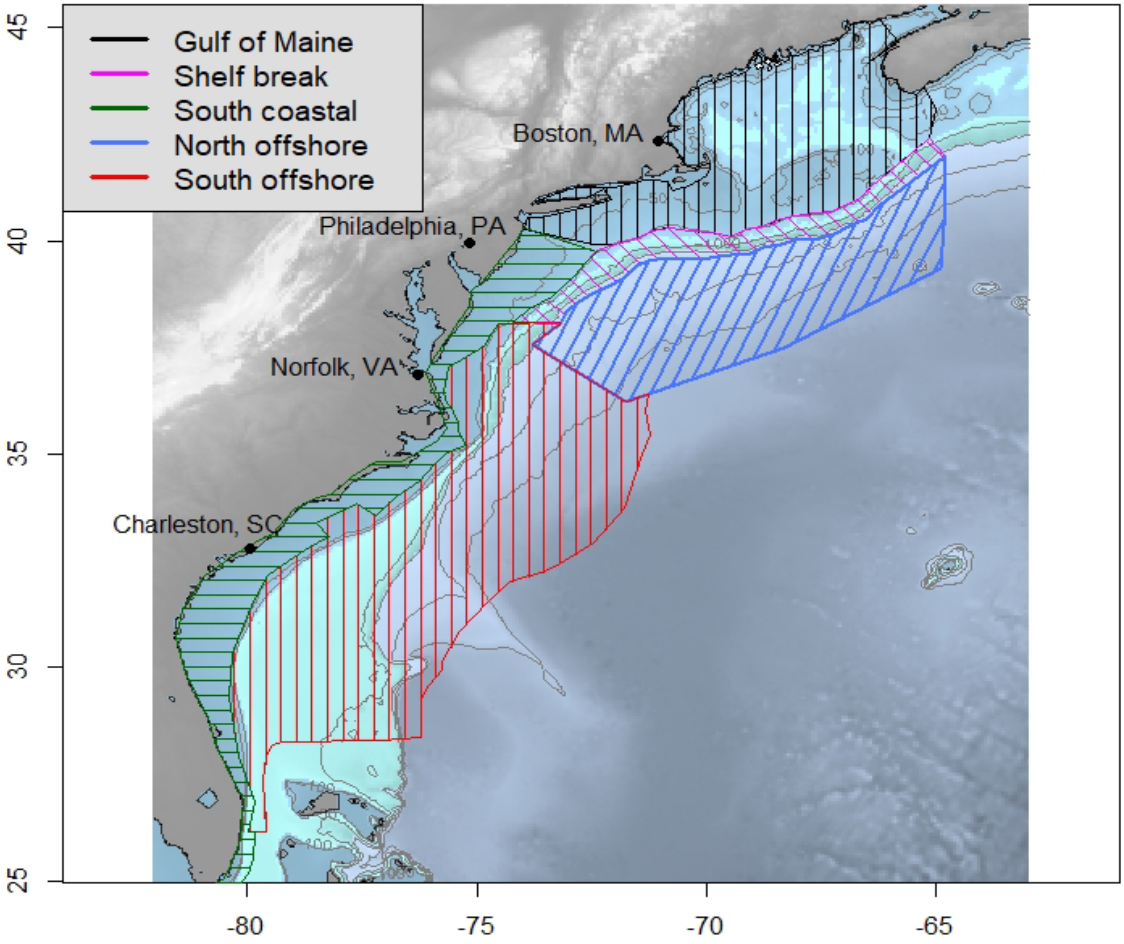

Figure 5-14 Strata used to estimate abundance

Table 5-6 Contemporaneous habitat covariates explored in MARSS trend analyses

Abbreviation	Description	Source
AMO	Unsmoothed average of the Atlantic multidecadal Oscillation index. **Original spatial resolution:** North Atlantic Ocean derived from the Kaplan SST dataset (5x5 degree resolution). **Original temporal resolution:** monthly for each year between 1992 and 2016. **Processed time series:** month-year (Figure 5-16).	Enfield et al. (2001) https://psl.noaa.gov/data/timeseries/AMO/ Downloaded on 04 Oct 2019.
GS	Average of 1st principal component for the latitudual position of the North Wall of the Gulf Stream **Original spatial resolution**: 79°W to 65°W. **Original temporal resolution:** monthly for each year between 1992 and 2016. **Processed time series:** month-year (Figure 5-16).	McCarthy et al. (2018) http://www.pml-gulfstream.org.uk/data.htm Downloaded on 29 Apr 2020.
NAO	North Atlantic Oscillation smoothed index. **Original spatial resolution:** North Atlantic Ocean standardized height anomalies within 20°N to 90°N. **Original temporal resolution:** monthly mean for each year between 1992 and 2016. **Processed time series:** month-year (Figures 5-16 and 5-18).	Chen and van den Dool (2003) https://www.cpc.ncep.noaa.gov/products/precip/CWlink/pna/nao.shtml. Downloaded on 4 October 2019.
SST	Mean sea surface temperature (°C) using COBE data provided by the NOAA/OAR/ESRL PSD. **Original spatial resolution:** Originally gridded to 1x1 degree (Figure 5-15A). Processed to calculate mean value of grids within each stratum. **Original temporal resolution:** monthly for each year between 1992 and 2016. **Processed time series:** month-year-stratum (Figure 5-18).	Folland and Parker (1995) Ishii et al. (2005) https://psl.noaa.gov/data/gridded/data.cobe.html Downloaded on 4 Oct 2019.
Zooplankton	Density (number/100m^3) of zooplankton taxa (Table 5-7) and a zooplankton total biomass index. **Original spatial resolution:** Virginia to Nova Scotia, from shore line to about 200 m depth contour (Figure 5-15B). Originally gridded to 0.1x0.1 degrees. Processed to calculate mean value of grids within each stratum. **Original temporal resolution:** spring for each year between 1992 and 2016 and fall for each year between 1992 and 2016. **Processed time series:** month-year-stratum-taxa group (Figures 5-17 and 5-18).	Friedland et al. (2020). Data provided by K. Friedland, Northeast Fisheries Science Center. Data collected from spring and fall NEFSC Ecosystem Montioring Program surveys.
BotTemp	Bottom temperture (°C). **Original spatial resolution:** Virginia to Nova Scotia, from shoreline to about 200 m depth contour (Figure 5-15B). Originally gridded to 0.1x0.1 degrees. Processed to calculate mean value of grids within each stratum. **Original temporal resolution:** spring for each year between 1992 and 2016 and fall for each year between 1992 and 2016. **Processed time series:** month-year-stratum.	Data provided by K. Friedland. Data collected from spring and fall NEFSC Ecosystem Montioring Program surveys.

Table 5-7 Zooplankton covariates used in MARSS trend analyses
Taken from Friedland et al. (2020).

Abbreviation	Full name	Description
Acarspp	*Acartia spp.*	Marine calanoid copepods
Calfin	*Calanus finmarchicus*	Marine calanoid copepod
Chaeto	Chaetognatha	Predatory marine worms
Cham	*Centropages hamatus*	Copepod
Cirr	Cirripedia	Barnacle
Ctyp	*Centropages typicus*	Copepod
Echino	Echinodermata	Star fish, urchin, sand dollar, sea cucumber
Evadnespp	*Evadne spp.*	Plankton
Gas	Gastropoda	Snail, slug
Hyper	Hyperiidea	Amphipods
Larvaceans	Appendicularians	Tunicates
Mlucens	*Metridia lucens*	Copepod
Oithspp	*Oithona spp.*	Crustacean
Para	*Paracalanus parvus*	Copepod
Penilia	*Penilia* spp.	Ctenopod
Pseudo	*Pseudocalanus spp.*	Copepod
Salps	Salpa	Tunicate
Tlong	*Temora longicornis*	Copepod
Volume	Zooplankton bio-volume	Bio-volume of all zooplankton species

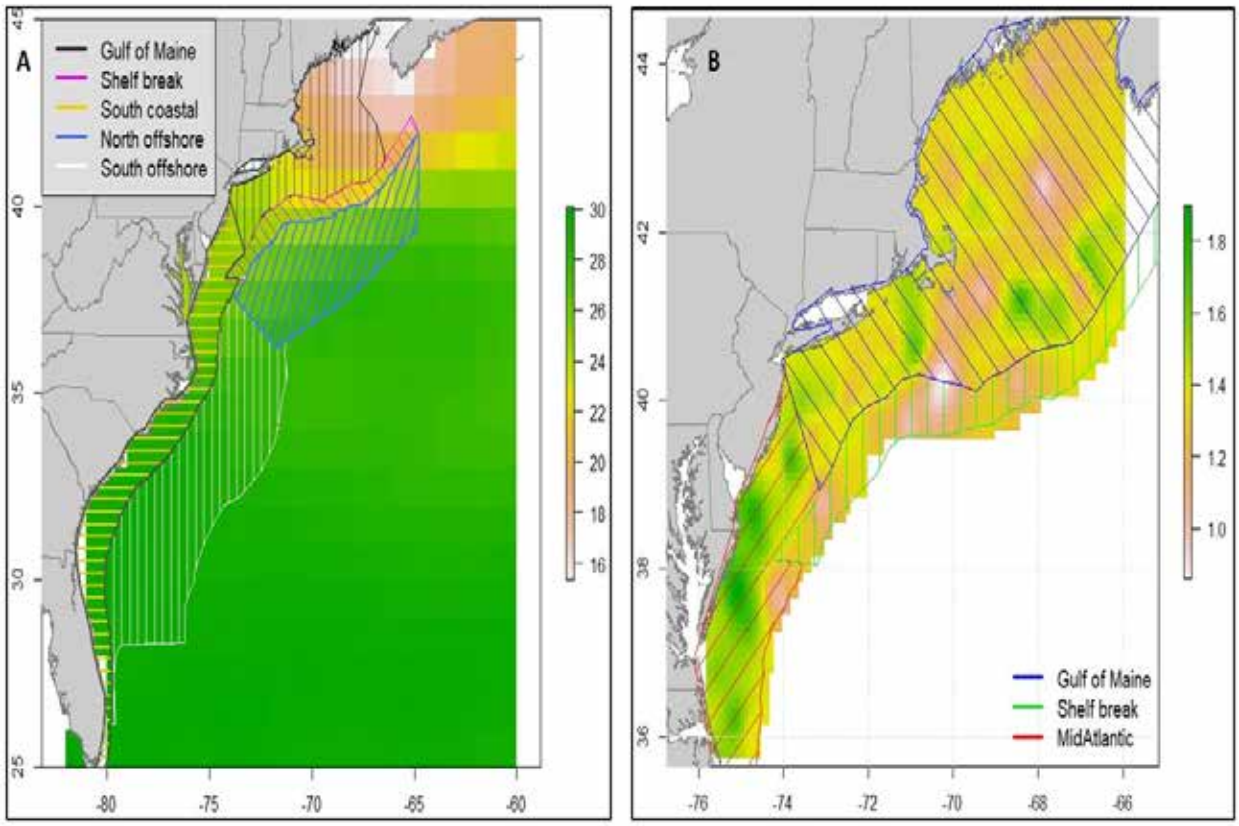

Figure 5-15 Average SST for August 2016 (A) and total zooplankton biomass for fall 2016 (B)
Examples of the spatially explicit gridded covariates with the strata overlaid. Area displayed in plot B is the same for all zooplankton species groups and for bottom temperature.

Figure 5-16 Time series for each fall plankton species grouping for each stratum
Species abbreviations explanations are in Table 5-7. Fall time series from 1990 to 2018. Abundance spatial strata displayed in Figure 5-14 and 5-15.

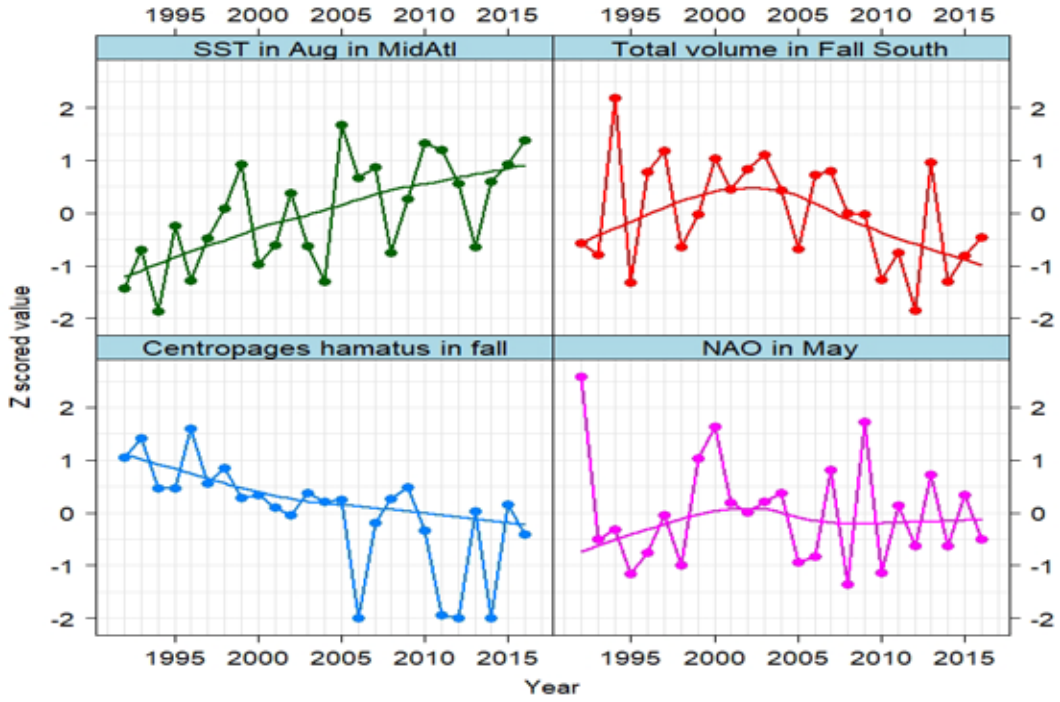

Figure 5-17 Month-annual trends of the standardized z-score of 4 habitat covariates

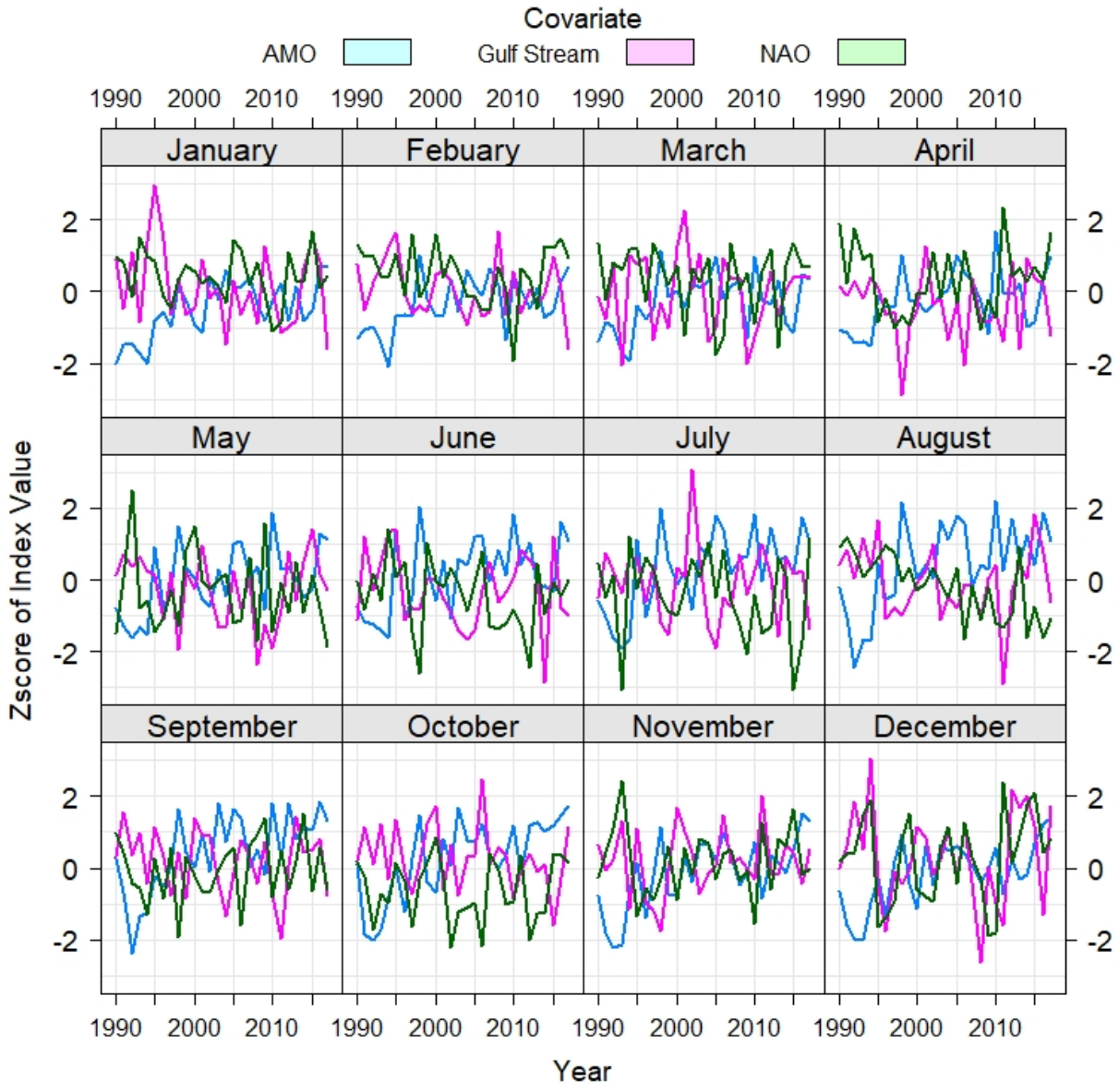

Figure 5-18 Time series for each month of the indices of the AMO, Gulf Stream, and NAO
These 3 indices are representative of the entire North Atlantic Ocean. To easily compare the indices values of the time series we standardized each time series by the standard Z-score.

5.7.3 Results and Discussion

5.7.3.1 Harbor porpoise

The standardized abundance time series for harbor porpoises showed a large amount of variability especially at the end of the time series (blue dots in Figure 5-19). The best one-covariate model that captured the general trend pattern incorporated the August SST time series for the Mid-Atlantic region (Figures 5-15A and 5-17). This model attributed the variability about the predicted trend line (red line in Figure 5-19) as a large amount of observation error, *R* (Table 5-8). When we added a second covariate

(fall density of the copepod *Centropages hamatus*; Figure 5-17) the predicted trend line captured the large interannual variable in the estimated abundance estimates (Figure 5-19B). The 2-variable model now attributed much of the variability to the state process and so reduced the variability attributed to observation error (Table 5-8). From the best fitting model, we estimated the population increased on average by about 1.7% per year between 1992 and 2016. It also showed that during 1992 to about 1999 the rate of increase was fast (about 8%). This was during the same time that the harbor porpoise bycatch decreased rapidly (green line in Figure 5-19B). During the years 2000 to 2009, although bycatch increased, there was no apparent abundance change in the study area.

The harbor porpoise estimated abundance trend was statistically correlated to the trend of fall copepod density (Figure 5-20). This relationship suggested a hypothesis for a potential reason for the large standardized abundance estimate in 2011. That is, the high SST in 2011 could have resulted in larger that usual densities of plankton in the Gulf of Maine. This then may have attracted harbor porpoises that usually reside in Canadian waters outside of the study area. Another hypothesis is, in 2011 the survey observation error due to survey measurement uncertainty could have been particularly large. The density-habitat models as reported in Chapter 6 and Appendix I also show the interannual variability in abundance estimates (Appendix I, Figure 19-5).

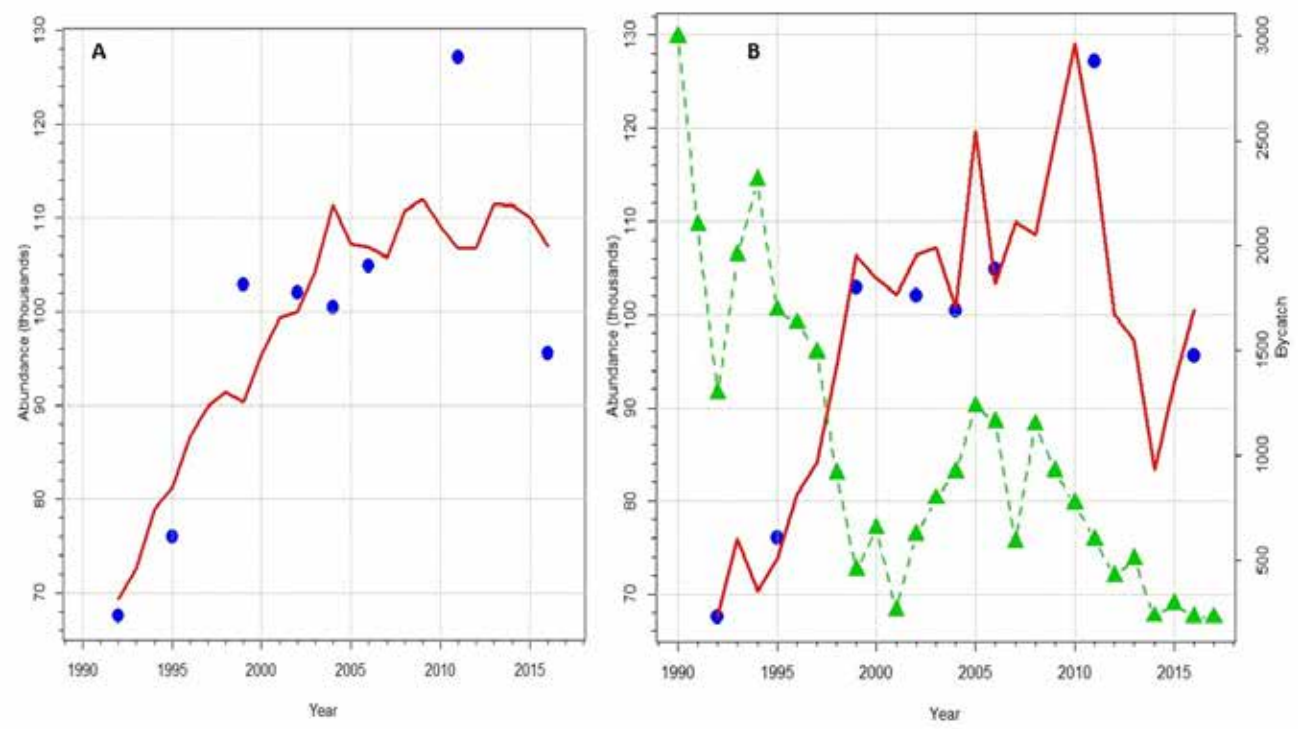

Figure 5-19 Harbor porpoise abundance trend
(A) Abundance trend as estimated by a MARSS model with 1 state habitat covariate, average SST for May in the South Coastal stratum. (B) Abundance trend as estimated by a MARSS model with 2 state habitat covariates, time series of SST index for May in the South Coastal stratum, and the time series of the density of a copepod during fall. Red lines are the predicted trend. Blue points are the standardized annual abundance estimates. Green dashed line with triangle annual points is the time series of estimated harbor porpoise bycatch in the Northeast and Mid-Atlantic gillnet fisheries.

Table 5-8 Coefficients of harbor porpoise MARSS models

State Covariate	R (observation error)	U (rate of change)	Q (process error)	x0 (initial log abundance)	State Covar 1	State Covar 2	AICc
SST Aug South Coastal	0.0096	0.020	0	11.077	-0.035	NA	25.5
Above + Copepod fall	0.0017	0.017	0	11.101	0.1083	0.0774	67.7

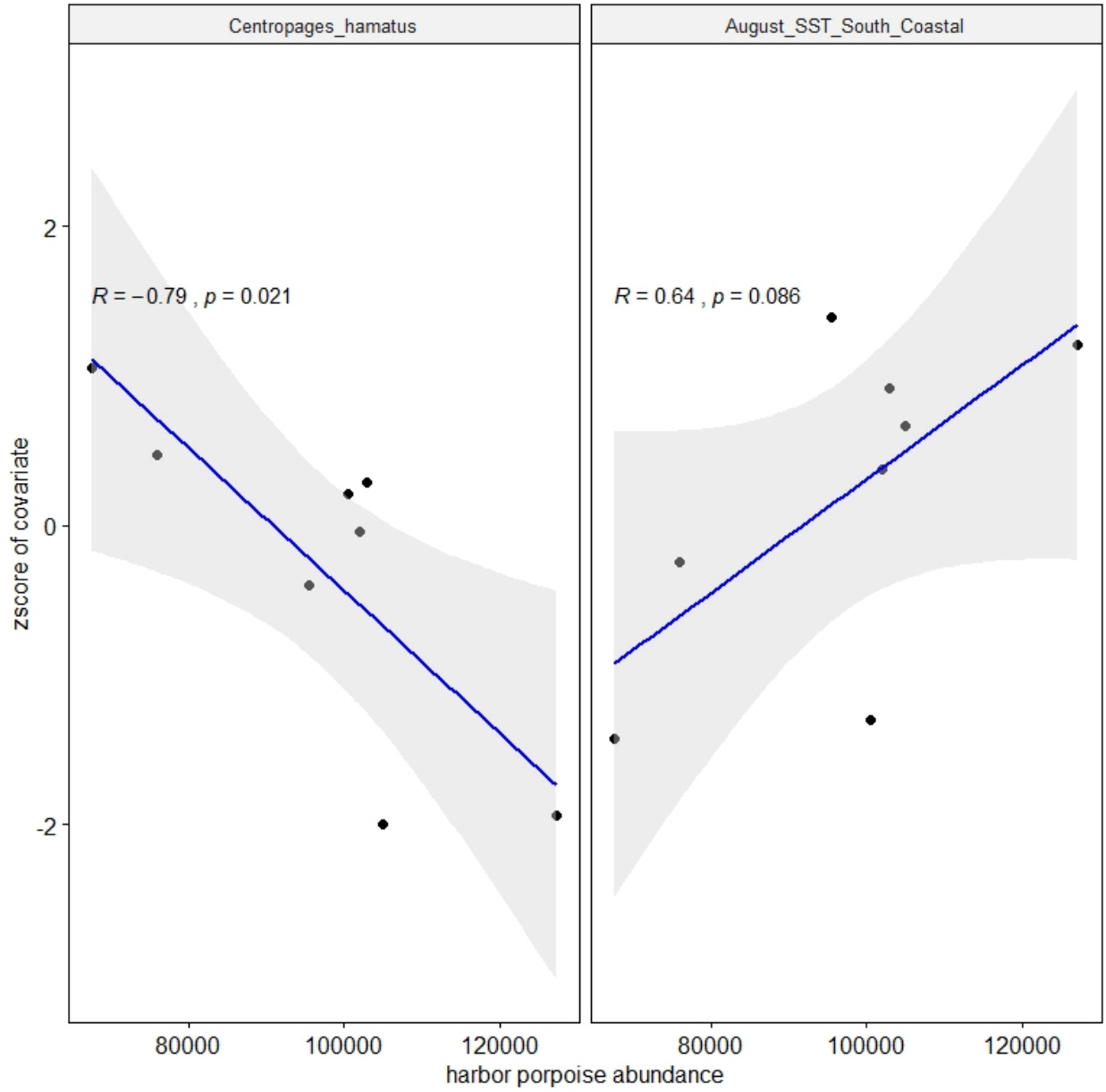

Figure 5-20 Relationship between harbor porpoise abundance and 2 state covariates

5.7.3.2 Common dolphins

The standardized abundance estimates of common dolphins varied within an ecosystem strata (Figure 5-21A). Ignoring habitat covariates, we first explored 5 potential combinations of the ecosystem strata:

a) 4 separate strata (GOM, shelfbreak, south offshore and north offshore);
b) warm versus cool waters: south offshore+north offshore versus GOM+shelfbreak;
c) very warm versus warm versus cool waters: north offshore versus south offshore+shelfbreak versus GOM;
d) coastal versus offshore waters: GOM+south offshore versus shelfbreak+north offshore; and
e) coastal versus offshore versus very offshore: GOM+south offshore, versus shelfbreak versus north offshore.

In addition, we tested 4 possible structures of the process error model (using the MARSS language): "diagonal and equal", "diagonal and unequal", "equal variance covariance", and "unconstrained". The data supported the warm versus cool waters (south offshore+north offshore versus GOM+shelfbreak) ecosystem strata division and the "diagonal and equal" structure of the state variance matrix *Q*. When we allowed *Q* to be unconstrained, we could calculate the correlation between the 2 strata, which was high (0.98). We can interpret this to mean that the data support a collection of 2 subpopulations within the common dolphin population that experience different apparent population growth rates and there is temporal correlation in the year-to-year variability experienced by both subpopulations.

When assuming the 2 subpopulations, the top 2 MARSS models with habitat covariates in the state process equation involved the NAO index for May time series (AICc = 63.4; Table 5-9) and the time series of the total biovolume of zooplankton from fall in the SE ecosystem strata (AICc = 49.8; Table 5-9). We could interpret this model to mean that these 2 habitat covariates explained the inter-annual variability in the abundance trend patterns of the 2 subpopulations. During 1995 to 2004, the abundance in both subpopulations increased at a similar fast rate. During 2004 to about 2009, the subpopulations' abundance leveled off. Then from 2010 onwards, the numbers of animals in the warm waters decreased markedly and the numbers in the cool water increased just as markedly.

Over the entire time series, the average rate of increase for common dolphins in warm and cool waters was about -7% and +12%, respectively.

Table 5-9 Coefficients of common dolphin MARSS models

Covariate	R (observation error)	U-change rate (cool)	U-change rate (warm)	Q (process error)	State Covar - cool	State Covar-warm	AICc
Zooplankton volume	0.041	0.119	-0.069	0.025	0.198	0.579	49.8
NAO for May	0.064	0.122	-0.407	0.139	0.082	0.535	63.4

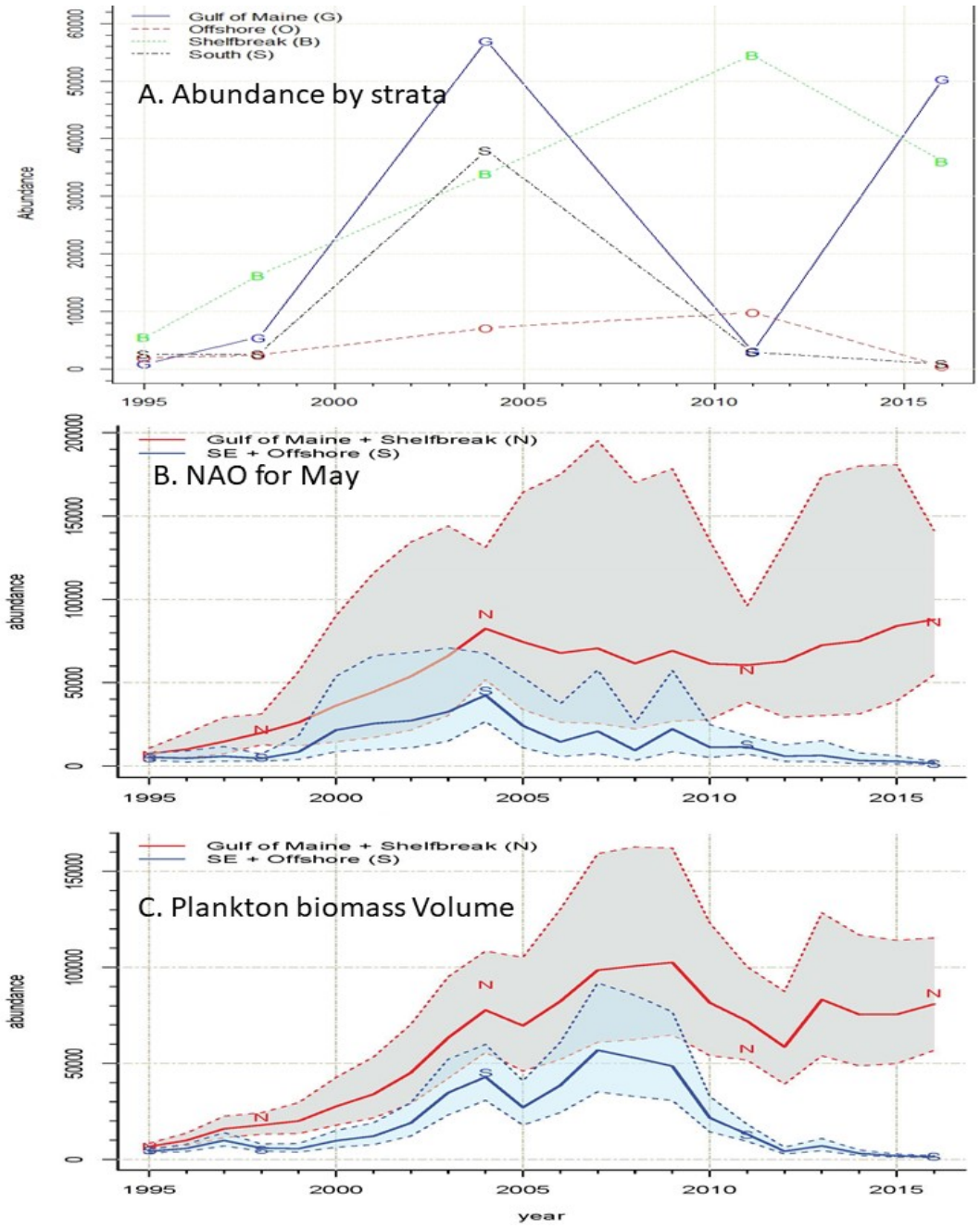

Figure 5-21 Abundance trends of 2 subpopulations of common dolphins
(A) Standardized absolute abundance estimates for the 4-ecosystem survey strata. (B) Abundance trends of the 2 subpopulations estimated by a MARSS model with the time series of May NAO indices (Figure 5-17) as a state habitat covariate. (C) MARSS model included the plankton biomass volume (number/100m^3) time series (Figure 5-17) as a state habitat covariate. Solid colored lines are the predicted trend. Dashed colored lines and the shading represent the 95% confidence intervals for the trend line. Letters are the annual abundance estimates from the 4 original ecosystem strata [Gulf of Maine (G), shelfbreak (S), southeast (E), and offshore (O)] and 2 subpopulation groupings [warm (W) and cool (C) waters]. Blue lines and letters indicate the warm waters of the southeast and offshore strata. Red lines and letters indicate the cooler Gulf of Maine and shelfbreak ecosystem strata.

5.7.4 Key Findings

This exploratory project showed that MARSS models were a feasible technique to estimate the rate of change in the abundance of 2 cetacean species (harbor porpoises and common dolphins). These models were also able to use habitat covariate patterns, process error, and observation error to explain most of the annual variability in the population standardized absolute abundance estimates.

The numbers of harbor porpoises that inhabit the Gulf of Maine during the summer fluctuated over the years, especially since 2010. The results from the models imply these fluctuations are probably due to more than just fluctuating observation error, but they are also due to (or at least are correlated with) changes in environmental habitat values of SST and densities of zooplankton. The common dolphin example demonstrated how changes in the habitat (as represented by zooplankton density patterns) related to shifts in distribution patterns of the dolphins.

5.7.5 Data Gaps and Future Work

We lack an understanding of what drives (or at least what is related to) the distribution and abundance spatiotemporal patterns. Insight into the drivers can inform management actions that aim to reduce bycatch in fisheries. This insight can also inform the interpretation of changes related to other human activities such as the installation of a wind farm or conducting naval activities. Using MARSS models, in addition to the density-habitat models explored in Chapter 6 is a technique that can assist us in understanding the potential drivers.

The trends in cetacean abundance corresponded with trends in density of zooplankton, suggesting a trophic link. We could learn more about the trophic link drivers behind the changes in distribution and abundance if we learned more about the predator-prey relationships. For example, more predator-prey (feeding habitat) studies could provide better choices of potential covariates to use in trend models. Investigating time series of fish density as additional covariates could provide better fitting models since many cetaceans directly prey on fish, not plankton.

Future work related to the development of MARSS models includes developing standardized abundance estimates for all cetacean species, and including other potential habitat covariates that cover the timeframe of the available abundance data (1992 to the present). We could explore if any of the covariates affect the observation error in addition to, or instead of, the process error using the present study. In addition, we could investiagate other frameworks, such as the spatial hierarchical state-space approach developed in Nadeem et al. (2016). Technical issues we should consider when using the MARSS framework include developing appropriate confidence intervals and exploring the starting points to ensure the fit is appropriate. In addition, because multiple species share the same waters at the same time, it is important to explore the inter-species interactions and correlations with the habitat using with complex MARSS models. Such multi-species models can also estimate resilience, stability metrics, and other community dynamics.

5.8 New Availability Bias Correction Factors

The objective of this analysis was to develop availability bias correction factors using newly acquired DTAG data. Dr. Andrew Read and colleagues from Duke University kindly provided DTAG time-depth data from 52 short-finned pilot whales (similar to Quick et al. 2017, Thorne et al. 2017, and Foley 2018) and 2 Cuvier’s beaked whales (similar to Foley 2018, and Shearer et al. 2019) that they tagged off Cape Hatteras, NC.

5.8.1 Methods

A description of the data and analysis methods are in sections 5.2.4 and 5.2.6, respectively. The data and analysis of the True's beaked whale tagged on Georges Bank (described in Chapter 7) is still underway. This section describes the availability bias correction factors derived from the Duke DTAG data.

5.8.2 Results

The dive patterns of the whales varied by individuals, where a few examples of short-finned pilot whales are in Figure 5-22, and the Cuvier's beaked whales are in Figure 5-23. Both species demonstrated the typical pattern of a series of shallow dives interspersed with deeper dives, where the maximum depths of a dive varied between individual whales.

To calculate the average surface and dive times, by using the random effects regression models, we defined the depth observers could see a whale at the "surface" as when the tagged whale recorded depth was 2, 3, or 4 m (Table 5-10). We also divided the dive patterns into those preformed during the daytime when an observer could detect the whale and dives performed at nighttime. To calculate the availability bias correction factor we defined the surface time as the amount of time the tag recordings were 3 m or less (Table 5-11). For reference, the average surface and dive times along with the correction factors are in Table 5-12.

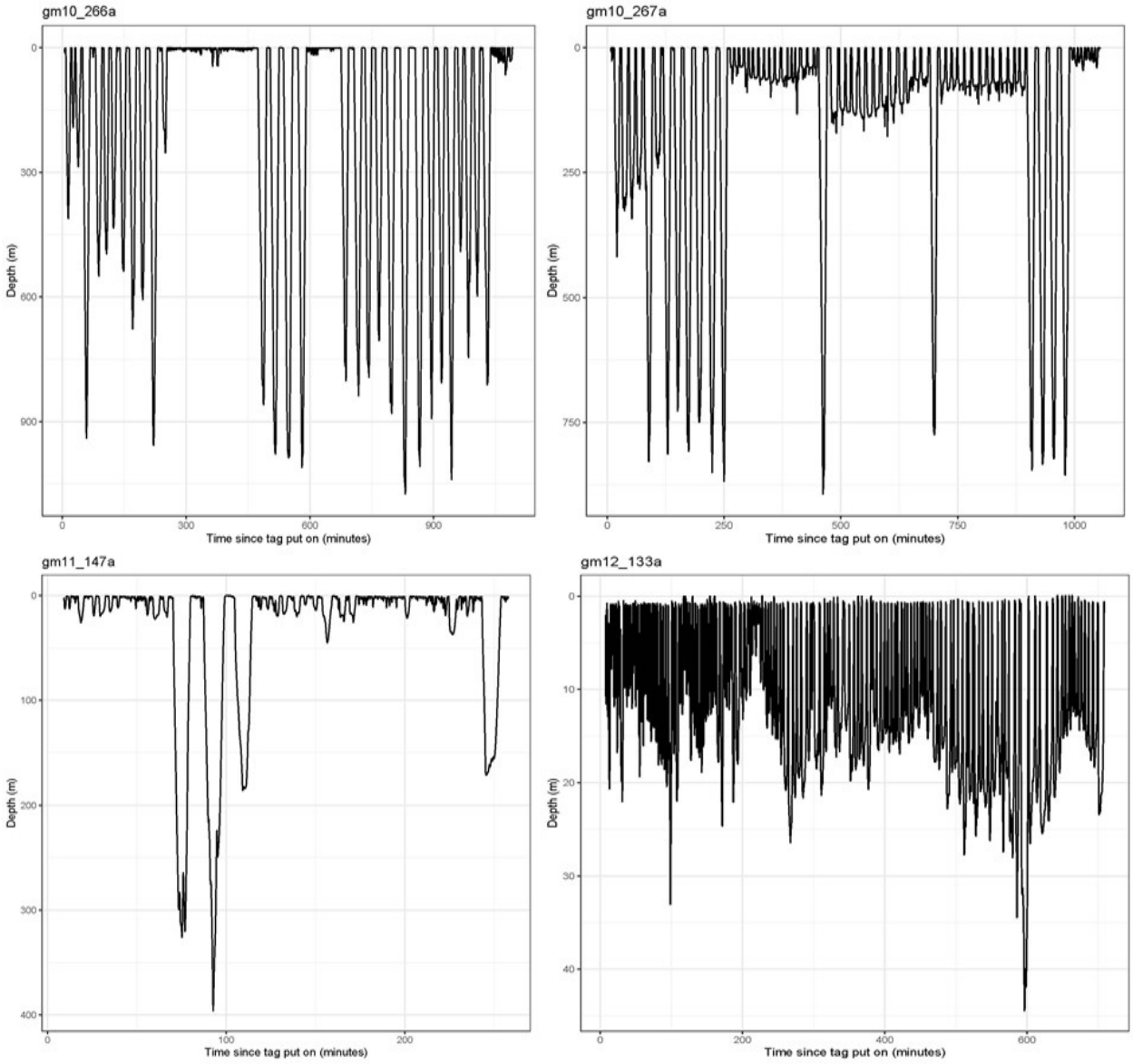

Figure 5-22 Dive patterns from 4 short-finned pilot whales equipped with DTAGs
Each plot is a trace of the depth that the animal was at during the time the tag was on the animal. The tag number is above the plot. Each plot displays the depth (in meters) on the y-axis, where the surface is depth 0. The x-axis is time (in minutes), where time 0 is when the tag was activated and on the animal. Note the depth and time scales are different for each animal.

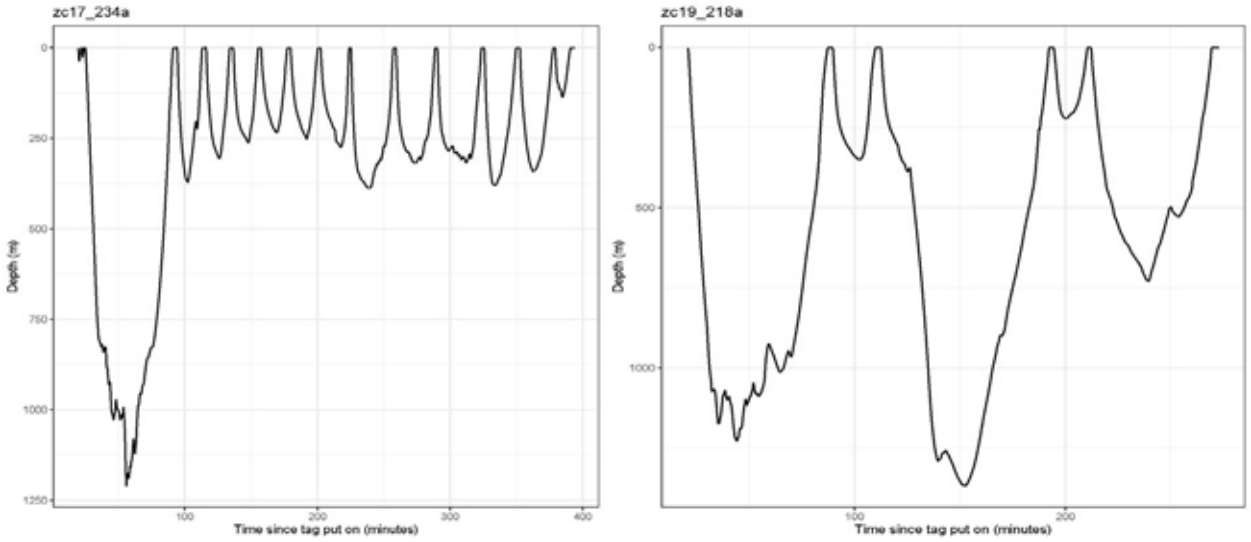

Figure 5-23 Dive patterns from Cuvier's beaked whales equipped with DTAGs
Each plot is a trace of the depth that the animal was at during the time the tag was on the animal. The tag number is above the plot. Each plot displays the depth (in meters) on the y-axis, where the surface is depth 0. The x-axis is time (in minutes), where time 0 is when the tag was activated and on the animal. Note the depth and time scales are different for each animal.

Table 5-10 Average surface and dive times (in minutes) calculated from tagged whales data
We defined surface time as the time that the tag was at a depth less than the depth in the first column (2, 3, or 4 m). The corresponding dive time is the time that the tag was at a depth greater than that in the first column. % surface time is the percent of time within a dive cycle (surface+dive time) that was spent at the surface [surface time/(surface time+dive time)]. Since we conducted the abundancesurveys only during the day, the dive and surface times used in the correction factors were only those times recorded in the daytime.

Surface Depth (m)	Attribute	Statistic	Cuvier's Beaked Whale - Daytime	Short-finned Pilot Whale - Daytime	Short-finned Pilot Whale - Nighttime
2	Surface time	Mean	2.20	4.20	3.76
2	Surface time	%CV	7.00	11.00	23.00
2	Dive time	Mean	34.44	4.92	6.26
2	Dive time	%CV	36.00	9.00	18.00
2	% surface time	Mean	6	45	36
2	% surface time	%CV	83.00	4.00	11.00
3	Surface time	Mean	2.28	5.30	4.72
3	Surface time	%CV	7.00	11.00	24.00
3	Dive time	Mean	34.34	5.33	6.66
3	Dive time	%CV	37.00	9.00	17.00
3	% surface time	Mean	7	49	39
3	% surface time	%CV	71.00	4.00	10.00
4	Surface time	Mean	2.35	5.39	5.13
4	Surface time	%CV	6.00	9.00	23.00
4	Dive time	Mean	34.28	5.61	6.83
4	Dive time	%CV	37.00	9.00	16.00
4	% surface time	Mean	7	50	40
4	% surface time	%CV	71.00	4.00	10.00

Table 5-11 Availability bias correction factor for aerial and shipboard surveys using new tag data

Species	Aerial	Shipboard
Cuvier's beaked whale	0.154	0.698
Short-finned pilot whale	0.653	1.000

Table 5-12 Availability bias correction factors from Palka et al. (2017)

Species	Aerial Correction Factor	CV	Shipboard Correction Factor	CV
Atlantic white-sided dolphin	0.890	0.186	1	-
Common bottlenose dolphin	0.785	0.364	1	-
Cuvier's beaked whale	0.142	0.462	0.764	0.246
Fin whale	0.374	0.336	1	-
Harbor porpoise	0.628	0.299	1	-
Humpback whale	0.649	0.185	1	-
Long/short finned pilot whale	0.679	0.241	1	-
Minke whale	0.307	0.397	1	-
Risso's dolphin	0.850	0.173	1	-
Right whale	0.265	0.060	1	-
Sei whale	0.417	0.517	1	-
Common dolphin	0.930	0.138	1	-
Sperm whale	0.145	0.005	0.613	0.247
Striped dolphin	1.000	-	1	-
Pygmy/dwarf sperm whale	unknown	-	0.539	0.307

5.8.3 Key Findings

Dr. A. Read from Duke University kindly provided DTAG data that they attached to short-finned pilot whales and Cuvier's beaked whales who were initially tagged off Cape Hatteras, NC (within the AMAPPS study area). The availability bias correction factors derived from the Atlantic Cuvier's beaked whale data from this analysis (aerial = 0.154; shipboard = 0.698) were surprisingly similar to the correction factors derived from Cuvier's beaked whale data that were tagged in Southern California (aerial = 0.142; shipboard = 0.764). The new Atlantic short-finned pilot whale correction factors were also similar to the Atlantic short-finned pilot whale factors from Palka et al. 2017, where 20 of the 52 tags were the same animals in both analyses. So more than doubling the sample size with animals from different years, though in the same general region, did not change the average dive patterns.

5.8.4 Data Gaps and Future Work

Quick et al. (2017) who analyzed a subset of these short-finned pilot whale DTAG data showed the animals dove in clustered bouts of 4 diving states (1 state was interpreted as non-foraging and 3 states represented different modes of foraging behavior that reached different depths). Using data from short-finned pilot whales from the Cape Hatteras, NC area that were equipped with satellite tags, Thorne et al. (2017) showed the animals travel from Cape Lookout, NC to Georges Bank using both continental shelfbreak and deeper offshore waters in meanders of the Gulf Stream (also shown in the density surface models in Appendix I). Together, these data, suggest the hypothesis that the availability bias correction factors could be different in regions with different bathymetric features and thus different dive profiles. We would like to further inspect the DTAG data to test this hypothesis.

We divide the estimate of uncorrected abundance by the correction factor to estimate the absolute abundance. Thus, the smaller the correction factor, the larger the magnitude of the change in abundance between uncorrected and corrected (absolute) estimate. For all species, the availability bias correction

factor for aerial surveys is smaller than the corresponding correction factor for shipboard surveys. This pattern is because the time an animal is available to the observer is much less when observing from a fast traveling plane, in contast to a slow traveling ship. Thus, the value of the correction factor can highly influence the absolute abundance estimate. Given its influence, we (and/or collaborators) should tag more animals in different regions of the study area and in different seasons to fill a large, potentially highly influential data gap. In the absence of applying more tags, we are currently collating additional dive patterns documented in published papers and attempting to access the raw data to process them in a similar manner as done in this section. The goal is to publish a paper with as much dive data for as many species as feasible. In addition, our plan is to add availability bias correction factors for groups that we calculated from focal follow data we collected during the NEFSC shipboard abundance survey, if appropriate.

5.9 Summary of Other Projects That Used AMAPPS Sighting Data

The AMAPPS line transect visual sightings data are available to the public to conduct other types of projects. Below is a summary of 2 such projects. We have summarized additional ongoing or completed projects that relate to density surface models in section 6.5.

Laura Howes, a PhD Environmental Biology student at the University of Massachusetts Boston, working under Dr. Scott Kraus and Dr. Stephanie Wood downloaded the data collected under AMAPPS I and II from the OBIS-SEAMAP website. Their research project, in partnership with the New England Aquarium and Charles River Analytics, entails developing and field testing a large whale automatic detection system. The shipboard automatic detection system incorporates infrared, electro-optical, and acoustic sensors. They will be incorporating the knowledge of whale distributions into the detection algorithm to show the likelihood of where certain species are threatened. A goal of the research is to create a critical and comprehensive single spatial dataset for the Gulf of Maine and Georges Bank of all large whale species. A variety of data sources (which includes the North Atlantic Right Whale Consortium and AMAPPS databases) from Gulf of Maine/George's Bank will be combined to create a probability of detection into the system with georeferenced layers by calculating unified sightings per unit effort for several large whale species in the Gulf of Maine and George’s Bank. We will use spatial statistical methods to adjust for variability in data and to calculate the likelihood of species detection throughout the region. We will be using methods similar to Pittman et al. (2006) to combine multiple survey data, and calculate the sightings per unit effort.

Dr. Timothy White and others from BOEM used AMAPPS surveys to identify areas important to sensitive marine mammal, seabird, and turtle communities. BOEM will be publishing some of this work in their upcoming Oil and Gas Leasing Environmental Impact Statement.

5.10 Acknowledgements

We would like to acknowledge all of the many scientific observers, NOAA pilots, and NOAA ships’ crewmembers who have spent hours on projects throughout the Atlantic Ocean. With their dedication, we were able to collect large amounts of high quality data, resulting in many abundance estimates. We also would like to thank Dr. Andrew Read (from Duke University) and his fellow researchers who kindly provided us the DTAG data from the Cuvier’s beaked whales and short-finned pilot whales that they tagged in waters off North Carolina. We also would like to thank Dr. Kevin Friedland (from the Northeast Fisheries Science Center in Woods Hole, MA) who shared the zooplankton and bottom temperature data used in section 5.7.

5.11 References Cited

Adamczak SK, McLellan WA, Read AJ, Wolfe CLP, Thorne LH. 2020. The impact of temperature at depth on estimates of thermal habitat for short-finned pilot whales. Mar. Mammal Sci. 20:1–14.

Barlow J, Taylor JB. 2005. Estimates of sperm whale abundance in the northeastern temperate Pacific from a combined acoustic and visual survey. Mar. Mammal Sci. 21(3):429-445.

Chen WY, van den Dool H. 2003. Sensitivity of teleconnection patterns to the sign of their primary action center, Mon. Wea. Rev. 131:2885-2899.

DeAngelis A, Valtierra R, Van Parijs S, Cholewiak D. 2017. Using multipath reflections to obtain dive depths of beaked whales from a towed hydrophone array. J. Acoust. Soc. Am. 142(2):1078-1087.

Enfield DB, Mestas-Nunez AM, Trimble PJ. 2001. The Atlantic Multidecadal Oscillation and its relationship to rainfall and river flows in the continental U.S. Geophys. Res. Lett. 28:2077-2080.

Fleming AH, Yack TM, Redfern JV, Becker EA, Moore TJ, Barlow J. 2018. Comparing acoustic and visual habitat models of Dall's porpoise in the California Current. Ecol. Model. 384:198-208.

Foley HJ. 2018. Spatial ecology and movement patterns of deep-diving odontocetes in the Western North Atlantic Ocean. Master of Science thesis from the North Carolina State University, Raleigh, NC.

Folland CK, Parker DE. 1995. Correction of instrumental biases in historical sea surface temperature data. Q. J. R. Meteorol. Soc. 121:319-367.

Friedland KD, Langan JA, Large SI, Selden RL, Link JS, Watson RA, Collie JS. 2020. Changes in higher trophic level productivity, diversity, and niche space in a rapidly warming continental shelf ecosystem. Sci. Total Environ. 704:135270.

Garrison LP. 2016. Abundance of marine mammals in waters of the U.S. east coast during the summer 2011. Southeast Fisheries Science Center, Protected Resources and Biodiversity Division, 75 Virginia Beach Dr., Miami, FL 33140. PRBD Contribution # PRBD-2016-08; 21 pp.

Garrison LP. 2020. Abundance of marine mammals in waters of the U.S. East Coast during summer 2016. Southeast Fisheries Science Center, Protected Resources and Biodiversity Division, 75 Virginia Beach Dr., Miami, FL 33140. PRBD Contribution #PRBD-2020-04; 17 pp.

Garrison LP, Rosel PE. 2017. Partitioning short-finned and long-finned pilot whale bycatch estimates using habitat and genetic information. Southeast Fisheries Science Center, Protected Resources and Biodiversity Division, 75 Virginia Beach Dr., Miami, FL 33149. PRBD Contribution # PRBD-2016-17; 24 pp.

Garrison LP, Stokes L. 2020. Estimated bycatch of marine mammals and sea turtles in the U.S. Atlantic Pelagic Longline fleet during 2017. Southeast Fisheries Science Center, Protected Resources and Biodiversity Division, 75 Virginia Beach Dr., Miami, FL 33149. PRD Contribution # PRD-2020-05; 58 pp.

Garrison LP, Barry K, Hoggard W. 2017. The abundance of coastal morphotype bottlenose dolphins on the U.S. east coast: 2002-2016. Southeast Fisheries Science Center, Protected Resources and

Biodiversity Division, 75 Virginia Beach Dr., Miami, FL 33140. PRD Contribution # PRBD-2017-01; 37 pp.

.Garrison LP, Palka D. 2018. Abundance of short-finned pilot whales along the U.S. east coast from summer 2016 vessel surveys. Southeast Fisheries Science Center, Protected Resources and Biodiversity Division, 75 Virginia Beach Dr., Miami, FL 33140. PRD Contribution # PRBD-2018-07; 18p.

Gerrodette T, Taylor BL, Swift R, Rankin S, Jaramillo A, Rojas-Bracho L. 2011. A combined visual and acoustic estimate of 2008 abundance, and change in abundance since 1997, for the vaquita, *Phocoena sinus*. Mar. Mammal Sci. 27:E79–E100.

Gillespie D, Gordon J, McHugh R, McLaren D, Mellinger DK, Redmond P, Thode A, Trinder P, Deng X. 2008. PAMGUARD: semiautomated, open source software for real-time acoustic detection and localisation of cetaceans. Proc. Inst. Acoust. 30:54–62.

Hayes SA, Josephson E, Maze-Foley K, Rosel P. eds. 2020. U.S. Atlantic and Gulf of Mexico Marine Mammal Stock Assessments - 2019. NOAA Tech Memo NMFS NE-264; 479 pp.

Hilborn R, Amoroso RO, Anderson CM, Baum JK, Branch TA, Costello C, de Moor CL, Faraj A, Hively D, Jensen OP, Kurota H, Little LR, Mace P, McClanahan T, Melnychuk MC, Minto C, Osio GC, Parma AM, Pons M, Segurado S, Szuwalske CS, Wilson JR, Ye Y. 2020. Effective fisheries management instrumental in improving fish stock status. PNAS 117(4):2218-2224.

Hogarth BT. 2001. A notice published in the Federal Register on October 24, 2001 (66 FR 53782) announced the establishment of the BDTRT and the first BDTRT meeting.

Holmes EE, Ward EJ, Scheuerell MD. 2020. Package 'MARSS' October 21, 2020.

Holmes EE, Ward EJ, Wills K. 2012. MARSS: Multivariate autoregressive state-space models for analyzing time-series data. The R Journal 4:11-19.

Ishii M, Shouji A, Sugimoto S, Matsumoto T. 2005. Objective analyses of sea-surface temperature and marine meteorological variables for the 20th century using ICOADS and the Kobe Collection. Int. J. Climatol. 25:865-879.

Laake JL, Calambokidis J, Osmek SD, Rugh DJ. 1997. Probability of detecting harbor porpoise from aerial surveys: Estimating g(0). J. Wildl. Manag. 61(1):63-75.

Laake JL, Borchers DL. 2004. Methods for incomplete detection at distance zero. In: Buckland ST, Anderson DR, Burnham KP, Laake JL, Thomas, L, editors. Advanced distance sampling. New York (NY): Oxford University Press. p. 108-189.

Laake J, Borchers D, Thomas L, Miller D, Bishop, J. 2020. mrds: Mark-Recapture Distance Sampling. R package version 2.2.1.

Lindenmayer DB, Likens GE. 2009. Adaptive monitoring: a new paradigm for long-term research and monitoring. Trends Ecol. Evol. 24(9):482-486.

Lyssikatos MC, Garrison LP. 2018. Common bottlenose dolphin (*Tursiops truncatus*) gillnet bycatch estimates along the US mid-Atlantic coast, 2007-2015. US Dept Commer, Northeast Fish Sci Cent Ref Doc. 18-07; 43pp.

Lawson J, Gosselin J-F. 2018. Estimates of cetacean abundance from the 2016 NAISS aerial surveys of eastern Canadian waters, with a comparison to estimates from the 2007 TNASS. NAMMCO SC/25/AE/09.

Madsen P, Wahlberg M, Møhl B. 2002. Male sperm whale (*Physeter microcephalus*) acoustics in a high-latitude habitat: implications for echolocation and communication. Behav. Ecol. Sociobiol. 53:31-41.

Marques FC, Buckland ST. 2003. Incorporating covariates into standard line transect analysis. Biometrics 59:924-935.

Marques TA, Thomas L, Martin SW, Mellinger DK, Ward JA, Moretti DJ, Harris D, Tyack PL. 2013. Estimating animal population density using passive acoustics. Biol. Rev. 88(2):287-309.

McCarthy GD, Joyce TM, Josey SA. 2018. Gulf Stream variability in the context of quasi-decadal and multidecadal Atlantic climate variability. Geophys. Res. Lett. 45:11,257–11,264.

McCullagh P, Nelder JA. 1989. Generalized linear models. London: Chapman & Hall.

McLaren IA. 1961. Methods of determining the numbers and availability of ringed seals in the eastern Canadian Arctic. Arctic 14:162-175.

Nadeem K, Moore JE, Zhang Y, Chipman H. 2016. Integrating population dynamics models and distance sampling data: a spatial hierarchical state-space approach. Ecology 97(7):1735-1745.

NOAA National Centers for Coastal Ocean Science (NCCOS) 2006. An ecological characterization of the Stellwagen Bank National Marine Sanctuary region: Oceanographic, biogeographic, and contaminants assessment. Prepared by NCCOS's Biogeography Team in cooperation with the National Marine Sanctuary Program. Silver Spring, MD. NOAA Tech Memo NOS NCCOS-45; 356 pp.

Palka DL. 2012. Cetacean abundance estimates in US northwestern Atlantic Ocean waters from summer 2011 transect survey. US Dept Commer, Northeast Fish Sci Cent Ref Doc. 12-29; 37 pp.

Palka DL, Rossman MC. 2001. Bycatch estimates of coastal bottlenose dolphin (*Tursiops truncatus*) in US mid-Atlantic gillnet fisheries for 1996 to 2000. US Dept Commer, Northeast Fish Sci Cent Ref Doc. 01-15; 77p.

Palka DL, Chavez-Rosales S, Josephson E, Cholewiak D, Haas HL, Garrison L, Jones M, Sigourney D, Waring G (retired), Jech M, Broughton E, Soldevilla M, Davis G, DeAngelis A, Sasso CR, Winton MV, Smolowitz RJ, Fay G, LaBrecque E, Leiness JB, Dettlof M, Warden M, Murray K, Orphanides C. 2017. Atlantic marine assessment program for protected species: 2010- 2014. US Dept. of the Interior, Bureau of Ocean Energy Management, Atlantic OCS Region, Washington, DC. OCS Study BOEM 2017-071; 211 pp.

Palka D. 2020. Cetacean abundance in the US Northwestern Atlantic Ocean summer 2016. US Dept Commer, Northeast Fish Sci Cent Ref Doc. 20-05; 60pp.

Pittman S, Costa B, Connie K, Wiley D, Kenney RD. 2006. Cetacean distribution and diversity. IN: An ecological characterization of the Stellwagen Bank National Marine Sanctuary Region: Oceanographic, biogeographic, and contaminants assessment. Chapter: Cetacean distribution and diversity. NOAA Tech Memo NOS NCCOS-45; 20 pp.

Quick NJ, Isojunno S, Sadykova D, Bowers M, Nowacek DP, Read AJ. 2017. Hidden Markov models reveal complexity in the diving behaviour of short-finned pilot whales. Sci Rep 7:45765.

Rone BK, Pace RM. 2012. A simple photograph-based approach for discriminating between free-ranging long-finned (*Globiephala melas*) and short-finned (*G. macrorhynchus*) pilot whales off the east coast of the United States. Mar. Mammal Sci. 28(2):254-275.

Rosel PE, Hansen L, Hohn AA. 2009. Restricted dispersal in a continuously distributed marine species: Common bottlenose dolphins (*Tursiops truncatus*) in coastal waters of the western North Atlantic. Mol. Ecol. 18:5030–5045.

Royle JR, Dorazio RM. 2008. Hierarchical modeling and inference in ecology: The analysis of data from populations, metapopulations and communities. Elsevier's Science and Technology, Oxford, UK.

Shearer JM, Quick NJ, Cioffi WR, Baird RW, Webster DL, Foley HJ, Swaim ZT, Waples DM, Bell JT, Read AJ. 2019. Diving behaviour of Cuvier's beaked whales (*Ziphius cavirostris*) off Cape Hatteras, North Carolina. R. Soc. Open Sci. 6:181728.

Thorne LH, Foley HJ, Baird RW, Webster DL, Swaim ZT, Read AJ. 2017. Movement and foraging behavior of short-finned pilot whales in the Mid-Atlantic Bight: Importance of bathymetric features and implications for management. Mar. Ecol. Prog. Ser. 584:245-257.

Thorne LH, Baird RW, Webster DL, Stepanuk JE, Read AJ. 2019. Predicting fisheries bycatch: A case study and field test for pilot whales in a pelagic longline fishery. Divers. Distrib. 25:909-923.

Torres LG, Rosel PE, D'Agrosa C, Read AJ. 2003. Improving managment of overlapping bottlenose dolphin ecotypes through spatial analysis and genetics. Mar. Mammal Sci. 19:502-514.

Ward EJ, Chirakkal H, Gonzalez-Suarez M, Aurioles-Gambia D, Holmes EE, Gerber L. 2010. Inferrring spatial structure from time-series data: using multivariate state-space models to detect metapolulation structure of California sea lions in the Gulf of California, Mexico. Journal of Applied Ecology 47:47-56.

Waring GT, Josephson E, Maze-Foley K, Rosel, PE, editors. 2014. U.S. Atlantic and Gulf of Mexico Marine Mammal Stock Assessments -- 2013. NOAA Tech Memo NMFS NE-228; 464 pp.

Wahlberg M. 2002. The acoustic behaviour of diving sperm whales observed with a hydrophone array. J. Exp. Mar. Biol. Ecol. 281(1-2):52-62.

Watwood SL, Miller PJO, Johnson M, Madsen PT, Tyack PL. 2006. Deep-diving foraging behavior of sperm whales (*Physeter macrocephalus*). J. Anim. Ecol. 75:814-825.

6 Density Surface Models

Primary authors: Samuel Chavez-Rosales, Doug Sigourney, Elizabeth Josephson, Debra Palka, Lance Garrison, Laura Aichinger Dias, and Chris Orphanides

6.1 Introduction

Managing the impacts of activities on marine life requires an understanding of the distribution, abundance, and habitat use by the species. Understanding processes that drive spatiotemporal variation in animal abundance and distribution is important to identify population trends and understanding distribution patterns. The AMAPPS objectives (Chapter 3) reflect the desire to achieve this understanding by including the collection and analysis of seasonal distribution and abundance data of marine mammals, marine turtle, and seabirds using visual, acoustic and telemetry data, in addition to collecting data on other components of the animal's habitat, like potential prey and physical oceanographic characteristics. This chapter addresses aspects of 4 of the 7 AMAPPS objectives (taken from the complete list of objectives in Chapter 3):

1) Collect broad-scale data over multiple years on the seasonal distribution and abundance of marine mammals (cetaceans and pinnipeds), marine turtles, and seabirds using fixed passive acoustic monitoring and direct aerial and shipboard surveys of coastal U.S. Atlantic Ocean waters;
2) Collect similar data at finer scales at several sites of particular interest to BOEM, NOAA, and partners using visual and acoustic survey techniques;
5) Identify currently used, viable technologies and explore alternative platforms and technologies to improve population assessment studies, if necessary;
6) Assess the population size of surveyed species at regional scales; and develop models and associated tools to translate these survey data into seasonal, spatially explicit density estimates incorporating habitat characteristics.

Under AMAPPS I, we developed spatiotemporal abundance estimates and maps incorporating habitat characteristics (AMAPPS objective 6) by using data collected during 2010 to 2013 (AMAPPS objectives 1 and 2). For the spatiotemporal density-habitat models developed under AMAPPS II, we expanded the time series with new shipboard and aerial survey data spanning 2010 to 2017, expanded the number of candidate habitat covariates for the density-habitat models, and expanded the statistical frameworks that developed the density-habitat models. These modifications resulted in more precise and detailed results.

We developed density-habitat models from the visual line transect data that we summarized as seasonal spatially explicit density maps and abundance estimates. Density-habitat models use known locations of individuals of a species and information on environmental conditions at those locations, to predict the species distribution patterns. The most commonly used model structure is correlative, where we use an algorithm to estimate the relationships between species locations and environmental conditions. We then use this correlative model to predict and map the estimated density of the species of interest in the area of interest. Examples of such correlative models include those we developed under AMAPPS I (Palka et al. 2017; Chavez-Rosales et al. 2019), those in this chapter, and those developed by others (Forney et al. 2012; Roberts et al. 2016, 2017, 2018; Becker et al. 2019).

Determining the relationships between species locations and environmental conditions is not a new concept. Early cetacean naturalists documented that large whales were associated with specific habitat types (Southwell 1898). During the 1940s to 1960s, commercial whalers understood that oceanographic conditions relate to locations of marine mammals. For example, the Japanese concluded that temperature and current fronts delineated favorable whaling grounds in the North Pacific and Southern Ocean (e.g. Uda 1954; Nasu 1966). Eventually, with the evolution of scientific methods, this led to the development

of some of the earliest predictive models of marine mammal habitats using visually detected observation data and limited habitat data (Palka 1995; Moses and Finn 1997; Cañadas and Sagarminaga 2000; Forney 2000; Gregr and Trites 2001). Over the past decade or so, passive acoustic monitoring (Chapter 7) and satellite telemetry (Chapter 8) have provided valuable new sources of observational data. However, at this time we have not incorporated these data sources into our density-habitat models. Today there are numerous analytical methods available to combine the observational and habitat data, although there are challenges inherent to each method (e.g., Guisan and Zimmermann 2000; Elith et al. 2006; Redfern et al. 2006; Robinson et al. 2011). We have employed 2 different statistical frameworks to combine observational and habitat data to develop spatiotemporal species density and abundance estimates and maps.

In section 6.2, we produced density distribution maps developed under the "2-stage" generalized additive model (GAM) framework (Miller et al. 2013). In the first stage, we estimated the observational processes that involve the probability of observing the individuals, given the true density and detection process during the line-transect surveys that account for visibility biases. In the second stage, we estimated the ecological state processes by modeling the relationship between the animal densities developed in the first stage to contemporaneous environmental habitat characteristics. In this section, we used GAMs to model the density-habitat relationship in the second stage.

In section 6.3, we applied the same input data used by the 2-stage GAM framework to a "single-stage" Bayesian hierarchical framework. In this framework, we simultaneously estimated all aspects in the 2-stage framework. An advantage of this process is that it allows the propagation of all uncertainties to the final estimates of density (and abundance). A disadvantage is that it requires long computing times, so model selection in the Bayesian framework was prohibitive, at least at this time. Thus, we are still in the process of developing an optimization of this framework. For now, we conducted model selection outside of the Bayesian hierarchical framework.

Nearly all of the habitat candidate covariates used previously in typical density-habitat models are variables that measure characteristics of the sea surface (e.g. sea surface temperature (SST) and chlorophyll-a derived from satellite sources) or sea bottom characteristics (e.g. bottom depth and slope). More recently, like in sections 6.2 and 6.3, we also used habitat candidate covariates that describe water-column characteristics (e.g. mixed layer depth or bottom temperature derived from ocean models like HYCOM (HYbrid Coordinate Ocean Model)). Although the density-habitat models that use these types of covariates provide good representations of the observed data, they explain only some of the observed data variability. This could partially be because we are assuming that these readily available covariates are appropriate proxies for what actually directly influences the distribution and abundance patterns. Palacios et al. (2013) concluded that important factors influencing the distribution and abundance of marine mammals include prey production and concentration, prey behavior and life history, reproduction, intra- and interspecies interactions. However, many of these factors are simply not available or difficult to incorporate directly into the density-habitat models; thus triggering the need to use proxies in the modeling frameworks.

In section 6.4, we took a step towards integrating information of potential prey species into density-habitat models with the goal to enhance our understanding of the distribution and abundance of marine mammals. So far, we have conducted an exploratory study where we developed density-habitat models of the abundance patterns of several marine mammal species located along the shelfbreak south of New England as related to the spatial structure patterns of organism groups derived from backscatter acoustic data that represent potential prey species. The results presented here are exemplary to illustrate our advances. We discuss future steps towards the longer-term goal of incorporating prey and water column structure into future marine mammal abundance and distribution estimates.

In section 6.5, we provided a brief summary of some of the work that other researchers have done or are doing with the visual line transect data collected under AMAPPS I and II that we made publicly available in several places and in several formats (see Chapter 11 for more details).

6.2 Two-Stage Framework

6.2.1 Methods

We based the spatiotemporal density estimates and maps on density-habitat models that we fitted to visual shipboard and aerial survey line-transect data, associated survey conditions, animal group characteristics, spatially- and temporally-explicit static and dynamic contemporaneous environmental characteristics, and species-specific availability bias correction factors. We applied the basic analysis methods (section 5.2) to all of the shipboard and aerial data collected during 2010 to 2017 (sections 5.2.2 and 5.2.3) that we stratified into spatial (10 km x 10 km) and temporal (8-day) strata, hereafter referred to as spatiotemporal strata. We then used the spatiotemporal strata with survey track lines to develop density-habitat models using the suite of candidate contemporaneous habitat covariates (Tables 6-1 and 6-2; Figures 6-1 to 6-4; section 11.2). We then used the resulting models and the habitat values from all the spatiotemporal strata to predict the density (and abundance) for each spatiotemporal stratum in the study area. We then displayed the results in map and table formats where we summed the results over several spatial regions (the entire study area and the wind-energy study areas) and over several timeframes (annual and seasonal).

We summarized the general workflow below, with details in Palka et al. (2017) and Chavez-Rosales et al. 2019):

1) **Define study area.** We defined the study area and strata by dividing all data into standardized spatial strata (10 km x 10 km) and standardized temporal strata (8-days) starting with 4 January of each year.

   We chose the size of the spatial (10 km x 10 km) and temporal (8-day) strata to reflect a compromise between not too small (and thus implying too much accuracy on such a fine scale) and not too large (and thus not providing the information our stakeholders are looking for). Because the target species (marine mammals, seabirds, and sea turtles) are mobile, providing information on a very fine scale will be statistically inaccurate and have high uncertainty. In addition, scientists often smooth the satellite-dervied data to an 8-day timeframe. Thus, if we use these data, we benefit from their corrections for issues such as cloud cover when we associate our sightings data to a contemporaneous habitat covariate.

2) **Conduct quality checks.** We conducted quality control checks, processed the input data into a format needed by the analysis methods, and collated the data into a common database (Chapter 11).

3) **Confirm species ids.** We assigned a specific species identification to some sightings that we ambiguously identified in the field. We then pooled these newly assigned sightings with the positively identified sightings for the rest of the modeling process.

   a. Using a binomial logistic regression model documented in Palka et al. (2017), we assigned a species identification to sightings that we ambiguously identified in the field as being either a fin or sei whale. The regression model to predict the probability that a sighting was a fin whale was a function of sea surface temperature, primary productivity, and distance to shore.

   b. Using a binomial logistic regression model documented in Garrison and Rosel (2017) and section 5.5 in this report, we assigned sightings identified in the field as an ambiguous pilot whale spp. to either long-finned pilot whales or short-finned pilot whales. The logistic

regression model to predict the probability that a sighting was a short-finned pilot whale was a function of SST, latitude, and month of the pilot whale sightings.

4) **Estimate surface density accounting for perception bias.** We estimated species and platform specific ocean surface density accounting for perception bias for each species (or species guild) within each spatiotemporal stratum that we surveyed in by using distance analysis techniques (Thomas et al. 2010). We applied this process to the 4 sighting platforms (northeast (NE) ship, NE plane, southeast (SE) ship, and SE plane). The NEFSC conducted the NE surveys, and the SEFSC conducted the SE surveys. The distance analysis methods that account for perception bias involved the estimation of a detection function, and *p(0)* – the probability of detecting a group on the track line – using significant survey related covariates, such as sighting conditions, group size, animal behavior, etc. (section 5.2.5). For each platform, we created datasets with species with similar characteristics that affect their detectability, such as the size of the animal, usual group sizes, diving patterns, and behavior of the animals when at the surface. These groupings ensured that all species observed were included in a set and the sample sizes were sufficient for the analysis of each set.

5) **Estimate availability bias correction factor.** We estimated a species- and platform-specific availability bias correction factor using information on the average surface and dive times, group sizes, and viewing area from the platform (section 5.2.6).

6) **Estimate corrected density for perception and availability bias (Stage 1).** We estimated the bias-corrected density that accounted for availability and perception bias for each spatiotemporal stratum that we surveyed in, by applying the estimate of the species- and platform-specific availability bias correction factor to the species- and platform-specific ocean surface density estimate that accounted for perception bias.

7) **Develop density-habitat model (Stage 2).** For each spatiotemporal stratum we surveyed in, we developed species-specific density-habitat models by using GAMs to predict the animal's bias-corrected density estimate using static and contemporaneous dynamic habitat covariates. We used several goodness-of-fit tests to choose the best fitting model.

8) **Predict density.** For all spatiotemporal strata, we predicted animal density and its associated uncertainty by using the modeled animal density-habitat relationship and the values of the static and contemporeous habitat covariates within each stratum. The definition of the seasons used throughout this analysis is:

   spring (1 March to 31 May)
   summer (1 June to 31 August)
   fall (1 September to 30 November)
   winter (1 December to 28 (29) February), unless specified.

9) **Display results.** Finally, we displayed the results by plotting maps of spatially explicit densities and associated measures of uncertainty, in addition to trend lines of abundance and their associated uncertainties. We also summarized the results for ecologically important groups of species by displaying hot spot maps.

When defining the wind-energy study areas, in several cases we merged together areas that were relatively small and close together. In addition, we added a 10 km buffer zone to all of these offshore wind energy areas to designate an area in which activities occurring within the wind energy area may influence an animal group. We refer to the wind energy area and 10 km buffer zone as a wind-energy study area. The size of an appropriate buffer is dependent on a variety of factors. Dependent factors include species-specific factors, such as the species of interest, individual animal's activities and natural short-term foraging and movement patterns that could then influence the animal's response and sensitivity to a wind-energy related activity. Other dependent factors include operation-specific factors, such as

sound source levels, sound propagation properties, and types of activity conducted in the wind energy area. In addition, dependent factors include area-specifc factors, such as the physical topography and oceanographic features within and surrounding the wind energy areas. For example, several studies indicate 20 km may be an appropriate buffer when interested in effects of pile driving on harbor porpoises (Brandt et al. 2011; 2016). Alternatively, perhaps we should not include a buffer for less mobile species or during certain operational phases. Another practical reason for the 10 km buffer is, since the model output is for 10 km x 10 km cells, the buffer insures all of the irregularly shaped wind energy areas are included in the wind-energy study area.

The response variable of the GAM density-habitat model was the Horvitz-Thompson like estimator of the density of individuals of a species (or species guild) accounting for perception and availability bias for each spatiotemporal stratum (*i*) that had survey effort, :

___

where

n_i = number of groups in spatiotemporal stratum *i*,
s_{ir} = size of the *r*th group in spatiotemporal stratum *i*,
= probability of detection within the search area of a spatiotemporal stratum *i* accounting for perception bias,
A_i = area (in km^2) searched in spatiotemporal stratum *i*, = $2wl_i$, where *w* is the truncation distance and l_i is the length of the track lines in cell *i*, and
= estimate of the species-specific availability bias correction factor.

Note, the 's from the aerial survey data were calculated slightly differently than that from the shipboard survey data due to the asymmetry of the aerial viewing areas for the 2 teams (see section 5.2.5 for more details).

The GAM density-habitat model related the response variable to a series of *j* static and contemporaneous dynamic habitat covariates (z_j; Tables 6-1 and 6-2; Figures 6-1 to 6-4):

where $_0$ is an intercept term and are *j* linear, smoothed, or tensor product smooth functions of the habitat covariate *z*. We described the procedures used to download and process the habitat covariates in Chapter 11. We used the R package *mgcv* and assumed the data followed an overdispersed Tweedie distribution. We used several goodness-of-fit tests to choose the best fitting GAM density-habitat model (Table 6-3).

Table 6-1 Dynamic contemporaneous habitat covariates considered in the modeling frameworks
We defined all covariate values (except for the North Atlantic Oscillation index (NAO)) for the location of the center of each 10 km x 10 km spatial stratum and averaged over each 8-day temporal stratum starting 4 January of each year. The North Atlantic Oscillation index is an index for the entire North Atlantic Ocean, so we defined it as the average over each 8-day timeframe for each year. Example maps of the covariate values during temporal layer 25 in 2016 (4 to 11 July 2016) are in Figures 6-1 to 6-4.

Dynamic Covariate	Description	Original Resolution	Source
SSTMUR	SST multi-scale ultra-high resolution (MUR) (ºC)	1 km mapped to 2 km	https://podaac.jpl.nasa.gov/dataset/ MUR-JPL-L4-GLOB-v4.1
SSTFMA	Strength of SST fronts using Modis Aqua data (unitless)	1 km mapped to 2 km	Original source data - https://oceancolor.gsfc.nasa.gov/, fronts calculated using Belkin & O'Reilly (2009)
SSTFMT	Strength of SST fronts using data from Modis Terra (unitless)	1 km mapped to 2 km	Original source data - https://oceancolor.gsfc.nasa.gov/, fronts calculated using Belkin & O'Reilly (2009)
CHLA	Chlorophyll-a concentration (mg/m^3)	1 km mapped to 2 km	Original source data - https://oceancolor.gsfc.nasa.gov/ Then derived by OCI algorithm
CHLFMA	Strength of chlorophyll fronts using Modis Aqua data (unitless)	1 km mapped to 2 km	Original source data - https://oceancolor.gsfc.nasa.gov/, fronts calculated using Belkin & O'Reilly (2009)
PIC	Particulate inorganic carbon (mol/m^3)	1 km mapped to 2 km	https://oceancolor.gsfc.nasa.gov/
POC	Particulate organic carbon (mg/m^3)	1 km mapped to 2 km	https://oceancolor.gsfc.nasa.gov/
PP	Primary productivity ($mgCarbon/(m^2 \cdot yr)$	1 km mapped to 2 km	Original source data - https://podaac.jpl.nasa.gov/dataset/MUR-JPL-L4-GLOB-v4.1 and https://oceancolor.gsfc.nasa.gov/, PP calculated using Behrenfeld and Falkowskip (1997) and Eppley (1972)
SLA	Sea Surface Height Anomaly (Heat contents/ thermal expansion)	1/4°	https://www.aviso.altimetry.fr/en/data/products/sea-surface-height-products
MLD	Mixed layer depth, depth at which the density changes from the surface by 0.03 kg/m^3 (m)	1/12°	https://hycom.org/dataserver/glb-analysis
MLP	Mixed layer thickness (m)	1/12°	https://hycom.org/dataserver/glb-analysis
SALINITY	Surface salinity (psu)	1/12°	https://hycom.org/dataserver/glb-analysis
BTEMP	Bottom temperature (ºC)	1/12°	https://hycom.org/dataserver/glb-analysis
DGSNW	Distance to the Gulf Stream north wall (m)		https://ocean.weather.gov/gulf_stream.php
DGSSW	Distance to the Gulf Stream south wall (m)		https://ocean.weather.gov/gulf_stream.php
NAO	North Atlantic Oscillation index (not spatially explicit)	Daily	ftp://ftp.cpc.ncep.noaa.gov/cwlinks/ norm.daily.aao.index.b790101.current.ascii

Table 6-2 Static spatial habitat covariates considered in the modeling frameworks
We defined all covariate values for the location of the center of each 10 km x 10 km spatial stratum and averaged over each 8-day temporal stratum starting 4 January of each year. Example maps of the covariate values during temporal layer 25 in 2016 (4 to 11 July 2016) are in Figure 6-4.

Static Covariates	Description	Original Resolution	Source
Depth	Bathymetry (m)	3 arc-sec	http://www.ngdc.noaa.gov/mgg/global/ global.html
Dist2shore	Distance to coastline (km)	0.04°	https://oceancolor.gsfc.nasa.gov/docs/distfromcoast/
Slope	Seafloor slope (degrees)	3 arc-sec	http://www.ngdc.noaa.gov/mgg/global/ global.html
Dist200	Distance to the 200 m isobath/contour (m)		Original source data – http://www.ngdc.noaa.gov/mgg/global/ global.html Then calculated in R script
Dist125	Distance to the 125 m isobath/contour (m)		Original source data - http://www.ngdc.noaa.gov/mgg/global/ global.html Then calculated in R script
Dist1000	Distance to the 1000 m isobath/contour (m)		Original source data - http://www.ngdc.noaa.gov/mgg/global/ global.html Then calculated in R script

Table 6-3 Diagnostic tests and criteria used to evaluate density-habitat model performance

Test	Description	Criteria	Calculated From	Formula
DE	Percentage of deviance explained from the model	Higher value	GAM model	
R^2	Coefficient of determination from the model	Higher value	GAM model	
RHO	Spearman's rank correlation	Higher value	None-zero data. 1) Initial testing and; 2) k-fold cross-validation.	
ASPE	Mean square prediction error	Lower value	All data. 1) Initial testing and; 2) k-fold cross-validation	
MAPE	Mean absolute percentage error	Lower value	None-zero data. 1) Initial testing and; 2) k-fold cross-validation	
MAE	Mean absolute error	Lower value	All data. 1) Initial testing and; 2) k-fold cross-validation.	

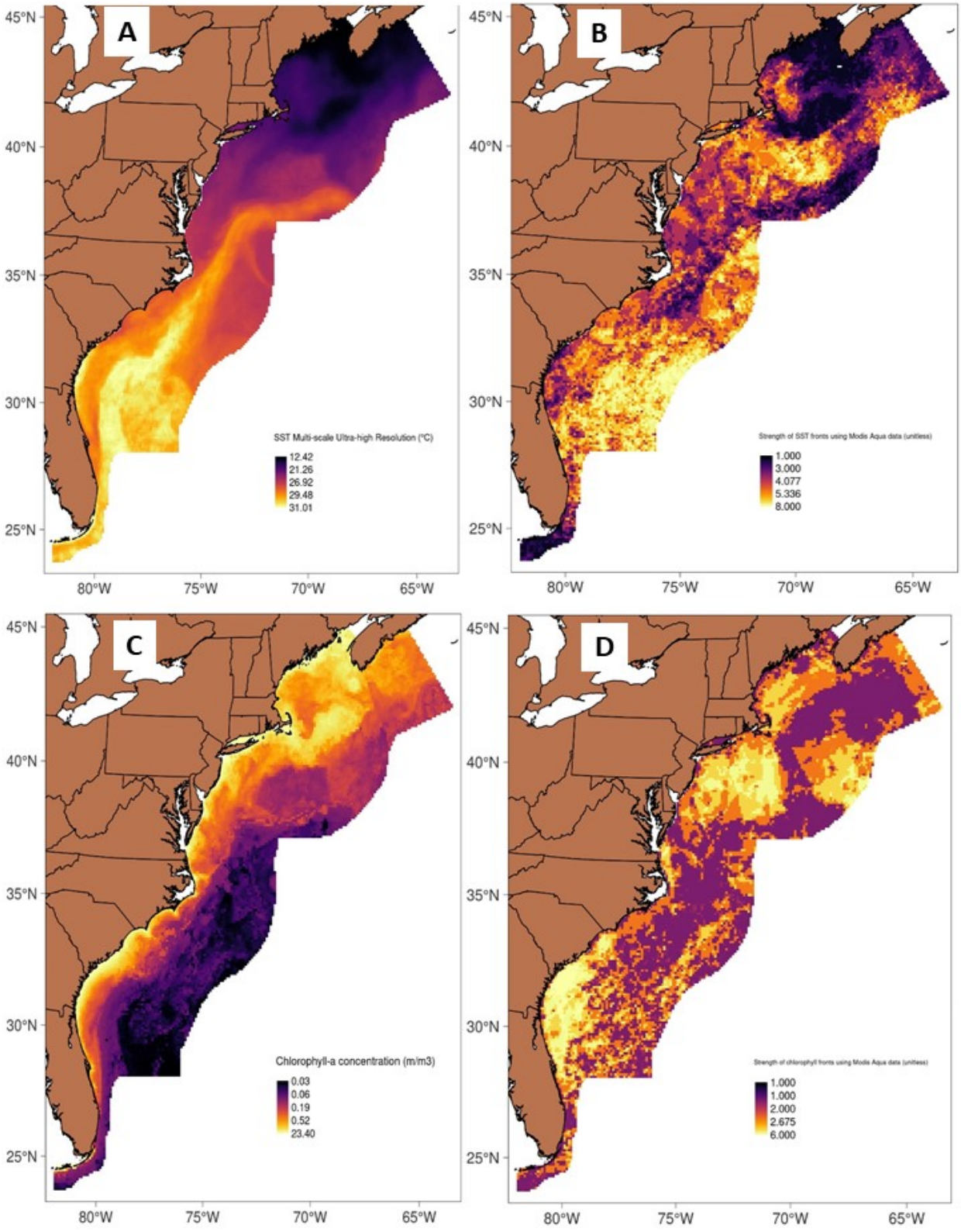

Figure 6-1 Habitat covariate maps – SST, SST fronts, chlorophyll concentration and fronts
Each map displaces the covariate values from temporal layer 25 in 2016 (4 to 11 July 2016) for all spatial strata in the study area.

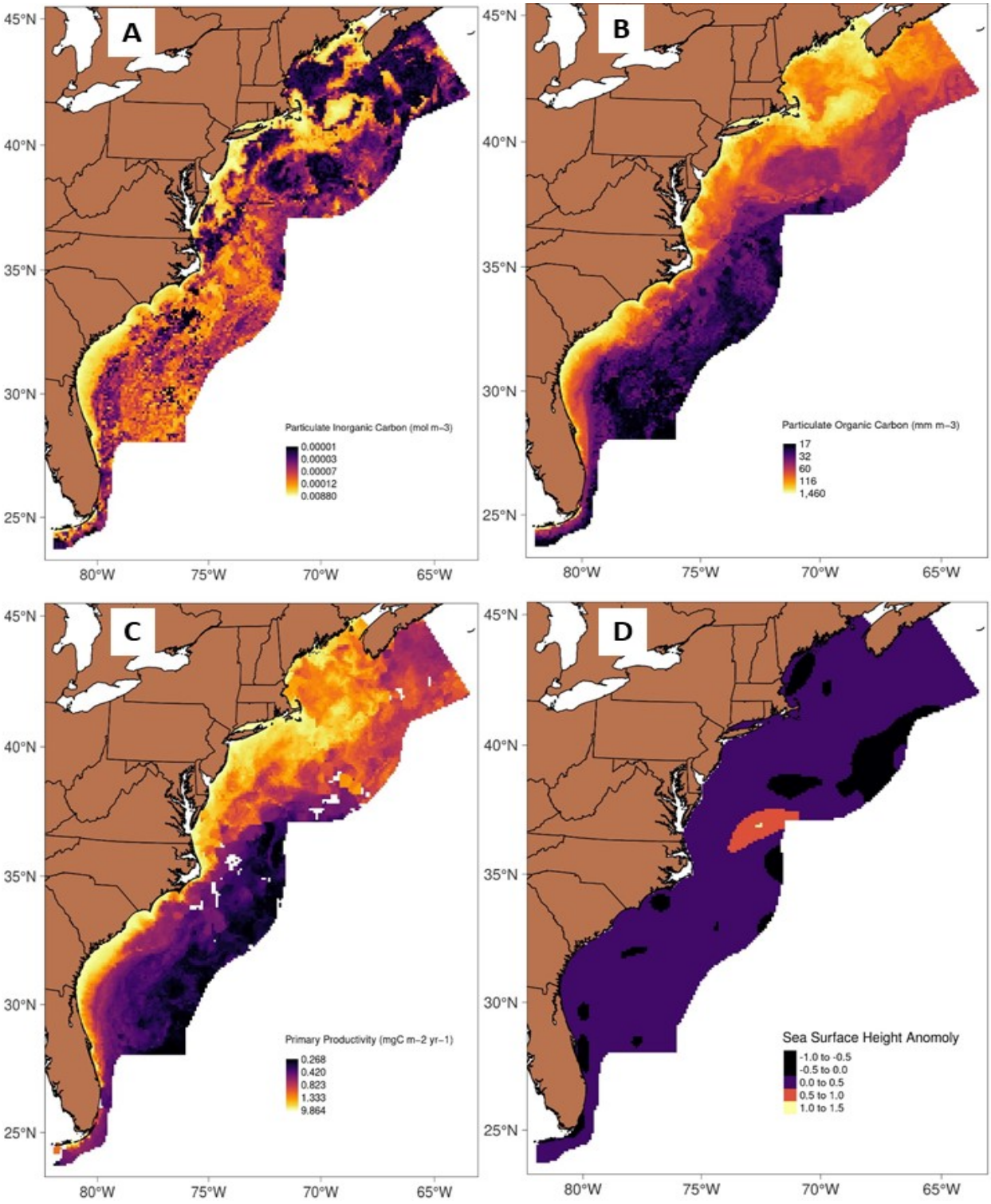

Figure 6-2 Habitat covariate maps – PIC, POC, PP, SLA
Each map displaces the covariate values from temporal layer 25 in 2016 (4 to 11 July 2016) for all spatial strata in the study area. (A) particulate inorganic carbon (PIC); (B) particulate organic carbon (POC); (C) Primary productivity (PP); (D) sea surface height anomaly (SLA).

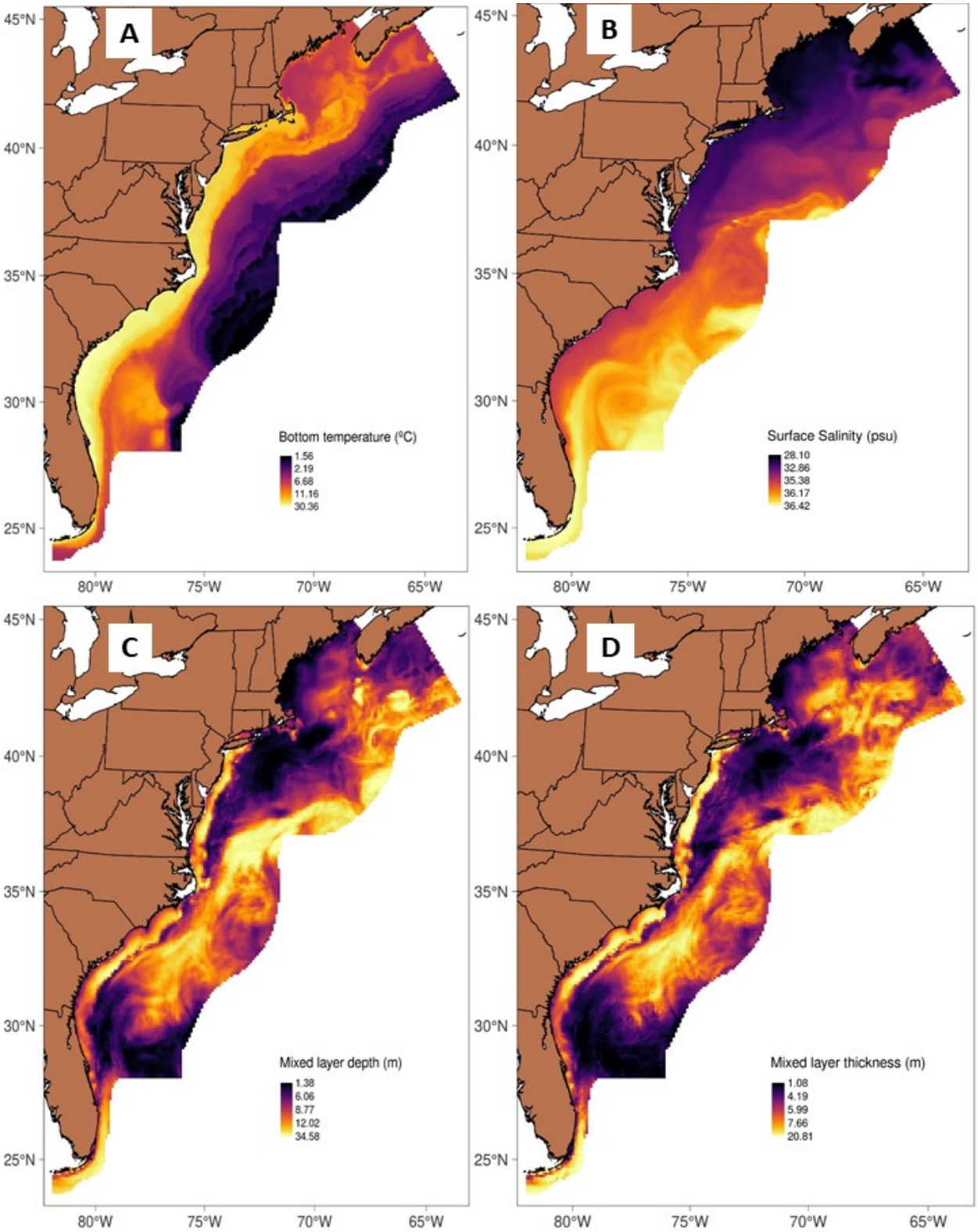

Figure 6-3 Habitat covariate maps – BTEMP, SALINITY, MLD, and MLP
Each map displaces the covariate values from temporal layer 25 in 2016 (4 to 11 July 2016) for all spatial strata in the study area.

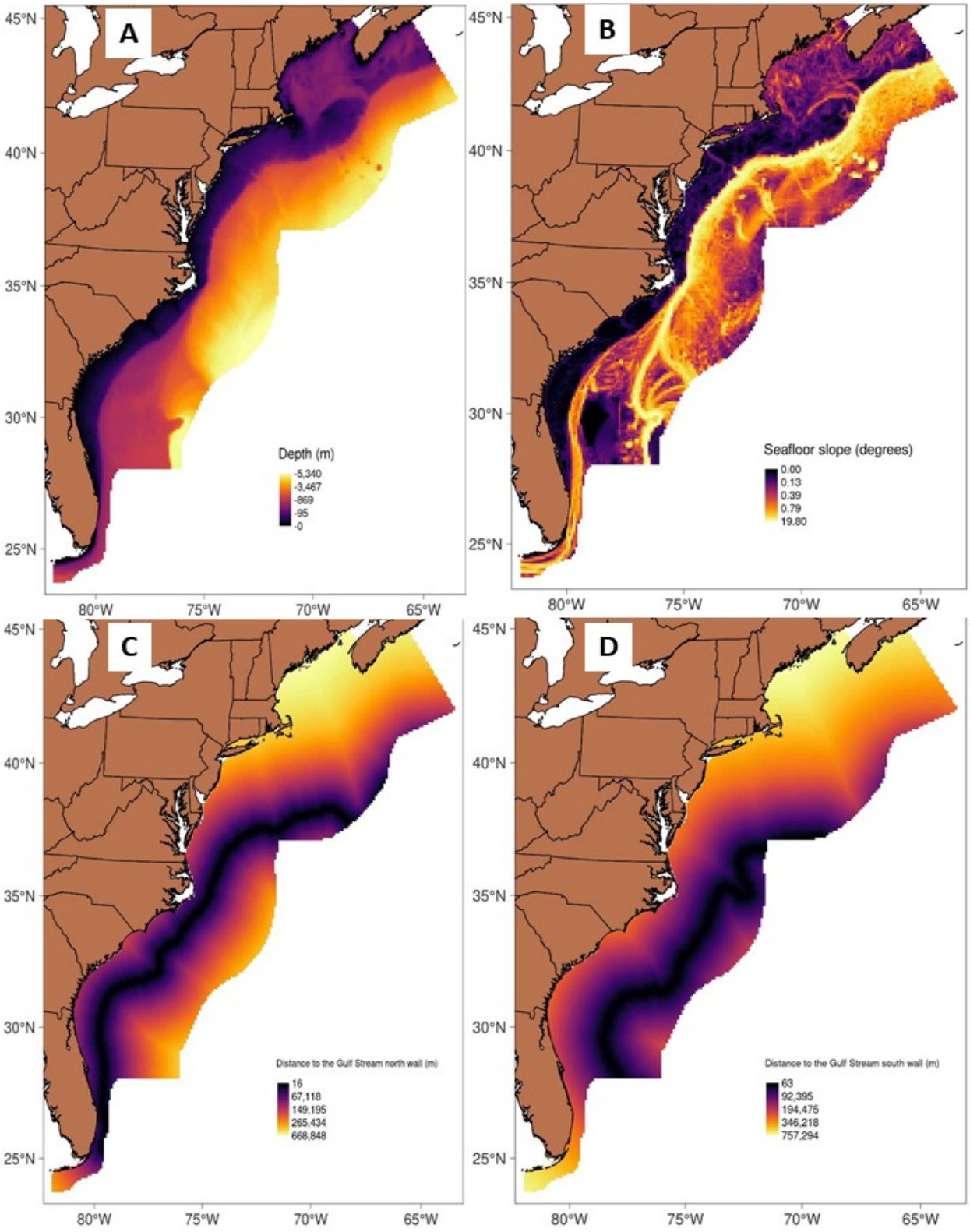

Figure 6-4 Habitat covariate maps – Depth, Slope, DGSNW, DGSSW
Each map displaces the covariate values from temporal layer 25 in 2016 (4 to 11 July 2016) for all spatial strata in the study area.

6.2.2 Results

6.2.2.1 Survey Efforts

We developed 16 GAM density-habitat models of single species and 2 models of species' guilds (pygmy/dwarf sperm whales and unidentified beaked whales) using the 2010 to 2017 line-transect visual sightings data collected under AMAPPS. We used data from all 4 seasons in the species density-habitat models, with 2 exceptions. One exception was the use of only summer data for species and species' guilds that inhabit only deeper shelfbreak and offshore waters, which we surveyed only in the summer by ship. These deep-water species included pygmy/dwarf sperm whales, Cuvier's beaked whales, Sowerby's beaked whales, and unidentified beaked whales. Another exception was for harbor porpoises where we developed 2 density-habitat models that represented distinct distribution behaviors in different times of the year. One harbor porpoise model included data from only warmer months (June to October) when the harbor porpoises clustered mainly in the northern Gulf of Maine. The other model represented cooler months (November to May) when harbor porpoises dispersed throughout much of the study area.

The 2010 to 2017 data we used in the density-habitat models came from over 250,000 km of on-effort track lines from AMAPPS shipboard and aerial surveys (Table 6-4; Figures 6-5 to 6-7). Aerial surveys were closer to shore, within about the 200 m or 2000 m depth contour, depending on location (Figure 6-6). Shipboard surveys were mostly in summer months in shelfbreak and offshore waters; we did not conduct shipboard surveys in the winter (Figure 6-7). We are planning to have a shelfbreak and offshore winter/spring shipboard survey during AMAPPS III in 2021.

The shipboard and aerial surveys resulted in the detection of nearly 9,000 sightings of groups of cetaceans that consisted of over 94,000 individuals (Tables 6-5 to 6-8). We defined a group (also referred to as a sighting) as either a single individual spatially separated from other individuals (that is, a group of size 1) or a spatially cluster of individuals that were within a few body lengths of each other (that is, a group of size 2 or more). Note the term sighting and group are interchangeable and represent the same thing. About 68% of the groups were within the northern shipboard and aerial surveys.

We did not attempt to create density-habitat models of North Atlantic right whales because currently there is another extensive research effort to create density-habitat models with the North Atlantic right whale data from not only the AMAPPS surveys but also many other datasets. We also did not create density-habitat models of species rarely detected (such as, Clymene's dolphins and killer whales) due to the limited number of sightings available. In addition, we did not use sightings of groups with broad categories of identification (such as unidentified dolphin or unidentified whales). Although it is possible to use the data from the unidentified sightings, we would have to make broad assumptions. We would have to do a more extensive investigation into the best way to accurately use these data, which we would like to conduct during AMAPPS III. Distribution maps of the detected sighting locations of the North Atlantic right whale, rare species, fish, seals, and undifferentiated identified species are in Appendix II. We discussed in detail the turtle sightings data collected during these surveys in Chapter 8, and the seabird sightings data in Chapter 9.

Table 6-4 On-effort track line effort (km) from 2010 to 2017 by season and platform
Survey effort used in the species density-habitat models.

Platform	Spring 1 Mar to 31 May	Summer 1 Jun to 31 Aug	Fall 1 Sep to 30 Nov	Winter 1 Dec to 29 Feb	TOTAL
NE Shipboard	0	37,529	1,065	0	38,594
NE Aerial	13,314	25,867	37,850	12,179	89,210
SE Shipboard	8,853	12,968	3,012	0	24,833
SE Aerial	41,293	28,236	18,974	8,950	97,453
Subtotal ship	8,853	50,497	4,077	0	63,427
Subtotal aerial	54,607	54,103	56,824	21,129	186,663
TOTAL	63,460	104,600	60,901	21,129	250,090

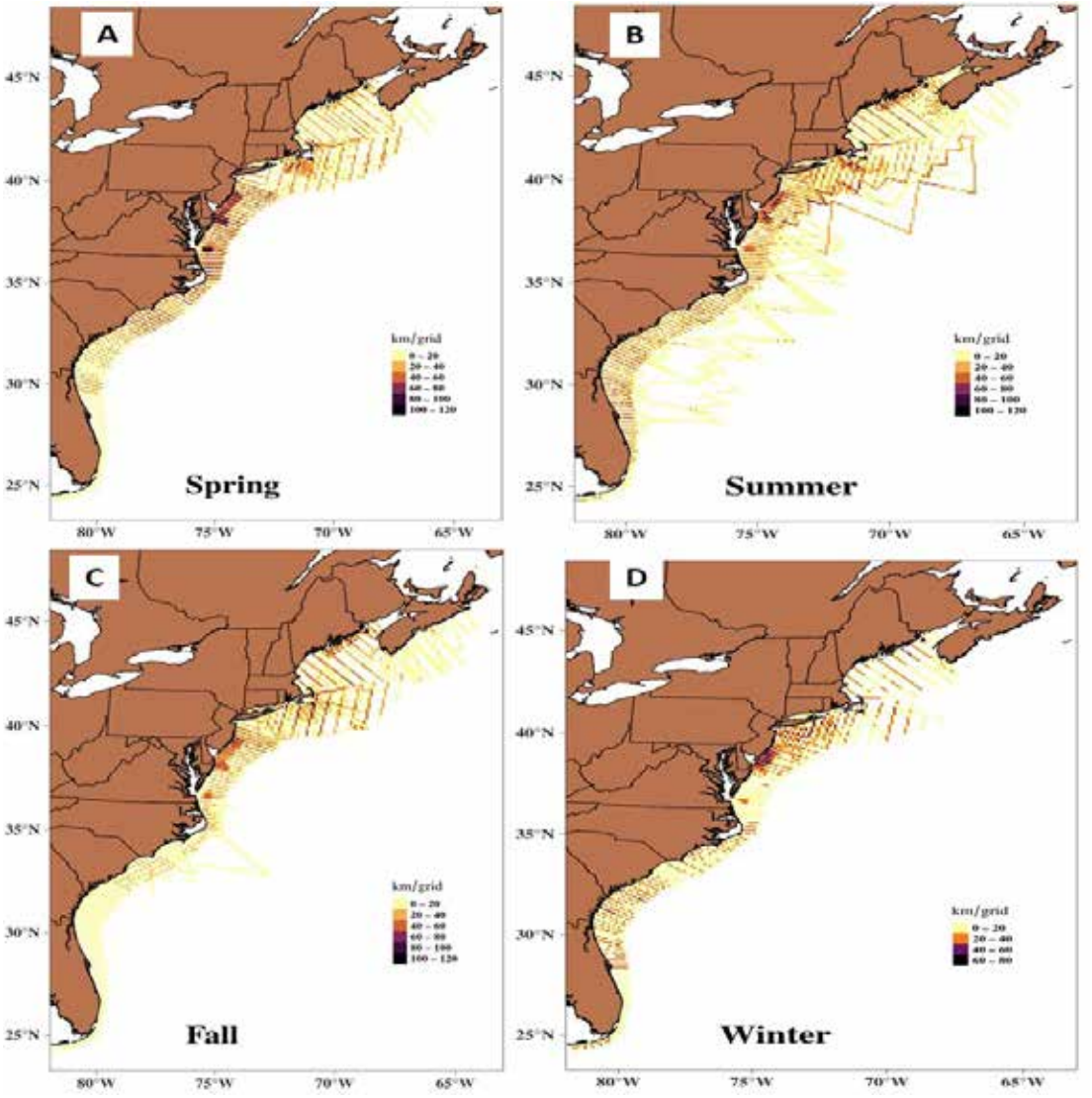

Figure 6-5 Spatial distribution of all survey effort used in density-habitat models, by season
We displayed the amount of survey effort (trackline length (km)) within each spatial stratum for the entire season conducted during the 2010 to 2017 AMAPPS shipboard and aerial surveys used in the density-habitat models. Spring is 1 Mar to 31 May; summer is 1 Jun to 31 Aug; fall is 1 Sep to 30 Nov; winter is 1 Dec to 29 Feb.

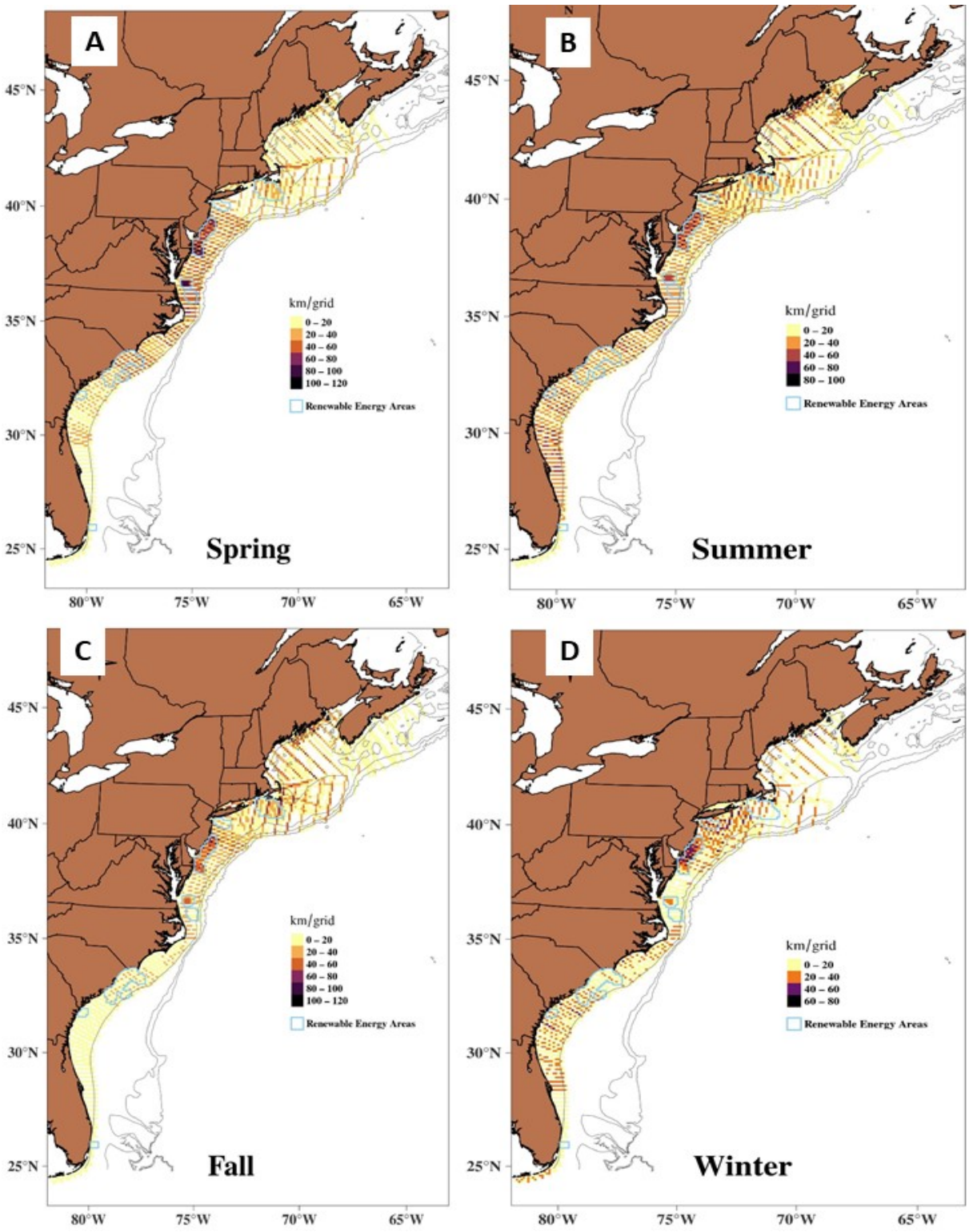

Figure 6-6 Aerial survey effort spatial distribution used in density-habitat models, by season
We displayed the amount of survey effort (trackline length (km)) within each spatial stratum for the entire season conducted during the 2010 to 2017 AMAPPS aerial surveys used in the density-habitat models. Spring is 1 Mar to 31 May; summer is 1 Jun to 31 Aug; fall is 1 Sep to 30 Nov; winter is 1 Dec to 29 Feb.

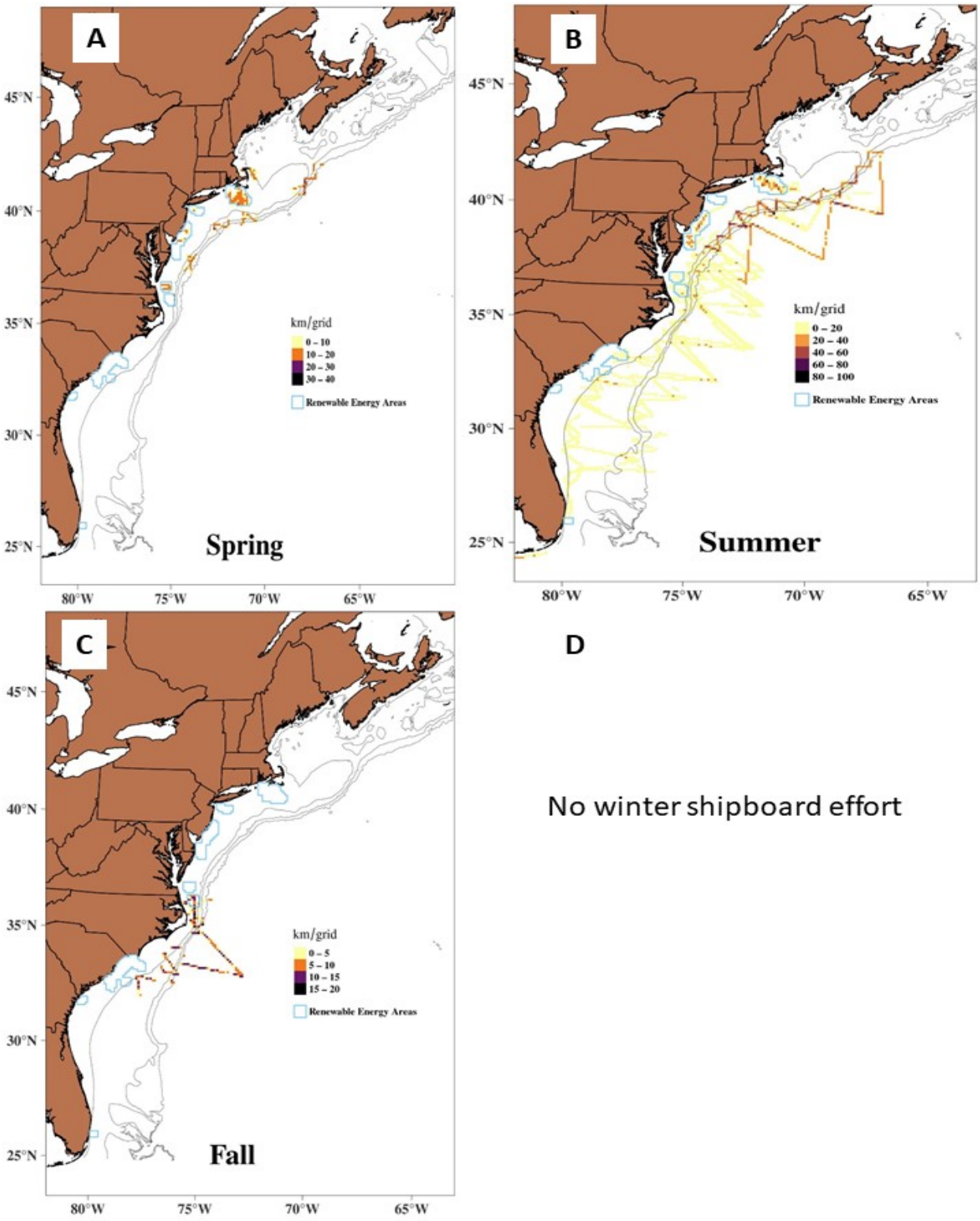

Figure 6-7 Shipboard survey effort spatial distribution used in density-habitat models
We displayed the amount of survey effort (trackline length (km)) within each spatial stratum for the entire season conducted during the 2010 to 2017 AMAPPS shipboard surveys used in the density-habitat models. Spring is 1 Mar to 31 May; summer is 1 Jun to 31 Aug; fall is 1 Sep to 30 Nov; winter is 1 Dec to 29 Feb.

Table 6-5 Species in Northeast shipboard mark-recapture distance sampling analysis sets
For each species in an analysis set, we provided the numbers of groups and of individuals, by season. Analysis sets are pooled data from species with similar detectability that we analyzed using mark-recapture distance sampling methods in Stage 1. We did not conduct spring or winter Northeast shipboard surveys. Spring is 1 Mar to 31 May; summer is 1 Jun to 31 Aug; fall is 1 Sep to 30 Nov; winter is 1 Dec to 29 Feb.

Set	Species	Groups Summer	Groups Fall	Individual Summer	Individual Fall	Total Groups	Total Individuals
1	Atlantic spotted dolphin	60	3	1,760	75	63	1,835
	Pantropical spotted dolphin	1	0	6	0	1	6
2	Striped dolphin	229	8	9,511	437	237	9,948
3	Common bottlenose dolphin	345	16	3,865	186	361	4,051
4	Risso's dolphin	486	23	3,131	218	509	3,349
	Killer whale	1	0	4	0	1	4
	Rough-toothed dolphin	6	0	59	0	6	59
	Pygmy killer whale	1	0	1	0	1	1
	False killer whale	8	0	57	0	8	57
5	Common dolphin	444	5	19,802	280	449	20,082
	White-sided dolphin	3	0	61	0	3	61
	Harbor porpoise	4	0	6	0	4	6
	Clymene dolphin	1	0	3	0	1	3
6	Unidentified Ziphiidae	194	3	493	8	197	501
	Blainville's beaked whale	2	0	4	0	2	4
	Gervais' beaked whale	16	0	60	0	16	60
	Cuvier's beaked whale	148	4	404	6	152	410
	Sowerby's beaked whale	28	0	29	0	28	29
	True's beaked whale	10	0	27	0	10	27
	Unidentified Mesoplodon	15	0	36	0	15	36
	Dwarf sperm whale	30	2	58	3	32	61
	Pygmy sperm whale	34	0	46	0	34	46
	Pygmy or Dwarf sperm whale	36	1	51	1	37	52
7	Long-finned pilot whale	41	0	666	0	41	666
	Short-finned pilot whale	230	2	2,050	32	232	2,082
8	Humpback whale	157	0	370	0	157	370
9	Sperm whale	298	27	491	45	325	536
10	Fin whale	345	1	533	1	346	534
	Sei whale	20	0	28	0	20	28
	Minke whale	32	0	32	0	32	32
	Blue whale	9	0	0	19	9	19
	Right whale	2	0	4	0	2	4
	TOTAL	3,236	95	43,648	1,311	3,331	44,959

Table 6-6 Species in Southeast shipboard mark-recapture distance sampling analysis sets

For each species in an analysis set, we provided the numbers of groups and of individuals, by season. Analysis sets are pooled data from species with similar detectability that we analyzed using mark-recapture distance sampling methods in Stage 1. We did not conduct winter Southeast shipboard surveys.

Set		Groups Spring	Groups Summer	Groups Fall	Individual Spring	Individual Summer	Individual Fall	Total Groups	Total Individual
1	Atlantic spotted dolphin	0	76	31	0	2,817	959	107	3,776
	Pantropical spotted dolphin	0	9	1	0	320	30	10	350
	Striped dolphin	4	11	0	66	1,397	0	15	1,463
	Common dolphin	63	6	0	1,648	575	0	69	2,223
	Clymene dolphin	0	4	0	0	328	0	4	328
	White-sided dolphin	27	0	0	261	0	0	27	261
2	Common bottlenose dolphin	26	134	55	390	2,352	1,213	215	3,955
	Harbor porpoise	11	0	0	21	0	0	11	21
3	Short-finned pilot whale	4	85	18	32	1,461	495	107	1,988
	Long-finned pilot whale	44	0	0	312	0	0	44	312
	Risso's dolphin	18	26	12	91	292	120	56	503
	False killer whale	0	2	0	0	20	0	2	20
	Rough-toothed dolphin	0	1	3	0	31	50	4	81
	Killer whale	1	1	0	4	5	0	1	9
4	Cuvier's beaked whale	5	19	6	6	45	10	30	61
	Blainville's beaked whale	0	1	3	0	1	7	4	8
	Unidentified Ziphiidae	15	54	9	15	112	16	78	143
	Unidentified Mesoplodon	0	35	8	0	89	17	43	106
	Gervais' beaked whale	0	1	0	0	1	0	1	1
	Sowerby's beaked whale	0	1	0	0	1	0	1	1
	True's beaked whale	0	0	0	0	0	0	0	0
5	Fin whale	34	5	3	48	8	9	42	65
	Humpback whale	45	1	0	76	1	0	46	77
	Right whale	0	1	0	0	1	0	1	1
	Sperm whale	38	70	12	44	156	38	120	238
	Minke whale	8	1	0	11	1	0	9	12
	Killer whale	0	1	0	0	5	0	1	5
	Blue whale	0	0	0	0	0	0	0	0
	Sei whale	28	0	0	33	0	0	28	33
6	Pygmy or Dwarf sperm whale	0	74	15	0	139	29	89	168
	Dwarf sperm whale	0	5	1	0	8	1	6	9
	Pygmy sperm whale	0	2	0	0	4	0	2	4
	TOTAL	370	626	177	3,054	10,170	2,994	1,173	16,218

Table 6-7 Species in Northeast aerial mark-recapture distance sampling analysis sets

For each species in an analysis set, we provided the numbers of groups and of individuals, by season. Analysis sets are pooled data from species with similar detectability that we analyzed using mark-recapture distance sampling methods in Stage 1. Spring is 1 Mar to 31 May; summer is 1 Jun to 31 Aug; fall is 1 Sep to 30 Nov; winter is 1 Dec to 29 Feb.

Set		Groups Spring	Groups Summer	Groups Fall	Groups Winter	Individual Spring	Individual Summer	Individual Fall	Individual Winter	Total Groups	Total Individual
1	Fin whale	25	31	55	4	36	31	60	4	115	131
	Sei whale	13	5	6	2	33	6	12	5	26	56
2	Minke whale	10	60	37	5	11	65	52	5	112	133
	Unidentified Ziphiidae	4	5	4	1	8	14	7	3	14	32
	Cuvier's beaked whale	1	1	0	0	4	1	0	0	2	5
	Sowerby's beaked whale	0	0	1	0	0	0	1	0	1	1
3	Humpback whale	13	68	75	7	20	88	101	10	163	219
	Blue whale	0	0	1	0	0	0	1	0	1	1
	Right whale	9	1	3	4	9	1	3	9	17	22
	Northern beaked whale	0	3	0	0	0	15	0	0	3	15
4	Common bottlenose dolphin	38	28	46	7	256	178	623	36	119	1,093
5	Harbor porpoise	181	341	390	135	264	757	1,547	258	1,047	2,826
6	Risso's dolphin	14	22	55	24	34	249	481	61	115	825
7	Short-finned pilot whale	0	21	15	0	0	156	82	0	36	238
	Long-finned pilot whale	6	18	19	2	7	86	78	3	45	174
8	White-sided dolphin	62	82	144	25	536	929	2,675	208	313	4,348
	White-beaked dolphin	0	0	2	0	0	0	21	0	2	21
9	Common dolphin	8	223	223	136	215	5,570	5,823	3,558	590	15,166
	Striped dolphin	1	5	8	2	100	86	385	50	16	621
	TOTAL	385	914	1,084	354	1,533	8,232	11,952	4,210	2,737	25,927

Table 6-8 Species in Southeast aerial mark-recapture distance sampling analysis sets

For each species in an analysis set, we provided the numbers of groups and of individuals, by season. Analysis sets are pooled data from species with similar detectability that we analyzed using mark-recapture distance sampling methods in Stage 1. Spring is 1 Mar to 31 May; summer is 1 Jun to 31 Aug; fall is 1 Sep to 30 Nov; winter is 1 Dec to 29 Feb.

Set	Species	Groups Spring	Groups Summer	Groups Fall	Groups Winter	Individual Spring	Individual Summer	Individual Fall	Individual Winter	Total Groups	Total Individual
1	Atlantic spotted dolphin	70	64	37	5	1,346	1,259	580	71	176	3,256
2	Common bottlenose dolphin	466	312	212	83	4,139	3,144	2,233	812	1,073	10,328
3	Common dolphin	125	11	5	36	6,520	784	254	1,625	177	9,183
	Striped dolphin	1	0	0	0	110	0	0	0	1	110
4	Fin whale	16	5	6	1	21	7	10	2	28	40
	Minke whale	11	0	3	1	14	0	3	1	15	18
	Humpback whale	8	0	3	2	9	0	6	2	13	17
	Right whale	1	0	0	1	5	0	0	2	2	7
	Sperm whale	7	3	0	0	7	3	0	0	10	10
	Cuvier's beaked whale	3	0	0	0	6	0	0	0	3	6
	Sowerby's beaked whale	0	1	0	0	0	1	0	0	1	1
	Unidentified Ziphiidae	0	0	0	2	0	0	0	2	2	2
	Unidentified Mesoplodon	0	1	0	0	0	2	0	0	1	2
5	Risso's dolphin	36	14	2	8	207	227	10	105	60	549
	Short-finned pilot whale	10	26	31	4	269	712	485	25	71	1,491
	Rough-toothed dolphin	0	1	0	0	0	7	0	0	1	7
	False killer whale	0	1	0	0	0	9	0	0	1	9
	TOTAL	754	439	299	143	12,653	6,155	3,581	2,647	1,635	25,036

6.2.2.2 Stage One

We divided the line transect data into analysis sets of similar species within the 4 area-platform combinations (NE shipboard, SE shipboard, NE aerial and SE aerial) to estimate perception bias-corrected surface density estimates using mark-recapture distance sampling analysis methods (MRDS; Tables 6-5 to 6-8).

The predicted mark-recapture distance sampling models that we developed to estimate the perception bias corrected densities of the spatiotemporal strata that we surveyed fit the observed data well, as demonstrated by the resulting Chi-squared, Kolmogorov-Smirnov and Cramer-von Mises (CvM) goodness-of-fit tests (Tables 6-9 and 6-10; Tables 4 in each chapter of Appendix I). To model the distance sampling detection function component, sighting conditions (Beaufort sea state and amount of glare) were the most common significant covariates (Figures 6-8 to 6-11); for only the NE shipboard data, swell height was also a common significant covariate (Figure 6-8). For the mark-recapture component models, observer team was a significant covariate in most of the analysis sets, indicating the position of the teams and/or observer composition between the teams resulted in different shapes of the detection function (Figures 6-8 to 6-11). In addition, Beaufort sea state and group size were also commonly significant covariates for the mark-recapture component models.

Table 6-9 Results of the mark-recapture distance sampling analyses for aerial survey data

Analysis Set	Truncation (m)* Step 1/Step2	Primary Team	CV[ ]	CvM* p-value
NE aerial-1	600/600	0.67	0.16	0.99
NE aerial-2	600/ LT35-600	0.62	0.19	0.91
NE aerial-3	1500/1500	0.67	0.09	0.94
NE aerial-4	450/450	0.62	0.13	0.96
NE aerial-5	210/350	0.52	0.10	0.78
NE aerial-6	300/300	0.62	0.16	0.98
NE aerial-7	400/400	0.54	0.30	1.00
NE aerial-8	400/400	0.57	0.10	0.90
NE aerial-9	300/300	0.56	0.10	0.84
SE aerial-1	330/ LT30-330	0.65	0.10	0.90
SE aerial-2	340/340	0.86	0.02	0.70
SE aerial-3	300/ LT20-300	0.78	0.08	1.00
SE aerial-4	300/ LT43-300	0.86	0.18	0.95
SE aerial-5	320/ LT50-360	0.74	0.15	0.98

*LT = left truncation CvM = Cramer-von Mises goodness-of-fit test.

Table 6-10 Results of the mark-recapture distance sampling analyses for shipboard survey data

Analysis Set	Truncation (m)	Primary Team	CV[ ]	CvM* p-value
NE ship-1	2000	0.87	0.08	0.92
NE ship-2	5000	0.72	0.07	0.94
NE ship-3	4000	0.59	0.10	0.97
NE ship-4	2220	0.50	0.11	0.62
NE ship-5	3800	0.52	0.08	0.78
NE ship-6	3800	0.42	0.13	0.88
NE ship-7	3500	0.66	0.10	0.91
NE ship-8	7000	0.39	0.24	0.99
NE ship-9	4600	0.58	0.11	0.97
NE ship-10	6000	0.48	0.10	0.95
SE ship-1	2700	0.62	0.09	0.98
SE ship-2	2800	0.69	0.09	0.95
SE ship-3	2700	0.71	0.08	0.81
SE ship-4	2800	0.32	0.40	1.00
SE ship-5	6000	0.57	0.11	0.65
SE ship-6	2800	0.48	0.26	0.99

[1]CvM = Cramer-von Mises goodness-of-fit test.

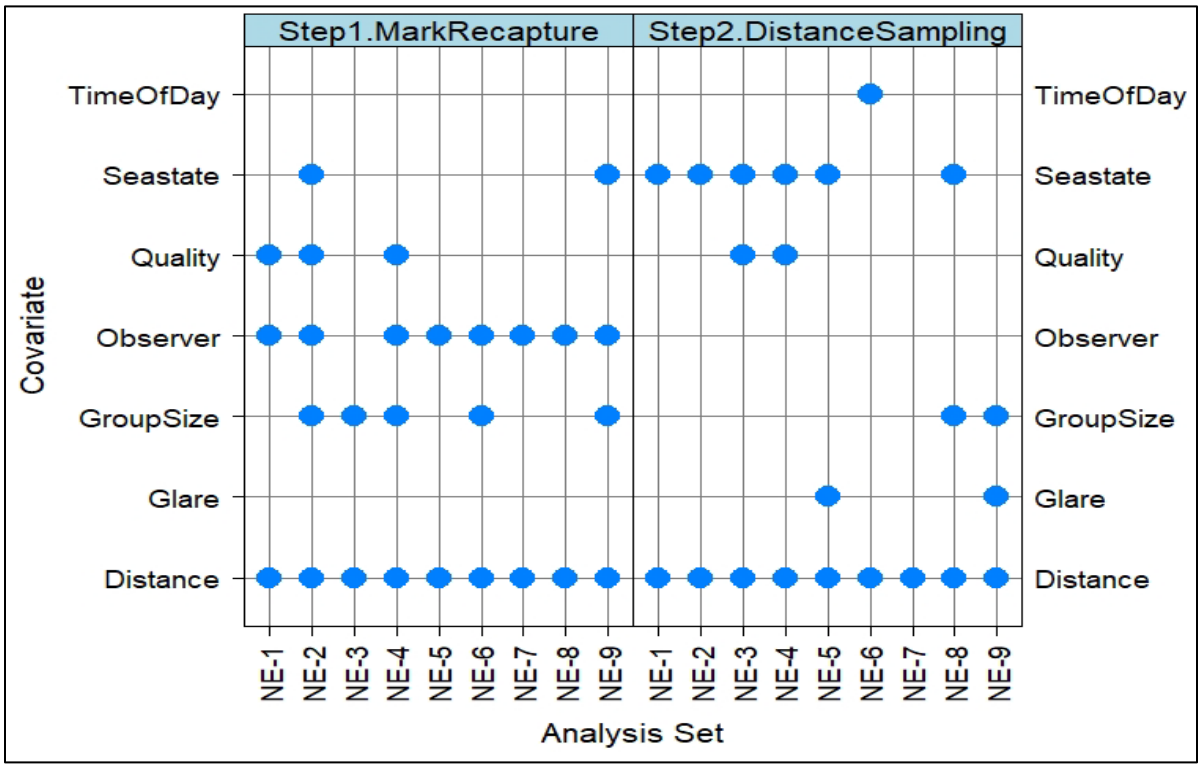

Figure 6-8 NE aerial distance sampling and mark-recapture models significant covariates

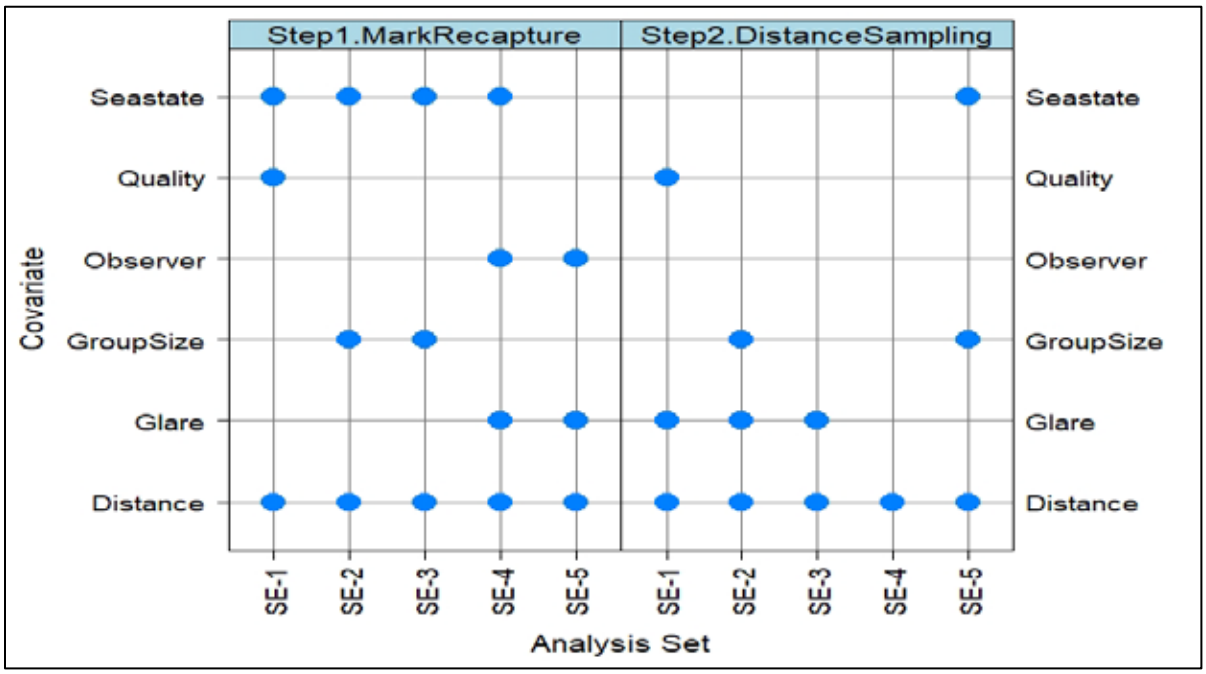

Figure 6-9 SE aerial distance sampling and mark-recapture models significant covariates

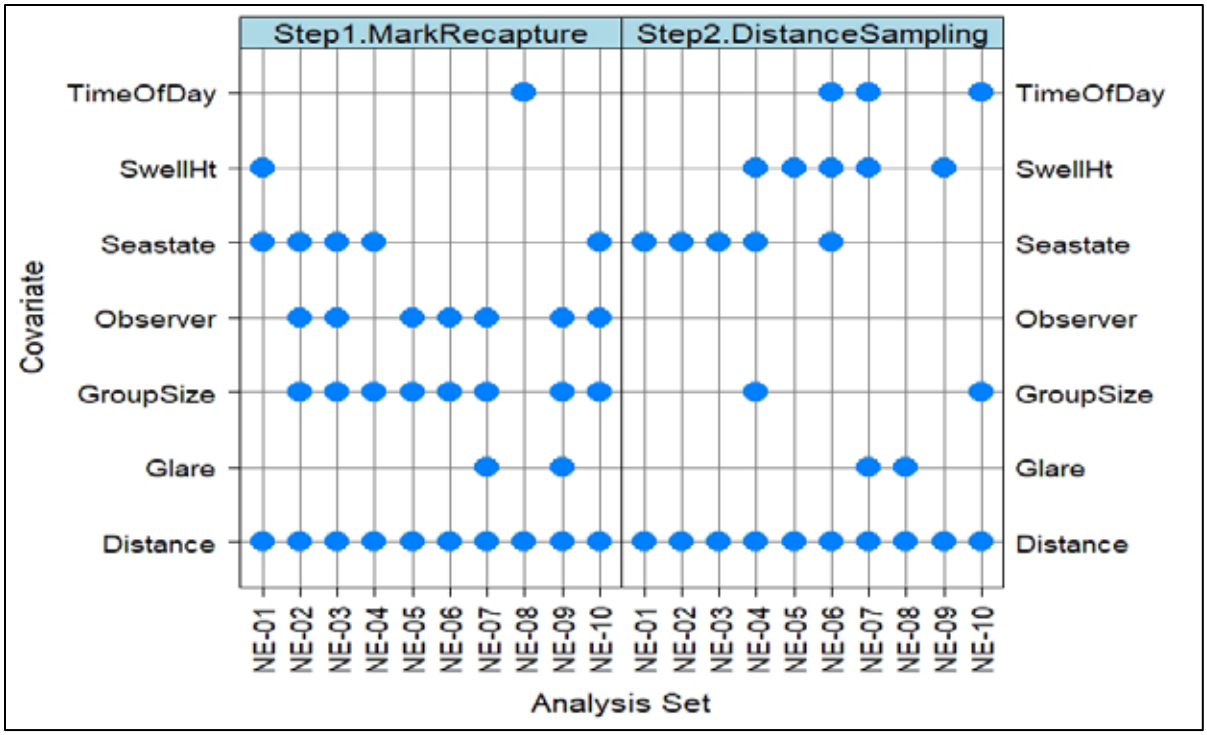

Figure 6-10 NE shipboard distance sampling and mark-recapture models significant covariates

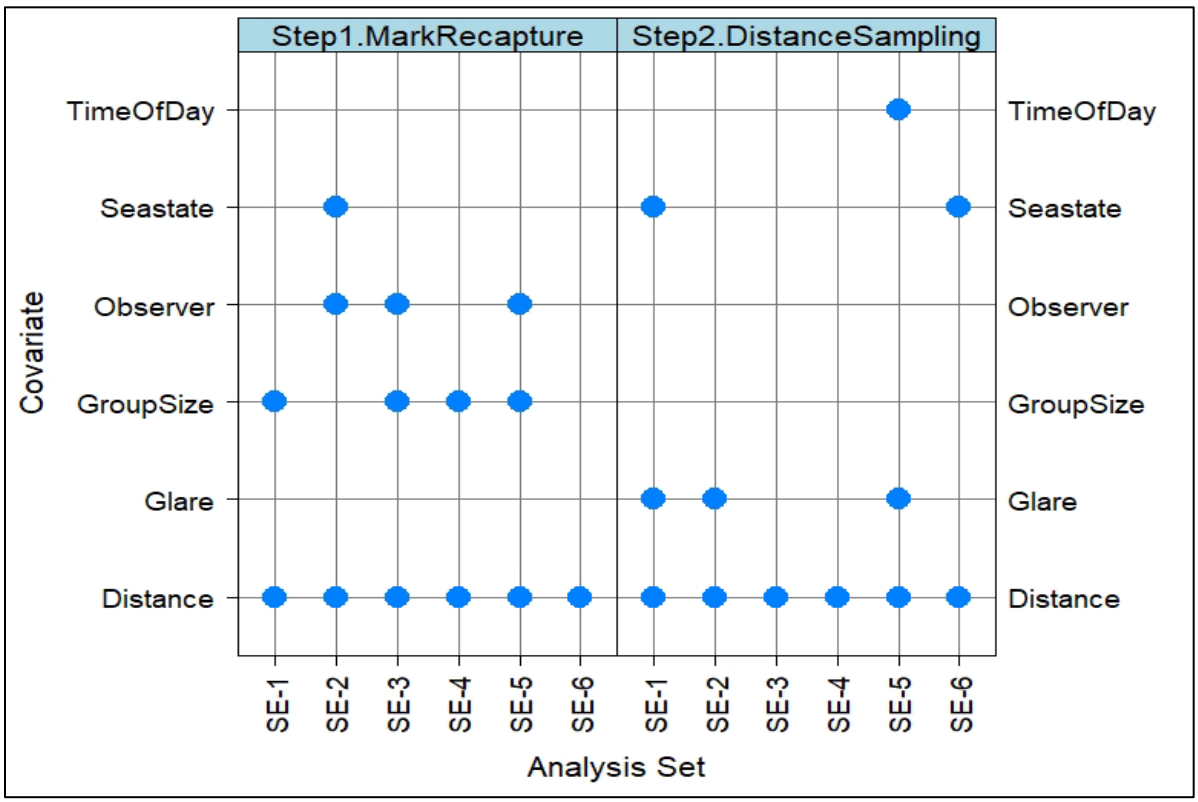

Figure 6-11 SE shipboard distance sampling and mark-recapture models significant covariates

6.2.2.3 Stage Two

The GAM density-habitat models of the relationship between the density estimates (perception and availability bias-corrected) and corresponding values of the static and contemporeous dynamic habitat covariates fit well according to the 4 diagnostic tests employed (Table 6-11). On average, the GAM density-habitat models explained 44% of the deviance (Figures 6-12 and 6-13). The percent deviance ranged from 24% (unidentified beaked whales) to 72% (striped dolphins), where, in general the dolphin models fit better than the large whale models. Latitude, bottom temperature, distance to the 1,000 m depth contour and SST were the most frequently chosen significant habitat covariates (Figure 6-14). In contrast, sea surface height anomaly and particulate organic carbon were the least frequently chosen. Interestingly, bottom temperature was a significant covariate twice as often as the commonly used SST covariate.

Several species displayed large differences within and between years. To develop a good fitting GAM density-habitat model under this situation, we used an interaction-like term between the temporal covariate we called “layer” and a habitat covariate, such as chlorophyll concentration, SST, or distance to the southern wall of the Gulf Stream. The covariate “layer” represented the 8-day timeframe within each year (for example, [year.8-day timeframe] 2010.1, 2010.2, …, 2010.46, 2011.1, 2011.2, …, 2011.46, … 2017.45, 2017.46). The species requiring an interaction-like term included Atlantic white-sided dolphins, common dolphins, common bottlenose dolphins, fin whales, harbor porpoises, humpback whales, and sei whales. When investigating long-term trends of the summer abundance estimates of common dolphins and harbor porpoises (section 5.7), we also found large inter-annual variability that we could explain by relationships with habitat covariates.

Table 6-11 Results of diagnostic tests to evaluate fit of the GAM density-habitat models
Diagnostic tests are the Spearman's rank correlation (RHO), mean absolute percentage error (MAPE) and mean absolute error (MAE). See Table 6-3 for more details on the tests.

Species	Non-Zero RHO[1]	Non-Zero MAPE	Random RHO	Random MAE
Atlantic spotted dolphin	0.101	95.64	0.123	0.040
Atlantic white-sided dolphin	0.104	91.00	0.097	0.012
Beaked whale – Cuvier's	0.187	85.39	0.110	0.003
Beaked whale – Sowerby's	0.185	91.29	0.142	0.006
Beaked whale – Unidentified	0.140	80.33	0.210	0.025
Common dolphin	0.358	99.14	0.169	0.146
Common bottlenose dolphin	0.325	83.80	0.181	0.069
Fin whale	0.190	89.90	0.124	0.002
Harbor porpoise – spread	0.318	94.43	0.157	0.143
Harbor porpoise – compact	0.318	81.18	0.181	0.377
Humpback whale	0.272	90.70	0.107	0.001
Pygmy or dwarf sperm whale	0.336	88.45	0.152	0.014
Minke whale	0.153	97.41	0.121	0.001
Pilot whale – long finned	0.374	87.76	0.189	0.005
Pilot whale – short finned	0.284	85.55	0.136	0.018
Risso's dolphin	0.251	84.20	0.165	0.023
Sei whale	0.335	98.75	0.063	0.0001
Sperm whale	0.187	86.82	0.146	0.002
Striped dolphin	0.233	76.88	0.138	0.039

[1]Color coding is:

Poor= x<0.05	Fair to good =0.05<=x<0.3	Excellent= x>0.3
Poor= x>150%	Fair to good= 150%>=x>50%	Excellent= x<=50%
Poor= x>1	Fair to good = 1>=x>0.25	Excellent= x<=0.25

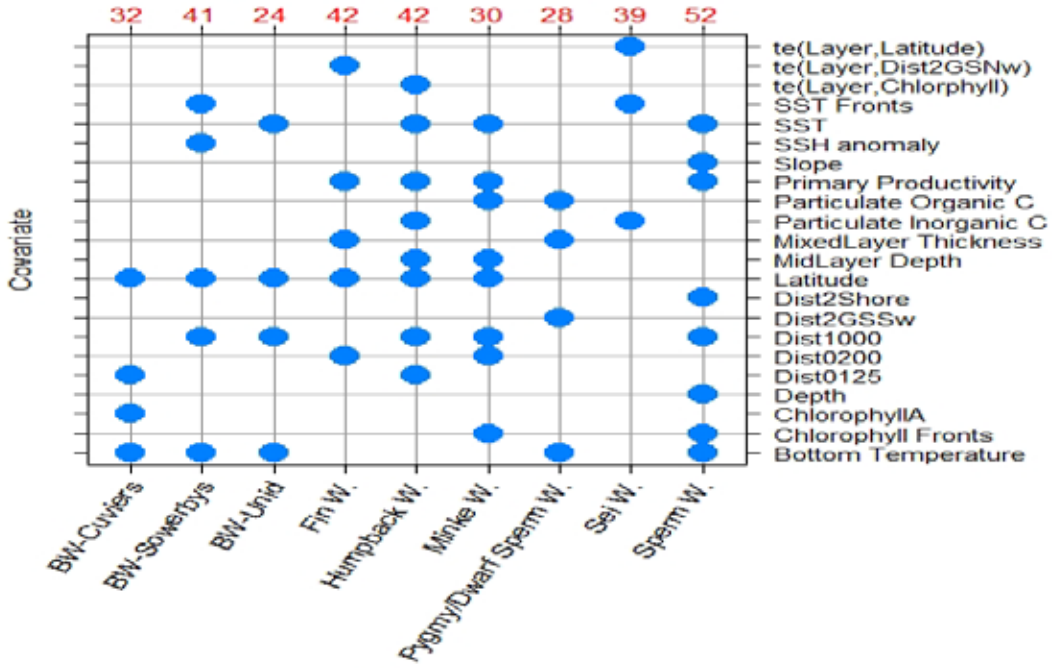

Figure 6-12 Significant habitat covariates for the GAM density-habitat models for whales
Percent deviance explained are the red numbers on top axis. Habitat covariates are described in Tables 6-1 and 6-2. BW = beaked whale. W = whale.

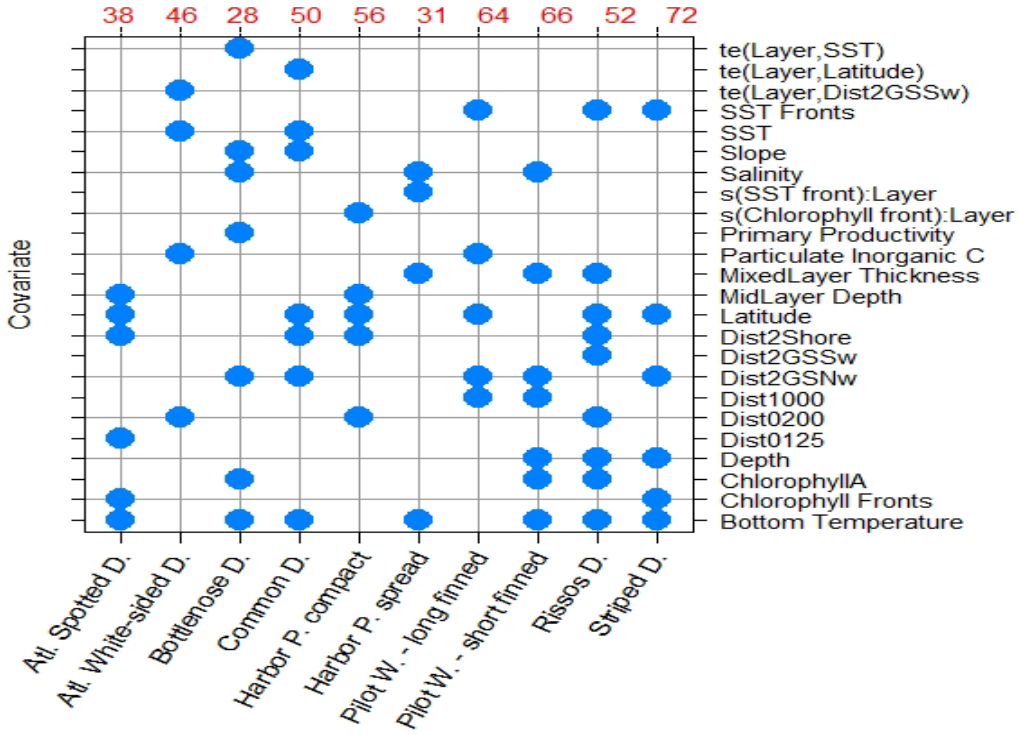

Figure 6-13 Significant habitat covariates for the GAM density-habitat models for dolphins
Percent deviance explained are the red numbers on top axis. Habitat covariates are described in Tables 6-1 and 6-2. D=dolphin. W=whale. P=porpoise.

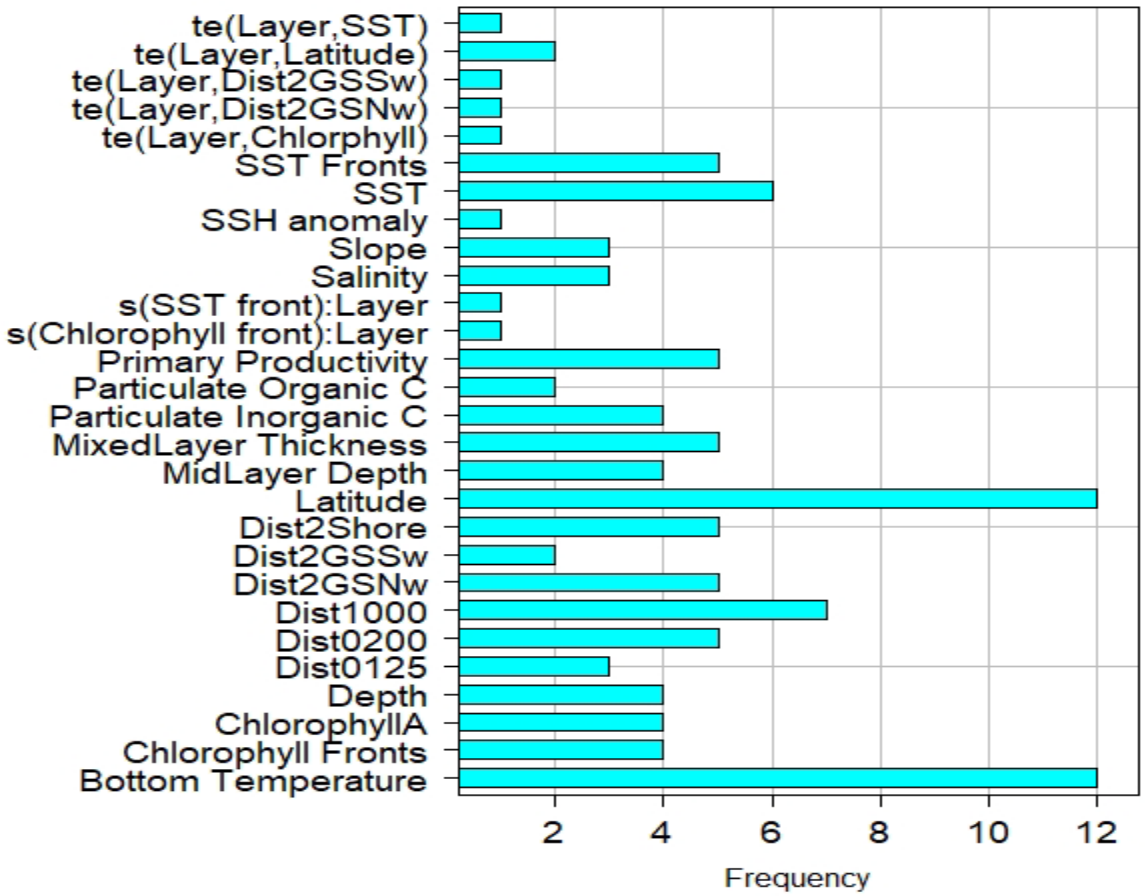

Figure 6-14 Frequency of habitat covariates in the GAM density-habitat models

6.2.2.4 Seasonal Abundance Estimates and Trends

A summary of the average seasonal abundance estimates for the entire AMAPPS study area for each of the cetacean species/species guilds is in Table 6-12. More details on the abundance estimates as divided by species are in Appendix I and as divided by wind-energy study areas are in Appendix III. We nearly always detected pygmy/dwarf sperm whales and beaked whales in only deep offshore waters that we predominately surveyed only in the summer. Consequently, we estimated their abundance for the summer season only.

Seasonal abundance patterns of a species/species guild were evident in the average seasonal abundance estimates (Table 6-12; Table 5 in each chapter in Appendix I) and in the annual abundance trend plots (Figure 5 in each chapter in Appendix I) summarized in Figure 6-15. Within a year, many species migrate up and down the coast and/or inside and outside of the AMAPPS study area (in other words, US waters), though at slightly different schedules resulting in peak abundance estimates in the AMAPPS study area at different times of the year (Figure 6-15). The species that had peak average abundance estimates during summer included the following: Atlantic spotted dolphins, common bottlenose dolphins, fin whales, Risso's dolphins, short-finned pilot whales, and striped dolphins. Species with a peak in late spring/early summer included humpback whales and minke whales. Species with a peak in late summer/early fall included harbor porpoises, short-finned pilot whales, and sperm whales. In addition, the species that had 2 peaks in average abundance with a decline in abundance during summer (August to September) were Atlantic white-sided dolphins, common dolphins, and sei whales.

Table 6-12 Average 2010 to 2017[1,2] seasonal abundances for each species or species guild
We also provided the coefficient of variation (CV) of the abundance and its lower and upper 95% confidence interval for the abundance (CI 2.5% and CI 97.5%, respectively).

Species and Season	Average Abundance	CV	CI 2.5%	CI 97.5%
Atlantic spotted dolphin				
Spring (Mar-May)	17,464	0.32	9,470	32,205
Summer (Jun-Aug)	44,947	0.30	25,282	79,907
Fall (Sep-Nov)	20,836	0.33	11,095	39,128
Winter (Dec-Feb)	3,855	0.40	1,812	8,203
Atlantic white-sided dolphin				
Spring	8,002	0.59	2,741	23,357
Summer	2,938	0.48	1,204	7,172
Fall	3,794	0.46	1,608	8,954
Winter	7,084	0.55	2,586	19,403
Beaked whales - summer				
Cuvier's	4,688	0.36	2,365	9,293
Sowerby's	1,001	0.49	403	2,485
Unidentified and others	9,592	0.20	6,506	14,141
Sum of all beaked whales	15,281	0.17	9,274	25,919
Common bottlenose dolphin				
Spring	30,423	0.29	17,431	53,099
Summer	55,040	0.27	32,725	92,571
Fall	44,812	0.27	26,644	75,369
Winter	25,912	0.28	15,123	44,398
Common dolphin				
Spring	34,295	0.42	15,565	75,566
Summer	77,109	0.34	40,325	147,449
Fall	80,751	0.37	40,017	162,949
Winter	38,748	0.39	18,533	81,011
Fin whale				
Spring	1,648	0.35	846	3,209
Summer	2,285	0.34	1,195	4,369
Fall	1,343	0.35	690	2,615
Winter	613	0.34	321	1,172
Harbor porpoise[1]				
Spring	29,006	0.58	10,095	83,342
Summer	60,388	0.26	36,580	99,691
Fall	39,137	0.32	21,233	72,172
Winter	27,454	0.53	10,353	72,801
Humpback whale				
Spring	581	0.44	238	1,238
Summer	1,366	0.42	599	2,908
Fall	414	0.42	184	892
Winter	111	0.46	44	248
Minke whale				
Spring	1,334	0.43	595	2,991
Summer	1,197	0.33	637	2,248
Fall	616	0.32	334	1,136
Winter	24	0.39	11	50
Pilot whale, long-finned[2]				
Spring	6,765	0.56	2,431	18,829

Summer	9,901	0.59	3,392	28,900
Fall	12,888	0.58	4,485	37,031
Winter	4,909	0.56	1,764	13,664
Pilot whale, short-finned				
Spring	8,497	0.34	4,444	16,248
Summer	29,091	0.31	16,066	52,675
Fall	11,654	0.32	6,320	21,491
Winter	1,961	0.44	860	4,473
Pygmy or dwarf sperm whale				
Summer	8,132	0.24	5,114	12,931
Risso's dolphin				
Spring	11,221	0.34	5,868	21,457
Summer	23,884	0.32	12,952	44,044
Fall	17,939	0.32	9,728	33,081
Winter	8,971	0.37	4,446	18,103
Sei whale[1]				
Spring	43	0.47	18	103
Summer	32	0.50	13	81
Fall	28	0.50	11	71
Winter	42	0.48	17	103
Sperm whale				
Spring	2,536	0.33	1,350	4,762
Summer	4,073	0.28	2,377	6,979
Fall	3,098	0.29	1,775	5,407
Winter	1,778	0.31	982	3,219
Striped dolphin				
Spring	50,904	0.33	27,107	95,593
Summer	61,195	0.33	32,587	114,919
Fall	48,944	0.34	25,595	93,591
Winter	46,238	0.34	24,180	88,417

[1] Harbor porpoise and sei whale estimates are for only the more recent timeframe 2014 to 2017.

[2] Long-finned pilot whale estimates are for only the more recent timeframe 2015 to 2017.

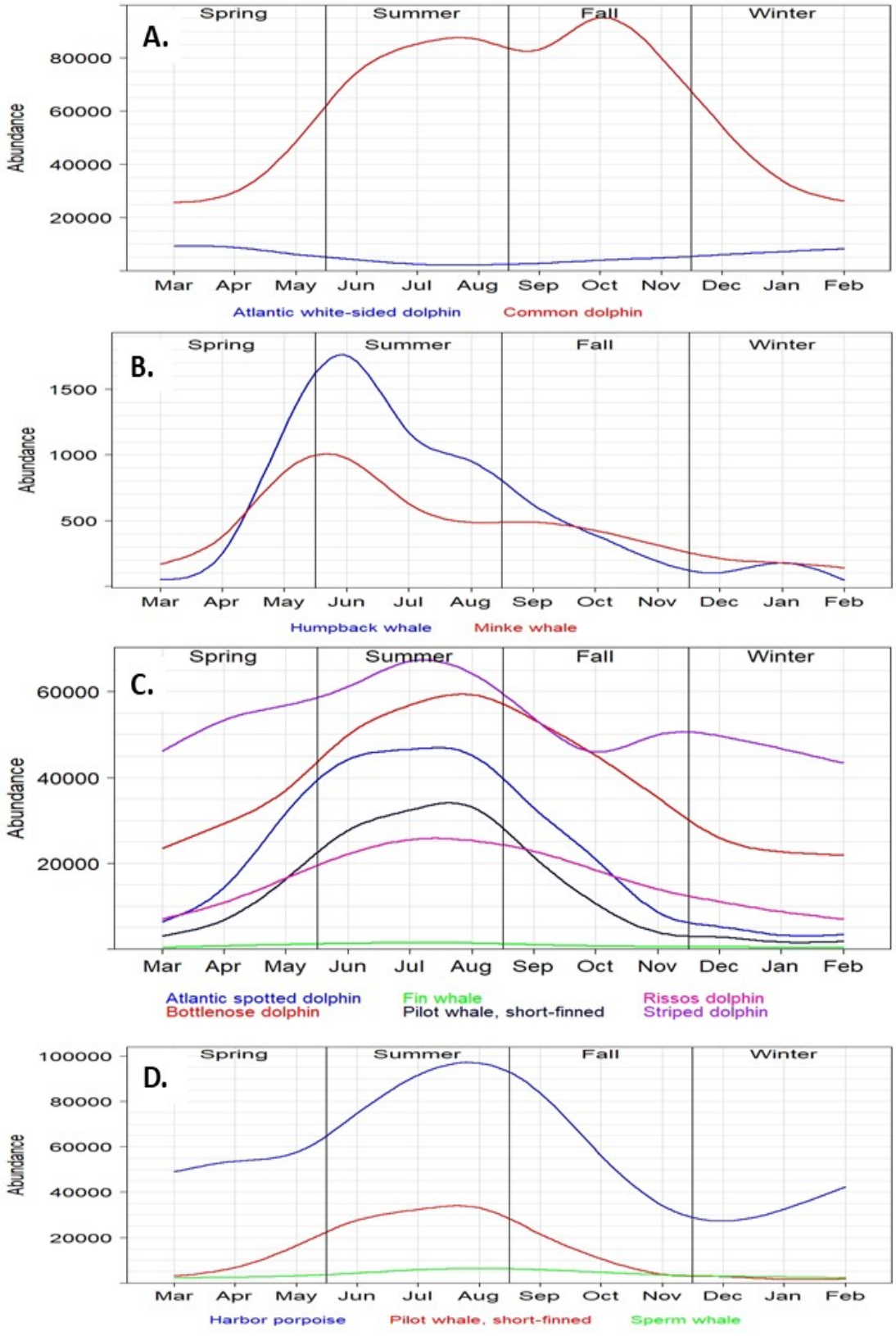

Figure 6-15 Average monthly abundance trends, by species

The results from the GAM density-habitat models also highlighted the interannual variability in the abundance of species in the AMAPPS study area, with dramatic effects from some species. For example, sei whale (Figure 6-16A; Figure 4-5 in Appendix I) abundance estimates varied dramatically before and after 2014. The GAM density-habitat model that best fit to the 2010 to 2017 data included the dynamic contemporeous habitat covariates SST fronts and particulate inorganic carbon, in addition to the interaction-like term between latitude and a temporal term (year-8 day layer). The interaction-like term explained most of the abundance patterns in this model, resulting in much larger predicted seasonal abundance estimates during 2010 to 2013 as compared to 2014 to 2017.

Another example of large interannual abundance variability is the annual abundance of harbor porpoises (Figure 6-16B; Figure 19-5 in Appendix I). As mentioned before, because of the clear spatial clustering patterns that changed dramatically throughout the year, we developed 2 GAM density-habitat models using data from warm versus cool times of the year. During warmer months (June to October), harbor porpoises were spatially clustered mostly in the Gulf of Maine. During cooler months (November to May), harbor porpoises were found dispersed throughout the study area. Even when accounting for this variability, the GAM density-habitat models for the 2 times of the year, still required a time varying interaction-like relationship with the strength of SST fronts or chlorophyll fronts. The interaction-like term was the second most important covariate (that is, a large contribution to the deviance in Table 19-3 in Appendix I). As a result, the average abundance estimates during 2010 to 2013 were larger within the AMAPPS area than that during 2014 to 2017. The difference in abundance between the 2 timeframes was largest in the summer and smallest in the winter (Figure 6-16B). During the summer, the 2016 spatially explicit estimates were smallest along the coasts of the U.S. and Canada (that is, the value of the 2016 average density estimate minus that from 2011 was the largest negative values in Figure 6-17A). This location is where the 2016 strength of the chorophyll fronts were the weakest (Figure 6-17B).

The GAM density-habitat model developed for long-finned pilot whales using data from 2010 to 2017 illustrated a temporal trend, whereas the abundance estimates during the more recent years (2015 to 2017) were larger than the previous years. However, when we fit a density-habitat model to only the 2015 to 2017 data, we produced a much better fitting model. Perhaps this discrepency indicates that the factors affecting the spatiotemporal density relationship to the habitat covariates varied between the 2 timeframes (before and after 2015). We couls also interpret this discrepancy to mean the GAM density-habitat model developed from the entire time series (2010 to 2017) was not able to accurately capture the interannual variability. Therefore, the information for long-finned pilot whales in Appendix I and Table 6-12 pertains to only the more recent timeframe, 2015 to 2017.

The habitat covariates involved in the interaction-like terms with time from GAM density-habitat models for other species were distance to the south wall of the Gulf Stream (Atlantic white-sided dolphin model), SST (common bottlenose dolphin), latitude (common dolphin), distance to the north wall of the Gulf Stream (fin whale), and chlorophyll front strength (humpback whale). Another way that we displayed the interannual differences is with the seasonal spatial location of the core habitat in different years, such as that done for common dolphins in Chavez-Rosales et al. (2019; Figure 6-18). We defined the core habitat as the location of spatiotemporal strata with the upper 80th percentile of the density estimates. These plots clearly show that in 2017, common dolphins tended to move farther north and spread out more than that seen earlier in 2010.

Species that demonstrated what appears to be mostly random interannual varability and no obvious interannual temporal trend included the warm-water offshore species (many of which were only modeled for summer): Cuvier’s beaked whales, Sowerby’s beaked whales, unidentified beaked whales, unidentified Kogia spp. (pygmy or dwarf sperm whales), short-finned pilot whales, Risso’s dolphins, Atlantic spotted dolphins, and striped dolphins.

Beaked whales are difficult to identify because they do not stay at the surface for long and do not expose a large portion of their bodies. Thus, we were only able to identify many sightings as some sort of beaked whale. However, our ability to identify the more common species like Cuvier's, Sowerby's and True's beaked whales has been improving each year. The average abundance for positively identified Cuvier's beaked whales (Figure 7-5 in Appendix I) in the more recent years is slightly higher than in previous years. This increase could be due to our increased ability to identify this species in recent years, environmental habitat variability, or random survey observation error. However, we did not see this trend when we added together the abundance estimates for all 3 categories of beaked whales (Figure 6-19). Thus, this indicates the Cuvier's beaked whale abundance trend was mostly due to our increasing ability to identify these species.

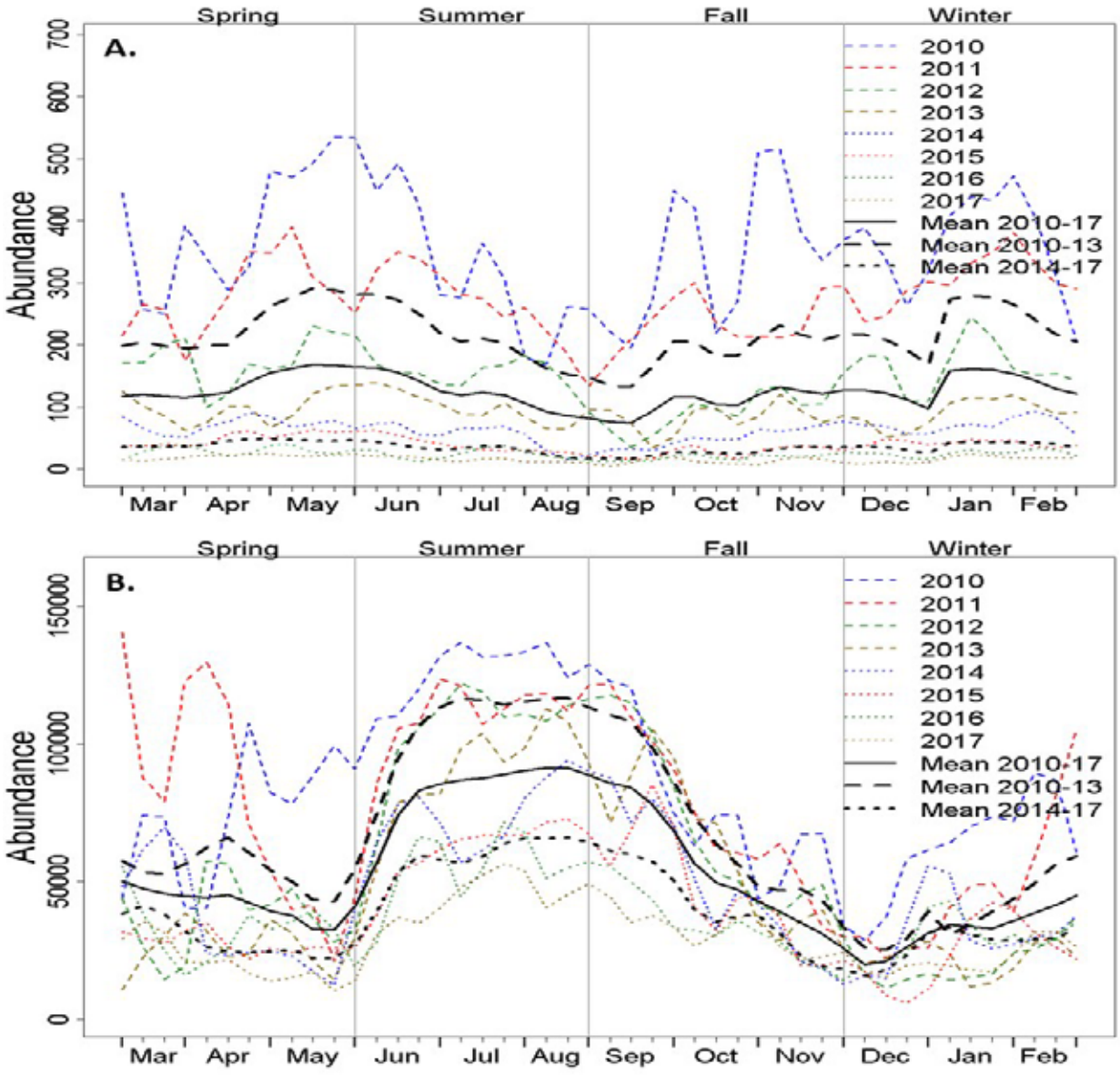

Figure 6-16 Predicted annual abundance trends for sei whales (A) and harbor porpoises (B)

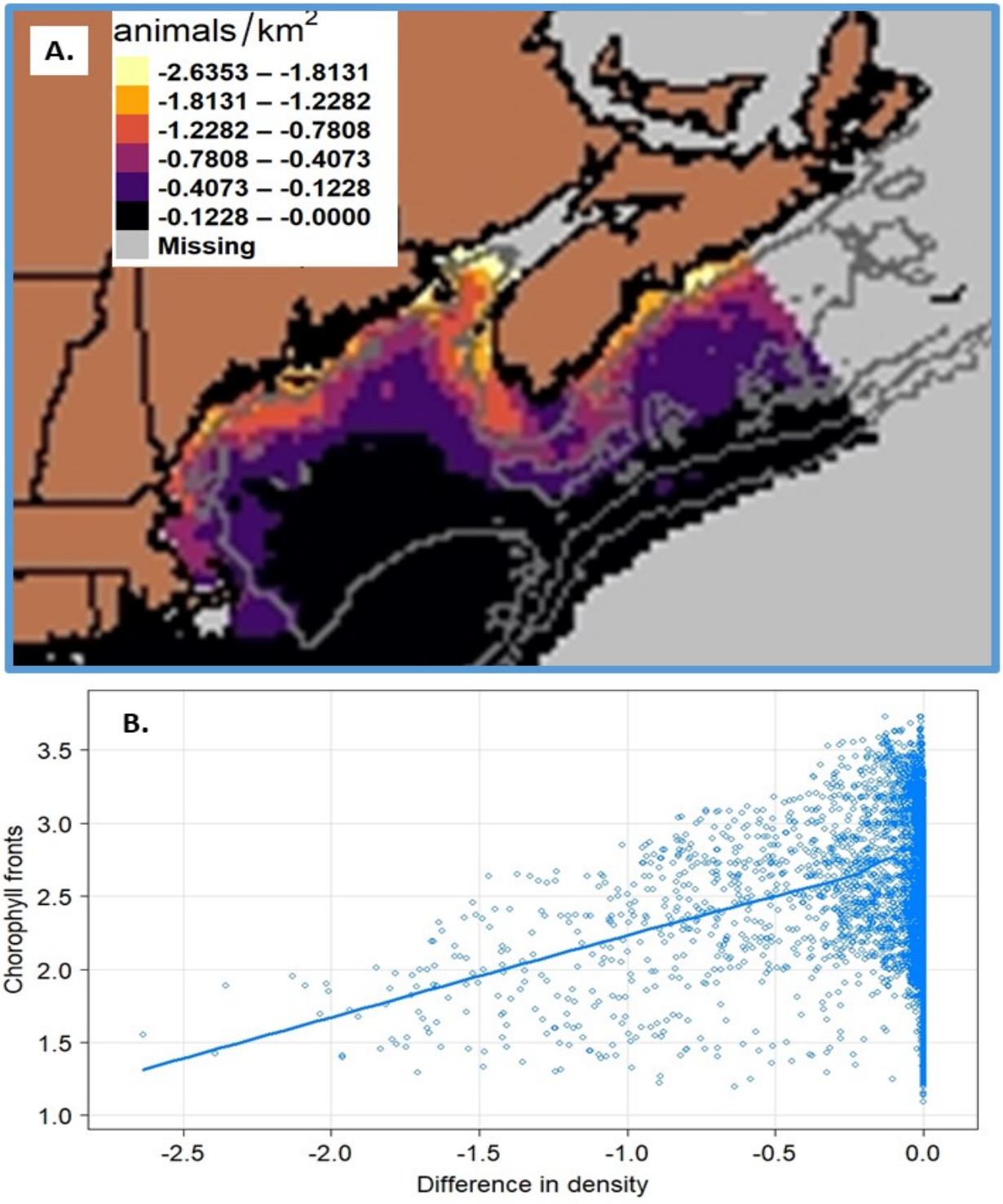

Figure 6-17 Difference between the harbor porpoise predicted summer density in 2011 and 2016 (A) Map of the spatial distribution of the summer density difference (2016 density minus 2011 density). (B) Relationship between density difference and values of the strength of chlorophyll fronts in 2016 for each spatiotemporal stratum.

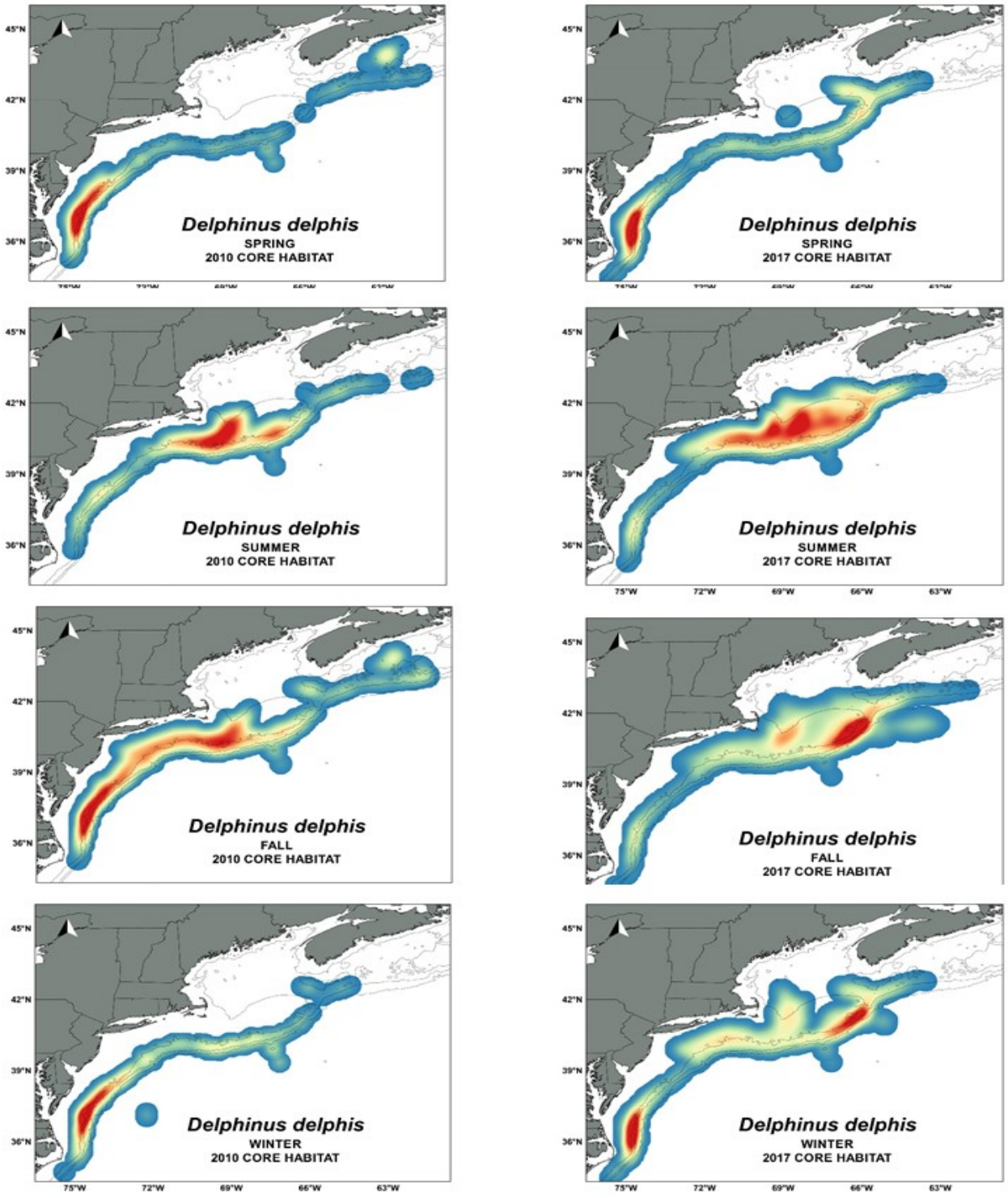

Figure 6-18 Contrasting spatial seasonal core habitat of common dolphins between 2010 and 2017
Core habitat defined as the top 80th percentile of the abundance. Figure from Chavez-Rosales et al. (2019). Red regions have the highest densities and dark blue the lowest densities.

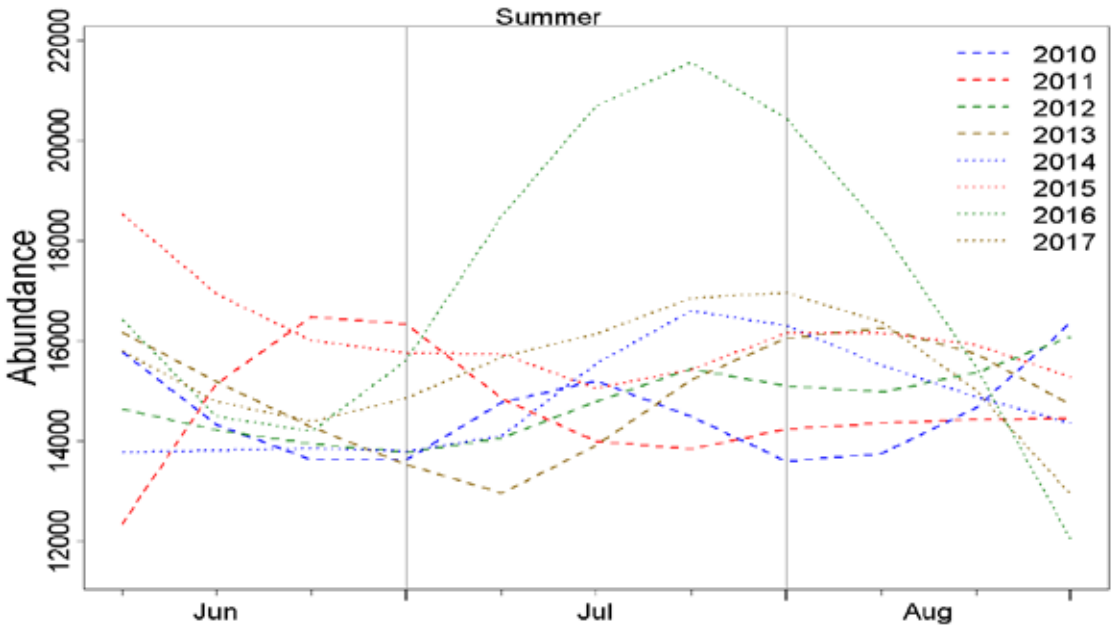

Figure 6-19 Annual abundance trends of the sum of all beaked whales, by year

6.2.2.5 Wind Energy Areas

The U.S. Atlantic wind-energy study areas (Figure 2-1) are in waters that are less than 100 m deep. This location influences which species inhabitat the waters in and around the wind-energy study areas. Details related to the survey efforts and resulting species abundance/density estimates within each wind-energy study area are in Appendix III. In summary, the wind-energy study areas north of Cape Hatteras, NC, are the most diverse, where 13 to 16 species utilized the waters in the wind-energy study areas, at least for part of the year and/or region within the wind-energy study areas (Table 6-13). The Rhode Island/Massachusetts wind-energy study area had the highest average (2,080 animals) of the 4 seasonal abundance estimates for all species, where the average was over the years of 2010 to 2017. Common dolphins, harbor porpoises, and bottlenose dolphins were the most abundant species. Humpback whales and minke whales were the most abundant large whales. The North Carolina/South Carolina wind-energy study area had the second highest average annual abundance (1,473 animals from only 7 species). Bottlenose dolphins and Atlantic spotted dolphins were the most abundant species. Large whales were only infrequent visitors.

Table 6-13 Average seasonal abundance of all cetaceans in each wind-energy study area

Wind Energy Study Area	Number of Species	Average Abund - Spring	Average Abund - Summer	Average Abund - Fall	Average Abund - Winter	Average of Seasonal Abund
Rhode Island/ Massachusetts	14	1,393	3,137	2,235	1,552	2,079.5
New York	14	373	248	188	391	300.1
New Jersey	13	903	378	443	1,126	712.4
Delaware/Maryland	13	566	251	337	820	493.5
Virginia	13	426	232	319	613	397.4
North Carolina	16	727	646	576	735	671.1
North Carolina/ South Carolina	7	1,096	2,366	1,696	732	1,472.7

The species that inhabited the wind-energy study areas and was sensitive to high frequency sounds was the harbor porpoise. Although pygmy or dwarf sperm whales infrequently visited the North Carolina wind-energy study area. During the nonsummer months, harbor porpoises visited mostly the northernly wind-energy study areas (Figure 6-20).

Species sensitive to medium frequency sounds that inhabited the wind-energy study areas included Atlantic spotted dolphins, Atlantic white-sided dolphins, all beaked whales, common bottlenose dolphins, common dolphins, pilot whales, Risso's dolphins, sperm whales, and striped dolphins. The largest numbers of these species were in the Rhode Island/Massachusetts and North Carolina/South Carolina wind-energy study areas (Figure 6-21A-B). The temporal abundance patterns throughout the year varied by the wind-energy area, as the species migrated in different directions relative to each other causing pulses of animals within the wind-energy study areas. For example, bottlenose dolphins are the most abundant species in the New Jersey wind-energy study area during the summer. However, in the spring and fall, common dolphins and harbor porpoises arrived in the New Jersey wind-energy study area and become the most abundant species (Appendix III).

Species sensitive to low frequency sounds that inhabited the wind-energy study areas included fin whales, humpback whales, minke whales, and sei whales. These species were mostly in the northern wind-energy study areas: Rhode Island/Massachusetts, New York, and New Jersey (in that order; Figure 6-21C-D). In all of the wind-energy study areas, the largest numbers of low-frequency sensitive species occurred from late spring to midsummer (May to July), with the lowest numbers in the winter (December to February).

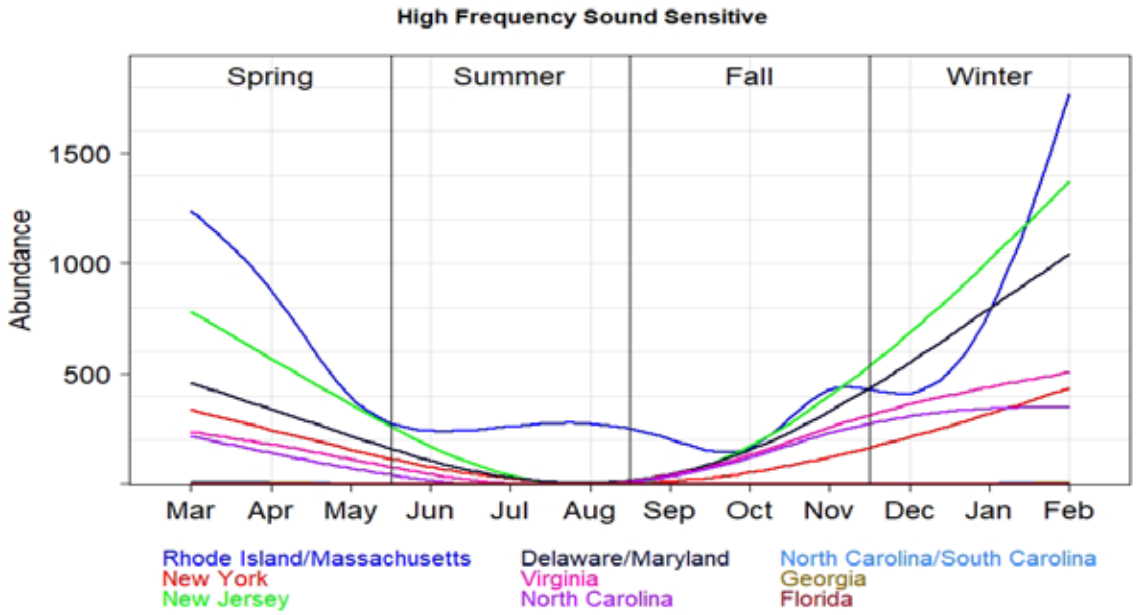

Figure 6-20 Abundance of high frequency sensitive species, by wind-energy study area
High frequency sensitive species include harbor porpoises, dwarf sperm whales, and pygmy sperm whales

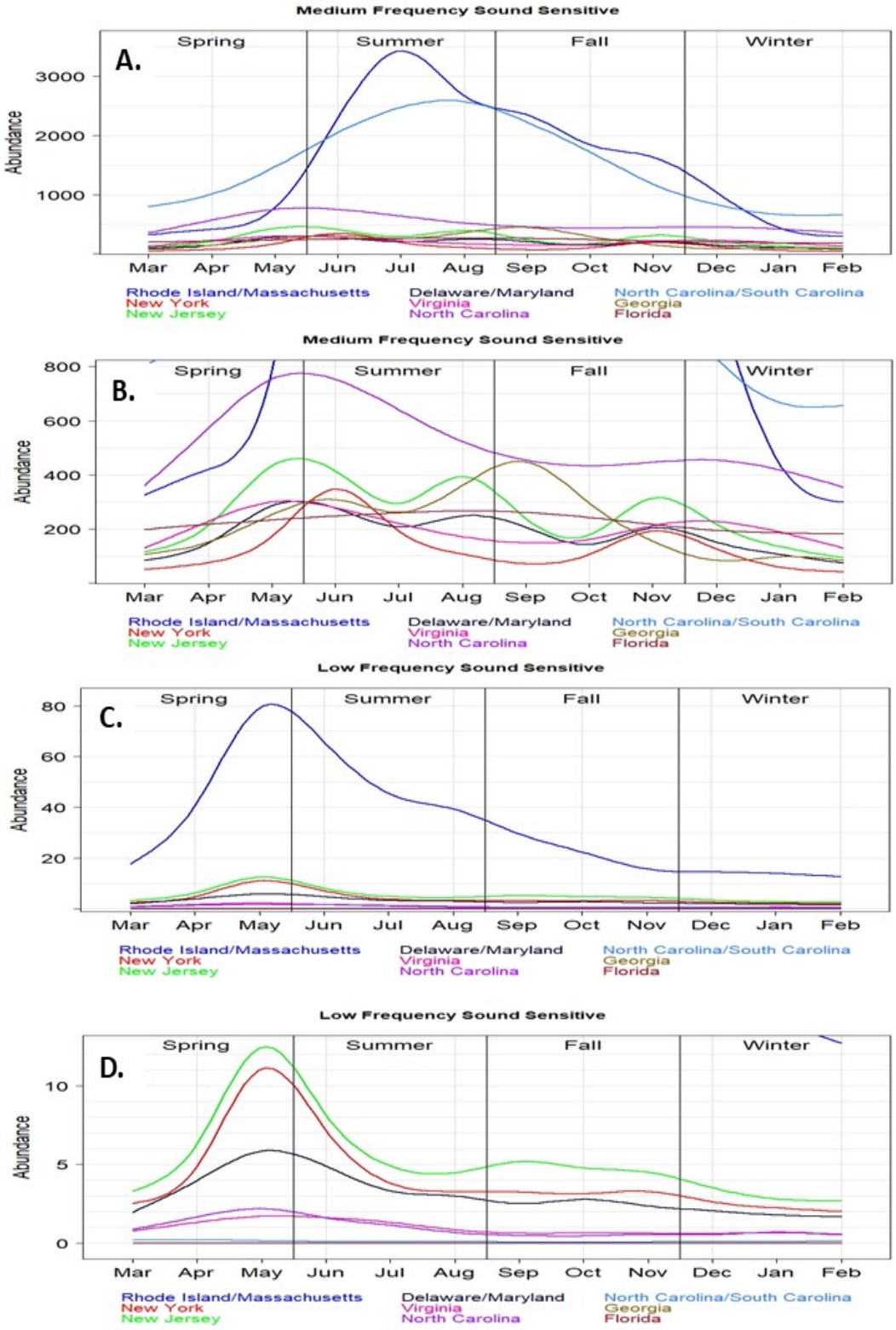

Figure 6-21 Abundance of medium/low frequency sensitive species, by wind-energy study area
Medium frequency sensitive species include Atlantic spotted dolphins, Atlantic white-sided dolphins, all beaked whales, common bottlenose dolphins, common dolphins, pilot whales, Risso's dolphins, sperm whales, and striped dolphins. Low frequency sensitive species include fin whales, humpback whales, minke whales, and sei whales.

6.2.3 Comparison to Other Studies

The spatiotemporal maps and abundance estimates that we developed in this chapter used visual sightings data collected from aerial and shipboard AMAPPS surveys conducted during 2010 to 2017 (Tables 11-3 to 11-6), in addition to contemporaneous dynamic spatial covariates (Table 6-1) and static habitat covariates (Table 6-2). We collected the AMAPPS data over a broad scale and developed spatiotemporal density-habitat models that predicted the distribution on a relatively small spatial scale (10 km x10 km) and short temporal scale (8-days). Then, to summarize the animal's distribution patterns we produced average seasonal density maps. However, other data sources also provide insights into the animal's distribution patterns. For example, some researchers collected fine-scale visual sighting data from parts of the AMAPPS study area, while other researchers collected data from various sources, such as animal-borne tags, species identification photographs, and passive acoustics. Each type of data provides a focus on different spatiotemporal scales and each have pros and cons when it comes to interpreting the resulting distribution and abundance patterns for a species. Nevertheless, gathering all data sources together provides the most complete picture of the spatiotemporal distribution and abundance. Here we highlight the consistent and inconsistent distribution patterns derived from other studies as compared to the contemporaneous density-habitat models derived from the AMAPPS data. In most cases, the distribution patterns were similar. However, in a few cases, the places with inconsistencies highlight where we can improve our density-habitat models or improve our data collection. In addition, in a few cases, it is impossible to discern which interpretation is most accurate.

6.2.3.1 Atlantic Spotted Dolphins

In summary, observed distribution patterns of Atlantic spotted dolphins from other studies were consistent with those predicted by the AMAPPS model (Appendix I, chapter 16).

In the New York bight from Long Island to the 1000 m depth contour 2 survey programs collected distribution data: the New York bight visual aerial surveys flew during March 2017 to February 2020 (Tetra Tech and LGL 2020) and the NYSERDA ultra-high resolution digital aerial surveys flew during summer 2016 to spring 2019 (Normandeau and APEM 2020). The digital surveys infrequently detected Atlantic spotted dolphins in waters about 50 to 200 m deep during the fall and spring. The visual surveys did not postitively identify this species.

McAlarney et al. (2018a, b) conducted several aerial surveys focused on waters from the midshelf to about the 2000 m depth contour from Chesapeake Bay, VA to Cape Hatteras, NC in 2017 during May to August, with less searching efforts in Feburary and September. They detected Atlantic spotted dolphins dispersed throughout their study area, although they detected this species most frequently in shallow waters less than 100 m and in waters deeper than 1000 m.

Off Jacksonville, FL, Foley et al. (2019) conducted aerial surveys from January 2009 through November 2017 spanning waters 100 to 1200 m deep. They detected Atlantic spotted dolphins year-round mostly in shallow shelf water.

6.2.3.2 Beaked Whales

In summary, observed distribution, patterns of beaked whales from other studies were consistent with those predicted by the AMAPPS models (Appendix I, chapters 7-9).

In the New York bight from Long Island to the 1000 m depth contour, 2 survey programs collected distribution data: the New York bight visual aerial surveys flew during March 2017 to February 2020 (Tetra Tech and LGL 2020) and the NYSERDA ultra-high resolution digital aerial surveys flew during summer 2016 to spring 2019 (Normandeau and APEM 2020). These surveys detected beaked whales (usually not identified to species) in waters deeper than 200 m year-round.

Engelhaupt et al. (2016, 2017, 2018, 2019, and 2020a, b) conducted shipboard sighting surveys off Chesapeake Bay, VA from the coast to about the 1500 to 2000 m depth contours. The beaked whale sightings (Cuvier's, Sowerbys, True's, and unidentified mesoplodon) they detected were in waters deeper than the 1000 m depth contour. This is consistent with the beaked whale AMAPPS models, where the density off Chesapeake Bay (and further north) in deeper waters off the shelf is high, and that on the shelf is nearly zero.

Cuvier's beaked whales: The distribution of the locations of visual sightings (Engelhaupt et al. 2016, 2017, 2018, 2019, and 2020a, b; McAlarney et al. 2018a, b; McLennan et al. 2018), tag tracks (Foley 2018; Baird et al. 2019, and vocalization patterns detected on HARPs (high-frequency recording packages; Stanistreet 2017; Rafter et al. 2020a, b) were consistent with the AMAPPS model. Around Cape Hatteras, NC, the visual sightings and tag tracks indicated highest densities in waters deeper than 1000 m and north of Cape Hatteras, NC. Stanistreet (2017) detected vocalizations of Cuvier's beaked whales throughout the year off Cape Hatteras, NC (listening sites were in waters 850 to 1000 m depth). The frequency of vocalizations (hrs per week) was much less near Norfolk Canyon, VA (980 m) and on Georges Bank (800 m), while nearly absent at Onslow Bay, NC (south of Cape Hatteras, NC in 900 m water) and off Jacksonville, FL (800 m). The distribution patterns resulting from the AMAPPS model were consistent with these general patterns. However, in waters deeper than the locations of the HARP listening sites (that is in waters deeper than 1000 m) the AMAPPS model predicted the relative summer densities were higher than that where the HARPs were located. The model predicted particularly high densities south of Georges Bank in US and Canadian waters.

Foley (2018) showed that the environmental predictors associated with the locations of tagged Cuvier's beaked whales were distance to shelfbreak, latitude, and bottom slope. Similarly, the environmental predictors that best fit the AMAPPS model visual sightings data included similar static covariates (latitude, bottom depth, and distance to the 125 m depth contours). However, the Cuvier's beaked whale AMAPPS model also included the contemporaneous dyamic factors surface chlorophyll concentration and bottom temperature. Latitude and bottom temperature were the most important covariates in the AMAPPS model.

Sowerby's beaked whales: Engelhaupt et al. (2019; 2020a) reported on sightings, photo-identification and tagged Sowerby's beaked whales near Norfolk Canyon off Virginia. All encounters were in waters deeper than about 1000 m, and the tagged animal moved north for about 135 km. Stanistreet (2017) indicated that the HARP passive acoustic monitoring sites located south of the Gully (south of Nova Scotia) could not reliably detect Sowerby's high frequency clicks. Despite this, they did detect some vocalizations on Georges Bank (800 m deep) and near Norfolk Canyon, off Virginia (980 m). Off Cape Hatteras, NC in waters about 1000 to 1400 m deep, Rafter et al. (2020) detected small numbers of Sowerby's beaked whales with several occurrences in January and February 2019. Off Jacksonville, FL in 800 m waters, Rafter et al. (2020) reported a single vocalization of a Sowerby's beaked whale in September 2018. The AMAPPS model predicted densities to be greatest in waters deeper than 1000 m, which is deeper than the locations of most of the HARPs mentioned above.

Gervais' beaked whale: Passive acoustic monitoring detected Gervais'/True's beaked whale vocalizations from Georges Bank to offshore of Jacksonville, FL (Stanistreet 2017). The highest frequency of vocalizations was at Onslow Bay (south of Cape Hatteras, NC), and the next highest off Cape Hatteras, NC. There were only a few vocalizations at the Georges Bank (800 m) and Jacksonville, FL (800 m) sites. Rafter et al. (2020) detected Gervais'/True's beaked whales intermittently off Cape Hatteras, NC with most detections from April to May 2019 in waters that were about 1000 to 1400 m deep. McLellan et al. (2018) detected Gervais' beaked whales in waters deeper than 1000 m, where most were south of Cape Hatteras, NC in Onslow Bay and only a few north of Cape Hatteras, NC.

Blainville's beaked whales: Stanistreet (2017) reported Blainsville's beaked whale vocalizations on only 1% of the monitored days at Cape Hatteras, NC, 5% at Onslow Bay, NC and 0.7% at Jacksville, FL. No Blainville's beaked whale vocalizations were on the 3 HARPs during June 2018 to September 2019 off Cape Hatteras, NC (located in waters about 1000 to 1400 m deep; Rafter et al. 2020).

6.2.3.3 Common Dolphins

In summary, observed distribution patterns of common dolphins from other studies were consistent with those predicted by the AMAPPS model (Appendix I, chapter 15).

In the New York bight from Long Island to the 1000 m depth contour, 2 survey programs collected distribution data: the New York bight visual aerial surveys flew during March 2017 to February 2020 (Tetra Tech and LGL 2020) and the NYSERDA ultra-high resolution digital aerial surveys flew during summer 2016 to spring 2019 (Normandeau and APEM 2020). Both survey programs detected common dolphins throughout the study area year-round.

Within and around the Maryland wind energy area, Bailey et al. (2019) recorded common dolphin vocalizations only offshore of the wind energy area and only from December to May.

Off Virginia and North Carolina, McAlarney et al. (2018a, b) conducted several aerial surveys focused on waters from the midshelf to about the 2000 m depth contour from Chesapeake Bay, VA to Cape Hatteras, NC in 2017 during May to August, with less searching efforts in Feburary and September. In addition, Engelhaupt et al. (2016, 2017, 2018, 2019, and 2020a) conducted shipboard sighting surveys in waters off Chesapeake Bay, VA, that spanned from the coast to offshore of the shelfbreak. These surveys detected common dolphins mostly on the shelf slope in waters 100 to 1000 m deep, with only a few sightings in waters shallower than 100 m deep.

6.2.3.4 Common Bottlenose Dolphins

In summary, observed distribution patterns of common bottlenose dolphins from other studies were consistent with those predicted by the AMAPPS model (Appendix I, chapter 18).

In the New York bight from Long Island to the 1000 m depth contour, 2 survey programs collected distribution data: the New York bight visual aerial surveys flew during March 2017 to February 2020 (Tetra Tech and LGL 2020) and the NYSERDA ultra-high resolution digital aerial surveys flew during summer 2016 to spring 2019 (Normandeau and APEM 2020). Both survey programs detected common bottlenose dolphins throughout the study area year-round.

In and around the Maryland wind energy area, Bailey et al. (2019) recorded common bottlenose dolphin vocalizations year-round within and inshore of the wind energy area, but limited to summer and fall offshore of the wind energy area.

Off Virginia and North Carolina, McAlarney et al. (2018a, b) conducted several aerial surveys focused on waters from the midshelf to about the 2000 m depth contour from Chesapeake Bay, VA to Cape Hatteras, NC in 2017 during May to August, with less searching efforts in Feburary and September. In addition, Engelhaupt et al. (2016, 2017, 2018, 2019, and 2020a) conducted shipboard sighting surveys in waters off Chesapeake Bay, VA, that spanned from the coast to offshore of the shelfbreak. These surveys detected common bottlenose dolphins mostly either close to land or on the shelfbreak in waters shallower than 1000 m deep.

Off Jacksonville, FL, Foley et al. (2019) conducted aerial surveys from January 2009 through November 2017 spanning waters 100 to 1200 m deep. They detected common bottlenose dolphins year-round mostly in waters about 100 to 700 m deep. The AMAPPS model was consistent with these patterns.

6.2.3.5 Fin Whales

In summary, the AMAPPS fin whale model (Appendix I, chapter 3) produced spatiotemporal distribution and density patterns that were consistent with patterns depicted from other studies, particularly in waters north of Cape Hatteras, NC. The modeled patterns south of Cape Hatteras, NC were less certain and perhaps biased low due to low survey efforts. Interestingly, a fin whale tagged off close to the Virginia coast traveled beyond the offshore edge of the AMAPPS study region off South Carolina through a region predicted to have very low density.

In the New York bight from Long Island to the 1000 m depth contour, 2 survey programs collected distribution data: the New York bight visual aerial surveys flew during March 2017 to February 2020 (Tetra Tech and LGL 2020) and the NYSERDA ultra-high resolution digital aerial surveys flew during summer 2016 to spring 2019 (Normandeau and APEM 2020). Both survey programs concluded that fin whales were the most common whale, with a peak in the summer months. The fin whales were located throughout the study area with a peak on the shelfbreak (100 to 1000 m deep).

In and around the Maryland wind energy area, Bailey et al. (2019) found fin whale vocalizations to be the most frequently acoustically detected large whale. The vocalizations were mostly offshore of the wind energy area and in the winter and spring months (November to March). The AMAPPS fin whale model for this area, predicted a low nearly constant year-round abundance (less than 5 fin whales on average on any day), contradicting the reported acoustic temporal pattern but consistent with the acoustic spatial pattern.

In and around the Virginia wind energy area, Salisbury et al. (2019) found fin whales vocalizations to be the most frequently acoustically detected large whale. They recorded fin whale vocalizations throughout the shelf off the mouth of Cheaspeake Bay, VA, with a peak closer to the shelfbreak. The vocalizations were present year-round with a peak during winter (October through February) and the least during summer (June through August). The AMAPPS fin whale model for this area, predicted a low nearly constant year-round abundance (less than 2 fin whales on average on any day), contradicting the reported acoustic temporal pattern but consistent with the acoustic spatial pattern. However, Salisbury et al. (2019) reported that it is difficult to define peak seasonal presence due to the large inter-annual variability, so the 2 data sources may not actually present contradictory results.

Off Virginia and North Carolina, McAlarney et al. (2018a, b) conducted several aerial surveys focused on waters from the midshelf to about the 2000 m depth contour from Chesapeake Bay, VA to Cape Hatteras, NC in 2017 during May to August, with less searching efforts in Feburary and September. In addition, Engelhaupt et al. (2016, 2017, 2018, 2019, and 2020a) conducted shipboard sighting surveys in waters off Chesapeake Bay, VA, that spanned from the coast to offshore of the shelfbreak. These surveys infrequently detected fin whales on the midshelf (in waters 30 to 100 m deep), while most were offshelf in waters deeper than about 1000 m. The Baumgartner (2019) January 2019 glider surveys acoustically detected a couple fin whales just north of Cape Hatteras, NC, on the midshelf, and a couple possible fin whales south of Cape Hatteras, NC on the shelf. Engelhaupt et al. (2020a) initially photographed 13 fin whales on the shelf and then re-photographed the same individuals again on the shelf, where for some individuals they took the subsequent photographs over 200 days after the initial photograph. Six fin whales tagged on the shelf in 2017 off Chesapeake Bay, VA stayed mostly on the shelf, a few visited water close to the coast, and a few visited the offshelf waters that were up to 1800 m deep (Engelhaupt et al. 2018). A unique track was from a fin whale tagged in March 2017 north of Cheasapeake Bay, VA close to the coast. This animal traveled south to the offshelf waters outside of the AMAPPS region (about 30°N 70°W) and then back to shelfbreak waters off Chesapeake Bay, VA. This animal's tracks traveled through areas south of Cape Hatteras, NC where the fin whale AMAPPS model predicted the density was nearly 0. The AMAPPS fin whale model was consistent with the above midshelf and offshelf patterns.

The passive acoustic monitoring devices described in Chapter 7 (Figures 7-12 to 7-13) detected fewer fin whale vocalizations south of Cape Hatteras, NC compared to north of Cape Hatteras, NC. Most of the southern vocalizations were during the winter months on the Blake Plateau and Blake Spur off Florida, which were in waters deeper than the AMAPPS surveys. The fin whale AMAPPS model was not able to predict this winter presence off Florida, although the 95% confidence interval map did predict low densities in these southern waters.

6.2.3.6 Harbor Porpoises

In summary, observed distribution patterns of harbor porpoises from other studies were consistent with those predicted by the AMAPPS model (Appendix I, chapter 19).

In the New York bight from Long Island to the 1000 m depth contour, 2 survey programs collected distribution data: the New York bight visual aerial surveys flew during March 2017 to February 2020 (Tetra Tech and LGL 2020) and the NYSERDA ultra-high resolution digital aerial surveys flew during summer 2016 to spring 2019 (Normandeau and APEM 2020). Both survey programs infrequently detected harbor porpoises mostly in waters shallower than 100 m mostly in the winter and spring. Although the digital surveys detected a few harbor porpoises in waters deeper than 200 m in the winter.

In and around the Maryland wind energy area, Bailey et al. (2019) and Wingfield et al. (2017) recorded harbor porpoise vocalizations throughout the study area from November to June, with a peak between January and May. The AMAPPS model is consistent with this spatiotemporal pattern. Bailey et al. (2019) highlighted fine scale interannual differences. They found that during the first year of their study harbor porpoise vocalizations were most commonly detected within and offshore of the wind energy area, whereas in the following 2 years they were detected more commonly within and inshore of the wind energy area.

Off Virginia and North Carolina, McAlarney et al. (2018a, b) conducted several aerial surveys focused on waters from the midshelf to about the 2000 m depth contour from Chesapeake Bay, VA to Cape Hatteras, NC in 2017 during May to August, with less searching efforts in Feburary and September. In addition, Engelhaupt et al. (2016, 2017, 2018, 2019, and 2020a) conducted shipboard sighting surveys in waters off Chesapeake Bay, VA, that spanned from the coast to offshore of the shelfbreak. These surveys infrequently detected harbor porpoises in waters about 30 to 40 m deep during April and May.

6.2.3.7 Humpback Whales

In summary, observed distribution patterns of humpback whales from other studies were consistent with those predicted by the AMAPPS model (Appendix I, chapter 2).

In the New York bight from Long Island to the 1000 m depth contour, 2 survey programs collected distribution data: the New York bight visual aerial surveys flew during March 2017 to February 2020 (Tetra Tech and LGL 2020) and the NYSERDA ultra-high resolution digital aerial surveys flew during summer 2016 to spring 2019 (Normandeau and APEM 2020). Both survey programs detected humpback whales from the shoreline to about 100 m deep. The visual surveys detected humpback whales year-round, mostly in the summer and fall. In contrast, the digital surveys detected humpback whales mostly in the spring and fall, with only 1 detection in the summer. In 2008 and 2009 at a site in about 90 m of water off the coast of Long Island, NY, Zeh et al. (2020) detected male humpback whale songs mostly during mid-winter through spring, and none during the summer (June to August).

In and around the Maryland wind energy area, Bailey et al. (2019) recorded humpback whale vocalizations most frequently in the winter to spring (November to May). Few recordings were close to shore and more (though not many) within and offshore of the wind energy area.

In and around the Virgina wind energy area, peak periods of detected humpack vocalizations were from February through April and lowest from June through August; except in 2012 when humpback whale vocalizations were frequently detected in the summer (Salisbury et al. 2019). This study reported that detects were located infrequently close to the mouth of the Chesepeake Bay, VA, more frequently within the wind energy area, and the most frequent farther offshore close to the shelfbreak.

Off Virginia and North Carolina, McAlarney et al. (2018a, b) conducted several aerial surveys focused on waters from the midshelf to about the 2000 m depth contour from Chesapeake Bay, VA to Cape Hatteras, NC in 2017 during May to August, with less searching efforts in Feburary and September. In addition, Engelhaupt et al. (2016, 2017, 2018, 2019, and 2020a) conducted shipboard sighting surveys in waters off Chesapeake Bay, VA, that spanned from the coast to offshore of the shelfbreak. Aschettino et al. (2018; 2020) conducted visual surveys and tagging efforts targeting humpback whales. These surveys detected humpback whales dispersed from the inside the mouth of the Chesapeake Bay, VA to waters deeper than 1000 m. Most were in waters deeper than 1000 m. Although they also detected humpback whales nearly year-round inside and just outside the mouth of the Chesapeake Bay, VA. Using photo-identification techniques, Aschettino et al. (2018; 2020) identified about 30 to 50 unique individuals near the mouth of the Chesapeake Bay each year.

Engelhaupt et al. (2018) and Waples and Read (2020) photographed the same individual humpback whales at locations near Cape Hatteras, NC and Chesapeake Bay, VA. They also tagged humpback whales that traveled between these 2 locations. Glider passive acoustic surveys conducted on the shelf north and south of Cape Hatteras, NC detected more humpback whales north of Cape Hatteras, NC. Aerial surveys conducted during 2017 from Chesapeake Bay, VA to Cape Hatteras, NC from midshelf to about 1200 m depth, detected 3 groups of humpback whales that spanned the entire study area (McAlarney et al. 2018a, b). One group was at the mouth of Chesapeake Bay, VA, 1 on the midshelf north of Cape Hatteras, NC, and 1 in waters deeper than 2000 m.

Off Jacksonville, FL, Foley et al. (2019) conducted aerial surveys from January 2009 through November 2017 spanning waters 100 to 1200 m deep. They detected humpback whales infrequently dispersed in waters about 150 to 800 m in the winter only.

6.2.3.8 Minke Whales

In summary, observed distribution patterns of minke whales from other studies were consistent with those predicted by the AMAPPS model (Appendix I, chapter 5).

In the New York bight from Long Island to the 1000 m depth contour, 2 survey programs collected distribution data: the New York bight visual aerial surveys flew during March 2017 to February 2020 (Tetra Tech and LGL 2020) and the NYSERDA ultra-high resolution digital aerial surveys flew during summer 2016 to spring 2019 (Normandeau and APEM 2020). Both survey progrms detected minke whales mostly in waters shallower than 100 m in all seasons.

In and around the Maryland wind energy area, Bailey et al. (2019) occasionally recorded minke whales vocalizations. Most of the vocalizations were offshore of the wind energy area during January to May.

In and around the Virginia wind energy area, Salisbury et al. (2019) rarely recorded minke whale vocalizations. When they did, they were mostly during September and March with large interannual variability. The vocalizations were mostly from the shelfbreak, with none close to the mouth of the Chesepeake Bay, VA.

Off Virginia and North Carolina, McAlarney et al. (2018a, b) conducted several aerial surveys focused on waters from the midshelf to about the 2000 m depth contour from Chesapeake Bay, VA to Cape Hatteras, NC in 2017 during May to August, with less searching efforts in Feburary and September. In addition,

Engelhaupt et al. (2016, 2017, 2018, 2019, and 2020a) conducted shipboard sighting surveys in waters off Chesapeake Bay, VA, that spanned from the coast to offshore of the shelfbreak. These surveys detected a few minke whales on the midshelf in about 30 to 60 m depth.

Off Jacksonville, FL, Foley et al. (2019) conducted aerial surveys from January 2009 through November 2017 spanning waters 100 to 1200 m deep. Minke whale sightings were in deeper waters (about 300 to 1000 m) in the winter months.

6.2.3.9 Pilot Whales

In summary, observed distribution patterns of short-finned and long-finned pilot whales from other studies were consistent with those predicted by the AMAPPS model (Appendix I, Chapters 11 and 12).

In the New York bight from Long Island to the 1000 m depth contour, 2 survey programs collected distribution data: the New York bight visual aerial surveys flew during March 2017 to February 2020 (Tetra Tech and LGL 2020) and the NYSERDA ultra-high resolution digital aerial surveys flew during summer 2016 to spring 2019 (Normandeau and APEM 2020). Both survey programs detected unidentified pilot whales in waters deeper than about 100 m during spring to summer, where the most detections were in the summer.

Off Virginia and North Carolina, McAlarney et al. (2018a, b) conducted several aerial surveys focused on waters from the midshelf to about the 2000 m depth contour from Chesapeake Bay, VA to Cape Hatteras, NC in 2017 during May to August, with less searching efforts in Feburary and September. In addition, Engelhaupt et al. (2016, 2017, 2018, 2019, and 2020a) conducted shipboard sighting surveys in waters off Chesapeake Bay, VA, that spanned from the coast to offshore of the shelfbreak. These surveys detected pilot whales (short-finned and unidentified pilot whales) dispersed through the study areas, although most were in waters about 150 to 1500 m deep.

Off Virginia and North Carolina, Engelhaupt et al. (2018) documented photo-id matches of short-finned pilot whales in the Cape Hatteras, NC and Viriginia areas. Researchers tagged short-finned pilot whales off Cape Hatteras, NC during 2014 to 2015 (Thorne et al. 2017) and during 2014 to 2018 (Baird et al. 2019), confirming the species identity using genetic analyses. The tagged whales used shelfbreak waters between Cape Hatteras, NC and Hudson Canyon off New Jersey, with a particular affinity for waters 200 to 1000 m deep.

Thorne et al. (2019) used mixed effects generalized additive models to describe the relationship between habitat covariates and the presence/absence of the locations of satellite tagged short-finned pilot whale. Their preferred model included SST, slope, distance to SST fronts, sea level anomaly, and distance to the 200 m isobath (shelfbreak). The habitat covariates included in the AMAPPS model were similar: distance to the north wall of the Gulf Stream, bottom temperature, distance to the 1000 m depth contour, chlorophyll concentration in surface waters, mixed layer thickness, salinity concentration in surface waters, and bottom depth, in that order of importance. The predicted maps from the 2 models shared similar distribution patterns. Some of the tagged animals stayed on the shelfbreak while others followed offshore meanders of the Gulf Stream.

Off Jacksonville, FL, Foley et al. (2019) conducted aerial surveys from January 2009 through November 2017 spanning waters 100 to 1200 m deep. They detected short-finned pilot whales April through October mostly in waters 200 to 1200 m deep.

The tracks of short-finned pilot whales tagged off Florida (Foley 2018; Baird et al. 2019) are also consistent with the AMAPPS model for waters south of Cape Hatters, NC. The tracks of the tagged animals were consistent with the AMAPPS predicted seasonal patterns of a higher density along the shelfbreak off Florida but still ranging out to the 1000 m and beyond in waters off Florida on the Blakes

Plateau. During winter, the tagged short-finned pilot whales stayed mostly in southern waters, centered on Cape Hatteras, NC. Then during summer/early fall, they moved north even to the southern flank of Georges Bank.

6.2.3.10 Pygmy and Dwarf Sperm Whales

In summary, observed distribution patterns of pygmy and dwarf whales from other studies were consistent with those predicted by the AMAPPS model (Appendix I, chapter 10) in the region we modeled. For the AMAPPS model, we assumed there were no pygmy or dwarf whales in the waters off Florida in waters shallower than about the 1000 m depth contour. However, other studies documented infrequent detections off Florida in waters deeper than 500 m, so our assumption was incorrect. Therefore, we will consider extending our model in southern waters for future modeling exercises.

In the New York bight from Long Island to the 1000 m depth contour, 2 survey programs collected distribution data: the New York bight visual aerial surveys flew during March 2017 to February 2020 (Tetra Tech and LGL 2020) and the NYSERDA ultra-high resolution digital aerial surveys flew during summer 2016 to spring 2019 (Normandeau and APEM 2020). The digital surveys infrequently detected pygmy or dwarf sperm whales in waters deeper than 200 m in the fall and spring. The visual surveys did not positively identify any pygmy or dwarf sperm whales.

Off Virginia and North Carolina, McAlarney et al. (2018a, b) conducted several aerial surveys focused on waters from the midshelf to about the 2000 m depth contour from Chesapeake Bay, VA to Cape Hatteras, NC in 2017 during May to August, with less searching efforts in Feburary and September. In addition, Engelhaupt et al. (2016, 2017, 2018, 2019, and 2020a) conducted shipboard sighting surveys in waters off Chesapeake Bay, VA, that spanned from the coast to offshore of the shelfbreak. These surveys detected pygmy or dwarf sperm whales only once in waters 1500 to 2000 m deep.

Off Virginia and North Carolina, using passive acoustic monitoring HARPs, Rafter et al. (2020) and Hodge et al. (2018) detected dwarf or pygmy sperm whale echolocation clicks off Norfolk Canyon, VA in waters 980 m deep, off Cape Hatteras, NC in waters 1000 to 1400 m deep, and off Onslow Bay, NC in 850 to 950 m.

Off Jacksonville, FL, Foley et al. (2019) conducted aerial surveys from January 2009 through November 2017 spanning waters 100 to 1200 m deep. They detected pygmy/dwarf sperm whales infrequently mostly in waters 500 to 1200 m deep in the summer and fall. In addition, off Jacksonville, FL, Hodge et al. (2018) infrequently recorded pygmy/dwarf sperm whale vocalizations from a HARP in 810 m of water during July 2014 to May 2015. In addition, Rafter et al. (2020) detected pygmy/dwarf sperm whale vocalizations throughout their study period (Jun 25 2017 to 26 May 2019) from a HARP off Jacksonville, FL in 740 m of water, where most detections were in the winter (November 2018 to January 2019). For the AMAPPS model, we assumed that there were no pygmy or dwarf whales off Florida in waters shallower than 1000 m, because we had limited survey coverage and no visual sightings in these waters. This was an incorrect assumption. Therefore, we will consider extending the model to 500 m depth off Florida during our next modeling exercise.

6.2.3.11 Risso's Dolphins

In summary, observed distribution patterns of Risso's dolphins from other studies were consistent with those predicted by the AMAPPS model (Appendix I, chapter 13).

In the New York bight from Long Island to the 1000 m depth contour, 2 survey programs collected distribution data: the New York bight visual aerial surveys flew during March 2017 to February 2020 (Tetra Tech and LGL 2020) and the NYSERDA ultra-high resolution digital aerial surveys flew during

summer 2016 to spring 2019 (Normandeau and APEM 2020). Both survey programs detected Risso's dolphins year-round in waters deeper than 100 m.

Off Virginia and North Carolina, McAlarney et al. (2018a, b) conducted several aerial surveys focused on waters from the midshelf to about the 2000 m depth contour from Chesapeake Bay, VA to Cape Hatteras, NC in 2017 during May to August, with less searching efforts in Feburary and September. In addition, Engelhaupt et al. (2016, 2017, 2018, 2019, and 2020a) conducted shipboard sighting surveys in waters off Chesapeake Bay, VA, that spanned from the coast to offshore of the shelfbreak. These surveys detected Risso's dolphins near the Norfolk Canyon, VA.

Off Jacksonville, FL, Foley et al. (2019) conducted aerial surveys from January 2009 through November 2017 spanning waters 100 to 1200 m deep. They detected Risso's dolphins year-round mostly in waters 200 to 500 m deep, with fewer in deeper waters.

6.2.3.12 Sei Whales

In summary, observed distribution patterns of sei whales from other studies were consistent with those predicted by the AMAPPS model (Appendix I, chapter 4), particularly for waters north of North Carolina.

Davis et al. (2020) and Parry et al. (2018) showed by using passive acoustic monitoring at selected sites located from Greenland to the Caribbean during 2004 and 2014 that sei whales seasonally migrate from summer concentrations in waters around Greenland to winter where densities were low everywhere but dispersed throughout the waters from Greenland to the Caribbean. The daily acoustic presence from 2015 to 2019 reported in Chapter 7 (Figure 7-12) demonstrated that within waters from Massachussetts and south on the shelfbreak, most sei whale acoustic detections were north of Wilmington Canyon off Delaware, where the density gradient increased north of Delaware. Within this region, most acoustic detections were during spring, with nearly none in the summer.

In the New York bight from Long Island to the 1000 m depth contour, 2 survey programs collected distribution data: the New York bight visual aerial surveys flew during March 2017 to February 2020 (Tetra Tech and LGL 2020) and the NYSERDA ultra-high resolution digital aerial surveys flew during summer 2016 to spring 2019 (Normandeau and APEM 2020). The visual surveys detected a few sei whales in deep waters (deeper than 200 m) and only in the spring and early summer. The digital surveys detected sei whales throughout the study area and in all seasons, though most were in the spring.

The AMAPPS sei whale model was consistent with these spatial patterns. Both the AMAPPS model and passive acoustic monitoring picked up the shelfbreak pattern of a density gradient with higher densities on the shelfbreak closer to Canadian waters and lower densities on the shelfbreak closer to New York.

Both data sources also documented lower occurences in August and September in the AMAPPS study area, though there was interannual and spatial variablitiy. Davis et al. (2020) and at the southern Georges Bank sites at Heezen Canyon (HZ), Oceanographer Canyon (OC), and Nantucket Canyon (NC) in Figures 7-12 and 7-13 and Table 7-8 showed that in the summer (July to September), the passive acoustic monitors recorded only a few sei whale vocalizations. However, when Parry et al. (2018) monitored more sites on the shelfbreak (southern flank of Georges Bank), they documented sei whale vocalizations in July and August. The AMAPPS visual shipboard surveys also documented a few sei whale sightings in the summer on the southern flank of Georges Bank (Palka et al. 2017; this report in Appendix I).

Interannual variability was present in the summer acoustic detections at the Nantucket site (Figure 7-12) as seen when comparing July and August in 2016 versus 2017. Interannual variability was also present in the visual modeled data, where the estimated abundance for years before 2014 were larger than that estimated after 2014 (Figure 4-5 in Appendix I). Although the general summer patterns documented by the 2 sources of data were similar, the visual sightings estimated density appears to be larger than the

detection rate of summer acoustic vocalizations. There are several possible explanations for this apparent difference between the sei whale distribution patterns recorded from visual sightings and acoustic detections. These explanations include the possibility that sei whales vocalize less or use different vocalizations during summer; or due to the locations of the monitors on southern Georges Bank, a sampling rate less than 100%, and large interannual variability, the acoustic monitoring results for the summer were no able to document these rare events.

Off Virginia and North Carolina, passive acoustic monitoring (Davis et al. 2020; Parry et al. 2018; Chapter 7 in this document), and other studies of visual sighting surveys, photo-identification, tagging and glider studies (Engelhaupt et al. 2016, 2017, 2018, 2019, and 2020a) infrequently documented sei whales, though when detected they were generally in waters 800 m or deeper. Although passive acoustic monitoring during 2012 to 2017 in and around the Virginia wind energy area did not document sei whale vocalizations (Salisbury et al. 2019).

Due to the lack of sei whale sightings in the AMAPPS surveys in waters south of Virgina, we did not attempt to model the sei whale distribution south of Virginia. The lack of sightings is understandable not only because of the limited AMAPPS effort in deeper waters south of North Carolina, but also because of the presumed very low densities of sei whales in these waters (according to the acoustic recordings).

6.2.3.13 Sperm Whales

In summary, observed distribution patterns of sperm whales from other studies were consistent with those predicted by the AMAPPS model (Appendix I, chapter 6).

In the New York bight from Long Island to the 1000 m depth contour, 2 survey programs collected distribution data: the New York bight visual aerial surveys flew during March 2017 to February 2020 (Tetra Tech and LGL 2020) and the NYSERDA ultra-high resolution digital aerial surveys flew during summer 2016 to spring 2019 (Normandeau and APEM 2020). Both survey programs detected sperm whales only in waters deeper than 200 m year-round, although most frequently in summer, and least frequently in winter.

Off Virginia and North Carolina, McAlarney et al. (2018a, b) conducted several aerial surveys focused on waters from the midshelf to about the 2000 m depth contour from Chesapeake Bay, VA to Cape Hatteras, NC in 2017 during May to August, with less searching efforts in Feburary and September. In addition, Engelhaupt et al. (2016, 2017, 2018, 2019, and 2020a) conducted shipboard sighting surveys in waters off Chesapeake Bay, VA, that spanned from the coast to offshore of the shelfbreak. These surveys detected sperm whales only in waters deeper than 1000 m. Sperm whales tagged off Chesapeake Bay, VA traveled generally in waters deeper than 1000 m. Some tagged animals traveled northward to the tip of Georges Bank in Canadian waters, some traveled offshore to the Gulf Stream, while others traveled southward on the Blakes Plateau off Florida (about 32°N 75°W).

Off Jacksonville, FL, Foley et al. (2019) conducted aerial surveys from January 2009 through November 2017 spanning waters 100 to 1200 m deep. They detected sperm whales infrequently in waters 200 to 700 m deep only in the winter and spring.

Stanistreet et al. (2018) commonly detected sperm whale echolocation clicks year-round between New England and North Carolina, but only infrequently off Florida (in 800 m depths). At the listening sites on Georges Bank (in 800 m) and Norfolk Canyon off Virginia (in 908 m), they recorded slightly more acoustic detections in spring over the other seasons. While at the Cape Hatteras, NC listening stations (850 to 970 m depth), winter had on average more acoustic detections then the other seasons. There did not appear to be seasonal differences in the acoustic detections at the Onslow Bay, NC site (south of Cape Hatteras, NC in 850 to 950 m depths). The sperm whale AMAPPS model predicted summer had slightly

higher estimated abundance over the other seasons for the approximate spots where the acoustic sites were, though the areas with the highest modeled density of sperm whales were in waters deeper than the locations of the acoustic recorders. In addition, the model predicted a steep abundance gradient in waters between 500 and 1500 m of water, with more animals in the deepest waters. Thus, it is not clear if the apparent differences between the acoustic versus visual patterns are truly different. Alternatively, the differences could simply be due to the acoustic recorders being in relatively shallow waters for sperm whales, the particularly low 10% duty-cyled recording schedule at the Georges Bank listening station, or the higher summer visual coverage in waters greater than 200 m deep.

6.2.3.14 Striped Dolphins

In summary, observed distribution patterns of striped dolphins from other studies were consistent with those predicted by the AMAPPS model (Appendix I, chapter 17).

In the New York bight from Long Island to the 1000 m depth contour, 2 survey programs collected distribution data: the New York bight visual aerial surveys flew during March 2017 to February 2020 (Tetra Tech and LGL 2020) and the NYSERDA ultra-high resolution digital aerial surveys flew during summer 2016 to spring 2019 (Normandeau and APEM 2020). Only the digital surveys detected striped dolphins year-round mostly in waters deeper than 100 m, with the most detectings in the winter.

Off Virginia and North Carolina, McAlarney et al. (2018a, b) conducted several aerial surveys focused on waters from the midshelf to about the 2000 m depth contour from Chesapeake Bay, VA to Cape Hatteras, NC in 2017 during May to August, with less searching efforts in Feburary and September. In addition, Engelhaupt et al. (2016, 2017, 2018, 2019, and 2020a) conducted shipboard sighting surveys in waters off Chesapeake Bay, VA, that spanned from the coast to offshore of the shelfbreak. These surveys detected striped dolphins mostly near Norfolk Canyon in waters deeper than 1000 m, although a few were off Cape Hatteras, NC in waters deeper than 1000 m. The AMAPPS model was consistent with this pattern, although we predicted most striped dolphins farther offshore and north of these survey areas.

6.2.4 Key Findings

We developed GAM density-habitat models for 18 species or species guilds. With the incorporation of the new shipboard and aerial survey data collected under AMAPPS II, we were able to confidently develop winter GAM density-habitat models for most of the species or species guilds. The results highlighted the known seasonal migratory shifts in distribution and abundance, but also highlighted how these seasonal shifts changed over the years. For example, sei whale and harbor porpoise abundance estimates in US Atlantic waters decreased dramatically after 2014. The changes in harbor porpoise abundance corresponded to changes in the strength of the chlorophyll fronts in US coastal waters. In contrast, the abundance of long-finned pilot whales in US Atlantic waters increased dramatically after 2015. Other species demonstrating less dramatic, but still visible interannual variability associated to changes of comtemporeous environment covariates. These species included humpback whales (associated with chlorophyll front strength), fin whales (associated with the location of the north wall of the Gulf Stream), Atlantic white-sided dolphins (associated with the location of the south wall of the Gulf Stream), and common bottlenose dolphins (associated with SST).

The seasonal predictions also highlighted which species would likely be within the wind energy areas along the US Atlantic coast. The wind-energy study areas north of Cape Hatteras, NC, have the higher species diversity, where 13 to 16 species utilized the waters in the wind-energy study areas, at least for part of the year and/or part of the wind-energy study area. The Rhode Island/Massachusetts wind-energy area had the highest average (2,080 animals) of the 4 seasonal abundance estimates of all species averaged over 2010 to 2017. The North Carolina/South Carolina wind-energy study area had the second highest average annual abundance (1,473 animals from only 7 species). Harbor porpoise was the main

species sensitive to high frequency sounds that inhabitated the wind-energy study areas. The largest numbers of the species sensitive to medium and low frequency sounds were in the Rhode Island/Massachusetts and North Carolina/South Carolina wind-energy study areas. In all of the wind-energy study areas, the largest numbers of low-frequency sensitive species inhabited the areas during late spring to summer (May to July), with the lowest in winter (December to February).

6.2.5 Data Gaps and Future Work

Some of the density-habitat models had higher levels of uncertainty in the winter and in waters south of North Carolina. This is mainly due to low sighting rates both because there appears to be fewer animals in these waters, and because there was low survey efforts. Thus, in the future we could survey these waters more often, especially in the winter and farther offshore. Also given the relatively high densities of cetaceans and large diversity of species in the region between Cape Hatteras, NC and Cheaspeake Bay, VA and the presence of wind-energy development areas in this region, we would be able to more precisely model this region if we increase the survey effort by adding more track lines in this region.

Several analytical issues with respect to the density-habitat modeling methodology warrant future work. For example, as discussed in section 6.3, we did not propagate the uncertainity from the stage 1 analyses into the final estimate of uncertainty. Currently, researchers, other than that developed in section 6.3, are developing methodological advances to propagate the uncertainty to the final estimates when using 2-team mark-recapture distance sampling methods. We plan to use these new methods in the near future.

Another issue we need to explore in the near future is how to accurately use the sightings that we identified as an ambiguous species grouping, such as unidentified beaked whales and pygmy/dwarf sperm whale. We will be exploring ways to use the positively identified beaked whales detected on the hydrophone array towed behind the survey ships. We are planning to explore using habitat covariates to model the presence/absence of acoustic detections of each positively identified species. If the models are sufficiently robust, we would like to use the habitat relationships to assign a species to the ambiguous visual whale sightings.

The long-term passive acoustic studies and tagging studies provide great insight into the spatiotemporal distribution patterns of a variety of species. We could investigate other statistical techniques such as occupancy models to combine the inferences resulting from passive acoustic, tagging, and visual sighting surveys into perhaps a more accurate spatiotemporal distribution model and resulting maps.

6.3 Development of a Bayesian Hierarchical Framework

6.3.1 Introduction

The objective of this study was to further explore a framework that estimates Bayesian hierarchical density-habitat models resulting in spatially- and temporally-explicit abundance estimates and associated density maps (Sigourney et al. 2020). This one-stage Bayesian hierarchical framework allows for the simultaneous fitting of both the detection function model (stage 1 in the 2-stage GAM framework described in section 6.2) and the density-habitat model (stage 2 in 2-stage GAM framework).

Applications of one-stage Bayesian hierarchical framework are less common than the 2-stage framework although there are a number of examples (Conn et al. 2012; Pardo et al. 2015; Pavanato et al. 2017). In this study, we aimed to expand the existing Bayesian hierarchical frameworks. We accommodated 2-team data from both aerial and shipboard platforms. We added semi-parametric smooth terms to the model framework that allow for more flexibility in the density-habitat relationships. We included a Compound Poisson-Gamma distribution that is a special case of the Tweedie distribution used in the 2-Stage GAM framework. In addition, we also incorporated prior information on surface availability estimated from

DTAG data. An important implication of the output from a one-stage Bayesian hierarchical framework is that estimates include more sources of uncertainty in comparison to traditional 2-stage frameworks. The 2-stage framework typically did not propagate the uncertainty from stage 1 analyses into the results from the stage 2 analyses. Although with recent developments (Bravington et al. 2021), the variance from stage 1 can be propagated to stage 2.

In this section, we describe the updated Bayesian hierarchical framework and apply it to the minke whale data collected under AMAPPS from 2010 to 2017 with the intention of assessing the performance of this method. For comparison, we aimed to keep as many components of the one-stage Bayesian hierarchical framework as consistent as possible with the 2-stage GAM framework including detection functions, habitat covariates, and the model likelihood. We also discuss plans for continued analyses using the one-stage Bayesian hierarchical framework.

6.3.2 Methods

6.3.2.1 Overview of the Bayesian hierarchical framework

Sigourney et al. (2020) provided a detailed description of the Bayesian hierarchical framework, an example application to fin whale data, and compared those results to results from the standard 2-stage framework. Here we provided a brief summary of the framework that contains 4 sub-models:

model to estimate Mark-Recapture Distance-Sampling detection probability for each survey platform,
model of the species- and platform-specific availability bias correction factor,
model of the average group size, and
model of density-habitat relationship.

The structure of the one-stage Bayesian hierarchical framework followed the general approach outlined by Miller et al. (2013) and the 2-stage GAM framework (as outlined in section 6.2), where we divided our data into spatial (10 km x 10 km) and temporal (8-day) stratum. We calculated the expected number of groups in spatiotemporal stratum *i*, by:

The product acts as an offset parameter. Then to estimate the density of individuals in each spatiotemporal stratum we multiplied the prediction by the estimate of average group size from the group size sub-model.

We are still exploring the most efficient way to select significant covariates for the density-habitat model within the one-stage Bayesian hierarchical framework. Therefore, at this time we used the results from the 2-stage framework to define the covariates for the density-habitat model in the Bayesian hierarchical framework. This also allowed us to directly compare outputs from the 2 frameworks. We fit the one-stage Bayesian hierarchical model using the following steps to estimate density of individuals in each spatiotemporal stratum:

1) For shipboard data, we estimated in custom-built mark-recapture density sampling Bayesian models using the set of covariates selected in the 2-stage GAM framework.
2) For aerial data, we estimated the probability of detection (not accounting for perception bias) for each stratum, , in custom-built mark-recapture density sampling Bayesian models using the set of covariates selected in the 2-stage GAM framework. We used estimates and CVs for developed in the 2-step aerial 2-stage GAM framework as informative Beta

priors. The Bayesian estimate of the aerial was the product of the Bayesian and a value from the prior distribution of .

3) We used estimates and CVs for the species- and platform-specific availability bias correction factors developed in section 5.2.6 as informative Beta priors. For both the shipboard and aerial data, we estimated the Bayesian that accounted for perception and availability bias as the product of the appropriate Bayesian and a value from the prior of the species- and platform-specific availability bias correction factor $_F$.
4) We used the *jagam* function from the *mgcv* package (Wood 2017) to construct the smooth terms in Equation 6-3.
5) For parameter estimation, we implemented Markov Chain Monte Carlo sampling in the JAGS software (Plummer 2003). We used a burn-in of 20,000 samples and 2 chains of 50,000 samples with a thinning rate of 50 samples.
6) Using the posterior distributions from the final model, we estimated the density of individuals within a spatiotemporal stratum *i* as the product of the spatiotemporal stratum specific estimated Bayesian density of groups and a value from the prior of the average group-size model.

6.3.2.2 Comparison to the 2-Stage GAM Framework

Even though we used the same input data and covariate variables in both analyses, the structure of the one-stage Bayesian hierarchical framework differs from the structure of the 2-stage GAM framework (section 5.2.3.4) in several fundamental ways. Because of these differences, our expectations and results from the 2-stage GAM and one-stage Bayesian hierarchical frameworks may differ in terms of the predicted point estimates and their corresponding estimated uncertainty.

One difference relates to the group size estimate. The 2-stage GAM framework used a Horvitz-Thompson estimator to estimate density of individuals in each spatiotemporal stratum, which used the observed number of animals within a spatiotemporal stratum. In the one-stage Bayesian hierarchical framework, we estimated the density of individuals within a spatiotemporal stratum as the product of the predicted density of groups in each spatiotemporal stratum derived from the density-habitat model and the study area's overall average group size and its associated variability. Using the overall average group size was a simplification that was appropriate for large whales since the group sizes of these species were usually one. However, we will have to modify this simplification for species found in larger groups, especially if the group size varies spatially or relates to some other factor.

Another difference relates to the response variable and distribution of the density-habitat model. The 2-stage GAM framework used an overdispersed Tweedie distribution. To mimic this, we developed a Tweedie distribution in the Bayesian hierarchical framework using a Compound Poisson-Gamma approach described in Sigourney et al. (2020). However, the response variable in the one-stage Bayesian hierarchical framework (Equation 6-3) is the discrete value of the number of groups, where the response variable in the 2-stage GAM framework is a continuous value of the estimate of density of individuals that accounts for perception and availability bias.

Finally, in the 2-stage GAM framework, we were not able to propagate the uncertainty from the detection function derived in its first stage to the final density estimates derived for its second stage. Thus, we expect the estimate of variability from the one-stage Bayesian hierarchical framework to be larger and more realistic than that from the 2-stage GAM framework.

6.3.3 Results

Estimated environmental relationships from the one-stage Bayesian hierarchical framework were similar to the relationships estimated from the 2-stage GAM framework (Figure 6-22). However, the credible

levels around each relationship (gray shading in Figure 6-22) were greater in the one-stage Bayesian hierarchical framework.

Average seasonal abundance estimates calculated from the one-stage Bayesian hierarchical framework ranged from 702 animals in the winter to 1,476 animals in the spring (Table 6-14). When comparing the results from 2 frameworks, the confidence intervals of the seasonal averages (Table 6-14 and Figure 6-23) and annual trend patterns (Figure 6-24) were similar. The Bayesian hierarchical framework predicted slightly higher seasonal average abundance point-estimates. Considering the confidence intervals, the estimates were not statistically different, except for in the winter.

In both frameworks, the abundance peaked in late spring and early summer declining to lower numbers in the fall and winter. The large-scale overall spatial patterns in distribution resulting from both frameworks were similar, showing highest densities concentrated north of New Jersey in the summer, more dispersion from North Carolina to Nova Scotia in the spring and fall, and the lowest density in the winter months (Figures 6-25 to 6-28). However, there were fine scale differences in the magnitude of density, even though both frameworks used the same set of habitat covariates. Overall, patterns in distribution from the one-stage Bayesian hierarchical framework were comparable to patterns predicted in the 2-stage GAM framework.

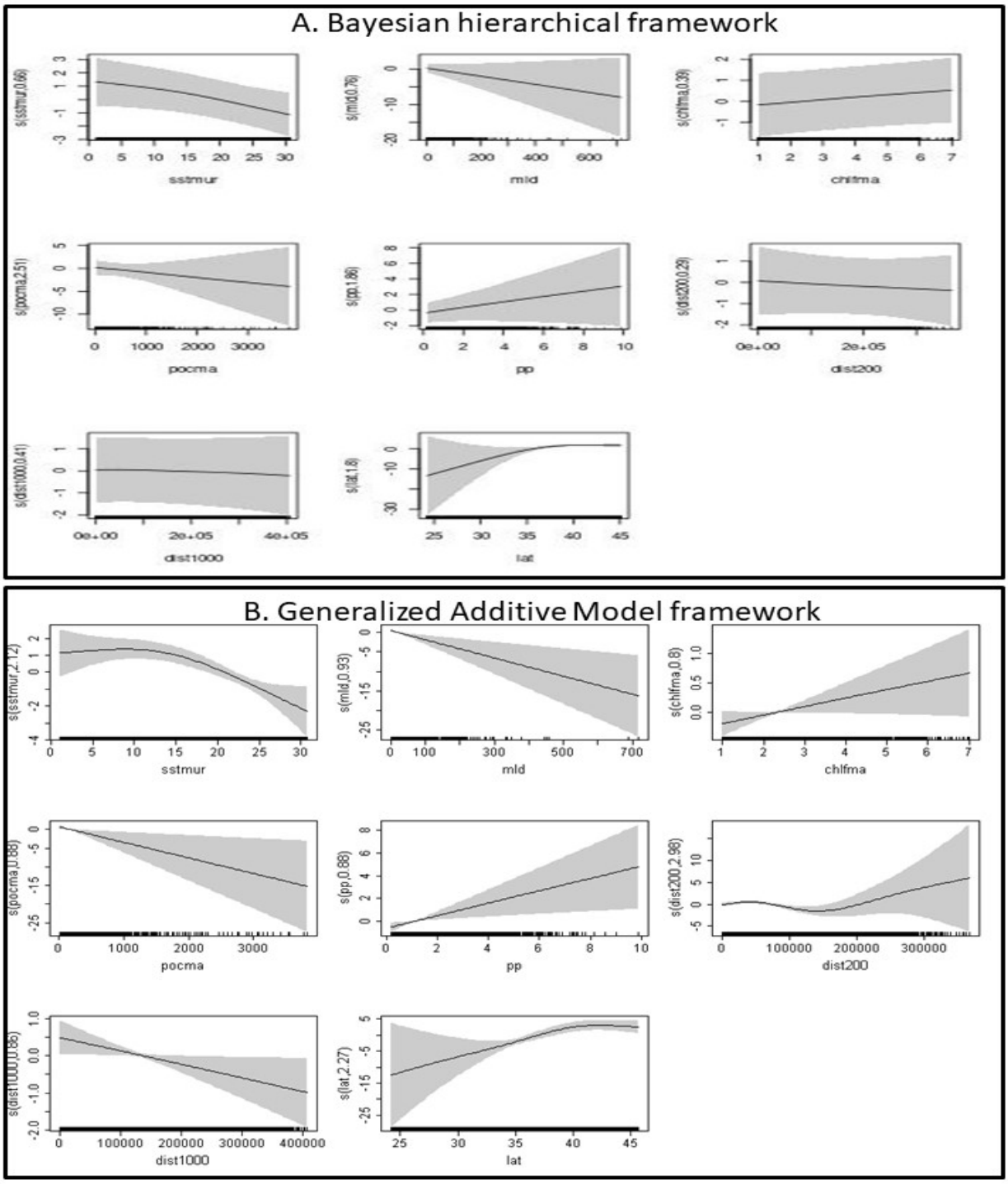

Figure 6-22 Minke whale density relative to significant habitat covariates from both frameworks

Table 6-14 Minke whale average seasonal abundance estimates from both frameworks
BH is the one-stage Bayesian hierarchical framework. GAM is the 2-stage GAM framework

Season	Abund BH	Abun GAM	CV BH	CV GAM	Lower 97.5% CI BH	Lower 97.5% CI GAM	Upper 2.5% CI BH	Upper CI 2.5% GAM
Spring	1,476	1,334	0.43	0.43	503	595	3,040	2,991
Summer	1,321	1,197	0.33	0.33	742	637	2,543	2,248
Fall	1,014	616	0.29	0.32	537	334	1,731	1,136
Winter	702	24	0.44	0.39	290	11	1,562	50

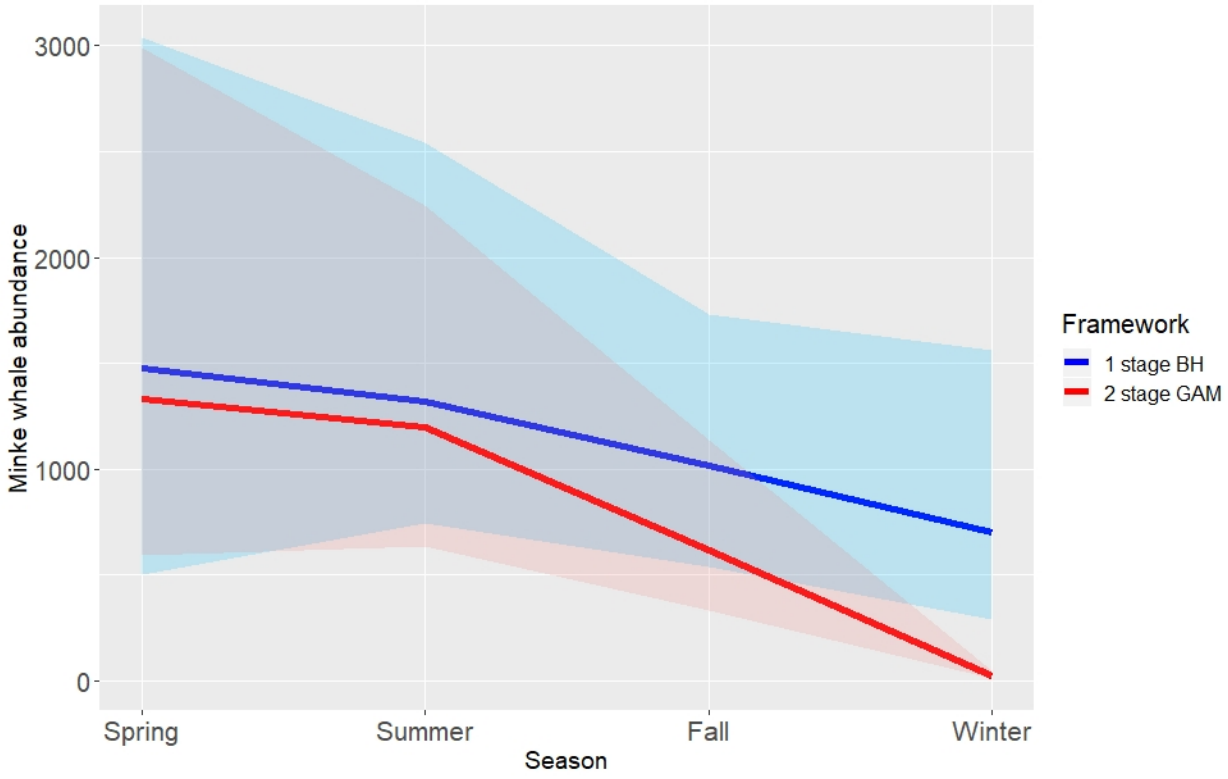

Figure 6-23 Minke whale average abundance estimates resulting from the 2 frameworks
Shaded regions are the 95% confidence intervals. BH = Bayesian hierarchical framework. GAM = Generalized additive model framework.

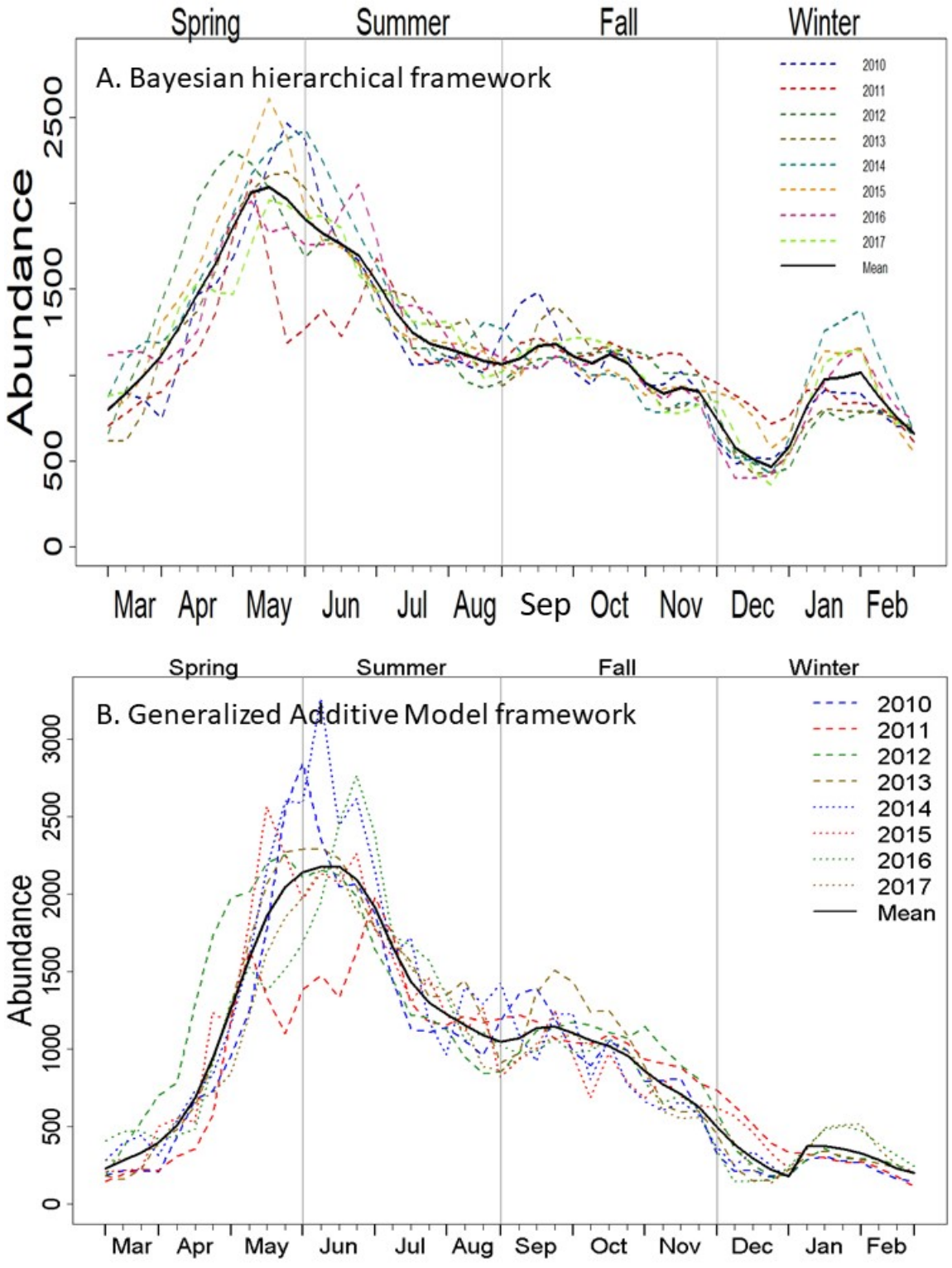

Figure 6-24 Annual abundance trends for minke whales resulting from both frameworks

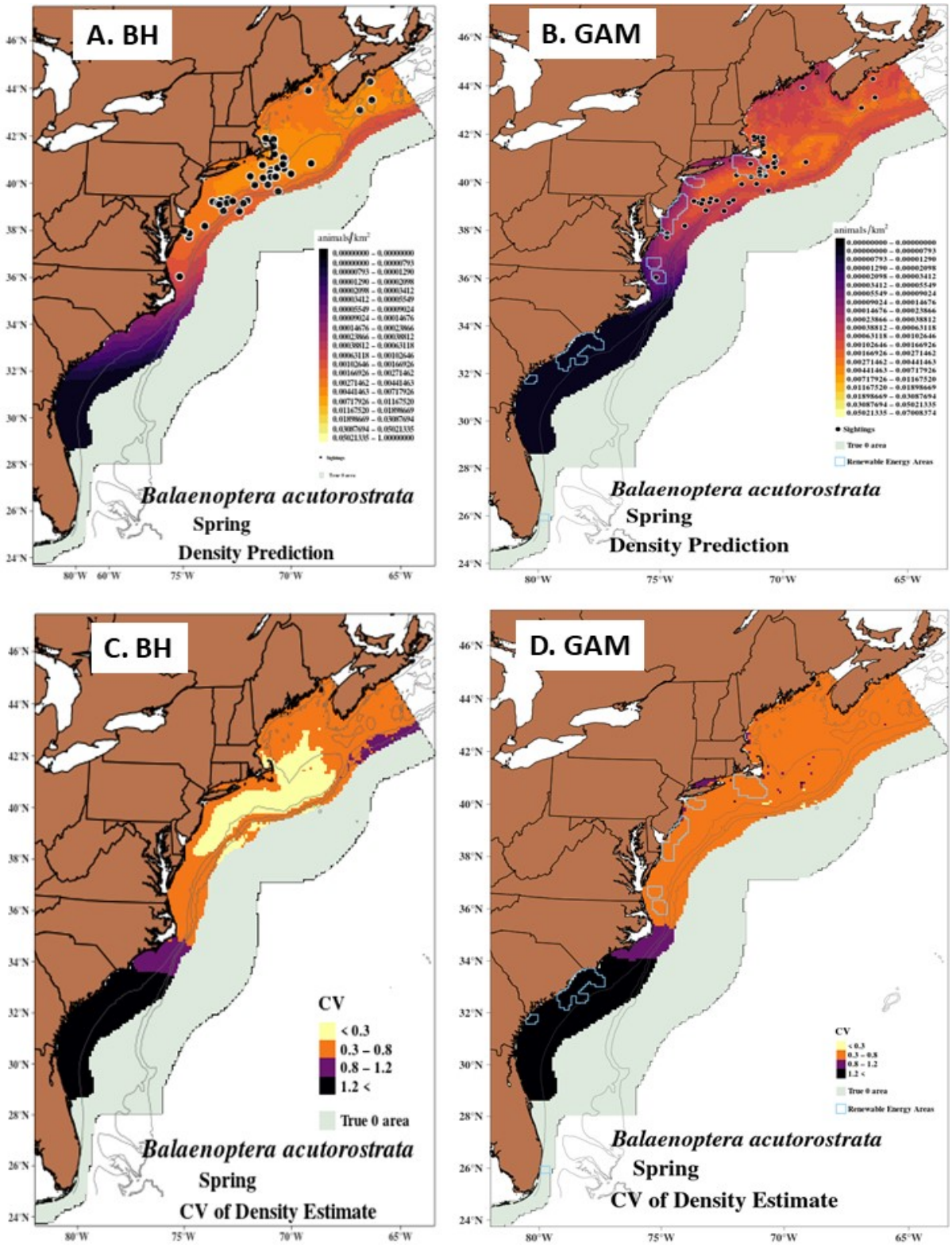

Figure 6-25 Minke whale spring maps from both frameworks
(A) Density prediction by the one-stage Bayesian hierarchical (BH) framework; (B) Density prediction by the 2-stage generalized additive model (GAM) framework; (C) CV of density by BH framework; (D) CV of density by GAM framework.

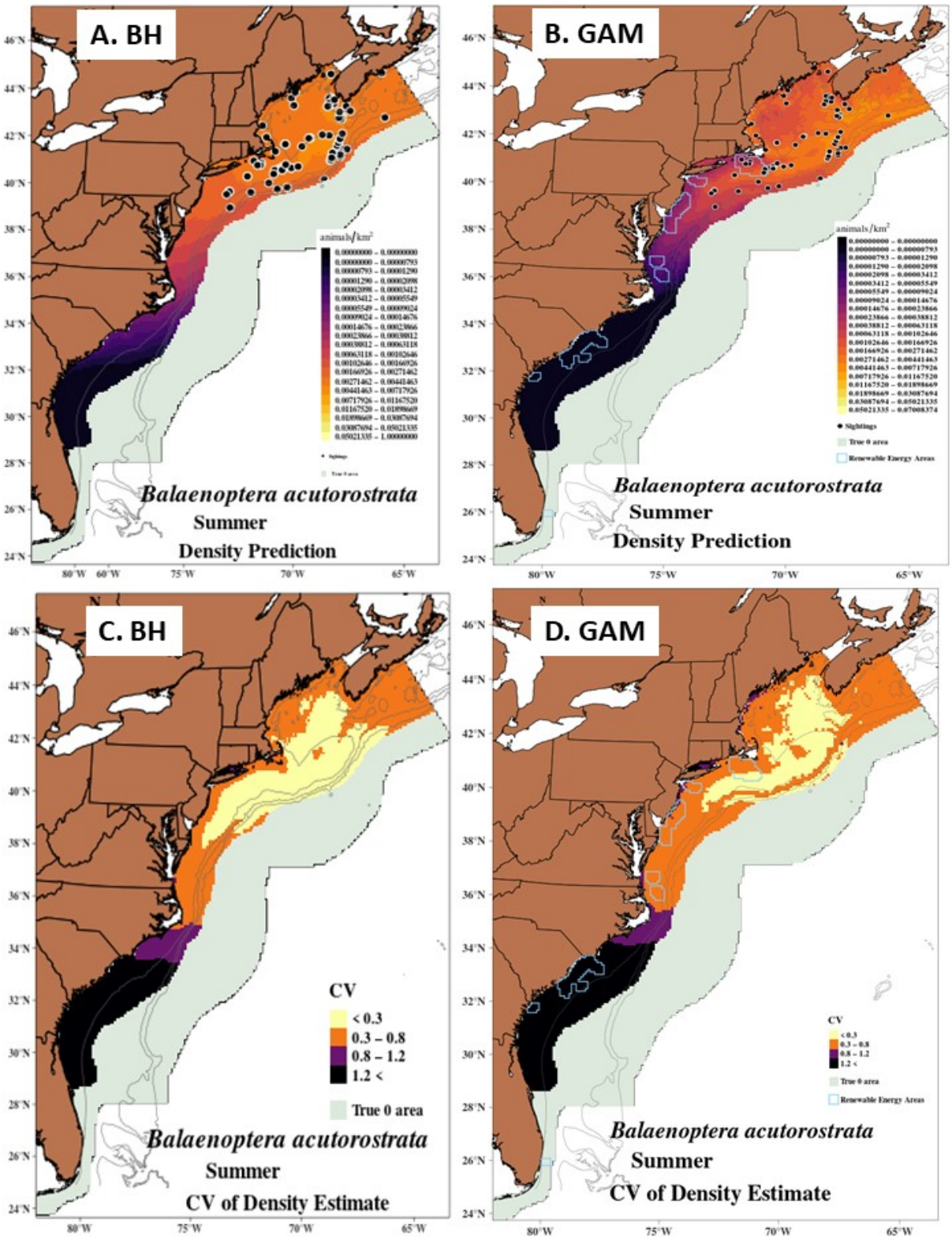

Figure 6-26 Minke whale summer maps from both frameworks
(A) Density prediction by the one-stage Bayesian hierarchical (BH) framework; (B) Density prediction by the 2-stage generalized additive model (GAM) framework; (C) CV of density by BH framework; (D) CV of density by GAM framework.

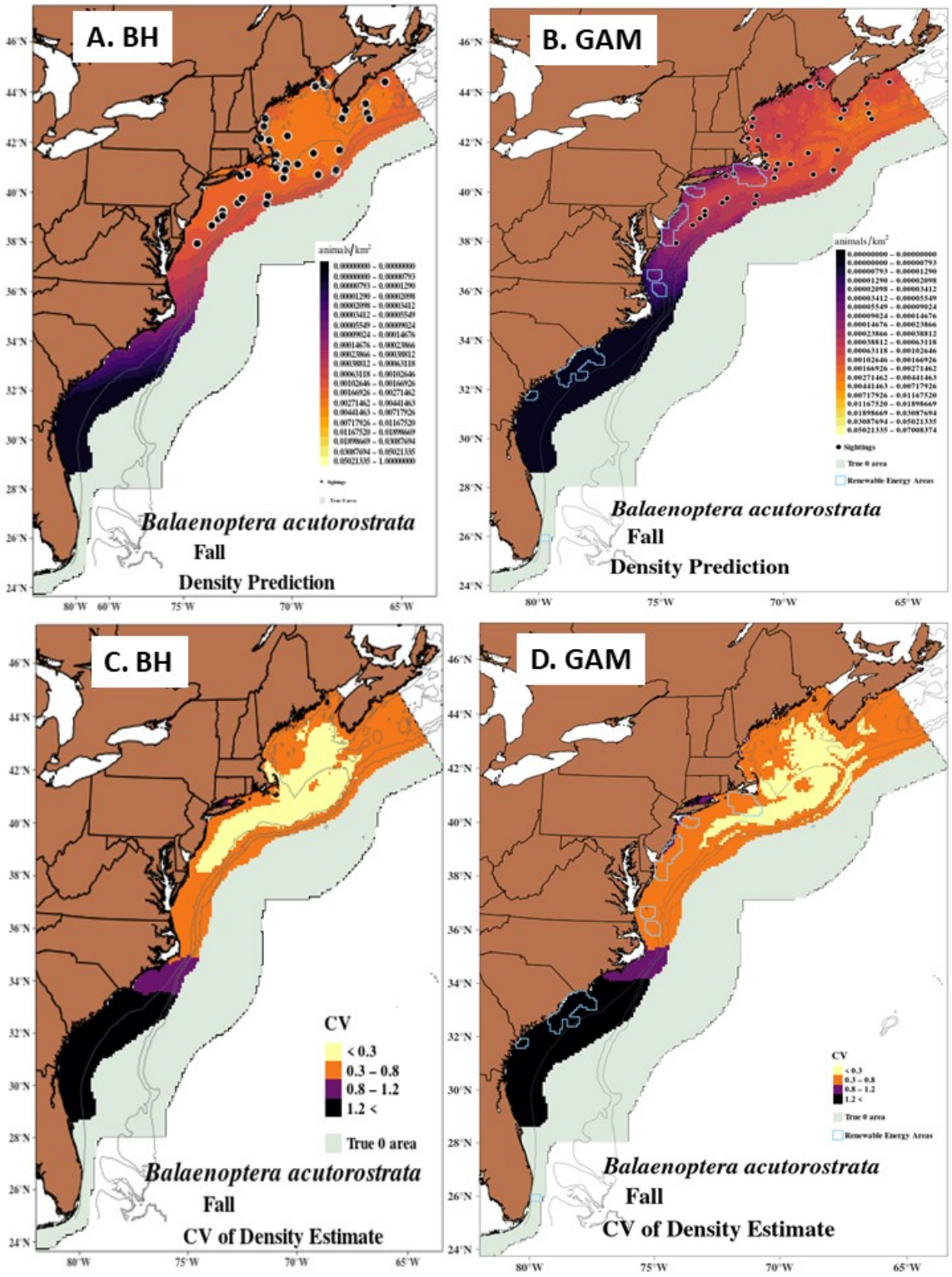

Figure 6-27 Minke whale fall maps from both frameworks
(A) Density prediction by the one-stage Bayesian hierarchical (BH) framework; (B) Density prediction by the 2-stage generalized additive model (GAM) framework; (C) CV of density by BH framework; (D) CV of density by GAM framework.

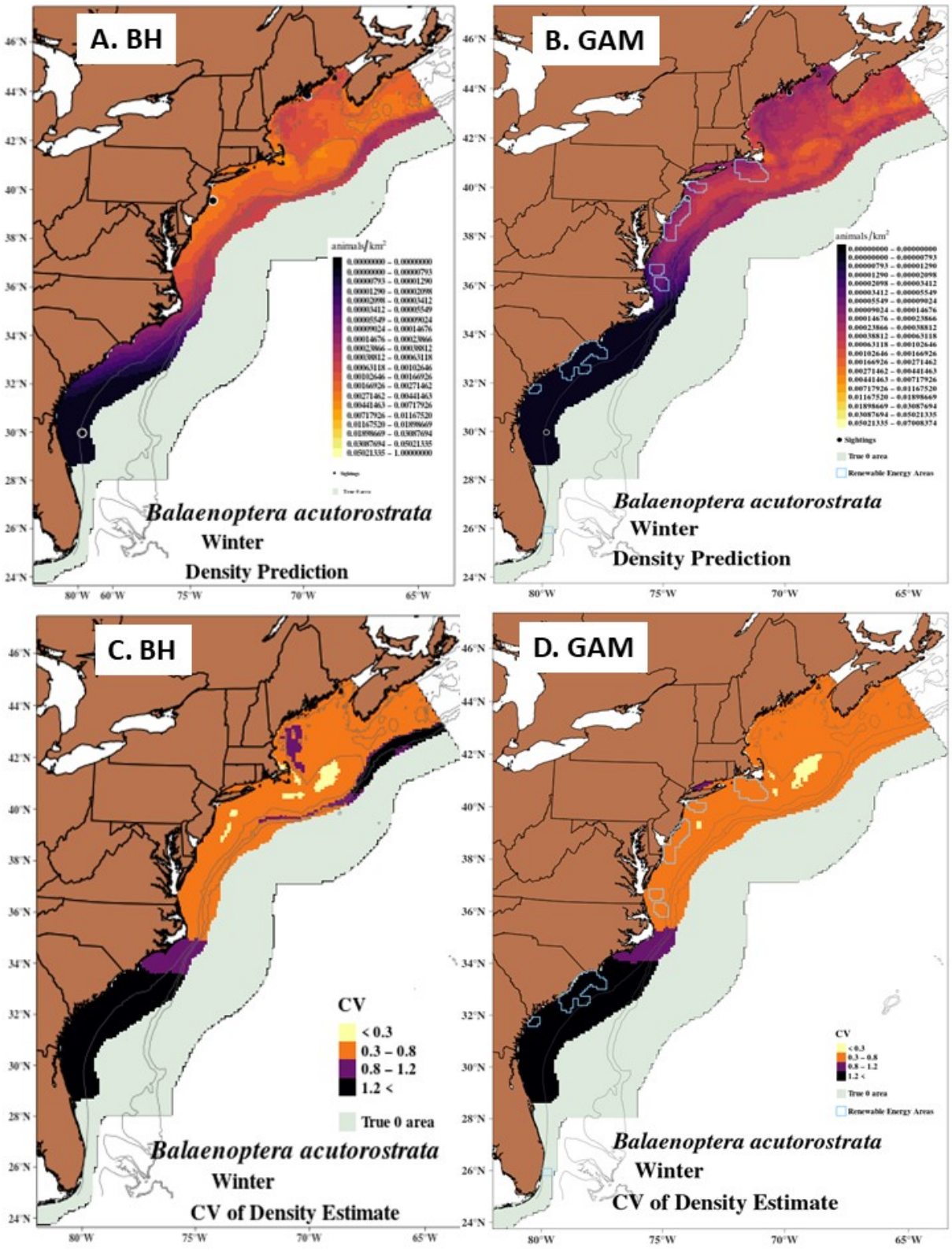

Figure 6-28 Minke whale winter maps from both frameworks
(A) Density prediction by the one-stage Bayesian hierarchical (BH) framework; (B) Density prediction by the 2-stage generalized additive model (GAM) framework; (C) CV of density by BH framework; (D) CV of density by GAM framework.

6.3.4 Discussion

Our analysis demonstrates that the one-stage Bayesian hierarchical framework is a viable framework to estimate spatial densities of large whales. We have successfully extended the model presented in Sigourney et al. (2020) to minke whales. Overall, we found spatial densities and seasonal abundance estimates were comparable to estimates from the 2-stage GAM framework with 1 notable difference. As compared to the 2-stage GAM framework results, the one-stage Bayesian hierarchical framework predicted a less pronounced decline in abundance going from fall to winter, and a larger average point estimate for winter. This difference is not surprising as the relationships between the habitat covariates and density (Figure 6-22) are slightly different.

One important implication of the output from a one-stage Bayesian hierarchical framework is that estimates include more sources of uncertainty in comparison to a 2-stage GAM framework, which does not incorporate the uncertainty from the detection process (Sigourney et al. 2020). The increase in sources of uncertainty in the Bayesian hierarchical framework has direct implications for management decisions (Taylor et al. 2000). A number of studies have demonstrated how inadequate consideration of uncertainty can result in poor management decisions (Regan et al. 2002; Artelle et al. 2013). By propagating additional sources of uncertainty from all model components into the final estimate, the Bayesian hierarchical framework estimates and associated uncertainty is more representative of the situation; thus providing managers the information they need to make appropriate management actions. In addition to propagating uncertainty, we can easily interpret output from a Bayesian analysis in terms of probabilities, and thus we can easily integrate results into a decision analysis framework. For these reasons, Wade (2000) advocated for Bayesian methods as an effective alternative to more traditional frequentist methods for conservation biology.

6.3.5 Key Findings

We developed a one-stage Bayesian hierarchical framework to estimate species density-habitat models and successfully applied it. The Bayesian hierarchical framework incorporates the following: 1) semi-parametric smooth functions, 2) compound Poisson-Gamma distributions that are a special case of a Tweedie distribution, 3) mark-recapture distance sampling functions, and 4) informative prior information on surface availability. We found that we can fit the one-stage Bayesian hierarchical framework to large whale data and achieved similar density estimates as the established 2-stage GAM framework.

6.3.6 Data Gaps and Future Work

Future work will focus on expanding our application of the one-stage Bayesian hierarchical framework to more species. Because we plan to apply this method to species with large group sizes, we will also determine the most appropriate approach for modelling group size. In addition, we plan to conduct model selection and model averaging so that we can complete an analysis within the Bayesian hierarchical framework independent of results from the 2-stage GAM framework. We will also implement hierarchical distance sampling within this framework (Sollmann et al. 2016) to deal with the situation where we have to pool several species into 1 model for the distance-sampling component. Because the Bayesian hierarchical framework is already in a hierarchical structure, we can also incorporate hierarchical distance sampling into our model so that we have species-specific detection functions derived from the data pooled across species. Finally, in an effort to reduce computation time we will experiment fitting Bayesian hierarchical models with other methods and software programs such as STAN, TMB, or Nimble.

6.4 Development of Incorporation of Potential Prey Data

6.4.1 Introduction

The objective of this exploratory study was to use data collected on a large-scale abundance survey involving numerous species and relate the spatial cetacean distribution and density to the spatial distribution and density of potential prey as measured by an acoustic echosounder. Some of the commonly used habitat covariates in density-habitat models (e.g., SST and chlorophyll-a derived from satellite data), while proven useful, act as proxies for water-column characteristics that actually have a more direct influence on marine mammal distribution and abundance. A few studies have examined spatial organism structure within the water column as it relates marine mammal distribution (e.g. Benoit-Bird and McManus 2012, Benoit-Bird et al. 2013).

Biological acousticians have done extensive research to distinguish marine organisms from their acoustic backscatter (Benoit-Bird and Lawson 2016; Stanton et al. 1998; Stanton and Chu 2000) and validated these approaches in both controlled (Wiebe et al. 1990; Stanton et al. 2004) and field tests (Wiebe et al. 1996; Lawson et al. 2001; Lawson et al. 2004). An organism's characteristic backscatter depends on the acoustic frequency encountering the organism, as well as the organism's shape, orientation, and body structure. This study employs relative frequency response, which is an approach that uses the fact that organisms have a characteristic backscattering response to particular echosounding frequencies, allowing researchers to associate unique acoustic patterns to a class of organism.

We hope the results of this study could spur incorporation of prey and water column structure into future marine mammal density-habitat models that result in estimates abundance and distribution patterns.

6.4.2 Methods

In this study, we employed the organism classification algorithm developed by Trenkel and Berger (2013) to quantify the acoustic response into 4 organism types (fish with swim bladders, larval fish and phytoplankton, fluid-like zooplankton, and fish with no swim bladder). We then used the categorized backscatter to model marine mammal distribution along the track lines (Orphanides 2019).

We collected marine mammal and echosounder data on the 2013 AMAPPS abundance survey conducted on the NOAA ship *Henry B. Bigelow* (see Chapter 10 for more details on this survey). In this exploratory study, we used 24 transects that traversed the continental shelfbreak (Figures 6-29). Echosounding equipment was set to passive mode (listening, but not actively pinging) for portions of the survey to fulfill multiple cruise objectives. So in this analysis, we only considered the portions of transects when the echosounder was actively recording data and the marine mammal observer team were active.

We described the marine mammal observing data collection protocols and acoustic processing procedures in Chapters 5 and 10, respectively. In this study, we analyzed data from only the upper team, 1 of the 2 teams described in section 5.2.3. The echosounder data records water characteristics below the ship because the sensors were on the bottom of the ship's hull. To ensure these data represented waters nearest the locations of the sightings (which we recorded as locations in front of the ship), we assigned to each sighting the echosounder data collected at the time the sighting was nearest the ship. For example, if observers recorded a sighting at a distance of 1,700 m in front of the ship along the track line from the ship's position, we assigned that sighting a time stamp associated with the approximate position of the ship when it was 1,700 m ahead of the initial sighting location, using the ship's mean speed. This way, the echosounding data used to represent marine mammal prey data match that of the animal's location.

We collected echosounding data using a keel-mounted Simrad EK60 system consisting of 18, 38, 70, 120, and 200 kHz transducers. We calibrated the system prior to the cruise with standard calibration techniques

(Foote et al. 1987; Demer et al. 2015). The echosounding data were then cleaned by removing impulse noise, transient nose and background noise using methods described in Ryan et al. (2015) and implemented in Echoview version 9.0 (Echoview 2018). After the primary data cleaning, we applied the Echoview school detection function for each frequency to further reduce the impact of noise on the analysis and to focus analysis on sizeable aggregations of organisms. We then processed the data with the multi-frequency indicator algorithm published by Trenkel and Berger (2013). This classified the acoustic backscatter into 4 specific species groups: 1) fish swim with bladders and large gas bubbles, 2) larval fish, zooplankton, and small resonant bubbles, 3) fluid like zooplankton (copepods & euphausiids), and 4) fish with no swim bladder (e.g., mackerel). Next we extracted the volume backscatter strength (S_v) (dB re $1m^{-1}$) associated with the assignment of a specific species group from the frequency most associated with that species group. The resulting Area Backscattering Coefficient (ABC) values (m^2m^{-2}) associated with each multi-frequency indicator classification were then summarized by bins 1000 m in length and either 50 or 200 m in depth (Figure 6-30). Then we merged the marine mammal sightings data along with the acoustic variables that represented phytoplankton and fish larvae, zooplankton, swim-bladder fish, and non-swim bladder fish at 3 depths: 0-50 m, 50-100m, and 0-200m, where all data were divided into 1000 m segments of the transects.

We built Generalized Additive Models (GAMs) (Hastie 1990, Wood 2017) to explain the density of marine mammals observed along the transects using the *mgcv* package (Wood 2011) implemented in the R statistical language (v. 3.5.2). We built density models for 6 species (common dolphin, common bottlenose dolphin, Risso's dolphin, striped dolphin, sperm whale, and fin whale and 1 species guild of short-finned and long-finned pilot whales). We converted counts of detected marine mammals in each of the 1000 m segments to density estimates (D) using where S is the number of groups per cell, G is the mean group size per cell, and L is the length of the cell (1000 m). Model building used the same techniques described in section 6.2.

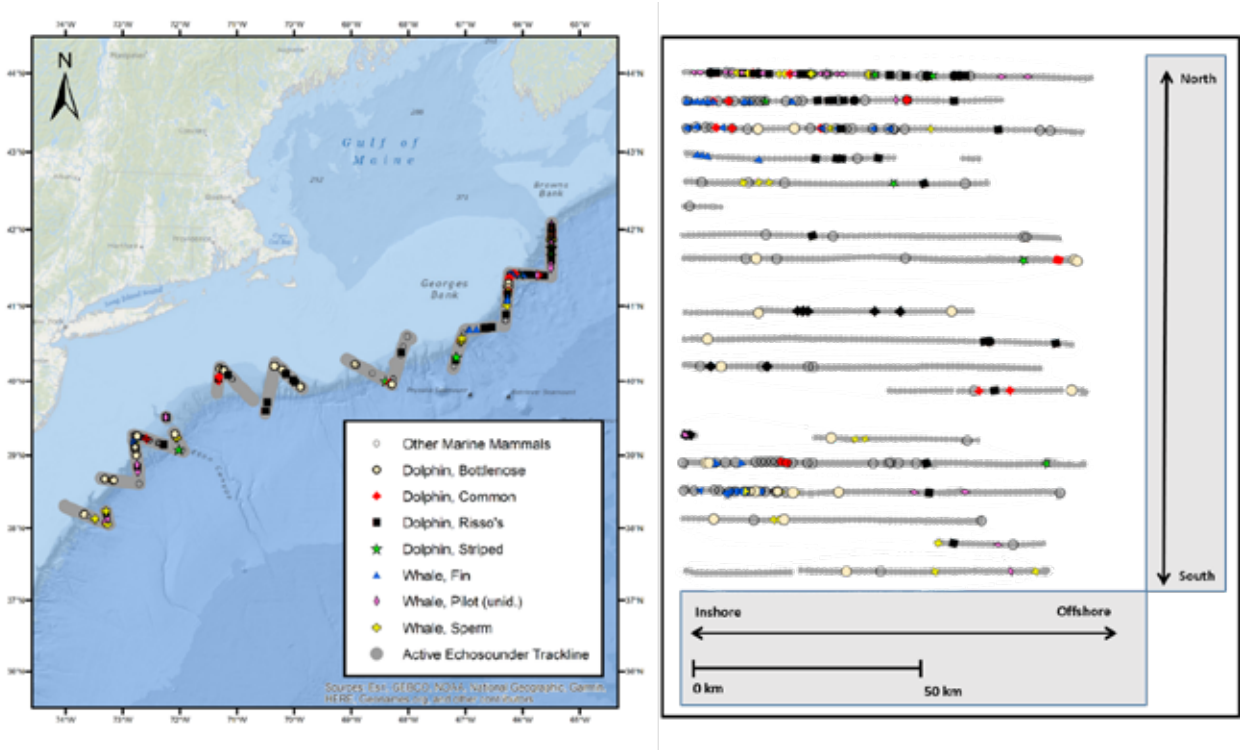

Figure 6-29 Locations of marine mammal sightings and active echosounding data

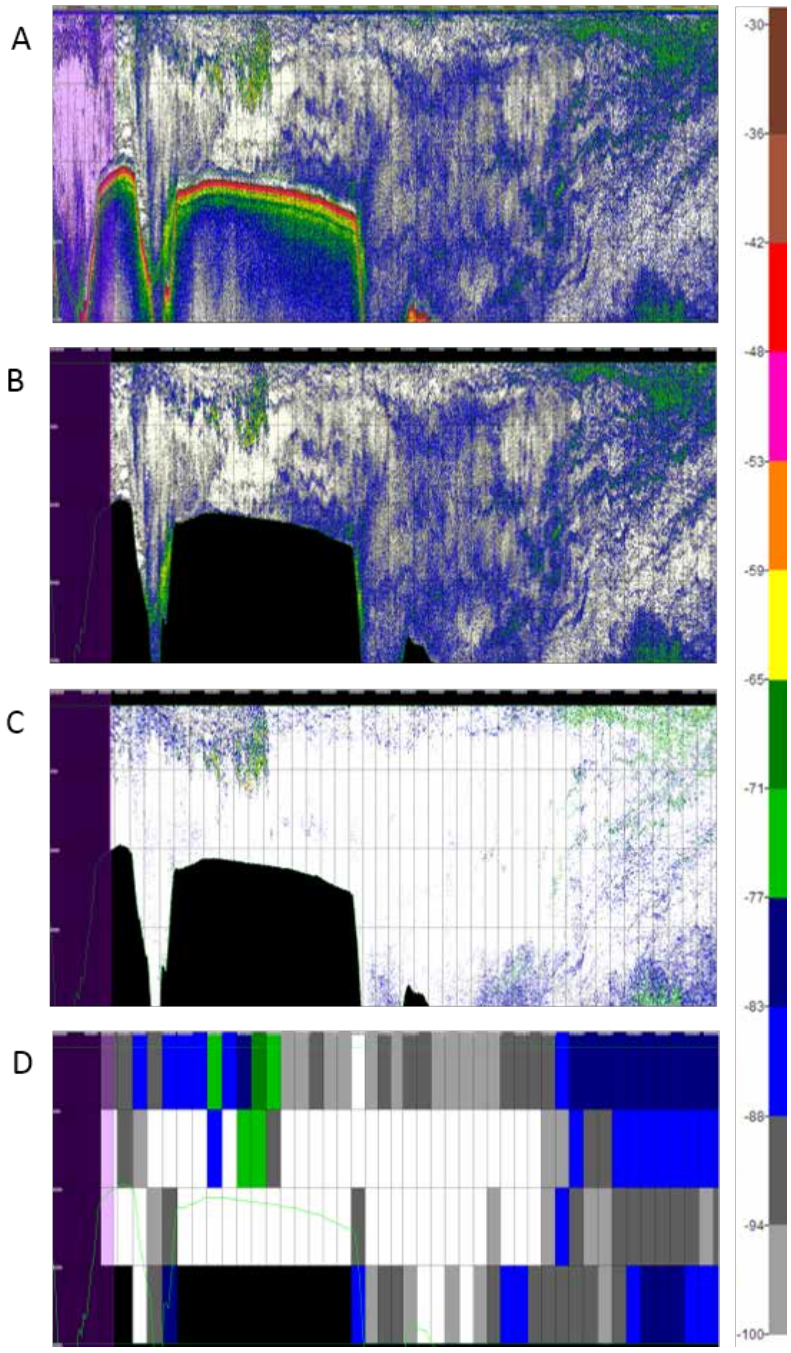

Figure 6-30 Example of echosounding transect data processing
A) Original 38 kHz data, B) cleaned 38 kHz data with noise processing applied, below bottom removed, and off-transect areas removed, C) 38 kHz data classified as swim-bladder fish, D) 38 kHz data classified as swim bladder fish and binned to 50 m (vertical) by 1000 m (horizontal) bins (scale is distorted in the y direction). Note: Data displayed is S_v (volume backscattering coefficient) (dB re 1 m^{-1}), or the mean volume backscattering strength. Data used for analysis was ABC (area backscattering coefficient) (m^2m^{-2}), where ABC = (10 ^S_v/10) x T, and where T is the mean thickness of the integrated cell.

6.4.3 Results

Using the 1,242 one-km horizontal cells (Figure 6-31), we built GAM species density models for 7 species/species guilds with the 12 candidate acoustic variables, where we allowed only 1 variable in combinations of highly correlated acoustic variables. We took care to limit inclusion of highly correlated acoustic variables in the species models, except for the case of the common dolphin model. The correlation matrix showed 2 surprisingly consistent patterns: correlations between swim-bladder fish and phytoplankton/fish larvae, and between non-swim bladder fish and zooplankton.

Model fits varied by species, from strong fits for common dolphin and fin whales, to no viable model for sperm whale (no significant predictors) (Table 6-15). The common dolphin model had the highest deviance explained, but also the highest effective degrees of freedom, a poor RHO value, and 1 of the lower numbers of group sightings, and therefore could be over-fit. Fin whales, which had the second highest number of groups (39), had a respectable amount of deviance explained (25.4%) and among the best error fits, particularly for the RHO value (0.122) derived from the k-fold cross validation. The striped dolphin model explained 11.0% of deviance, and fair to excellent k-fold cross validation test statistics, but had the smallest group sightings size (10). The Risso's dolphin model, which had the most frequently sighted groups (51), was fit with only 1 variable (swim bladder fish at 0-200 m), had fair to excellent and qualitative valuation metrics, but only explained 3.6% of deviance. Pilot whale and bottlenose dolphin models both explained nearly 6% of the deviance, and their MAPE and MAE values evaluated in the fair to good range, however, the pilot whale RHO fell just within the poor classification range. In general, MAE values suggested much better fits than the other metrics across all species.

Common dolphins, bottlenose dolphins, and fin whales all appeared to have significant relationships with potential prey in their final models. Densities of common dolphins and bottlenose dolphins showed a positive relationship with swim bladder fish density (Figure 6-32). Densities of fin whales showed a positive relationship with zooplankton density (Figure 6-33).

Table 6-15 GAM results from cetacean density model using potential prey predictors
Results include variables in each model, model effective degrees of freedom (EDF), percent deviance explained (% dev), and 3 measures of goodness-of-fit: mean absolute percentage error (MAPE), mean absolute error (MAE) and Spearman's rank correlation coefficient (RHO) results for k-fold cross validation[1].

Species	p(0)	Zoo-plankton (m)	Phyto-plankton and fish larvae (m)	Swim Bladder Fish (m)	EDF	Percent Dev	MAPE	MAE	RHO
Common dolphin	0.060	0-50*	0-50***	0-50**	4.82	36.8	98.89	0.243	0.019
Common bottlenose dolphin	0.643	0-50**		0-50*	2.42	6.8	96.25	0.0002	0.096
Striped dolphin	0.764			0-200*	1.79	11.0	98.56	0.0007	0.098
Risso's dolphin	0.674			0-200**	1.81	3.6	90.38	0.0002	0.060
Pilot whale	0.740	50-100*			1.74	5.7	96.56	0.0003	0.049
Sperm whale	0.605				NA	<1	NA	NA	NA
Fin whale	0.513	0-200****	0-200***		2.84	25.4	95.23	0.00007	0.122

**** p=0

*** p<0.001	Excellent	x>0.03	x<0.025	x>150%
** p<0.05	Fair to good	0.05<=x<0.3	1>x>0.025	150>=x>50
* p<=0.10	Poor	x<0.05	x>1	x<50

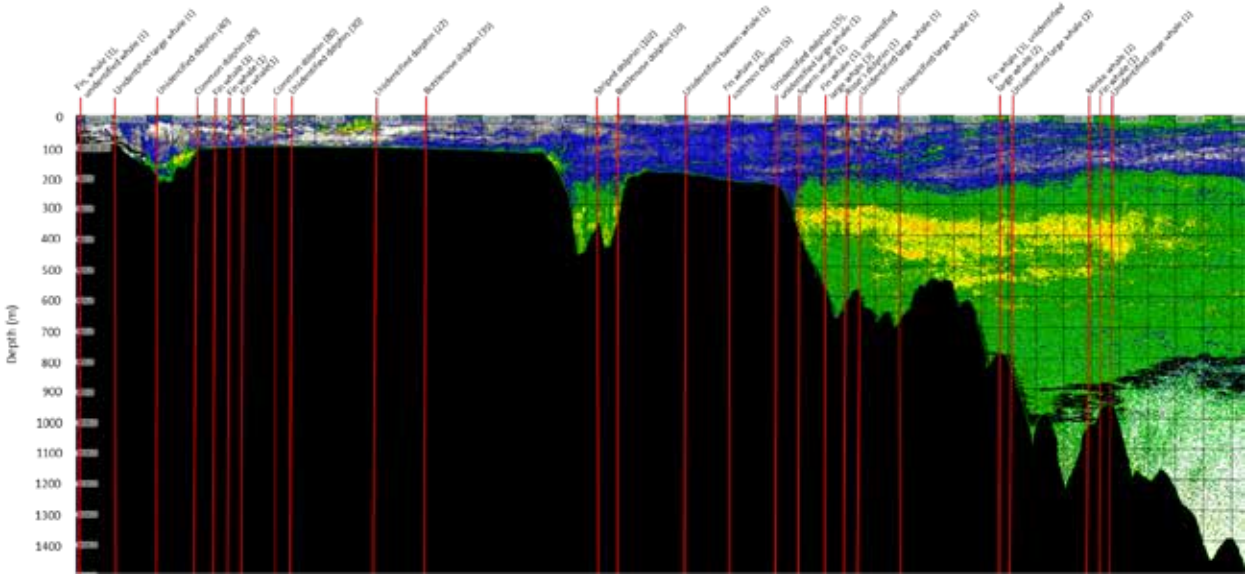

Figure 6-31 Example shelf edge transect in the area of Georges Bank that crosses canyon mouths
Marine mammal sightings (red lines) overlaid with 38 kHz S_v (volume backscattering coefficient) (dB re 1 m^{-1}). Grid intervals are 50 m in depth and 1000 m horizontally.

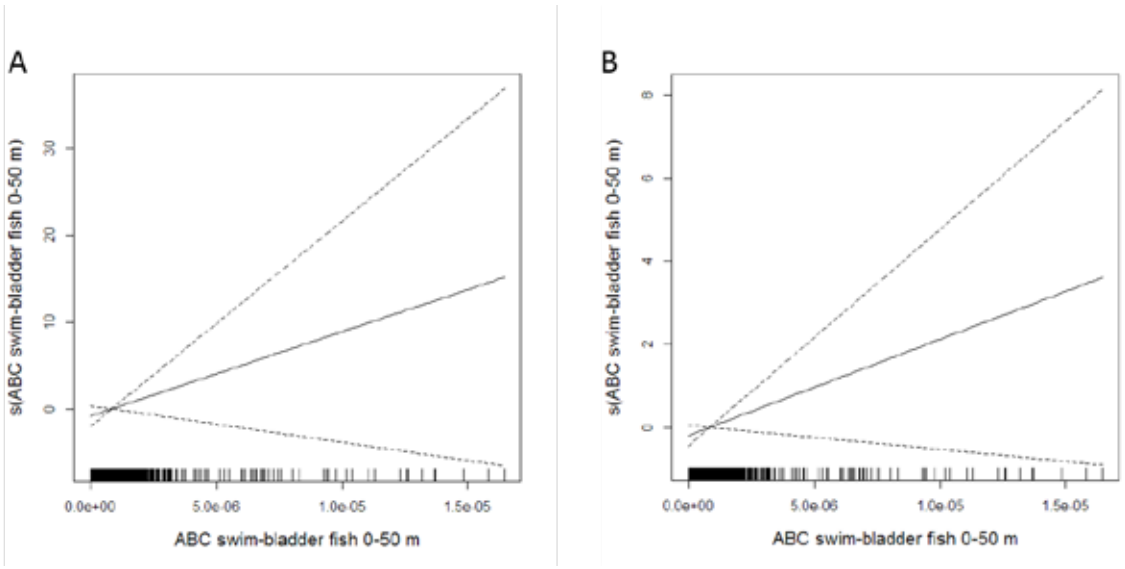

Figure 6-32 GAM results for common (A) and common bottlenose (B) dolphins
Shows relationship with Area Backscatter Coefficient (ABC) from swim-bladder fish in the first 50 m of the water column

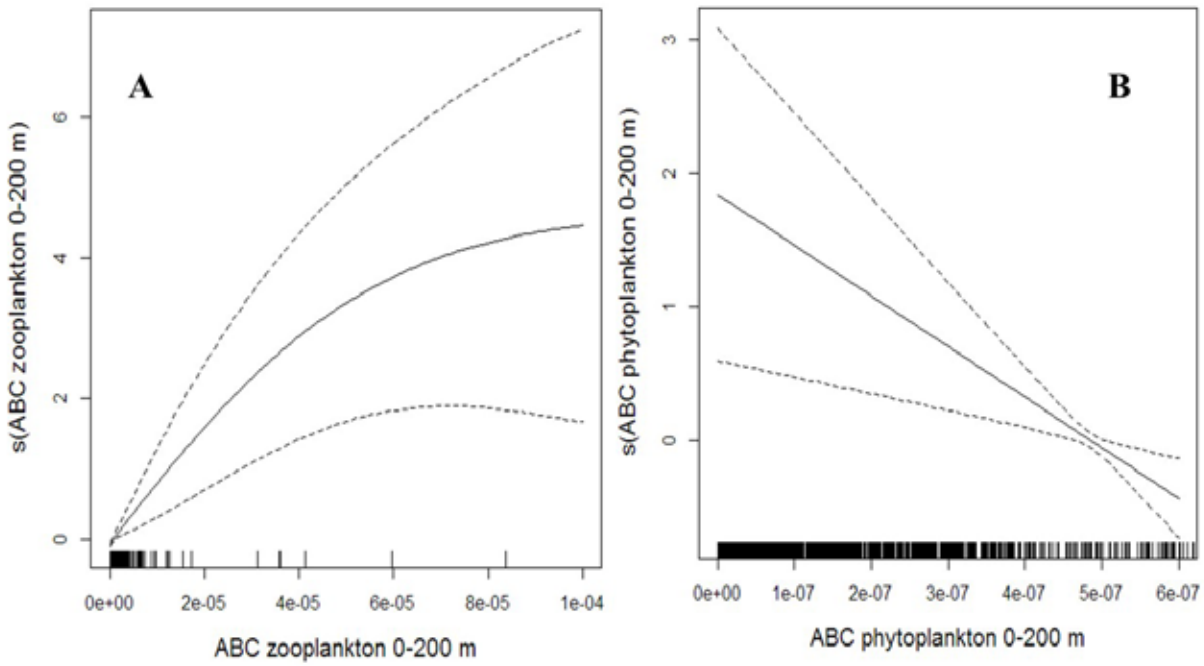

Figure 6-33 GAM plots for fin whale model
We truncated the plot in the x-direction to exclude a couple outliers and better display region with the vast majority of observations of the ABC from zooplankton and phytoplankton.

6.4.4 Discussion

Marine mammal abundance models prepared by Palka et al. (2017) and Chavez-Rosales et al. (2019) for the east coast of the U.S. and part of Canada (including the data used in this exploratory study) explained between 16% to 69% of deviance, based on data from 2010 to 2013. Their study developed models from 17 potential predictor variables, though most final models contained 5 predictor variables. Models often included aerial survey data from other seasons and areas other than the shelfbreak region, so evaluations between the Chavez-Rosales et al. (2019) models and those presented here are not directly comparable. That said, they are useful for a general validation of modelling with acoustic variables. The explained deviance was similar in this study for common dolphin (36.8% vs 42.1%) and fin whale (25.4% vs 34.7%). Models from our study did not compare as well when the species typically feed more deeply or more concentrated on squid. Models of Risso's dolphins, pilot whales, and sperm whales explained much less deviance than the Chavez-Rosales et al. (2019) study (3.6% vs 49.6% for Risso's dolphins, 5.7% vs 56.2% for pilot whales, and no deviance explained vs 33.5% for sperm whales).

We chose a horizontal distance of 1000 m in this study in an attempt to retain the potential fine-scale relationships that drive predator-prey interactions. Recent research into marine patchiness examining the scales shaping zooplankton, fish, and seabird distribution via acoustics found that sub-mesoscale processes from 100 m to 1 km play a significant role in shaping the pelagic seascape (Bertrand et al. 2014). Use of an overly small horizontal scale could result in autocorrelation and artificially inflate explanatory power; however, GAMs limit that possibility since they are generally robust to autocorrelation. Furthermore, recent analysis of acoustic observations near seamounts have found that autocorrelation was not present at scales greater than 1 km (Cascão et al. 2017), suggesting that a comparable relationship may apply in a similarly high relief area such as the continental shelfbreak.

6.4.5 Key Findings

This exploratory study demonstrated that acoustic-based measures of organism structure alone might explain a large amount of variance when describing marine mammal density patterns, at least for some species. The top 2 models explained 37% and 25% of model deviance when using just the prey information, with an average of 15% deviance explained across all models except sperm whale. These fits are similar to previous studies modelling marine mammal distribution in this same region and off the east coast of the U.S that often needed many covariates that were proxies for prey densities. Thus, the incorporation of prey density covariates has the potential to improve future distribution and abundance models, while also making them more robust to potential future ecological, oceanographic, and climatic changes.

6.4.6 Data Gaps and Future Work

Future research should include additional years of data to ensure robust models, and areas off the shelfbreak should be included to allow for abundance estimations over a wider region. We are currently expanding the research described in this study to include data collected in 2011 and 2016. This expansion should result in findings that are more robust. To best employ water column characteristics in a modeling framework, future models should combine acoustically sensed prey layers with more traditional variables like sea surface temperature and latitude that could provide structure for which acoustic variables may become more informative, improving accuracy and possibly informing the reasons behind some acoustic relationships. To achieve prediction in areas not on the ship track, we would apply a 2- or 3-dimensional surface of characteristics of the water column prey across the full study area. Currently, acoustic sampling in areas along and off the shelfbreak, are rare outside of the repeated AMAPPS ship tracks. Interpolating

only using the AMAPPS ship tracks would result in large areas with high uncertainty. An alternative approach is to model prey layers relative to existing variables such as bathymetry, satellite-derived oceanographic variables, and ocean models, then use the modeled prey layers in a marine mammal distribution model.

Palacios et al. (2013) considered prey was the single most desirable predictor variable for modelling marine mammal distributions. Thus by directly modelling prey abundances in density-habitat models we could result in modeled estimated that are more accurate and more responsive to changing ocean conditions. This approach would get closer to a mechanistic prediction of distribution. The next step would be to include physical processes that drive the lower trophic level prey aggregations. These improved models would assist in managing human impacts on marine mammals as climate shifts preferred habitats and as human use of the ocean for energy resources increases.

6.5 Summary of Other Projects that used AMAPPS Sighting Data

The AMAPPS line transect visual sightings data are available to the public to conduct other types of analyses. Below are summaries of some of the recently published and ongoing work on species density models.

6.5.1 Cetacean Density Surface Models

The Duke Marine Geospatial Ecology Lab, in collaboration with scientists from NEFSC and SEFSC and other partnering organizations, incorporated AMAPPS I (2010 to 2014) survey data into cetacean density surface models released in 2017 and 2018 (Roberts et al. 2017, 2018), which updated models originally published in 2016 (Roberts et al. 2016). Roberts presented these models at the 2017 conference of the Society for Marine Mammalogy. These models informed various management and regulatory contexts. For example, NOAA Fisheries used them to inform the development of regulations for geological and geophysical surveying of U.S. Atlantic waters, and the related incidental harassment permits, as well as incidental harassment permits for offshore wind-energy projects. Regional ocean planning bodies incorporated and utilized these models in the northeast (Northeast Regional Ocean Council) and mid-Atlantic (Mid-Atlantic Regional Council on the Oceans).

Duke Marine Geospatial Ecology Lab, NEFSC, SEFSC, and other partners initiated development of a new set of density models for all extant cetacean taxa sighted off the U.S. east coast for the Navy to develop the Phase IV Environmental Impact Statement for the Atlantic Fleet Testing and Training area. These models will utilize all survey data from AMAPPS I and II, and any from AMAPPS III made available by NOAA Fisheries. In addition, these partners developed a revised right whale density model, incorporating data from many surveys, including those conducted under AMAPPS I and II. The right whale model became part of the Right Whale Decision Support Tool that is informing new right whale regulations.

6.5.2 Deep-diving Cetaceans

Virgili et al. (2018) combined data from multiple visual surveys to model the habitat of deep-diving cetaceans (ziphiids, physeteriids, and kogiids) at the basin scale. They used data from 11 different survey groups that surveyed waters ranging from the western North Atlantic (AMAPPS) to the Mediterranean, where most surveying was between 30°N and 60°N. To model habitat preferences, they used GAMs with a Tweedie distribution to model the mean number of individuals per track line segment with smooth nonlinear functions of candidate environmental predictors. These predictors included static covariates (depth, bottom slope, and surface area of canyons and seamounts) and dynamic covariates (SST, sea surface height, net primary production, and eddy kinetic energy). They found that the deeper areas of the North Atlantic gyre were mostly environmental extrapolation in the predictions, thereby highlighting gaps

in sampling across the different surveys. For the 3 species groups, they found the highest relative densities were along continental slopes, particularly in the western North Atlantic Ocean where the Gulf Stream creates dynamic frontal zones and eddies.

6.5.3 Giant Manta Ray

The NMFS Southeast Regional Office used AMAPPS and GOMMAPPS (Gulf of Mexico marine assessment for protected species) sightings and effort for ESA-listed giant manta ray (*Manta birostris*) to develop a species distribution model. This model controls for effective survey effort and predicts the probability of manta sightings based on environmental conditions such as sea surface temperature, thermal frontal gradients, water depth, and primary productivity (Nicholas et al. in prep). They recently presented the draft results of this effort to our Southeast Region Office Section 7 teams to facilitate their conservation efforts.

6.5.4 Short-term Forecasts of Marine Mammal Distributions

Julia Stepanuk, a student at Stony Brook University is currently working on a PhD dissertation, under Dr. Lesley Thorne, that incorporates environmental and prey distribution covariates into present-absent models for Northeast Atlantic humpback and fin whales. Prey data are from the NEFSC bottom trawl surveys and the whale data were from standardized marine mammal line transect surveys, including those from AMAPPS. She also is using output from the NOAA Subseasonal Experiment forecasts to generate probabilistic predictions of forage fish, humpback whale, and fin whale distributions. This work represents a first step towards the development of a subseasonal forecast for large whale distributions. These forecasts could provide fishers and managers with information about times and areas where whales are likely to occur, for example high risk areas to ship strikes and entanglements.

6.6 Acknowledgements

We would like to thank the many scientists that spent months collecting the data analyzed in this chapter. We also thank the crews of the NOAA ships *Henry B. Bigelow* and *Gordon Gunter*, along with the pilots that flew the NOAA Twin Otters. In addition, we would like to thank David Chevier from the Northeast Fisheries Science Center in Woods Hole, MA who created and updated the AMAPPS Cetacean Model Viewer website that houses the results of the density-habitat model predictions.

6.7 References Cited

Artelle KA, Anderson SC, Cooper AB, Paquet PC, Reynolds JD, Darimont CT.2013. Confronting uncertainty in wildlife management: Performance of grizzly bear 550 management PLOS ONE (8):e78041.

Aschettino JM, Engelhaupt D, Engelhaupt A, Richlen M, DiMatteo A. 2018. Mid-Atlantic humpback whale monitoring, Virginia Beach, Virginia: 2017/18 annual progress report. Final Report. Prepared for U.S. Fleet Forces Command. Submitted to Naval Facilities Engineering Command Atlantic, Norfolk, Virginia, under Contract N62470-15-8006, Task Order 17F4013, issued to HDR, Inc., Virginia Beach, Virginia. June 2018.

Aschettino JM, Enelhaupt DT, Engelhaupt AG, DiMatteo A, Pusser T, Richlen MF, Bell JT. 2020. Satellite telemetry reveals spatial overlap between vessel high-traffic areas and humpback whales (*Megaptera novaeangliae*) near the mouth of the Chesapeake Bay. Front. Mar. Sci 7:121.

Bailey H, Rice A, Wingfield JE, Hodge KB, Estabrook BJ, Hawthorne D, Garrod A, Fandel AD, Fouda L, McDonald E, Grzyb E, Fletcher W, Hoover AL. 2019. Determining habitat use by marine mammals and ambient noise levels using passive acoustic monitoring offshore of Maryland. Sterling (VA): US Department of the Interior, Bureau of Ocean Energy Management. OCS Study BOEM 2019-018; 232 pp.

Baird RW, Webster DL, Swaim ZT, Aschettino JM, Foley HJ, Cioffi WR, Anderson DB, Read AJ. 2019. Spatial Use of Cuvier's Beaked Whales and Short-finned Pilot Whales Satellite Tagged off Cape Hatteras, North Carolina: 2018 Annual Progress Report. Prepared for U.S. Fleet Forces Command. Submitted to Naval Facilities Engineering Command Atlantic, Norfolk, Virginia, under Contract No. N62470-15-D-8006, Task Order 18F4036, issued to HDR Inc., Virginia Beach, Virginia. June 2019.

Baumgartner M. 2019. North Atlantic right whale automomous acoustic monitoring. Final report to contract number N62470-15-D-8006-18N4109. Available on US Navy Marine Species Monitoring website.

Becker EA, Forney KA, Redfern JV, Brlow J, Jocox MC, Roberts JJ, Palacios DM. 2019. Predicting cetacean abundance and distribution in a changing climate. Divers. Distrib. 25(4):626-643.

Behrenfeld MJ, Falkowski PG. 1997. Photosynthetic rates derived from satellite-based chlorophyll concentration. Limnol. Oceanogr. 42(1):1-20.

Belkin IM, O'Reilly JE. 2009. An algorithm for oceanic front detection in chlorophyll and SST satellite imagery. Journal of Marine Systems 78:319-326.

Benoit-Bird KJ, Lawson GL. 2016. Ecological insights from pelagic habitats acquired using active acoustic techniques. Annu. Rev. Mar. Sci. 8:463-490.

Benoit-Bird KJ, McManus MA. 2012. Bottom-up regulation of a pelagic community through spatial aggregations. Biol. Lett. 8:813-816.

Benoit-Bird KJ, Battaile BC, Heppell SA, Hoover B, Irons D, Jones N, Kuletz KJ, Nordstrom CA, Paredes R, Suryan RM, Waluk CM, Trites AW. 2013. Prey patch patterns predict habitat use by top marine predators with diverse foraging strategies. PLOS ONE 8:e53348.

Brandt MJ, Diederichs A, Betke K, Nehls G. 2011. Responses of harbour porpoises to pile driving at the Horns Rev II offshore wind farm in the Danish North Sea. Mar. Ecol. Prog. Ser. 421:205-216.

Brandt MJ, Dragon A-C, Diederichs A, Schubert A, Kosarev V, Nehls G, Wahl V, Michalik A, Braasch A, Hinz C, Ketzer C, Todeskino D, Gauger M, Laczny M, Piper W. Effects of offshore pile driving on harbour porpoise abundance in the German Bight. Assessment of noise effects. Final report. 2016. Prepared for Offshore Forum Windenergie.

Bravington MV, Miller DL, Hedley SL. 2021. Variance propagation for density surface models. J. Agric. Biol. Environ. Stat.

Cañadas A, Sagarminaga R. 2000. The Alboran Sea, an important breeding and feeding ground for the long-finned pilot whale (*Globicephala melas*) in the Mediterranean Sea. Mar. Mammal Sci. 16:513-529.

Cascão I, Domokos R, Lammers MO, Marques V, Domínguez R, Santos RS, Silva MA. 2017. Persistent enhancement of micronekton backscatter at the summits of seamounts in the Azores. Front. Mar. Sci. 4:25.

Chavez-Rosales S, Palka DL, Garrison L, Josephson E. 2019. Environmental predictors of habitat suitability and occurrence of cetaceans in the western North Atlantic Ocean. Sci. Rep. 9:5833.

Conn PB, Laake JL, Johnson DS. 2012. A hierarchical modeling framework for multiple observer transect surveys. PLOS ONE 7:e42294.

Davis GE, Baumgartner MF, Corkeron PJ, Bell J, Berchok C, Bonnell JM, Thornton BJ, Brault S, Buchanan GA, Cholewiak DM, Clark CW, Delarue J, Hatch LT, Klinck H, Kraus SD, Martin B, Nieukirk S, Nowacek DP, Parks SE, Parry D, Pegg N, Read AJ, Rice AN, Risch D, Scott A, Soldevilla MS, Stafford KM, Stanistreet JE, Summers E, Todd S, Van Parijs SM. 2020. Exploring movement patterns and changing distributions of baleen whales in the western North Atlantic using a decade of passive acoustic data. Glob. Change Biol. 26(9):4812-4840.

Demer DA, Berger L, Chabot D, Bernasconi M, Bethke E, Boswell K, Chu D, Domokos R, Dunford A, Fässler S, Stéphane G, Hufnagle LT, Jech JM, Bouffant N, Lebourges-Dhaussy A, Lurton X, Macaulay GJ, Perrot Y, Ryan T, Parker-Stetter S, Stienessen S, Weber T, Williamson N. 2015. Calibration of acoustic instruments. International Council for the Exploration of the Sea, Copehangen, Denmark.

Echoview. 2018. Echoview software. Echoview Software Pty Ltd, Hobart, Australia.

JR, Lehmann A, Li J, Lohmann LG, Loiselle BA, Manion G, Moritz C, Nakamura M, Nakazawa Y, Overton J McC, Peterson AT, Phillips SJ, Richardson KS, Scachetti-Pereira R, Schapire RE, Sobero´n J, Williams S, Wisz MS, Zimmermann NE. 2006. Novel methods improve prediction of species' distributions from occurrence data. Ecography 29:129-151.

Engelhaupt A, Aschettino JM, Engelhaupt D, Richlen M, Cotter M. 2020a. VACAPES Outer continental shelf cetacean study, Virginia Beach, Virginia: 2019 Annual progress report. Prepared for U.S. Fleet Forces Command. Submitted to Naval Facilities Engineering Command Atlantic, Norfolk, Virginia, under Contract No. N62470-15-8006, Task Orders 18F4082 and 19F4068, issued to HDR Inc., Virginia Beach, Virginia. April 2020.

Engelhaupt DT, Pusser T, Aschettino JM, Engelhaupt AG, Cotter MP, Richlen MF, Bell JT. 2020b. Blue whale (*Balaenoptera musculus*) sightings off the coast of Virginia. Mar. Biodivers. Rec. 13:6.

Engelhaupt A, Aschettino JM, Engelhaupt D, DiMatteo A, Richlen M, Cotter M. 2019. VACAPES Outer continental shelf cetacean study, Virginia Beach, Virginia: 2018 Annual progress report. Prepared for U.S. Fleet Forces Command. Submitted to Naval Facilities Engineering Command Atlantic, Norfolk, Virginia, under Contract No. N62470-15-8006, Task Order 18F4082, issued to HDR Inc., Virginia Beach, Virginia. July 2019.

Engelhaupt A, Aschettino JM, Engelhaupt D. 2018. VACAPES Outer continental shelf cetacean study, Virginia Beach, Virginia: 2017 Annual progress report. Prepared for U.S. Fleet Forces Command. Submitted to Naval Facilities Engineering Command Atlantic, Norfolk, Virginia, under Contract No. N62470-15-8006, Task Order 35, issued to HDR Inc., Virginia Beach, Virginia. May 2018.

Engelhaupt A, Aschettino JM, Engelhaupt D. 2017. VACAPES Outer continental shelf cetacean study, Virginia Beach, Virginia: 2016 Annual progress report. Prepared for U.S. Fleet Forces Command. Submitted to Naval Facilities Engineering Command Atlantic, Norfolk, Virginia, under Contract Nos. N62470-10-3011, Task Orders 03 and 54, and N62470-15-8006, Task Order 35, issued to HDR Inc., Virginia Beach, Virginia. 31 August 2017.

Engelhaupt A, Aschettino J, Jefferson TA, Engelhaupt D, Richlen M. 2016. Occurrence, distribution, and density of marine mammals near naval station Norfolk and Virginia Beach, Virginia: 2016 Final report. Prepared for U.S. Fleet Forces Command. Submitted to Naval Facilities Engineering Command Atlantic, Norfolk, Virginia, under Contract No. N62470-10-3011, Task Orders 03 and 043, issued to HDR Inc., Virginia Beach, Virginia. 12 October 2016.

Eppley RW. 1972. Temperature and phytoplankton growth in the sea. Fish. Bull. 70:1063-1085.

Foley HJ. 2018. Spatial ecology and movement patterns of deep-diving odontocetes in the Western North Atlantic Ocean. Master's thesis under the direction of Dr. Krishna Pacifici at North Carolina State University, Raleigh, NC.

Foley HJ, Paxton CGM, Cummings EW, McAlarney RJ, McLellan WA, Pabst DA, Read AJ. 2019. Occurrence, distribution, and density of protected species in the Jacksonville, Florida, Atlantic fleet training and testing (AFTT) study area. Prepared for U.S. Fleet Forces Command. Submitted to Naval Facilities Engineering Command (NAVFAC) Atlantic, Norfolk, Virginia, under Contract No. N62470-15-D-8006, Task Orders 29 and 48, issued to HDR, Inc., Virginia Beach, Virginia. May 2019.

Foote KG, Knudsen HP, Vestnes G, MacLennan DN, Simmonds EJ. 1987. Calibration of acoustic instruments for fish density estimation: A practical guide. International Council for the Exploration of the Sea, Copenhagen Denmark.

Forney KA. 2000. Environmental models of cetacean abundance: reducing uncertainty in population trends. Conserv. Biol. 14:1271-1286.

Forney KA, Ferguson MC, Becker EA, Fiedler PC, Redfern JV, Barlow J, Vilchis IL, Ballance LT. 2012. Habitat-based spatial models of cetacean density in the eastern Pacific Ocean. Endang Species Res 16:113-133.

Garrison LP, Rosel PE. 2017. Partitioning short-finned and long-finned pilot whale bycatch estimates using habitat and genetic information. Southeast Fisheries Science Center, Protected Resources and Biodiversity Division, 75 Virginia Beach Dr., Miami, FL 33140. PRBD Contribution # PRBD-2016-17; 24 pp.

Gregr EF, Trites AW. 2001. Predictions of critical habitat for five whale species in the waters of coastal Britsh Columbia. Can J Fish Aquat Sci 58:1265-1285.

Guisan A, Zimmermann NE. 2000. Predictive habitat distribution models in ecology. Ecol. Model. 135:147-186.

Hastie T, Tibshirani, R. 1990. Generalized Additive Models. Chapman & Hall, London.

Hodge LEW, Baumann-Pickering S, Hilderbrand JA, Bell JT, Cummings EW, Foley HJ, McAlarney RJ, McLellan WA, Pabst DA, Swaim ZT, Waples DM, Read AJ. 2018. Heard but not seen: Occurrence of *Kogia* spp. along the western North Atlantic shelf break. Mar. Mammal Sci. 34(4):1141-1153.

Lawson GL, Barange M, Fréon P. 2001. Species identification of pelagic fish schools on the South African continental shelf using acoustic descriptors and ancillary information. ICES J. Mar. Sci. 58: 275-287

Lawson GL, Wiebe PH, Ashjian CJ, Gallager SM, Davis CS, Warren JD. 2004. Acoustically-inferred zooplankton distribution in relation to hydrography west of the Antarctic Peninsula. Deep Sea Res. Part II: Topical Studies in Oceanography 51:2041-2072

McAlarney R, Cummings E, McLellan B, Pabst A. 2018a. Aerial surveys for protected marine species in the Cape Hatteras study area: 2017 Annual progress report. Prepared for U.S. Fleet Forces Command. Submitted to Naval Facilities Engineering Command Atlantic, Norfolk, Virginia, under Contract No. N62470-15-D-8006 Task Orders 05, 29 and 48, issued to HDR, Inc., Virginia Beach, Virginia. April 2018.

McAlarney R, Cummings E, McLellan W, Pabst A. 2018b. Aerial surveys for protected marine species in the Norfolk Canyon region: 2017 Annual progress report. Prepared for U.S. Fleet Forces Command. Submitted to Naval Facilities Engineering Command Atlantic, Norfolk, Virginia, under Contract No. N62470-15-D-8006 Task Orders 05, 29 and 48, issued to HDR, Inc., Virginia Beach, Virginia. April 2018.

McLennan WA, McAlarney RJ, Cummings EW. 2018. Distribution and abundance of beaked whales (Family Ziphiidae) off Cape Hatteras, North Carolina, USA. Mar. Mammal Sci. 34(4):997-1017.

Miller DL, Burt ML, Rexstad EA, Thomas L. 2013. Spatial models for distance sampling data: Recent developments and future directions. Methods Ecol. Evol. 4:1001-1010.

Moses E, Finn JT. 1997. Using geographic information systems to predict North Atlantic right whale (*Eubalaena glacialis*) habitat. J. Northwest Atl Fish Sci 22: 37-46.

Nasu K. 1966. Fishery oceanographic study on the baleen whaling grounds. Sci. Rep. Whales Res. Inst. 20:157-210.

Nicholas A, Farmer, Garrison LP, Horn C, Miller M, Gowan T, Kenney RD, Rappucci G, Aichinger Dias L, Vukovich M, Willmott JR, Pate J, Webb HD, Hickerson E, Stewart J, Bassos-Hull K, Jones D, Adams D, Carlson J, Kaijura S, Waldron J, Marshall A. In Prep. The distribution of manta rays in the northwestern Atlantic Ocean and Gulf of Mexico.

Normandeau Associates Inc., APEM Ltd. 2020. Digital aerial baseline survey of marine wildlife in support of offshore wind energy. Third annual report. Summer 2016 – Spring 2019. Available online.

Orphanides CD. 2019. Relating marine mammal distribution to prey abundance. Ph.D. Dissertation. Graduate School of Oceanography, University of Rhode Island, Kingston, RI.

Palacios DM, Baumgartner MF, Laidre KL, Gregr EJ. 2013. Beyond correlation: integrating environmentally and behaviourally mediated processes in models of marine mammal distributions. Endang Species Res 22:191-203.

Palka D. 1995. Influences on spatial patterns of Gulf of Maine harbor porpoises. Dev. Mar. Biol. 4:69-75.

Palka DL, Chavez-Rosales S, Josephson E, Cholewiak D, Haas HL, Garrison L, Jones M, Sigourney D, Waring G (retired), Jech M, Broughton E, Soldevilla M, Davis G, DeAngelis A, Sasso CR, Winton MV, Smolowitz RJ, Fay G, LaBrecque E, Leiness JB, Dettlof M, Warden M, Murray K, Orphanides C. 2017. Atlantic marine assessment program for protected species: 2010- 2014. US Dept. of the Interior, Bureau of Ocean Energy Management, Atlantic OCS Region, Washington, DC. OCS Study BOEM 2017-071; 211 pp.

Pardo MA, Gerrodette T, Beier E, Gendron D, Forney KA, Chivers SJ, Barlow J, Palacios DM. 2015. Inferring cetacean population densities from the absolute dynamic topography of the ocean in a hierarchical Bayesian framework. PLOS ONE 10(3):e0120727.

Parry DM, Van Parijs SM, Baumgartner MF, Davis GE. 2018. Tracking sei whales in the Western North Atlantic using passive acoustics. Poster.

Pavanato HJ, Wedekin LL, Guilherme-Silveira FR, Engel MH, Kinas PG. 2017. Estimating humpback whale abundance using hierarchical distance sampling. Ecol. Model. 358:10-18.

Rafter MA, Trickey JS, Rice AC, Merrifield M, Thayre BJ, O'Neill E, Wiggins SM, Baumann-Pickering S, Frasier KE, Hildebrand JA. 2020. Passive acoustic monitoring for marine mammals in the Jacksonville Range Complex, June 2017 – 2019. Final Report. Marine Physical Laboratory Technical Memorandum 649. June 2020. Submitted to Naval Facilities Engineering Command (NAVFAC) Atlantic, Norfolk, Virginia, under Contract No. N62470-15-D-8006 Subcontract #383-8476 (MSA2015-1176 Task Order 003) issued to HDR, Inc.

Plummer M. 2003. JAGS: A program for analysis of Bayesian graphical models using Gibbs sampling.

Redfern JV, Ferguson MC, Becker EA, Hyrenbach KD, Good C, Barlow J, Kaschner K, Baumgartner MF, Forney KA, Balance LT, Fauchald P, Halpin P, Hamazaki T, Pershing AJ, Qian SS, Read A, Reilly SB, Torres L, Werner F. 2006. Techniques for c Mar. Ecol. Prog. Ser. 310: .

Regan HM, Colyvan M, Burgman MA. 2002. A taxonomy and treatment of uncertainty for ecology and conservation biology. Ecol. Appl. 12:618-628.

Roberts JJ, Best BD, Mannocci L, Fujioka E, Halpin PN, Palka DL, Garrison LP, Mullin KD, Cole TVN, Khan CB, McLellan WA, Pabst DA, Lockhart GG. 2016. Habitat-based cetacean density models for the US Atlantic and Gulf of Mexico. Sci. Rep. 6:22615.

Roberts JJ, Mannocci L, Halpin PN. 2017. Final project report: Marine species density data gap assessments and update for the AFTT study area, 2016-2017 (Option year 1), Document version 1.4. Duke University Marine Geospatil Ecology Lab, Durham, NC. Pg 87.

Roberts JJ, Mannocci L, Schick RS, Halpin PN. 2018. Final project report: Marine species density data gap assessments and update for the AFTT study area, 2017-2018 (Option year 2), Document version 1.2. Duke University Marine Geospatial Ecology Lab, Durham, NC; 114pp.

Robinson LM, Elith J, Hobday AJ, Pearson RG, Kendall BE, Possingham HP, Richardson AJ. 2011. Pushing the limits in marine species distribution modelling: lessons from the land present challenges and opportunities. Glob. Ecol. Biogeogr. 20:789-802.

Ryan TE, Downie RA, Kloser RJ, Keith G. 2015. Reducing bias due to noise and attenuation in open-ocean echo integration data. ICES J. Mar. Sci. 72:2482-2493.

Salisbury DP, Estabrook BJ, Klinck H, Rice AN. 2019. Understanding marine mammal presence in the Virginia Offshore Wind Energy Area. Sterling (VA): US Department of the Interior, Bureau of Ocean Energy Management. OCS Study BOEM 2019-007; 103 pp.

Sigourney DB, Chavez-Rosales S, Conn PB, Garrison L, Josephson E, Palka D. 2020. Developing and assessing a density surface model in a Bayesian hierarchical framework with a focus on uncertainty: insights from simulations and an application to fin whales (*Balaenoptera physalus*). PeerJ, DOI 10.7717/peerj.8226.

Sollman R, Gardner B, William KA, Gilbert AT, Veit RR. 2016. A hierarchical distance sampling model to estimate abundance and covariate associations of species and communities. Methods Ecol. Evol. 7:529-537.

Southwell T. 1898. The migration of the right whale (*Balaena mysticetus*). Nat. Sci. 12:397-414.

Stanistreet JE, Nowacek DP, Bell JT, Cholewiak DM, Hildebrand JA, Hodge LE, Van Parijs SM, Read AJ. 2018. Spatial and seasonal patterns in acoustic detections of sperm whales *Physeter microcephalus* along the continental slope in the western North Atlantic. Endang Species Res 35:1-13.

Stanistreet JE. 2017. Ecology of beaked whales and sperm whales in the Western North Atlantic Ocean: Insights from passive acoustic monitoring. Thesis from Duke University, University Program in Ecology; 164 pp.

Stanton TK, Chu D. 2000. Review and recommendations for the modelling of acoustic scattering by fluid-like elongated zooplankton: euphausiids and copepods. ICES Journal of Marine Science 57:793-807.

Stanton TK, Chu D, Wiebe PH. 1998. Sound scattering by several zooplankton groups. II. Scattering models. J Acoust. Soc. Am. 103(1):236-253.

Stanton TK, Dezhang C, Reeder DB. 2004. Non-Rayleigh acoustic scattering characteristics of individual fish and zooplankton. IEEE J. Ocean. Eng. 29:260-268.

Taylor BL, Wade PR, DeMaster DP, Barlow J. 2000. Incorporating uncertainty into management models for marine mammals. Conserv. Biol. 14(5):1243-1252.

Tetra Tech and LGL. 2020. Final comprehensive report for New York Bight whale monitoring aerial surveys, March 2017 – February 2020. Technical report prepared by Tetra Tech, Inc. and LGL Ecological Research Associates, Inc. 211 pp. + appendices. Prepared for New York State Department of Environmental Conservation, Division of Marine Resources, East Setauket, NY. May 18, 2020.

Thomas L, Buckland ST, Rexstad EA, Laake JL, Strindberg S, Hedley SL, Bishop JRB, Marques TA, Burnham KP. 2010. Distance software: design and analysis of distance sampling surveys for estimating population size. J. Appl. Ecol. 47:5-14.

Thorne LH, Foley HJ, Baird RW, Webster DL, Swaim ZT, Read AJ. 2017. Movement and foraging behavior of short-finned pilot whales in the Mid-Atlantic Bight: Importance of bathymetric features and implications for management. Mar. Ecol. Prog. Ser. 584:245-257.

Thorne LH, Baird RW, Webster DL, Stepanuk JE, Read AJ. 2019. Predicting fisheries bycatch: A case study and field test for pilot whales in a pelagic longline fishery. Divers. Distrib. 25:909-923.

Trenkel VM, Berger L. 2013. A fisheries acoustic multi-frequency indicator to inform on large scale spatial patterns of aquatic pelagic ecosystems. Ecol. Indic. 30:72-79.

Uda M. 1954. Studies of the relation between the whaling grounds and the hydrographical conditions (I). Sci. Reo. Whales Res. Inst. 9:179-187.

Virgili A, Authier M, Boisseau O, Canadas A, Claridge D, Cole T, Corkeron P, Doremus G, David L, DiMeglio N, Dunn C, Dunn TE, Garcia Baron I, Laran S, Lewis M, Louzao M, Mannocci L, Martinez-Dedeira J, Palka D, Panigada S, Pettex E, Roberts J, Ruiz Sancho L, Santos MB, VanCannery O, Vazquez Bonales JA, Monestiez P, Ridoux V. 2018. Combining multiple visual surveys to model habitats of deep diving cetaceans at the basin level. Glob. Ecol. Biogeogr. 28(3):300-314.

Wade PR. 2000. Bayesian methods in conservation biology. Conserv. Biol. 14(5):1308-1316.

Waples DM, Read AJ. 2020. Photo-Identification Analyses in the Cape Hatteras Study Area: 2019 Annual Progress Report. Prepared for U.S. Fleet Forces Command. Submitted to Naval Facilities Engineering Command Atlantic, Norfolk, Virginia, under Contract No. N62470-15-D-8006, Task Order 19F4026 issued to HDR, Inc., Virginia Beach, Virginia. April 2020.

Wiebe PH, Greene CH, Stanton TK, Burczynski J. 1990. Sound scattering by live zooplankton and micronekton: Empirical studies with J. Acous. Soc. Am. 88:2346-2360.

Wiebe PH, Mountain DG, Stanton TK, Greene CH, Lough G, Kaartvedt S, Dawson J, Copley N. 1996. Acoustical study of the spatial distribution of plankton on Georges Bank and the relationship between volume backscattering strength and the taxonomic composition of the plankton. Deep Sea Res. Part II: Topical Studies in Oceanography 43:1971-2001.

Wingfield JE, O'Brien M, Lyubchich V, Roberts JJ, Halpin PN, Rice AN, Bailey H. 2017. Year-round spatiotemporal distribution of harbour porpoises within and around the Maryland wind energy. PLOS ONE 12(5):e0176653.

Wood SN. 2011. Fast stable restricted maximum likelihood and marginal likelihood estimation of semiparametric generalized linear models. J. R. Stat. Soc. Series B 73:3-36.

Wood SN. 2017. Generalized Additive Models: An Introduction with R. Chapman and Hall/CRC

Zeh JM, Rekdahl ML, Rice AN, Clark CW, Rosenbaum HC. 2020. Detections of humpback whale (*Megaptera novaeangliae*) vocalizations on an acoustic sensor in the New York Bight. Mar. Mammal Sci. 37:751-760.

7 Cetacean Ecology and Passive Acoustic Research

Primary authors: Danielle Cholewiak, Genevieve Davis, Annamaria DeAngelis, Liam Mueller-Brennan, Nicole Pegg, Melissa Soldevilla, and Debra Palka.

7.1 Introduction

To better understand species distribution, abundance trends, and habitat use throughout U.S. waters, we need effective marine mammal monitoring programs. Anthropogenic activities are steadily increasing along coastal and offshore areas concurrent with important cetacean habitats. In many cases, the effects of these activities on cetacean populations are unknown. Both baseline monitoring, and detailed studies of fine-scale cetacean habitat use and ecology, are necessary to better understand the drivers of cetacean distribution and the potential effects of anthropogenic activities.

In this chapter, we focus on 2 main research areas that address aspects of 5 of the 7 AMAPPS objectives (taken from the complete list of objectives in Chapter 3):

1) Collect broad-scale data over multiple years on the seasonal distribution and abundance of marine mammals (cetaceans and pinnipeds), marine turtles, and seabirds using fixed passive acoustic monitoring and direct aerial and shipboard surveys of coastal U.S. Atlantic Ocean waters;
2) Collect similar data at finer scales at several sites of particular interest to BOEM, NOAA, and partners using visual and acoustic survey techniques;
4) Collect additional data on life-history and ecology, including habitat use, residence time, frequency of use, and behavior;
5) Identify currently used, viable technologies and explore alternative platforms and technologies to improve population assessment studies, if necessary;
7) Collect long-term ambient noise data in U.S. Atlantic Ocean waters.

The first main research area discussed in this chapter relates to the distribution, habitat use and ecology of offshore deep-diving species, particularly beaked whales (Ziphiidae), pygmy sperm whales (*Kogia breviceps*) and dwarf sperm whales (*Kogia sima*). Beaked whales are notoriously difficult to detect via standard visual survey methods (Barlow et al. 2005), as they are inconspicuous while at the surface and spend a long time submerged on foraging dives. Thus, this is 1 of the reasons that the International Union for Conservation for Nature Red List considers most beaked whales as data deficient. Their low visual detection rates and difficulty to identify to species make it difficult to develop robust abundance estimates. In addition, beaked whales are of particular concern for impacts from offshore activities, as they are sensitive to anthropogenic sound in a variety of circumstances (Cox et al. 2006).

During AMAPPS II, we conducted a broad-scale cetacean abundance survey in 2016, as well as 3 fine-scale surveys during 2015 to 2019 as part of the Integrated Technologies for Deep Diving Cetaceans Program (ITS.DEEP). In the latter surveys, we combined visual and passive acoustic data collection with tagging, genetic sampling, and oceanographic data collection. Passive acoustic technologies have become a critical component of marine mammal monitoring, providing valuable information about the spatial and temporal distribution of a variety of species, as well as contributing new insights into their behavior and ecology (Davis et al. 2017). Passive acoustics are a primary component of the studies described in this chapter. We used the AMAPPS II data to document the distribution of beaked whales and pygmy or dwarf sperm whales (*Kogia* spp.) along the U.S. eastern seaboard. We provided a preliminary assessment of beaked whale dive depths. In addition, we presented results of our focused studies on True's beaked whales (*Mesoplodon mirus*) in the Georges Bank region of the western North Atlantic, where this is the first detailed study on this species.

The second main research area discussed in this chapter is the use of long-term passive acoustic monitoring, aimed at assessing cetacean distribution and anthropogenic activities at fixed sites along the entire U.S. eastern seaboard. From 2015 to 2018, we collected data along the continental shelf using marine autonomous recording units (MARUs), deployed across 5 lines spanning shelf waters from Massachusetts to Georgia. We also deployed a suite of high-frequency recording packages (HARPs) at 8 sites along the shelfbreak, from the Georges Bank region through to the Blake Plateau.

In our region, data collected from acoustic studies have already provided important new insights on species distributions, including demonstrating the extended occurrence of baleen whales beyond seasons and regions where they were previously documented (e.g. Risch et al. 2013; Risch et al. 2014; Davis et al. 2017; Davis et al. 2020). Previous AMAPPS acoustic research has helped us to better understand the characteristics of the acoustic signals from multiple species (Cholewiak et al. 2013; Soldevilla et al. 2017; DeAngelis et al. 2018), the effects of anthropogenic noise (Cholewiak et al. 2017), and the use of towed hydrophone arrays to estimate dive depths for deep diving species (DeAngelis et al. 2017). The current AMAPPS studies expand on this work to improve our understanding of cetacean ecology, provide new information for species classification and stock delineations, improve abundance estimation, and further our understanding of the spatial and temporal distribution of baleen whales and more cryptic odontocete species along the western North Atlantic.

7.2 Offshore Cetacean Ecology Studies

7.2.1 Methods

7.2.1.1 Overview

In this chapter, we discuss the visual, passive acoustic, genetic, and oceanographic data collected during 7 shipboard surveys between 2015 and 2019. In 2016, the NEFSC and SEFSC each conducted a broad-scale cetacean abundance survey along the U.S. east coast, during which visual and passive acoustic teams collected data following line-transect methodologies (Figure 7-1A; Table 7-1). We used these data to assess the distribution of beaked whale species and pygmy/dwarf sperm whales along the U.S. east coast, as well as providing data for an assessment of beaked whale dive depths by using towed hydrophone arrays.

From 2017 to 2019, the NEFSC conducted 3 focused cetacean surveys in the Georges Bank region (Figure 7-1B; Table 7-1). These surveys were part of a project entitled “Integrated Technologies for Deep Diver Ecology Program” (ITS.DEEP), in which the goal was to study the ecology and fine-scale habitat use of offshore, deep-diving cetaceans by integrating multiple technological tools. These surveys focused primarily on beaked whales, specifically the little-known True’s beaked whale. We collected visual and passive acoustic data from a variety of platforms, genetic data via eDNA and biopsy sampling, and deployed the first digital acoustic recording tag (DTAG) on a True’s beaked whale. Our design plan for data collection during these surveys included 2 modes:

1) “exploratory”, during which time the visual and acoustic teams collected data on all species using modified line-transect methodologies, and
2) “focal follow”, during which time we collected data on positions, surfacing intervals, and behavior of target groups of animals, in addition to noting the presence of nearby groups of animals.

Additionally, in 2015 the NEFSC conducted both a cetacean survey and a turtle ecology survey in the Georges Bank region. While we did not focus on beaked whales during these surveys, we did incorporate limited passive acoustic data collection that also contributed to our knowledge of the distribution of beaked whales and other deep-diving cetaceans in this region.

Additional details on these surveys are in Chapter 11 and previous AMAPPS annual reports that are on the AMAPPS website.

Table 7-1 Overview of shipboard surveys included in the offshore cetacean ecology studies

HB1503-1	2015	Sei whale survey	10-Jun	19-Jun
HB1503-2	2015	Turtle tagging survey	24-Jun	1-Jul
HB1603	2016	NEFSC shipboard abundance survey	28-Jun	24-Aug
GU1605	2016	SEFSC shipboard abundance survey	1-Jul	24-Aug
HRS1701	2017	Offshore deep-diving cetacean survey	8-Sep	17-Sep
GU1803	2018	Offshore deep-diving cetacean survey	21-Jul	1-Aug
HRS1910	2019	Offshore deep-diving cetacean survey	18-Aug	27-Aug

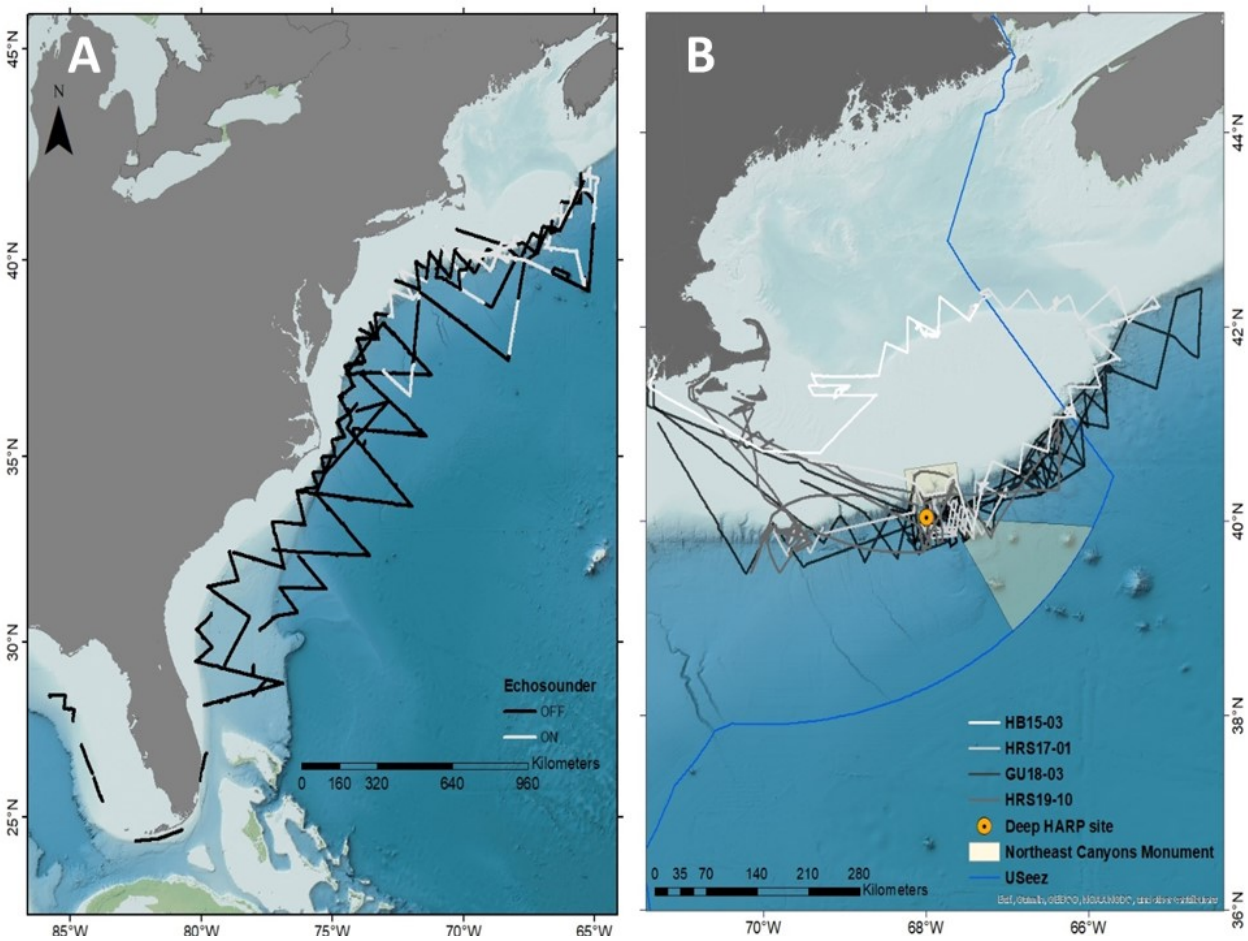

Figure 7-1 Track lines used in offshore cetacean ecology studies
A) Survey tracklines for NEFSC and SEFSC cetacean abundance surveys conducted in 2016. Note that during the NEFSC survey, echosounder status alternated between active ("on") and passive ("off") modes. B) Survey tracklines for NEFSC cetacean ecology surveys conducted on ships in 2015 and 2017 to 2019.

7.2.1.2 Visual and Oceanographic Data Collection

We collected visual data with 1 to 2 teams of trained observers using high-powered binoculars (25 x 150), handheld binoculars, and naked eye. We also collected data related to sighting conditions (i.e. Beaufort sea state, glare, haze, fog, etc.) and survey effort. During focal follow modes, we collected data on positions and surfacing intervals of target groups, behavior, the presence of nearby groups of animals, and any other relevant information. Most of our focal follow effort targeted groups of True's beaked whales, though we collected some additional data on groups of Sowerby's and Cuvier's beaked whales as well. In addition, an independent team of 1 to 2 people collected data on seabird occurrence and distribution (see Chapter 9 for more detail). The seabird team also assisted with marine mammal data collection when the team was operating in focal follow mode. Detail on our oceanographic data collection and results are in Chapter 10.

Passive Acoustic Data Collection and Analyses: Towed Hydrophone Arrays

From 2015 to 2019, we used several different towed hydrophone array configurations to collect passive acoustic data during shipboard surveys. We used custom-built linear arrays, each of which included an oil-filled section with a combination of hydrophones and a depth sensor. In 2018, we also tested a rigid tetrahedral array ("Trident" array, Proteus Technology). We recorded digitized acoustic data directly to hard drives or a desktop computer using the software program PAMGUARD (Gillespie et al. 2009), sampling at either 192 or 500 kHz.

Details on array design and recording methodologies are in the AMAPPS annual reports. In brief, we deployed the hydrophone arrays up to 300 m behind the ship, for up to 24 hr per day, depending on the survey. We typically deployed the array only in water depths of 100 m or greater. During the turtle survey in 2015, we collected passive acoustic data opportunistically at night. During the dedicated cetacean surveys conducted during 2017 to 2019, we often collected passive acoustic data for 24 hr per day. Our passive acoustic teams consisted of 1 to 4 people who monitored the hydrophone array(s) in real-time as much as possible. See Chapter 11 for an overall summary of the towed hydrophone array effort.

We used a suite of software packages to process the hydrophone array data, but we primarily processed our acoustic data using PAMGUARD. In 2018 and 2019, we were able to process most of our acoustic data in real-time, but other datasets required extensive post-processing. Our general methodology employed a 2 step-procedure to identify click trains of interest. First, we ran the PAMGUARD click detector over all sound files, with pre-filter, trigger filter, and threshold settings determined based on the analysis needs. We identified putative beaked whale events based on the frequency spectra, inter-click interval, and shape of the echolocation click. To classify beaked whale events, we referenced click information from the literature (Johnson et al. 2004; Zimmer et al. 2005; Johnson et al. 2006; Gillespie et al. 2009; Cholewiak et al. 2017; DeAngelis et al. 2018; Clarke et al. 2019). The structure of clicks from True's beaked whales and Gervais' beaked whales (*Mesoplodon europaeus*) are similar (DeAngelis et al. 2018). Thus, we assigned the species identification of events with this ambigous click structure to a category representing either a True's beaked whale or Gervais' beaked whale (referred to as the MmMe category: that is, *Mesoplodon mirus* or *Mesoplodon europaeus*). Additionally, for datasets analyzed only in real-time (2018 and 2019), clicks that appeared similar to True's or Gervais' clicks were placed into the MmMe category when we did not have corresponding visual species confirmation. For post-processed datasets, we assigned beaked whale events to categories depending on the duration and quality of event. We did not use these categories for the data processed in real-time. Whenever possible, we localized the beaked whale events by using Target Motion Analysis and the 2-demensional Simplex Optimisation algorithm within PAMGUARD. If the algorithm could not find a convergence point from the bearings, we used the GPS location of the vessel at the start of the event as its location. In real-time analyses, the GPS position of the vessel was from the start of the event as localizing in real time was not possible.

Limited information exists on the click characteristics of pygmy and dwarf sperm whales (Hildebrand et al. 2019; Merkens et al. 2018; Merkens and Oleson 2018). Based on these data, we identified putative pygmy or dwarf sperm whale events based on the frequency spectra, inter-click interval, and shape of the echolocation click. However, there is currently little consensus on reliably classifying acoustic detections between pygmy/dwarf sperm whale species (*Kogia* sp). Furthermore, the majority of visual sightings of pygmy or dwarf sperm whales also did not classify them to species. Therefore, to be conservative, we categorized our events as Kogia1 spp., Kogia2 spp., and Kogia3 spp. representing the differences in received frequency content between echolocation clicks (peak frequency for Kogia1 spp. = 126 kHz, peak frequency for Kogia2 spp. = 137 kHz, and peak frequency for Kogia3 spp. = 116 kHz), but we did not classify to species (Figure 7-2). At this time, we are unsure how to interpret these peak differences. The 3 different peak frequencies could be a result of propagation effects, or variations in click types within and/or between species (as occurs in Blainville's beaked whales; Keating et al. 2016).

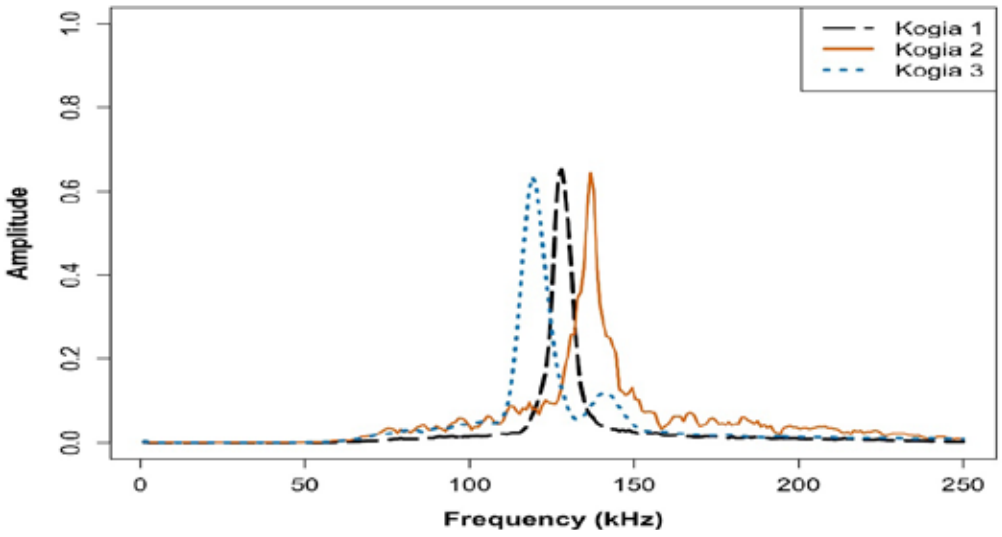

Figure 7-2 Click spectrum of 3 pygmy/dwarf sperm whale click types
Kogia1 spp. (black), Kogia2 spp. (brown) and Kogia3 spp. (blue) clicks show differences in the energy and frequency content of the 3 click types.

7.2.1.4 Passive Acoustic Data Collection and Analyses: Other Units

During the 2018 survey, we deployed a deep-water high-frequency acoustic recording package (Deep-HARP) at 1 offshore site for the duration of the survey. The Deep-HARP developed by Scripps Institution of Oceanography (Wiggins and Hildebrand 2007) collected data on presence of vocally active marine mammals by sampling at 200 kHz and recording continuously. We selected the site (Figure 7-1B) based on bottom depth and previous sightings of cetacean species of interest. We recovered the mooring during the survey, about 25 days later.

We also constructed 3 drifting autonomous spar buoy recorders (DASBRs) prior to the survey, as part of a pilot project to acoustically survey for animals distant from the ship. One of our goals for this pilot project was to assess whether cetacean acoustic detection rates varied without the ship's presence, as compared to acoustic detections using the hydrophone array towed from the ship. Our DASBR design was a modified version of that described in Griffiths and Barlow (2015; 2016). Each DASBR was equipped with an ST4300 SoundTrap (Ocean Instruments) and 2 hydrophones (HTI-96-min and HTI-92-WB, High Tech Inc.), as well as 2 satellite trackers (SPOT Trace) to track the buoy during deployment.

7.2.1.5 Digital high-frequency recording tag (DTAG) Data Collection and Analyses

During the 2017 and 2018 surveys, we used a small boat to approach focal groups of beaked whales to attempt to deploy digital high-frequency recording tags (DTAGs), developed by Woods Hole Oceanographic Institution (Johnson and Tyack 2003). In 2018, we deployed a single DTAGv3 on a True's beaked whale, on 1 individual in a group of 5 to 6 animals. We programmed the DTAG to stay on the animal for 12 hrs, record audio data at a sampling rate of 500 kHz, and additional sensor data at a sampling rate of 50 Hz. We collected surfacing and dive data on the group for approximately 2 hrs prior to tag deployment, and until sunset after tag deployment. The tag remained attached for approximately 13 hrs, after which we relocated it the following morning, approximately 11 km from the deployment site.

We analyzed the resulting data using custom-built MATLAB tools (MathWorks Inc., Natick, MA), as well as the software package Raven Pro 2.0 (Center for Conservation Bioacoustics 2019). Preliminary analyses quantified the number and depth of foraging and bounce dives, the intervals between dives, the duration of echolocation click periods for each foraging dive, and the number of foraging buzzes. Additional analyses examined the surfacing behavior of the whale in more detail, quantifying duration of time at the surface, number of breaths at the surface, and duration of flow noise indicating active swimming.

We also conducted an analysis of the "soundscape" of the tagged whale, quantifying the amount of time that sperm whales, dolphins, pygmy/dwarf sperm whales, other beaked whales besides the tagged whale and its group, and anthropogenic sound sources were audible on the tag (and presumably therefore to the whale). We are conducting further analyses and planning to publish the results in conjunction with the focal follow data.

7.2.1.6 Genetic Data Collection and Analyses

During the 2017 and 2018 surveys, we also collected genetic data during small boat deployments, via biopsy and eDNA sampling (see Chapter 11 for more details). We collected biopsy samples using a crossbow and a sampling bolt equipped with a 40mm stainless steel tip. For the eDNA sampling, we collected paired water samples in 1L bottles on either side of the small boat, typically in or near the flukeprint of an animal after it dove. Once back aboard the ship, we fractioned the biopsy samples. We preserved the skin in 90% ethanol, and froze the blubber dry, wrapped in aluminum foil. We filtered the analyses. At several locations, we also sampled water from depth through conductivity, temperature and depth (CTD) casts. We processed these samples in the same way as the eDNA water samples. We are conducting these analyses in collaboration with the Cetacean Conservation and Genomics Laboratory at the Marine Mammal Institute at Oregon State University.

7.2.2 Results

7.2.2.1 Overall visual and acoustic detections of beaked whales

We searched for beaked whale vocalizations in over 1,743 hrs of towed hydrophone array data collected during 7 cruises (Table 7-2). About 2% of this time, we found interfering noises masking the targeted vocalizations. The sources of the interference were primarily vocal schools of dolphins or snapping shrimp (for SEFSC data only) that were near the ship.

Table 7-2 Summary of analyzed AMAPPS II towed hydrophone array data

Science Center	Year	Cruise	Days with Acoustic Effort	Hours Analyzed for Beaked Whales	Hours Analyzed for Pygmy/Dwarf Sperm Whales
NEFSC	2015	HB1503 (1 and 2)	7	41.52	0
NEFSC	2016	HB1603	40	477.73	565.14
SEFSC	2016	GU1605	44	473.63	506.00
NEFSC	2017	HRS1701	9	171.43	0
NEFSC	2018	GU1803*	25	459.00**	404.86
NEFSC	2019	HRS1910*	9	120.06	0
TOTAL			134	1,743.37	1,476.00

* Hours reported as analysed for these cruises are for real-time monitoring, not post-processing
** This includes the number of hours analysed in post-processing when the array was unmonitored in real time

Throughout the 5 years of surveys, we sighted and acoustically detected 5 of the 6 beaked whale species that occur in the North Atlantic (Table 7-3). The species that we did not sight or acoustically detect was the Northern bottlenose whale (*Hyperoodon ampullatus*), which usually occurs to the north of our study area. Beaked whales tend to be cryptic at the surface and undertake long foraging dives. This behavior makes identifying species challenging, particularly during times when the sea states are rough or when we cannot dedicate time to resight the unidentified groups. Consequently, we could not visually identify nearly half of the beaked whale groups to species. Nevertheless, this is actually a high percentage when compared to previous surveys conducted by us and other researchers. This is because over the years we have developed a better understanding of the subtle physical and behavioral characteristics of the species, particularly Cuvier's and True's beaked whales.

We had more than twice as many acoustic detections of beaked whales as compared to sightings of groups (Table 7-3). However, an acoustic event may represent 1 or more animals within a group, and it could represent the same group recorded more than once because, for example, the group was the target of a focal follow. Multiple acoustic events occurring at the same time could represent individuals in a group spread out while foraging such that their click trains arrive at different bearing angles. Therefore, it is difficult to interpret the difference between the absolute numbers of sightings versus numbers of acoustic detections. Nevertheless, it is clear that we were able to acoustically identify both Blainville's beaked whales (*Mesoplodon densirostris*) and Gervais' beaked whales more often than visually, where the majority of these detections occurred during the SEFSC abundance survey in 2016. Acoustically, there were very few events that we considered "unidentified" beaked whale, as we were able to categorize most events to a species or species group. However, as mentioned above, distinguishing between the echolocation clicks of True's and Gervais' beaked whales is challenging, particularly in real-time. Therefore, our acoustic results include a True's/Gervais' category, to capture the events where we were not able to confidently distinguish between the 2 species without further information or analysis.

7.2.2.2 2016 Abundance Surveys: Distribution of Beaked Whales and Pygmy/Dwarf Sperm Whale Detections

Because our data collection methodology was so different between the line-transect abundance survey conducted in 2016, as compared to other years, we examined the visual and acoustic detections from the 2016 surveys separately to assess broad-scale patterns in species occurrence (Table 7-4). During our combined abundance survey between NEFSC and SEFSC in 2016, we sighted beaked whale groups 182 times. We identified 67% of the sightings as the undifferentiated beaked whale group and 24% as Cuvier's beaked whales. We acoustically detected beaked whale events over 500 times, with 46% of these representing Cuvier's beaked whales (Table 7-4; Figure 7-3). Gervais' and Blainville's beaked whales

were identified almost exclusively from the acoustic data, whereas we both sighted and acoustically detected multiple groups of Sowerby's and True's beaked whales (Table 7-4).

We detected pgymy/dwarf sperm whales on both surveys, with more during the SEFSC survey (Table 7-4). Only 1 detection was classified as Kogia2; the rest were classified as Kogia1 (Figure 7-3). We need more data to assess whether these 2 classifications are the result of intra-specific variation or represent the 2 species. We will be preparing a manuscript further examining the coast-wide distribution of beaked whale and pygmy/dwarf sperm whales species during AMAPPS III.

Table 7-3 Numbers of visually sighted beaked whale groups and acoustic detection events
Numbers were from all surveys, 2015 to 2019. Note that an acoustic detection event may represent 1 or more individuals and do not represent unique sightings/events, as they may include multiple resightings of the same group say during focal follow data collection. The exact correspondence between the number of True's beaked whale group sightings and acoustic detection events is coincidental.

Common Name	Visual Sightings (Groups)	Acoustic Detections (Events)
Blainville's beaked whale	1	46
Cuvier's beaked whale	167	819
Gervais' beaked whale	5	81
Sowerby's beaked whale	12	17
True's beaked whale	184	184
True's/Gervais' beaked whale *(acoustic only)*	*N/A*	354
Unidentified beaked whale	324	6
TOTAL	693	1507

Table 7-4 Numbers of beaked whale and pygmy/dwarf sperm whale groups during 2016
Acoustic detection events and visual group sightings may represent 1 individual or more individuals from a group. Both visual sightings and acoustic events can include multiple detections of the same group.

Common Name	Visual Group Sightings	Acoustic Detection Events
Blainville's beaked whale	1	46
Cuvier's beaked whale	43	233
Gervais' beaked whale	5	81
Sowerby's beaked whale	3	8
True's beaked whale	8	88
True's/Gervais' beaked whale *(acoustic only)*	N/A	23
Unidentified beaked whale	122	1
Pygmy/Dwarf sperm whale (*Kogia* spp.)	58	31
TOTAL	240	511

Latitude and habitat type were able to explain broadly the locations of the acoustic detections of beaked whale species (Figure 7-3). We detected Cuvier's beaked whales primarily along the shelfbreak from Cape Hatteras, NC to the north and on the Blake Ridge off Georgia. In contrast, Sowerby's beaked whales were mostly from Chesapeake Bay to the north. We detected True's beaked whales along the shelfbreak and abyssal waters north of Delaware, while we detected Gervais' beaked whales primarily south of Delaware in the abyssal waters. We detected events that were difficult to distinguish between True's and Gervais' (MmMe class) throughout the east coast. Finally, we detected Blainville's beaked whales south of Albemarle Sound in North Carolina, with a concentration in abyssal waters ranging from off southern North Carolina to the slope waters off central Florida.

Because Cuvier's and Sowerby's beaked whales were able to be visually identified at times, we were able to use the confirmed visual sightings to create spatially explicit density models that incorporated habitat covariates (Chapter 6). These models showed the same spatial patterns (Figure 7-4; Appendix I) as depicted by the acoustic detections (Figure 7-3).

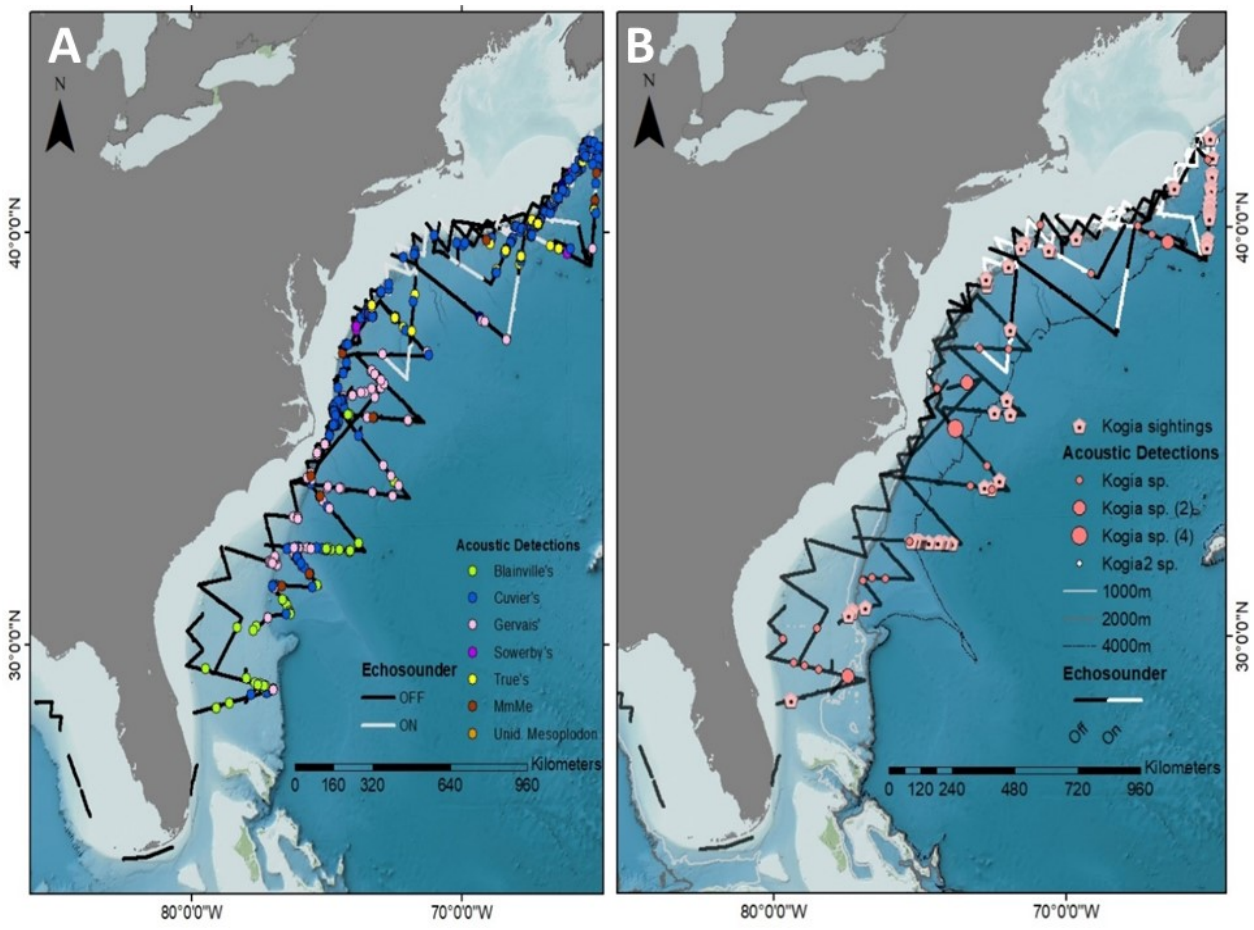

Figure 7-3 Acoustic detections of beaked whales and pygmy/dwarf sperm whale during 2016
Detections were from towed hydrophone arrays. The NEFSC survey used active mode of echosounder every other day. A) Beaked whales. B) Pygmy or dwarf sperm whales. Note the overlapping points identified by the legend "*Kogia* spp. (2)" indicates that there are 2 points in that location and, similarly, "*Kogia* spp. (4)" indicates that there are 4 points in that location.

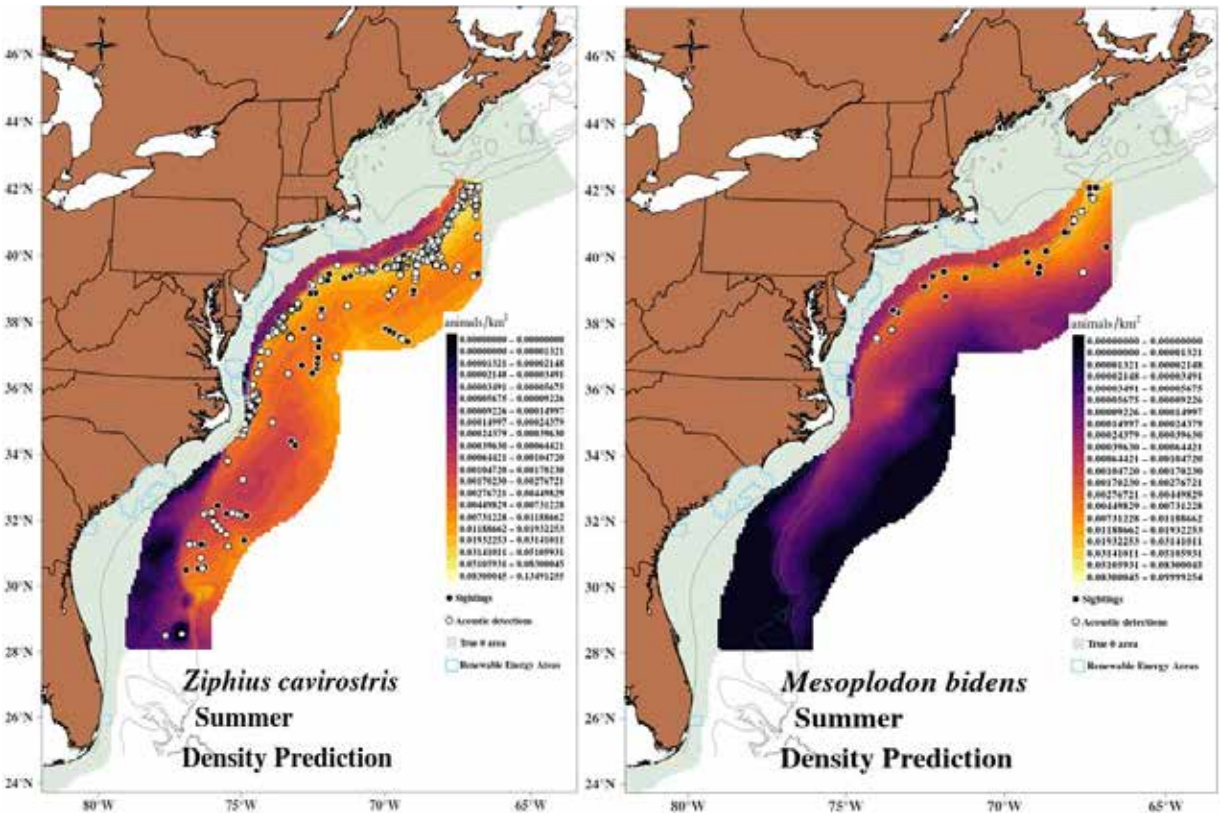

Figure 7-4 Predicted density of Cuvier's and Sowerby's beaked whales from visual sightings data
Colored shadings represent the predicted density, solid black dots are the locations of the visually detected groups, and open dots are locations of acoustic detections. See Chapter 6 and Appendix I for more information about these maps.

7.2.2.3 2016 Abundance Surveys: Effects of Echosounders on Beaked Whales

We also examined beaked whale acoustic event detections relative to shipboard echosounder status by using data from the NEFSC 2016 cetacean abundance survey. This built on previous work that we conducted during AMAPPS I (Cholewiak et al. 2017), where we found that we acoustically detected significantly less beaked whales when shipboard EK60 echosounder was in active mode as compared to passive mode. Active mode is when the EK60 produced sound pings at a variety of frequencies and then recorded received sounds. Active mode is when the EK60 did not produce any sounds but the system still recorded received sounds. See Chapter 10 for more information on the EK60. During the 2016 NEFSC survey, we alternated echosounder status daily between active and passive mode, consistent with our previous study. Similar to our previous results, in 2016 we had nearly 10 times as many detections when echosounders were operating in passive mode (197 events) as compared to active mode (20 events). During the 2016 SEFSC survey, in which shipboard echosounders operated in passive mode during all towed hydrophone array data collection, we detected 263 beaked whale events. This is in stark contrast to the 2013 SEFSC survey in which we found only 17 beaked whale events with the echosounders active during the entire survey (Palka et al. 2017).

Because we also analyzed the data for pygmy/dwarf sperm whales, we wanted to see if there was also a change in detection presence based on echosounder state. However, we did not have enough detections in the 2016 NEFSC dataset to statistically assess whether the effect of the ship's echosounders on pygmy/dwarf sperm whales. Preliminary observations find all 7 pygmy/dwarf sperm whale events when the echosounders were not actively transmitting signals.

7.2.2.4 2016 Abundance Surveys: Dive Depth Estimation

We are in the process of using the 2016 towed hydrophone array data from both the NEFSC and SEFSC surveys to expand on the DeAngelis et al. (2017) study to explore the dive depths of beaked whale species. The dive depths provide information on the animal's ecology and habitat utilization. In addition, we can use these data to correctly estimate the perpendicular distance between the animal and the track line when measured at the surface (as used in abundance estimation). We will attempt to include all 5 species detected on our surveys (as opposed to Cuvier's and MnMe as done in DeAngelis et al. (2017). Preliminary analyses have identified 84 beaked whale events in the NEFSC 2016 abundance survey data that meet our event duration criterion (longer than 2 mins) and our localization criterion (likely to be localizable). We have so far examined 44 of these acoustic events, 38 of which contain sufficient acoustic information to estimate dive depths (Figure 7.5). By species/species group, these included Cuvier's (n = 4), True's (n = 29), Gervais' (n = 1), Sowerby's (n = 1), and MmMe (n = 3). We will be continuing this analysis on the remaining 40 events from the NEFSC 2016 abundance survey data, as well as the 151 events identified from the SEFSC 2016 abundance survey data.

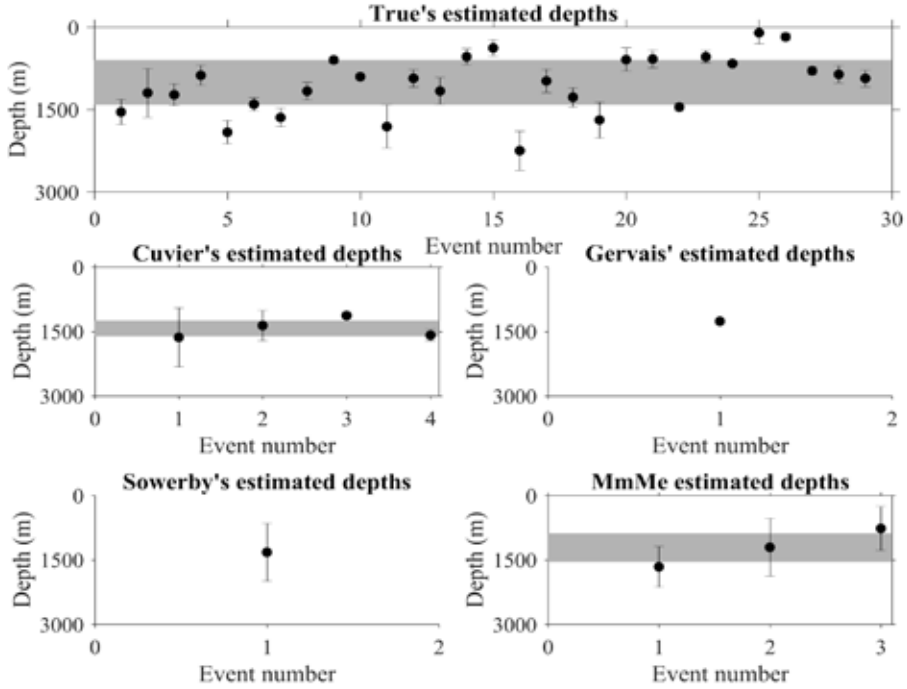

Figure 7-5 Preliminary dive depths for 5 beaked whale species/species groups
We calculated the dive depths by using the towed hydrophone array data collected during the NEFSC 2016 abundance survey, HB1603. Vertical grey bars indicate the interquartile range. Horizonal grey bars indicate the inter-quartile depth range for each species with a sample size greater than 1.

7.2.2.5 Cetacean Ecology Surveys: Detections of beaked whales and pygmy/dwarf sperm whales

During our dedicated cetacean ecology surveys in 2015 and 2017 to 2019, we had over 500 sightings of beaked whale groups and over 1000 acoustic detections (Table 7-5; Figure 7-6). These surveys targeted known beaked whale habitat (based on data collected in AMAPPS I) off Georges Bank in the northeast U.S., focusing on fine-scale studies of deep-diver ecology and habitat use, particularly of True's beaked whales. While 40% of our sightings were unidentified to species, we had nearly 180 sightings of True's beaked whales (57% of positively identified sightings) and over 120 sightings of Cuvier's beaked whales

(40% of positively identified sightings). Acoustically, over 50% of the detection events were of Cuvier's beaked whales, while over 40% of acoustic events were True's or True's/Gervais' beaked whales. The number of sightings and acoustic detections in the 2016 survey give a better representation of coast-wide distribution of beaked whales, whereas the sightings and detections from the cetacean ecology surveys represent data collected through dedicated effort surveying specific beaked whale habitat. These provide finer scale information such as dive cycle and group behavior.

From the cetacean ecology surveys, so far we only analyzed the 2018 data for pygmy/dwarf sperm whales. We had 2 visual sightings and 14 acoustic events detected, across 8 different days.

Table 7-5 Numbers of beaked whales and pygmy/dwarf sperm whale groups from ecology surveys
Surveys conducted in 2015 and 2017 to 2019. Acoustic detection events and visual group sightings may represent 1 individual or more individuals from a group. The numbers reported for the acoustic detections originate from both real-time monitoring and post-processing methods, depending on the survey and family. Both visual sightings and acoustic events include multiple detections of the same group, such as during focal follow data collection.

Common Name	Visual Group Sightings	Acoustic Detection Events
Cuvier's beaked whale	124	586
Gervais' beaked whale	0	0
Sowerby's beaked whale	9	9
True's beaked whale	176	96
True's/Gervais' beaked whale *(acoustic only)*	*N/A*	331
Unidentified beaked whale	202	5
Dwarf/pygmy sperm whale (*Kogia* spp.)	2	14*
TOTAL	511	1027

*2018 only

7.2.2.6 Focal Follow and Dive Behavior of True's Beaked Whales in 2018

During the 2018 NEFSC survey, the focal follow data that we collected on 10 groups of True's beaked whales across 7 different days included the locations, group composition, and behavior of all surfacings (or as many as feasible) of the focus group. We tracked all the focal groups through at least 1 bounce dive[2], and 6 groups through foraging dives[2]. One group was lost when it went on a foraging dive after only 1 "bounce" dive cycle. Of the remaining 9 groups, our focal follow tracking periods ranged from 1 to 7+ hrs, with an average of about 3 hrs. We had an estimated 85 documented surfacing of these 10 groups. We categorized repeat surfacings of focal groups as 'certain', 'probable', or 'possible'. Results from the 2 'possible' surfacing events are not included here.

We tracked focal groups across 56 bounce dives (Table 7-6), and 10 foraging dives (Table 7-7). Bounce dives lasted 13 mins on average, with a range of 3 to 25 mins. Foraging dives lasted 40 mins on average, with a range of 35 to 56 mins. However, it is possible (perhaps likely) that we missed a dive cycle after the group surfaced from foraging, particularly for group 9, which had the longest dive duration. We detected all 9 foraging dives on the towed hydrophone array[2], and once the group was on a foraging dive, we attempted to stay within visual or acoustic detection range of the group (i.e., within 1 to 2 km) and to use the acoustic information to assist the visual sightings team to relocate the group. On average, we

[2] Many whale species (including beaked whales) typically perform 2 types of dives: bounce and foraging dives (Watwood et al 2006; Shearer et al. 2019). A typical dive sequence consists of several short duration, shallow dives (referred to as bounce dives) followed by a long duration, deep dive (referred to as a foraging dive). During a forage dive, the animal produces echolocation clicks for only part of the forage dive (referred to as the vocal period), presumable when the animal is hunting.

detected echolocation clicks for 13 mins during a foraging dive. In several cases, it is likely that we moved out of acoustic detection range of the group while they were still actively echolocating and foraging. Thus, it is possible that the group vocal period[2] we detected does not fully represent the actual group vocal period.

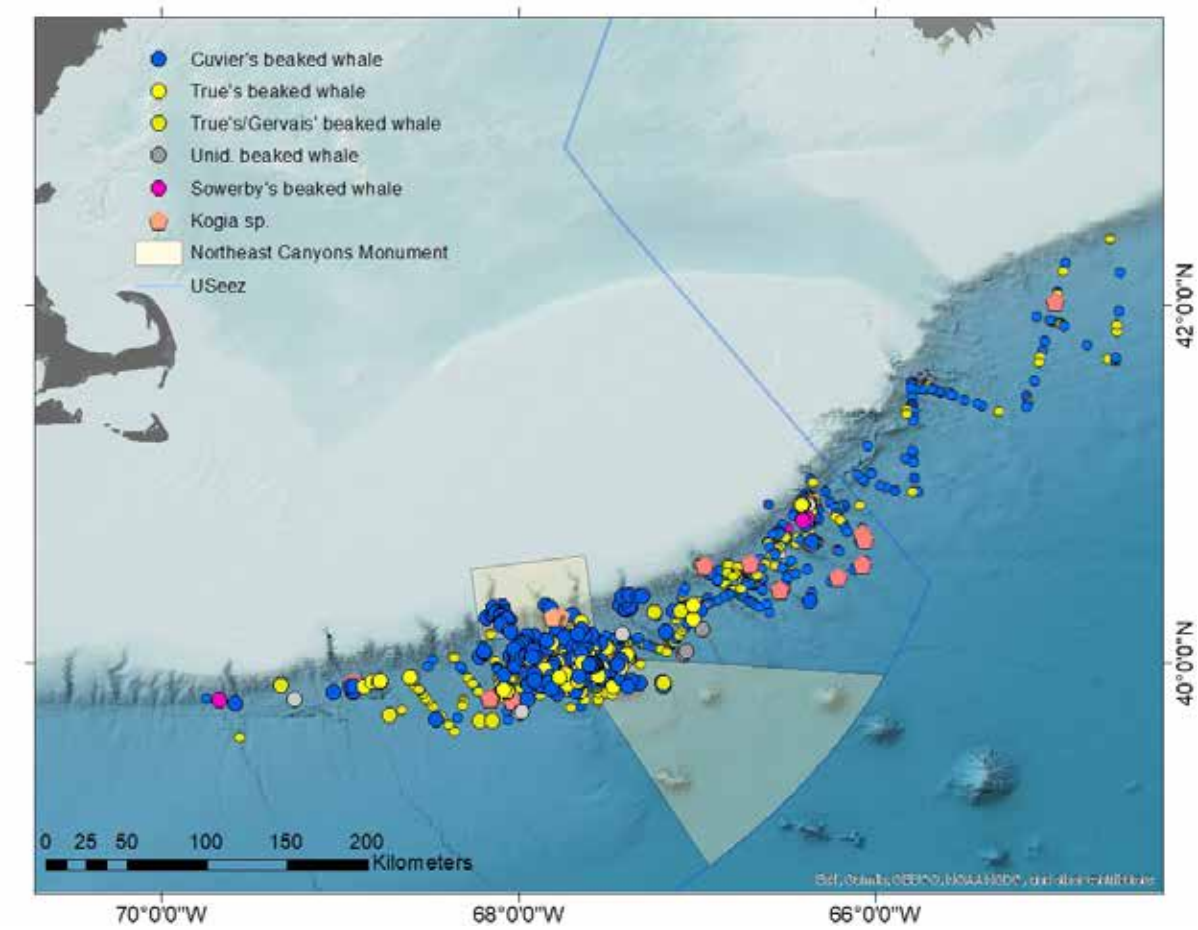

Figure 7-6 Locations of beaked whale and pymy/dwarf sperm whales from ecology surveys
Locations are from either a visually sighted group or an acoustically detected event. Surveys conducted in 2015 and 2017 to 2019.

Table 7-6 Summary of focal follow data on bounce dives
Focal follow data from the NEFSC 2018 cetacean ecology survey. Group size represents the minimum and maximum estimate over the course of all bounce dives, where the group size appeared to fluctuate throughout focal follow period.

Group Identification Number	Group Size (Min to Max)	Number of Dives	Average Dive Duration (min)	Minimum Dive Duration (min)	Maximum Dive Duration (min)
1	3-8	16	15	3	25
2	3-5	3	13	11	15
3	2-4	6	17	15	25
	4-5	18	10	5	20
5	3-5	1	16	16	16
6	2-4	1	15	15	15
7	2-4	2	15	15	16
8	4-5	1	14	14	14
9	2-6	2	13	12	15
10	2-5	6	12	4	25
TOTAL		56	13	3	25

Group includes the animal we tagged with a DTAG.

Table 7-7 Summary of focal follow data on foraging dives
Focal follow data from the NEFSC 2018 cetacean ecology survey. Group size represents minimum and maximum size estimates over the course of all dives. In some cases, group size appeared to fluctuate throughout focal follow period.

Group Identification Number	Group Size (Min to Max)	Number of Dives	Average Dive Duration (min)	Minimum Dive Duration (min)	Maximum Dive Duration (min)	Average Group Vocal Period (min)
1	6	4	39	36	46	14
2	5	1	42	42	42	8
	4-5	1	39	39	39	7
5	3-4	1	39	39	39	9
9	5-6	2	45	35	56*	16
10	5	1	35	35	35	19
TOTAL		10	40	35	56*	13

Group includes the animal we tagged with a DTAG.
* It is possible that we missed a bounce dive after this foraging dive, resulting in a long estimated dive period.

7.2.2.7 True's beaked whale DTAG data collected in 2018

The data from Group 4 (above) is the group that we deployed a DTAG on 1 individual on 10 August 2018 at 15:27 ET. We were able to collect data until sunset on the group with the tagged animal that was about 4 hrs after we deployed the tag (Tables 7-6 and 7-7). During this time, the group moved in a largely clockwise direction, within an area of approximately 5.5 km by 3 km (Figure 7-7). The tag remained attached to the whale for about 13 hrs, 11 min. During this time, the tagged animal undertook 9 foraging dives, 1 of them being while we were tracking the group, and the other 8 after sunset. The tagged animal's foraging dives lasted 32.7 min on average, ranging from 26.1 to 38.9 min, with an average of 18 min of echolocating. This average vocal period aligns well with what was tracked with the towed array, and also highlights the short group vocal periods where we definitely went out of detection range of the group (Groups 2, 4, and 5). Overall, the average dive time between surfacings for the tagged animal was 13.55 min (± 8.67 min). The whale was at the surface for an average of 2.95 min (± 2.43 min) between dives, and took an average of 9 breaths while in the surfacing phase. Over the duration of the tag attachment, the whale was at the surface for approximately 16% of the time (139 min / 851 min). We recovered the tag at

07:05 ET the following morning, about 2.5 hrs after release from the animal, about 8 km from the deployment site (Figure 7-7).

We analyzed the 'soundscape' of the tagged whale, to assess the biologic and anthropogenic contributors to the whale's acoustic environment by dividing the tag data into hourly time units and recording the presence of biological and anthropogenic contributors. Sound sources recorded on the tag were sounds produced/attributed to the tagged whale (such as foraging clicks, flow noise, and blows), foraging clicks from other animals in the tagged animal's group, Cuvier's beaked whale clicks, sperm whale clicks, dolphin clicks and whistles, and vessel noise and echosounders from the research vessel (Figure 7-8). Sperm whale clicks were present at least once within all hourly time units; dolphin vocalizations in 10 hourly time units (77% of the time) and Cuvier's beaked whales in only 2 hourly time units (15% of the time). We only detected vessel noise in the first 4 hrs of the tag deployment when the ship was conducting the focal follow of the group.

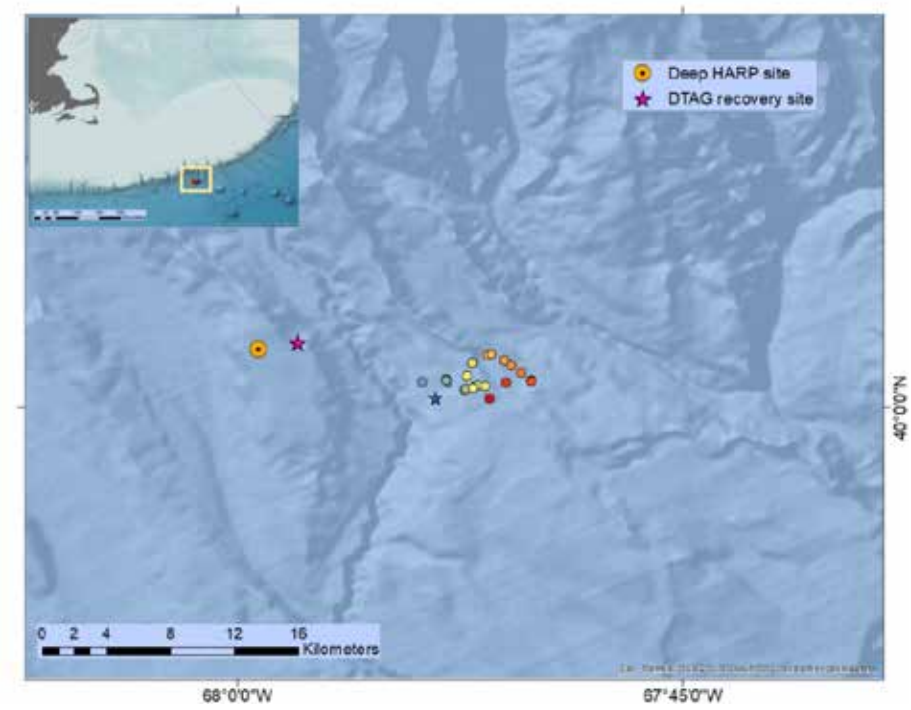

Figure 7-7 Locations of True's beaked whale group with tagged individual
The blue star is at the location of the group when we deployed the DTAG. Subsequent locations of resightings of focal followed group with tagged individual are circles colored blue to yellow to red by time, until group was lost at sunset. The magenta star is at the location where we recovered the tag the following morning.

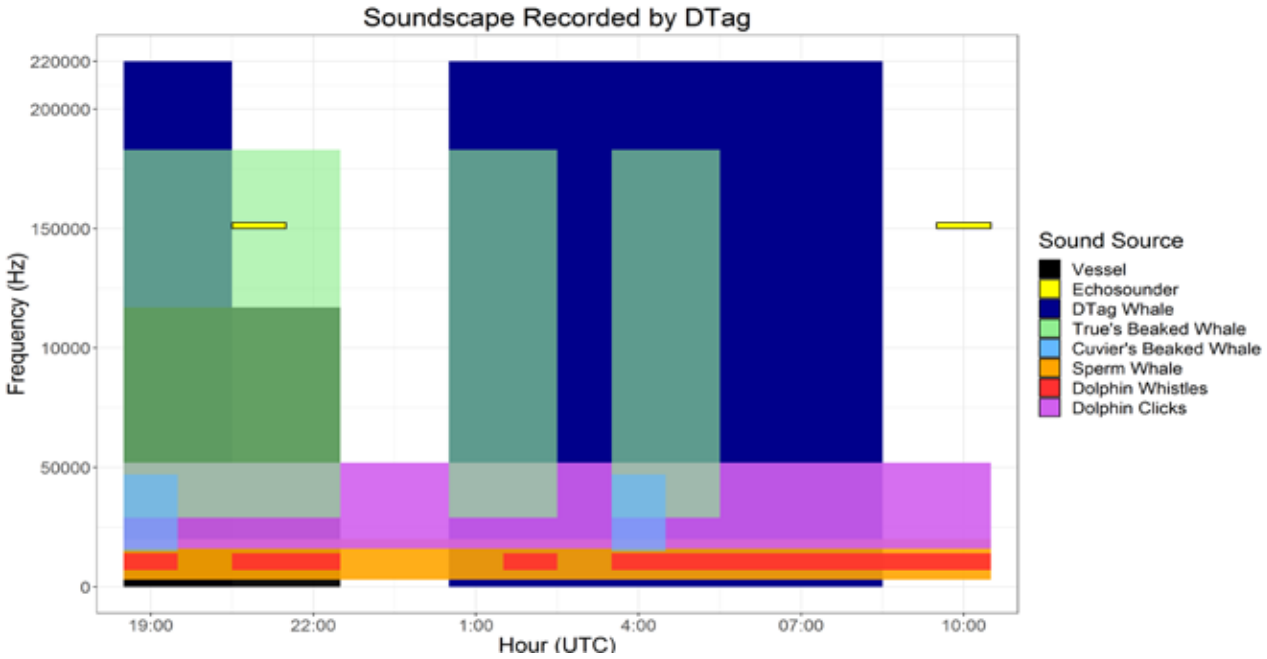

Figure 7-8 Contributors to the acoustic environment recorded on True's beaked whale DTAG
We summarized the presence of acoustic signals that were present on the tag in hourly time bins for the period that the tag was on the whale. The ship's ADCP was transmitting at 150 kHz, which was detectable during the initial 4-hr focal follow after tag deployment and just before tag retrieval.

7.2.2.8 Deep-HARP deployment

We evaluated the presence and persistence of True's and Cuvier's beaked whales, and pygmy/dwarf sperm whales in the 24 days of acoustic data recorded by the deep-HARP that we deployed during the 2018 shipboard survey (locations shown in Figures 7-1 and 7-7). The deep-HARP acoustic data recorded multiple deep diving species sharing their fine-scale habitat (Figure 7-9). We detected True's beaked whales on 21 of 24 days (total = 1,521 min), Cuvier's beaked whales on each day (total = 3,777 min), and pygmy/sperm whales on 15 days (total = 84 min). We detected all 3 species on the same day on 13 of the 24 deployment days, and in some cases, we detected multiple species at the same time.

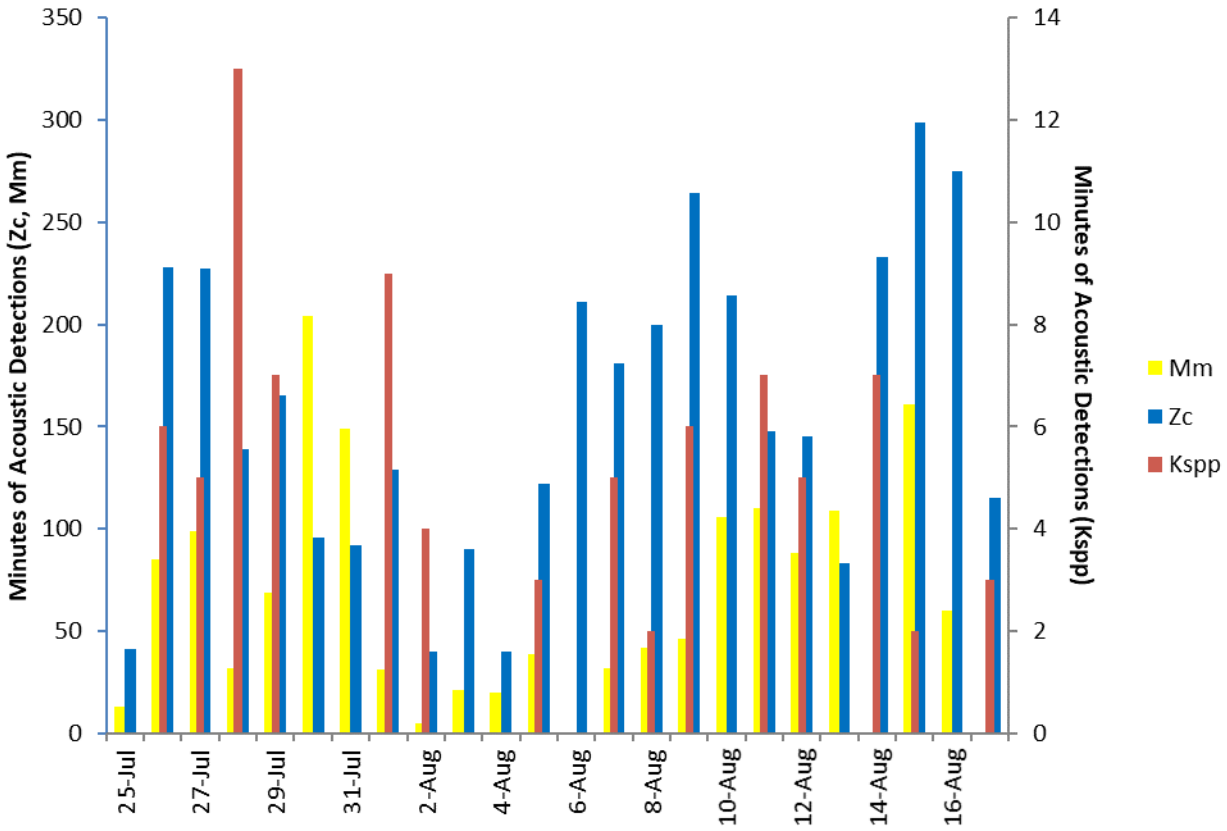

Figure 7-9 Duration of acoustic detections on deep-HARP
Detections were of True's beaked whales (Mm), Cuvier's beaked whales (Zc), and pygmy or dwarf sperm whales (Kspp). Note that the minutes of detection for the beaked whales are on the left-sided y-axis and pygmy/dwarf sperm whales are on the right-sided y-axis.

7.2.2.9 Description of True's beaked whale clicks

True's beaked whales were the last known beaked whale in the North Atlantic Ocean to have its vocalizations characterized acoustically. Until recently, information regarding the distribution, visual description, and diving behavior was limited to some sightings, but mainly strandings of dead specimens (MacLeod et al. 2006; Aguilar de Soto et al. 2017). In 2016 as part of the AMAPPS abundance survey, and 2017 as part of the ITS.DEEP project, we encountered and tracked True's beaked whales twice between both visual and acoustic teams, providing data to describe the click characteristics of this species. In 2016, we detected echolocation clicks from the hydrophone array for 26 min after the visual teams detected 3 groups of True's beaked whales within 1200 m of the NOAA ship *Henry B. Bigelow*. Using the R/V *Hugh R. Sharp* in 2017, we tracked a single group of 5 True's beaked whales for 5 hrs. During this time, we recorded 37 min of echolocation clicks during 3 of the 10 dives. These events taught us how to acquire the extensive acoustic tracking of True's beaked whales that we conducted in subsequent years.

We analyzed the acoustic data in PAMGUARD, to identify beaked whale clicks and localize them relative to the visual sighting's locations. Once identified as belonging to the same area as the sighted True's groups, those clicks were extracted from PAMGUARD and imported into MATLAB (MATLAB 2017) using custom built MATLAB scripts to characterize the clicks. We analyzed over 2000 echolocation clicks to describe their spectral and temporal characteristics. We found that the peak frequencies of True's beaked whale clicks were similar to those reported for likely Gervais' clicks collected from bottom mounted recorders, and Gervais' clicks recorded from a towed hydrophone array

(Gillespie et al. 2009). This similarity highlights the need for further research into collecting more instances of visually confirmed Gervais' with acoustic recordings. Currently, it seems that the best way to distinguish between these 2 species is to utilize the inter-click interval measurement (Figure 7-10). We published a manuscript detailing these findings; for further details, see DeAngelis et al. (2018).

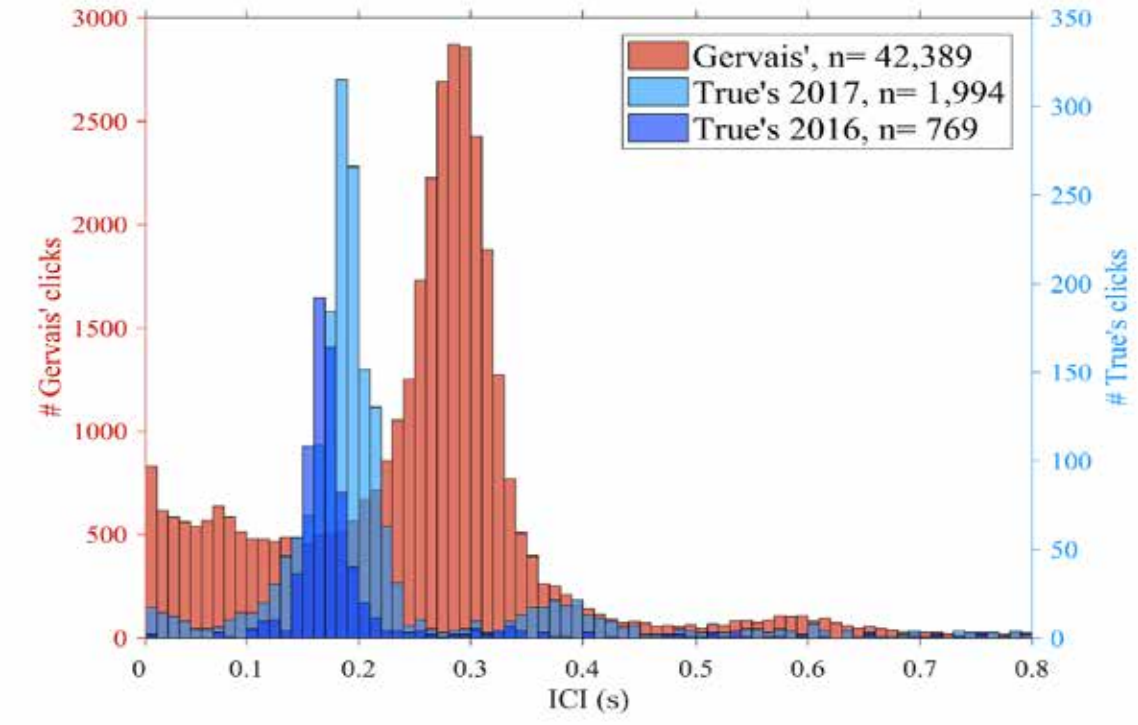

Figure 7-10 Distribution of inter-click intervals of True's and Gervais' beaked whales
True's beaked whale data are from DeAngelis et al. (2018) and the likely Gervais's beaked whale data are from Baumann-Pickering et al. (2013).

7.2.2.10 Genetic Analyses

We collected 14 eDNA samples in or near flukeprints of beaked whales during 2017, from 3 groups of True's beaked whales and 2 groups of Cuvier's beaked whales. The samples we collected near True's beaked whales revealed a new haplotype, not previously included in GenBank or described in the literature. This haplotype suggests the potential for differentiation between eastern and western North Atlantic stocks. These results demonstrate that eDNA is not only useful for confirming species identification of cryptic species, but also may provide new information relative to stock structure. We are still analyzing our samples from 2018, and our collaborators are preparing a manuscript examining the genetic differentiation between northern and southern hemisphere True's beaked whales.

7.2.3 Key Findings

The results from this suite of studies provide extensive new information on cryptic, poorly documented taxa for which we have traditionally lacked baseline data. Data from our combined NEFSC/SEFSC cetacean abundance survey conducted in 2016 provided a broad overview of beaked whale and pygmy or dwarf sperm whale distribution along the entire U.S. eastern seaboard. While we were able to identify to species 32% of visual beaked whale sightings, we were able to identify to species 95% of the acoustic detections of beaked whales. These acoustic detections have allowed us to better assess potential species-

specific differences in distribution and habitat use and to create a more thorough understanding of species' distributions. This is a good example of how passive acoustic data can complement and strengthen visually collected data.

Furthermore, the ITS.DEEP studies in 2015 and 2017 to 2019 have provided the first detailed data on True's beaked whales, a species that was virtually unknown in U.S. Atlantic waters. Confirmed True's beaked whales had been sighted a handful of times previously, but were primarily known from stranded specimens, and were not considered as a single species in NMFS' stock assessment reports or management priorities. Our studies have demonstrated that not only is this species present in our waters, but that the offshore Georges' Bank region, including waters of the Northeast Canyons and Seamount National Monument, provide important habitat for a community of deep-diving, poorly known cetaceans, including multiple species of beaked whales. We reliably found True's beaked whales and other beaked whale species, in this region over the course of multiple surveys and multiple years, indicating long-term utilization of this habitat. Our focal follow data provided baseline information on not only dive times and surfacing intervals, but on movements and behavior, all of which will serve to inform and improve our future abundance estimates. We deployed the first DTAG on this species, providing new insights into their dive and foraging behavior. And the suite of additional technologies that we incorporated into these studies: multiple forms of passive acoustic sampling, genetic sampling, and photo-ID, will provide new information on acoustic detection rates, stock structure, and population dynamics, all of which are shedding new light on this little-known species.

7.2.4 Data Gaps and Future Work

Though these studies seem extensive, in reality they are just the beginning of collecting important baseline data on the ecology and habitat use of offshore cetacean populations. Further work is needed to better acoustically characterize the differences between True's and Gervais' beaked whales, as well as to better document the long-term movements, persistence and site fidelity for the beaked whale populations in the U.S. North Atlantic region. Our data so far indicate that, at least in the summer and fall months, waters off the southern flank of Georges Bank is a site of high persistence, for a community of species known to be sensitive to anthropogenic disturbance. This puts them at risk in the event that anthropogenic activities increase in this region. In particular, if these species of beaked whales and pygmy/dwarf sperm whales exhibit high site fidelity, they would be vulnerable to acoustic disturbance from activities such as deep-sea bottom-mapping, seismic exploration, etc. To meet management and conservation needs and to improve our understanding of their habitat and movements, we need to apply satellite tags to individuals in these populations, as Shearer et al. (2019) did for Cuvier's beaked whales off Cape Hatteras, NC.

We are currently starting an investigation into the feasibility of using the small-scale habitat patterns in the passive acoustic detections of the different species to estimate the probability of the species identification of the visual sightings labeled as an ambiguous beaked whale or pygmy/dwarf sperm whales.

7.3 Long-Term Passive Acoustic Monitoring Studies

7.3.1 Methods

7.3.1.1 Bottom-mounted Recorder Data Collection

We collected archival, bottom-mounted recorder data associated with AMAPPS II from 2015 through 2018 or 2019, as part of 2 separate projects, where AMAPPS partially supported both projects.

In the first project ("Migratory Corridor 2.0"), we deployed 5 lines of MARUs (marine autonomous recording units; Cornell University) along the U.S. eastern seaboard from Massachusetts to Georgia

(Figure 7-11). We designed the distribution of these deployments in the northeast region to complement other ongoing passive acoustic monitoring projects conducted by external colleagues. We programmed the MARUs to record continuously at 2 kHz, for approximately 6 months at a time. Each line of MARUs included between 4 and 8 units; the exact number varied by deployment, and some units were lost due to storms and other external factors. We conducted this project in collaboration with the Center for Conservation Bioacoustics, Cornell University. Our primary goals for this project were to monitor the migratory movements of baleen whales along the continental shelf.

In the second project, we deployed 8 high-frequency acoustic recording packages (HARPs, Wiggins and Hildebrand 2007, Figure 7-11), in collaboration with SIO. We deployed the HARPs along the shelfbreak, from Georges Bank to the Blake Spur, at about 900 m depth. We programmed the HARPs to sample continuously at 200 kHz, for approximately a year at a time. We designed our deployment scheme such that the recorders were regularly spaced along the eastern seaboard, from the area near Heezen Canyon on Georges Bank (HZ in Figure 7-11), down through the Blake Spur off Georgia/Florida (BS in Figure 7-11). The distribution of recording sites complemented the concurrent MARU data collection described above, as well as data collection at 3 additional sites supported by Duke University and the U.S. Navy (Figure 7-11). Data analyses from the latter 3 sites are not included in this report. Our primary goals for this project were to monitor the acoustic ecology of shelfbreak and deep-water habitats, including the presence of baleen whales, toothed whales, and anthropogenic noise.

The combination of these datasets also complement earlier work conducted by Davis et al. (2017; 2020), which examined migratory movements of baleen whales along the U.S. eastern seaboard from 2004 to 2014, using an aggregation of passive acoustic datasets from many projects and collaborators. The MARU and HARP data that we collected during AMAPPS II provide the opportunity to extend the previous analyses, to examine baleen whale occurrence in the deeper waters of the Blake Plateau and the shelfbreak, which is particularly relevant for more pelagic species such as sei whales and blue whales.

Analyses for all of these projects are ongoing; we presented several highlights in this chapter. See Chapter 11 for more details on recorder positions and deployment timelines.

7.3.1.2 Bottom-mounted Recorder Data Analysis

We are analyzing all recording units for the daily presence of blue, fin, humpback, sei and North Atlantic right whales, using the low-frequency detection and classification system (Baumgartner and Mussoline 2011). This detection software creates conditioned spectograms and creates contours (“pitch tracks”) through tonal signals using a set of user-defined criteria. The software classifies potential baleen whale vocalizations based on a comparison to a pre-programmed call library for each individual species. We then manually review the pitch tracks to determine daily acoustic presence for each of the baleen whale species, following Davis et al. (2017; 2020). At this time, we will report on the completed analyses that we have for several species at some of the sites. The rest of the processing is ongoing. In particular, analyses are still ongoing for humpback whales and minke whales at all sites and therefore not presented in this report.

Our team and our collaborators at SIO are conducting additional analyses to assess the presence of odontocetes and anthropogenic noise at the HARP sites (Rafter et al. 2018). For these analyses, we used a combination of software packages and custom-built automated tools to assess the presence of beaked whales, sperm whales, pygmy/dwarf sperm whales, and delphinids. Using the custom software program Triton based in MATLAB (Mathworks, Natick, MA), we calculated long-term spectral averages with a time average of 5 sec and 10 Hz and 100 Hz, and trained analysts manually reviewed for echolocation. We analyzed the echolocation clicks by using a 2-stage automated detector, and we classified them based on spectral and temporal characteristics (Baumann-Pickering et al. 2013). We identified acoustic events to

species, to species group, or to click type when the species identification was unknown (as is the case for many delphinid species).

In addition, we are analyzing the HARP data for the presence of 4 types of anthropogenic signals: vessel sounds, airguns, explosions, and echosounders. As with the analyses of cetacean signals, these analyses incorporated a combination of automated detectors and manual review, using the software program Triton. Trained analysts manually detected vessels and echosounders, reviewing long-term spectral averages in 3-hr or 1-hr time bins. We detected explosions and seismic survey signals using automatic matched filter detectors, after which a trained analyst reviewed the detections. For both echosounders and seismic surveys, we conducted additional preliminary analyses. For the echosounders, we manually reviewed each event in the 2015 data to determine the peak frequencies of individual echosounders. For seismic surveys, we are manually reviewing seismic events on all sites in 2016 to determine the distribution of seismic survey detections across sites. In this chapter, we present some of the preliminary seismic survey analyses.

Finally, Rafter et al. (2018; 2020) conducted long-term ambient noise analyses with the HARP data, to evaluate the low frequency (<1000 Hz) soundscape across all 8 sites and across years. To determine ambient sound levels, they computed daily spectra by averaging 5, 5 sec sound pressure levels calculated from each 75 sec of acoustic data, and concatenated daily-average sound pressure levels in Hz bins to produce long-term spectrograms. These and the above analyses are an ongoing part of a study to assess the impacts of anthropogenic noise on cetacean vocal behavior.

In this section, we present highlights of the ongoing analyses on the combined MARU and HARP datasets. In particular, we present:

1) analyses of baleen whale occurrence across MARU and HARP sites;
2) an overview of the acoustic niche visualization results from the 3 HARPs deployed in 2015;
3) a preliminary summary of seismic survey analysis results from the 8 HARPs deployed in 2016; and
4) a subsample of long-term ambient noise analyses from 2 HARP sites.

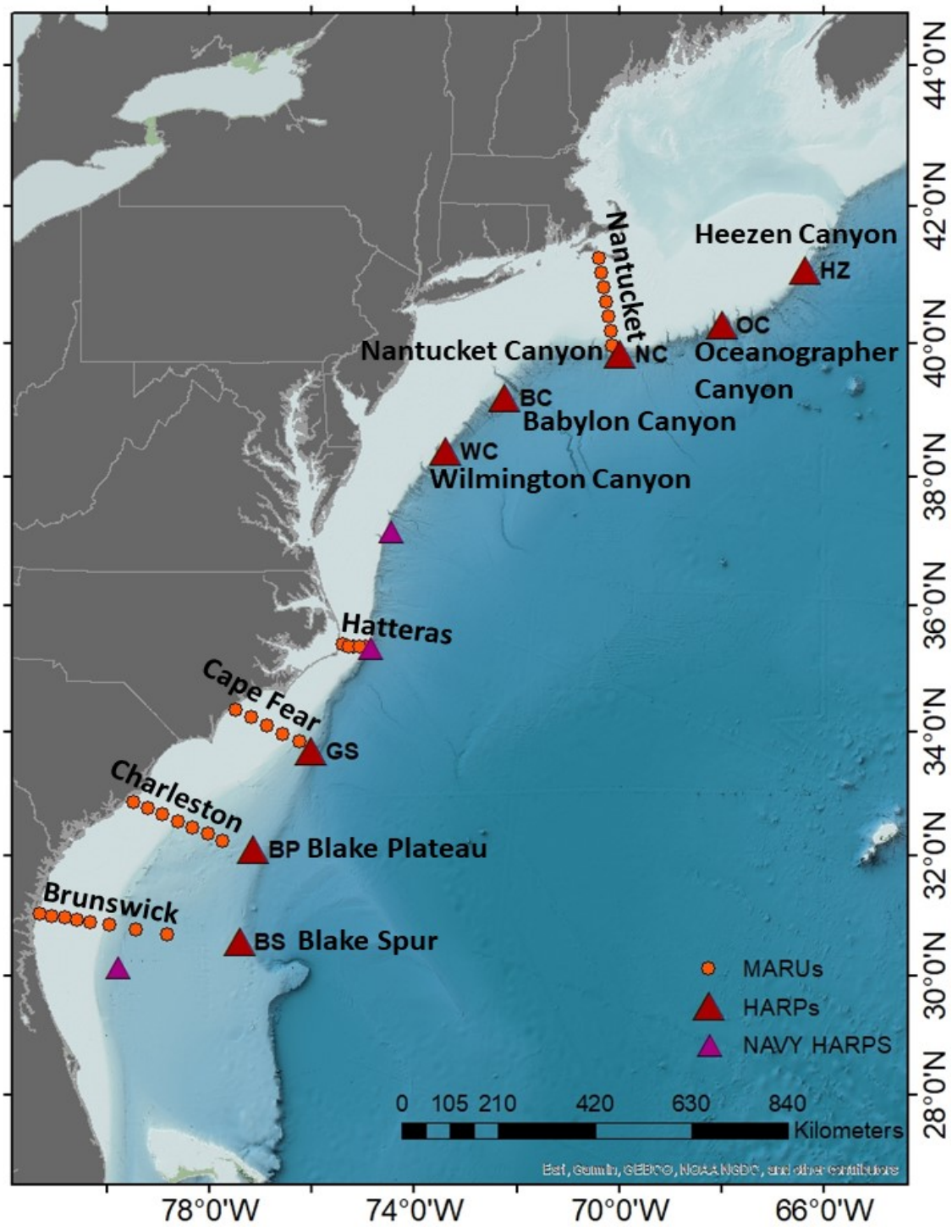

Figure 7-11 Locations of MARUs and HARPs deployed by NMFS between 2015 and 2019
AMAPPS II partially funded the red and orange deployments. The additional HARP sites supported by Duke University and the U.S. Navy are in purple. Note that exact positions and numbers of recorders varied between years, due to logistical constraints and recorder failures. Positions shown in map are approximate.

7.3.2 Results

7.3.2.1 Baleen Whale Occurrence

To assess general baleen whale occurrence latitudinally along the shelf, we grouped the results from the lines of MARUs according to region: Nantucket, Hatteras, Cape Fear, Charleston, and Brunswick. As was expected, we detected 4 species (blue, fin, humpback, and North Atlantic right whales) in every region, with the highest levels of daily acoustic presence generally recorded along the Nantucket MARU line (Figure 7-12). Right whales were present along the Nantucket line in all months of the year, with the highest levels of daily acoustic presence in the winter (November to February). They were present off Hatteras primarily in the winter, but with a few days of spring occurrence as well, and they were present off Brunswick primarily in the winter. Similarly, sei whales and fin were acoustically present in all seasons along the Nantucket line, though sei whale acoustic presence was highest in the spring and fin whales in the winter. Both species were primarily present in winter from Cape Hatteras to the south. Finally, blue whales were acoustically present in winter along the Nantucket line, with only 1 day of occurrence in fall or spring months in this region. However, they were present in both fall and winter off Cape Fear and Charleston, with no detections along the Cape Hatteras MARU or Brunswick lines.

Figure 7-12 Daily acoustic presence of 4 baleen whale species by region from 2015 to 2019
We pooled data from all MARUs within a region (see Figure 7-11 for locations) to summarize acoustic daily presence along each line. North Atlantic right whales (NARW) are shown in gold, sei whales in red, fin whales in purple, and blue whales in blue. Grayed out areas indicate periods where no data were collected.

Not surprisingly, the levels of baleen whale acoustic occurrence were quite different at the deeper HARP sites as compared to the MARUs deployed on the continental shelf. While we rarely detected right whales on the HARPs, we did detect them on several days at 4 sites between March and June in 2016 and 2017 (Figure 7-13; Table 7-8). However, the more pelagic balaenopterid species had high levels of daily acoustic occurrence, with clear seasonal patterns at each site. We frequently detected fin whales between September and March on sites north of Cape Hatteras, NC with fewer days with detections, primarily concentrated between December and February, on the 3 southern sites. We detected the sei whales detections slightly shifted into spring months, with highest levels of daily activity in March through May north of Cape Hatteras, NC. However, we detected them in the winter on all sites in 2016. Interestingly, we detected blue whales from September through March at the northernmost site, but then we detected most consistently from Wilmington Canyon and south, from August through September.

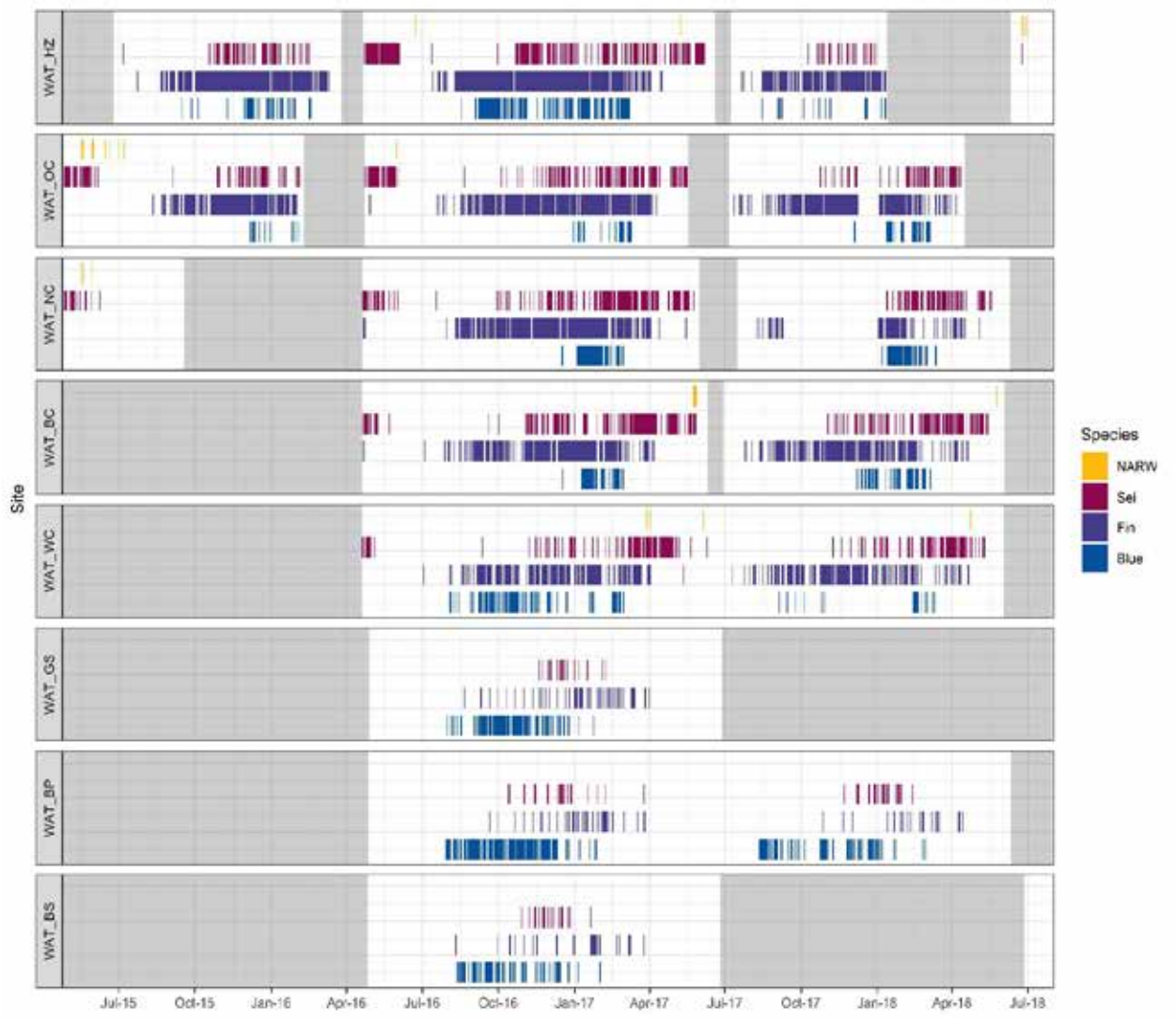

Figure 7-13 Daily presence of 4 baleen whale species by HARP site from 2015 to 2018
HARP sites ordered from north to south, starting with Heezen Canyon (HZ) and ending with Blake Spur (SC). See Figure 7-11 for more information on location. North Atlantic right whales (NARW) are shown in gold, sei whales in red, fin whales in purple, and blue whales in blue. Grayed out areas indicate periods where no data were collected or where analyses have not yet been conducted.

Table 7-8 Summary of daily detections of baleen whales across HARP sites
We tabulated the number of days per month with acoustic detections for each of the 4 baleen whale species, from April 2016 through July 2017. See Figure 7-10 for HARP site locations. Colored shading indicates relative proportion of detection days per cell, to provide a visual cue to interpret the seasonality between sites and species. Blank months represent those with no data. Information on deployment periods is in Table 11-11; the deployment and retrieval months for each site represent less than 1 month.

		2016									2017							
	Site	4	5	6	7	8	9	10	11	12	1	2	3	4	5	6	7	Total Number of Days
Blue whales	WAT_HZ	0	0	0	0	1	26	21	9	19	20	16	8	0	0	0	0	120
	WAT_OC	0	0	0	0	0	0	0	0	1	6	9	6	0	0		0	22
	WAT_NC	0	0	0	0	0	0	0	0	2	28	18	0	0	0		0	48
	WAT_BC	0	0	0	0	0	0	0	0	1	18	17	0	0	0	0	0	36
	WAT_WC	0	0	0	0	7	18	23	12	6	4	11	1	0	0	0	0	82
	WAT_GS	0	0	0	0	8	24	27	19	11	2	0	0	0	0	0		91
	WAT_BP	0	0	0	2	23	25	26	26	12	5	0	0	0	0	0	0	119
	WAT_BS	0	0	0	0	11	21	14	9	11	1	1	0	0	0	0		68
Fin whales	WAT_HZ	0	0	0	8	23	30	30	30	31	30	27	20	6	0	0	3	238
	WAT_OC	1	0	0	6	12	25	29	28	29	29	26	29	5	0		6	225
	WAT_NC	3	0	0	1	19	24	29	29	28	31	23	22	4	1		0	214
	WAT_BC	2	0	0	2	11	26	16	27	27	27	24	12	3	0	0	2	179
	WAT_WC	0	0	0	1	10	22	21	21	24	26	12	20	2	1	0	3	163
	WAT_GS	0	0	0	0	1	3	3	6	5	14	12	9	1	0	0		54
	WAT_BP	0	0	0	0	0	1	2	4	7	11	10	5	0	0	0	0	40
	WAT_BS	0	0	0	0	1	0	4	4	3	9	3	4	0	0	0		28
Right whales	WAT_HZ	0	0	**1**	0	0	0	0	0	0	0	0	0	0	**1**	0	0	2
	WAT_OC	0	**1**	0	0	0	0	0	0	0	0	0	0	0	0		0	1
	WAT_NC	0	0	0	0	0	0	0	0	0	0	0	0	0	0		0	0
	WAT_BC	0	0	0	0	0	0	0	0	0	0	0	0	0	**5**	0	0	5
	WAT_WC	0	0	0	0	0	0	0	0	0	0	0	**1**	**1**	0	**1**	0	3
	WAT_GS	0	0	0	0	0	0	0	0	0	0	0	0	0	0	0		0
	WAT_BP	0	0	0	0	0	0	0	0	0	0	0	0	0	0	0	0	0
	WAT_BS	0	0	0	0	0	0	0	0	0	0	0	0	0	0	0		0
Sei whales	WAT_HZ	7	30	4	1	0	1	10	21	19	8	15	18	10	19	6	0	169
	WAT_OC	5	25	1	0	1	0	4	4	19	9	20	19	13	14		0	134
	WAT_NC	8	13	1	1	0	1	6	7	18	8	24	26	13	18		0	144
	WAT_BC	7	7	0	0	0	1	1	17	15	7	12	27	19	15	0	0	128
	WAT_WC	8	2	0	0	0	1	0	6	10	6	6	21	26	3	1	0	90
	WAT_GS	0	0	0	0	0	0	0	3	9	4	2	0	0	0	0		18
	WAT_BP	0	0	0	0	0	0	2	6	10	2	1	1	0	0	0	0	22
	WAT_BS	0	0	0	0	0	0	1	9	9	1	0	0	0	0	0		20
	Sum of blue whale days	0	0	0	2	50	114	111	75	63	84	72	15	0	0	0	0	586
	Sum of fin whale days	6	0	0	18	77	131	134	149	154	177	137	121	21	2	0	14	1141
	Sum of right whale days	0	1	1	0	0	0	0	0	0	0	0	1	1	6	1	0	11
	Sum of sei whale days	35	77	6	2	1	4	24	73	109	45	80	112	81	69	7	0	725

We present the spatial distribution of the combined acoustic detections from the MARU and the HARP data in Figure 7-14. We detected blue whales are primarily along the shelfbreak and on the deepest HARP units on the Blake Plateau, with few detections on the continental shelf. Fin whales and sei whales show a similar pattern, though we detected both species at high levels across the line of Nantucket MARUs, demonstrating the importance of this habitat to both species. Like blue whales, we detected both fin and sei whales on the HARPs extending to the Blake Spur, and on several of the deeper MARUs on the Blake

Plateau. Finally, we detected North Atlantic right whales most commonly on the Nantucket MARUs, with few detections at the shelfbreak, reflecting the coastal distribution of this species.

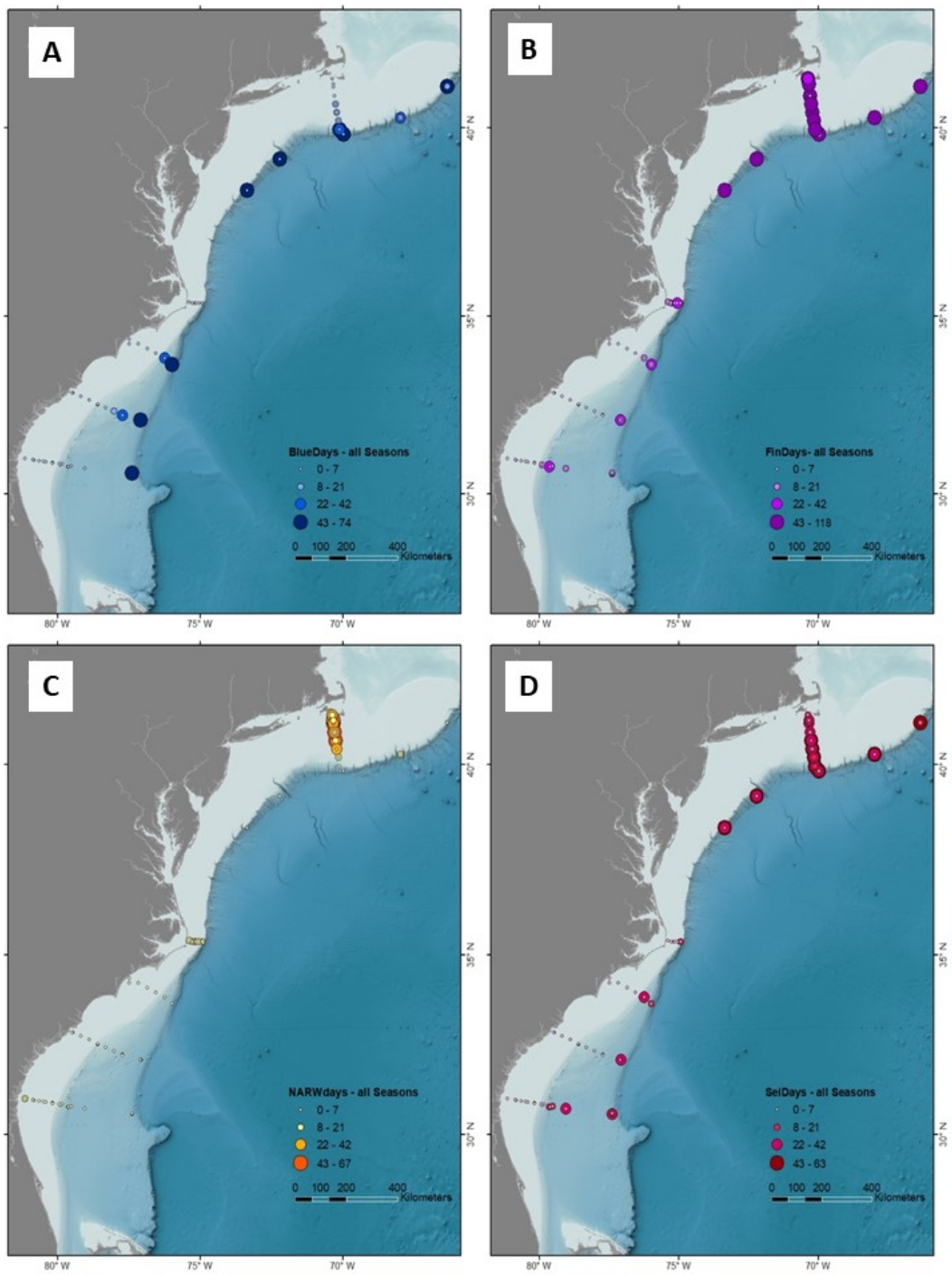

Figure 7-14 Daily presence of baleen whale species across MARU and HARP sites combined
Spatial distribution of acoustic detections for blue (A), fin (B), right (C), and sei whales (D), for all data analyzed to date (up to 2017 or 2018, depending on site). The size of the circle indicates the number of days with acoustic detections; note that the maximum number of days varies between species.

These results complement and extend those presented by Davis et al. (2020), which evaluated baleen whale occurrence over a 10-year period, using a compilation of recorders deployed along portions of the U.S. and Canadian eastern seaboard. For the pelagic blue, fin and sei whales, our results provide new information on seasonal occurrence in the deeper waters of the Blake Plateau and along the shelfbreak, demonstrating in particular the distributions of these species during fall and winter months in deep water habitats. These results also supplement those that are obtained through NMFS' visual surveys, as we have little effort in winter months in offshore waters and have had limited ability to assess the spatial distribution of these baleen whale species during those months.

We examine right whale detections in more detail (Figure 7-15). We assessed the spatial and temporal distribution of right whale acoustic daily detections relative to Seasonal Management Areas that are in place during winter and spring months. As our AMAPPS data do not include Cape Cod Bay or the Great South Channel, we will not discuss the northernmost protection areas in Figure 7-15. However, the Seasonal Management Areas from Block Island (west of Nantucket, MA) through Savannah ,GA are in place from November 1 to April 30, spanning the winter and spring months in Figure 7-15. The Southeast Seasonal Management Areas, which covers the calving and nursery grounds from southern Georgia to northern Florida, are in place from November 15 to April 15. We note several main findings from distribution of acoustic detections shown below. First, the highest level of right whale acoustic activity is on the MARUs south of Nantucket, MA, an area for which currently no mandatory protections exist. Right whales are acoustically present in this region year-round. Second, in winter and spring, right whales are acoustically present off Cape Hatteras, presumably, as animals migrate to and from the calving grounds in the southeast, an area that is also not in a Seasonal Management Areas. Right whales were also present on several days near Cape Fear. Finally, the Seasonal Management Areas from South Carolina to Florida encapsulate most of the detections on the MARU lines in that region, though we also detected right whales on MARUs outside of this protection zone on several days during the study period as well.

These results complement those presented in Davis et al. (2017), which examined the distribution of right whale acoustic detections from 2004 to 2014 over a broader range of the western North Atlantic. In particular, our results highlight that the region near Nantucket Shoals continues to be of high importance to right whales year-round, and that right whales continue to be acoustically present at low levels along the shelfbreak, from Delaware to Georges Bank, in the summer. Cape Hatteras continues to be a narrow corridor utilized by right whales in winter and spring. For the southeast region, our results support those of Davis et al. (2017), in that most acoustic detections were in nearshore waters, but with some sporadic occurrence in deeper waters. Davis et al. (2017) also found some further offshore detections off North Carolina and Georgia in winter months.

Finally, we compared the distribution of right whale detections along the Nantucket MARU line to the BOEM Wind Energy lease areas (WEAs) that are south of Cape Cod and the Islands (Figure 7-16). The areas of highest and most consistent acoustic activity overlap or are directly adjacent with the WEAs, emphasizing the importance of this habitat to right whales, extending previous results reported by Leiter et al. (2017) and Davis et al. (2017).

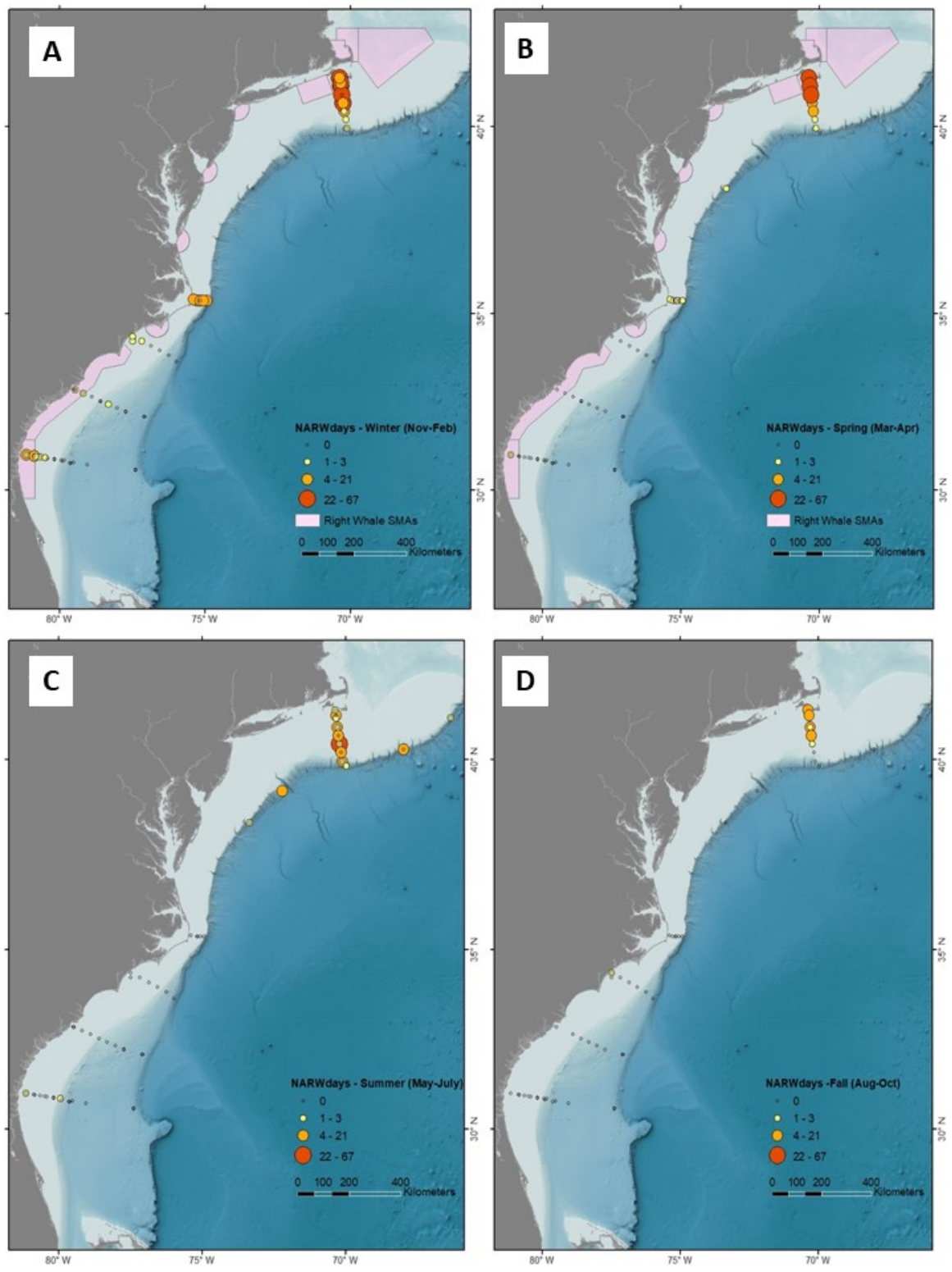

Figure 7-15 Daily presence of North Atlantic right whales on MARU and HARP sites by season
We displayed the spatial distribution of acoustic detections for right whales, from 2015 to 2018/2019 (depending on site). The size of the circle indicates the number of days with acoustic detections. The pink shading represents mandatory Seasonal Management Areas; for active times, see text.

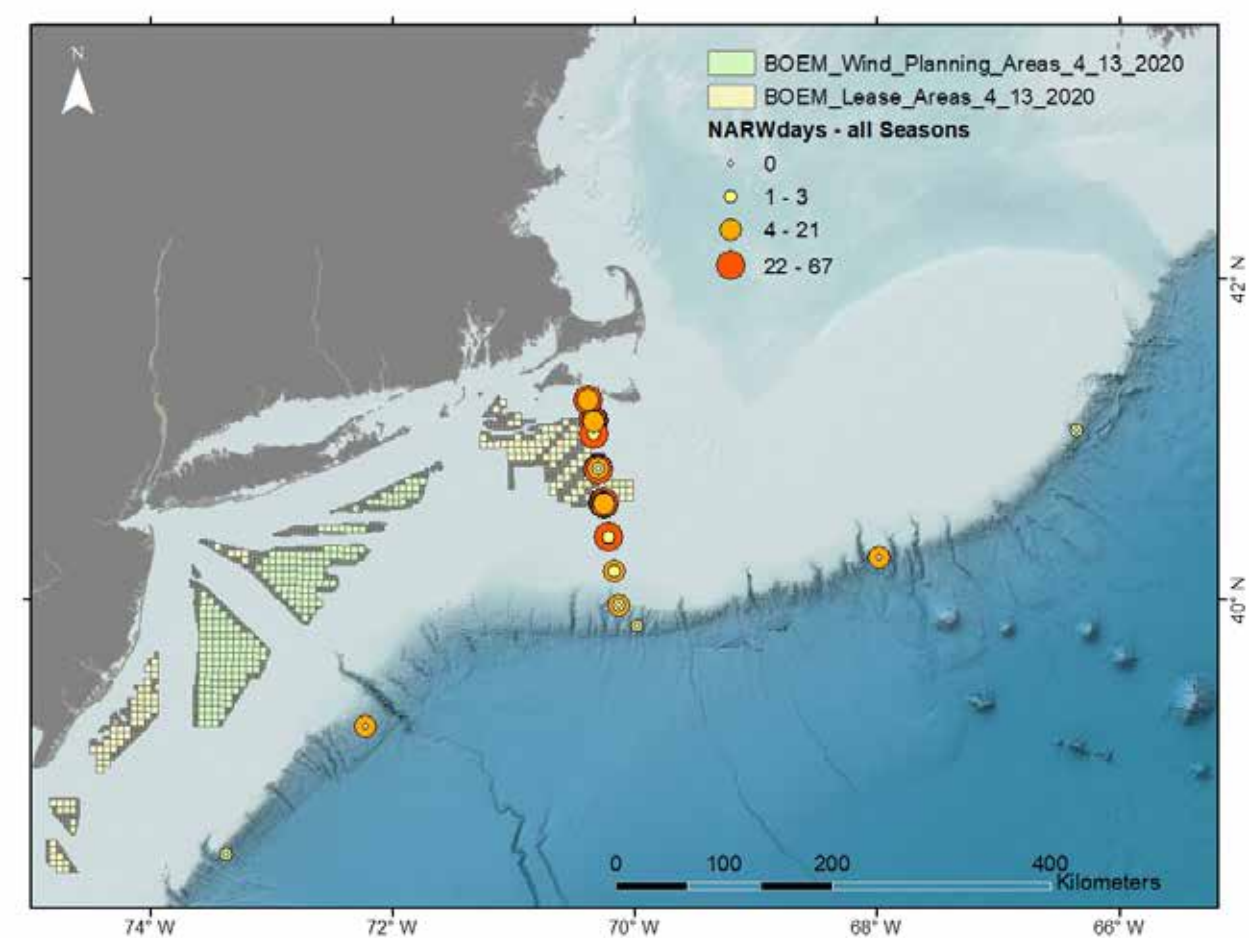

Figure 7-16 Daily presence of right whales near Massachusetts Wind Energy Areas
We displayed the spatial distribution of acoustic detections for right whales from 2015 to 2018/2019 (depending on site). The size of the circle indicates the number of days with acoustic detections. Wind planning and lease area maps accessed on 10/15/2020 from BOEM website.

7.3.2.2 Acoustic Niche Visualization of Complex Acoustic Data

We compiled the results of the baleen whale, toothed whale, and anthropogenic sounds analyses for the 3 northern HARPs deployed off Georges Bank in 2015, to examine the overlap in time and frequency bands between biological and anthropogenic signals. This work built on that published by Van Opzeeland and Boebel (2018), which explored the use of a spectrographic box plot display to examine the overlap in time and frequency between noise-producing anthropogenic activities and communication sounds produced by marine mammals. We assessed the daily presence of 5 baleen whale species (blue, fin, humpback, right and sei whales), 5 toothed whale species or species groups (delphinids, pygmy/dwarf sperm whales, sperm whales, Sowerby's beaked whales, and Cuvier's/True's/Gervais' beaked whales) and 4 anthopogenic activities (airguns, broadband ship noise, echosounders and explosions). Among cetaceans, we most frequently detected delphinid groups, sperm whales, and fin whales, with different cetacean groups present from 2% to 100% of days analyzed at each site. Among anthropogenic signals, we most frequently detected airgun noise from seismic surveys, present on 50% to 91% of days across sites. Ship noise was present on 15% to 65% of days, depending on site, while we detected shipboard echosounders on 1% to 14% of days. An example of the acoustic niche visualization is in Figure 7-17, which shows the

data from the Heezen Canyon HARP from May 2015 to February 2016. We observed a clear temporal occurrence and frequency band overlap between broadband ship noise and seismic survey exploration. Additionally, we observed an overlap in frequency between different echosounder categories and toothed whales. Weiss et al., currently in review with Marine Policy, provide more details and results.

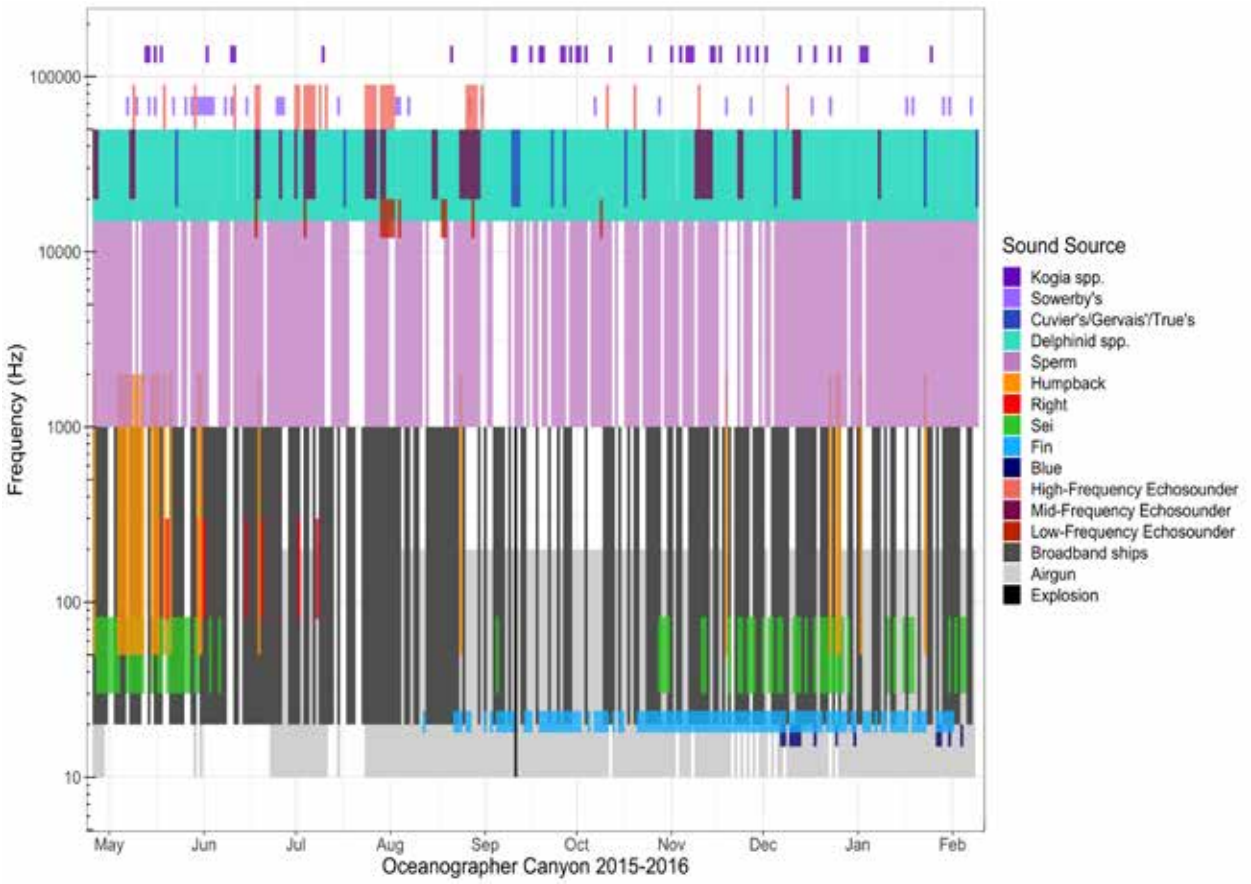

Figure 7-17 Acoustic niche visualization from Heezen Canyon, 2015 to 2016
Spectrographic box plot display showing daily occurrence (x-axis) and overall frequency range (y-axis) for 10 different cetacean species or species groups, and 4 types of anthropogenic signals. We subdivided echosounders into "low", "medium", and "high" categories to better characterize their overlap with different cetacean groups. Figure from Weiss et al. (in review).

7.3.2.3 Anthropogenic Signals

Building on the acoustic niche analyses that we conducted on the HARPS deployed in 2015, we are expanding our analyses of anthropogenic noise across all HARPs along the U.S. eastern seaboard. We are conducting a detailed analysis of seismic survey data in the 2016 to 2017 HARP dataset, to assess the prevalence of airgun noise across sites, the range at which these signals may be detected, and contribution of this noise to the soundscape of the U.S. shelfbreak ecosystem. In our analyses of the 2016 HARP dataset, we detected airgun signals at all 8 HARP sites, from Heezen Canyon to Blake Spur. In the first full month of deployment (May 2016), we detected airguns nearly the entire month (30/31 days) at Heezen, Oceanographer, Babylon and Wilmington Canyon areas (Table 7-8). Airgun detections were consistently high across all sites north of Cape Hatteras, NC with some similarly high months of activity at the sites south of Cape Hatteras, NC.

Table 7-8 Daily presence of airguns from April to September 2016 at HARP sites
For each site and month, we show the number of days with at least 1 airgun detection per number of analysis days, and the corresponding percentage of days with airguns present. Location of sites displayed in Figure 7-10.

Site	HZ	OC	NC	BC	WC	GS	BP	BS
Apr 2016	9/10 (90%)	7/7 (100%)	9/10 (90%)	10/11 (91%)	11/11 (100%)	0/2 (0%)	1/3 (33%)	0/4 (0%)
May 2016	30/31 (97%)	30/31 (97%)	26/31 (84%)	30/31 (97%)	30/31 (97%)	29/31 (94%)	28/31 (90%)	9/31 (29%)
Jun 2016	20/30 (67%)	21/30 (70%)	15/30 (50%)	20/30 (67%)	23/30 (77%)	25/30 (83%)	25/30 (83%)	21/30 (70%)
Jul 2016	22/31 (71%)	23/31 (74%)	25/31 (80%)	22/31 (71%)	22/31 (71%)	20/31 (65%)	14/31 (45%)	21/31 (68%)
Aug 2016	24/31 (77%)	16/31 (52%)	22/31 (71%)	24/31 (77%)	27/31 (87%)	3/31 (10%)	4/31 (13%)	4/31 (13%)
Sep 2016	27/30 (90%)	5/30 (17%)	11/30 (37%)	25/28 (89%)	23/28 (82%)	2/30 (7%)	1/2 (50%)	1/30 (3%)

To determine whether we were detecting the same seismic surveys across the entire eastern seaboard, or more locally specific surveys, we evaluated the first 2 months of data from each site to look for breaks in airgun activity that were unambiguously aligned between sites. Seismic surveys can often continue uninterrupted for days, but we found that it was not uncommon to see clear and sudden stops in airgun activity, occasionally followed by an abrupt start several minutes later, causing a recognizable gap (Figure 7-18).

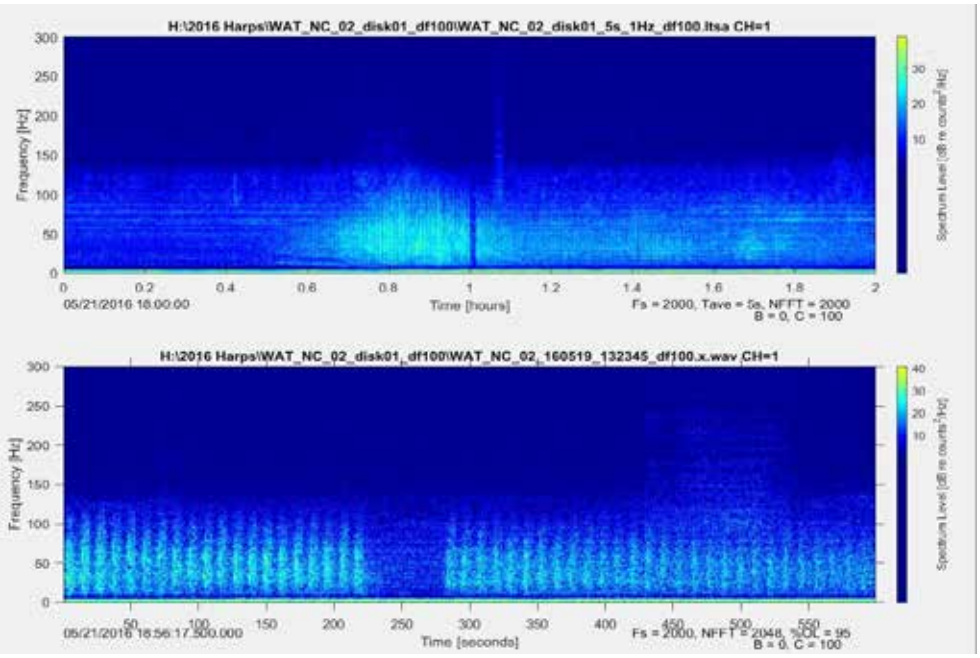

Figure 7-18 Example of airgun noise recorded on 21 May 2016 on the Nantucket Canyon HARP
The top panel shows a 2-hr long-term spectrogram, while the bottom panel shows a detail of 600 s (NFFT: 2048; 95% overlap). Notice the sudden stop and start of the airgun pulses at around 19:00:00.

Using the software package Triton, a trained analyst manually reviewed the data to note each occurrence of a stop, start, or gap in airgun activity. We compared the timing of these events across sites to determine across how many sites we could detect the same airgun pulse. From 2 May to 14 June 2016, we found at least 10 events that co-occurred across all 8 HARP sites, indicating we could acoustically detect the same seismic surveys across nearly the entire U.S. eastern seaboard (Table 7-9). We detected many more events across 5 to 7 of the HARP sites. We are continuing to conduct these analyses, where we will use these data to localize the seismic surveys and quantify their noise levels in the context of ambient soundscapes along the U.S. east coast. Additionally, we are conducting analyses of the effects of anthropogenic noise on cetacean vocalization rates; preliminary analyses of the impacts of navy sonar on beaked whale acoustic occurrence are underway.

Table 7-9 Results from preliminary analysis of airgun events across HARP sites
The number of distinct acoustic seismic survey events (sudden stops and starts) that we aligned across HARP sites during 2 May to 14 June 2016.

Number of HARPs	1	2	3	4	5	6	7	8
Number of events detected	70	29	27	18	36	30	46	10

7.3.2.4 Long-term Ambient Noise Analyses

Rafter et al. (2018; 2020) report on the details of the ambient noise analyses conducted on the 2016 to 2018 HARP data. Across all sites, anthropogenic sounds dominated the noise levels at the lowest frequencies between 10 and 100 Hz, primarily from vessel traffic and seismic exploration. In this frequency range, most sites had sound levels within 5 to 10 dB of each another. From 100 to 1000 Hz, sound pressure levels are primarily related to wind and sea state, with generally higher levels in the winter and lower levels in the summer. These sound levels varied between sites and years; for example, Heezen Canyon had the highest levels in March 2017, while the Oceanographer Canyon site had the highest levels in March 2018. Similarly, levels were lowest at the Blake Plateau site in September 2017 and at the Blake Spur site in 2018 (Figure 7-19). Additionally, we detected fin whale song seasonally at all 8 sites (Figure 7-19), which exhibited a characteristic peak in sound levels around 20 Hz. Fin whale song levels were highest at the northern sites. We also detected an unknown signal year-round at Heezen Canyon, between 400 and 800 Hz, which may be a fish call.

When comparing to the results of studies conducted in other regions, we find that the shelfbreak acoustic environment of the U.S. eastern seaboard has higher levels of low-frequency noise than some deep water habitats on the west coast, but shows similar patterns to the noise observed in the offshore waters of the U.S. northeast (Haver et al. 2018). Vessel noise and seismic surveys may be contributors to these low-frequency noise signatures. These analyses are still ongoing; we are awaiting completion of the analyses from the 2018 and 2019 datasets so that we can compile a comprehensive overview of ambient noise across the 3 yrs.

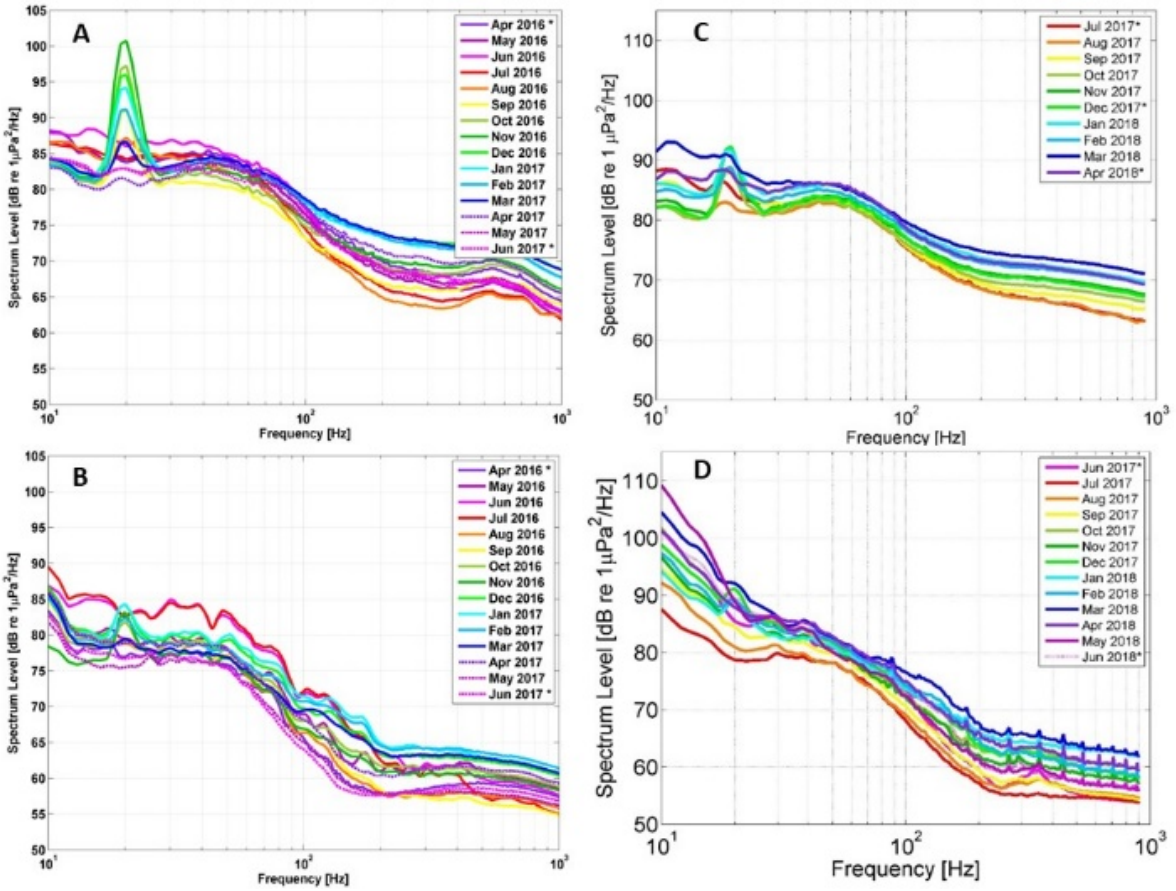

Figure 7-19 Low-frequency ambient soundscape
The soundscapes from April 2016 to June 2017 are from Heezen Canyon (A) and Blake Plateau (B). The soundscapes from June/July 2017 to April/June 2018 are from Oceanographer Canyon (C) and Blake Spur (D). The color of the line indicates the month. Note that the y-axis scale differs between the panels. The peak at 20 Hz at each site is due to fin whale song.

7.3.3 Key Findings

The multi-year, broad-scale passive acoustic monitoring efforts associated with AMAPPS II are yielding an enormous amount of new information on cetacean occurrence, distribution, and anthropogenic noise across the entire U.S. eastern seaboard. The results that we present here highlight a few of the many ongoing analyses.

With respect to baleen whales, our results complement and extend those published by Davis et al. (2017; 2020), and add to what we currently know about baleen whale seasonal distribution from visual surveys. For North Atlantic right whales, the key findings include the continued persistence of the region south of Cape Cod as a right whale hotspot from 2015 to 2019, supplementing data gathered from aerial surveys as well as previous passive acoustic monitoring work in the region. These results also demonstrate the significant overlap between right whale occurrence and the wind energy areas within this region, as well as the lack of mandatory seasonal protections. Our results also indicate some use of the deeper water and shelfbreak habitats by right whales in summer months in the northeast region, areas that historically we did not consider as high usage areas by this species; thus, warranting further monitoring in this region. For blue, fin, and sei whales, our passive acoustic monitoring results demonstrate a pelagic distribution of these species, with high levels of seasonal acoustic detections along the shelfbreak and the deeper HARPs on the Blake Plateau. These results provide additional data on the distribution of these species in winter

months, where we currently lack sufficient visual survey effort to adequately assess these species' occurrence and densities.

Our results of the acoustic niche visualization analysis, initially compiled using the 3 HARPs deployed along the northeast shelfbreak in 2015, provide a new mechanism for scientists and managers to visualize the overlap in time, space, and acoustic range, between protected species and anthropogenic activities. The results of this study show, for example, the overlap between low-frequency baleen whales and both vessel noise and seismic surveys. More surprising, perhaps, was the level at which we detected shipboard echosounders at these sites, and the potential for overlap between vessel-based echosounders and higher frequency toothed whale species. Because high-frequency echosounders propagate over relatively small distances, these results may provide information on the levels of site-specific vessel activity, such as from fishing vessels.

The preliminary results from the analyses of anthropogenic signals on the shelfbreak HARPs indicate a surprising level of chronic noise from seismic survey events along the entire U.S. eastern seaboard. This is despite the fact that currently U.S. offshore waters are not open for oil and gas exploration. The fact that we detected some of these seismic survey events across all 8 HARPs at the same time indicates that their origin is at quite a distance from the HARPs. We are currently working to assess how far away we can detect these seismic surveys. The implications of these results reinforce previous work that demonstrated the potentially extensive overlap between baleen whale acoustic vocalizations and airgun noise in the North Atlantic (Nieukirk et al. 2012).

7.3.4 Data Gaps and Future Work

Many of our analyses are ongoing, and so we expect will continue to produce new insights as we complete the processing and analyses of all datasets. We now have an extensive monitoring dataset for the continental shelf and slope waters. However, the region beyond the shelfbreak and out to the U.S. EEZ remains poorly studied. To better understand the distribution, densities, and habitat use of pelagic delphinid and baleen whale species, we need to expand our monitoring of offshore habitats.

In addition, we have critical data gaps regarding the acoustic characteristics and acoustic repertoires of many protected species, limiting our ability to fully utilize our existing passive acoustic monitoring datasets. For example, we lack basic acoustic repertoire data and information on which sexes are producing the vocalizations we monitor for many of the large whale species, such as sei whales. Without this information, we do not know whether we are monitoring males, females, or both. Furthermore, we do not know what additional call types, beyond those already identified, we could use for effective acoustic monitoring. Dedicated effort to collect passive acoustic data in conjunction with visual and behavioral observations, as well as genetic sampling, is necessary for us to develop an adequate understanding of baleen whale acoustic production. Similarly, for delphinids we need to develop better techniques to adequately distinguish between the echolocation and whistle characteristics of different species or species groups. Our AMAPPS data are contributing to ongoing efforts to better classify toothed whale signals.

Future work will expand on the studies highlighted here, to more fully assess the distribution of baleen whales and toothed whales, and to assess the impacts of anthropogenic noise on protected species vocal activity along the U.S. eastern seaboard.

7.4 Acknowledgements

The work highlighted in this chapter would not have been possible without extensive additional contributions in both time and funds from many sources. For contributions to data collection and/or analyses, we would like to thank the science crews that participated in the shipboard surveys from 2015 to 2019, particularly the teams that dedicated long hours to collecting focal follow and tag data to further our

understanding of beaked whales. We thank the crews of the NOAA ships *Henry B. Bigelow* and *Gordon Gunter*, as well as the University of Delaware and the crew of the *Hugh R. Sharp*. We thank Lance Garrison, Tony Martinez, and the Southeast Fisheries Science Center for use of their rigid hull inflatable boat during our 2018 shipboard survey. We also thank Nathan Keith for his tireless efforts in helping to secure ship time and charter vessels for the studies represented in this chapter, as well as Eric Matzen for his efforts with our HARP deployments. We thank Holger Klink, Edward Moore III, Chris Tessaglia-Hymes and the staff of the Center for Conservation Bioacoustics for their work with the deployments and extracting of the MARU data. Similarly, we thank John Hildebrand, Ryan Griswold, Erin O'Neill, Sean Wiggins, and the staff at Scripps Institution of Oceanography for assistance with the deployment and extraction of the HARP data. For additional assistance with data analyses, we thank Natasha Heisenberg Leigh Hickmott, Alyssa Scott, Allison Stokoe, Sarah Weiss, as well as Simone Baumann-Pickering, Kait Frasier, John Hildebrand, Jenny Trickey, and their staff at Scripps Institution of Oceanography. We received additional funding for data collection and analyses from NOAA and the Navy's N45 and Living Marine Resources programs.

7.5 References Cited

Aguilar de Soto NA, Martín V, Silva M, Edler R, Reyes C, Carrillo M, Schiavi A, Morales T, García-Ovide B, Sanchez-Mora A, Garcia-Tavero N. 2017. True's beaked whale (*Mesoplodon mirus*) in Macaronesia. PeerJ 5:e3059.

Barlow J, Taylor BL. 2005. Estimates of sperm whale abundance in the northeastern temperate Pacific from a combined acoustic and visual survey. Mar. Mammal Sci. 21:429-445.

Baumgartner M F, Mussoline SE. 2011. A generalized baleen whale call detection and classification system. J. Acous. Soc. Am. 129:2889-2902.

Baumann-Pickering S, McDonald MA, Simonis AE, Solsona Berga A, Merkens KP, Oleson EM, Roch MA, Wiggins SM, Rankin S, Yack TM, Hildebrand JA. 2013. Species-specific beaked whale echolocation signals. J. Acous. Soc. Am. 134:2293-301.

Center for Conservation Bioacoustics, Cornell Laboratory of Ornithology, 2019.

Cholewiak D, Baumann-Pickering S, Van Parijs SM. 2013. Description of sounds associated with Sowerby's beaked whales (*Mesoplodon bidens*) in the western North Atlantic Ocean. J. Acous. Soc. Am. 134:3905-3912.

Cholewiak D, DeAngelis AI, Palka D, Corkeron PJ, Van Parijs SM. 2017. Beaked whales demonstrate a marked acoustic response to the use of shipboard echosounders. R. Soc. Open Sci. 170940.

Clarke E, Feyrer LJ, Moors-Murphy H, Stanistreet J. 2019. Click characteristics of northern bottlenose whales (*Hyperoodon ampullatus*) and Sowerby's beaked whales (*Mesoplodon bidens*) off eastern Canada. J. Acous. Soc. Am. 146:307-315.

Cox TM, Ragen TJ, Read AJ, Vos E, Baird RW, Balcomb K, Barlow J, Caldwell J, Cranford T, Crum L. 2006. Understanding the impacts of anthropogenic sound on beaked whales. J. Cetacean Res. Manag. 7:177-187.

Davis GE, Baumgartner MF, Bonnell JM, Bell J, Berchok C, Bort Thorntom J, Brault S, Buchanan G, Charif RA, Cholewiak D, Clark CW, Corkeron P, Delarue J, Dudzinski K, Hatch L, Hildebrand J, Hodge L, Klinck H, Kraus S, Martin B, Mellinger DK, Moors-Murphy H, Nieukirk S, Nowacek DP,

Summers E, Todd S, Warde A, Van Parijs SM. 2017. Long-term passive acoustic recordings track the changing distribution of North Atlantic right whales (*Eubalaena glacialis*) from 2004 to 2014. Sci. Rep. 17: 13460.

Davis GE, Baumgartner MF, Corkeron PJ, Bell J, Berchok C, Bonnell JM, Thornton BJ, Brault S, Buchanan GA, Cholewiak DM, Clark CW, Delarue J, Hatch LT, Klinck H, Kraus SD, Martin B, Parry D, Pegg N, Read AJ, Rice AN, Risch D, Scott A, Soldevilla MS, Stafford KM, Stanistreet JE, Summers E, Todd S, Van Parijs SM. 2020. Exploring movement patterns and changing distributions of baleen whales in the western North Atlantic using a decade of passive acoustic data. Glob. Change Biol. 26(9):4812-4840.

DeAngelis A, Valtierra R, Van Parijs SM, Cholewiak D. 2017. Using multipath reflections to obtain dive depths of beaked whales from a towed hydrophone array. J. Acous. Soc. Am. 142:1078-1087.

DeAngelis AI, Stanistreet JE, Baumann-Pickering S, Cholewiak DM. 2018. A description of echolocation clicks recorded in the presence of True's beaked whale (*Mesoplodon mirus*). J. Acous. Soc. Am. 144:2691-700.

Gillespie D, Mellinger DK, Gordon J, McLaren D, Redmond P, McHugh R., Trinder P, Deng XY, Thode

localization of cetaceans. J. Acous. Soc. Am. 125:2547-2547.

Griffiths ET, Barlow J. 2015. Equipment performance report for the drifting acoustic spar buoy recorder (DASBR). NOAA Tech Memo NMFS SWFSC-543.

Griffiiths ET, Barlow J. 2016. Cetacean acoustic detections from free-floating vertical hydrophone arrays in the southern California Current. J. Acous. Soc. Am. 140(5):EL399-EL404.

Haver SM, Gedamke J, Hatch LT, Dziak RP, Van Parijs S, McKenna MF, Barlow J, Berchok C, DiDonato E, Hanson B, Haxel J. 2018. Monitoring long-term soundscape trends in U.S. waters: The NOAA/NPS ocean noise reference station network. Mar. Policy 90:6-13.

Hildebrand JA, Frasier KE, Baumann-Pickering S, Wiggins SM, Merkens KP, Garrison LP, Soldevilla MS, McDonald MA. 2019. Assessing seasonality and density from passive acoustic monitoring of signals presumed to be from pygmy and dwarf sperm whales in the Gulf of Mexico. Front. Mar. Sci. 6:66.

Johnson MP, Tyack PL. 2003. A Digital Acoutic Recording Tag for Measuring the Response of Wild Marine Mammals to Sound. IEEE J. Ocean. Eng. 28(1):3-12.

Johnson M, Madsen PT, Zimmer WM, De Soto NA, Tyack PL. 2004. Beaked whales echolocate on prey. Proc. R. Soc. Lond. B. 271:S383-S386.

Johnson M, Madsen PT, Zimmer WMX, De Soto NA, Tyack PL. 2006. Foraging Blainville's beaked whales (*Mesoplodon densirostris*) produce distinct click types matched to different phases of echolocation. J. Exp. Biol. 209(24):5038-5050.

Keating JL, Barlow J, Rankin S. 2016. Shifts in frequency-modulated pulses recorded during an encounter with Blainville's beaked whales (*Mesoplodon densirostris*). J. Acous. Soc. Am. 140(2):EL166-EL171.

Leiter SM, Stone KM, Thompson JL, Accardo CM, Wikgren BC, Zani MA, Cole TVN, Kenney RD, Mayo CA, Kraus SD. 2017. North Atlantic right whale Eubalaena glacialis occurrence in offshore wind energy areas near Massachusetts and Rhode Island, USA. Endang Species Res. 34:45-59.

MATLAB. 2017. Natick, Massachusetts: The MathWorks Inc.

MacLeod CD, D'Amico AN. 2006. A review of beaked whale behaviour and ecology in relation to assessing and mitigating impacts of anthropogenic noise. J. Cetacean Res. Manag. 7:211-221.

Merkens K, Mann D, Janik VM, Claridge D, Hill M, Oleson E. 2018. Clicks of dwarf sperm whales (*Kogia sima*). Mar. Mammal Sci. 34:963-978.

Merkens KP, Oleson EM. 2018. Comparison of high-frequency echolocation clicks (likely *Kogia*) in two simultaneously collected passive acoustic data sets sampled at 200 kHz and 320 kHz. NOAA Tech Memo. NMFS PIFSC-74; 21pp.

Nieukirk SL, Mellinger DK, Moore SE, Klinck K, Dziak RP, J. Goslin. 2012. Sounds from airguns and fin whales recorded in the mid-Atlantic Ocean, 1999–2009. J. Acoust. Soc. Am. 131:1102-1112

Palka DL, Chavez-Rosales S, Josephson E, Cholewiak D, Haas HL, Garrison L, Jones M, Sigourney D, Waring G (retired), Jech M, Broughton E, Soldevilla M, Davis G, DeAngelis A, Sasso CR, Winton MV, Smolowitz RJ, Fay G, LaBrecque E, Leiness JB, Dettlof M, Warden M, Murray K, Orphanides C. 2017. Atlantic marine assessment program for protected species: 2010- 2014. US Dept. of the Interior, Bureau of Ocean Energy Management, Atlantic OCS Region, Washington, DC. OCS Study BOEM 2017-071; 211 pp.

Rafter MA, Frasier KE, Thayre BJ, Ziegenhorn MA, Cohen R., O'Neill E, Wiggins SM, Baumann-Pickering S, Hildebrand JA, Cholewiak DM, Van Parijs SM. 2018. Passive Acoustic Monitoring for Marine Mammals in the Western Atlantic April 2016 – June 2017. Final Report. Marine Physical Laboratory Technical Memorandum 632. September 2018.

Rafter MA, Rice AC, Thayre BJ, O'Neill E, Wiggins SM, Frasier KE, Baumann-Pickering S, Hildebrand JA, Cholewiak DM, Van Parijs SM. 2020. Passive Acoustic Monitoring for Marine Mammals in the Western Atlantic June 2017–June 2018. Final Report. Marine Physical Laboratory Technical Memorandum 640. June 2020.

Risch D, Clark CW, Dugan PJ, Popescu M, Siebert U, Van Parijs SM. 2013.Minke whale acoustic behavior and multi-year seasonal and diel vocalization patterns in Massachusetts Bay, USA. Mar. Ecol. Prog. Ser. 489:279-295.

Risch D, Siebert U, Van Parijs SM. 2014. Individual calling behaviour and movements of North Atlantic minke whales (*Balaenoptera acutorostrata*). Behaviour 151(9):1335-1360.

Shearer JM, Quick NJ, Cioffi WR, Baird RW, Webster DL, Foley HJ, Swaim ZT, Waples DM, Bell JT, Read AJ. 2019. Diving behaviour of Cuvier's beaked whales (*Ziphius cavirostris*) off Cape Hatteras, North Carolina. R. Soc. Open Sci. 6:181728.

Soldevilla MS, Baumann-Pickering S, Cholewiak D, Hodge LE, Oleson EM, Rankin S. 2017. Geographic variation in Risso's dolphin echolocation click spectra. J. Acous. Soc. Am. 142:599-617.

Van Opzeeland I, Boebel O. 2018. Marine soundscape planning: Seeking acoustic niches for anthropogenic sound. J. Ecoacoustics 2:#5GSNT8.

Watwood SL, Miller PJO, Johnson M, Madsen PT, Tyack PL. 2006. Deep-diving foraging behaviour of sperm whales (*Physeter macrocephalus*). J. Anim. Ecol. 75:814-825.

Weiss SG, Cholewiak D, Frasier KE, Trickey JS, Baumann-Pickering S, Hildebrand JA, Van Parijs SM. In review. Monitoring the acoustic ecology of the shelf break of Georges Bank, Northwestern Atlantic Ocean – new approaches to visualizing complex acoustic data. Mar. Policy.

Wiggins SM, Hildebrand JA. 2007. High-frequency acoustic recording package (HARP) for broad-band, long-term marine mammal monitoring, International Symposium on Underwater Technology 2007 and International Workshop on Scientific Use of Submarine Cables and Related Technologies 2007. Institute of Electrical and Electronics Engineers, Tokyo, Japan. 551-557.

Zimmer WM, Johnson MP, Madsen PT, Tyack PL. 2005. Echolocation clicks of free-ranging Cuvier's beaked whales (*Ziphius cavirostris*). J. Acous. Soc. Am. 117:3919-3927.

8 Sea Turtle Research

Primary authors: Heather Haas and Chris Sasso, with contributions from Samir Patel, Joshua Hatch, Craig Harms, Kate Choate, Leah Crowe and Debra Palka

8.1 Introduction

There is an increasing concern over the effects of human activities on sea turtles and other marine wildlife. To assess the level of concern, scientists and managers need to understand the current distribution, habitat usage, and life history of the marine wildlife and attempt to predict future changes. This requires not only knowing where species are, but also why they are there, and what they are doing there. We need long term monitoring and we need to use a range of study tools to understand the ecology of marine wildlife within the complexities of their ecosystem (Wiebe et al. 2009). The Turtle Ecology task within the Atlantic Marine Assessment Program for Protected Species (AMAPPS) is following this strategy to contribute to aspects of 4 of the 7 AMAPPS objectives (taken from the complete list of objectives in Chapter 3):

3) Conduct tag telemetry studies of marine turtles to develop corrections for availability bias in the abundance survey data and to investigate behavior and ecology of species in areas of interest;
4) Collect additional data on life-history and ecology, including habitat use, residence time, frequency of use, and behavior;
5) Identify currently used, viable technologies and explore alternative platforms and technologies to improve population assessment studies, if necessary;
6) Assess the population size of surveyed species at regional scales; and develop models and associated tools to translate these survey data into seasonal, spatially explicit density estimates incorporating habitat characteristics.

In addition, the fieldwork conducted by the Turtle Ecology task members has also contributed to the following AMAPPS objective when we conducted visual line transects surveys, particularly those conducted on NOAA vessels:

1) Collect broad-scale data over multiple years on the seasonal distribution and abundance of marine mammals (cetaceans and pinnipeds), marine turtles, and seabirds using fixed passive acoustic monitoring and direct aerial and shipboard surveys of coastal U.S. Atlantic Ocean waters;

The National Marine Fisheries Service (NMFS) Northeast and Southeast Fisheries Science Centers (NEFSC and SEFSC), along with external colleagues, collaborated to address the above AMAPPS objectives related to turtle ecology data collection and analysis efforts. The portion of the AMAPPS I (and II) funds from BOEM and the U.S. Navy allocated for turtles funded primarily data collection efforts, with only a small fraction of the budget funding analysis and manuscript preparation related to turtle issues. Nevertheless, together with partners, during AMAPPS II data collected under AMAPPS contributed to several published research papers related to AMAPPS objectives.

During AMAPPS I (01 Oct 2010 to 30 Sept 2014), the Turtle Ecology task members tagged loggerhead turtles (*Caretta caretta*) in shelf waters off the southeastern and northeastern regions of the United States. During AMAPPS II (01 Oct 2014 to 30 Sep 2019), BOEM requested we deploy all loggerhead tags north of Cape Hatteras, NC and attempt to place tags on turtles in under sampled areas and on under sampled demographic groups. During AMAPPS II, we also started developing a research program for leatherback turtles (*Dermochelys coriacea*).

To understand the spatiotemporal distribution and abundance patterns of sea turtles (AMAPPS objectives 1, 2, 3, and 6), we used several study tools including animal-borne telemetry tags and visual shipboard

and aerial survey data. This chapter highlights how loggerhead tag data collected under AMAPPS and other collaborating projects contributed to spatially explicit relative distribution monthly maps (Winton et al. 2018). This chapter, along with Chapters 5 and 6, also highlights the ongoing AMAPPS project to use visual survey data for distribution information and the time-depth data from tags to account for surface availability. Together we are using this information to describe the abundance and distribution of turtle species and to develop density-habitat models resulting in spatiotemporal maps and absolute abundance estimates for the study area.

Animal-borne tags are a tool that also provides data used to understand the behavior and ecology of sea turtles (AMAPPS objectives 3 and 4). For example, we configured the tags to also collect temperature at depth. The time-depth-temperature data provided us a unique insight into the animal's behavior and utilization of the water column. This type of insight can inform marine spatial managers on the potential effect of anthropogenic activities in those waters. This chapter highlights these insights into loggerhead's behavior in the water column in the collaborative paper Patel et al. (2018).

Density-habitat models (such as those in Chapter 6) commonly use as input habitat covariates the output from ocean models of surface and water column characteristics (such as temperature and salinity). The U.S. Mid-Atlantic waters, where many cetaceans and sea turtles are, is a dynamic ecosystem that is difficult to model due to a combination of complex seasonal water masses and currents and a limited set of tools for taking *in situ* measurements. Thus, we realized that another contribution of these tag studies is that the temperature data collected on the tags can contribute to improving ocean temperature models.

Since we had to bring the turtles onboard a ship to tag them, we also had the opportunity for collaborators to collect biological and life history characteristics, ranging from morphometric measurements to blood biochemistry, which contributes to AMAPPS objective 4. Chapter 10 documents the types of biological data we collected. In this chapter, we highlighted the completed blood biochemistry analysis (Yang et al. 2019).

In addition, to learning more about the ecology and behavior of loggerheads, the turtle tagging cruises were an opportunity to explore alternative platforms (AMAPPS objective 5). Previously assessing sea turtle behavior on the foraging grounds was primarily limited to the interpretation of visual sightings and remotely sensed data, like tags. As a result, we had a general lack of detailed understanding of the habitat use of sea turtles during a phase that accounts for a majority of their lives. AMAPPS scientists and collaborators started addressing this data gap by using data collected from remotely operated vehicles (ROV). In this chapter, we highlighted the video data collected from ROVs in a collaborative project that contributed to learning about the habitat usage, foraging behavior and prey selection (Smolowitz et al. 2015; Patel et al. 2016).

We know we need long term monitoring to investigate the status of and changes within a population (relates to AMAPPS objective 6). However, a question is what should we monitor in the case of sea turtles? Traditionally, scientists monitored nest counts to assess the status of sea turtles (Whiting et al. 2014). Another potential method to monitor sea turtles is through the NMFS aerial surveys over oceanic waters. The aerial surveys focused on protected species, including sea turtles since 1983, and efforts increased in 2010 with the implementation of AMAPPS. Both types of monitoring techniques result in estimates that have a measurable sampling variability. However, natural spatial and inter-annual variability complicates the accuracy and precision of the estimates. One of the AMAPPS collaborators used the AMAPPS turtle tag data and line transect turtle data to evaluate nest counts and line-transect aerial surveys as annual loggerhead sea turtle population monitoring metrics to assess population level impacts (Warden et al. 2017).

In this chapter, we describe our approaches to data collection to address the AMAPPS objectives, summarize our results, discuss progress, and identify data gaps and future work.

8.2 Methods

8.2.1 Collaborative Approach

To optimize resources we developed a highly collaborative approach. We described our field sampling partnerships in the AMAPPS annual reports. During AMAPPS I we developed collaborations between SEFSC, NEFSC, Coonamessett Farm Foundation (CFF), and Virginia Aquarium & Marine Science Center. During AMAPPS II we also partnered on data sharing and analysis with Michael Arendt of the South Carolina Department of Natural Resources, Michael James of the Department of Fisheries and Oceans Canada (DFO), Megan Winton and Gavin Fay of University of Massachusetts Dartmouth, and Craig A. Harms, DVM, PhD of North Carolina State University's College of Veterinary Medicine. In addition to satellite tagging, we also collaborated to collect opportunistically biological and behavioral samples. When feasible, we collected morphometric measurements, blood for health assessment and sex determinations, multiple tissues for stable isotopes and genetic analysis, and behavioral data. Because these collaborations are coordinated with AMAPPS and support AMAPPS objectives, a summary of partners' activities are included here.

8.2.1.1 Coonamessett Farm Foundation

For over 10 years, the CFF has been researching the ecology and behavior of loggerhead sea turtles in areas that overlap with the interests of AMAPPS and the Northeastern scallop fishery. These areas include the Mid-Atlantic Bight, southern New England, and Georges Bank. The primary objectives are to examine sea turtle distributions, behavior and foraging habits; improve sea turtle bycatch estimates; identify factors impacting bycatch rates; and determine the role loggerheads play in impacting sea scallop health (Table 8-1). Through these efforts, CFF continues to advance the ability to locate, track, and observe loggerhead sea turtles through innovative use of Remotely Operated Vehicle (ROV) mounted video cameras, side-scan sonar, aerial surveys, and satellite tags. The information collected aids in assessing the ecology of sea turtles in wind development areas, improving loggerhead abundance estimates, developing scallop-harvesting strategies that minimize harm to sea turtles, and defining critical habitats for loggerheads.

A major source of CFF sea turtle funding has been from the NMFS Scallop Research Set-Aside program. This project spearheaded the development of an offshore tagging program for loggerheads in the Mid-Atlantic Bight. The Research Set-Aside program provided the ship time and staffing for the vast majority of AMAPPS satellite tag deployments. Over the past 5 years, Research Set-Aside funding purchased over 50 satellite tags that they parameterized and deployed consistent with AMAPPS objectives. They shared and stored these data in an NEFSC Oracle database. CFF staff and AMAPPS staff worked side by side on fieldwork and analysis. Both projects benefit from increased field capacity, sample sizes, and analytic capabilities.

CFF received two Saltonstall-Kennedy grants to fund modeling studies using CFF and AMAPPS data to provide estimates of potential loggerhead distribution under future climate scenarios and improve oceanographic forecast modelling for the region. In the first grant, a collaborative team characterized sea surface temperature (SST) and depth conditions encountered by loggerheads in the Mid-Atlantic Bight, and applied generalized linear models to identify SST and depth associated with loggerhead habitat usage by using data obtained from remotely sensed sources. Then they projected the results of the habitat model to predicted future conditions to illustrate how loggerhead distributions in the Mid-Atlantic Bight may shift in response to climate change over long-term time scales (i.e., 80 to 100 yrs) to show potential impacts over the lifetime of an individual turtle. The second grant aimed to improve oceanographic models used to forecast temperature within Mid-Atlantic Bight waters and produce continuously updated temperature products for fishers and managers. One goal of this grant is to incorporate several years of

temperature data accrued from animal-borne sensors, autonomous ocean gliders, commercial fishing gear, and trawl surveys to improve numerical modeling of the Cold Pool and greater Mid-Atlantic Bight.

Finally, CFF's Bycatch Reduction Engineering Program grant investigated leatherback sea turtle entanglements in vertical lines from fishing gear within the near shore waters adjacent to Cape Cod, MA using spotter pilots, videography, and anonymous fishers' surveys. This leatherback behavior study has interfaced with the burgeoning AMAPPS leatherback program. The Bycatch Reduction Engineering Program project has been working collaboratively with AMAPPS on aerial surveys to locate leatherbacks, leatherback satellite tagging, and leatherback suction cup tagging. CFF staff and AMAPPS staff work side by side on fieldwork and analyses. The approximate 35 hrs of direct leatherback video footage acquired through the Bycatch Reduction Engineering Program project could agument the dive-depth tag data to improve calculations of the availability bias correction factor for leatherbacks in the region.

8.2.1.2 NMFS National Protected Species Toolbox Initiative

During the fiscal years of 2018, 2019, and 2020 NMFS funded a project that supported AMAPPS objectives and utilized existing satellite telemetry data: "Analysis and Applications to Improve Protected Species Assessments in the Greater Atlantic Region". The project's principal investigators (Joshua Hatch and Heather Haas) partnered with the Greater Atlantic Regional Fisheries Office (Carrie Upite and Ellen Keane), Coonamessett Farm Foundation (Ronald Smolowitz and Samir Patel), University of Massachusetts Dartmouth (Gavin Fay and Megan Winton), and the NEFSC Geophysical Fluid Dynamics Laboratory (Vincent Saba). By working together with governmental and research partners, the team proposed to develop a set of analyses and web applications to improve protected species assessments in the Greater Atlantic Region (Maine through Cape Hatteras, NC).

The project consists of several components that relate to processing and utilizing data from animal-borne data loggers deployed on loggerhead sea turtles. Broadly speaking, the subcomponents involve developing an R Shiny interactive web application to reconstruct tracks from satellite-tag data; assessing the overlap of commercial fishing effort and loggerhead turtle distribution in space and time; working with collaborators to use climate change scenarios to project the possible future loggerhead turtle distribution in the Greater Atlantic Region. The development of the R Shiny application is particularly responsive to AMAPPS priorities because it can simplify future analysis of data from satellite tags deployed on sea turtles and other animals.

The project consists of several components that relate to processing and utilizing data from animal-borne data loggers deployed on loggerhead sea turtles. Broadly speaking, the subcomponents involve developing an R Shiny interactive web application to reconstruct tracks from satellite-tag data; assessing the overlap of commercial fishing effort and loggerhead turtle distribution in space and time; working with collaborators to use climate change scenarios to project the possible future loggerhead turtle distribution in the Greater Atlantic Region. The development of the R Shiny application is particularly responsive to AMAPPS priorities because it can simplify future analysis of data from satellite tags deployed on sea turtles and other animals.

The R Shiny interactive web application allows users to reconstruct tracks from satellite-tagged animals using a Continuous Time Correlated Random Walk movement model (Johnson et al. 2008; Albertsen et al. 2015; Winton et al. 2018). The reconstructed tracks can then serve as the basis for other AMAPPS research interests such as the collaborative work modeling the distribution of loggerhead turtles under current and potential future climatic changes, funded in part by AMAPPS, the National Protected Species Toolbox project, and Saltonstall-Kennedy grants. Other researchers not funded as part of AMAPPS have already used the web app to analyze satellite tags deployed on grey seals (Kimberly Murray, pers. comm.).

Table 8-1 List of Coonamessett Farm Foundation projects that are relevant to AMAPPS objectives
Funding sources were from Research Set-Asides (RSA), Saltonstall-Kennedy grants (SK), and the Bycatch Reduction Engineering Program (BREP).

Funding Info	Title	Principals	Collaborators/Partners
2019 RSA 04/19-03/20 $146,104	Understanding Impacts of the Sea Scallop Fishery on Loggerhead Sea Turtles through Satellite Tagging	Dr. Samir Patel, CFF Dr. Liese Siemann, CFF	Ronald Smolowitz, Coonamessett Farm James Gutowski, Viking Village Fisheries Roxanna Smolowitz, Roger Williams University
2018 RSA 04/19-03/20 $190,599	Understanding the Impacts of the Atlantic Sea Scallop Fishery on Loggerhead Sea Turtles	Dr. Samir Patel, CFF	Ronald Smolowitz, Coonamessett Farm James Gutowski, Viking Village Fisheries Roxanna Smolowitz, Roger Williams University
2017 RSA 03/18-02/18 $224,750	Understanding Impacts of the Sea Scallop Fishery on Loggerhead Sea Turtles through Satellite Tagging	Dr. Samir Patel, CFF	Ronald Smolowitz, Coonamessett Farm James Gutowski, Viking Village Fisheries Roxanna Smolowitz, Roger Williams University
2016 RSA 04/16-03/17 $223,015	Understanding Impacts of the Sea Scallop Fishery on Loggerhead Sea Turtles through Satellite Tagging	Dr. Samir Patel, CFF Shea Miller, CFF	Ronald Smolowitz, Coonamessett Farm James Gutowski, Viking Village Fisheries
2015 RSA 04/15-03/16 $199,260	Understanding Impacts of the Sea Scallop Fishery on Loggerhead Sea Turtles through Satellite Tagging	Coonamessett Farm Foundation	James Gutowski, Viking Village Fisheries
2018 SK 09/19-08/19 $35,770	Using climate change scenarios to project loggerhead distributions in the U.S. Mid-Atlantic	Dr. Samir Patel, CFF	Megan Winton, University of Massachusetts Gavin Fay, University of Massachusetts Ronald Smolowitz, Coonamessett Farm, Inc. Vincent Saba and Heather Haas, NEFSC
2018 SK 09/18-08/20 $257,534	Improving oceanographic models of bottom temperature within the Mid-Atlantic Bight through novel data assimilation and stakeholder input	Dr. Samir Patel, CFF Jason Clermont, CFF	Ronald Smolowitz- Coonamessett Farm, Inc. Peter Moore, Fisheries Development International LLC Wendell Brown, UMass Dartmouth/SMAST & MARACOOS Bill Bright, F/V Retriever, Loper-Bright Enterprises LLC Leah Crowe, Integrated Statistics James Manning, Heather Haas, NEFSC
2017 BREP 06/18-05/20 $168,803	Improving the Understanding of Sea Turtle Entanglement in Vertical Lines	Dr. Samir Patel, CFF Dr. Liese Siemann, CFF	Heather Haas, Henry Milliken, and Eric Matzen, NEFSC Michael James, Fisheries and Oceans Canada Aliki Panagopoulou, The Leatherback Trust John Pappalardo, Cape Cod Fishermen's Alliance Ronald Smolowitz, Coonamessett Farm George Breen, Pilot

Currently, the web app is on an internal NEFSC server and is only available to research scientists with access to the NEFSC network that lies behind the NMFS firewall (i.e., not public facing). To provide

better outreach to the public and our partners, AMAPPS funded an R Shiny Server Pro license to establish a web server accessible by the public. In the coming months, we hope to make the developed R Shiny web app available to the public, along with other web apps developed in R Shiny to support the AMAPPS mission (e.g., data access and dissemination). The advantage of the developed R Shiny web app is it eases the process of reconstructing animal tracks from satellite-tag data, as it does not require the user to know the R programming language. Additionally, the web app allows the process to reconstruct tracks from satellite-tag data to be streamlined and made more transparent, allowing for reproducible and repeatable analyses in a more interactive way than simply providing code for public use.

Prior to 2018, the National Protected Species Toolbox Inititive funded a project to evaluate quantitative methods for assessing the impact of anthropogenic activity on marine turtles: "Quantitative Tools to Assess Impact of Anthropogenic Activity on Sea Turtle Populations". This project used simulations to evaluate the relationship between sea turtle population monitoring metrics and population trends. This earlier phase of the Toolbox initiative did not routinely incorporate AMAPPS data (as is currently being done), but the project's objectives of assessing turtle populations and evaluating federal impacts paralleled some of the AMAPPS objectives. A paper from this earlier phase of the Toolbox Initiative (Warden et al. 2017, discussed later in this chapter) used information from published AMAPPS aerial surveys (NEFS and SEFSC 2011) to characterize the uncertainty associated with abundance estimates from line transect aerial surveys compared to nest count surveys.

8.2.1.3 Marine Health Program at North Carolina State

The Marine Health Program at North Carolina State Center for Marine Sciences and Technology (CMAST) has collaborated with AMAPPS to study leatherback sea turtle migratory patterns, movements, and health status. Dr. Craig Harms from CMAST is leading the health assessment component. Fieldwork occurred in 2018 and 2019 in Massachusetts and North Carolina. Leatherback sea turtles were captured at-sea using hoop nets deployed from small boats guided by an overhead spotter plane. Turtles spent about 15 minutes on an inflatable platform being measured and tagged (satellite, flipper, and microchip), having blood drawn (hematology, plasma chemistry analysis, blood gases, and nuclear magnetic resonance metabolomics), temperature recorded (leatherback sea turtles maintain an internal temperature warmer than their environment), fat thickness determined by ultrasound, and electrocardiogram monitored. Veterinary team members from NC State College of Veterinary Medicine CMAST and the NC Aquariums included Craig Harms, Michael Stoskopf, Emily Christiansen, Greg Scott, Heather Broadhurst, and Maria Serrano. The team assessed 7 turtles in 2018 and 13 in 2019. Having access to healthy migrating leatherbacks at-sea, versus nesting females or compromised stranded turtles, is a rare opportunity. An interesting finding has been anomalously low plasma total calcium values, compared with leatherbacks sampled elsewhere (mostly but not exclusively nesting females) and compared with other sea turtle species. Whether this represents an unusual mode of calcium metabolism related to diet and migration at this life stage, or is an unidentified laboratory artifact, is under further investigation. Wildlife capture events also provide the chance to evaluate the impacts of the capture method itself, to ensure the welfare of the study animals and the quality of post-release data. As assessed by blood gases, lactates, and heart rate, the hoop net capture method has relatively minor impacts on leatherbacks, although the features of some individual captures have been associated with somewhat higher lactate values than others, providing insights for continuous improvements in methods.

8.2.1.4 Additional Collaborations

We have been collaborating with Dr. Michael James of DFO on the loggerhead research cruises aboard the NOAA ship *Henry B. Bigelow* in 2015 and again in 2017. During these times, BOEM recommended that the AMAPPS satellite tags be deployed in times and areas that have been historically underrepresented, with a particular interest in having more tags deployed as far north as feasible. The collaboration with Dr. James allowed the dedicated AMAPPS Turtle Ecology cruise to benefit from the

real-time turtle-related knowledge of DFO and the Canadian Fishing Fleet. DFO also collaborated on AMAPPS objectives by providing labor and travel for their expert field staff to add in AMAPPS research cruises and small boat work and by providing multiple tags (satellite, hybrid, and archival suction cup).

During AMAPPS II, DFO and AMAPPS collaborated with University of North Carolina Wilmington's Professor Amanda Southwood and her student Tiffany Yang to analyze the loggerhead physiological data from previous blood draws. The collaboration led to Yang et al. (2019), details below.

We have also coordinated closely with stranding and disentanglement teams as well as other local sea turtle researchers. For example, in 2019, Dr. Charlie Innis (New England Aquarium) joined us on our small boat-tagging trip where we diverted our operations to help Dr. Innis tag a leatherback entangled in vertical line. Later on the same day, we received a notification from the Marine Animal Entanglement Response team at the Center for Coastal Studies of an additional entangled leatherback. In rapid response, we joined the Coast Guard to assist in locating, disentangling, and tagging that leatherback.

In addition, we have coordinated with the NMFS Sea Turtle Stranding and Salvage Network and their support of the NMFS Serious Injury Determination for sea turtles in the Greater Atlantic Region. In 2019, we observed and were able to capture video of a free-swimming leatherback with severe injuries consistent with entanglement in a vertical line. It is extremely rare to be able to record the movements of a free-swimming leatherback with impaired mobility and recent injuries consistent with entanglement restriction marks. This turtle had unhealed encircling scarring patterns on the neck and humerus area of the front right flipper, as well as the unhealed chafe marks on the corresponding anterior margin of the carapace. The impaired front right flipper mobility (most evident in asymmetrical flipper stroke biomechanics) suggested the possibility of deep muscle damage from blood flow restriction. We called the Marine Animal Entanglement Response team at the Center for Coastal Studies team who came to the scene to ensure that there was no line still attached to this turtle and to better document the situation. We have submitted the photographs and video of this turtle to the NMFS Sea Turtle Stranding and Salvage Network who will pass the information along to NMFS Greater Atlantic Region's Sea Turtle Serious Injury Working Group.

8.2.2 Tagging Study Sites

From October 2014 through September 2019, the AMAPPS Turtle Ecology task members sampled 4 primary study sites (Figure 8-1) ranging from coastal waters to farther offshore on the continental shelf and range from waters offshore of Florida to Massachusetts. The majority of the loggerhead satellite tagging work occurred in the Mid-Atlantic shelf in collaboration with other research organizations, though some searching and sampling effort also occurred further offshore. In the summers of 2015 and 2017, we undertook dedicated loggerhead cruises aboard the NOAA Ship *Henry B. Bigelow*. The coastal Florida sites were sampled during AMAPPS I (2010 and 2013). During AMAPPS II, at the request of BOEM, turtle sampling shifted further north. We sampled the Mid-Atlantic Bight throughout AMAPPS I and II.

Leatherback satellite tagging occurred at two primary coastal sites in North Carolina and Massachusetts (Figure 8-1).

With respect to loggerheads during AMAPPS II, we focused our captures and deployments in areas that historically were under-sampled. Details of the field operations are available in the AMAPPS annual reports as well as in Patel et al. (2018). Our sampling focused on demographic classes (juveniles and males) that were under-sampled in the past. We deployed tags in the Mid-Atlantic Bight and northeast because historically far fewer tagged loggerheads were in this more northern part of their range. Similarly, we focused on offshore (> 20 miles from shore) deployments because we suspected

inshore/offshore population structuring and there has been only limited offshore sampling in the Mid-Atlantic.

With respect to leatherbacks, our goal during AMAPPS II was to develop a small boat-based program that could satellite tag leatherbacks in an efficient and cost-effective manner. Leatherbacks present several challenges to researchers. Their large size makes leatherbacks more difficult to handle than the hard-shelled turtles, like loggerheads. Compared to loggerheads, leatherbacks are more ephemeral, both in terms of time at the surface of the water and in terms of time spent in a particular geographical area. Studying leatherbacks during AMAPPS II was also challenging because the majority of the funds were dedicated to loggerheads.

For these reasons, we invested time during AMAPPS II to build a leatherback research program that could be successful given the species-specific constraints. Our approach had several elements, the first of which was close collaboration between SEFSC and NEFSC, as well as with DFO and various academic, conservation, and research organizations. The second component was to move from a large research vessel program to a small boat-based program that could be more cost-effective and flexible. Third, we selected sampling regions where leatherbacks would be close to shore during relatively predictable periods. Fourth, we invested in low-cost innovations (like vessel modifications, the purchase of custom-made inflatable sampling platforms, and communication equipment) so that we could stretch the capabilities of our existing small boat fleet. This approach culminated in 35 small boat days at-sea dedicated to leatherback research in the final year of AMAPPS II.

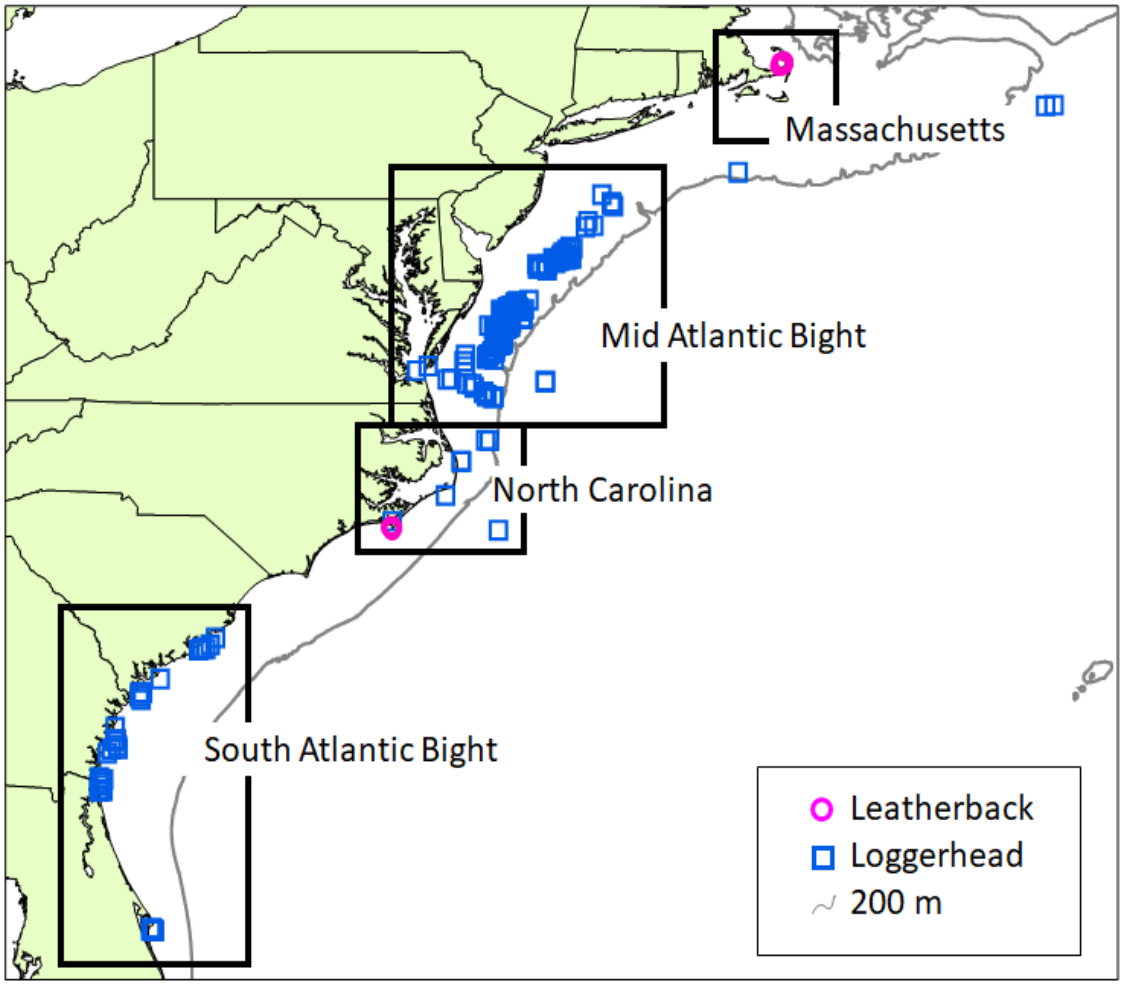

Figure 8-1 Locations of satellite tags deployed on loggerhead and leatherback sea turtles
Black boxes outline the locations of the 4 primary turtle tagging study sites.

In addition to developing a leatherback capture and satellite-tagging program in AMAPPS II, we also developed a high-resolution short-term tagging program based on suction cup tags placed on turtles while they are free-swimming. This work is in close collaboration with DFO and CFF through a project lead by CFF that focused on improving our understanding of sea turtle behavior in areas with entanglement risks. We deployed and tested several custom-made suction cup tags to describe surfacing behavior, foraging behavior, and dive behavior. One of the custom tags was an enhanced version of Loggerhead Instruments' AMX tag, which is an audio and motion datalogger that records animal motion and sound production and exposure simultaneously. This effort obtained 36 hrs of footage obtained from camera deployments on 24 leatherbacks. Video analysis to identify specific behaviors and environmental markers will occur during AMAPPS III.

8.2.3 Habitat Usage Studies

To understand how turtles are using their habitat, AMAPPS researchers and their collaborators used a suite of tools in the following studies that are at different stages of completion:

1) Relative spatiotemporal densities based on loggerhead tag location data
2) Water column usage of loggerheads based on ROV videos
3) Density-habitat modeling based on visual aerial and shipboard sightings

A study conducted to document the spatiotemporal distribution of loggerheads used the movement and location data collected via satellite-linked telemetry tags (Winton et al. 2018). Most applied telemetry studies aim to reconstruct the continuous utilization distribution underlying reported locations to characterize the relative intensity of space use. However, commonly applied space use estimators do not directly estimate the underlying distribution of interest and, perhaps more importantly, ignore correlations in space and time that may bias estimates. Here we used geostatistical mixed effects models to explicitly account for spatial and/or temporal correlation using Gaussian random fields to estimate utilization distributions from the satellite telemetry data. We also used simulation testing to compare the performance of the proposed models with several conventional space use estimators.

Smolowitz et al. (2015) represents the first documented use of a ROV to actively track sea turtles *in situ*. From 2008 to 2014, they deployed an ROV to track the at-sea behavior of loggerhead turtles in the Northwest Atlantic Ocean. They tracked 70 turtles, totaling 44.7 hrs of direct turtle footage. To obtain the video footage they first detected turtles from the boat. Then, when a turtle was within about 50 m of the boat, they deployed the ROV to track the turtle for as long as possible.

Patel et al. (2016) quantified the video data from Smolowitz et al. (2015) in the context of a behavioral ethogram. They aimed to understand loggerhead habitat usage by providing detailed information about the feeding habits, prey availability, buoyancy control, and water column usage. They accomplished this by using 45.7 hrs of video footage from 73 loggerhead turtles obtained from ROVs deployed during 2008 to 2014. They filmed turtles that used the entire water column and quantified the frequency of behaviors, such as flipper beats, breaths, defecations, feedings and reactions to the ROV. They developed an ethogram account for 27 potential environmental and behavioral parameters. They also used the ROV's depth sensor and visible cues (i.e., water surface or benthic zone in view) to distinguish depth zones and assess how the turtles used the water column. In addition, they quantified interactions with sympatric biota, including potential gelatinous and non-gelatinous prey species, fish (including sharks), marine mammals, and other sea turtles.

Density-habitat modeling based on visual aerial and shipboard sightings is an ongoing AMAPPS project. We described the data collection and analysis methods for the visual data in Chapters 5 and 6. As discussed in Chapters 5 and 6, absolute abundance estimates result from analyses that account for perception and availability bias. The data resulting from the two-team data collection protocols result in abundance estimates that account for perception bias. Because turtles routinely perform long dives, it is essential to account for the low chances of visually detecting a turtle on the surface during an aerial and shipboard abundance survey (that is, account for availability bias). Hatch et al. (in review) uses the dive depth information obtained from the tags to quantify the average time spent at the surface (where they could be detected during a visual survey) and at depth (where they are not detected during a visual survey). When we finalize this analysis, then we can use the methods described in section 5.2.5 to calculate a correction factor for availability bias. Dive patterns of all marine animals, including sea turtles, vary depending on many mostly unknown factors. For example, previous AMAPPS research (NEFSC and SEFSC 2011) showed dive patterns and therefore the correction factors were drastically different for loggerheads that were north and south of Cape Hatteras, NC. We are now in the process of improving the previous analyses to determine what the most appropriate correction factors are.

8.2.4 Biological Studies

AMAPPS researchers and collaborators collected biological data from the turtles that we brought onboard to apply tags (See Chapter 10 for more details). Morphometric measurements included animal weight, body depth, and carapace dimensions. We took biopsy samples for genetic and stable isotope analyses. We also took blood samples to analyze for testosterone levels to identify sex and used general blood chemistry for health assessments.

In a collaborative study, Yang et al. (2019) documented blood biochemistry and haematology of healthy loggerhead turtles in the Northwest Atlantic to establish clinical reference intervals for this threatened population. They analyzed blood samples from migratory loggerheads captured in 2011, 2012, 2013, and 2016 off the Mid-Atlantic coast of the U.S., including those collected under AMAPPS. They analyzed the blood to quantify blood characteristics by using a point-of-care analyser and a veterinary diagnostic laboratory service. They calculated 95% reference intervals with associated 90% confidence intervals for each blood variable. They then compared results obtained from the study of migratory loggerheads with published data from Kelly et al. (2015) for similarly sized loggerheads that were resident at a seasonal temperate latitude foraging area. They used a criterion of P 0.002 to identify significant differences (P 0.002) by using the Holm-Bonferroni adjusted p-values obtained from the Mann-Whitney U test. We discuss these results below in Section 8.3.

8.2.5 Monitoring Metrics

Variable detection probabilities can create uncertainty in trends and abundances estimated from point count surveys (e.g. nest counts), as well as from more expensive monitoring methods such as line transect surveys (e.g. aerial surveys). In a collaborative study, Warden et al. (2017) used a loggerhead sea turtle population model to generate stochastic 'known' populations from which they mimicked the information they would obtain from nest counts and from over-water aerial surveys. They then subjected the populations to environmental or anthropogenic impacts and compared trends in each monitoring metric with the trend in simulated turtle population size in terms of adult equivalents. We discuss these results below in Section 8.3.

8.3 Results

8.3.1 Collaborative Approach

Our collaborative approach to sea turtle capture and tagging has enabled us to tag and sample 278 non-nesting loggerhead sea turtles (Table 8-2), including those that were foraging offshore. Collaborations with CFF and other organizations contributed nearly 40% of the loggerhead satellite tags. We undertook loggerhead tagging in all years between 2009 and 2019, although 2009 had only two tags.

Leatherback work was also highly collaborative, but SEFSC purchased all satellite tags deployed on leatherbacks. We started developing the leatherback program in 2017, and then by 2019, we were able to deploy 22 leatherbacks tags (Table 8-3).

The size class distribution of tagged loggerhead and leatherback turtles remained relatively consistent throughout the years, with the most noticeable effect being an expansion of the range of size classes in years with high tagging efforts (Figure 8-2).

Table 8-2 Numbers of loggerhead turtle satellite tags deployed, by purchasing organization
Tag deployments were those consistent with AMAPPS protocols and stored in NMFS databases.

Year	NEFSC	SEFSC	CFF	Other	Total
2009	0	0	2	0	2
2010	14	30	0	0	44
2011	16	0	10	0	26
2012	15	0	15	2	32
2013	6	30	10	4	50
2014	7	0	13	0	20
2015	2	0	8	0	10
2016	17	0	5	0	22
2017	9	0	16	0	25
2018	18	0	19	0	37
2019	3	0	7	0	10
AMAPPS I (2010 – 2014)	58	60	50	6	174
AMAPPS II (2015 – 2019)	49	0	55	0	104
GRAND TOTAL	107	60	105	6	278

Table 8-3 Numbers of leatherback tags deployed in Massachusetts and North Carolina

Year	MA	NC	Total
2017	1	0	1
2018	1	7	8
2019	9	13	22
TOTAL	11	20	31

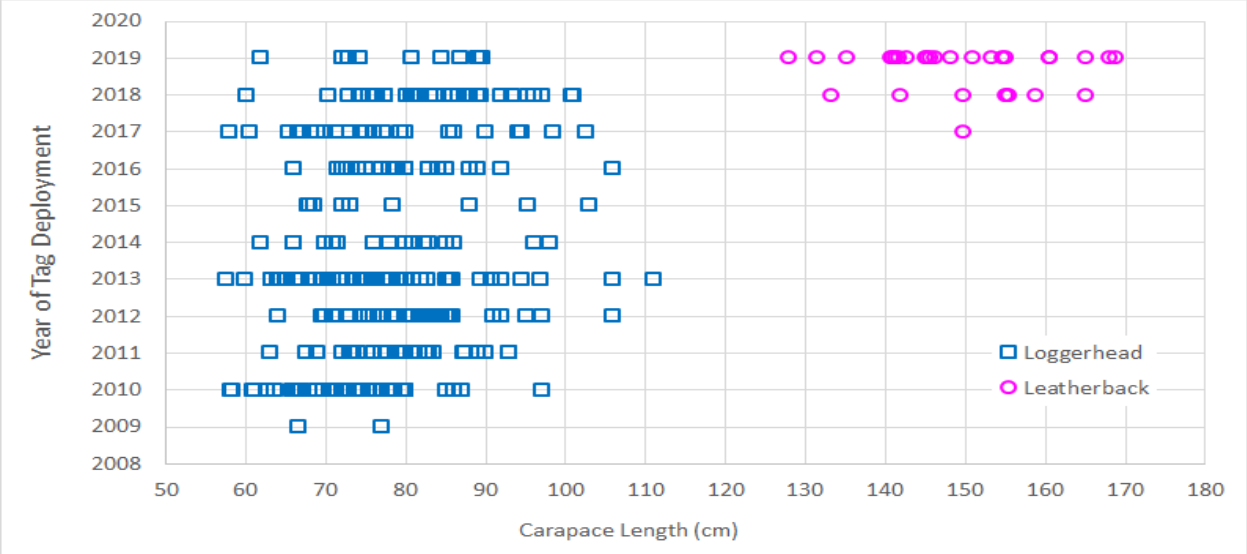

Figure 8-2 Carapace length of tagged loggerhead and leatherback sea turtles
These satellite tags were consistent with AMAPPS goals and purchased by NEFSC, SEFSC, and CFF.

8.3.2 Loggerhead Tags

Tags deployed on loggerhead turtles performed well and collected information as the turtles migrated from their initial tagging location (Figure 8-3). Reliable locations were from ARGOS location qualities 1 to 3 and Fastloc-GPS sources (residuals > 0 and < 25 using 5 or more satellites) collectively after we applied a 10 km/h filter (Douglas et al. 2012). Mean tag duration was 340.2 days (range: 23.3 – 703.0 days), almost half (44.4%) of the tags lasted the programmed 13 months (395 days) (Figure 8-4; Patel et al. 2018).

As the loggerhead-tagging program matured, we understood better how to tag turtles when they were likely to disperse widely after tagging. Dispersal after tagging extends the utility of the data by increasing the spatial areas covered and by decreasing the bias associated with initial tagging locations. The tagged loggerheads extensively covered all of the wind energy areas. In addition, many loggerheads took long migrations while tagged. Some migrated far offshore of the Mid-Atlantic or south of Georges Bank, some went towards the Bahamas, some went into the Gulf of Mexico, but most stayed on the continental shelf along the eastern United States (Figure 8-3).

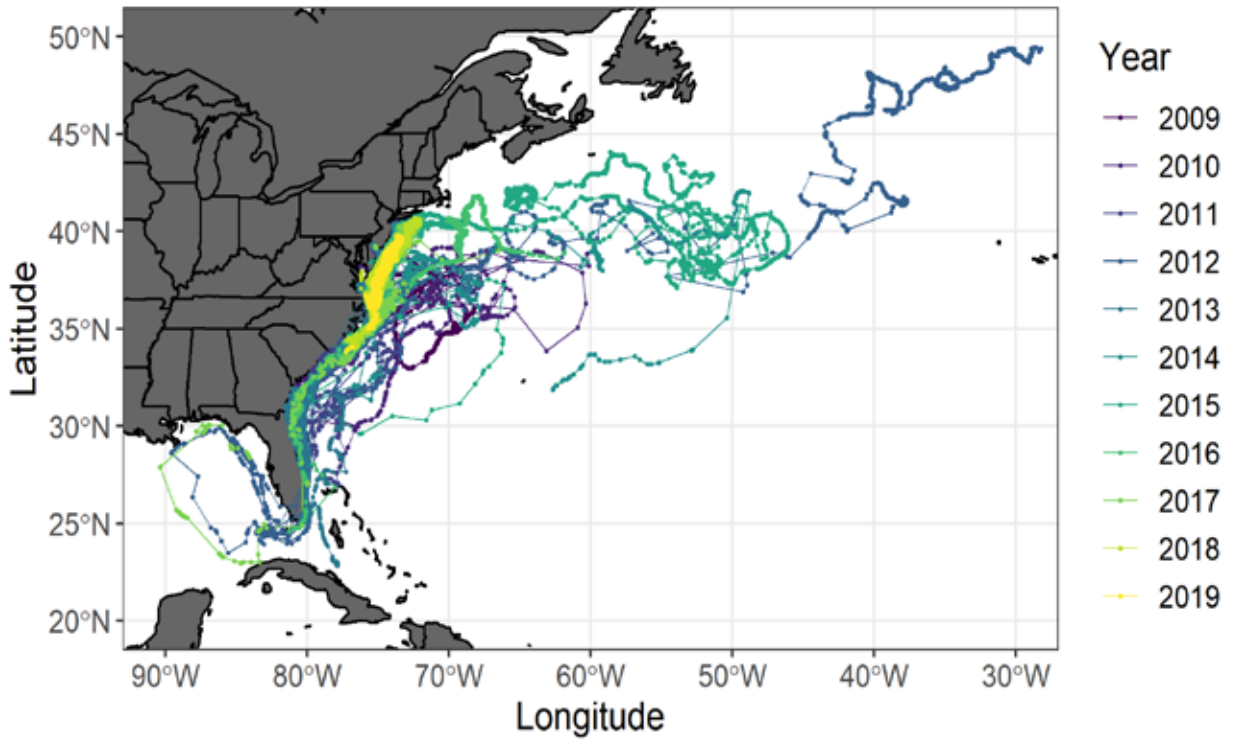

Figure 8-3 Tracks of all loggerheads tagged between 2009 and 2019

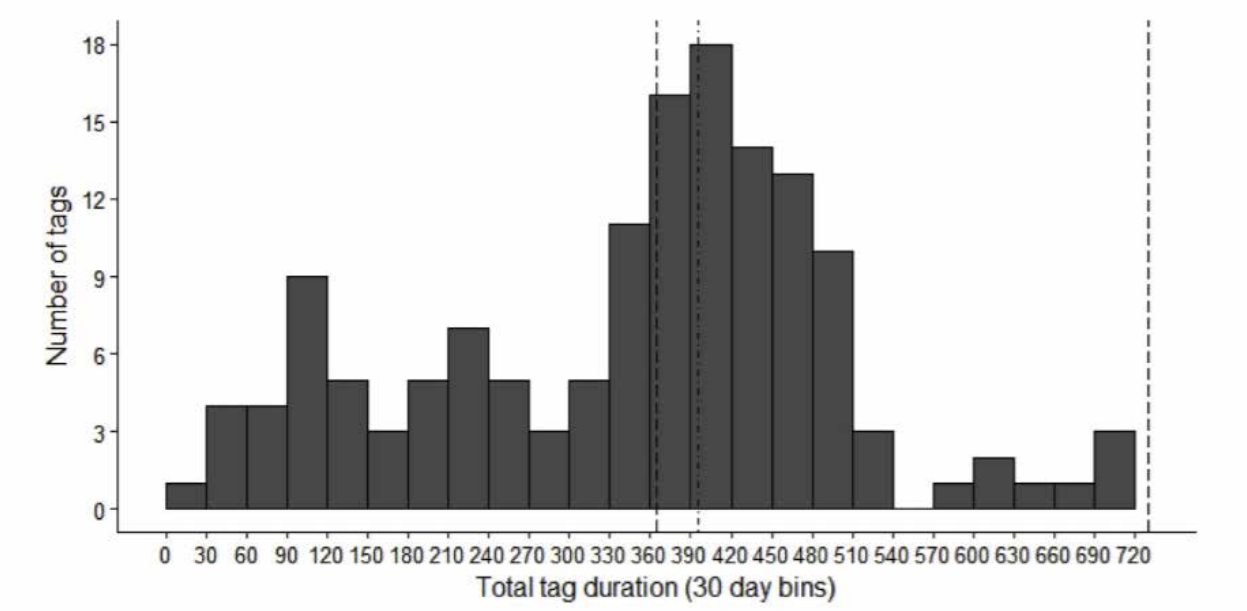

Figure 8-4 Satellite tag lifespans of loggerheads
Dash-dot line is the 13-month mark we parameterized the tags to achieve (Figure repurposed from Patel et al. 2018).

8.3.3 Leatherback Tags

Tags deployed on leatherback turtles also performed well and collected information as the turtles migrated from their initial tagging location (Figure 8-5). We were not concerned about whether leatherbacks would disperse enough after tagging (because leatherbacks are generally highly mobile), but we were concerned more about whether the tagged leatherbacks would stay in shelf waters long enough to collect data before moving offshore. Many of the tagged leatherbacks spent time in shelf waters from North Carolina, up the Mid-Atlantic shelf and into southern New England and the Gulf of Maine (Figure 8-5). After coastal residency, some leatherbacks undertook long migrations while tagged (Figure 8-6). Some migrated far offshore of the Mid-Atlantic, past Bermuda, even as far as the Mid-Atlantic Trench region. Others went towards Florida, the Caribbean, or Central America. Overall, the satellite tags were able to track the leatherbacks while they were in continental shelf waters as well as deep offshore waters.

We deployed the satellite tags without the intention of retrieval. Whereas we retrieved the suction cup tags that provided finer scale data to better explore feeding behavior. Leatherback satellite tags performed well in terms of tag duration, with the majority of tags transmitting data for 150 days or more (Figure 8-7). The video recorded from the suction cup tags provided over 1 hr of footage per most deployments, while several provided over 3 hrs of footage (Figure 8-8).

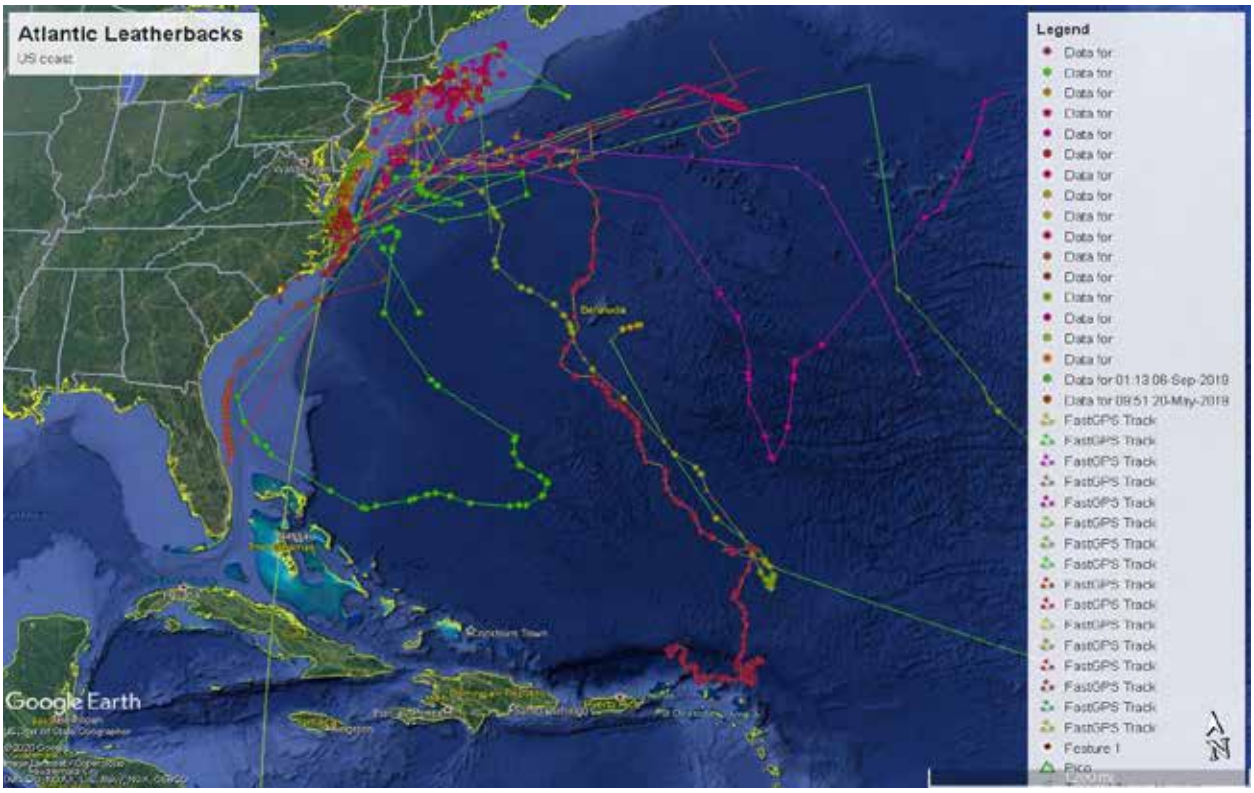

Figure 8-5 Tracks of leatherback sea turtles tagged off Massachusetts and North Carolina

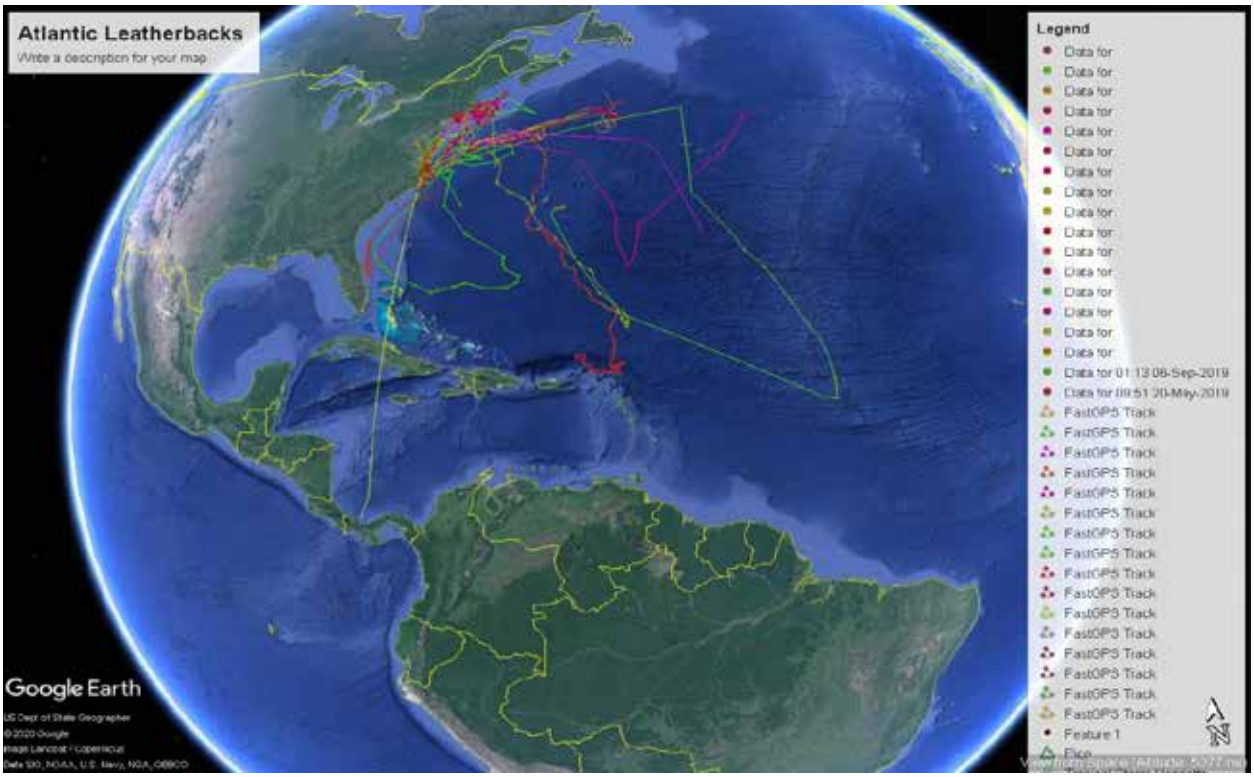

Figure 8-6 View of the longer migrations of the tagged leatherbacks

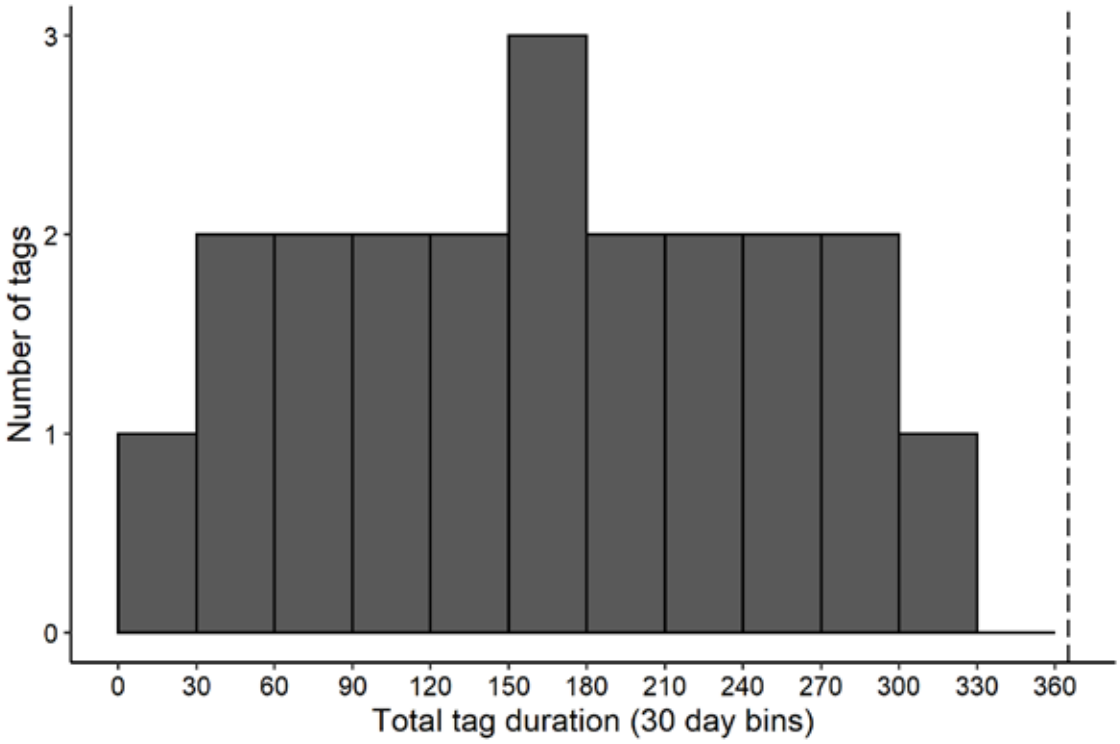

Figure 8-7 Satellite tag lifespans of leatherbacks
Data are from 21 leatherback satellite tag deployed in 2019.

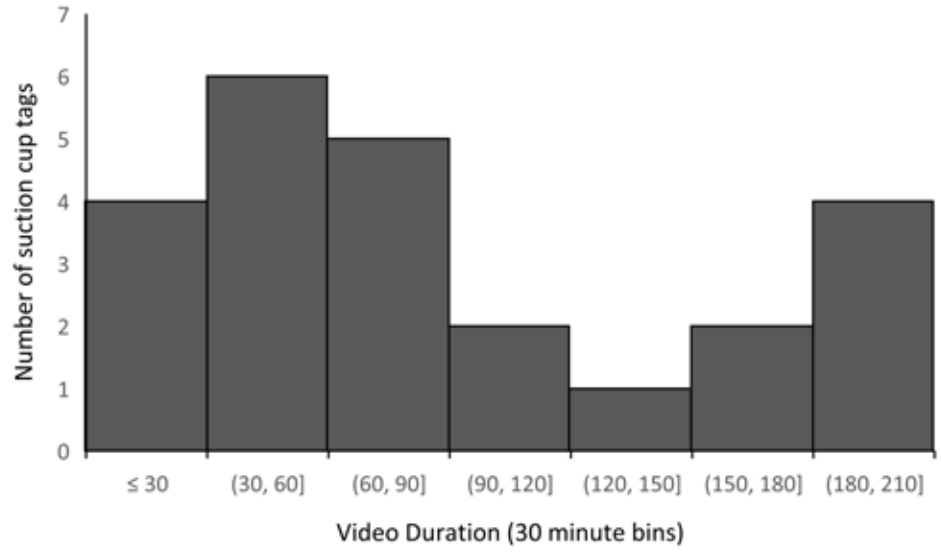

Figure 8-8 Video duration of leatherback suction-cup tags

8.3.4 Habitat Usage Studies

8.3.4.1 Tagging Studies

Data from animal-borne tags provided information on the spatiotemporal distribution along the U.S. Atlantic coast, in addition to information on how the animals use the water column.

Using the locations of 271 large juvenile and adult loggerhead turtles tagged in the western North Atlantic during 2004 to 2016, Winton et al. (2018) modeled the overall spatial distribution of tagged individuals, as well as seasonal shifts in densities at smaller time scales. This paper suggested that geostatistical mixed effects models outperform conventional estimators when the number of tag transmissions change over time, a common source of bias in satellite telemetry studies that others rarely addressed. For tagged loggerheads, overall predicted densities were greatest in the shelf waters along the U.S. Atlantic coast from Florida to North Carolina, but monthly predictions highlight the importance of summer foraging habitat in the Mid-Atlantic Bight.

By using data collected during 2009 to 2017, Patel et al. (2018) documented in a collaborative paper findings from the deployment of 167 satellite tags on loggerheads within the U.S. Mid-Atlantic Bight of the Northwest Atlantic Ocean. These tags collected and transmitted location, temperature, and depth information and yielded 18,790 temperature-depth profiles during the highly stratified season (01 June to 04 October) for the region. These included 16,371 profiles exceeding the mixed-layer depth, and, of those, 11,591 full water column profiles reaching the ocean floor. They suggested that the habitat usage of loggerhead turtles in the Mid-Atlantic Bight make them good ocean observers within this difficult to model, highly stratified region. The use of turtle-borne telemetry devices has the potential to improve resolution of *in situ* temperature through depth data and in turn improve oceanographic model outputs.

In a collaborative paper, Smolowitz et al. (2015) reported on tracked loggerhead turtles documented in video footage obtained from ROVs. For all video attempts, 43.5% of the usable video had a turtle in view for a minimum of 30 sec. The tracking durations lasted up to 426.1 min. The footage documented that often the loggerheads remained within about 10 m of the surface. However, on 12 occasions loggerheads went to the seafloor. Loggerheads were observed feeding on both pelagic species (lion's mane jellies (*Cyanea capillata*), comb jellies (Ctenophora), and salps (Salpidae) and benthic species (hermit crabs (Paguroidea), rock crabs (*Cancer irroratus*), and Atlantic sea scallops (*Placopecten magellanicus*), even where bottom temperatures reached as low as 7.1°C. The benthic foraging was especially noteworthy in that other prey resources were available in warmer pelagic waters, but loggerheads dove to the bottom to actively feed in temperatures that have been otherwise associated with lethargy and cold stunning (Spotila et al. 1997). They also captured inter- and intra-species interactions. For example, several varieties of fish remained associated with individual turtles for an extended time, even during benthic foraging dives. Additionally, they documented a variety of social interactions between loggerheads that were generally near the ocean surface, such as flapping their flippers with each other, carapace rubbing, nudging, biting, and generally being in close proximity. Overall, using the ROV provided great insight into loggerhead at-sea behavior, otherwise unattainable using previously established techniques.

Patel et al. (2016) quantified the video data from Smolowitz et al. (2015). They revealed that loggerheads tended to remain within the near surface and surface zones of the water column through the majority of the footage. During benthic dives, turtles consistently exhibited negative buoyancy and some turtles exhibited a dichotomous foraging behavior by first foraging within the water column, then diving to the benthic environment. Videography allowed them to combine behavioral observations and habitat features resulting in a broader understanding of loggerheads' ecological role in the U.S. Mid-Atlantic then they could have captured by traditional telemetry methods.

8.3.4.2 Visual Sighting Surveys

During the visual aerial and shipboard abundance surveys conducted under AMAPPS I and II, we detected 13,918 groups of sea turtles, where 47% were positively identified loggerheads and 5.4% positively identified leatherbacks (Table 8-4). Loggerhead turtles were by far the most commonly recorded sea turtle in the abundance surveys, though we detected very few in the Gulf of Maine and offshore of about the 100m depth contour (Figure 8-9). The visual survey data documented the loggerheads coastal migrate northward, where nearly all sightings in the winter (Figure 8-9D) were off the Florida coast, during the spring (Figure 8-9A) they were spread out from Florida to southern Virginia, and in the summer (Figure 8-9B) and fall (Figure 8-9C) they were the most abundant and dispersed from Florida to Massachusetts. After the classification of "undetermined hard-shell turtle", positively identified loggerhead turtles were the second most commonly recorded sea turtle identification in the visual surveys. The seasonal patterns of the sighting followed about the same seasonal migration patterns as the leatherbacks (Figure 8-10). Although during the summer and fall, we recorded more leatherbacks in the Gulf of Maine and off Nova Scotia. Kemp's ridley sea turtles (*Lepidochelys kempii*) were not commonly detected (Figure 8-11). Perhaps this is because they are small and hard to distinguish and/or because their density is truly low in U.S. Atlantic continental shelf waters. We also positively identified green turtles (*Chelonia mydas*) during the visual surveys that displayed similar seasonal migrations along the U.S. continental shelf (Figure 8-12). We detected the most during summer between North Carolina and New York, along the continental shelf. We only positively identified 2 hawksbill sea turtles (*Eretmochelys imbricata*), both south of Cape Hatteras (Figure 8-13). We also have many sea turtle sightings that we could not positively identify to a hardshell turtle species, though we knew the turtle sighting was not a leatherback turtle (Figure 8-14). The plan during AMAPPS III is to estimate abundance that account for perception and visibility bias using techniques similar to that shown in Chapter 6. We also will attempt to fully utilize the unidentified hardshell turtle sightings, as appropriate.

In addition, a cruise on a NOAA vessel that focused on capturing turtles to tag (HB1503-2) collected line-transect data on marine mammals and large fish that can be used in density-habitat models for the marine mammals (AMAPPS 2015 annual report and Chapter 11).

Table 8-4 Numbers of turtle groups and individuals detected visually during AMAPPS I and II
AMAPPS I was in effect during 1 October 2010 to 30 September 2014 and AMAPPS II was in effect in 1 October 2014 to 30 September 2019.

Turtle Species	Number of Groups in AMAPPS I	Number of Groups in AMAPPS II	Number of Individuals in AMAPPS I	Number of Individuals in AMAPPS II
Green	381	193	412	248
Hawksbill	0	3	0	3
Kemp's ridley	85	100	90	111
Leatherback	538	299	584	305
Loggerhead	3,797	2,826	4,485	3,217
Unidentified hardshell	2,968	2,728	3,415	3,518
TOTAL	7,769	6,149	8,986	7,402

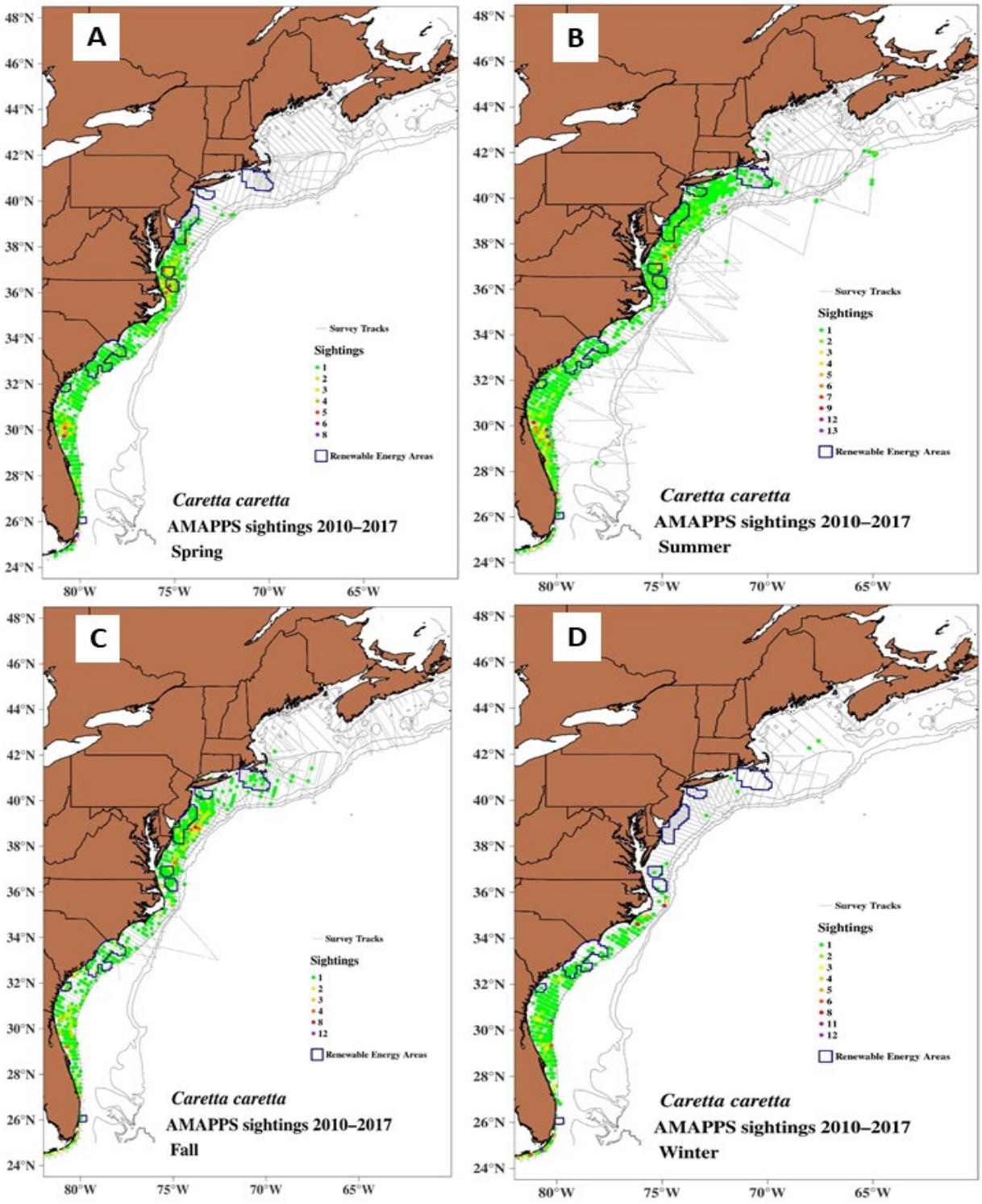

Figure 8-9 Locations of loggerhead turtle sightings collected in visual surveys, by season
Gray lines indicate track lines surveyed during the aerial and shipboard AMAPPS abundance surveys conducted during 2010 to 2017. Colored circles correspond to the sighting's group size. Spring is 1 March to 31 May; summer is 1 June to 31 August; fall is 1 September to 30 November; and winter is 1 December to 28 (29) February.

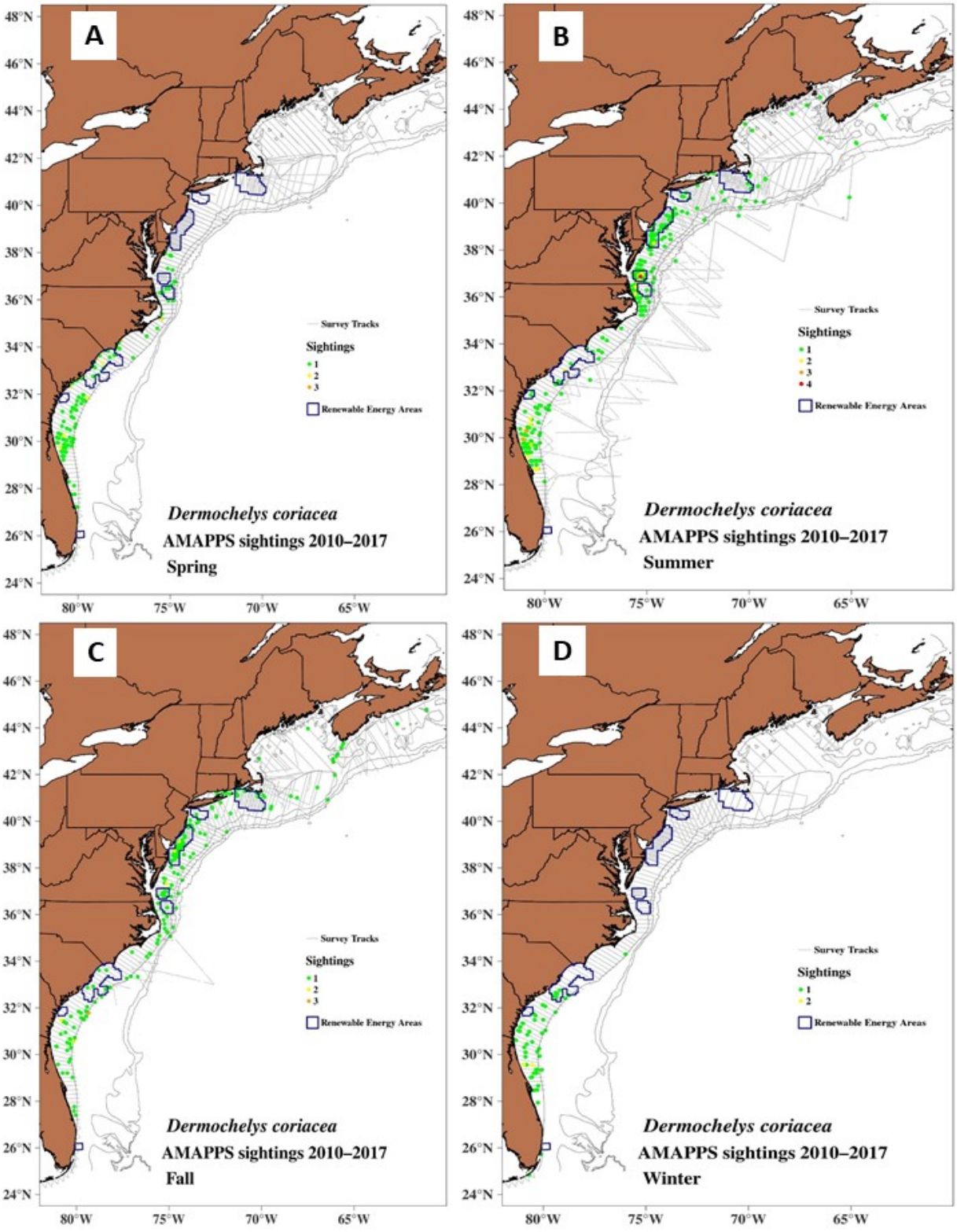

Figure 8-10 Locations of leatherback turtle sightings collected in visual surveys, by season
Gray lines indicate track lines surveyed during the aerial and shipboard AMAPPS abundance surveys conducted during 2010 to 2017. Colored circles correspond to the sighting's group size. Spring is 1 March to 31 May; summer is 1 June to 31 August; fall is 1 September to 30 November; and winter is 1 December to 28 (29) February.

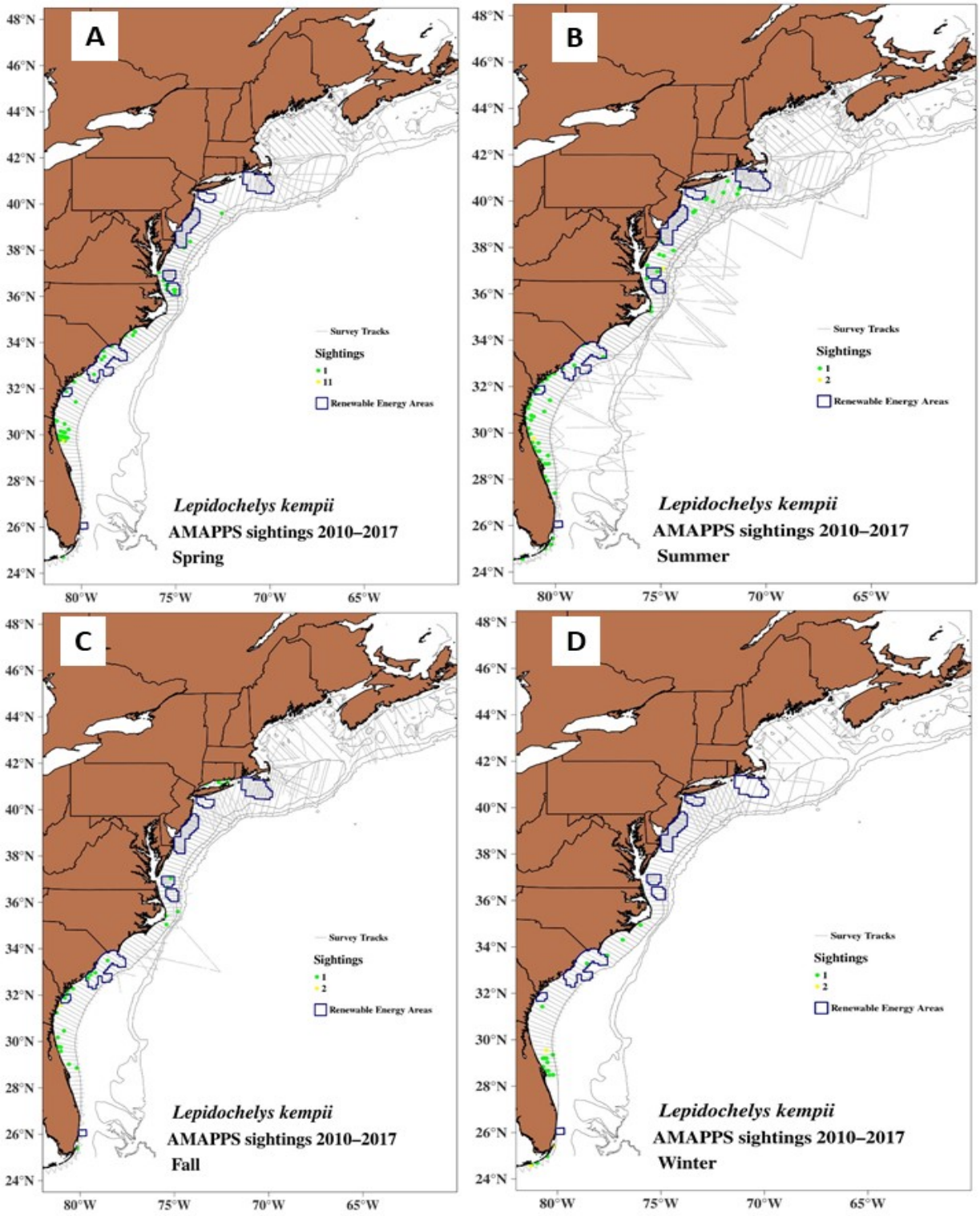

Figure 8-11 Locations of Kemp's ridley turtle sightings collected in visual surveys
Gray lines indicate track lines surveyed during the aerial and shipboard AMAPPS abundance surveys conducted during 2010 to 2017. Colored circles correspond to the sighting's group size. Spring is 1 March to 31 May; summer is 1 June to 31 August; fall is 1 September to 30 November; and winter is 1 December to 28 (29) February.

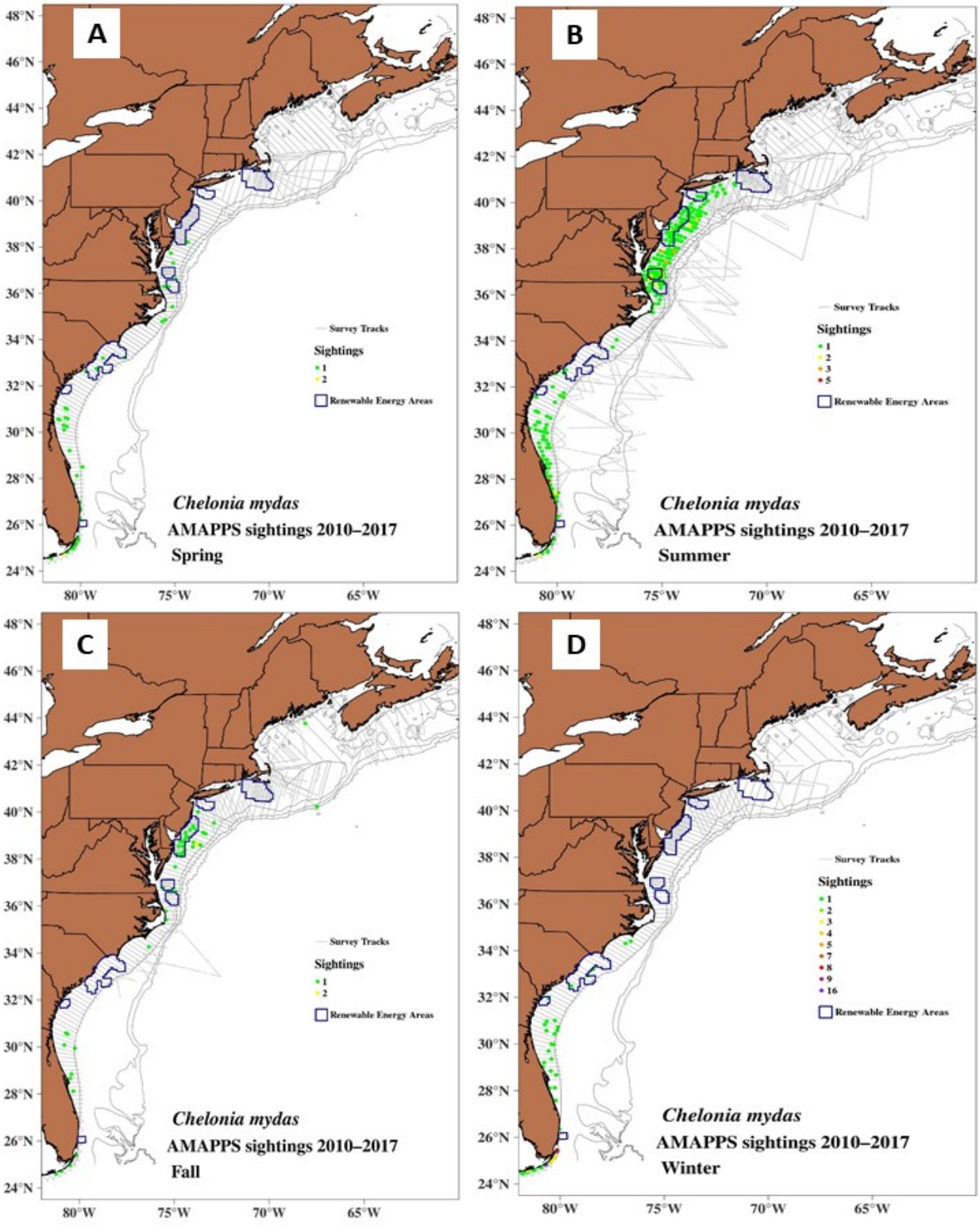

Figure 8-12 Locations of green turtle sightings collected in visual surveys, by season
Gray lines indicate track lines surveyed during the aerial and shipboard AMAPPS abundance surveys conducted during 2010 to 2017. Colored circles correspond to the sighting's group size. Spring is 1 March to 31 May; summer is 1 June to 31 August; fall is 1 September to 30 November; and winter is 1 December to 28 (29) February.

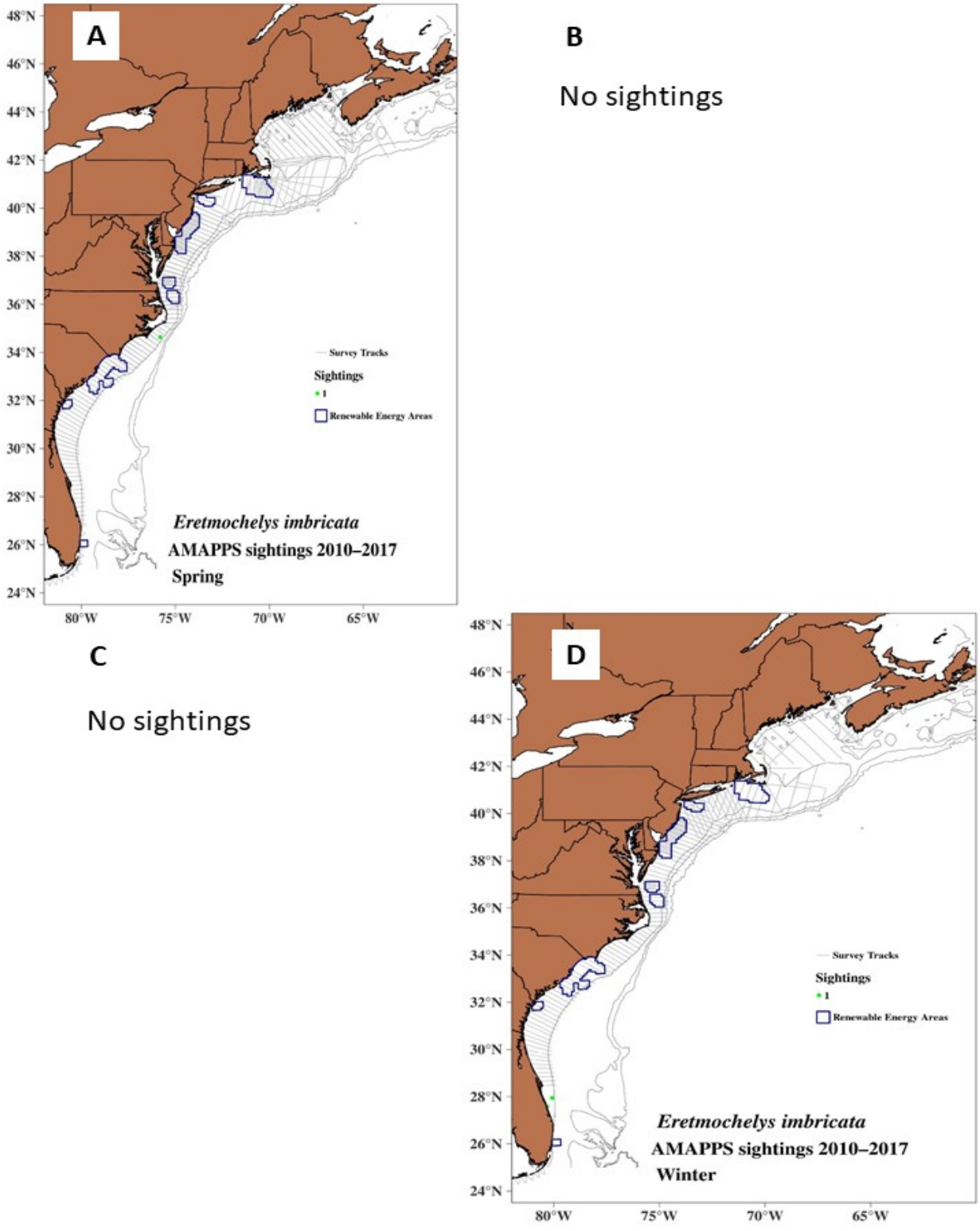

Figure 8-13 Locations of hawksbill turtle sightings collected in visual surveys, by season
Gray lines indicate track lines surveyed during the aerial and shipboard AMAPPS abundance surveys conducted during 2010 to 2017. Colored circles correspond to the sighting's group size. Spring is 1 March to 31 May; summer is 1 June to 31 August; fall is 1 September to 30 November; and winter is 1 December to 28 (29) February.

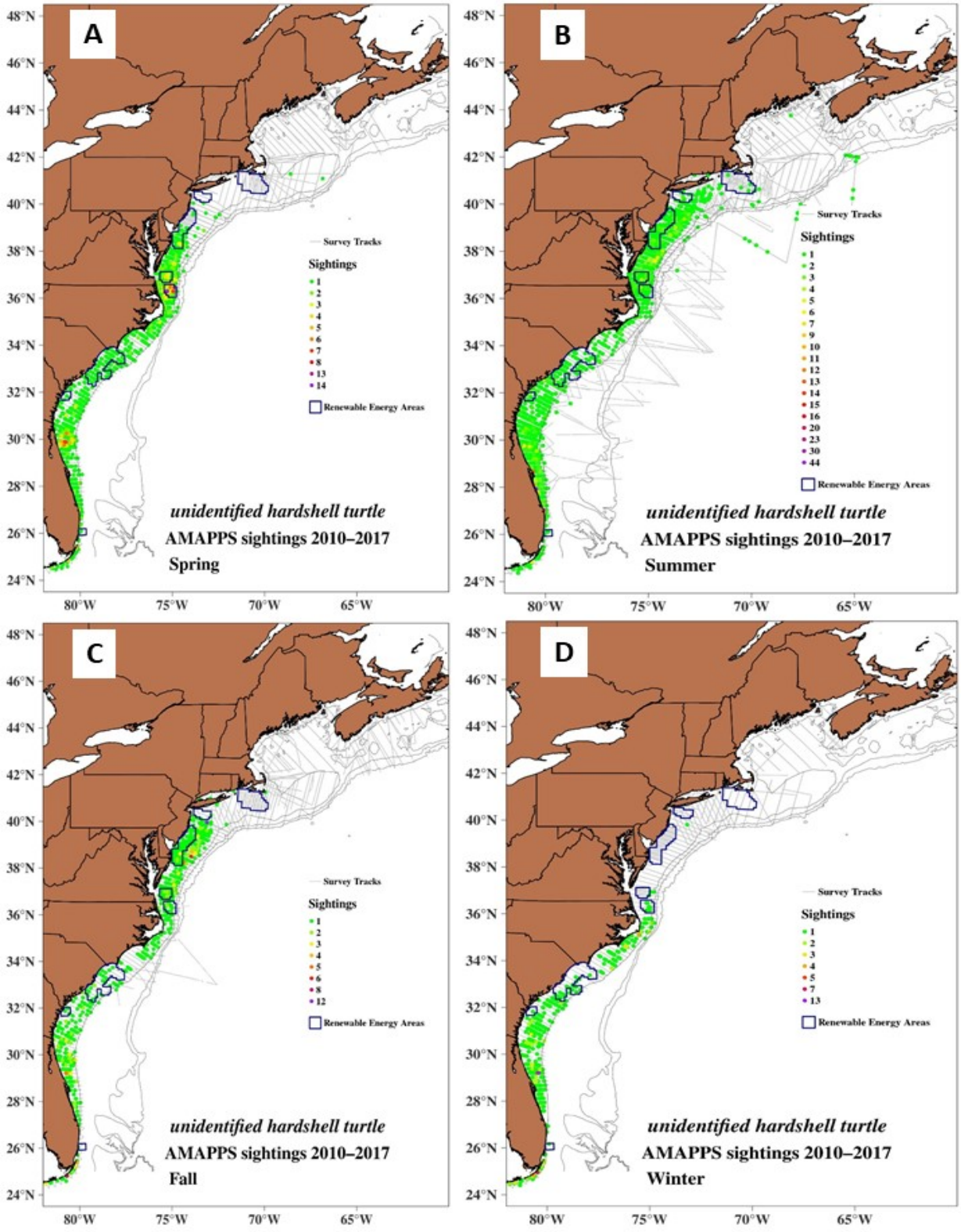

Figure 8-14 Locations of unidentified hardshell turtles collected in visual surveys, by season
Gray lines indicate track lines surveyed during the aerial and shipboard AMAPPS abundance surveys conducted during 2010 to 2017. Colored circles correspond to the sighting's group size. Spring is 1 March to 31 May; summer is 1 June to 31 August; fall is 1 September to 30 November; and winter is 1 December to 28 (29) February.

8.3.5 Biological Studies

Yang et al. (2019) documented significant differences in several blood characteristics between migratory and resident loggerhead turtles (Table 8-5) using the biological data collected during AMAPPS and other collaborative cruises. These differences provided insight into energetic and health status during different behavioral states. They found that temperature correlated significantly with several blood characteristics: lactate, partial pressure of carbon dioxide, sodium, hemoglobin, and lactate dehydrogenase. Their assessment of blood chemistry in healthy loggerhead turtles in the Northwest Atlantic provided a baseline for clinical comparisons with turtles impacted by anthropogenic and environmental threats. This baseline highlighted the importance of identifying unique aspects of biochemical and haematological profiles for sea turtles at the intra-population level.

Table 8-5 Comparison of blood characteristics between migratory and resident loggerheads
Descriptions of the blood characteristics and data from migratory loggerheads are in Yang et al. (2019). Data from resident loggerheads are from Kelly et al. (2015).

Characteristic	Sample size of Migratory Turtles	Migratory Median (Range)	Resident Median (Range)	Holm–Bonferroni adjusted P-value
SCL_NT (cm)		73.7 (54.9–100.8)	63.3 (50.4–85.6)	1.59E–14*
	52	275 (48–1120)	0 (0–1200)[b]	4.84E–15*
ABS AzurosMonos		300 (0–2960)	210 (0–1650)[b]	2.36E–02
	56	494 (0–3390)	300 (0–4800)[b]	2.02E–02
	63	3600 (900–8710)	4700 (0–21 600)[b]	7.44E–02
	64	5770 (240–10 800)	3400 (600–9200)[b]	3.61E–07*
	22	630 (0–2664)	1400 (0–1600)[b]	4.31E–05*
Albumin (g/dl)	61	1.0 (0.5–1.9)	1.1 (0.4–1.7)	1.00E+00
AST (U/l)	61	118 (71–1213)	161.0 (50.0–390.0)	1.43E–05*
BUN (mmol/l)	12	9.0 (3.1–16.2)	23.6 (6.1–67.8)	3.61E–06*
Ca (mg/dl)	61	7.4 (5.4–12.0)	7.6 (5.2–11.6)	1.00E+00
CK (U/l)	61	928 (285–2759)	1034.0 (153.0–13310.0)	1.00E+00
Cl (mmol/l)	12	105 (96–113)	115.0 (101.0–129.0)	5.52E–05*
Globulin (g/dl)	61	2.9 (1.7–4.6)	2.4 (1.3–4.6)[a]	1.65E–07*
Glucose (mg/dl)	55	74 (47–332)	104 (45.233)	8.71E–13*
K (mg/dl)	55	3.4 (2.6–4.8)	4.2 (2.5–6.1)	4.91E–12*
Na (mEq/l)	55	147 (136–163)	156.0 (145.0–168.0)	4.84E–15*
P (mg/dl)	61	5.4 (2.9–10.6)	6.8 (3.7–11.1)[a]	4.00E–09*
PCV (%)	54	37 (28–68)	31.0 (9.0–40.0)[b]	6.86E–15*
Total protein (g/dl)	61	3.9 (2.4–5.9)	3.5 (2.1–6.0)[a]	5.37E–04*
UA (mg/dl)	61	1.3 (0–3.3)	0.8 (0.1–2.8)[a]	1.53E–04*
WBC (THOUS.)	64	11.7 (3.5–15.0)	9.0 (2.0–27.0)[b]	1.59E–01

a Values from Kelly et al. (2015) that we converted to the units used in Yang et al. (2019)

b Resident turtle characteristics with 190 samples, in contrast to other resident turtle characteristics with 191 samples

8.3.6 Monitoring Metrics

Warden et al. (2017) used estimates of availability from satellite tags together with a simulation approach to evaluate nest counts and line-transect aerial surveys as loggerhead sea turtle population monitoring metrics. Over long timeframes, they found both the nest counts and in-water aerial survey monitoring

rate estimated from simulated adult equivalents). Over shorter timeframes, total adult females estimated from simulated nest counts generally tracked closer to adult equivalents than did abundance estimated

relative error. They showed that aerial surveys benefitted as a monitoring metric if population impacts affected young turtles (which can take 20 to 30 yrs to become nesters) or if impacts changed the structure of the population (e.g. changed the stable age distribution). They concluded that for effective monitoring over short timeframes we need both monitoring schemes.

8.4 Key Findings

Through AMAPPS and collaborative efforts, we deployed over 300+ satellite tags that collected data on location, surface availability, and behavior throughout the water column. Tagged turtles dispersed broadly throughout the AMAPPS study area, with extensive coverage in the wind energy areas, and dispersed coverage ranging from the Gulf of Mexico to the Mid-Atlantic Ridge (30°W).

Through AMAPPS and collaborative efforts, we collected more than just satellite tag data. Most deployed tags also collected temperature data, which can provide additional insights into turtle ecology. By closely examining and sampling individual turtles, we have collected data on animal size, health, physiology, sex, and forage. We can use these additional data sources to examine the connections between turtles and their physical environment and to assess behavior and habitat usage. As described in the AMAPPS III Interagency Agreement, life history and ecological information is important for assessing vulnerability to various human activities, and knowing why species are doing what they are doing can be helpful in understanding impacts of future development.

We designed Winton et al. (2018) as a core AMAPPS product. This paper made a methodological contribution to the process of estimating space utilization distributions from satellite telemetry data. Data contributions from outside of AMAPPS substantially increased the sample size. The resulting maps of the distribution of tagged loggerheads represent the first AMAPPS animal distribution maps published and are available in Winston et al. (2018). The shape files are available to download at sea turtle ecology and population dynamics in the Northeast website. We intended these maps to serve as input into several upcoming projects. This paper is also noteworthy in that it questions whether the Mid-Atlantic foraging ground is more important to the broader western North Atlantic loggerhead population than previously thought. That is, the preliminary analysis (NEFSC and SEFSC 2011) estimated only 5% of the surveyed loggerhead population occurred north of Cape Hatteras from June to September. In contrast, Winton et al. (2018) suggest that the Mid-Atlantic foraging grounds may support a larger proportion of the population, with over 50% of the predicted relative density of tagged loggerheads occurring north of Cape Hatteras from June to October.

Patel et al. (2018) documented that loggerhead habitat in the Mid-Atlantic included a highly stratified water column, an oceanographic situation that may be unique among loggerhead habitats in the Northwest Atlantic Ocean. The paper also documented the importance of continuing rigorous *in situ* sampling because current methods for determining temperature in this region lack appropriate small-scale resolution. This has consequences for the accuracy of density-habitat estimates based on modelled ocean temperature data.

Although foraging ecology was not our primary focus in AMAPPS II, we did collect data that can improve our understanding of foraging, particularly in the Mid-Atlantic. We collected stable isotope samples, which are available for later analysis. ROV and animal-borne cameras give us insight to prey availability as well as foraging selection. They have the potential to show trophic levels and broad-scale foraging patterns as well as availability of forage species and selection of prey. Smolowitz et al. (2015) pioneered a new way to study *in situ* turtle behavior, videotaping from ROVs. These new observations added to our knowledge of loggerheads in the offshore Mid-Atlantic shelf waters where foraging behavior has been largely undocumented. The documentation of cold-water benthic foraging added a new layer to our knowledge of habitat use on the Mid-Atlantic shelf, an area with plans for extensive wind development.

Despite widespread reliance on ethograms as scientific tools to summarize animal behavior, challenges associated with observing *in situ* sea turtle behavior had previously prevented this research in the Mid-Atlantic shelf region. Patel et al. (2016) provided the first ethogram of loggerhead behavior in the Mid-Atlantic Shelf region, a globally important loggerhead foraging ground. Our quantification of time spent at the surface, in the water column, and on the sea floor combined with data on prey's availability and consumption provided better understanding of habitat use than is possible with satellite telemetry alone. Foraging on gelatinous prey only occurred near surface or within the water column with an approximate depth range from 1 to 16 meters and a median depth of about 4 meters. In the companion paper, Smolowitz et al. (2015) examined the prey species and identified both pelagic and benthic prey. Pelagic prey included Lion's mane jellies (*Cyanea capillata*), comb jellies (*Ctenophora*) and salps (*Salpidae*), while benthic prey included hermit crabs (*Paguroidea*), rock crabs (*Cancer irroratus*), and Atlantic sea scallops (*Placopecten magellanicus*). Telemetry studies typically group turtles into benthic versus pelagic foragers based on the dive behavior and location; however, we identified turtles exhibiting both behaviors in sequential dives. Thus, loggerheads may have a higher level of diversity in their foraging approaches than typically recognized. Increasing our knowledge of "baseline" turtle behavior can help us better monitor future changes, including changes associated with development.

Yang et al. (2019) established baseline blood biochemistry and haematology profiles in the form of reference intervals for offshore migrating loggerheads, a first. The high metabolic demands of migration affect turtle physiology, and it is widely recognized that specific reference intervals are necessary to account for unique habitats and differences in behavior. As several blood variables differed between migratory and residential loggerhead turtles, the relevance of assessing this population during all its behavioral states is of great importance, particularly if scientists will use blood variables for assessing physiological impacts of anthropogenic disturbances. By using reference intervals to provide a physiological basis for the behavioral state of migratory loggerhead turtles at present, clinicians, and managers can make more confident conservation decisions in the future based on preserving the physiological migratory phenotypes currently expressed.

By using loggerhead tag and line-transect data and simulations, Warden et al. (2017) concluded that for effective monitoring over short timeframes we need to continue both beach nest counts and in-water aerial line-transect surveys as monitoring schemes.

8.5 Data Gaps and Future Work

The magnitude of deployed satellite tags, the extensive spatial coverage, and the consistency of deployments across this last decade combined to produce a powerful time series of data for loggerhead sea turtles. This dataset can serve as a baseline against which to measure future changes in turtle distribution and behavior in AMAPPS' areas of interest. Because we expect climate driven changes in turtle distribution and behavior, deploying additional tags during AMAPPS III will be an important step in the collection of baseline data to support analysis of impacts of future development.

We end AMAPPS II with drastically different magnitudes of data for leatherbacks and loggerheads. The leatherback program climbed the learning curve during AMAPPS II. We now have a cost- effective capture method in place at study sites where turtles are likely to occupy high interest shelf waters, and we have collaborations and technology in place to extend our research into the ecological underpinnings of behavior patterns. However, we do not have a large sample size in place yet. With leatherback satellite tagging sample sizes in the few dozen, we can begin to see the normal patterns for this group of sea turtles, but we fall short of being able to robustly define population parameters (Sequeira et al. 2019). As such, we will try to deploy more satellite tags before undertaking substantial data analysis. The loggerhead-tagging program, in contrast, is fully developed. We have had the program in place for long enough that we have amassed a substantial dataset. Loggerhead sample sizes number in the few hundreds, stretched over more than a decade. With this dataset, we can pursue more synthetic analyses and we can begin to look for temporal and spatial patterns (Sequeira et al. 2019).

During AMAPPS III, we plan to continue Turtle Ecology research in accordance with guidelines developed with Desray Reeb and Kyle Baker during AMAPPS III planning. We understand our species focus for AMAPPS III should be to continue but shrink the loggerhead-tagging program from North Carolina northwards, to increase the amount of leatherback research, and to generally avoid or do only minimal pilot work on other sea turtle species. In terms of field tools, we understand our focus should be on satellite telemetry to provide behavior data that spans large areas and timeframes. We understand that a strong secondary goal should be to obtain high-resolution data from short-term archival tags. Information from animal samples is still a goal; however, this should be a minor element. We had been hoping to perform laparoscopies to determine sex while aboard the NOAA ship *Gordon Gunter*, but we had to cancel the cruise due to the pandemic. The development or refinement of acoustic tags and acoustic trials are outside of the scope of AMAPPS III, but partnerships to advance these components are appropriate. Overall, as compared to work conducted under AMAPPS I and II, work conducted by the Turtle Ecology program under AMAPPS III should have a higher investment in database development and analysis.

We enter AMAPPS III with 4 loggerhead analysis projects well underway, and others starting to percolate. First, we have assembled and begun to analyze loggerhead behavior data in order to estimate the complex patterns of survey availability. In association with other funded projects, we have also begun an effort to estimate the projected shifts in loggerhead habitat in the Northwest Atlantic Ocean due to climate change. Also in association with other funded projects, we have a project underway that evaluates the overlap of federally authorized activities (scallop fishing effort) and loggerhead turtle distribution in space and time. A fourth well-developed project we bring into AMAPPS III is an investigation of loggerhead behavior during an oceanographic disturbance (Hurricane Irene). During AMAPPS III, we also anticipate using the substantial loggerhead database to explore environmental drivers of turtle behavior. With a decade of data in hand, we will have a new ability to examine trends in behavior over time. We are particularly interested in loggerhead use of the Mid-Atlantic and southern New England areas because we expect that loggerhead distribution will be changing with rapidly changing ocean conditions in these areas. We hope the continued sampling during AMAPPS III will allow the research topic to extend into the future and expand to other sea turtle species.

8.6 Acknowledgements

Additional funding for tags and biological sampling was provided by the National Marine Fisheries Service (award numbers: NA03NMF4720281, NA08NMF4720502, and NA13NMF4720182), the Bycatch Reduction and Engineering Program (award number: NA17NMF4720268) and the Sea Scallop Research Set-Aside program (award numbers: NA15NMF4540055, NA16NMF4540037, NA17NMFGC0031, NA18NMF4540011, NA19NMF4540015). Funding for additional data analyses was provided by the Saltonstall-Kennedy Grant Program (award numbers: NA18NMF4270190,

NA18NMF4270185) The authors thank J. Gutowski, Captain M. Francis and Captain C. Karch of Viking Village Fisheries as well as the Captain the crew of the R/V Henry Bigelow. We also thank the many individuals who have assisted with the small boat operations and tagging portions of this project, especially L. Crowe, E. Matzen, L. Conger, J. Hatch, M. James, G. Breen, L. Seimann, R. Smolowitz, A. Gorgone, L. Avens, M. Judge, J. McNeill, B. Price, J. Clark, and J. Summers. Finally, we want to acknowledge the contributions of L. Crowe, R. Rogers, and K. Choate in developing and documenting a database that makes the data more accessible for use.

8.7 References Cited

Albertsen CM, Whoriskey K, Yurkowski D, Nielsen A, Fleming JM. 2015. Fast fitting of non-Gaussian state-space models to animal movement data via Template Model Builder. Ecology 96(10):2598-2604.

Douglas DC, Weinzierl R, Davidson SC, Kays R, Wikelski M, Bohrer G. 2012. Moderating Argos location errors in animal tracking data. Methods Ecol. Evol. 3:999-1007.

Johnson DS, London JM, Lea MA, Durban JW. 2008. Continuous-time correlated random walk model for animal telemetry data. Ecology 89(5):1208-1215.

Hatch JM, Haas HL, Sasso CR, Patel SH, Smolowitz RJ. (in review). Estimating the complex patterns of survey availability for a highly mobile marine animal.

Kelly TR, McNeill JB, Avens L, Hall AG, Goshe LR, Hohn AA, Godfrey MH, Mihnovets AN, Cluse WM, Harms CA. 2015. Clinical pathology reference intervals for an in-water population of juvenile loggerhead sea turtles (*Caretta caretta*) in Core Sound, North Carolina, USA. PLOS ONE 10:e0115739.

Northeast Fisheries Science Center and Southeast Fisheries Science Center (NEFSC and SEFSC). 2011. Preliminary summer 2010 regional abundance estimate of loggerhead turtles (*Caretta caretta*) in northwestern Atlantic Ocean continental shelf waters. US Dept Commer, Northeast Fish Sci Cent Ref Doc. 11-03; 33 pp.

Patel SH, Dodge KL, Haas HL, Smolowitz RJ. 2016. Videography reveals in-water behavior of loggerhead turtles (*Caretta caretta*) at a foraging ground. Front Mar. Sci. 3:254.

Patel SH, Barco SG, Crowe LM, Manning JP, Matzen E, Smolowitz RJ, Haas HL. 2018. Loggerhead turtles are good ocean-observers in stratified mid-latitude regions. Estuar. Coast Shelf Sci. 213:128-136.

Sequeira AMM, Heupel MR, Lea MA, Eguíluz VM, Duarte CM, Meekan MG, Thums M, Calich HJ, Carmichael RH, Costa DP, Ferreira LC. 2019. The importance of sample size in marine megafauna tagging studies. Ecol. Appl. 29(6):e01947.

Smolowitz RJ, Patel SH, Haas HL, Miller S. 2015. Using a remotely operated vehicle (ROV) to observe loggerhead sea turtle (*Caretta caretta*) behavior on foraging grounds off the mid-Atlantic United States. J. Exp. Mar. Biol. Ecol. 471:84-91.

Warden ML, Haas HL, Richards PM, Rose KA, Hatch JM. 2017. Monitoring trends in sea turtle populations: walk or fly? Endang. Species Res. 34:323-337.

Whiting AU, Chaloupka M, Pilcher N, Basintal P, Limpus CJ. 2014. Comparison and review of models describing sea turtle nesting abundance. Mar. Ecol. Prog. Ser. .

Wiebe PH, Harris RP, Werner FE, Young BD. 2009. BASIN: Basin-scale analysis, synthesis, and integration. Science plan and implementation strategy. GLOBEC Report 27. Plymouth, UK.

Winton M, Fay G, Haas HL, Arendt M, Barco S, James MC, Sasso C, Smolowitz R. 2018. Estimating the distribution and relative density of satellite-tagged loggerhead sea turtles in the western North Atlantic using geostatistical mixed effects models. Mar. Ecol. Prog. Ser. 586:217-232.

Yang T, Haas HL, Patel SH, Smolowitz R, James MC, Williard A. 2019. Blood biochemistry and hematology of migrating loggerhead turtles (*Caretta caretta*) in the Northwest Atlantic: reference intervals and intrapopulation comparisons. Conserv. Physiol. 7(1):coy079.

9 Seabird Research

Primary authors: Harvey Walsh and Elizabeth Josephson

9.1 Introduction

The Oceans and Climate Branch of the Northeast Fisheries Science Center (NEFSC) conducts Ecosystem Monitoring (EcoMon) cruises to collect broad-scale data that aims to index the seasonal to decadal changes in ecosystem condition by sampling the full Northeast Atlantic U.S. shelf in every season. We conducted oceanographic and plankton sampling on full-shelf surveys, with measurements focused on the chemical, physical, and biological properties of the water column. Since 2017, we also conducted comprehensive visual surveys of seabirds, marine mammals, turtles, large pelagic fish, and marine debris on EcoMon research cruises under the Atlantic Marine Assessment Program for Protected Species (AMAPPS). This builds on other AMAPPS projects that collected seabird visual survey data on other AMAPPS shipboard cruises. Collecting seabird and marine mammal data in conjunction with other biotic and abiotic data that we collected concurrently will help to understand the spatiotemporal distributions of the species and relationships with other trophic levels within the changing marine ecosystem. In addition, we provided the data collected during the AMAPPS projects to other researchers such as, those who explored modeling efforts to map the distribution of seabirds (Winship et al. 2018) and to understand habitat usage (Veit et al. 2015; White and Veit 2020).

In this chapter, we describe the distribution of seabird data collected during 2011 to 2019, which addresses aspects of 3 of the 7 AMAPPS objectives (taken from the complete list of objectives in Chapter 3):

1) Collect broad-scale data over multiple years on the seasonal distribution and abundance of marine mammals (cetaceans and pinnipeds), marine turtles, and seabirds using fixed passive acoustic monitoring and direct aerial and shipboard surveys of coastal U.S. Atlantic Ocean waters;
2) Collect similar data at finer scales at several sites of interest to BOEM, NOAA, and partners using visual and acoustic survey techniques;
6) Assess the population size of surveyed species at regional scales; and develop models and associated tools to translate these survey data into seasonal, spatially explicit density estimates incorporating habitat characteristics.

9.2 Methods

9.2.1 Data Collection

The data collection protocol was based on a standardized 300 m strip transect methodology, like that used by various agencies in North America and Europe (Tasker et al. 1984; Anonymous 2011; Ballance 2011) including previous AMAPPS and Bureau of Ocean Energy Management (BOEM) surveys. Observers collected data on all seabirds within a 300 m strip on 1 side of the ship's track line. Observers searched from the bow to 90° to either the port or the starboard side, depending on which side had the best viewing conditions. Observers conducted surveys on the flying bridge of the ship, whenever possible. They collected data in sea states up to a Beaufort 7, in light rain, fog, and when ship speeds were between 8 and 12 kts (below 8 kts, the data becomes questionable to use for abundance estimates).

Beginning in 2018, observers used a new SeaScribe program (BRI 2020) for data entry. The SeaScribe app draws GPS coordinates, as well as time from a GPS device via Bluetooth, so each observation received data on the latitude-longitude position, time stamp, and ship's course. The standard data collected for observations included species identification, distance between the ship and the animal, number of

individuals, association, behavior, flight direction, flight height, and if possible or applicable, age, sex, and plumage status. While the designers of SeaScribe did not intend the application to collect data on other marine megafauna, observers also recorded other species that were both inside and outside of the 300 m strip survey zone.

On some surveys, SeaScribe was not able to update the sighting positions continuously because of issues with the location services/GPS positioning capabilities of the tablet device running the program. In these cases, observers recorded data using the SeeBird (version 4.3.7) data entry program from previous years. The data collected on SeeBird were similar to that described above for the SeaScribe data entry program.

During surveys, the on-effort observer utilized binoculars (10 x 42) to scan within the survey strip. When there were two observers onboard, they alternated 2-hr shifts, with a person on-effort collecting data and the other off-effort (not collecting data). If an animal proved elusive, observers used a pair of 20 x 60 Zeiss imaged-stabilized binoculars to attain positive identifications. To aide in approximating distance observers used custom-made range finders based on height above water and the observers' personal body measurement (Heinemann 1981).

9.2.2 Data Summary

We summarized bird sighting data to the lowest taxonomic identification level (henceforth referred to as species) and higher classification levels. Species distribution maps were plotted for the classification levels: Alcids, Gannet and Boobies, Gulls, Loons, Petrels, Shearwaters, Skuas, and Storm-petrels for cruises conducted by the NEFSC from 2011 to 2019. For each higher classification and species, we calculated the percent frequency of occurrence for the cruises conducted during 2017 to 2019 as the number of cruises with a positive sighting divided by the total number of cruises, which was then multiplying by 100. In addition, for each classification or species, we calculated the relative proportion of all birds counted on a cruise as the number sighted divided by the total number of birds counted, which was then multiplying by 100. Finally, we averaged the relative proportion of each higher classification and species across all cruises (2017 to 2019) analysed and sampling season: spring, summer, and fall, where the seasons are as follows:

spring (1 March to 31 May)
summer (1 June to 31 August)
fall (1 September to 30 November).

9.3 Results

NEFSC began collecting seabird visual survey data in 2011. During 2011 to 2016, NEFSC collected seabird visual data on 6 AMAPPS surveys that focused on abundance data, sei whales (*Balaenoptera borealis*), and beaked whales (Ziphiidae; Table 9-1). More information on these cruises is in Chapter 11. Placing observers on Oceans and Climate Branch EcoMon cruises and other opportunistic surveys as part of the AMAPPS II seabird project began in spring 2017. During 2017 to 2019, we deployed observer teams on 14 of 17 cruises (Table 9-1). Nine of these cruises were part of the EcoMon project; 3 cruises were in collaboration with NEFSC during NOAA ship transits between ports; and two cruises were part of a "Shelfbreak frontal dynamics: mechanisms of upwelling, net community production, and ecological implications" project led by the Woods Hole Oceanographic Institution and funded by the National Science Foundation (Table 9-1). In collaboration with the AMAPPS seabird project, visual seabird observers collected data on 3 beaked whale surveys in 2017 to 2018 using similar data collection protocols (Table 9-1).

9.3.1 Effort

Since 2011, observers logged over 45,000 km of visual survey effort in over 357 days-at-sea in waters from the Gulf of Mexico to the Gulf of Maine on NEFSC surveys (Table 9-1; Figure 9-1A). The greatest spatial coverage occurred during the summer when surveys covered both the Northeast Atlantic U.S. shelf (NEUS Shelf) and Southeast Atlantic U.S. shelf (SEUS Shelf) and adjacent offshore waters (Figure 9-1C). Coverage during the spring and fall occurred mainly on the NEUS Shelf (Figure 9-1B, D).

Since the AMAPPS II seabird project started in 2017, 188 days-at-sea and more than 25,000 km of visual survey effort has been logged (Table 9-1) Sampling occurred primarily over the NEUS Shelf and adjacent offshore waters.

9.3.2 Overall Seabird Sightings

Counts of seabirds within the survey zone totalled 23,116 on NEFSC surveys since 2011, and almost 14,000 counted since 2017 (Table 9-1). Observers counted 184 species of seabirds on cruises from 2017 to 2019 (Table 9-2). When looking at higher classification levels, Land birds and Shorebirds had the largest numbers of species: 58 and 27, respectively (Table 9-2). At least 1 species of Shearwater, Storm-petrel, and Skua were counted on all cruises (Table 9-2). Shearwaters and Storm-petrels totalled 48% of the mean cumulative relative proportion of sightings (Table 9-2). During the spring, Fulmars, Shearwaters, and Storm-petrels had the highest relative proportion of sightings (Table 9-2). Summer sightings were dominated by Shearwaters and Storm-petrels (Table 9-2). In the fall, Gannets, Shearwaters, and Storm-petrels had the highest relative proportion of sightings in fall (Table 9-2).

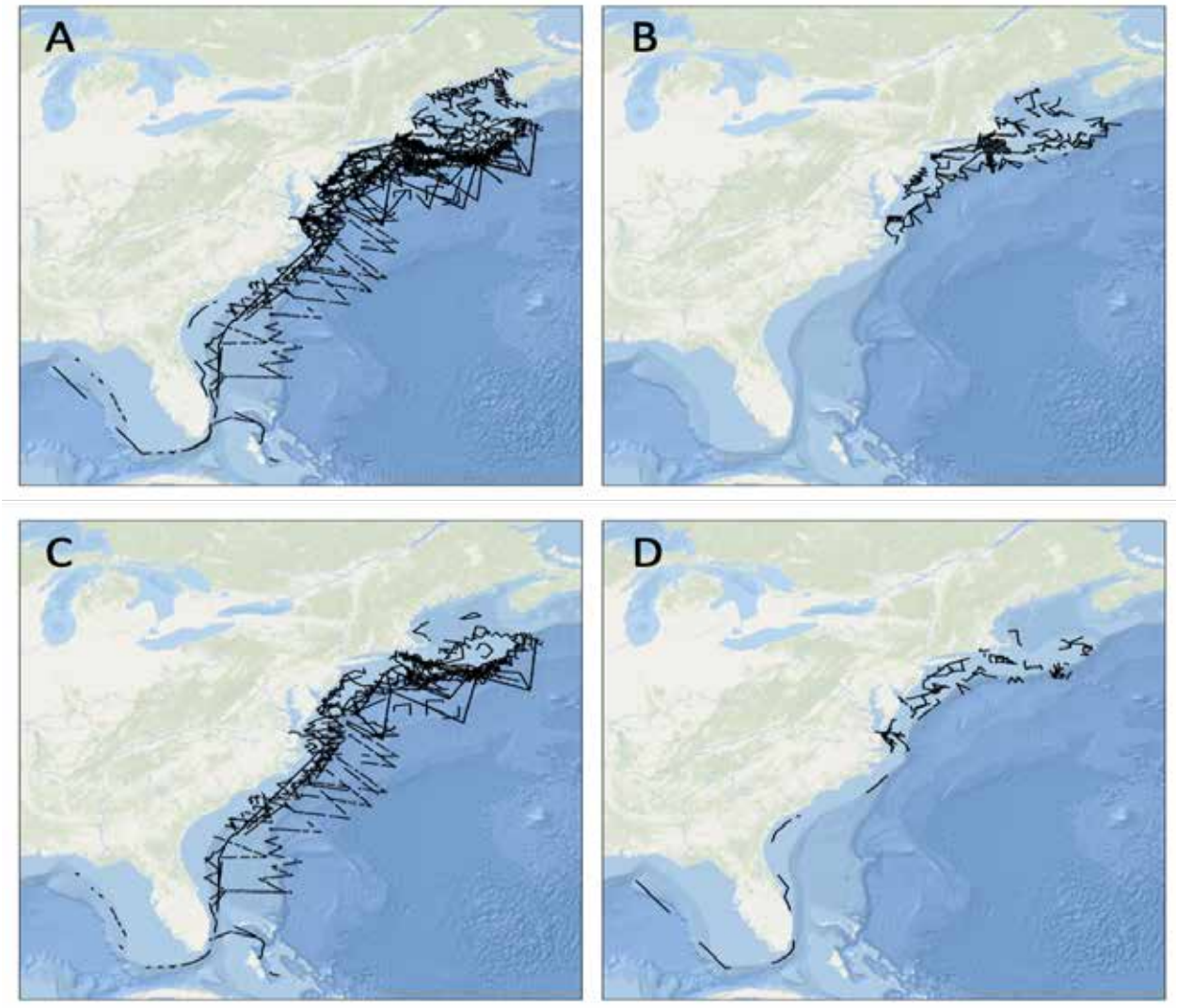

Figure 9-1 Visual survey lines of NEFSC cruises on which seabird observations were made
During 2011 to 2019 for all season (A), spring (B), summer (C) and fall (D). Spring is 1 March to 31 May; summer is 1 June to 31 August; and fall is 1 September to 30 November.

Table 9-1 NEFSC surveys since 2011 with seabird visual survey effort

Trip Identifier[1]	Year	Purpose	Start Date	End Date	Days with Sighting Effort	Visual Survey On-Effort (km)	Number Bird Sightings in Zone
HB1103	2011	shipboard abundance survey	2-Jun	1-Aug	40	4,973	1,135
HB1303	2013	shipboard abundance survey	2-Jul	18-Aug	38	5,021	2,207
GU1402	2014	shipboard abundance survey	12-Mar	27-Apr	33	4,014	2,493
HB1403	2014	beaked whale survey	25-Jul	30-Jul	5	740	336
HB1503-1	2015	sei whale survey	10-Jun	19-Jun	8	1,228	937
HB1603	2016	shipboard abundance survey	28-Jun	24-Aug	45	5,203	2,031
GU1701	2017	ecosystem monitoring	16-May	6-Jun	18	2,923	1,773
GU1702	2017	ecosystem monitoring	10-Jun	22-Jun	13	1,856	1,177
HRS1701	2017	beaked whale survey	8-Sep	17-Sep	10		255
GU1706	2017	ecosystem monitoring	31-Oct	9-Nov	10	1,083	861
HB1803	2018	ecosystem monitoring	23-May	4-Jun	13	2,214	1,516
GU18TN	2018	NOAA ship transit	11-Jul	16-Jul	6	1,213	371
GU1803	2018	beaked whale survey	21-Jul	1-Aug	13		522
HB18TN	2018	NOAA ship transit	1-Aug	6-Aug	6	1,213	485
GU1804	2018	ecosystem monitoring	22-Aug	30-Aug	9	1,537	636
GU18TS	2018	NOAA ship transit	2-Sep	9-Sep	8	1,216	327
HS1801	2018	ecosystem monitoring	1-Nov	12-Nov	10	1,099	1,282
RB1904	2019	WHOI/NSF[2]	13-May	24-May	11	2,422	202
HB1902	2019	ecosystem monitoring	24-May	5-Jun	13	2,614	1,510
TN368	2019	WHOI/NSF[2]	6-Jul	17-Jul	12	814	155
GU1902	2019	ecosystem monitoring	15-Aug	29-Aug	14	2,334	1,364
HRS1910	2019	beaked whale survey	18-Aug	27-Aug	8	580	441
GU1905	2019	ecosystem monitoring	15-Oct	30-Oct	14	1,675	1,100
TOTAL					357	45,972	23,116

[1] First couple letters of trip identifier indicated the ship. HB = NOAA ship ; GU = NOAA ship ; HRS = R/V ; TN = R/V ; RB =NOAA ship .

[2]WHOI/NSF = Woods Hole Oceanographic Institution/National Science Foundation

Table 9-2 Summary of birds at a higher classification level on NEFSC cruises during 2017 to 2019
Number of species (n), percent frequency of occurrence (% FO), and mean relative proportion of total birds counted on all cruises and seasonally (spring, summer, and fall) sorted from highest to lowest mean overall relative proportion.

Higher Classification	n	% FO	All	Spring	Summer	Fall
Shearwater	9	100	3.819	3.57	5.29	2.01
Storm-petrel	7	100	3.308	2.91	4.70	1.77
Fulmar	1	41	2.107	5.76	0	1.40
Gannet	5	82	1.516	0.70	0.19	4.18
Gull	10	88	0.788	0.72	0.31	1.52
Petrel	3	65	0.585	0.01	1.36	0.07
Tern	15	82	0.439	0.36	0.44	0.51
Duck	10	47	0.346	0.30	0	0.87
Kittiwake	1	29	0.291	0.02	0	0.97
Shorebird	27	94	0.274	0.70	0.07	0.14
Pelican	1	35	0.238	0	0.30	0.38
Booby	2	53	0.226	0.07	0.15	0.50
Loon	3	35	0.173	0.29	0.00	0.30
Skua	7	100	0.172	0.14	0.14	0.25
Noddy	1	18	0.126	0	0.26	0.06
Raptor	3	53	0.106	0.03	0.01	0.32
Heron	3	29	0.044	0.00	0	0.14
Alcid	8	53	0.043	0.10	0.00	0.04
Land Bird	58	88	0.033	0.01	0.02	0.08
Egret	4	12	0.023	0	0	0.08
Tropicbird	2	24	0.023	0	0.06	0
Skimmer	2	12	0.011	0.01	0.02	0
Goose	1	6	0.005	0	0	0.02
Grebe	1	6	0.005	0	0	0.02

9.3.3 Species Distribution Maps

We shared the seabird data collected on AMAPPS by NMFS (2011 to 2015) and FWS (2010 to 2014) with NOAA National Centers for Coastal Ocean Science Biogeography Branch. They used the AMAPPS survey data, in addition to about 80 other surveys spanning 4 decades to model the Atlantic at-sea density of marine birds (Winship et al. 2018). See section 9.3.5 for a brief summary of this work.

The following sections provide an update on seabird distribution information by focusing on recently collected data, 2017 to 2019.

9.3.3.1 Alcids

Observers detected 8 species of Alcids on NEFSC cruises from 2011 to 2019 (Figure 9-2), mostly in the spring. Atlantic Puffin, Dovekie, Razorbill had the highest relative proportion of sightings among the Alcids from 2017 to 2019 (Table 9-3). Atlantic Puffin and Dovekie were along the continental shelf-break of the NEUS Shelf and on Georges Bank, while Razorbills were over the NEUS Shelf waters (Figure 9-2).

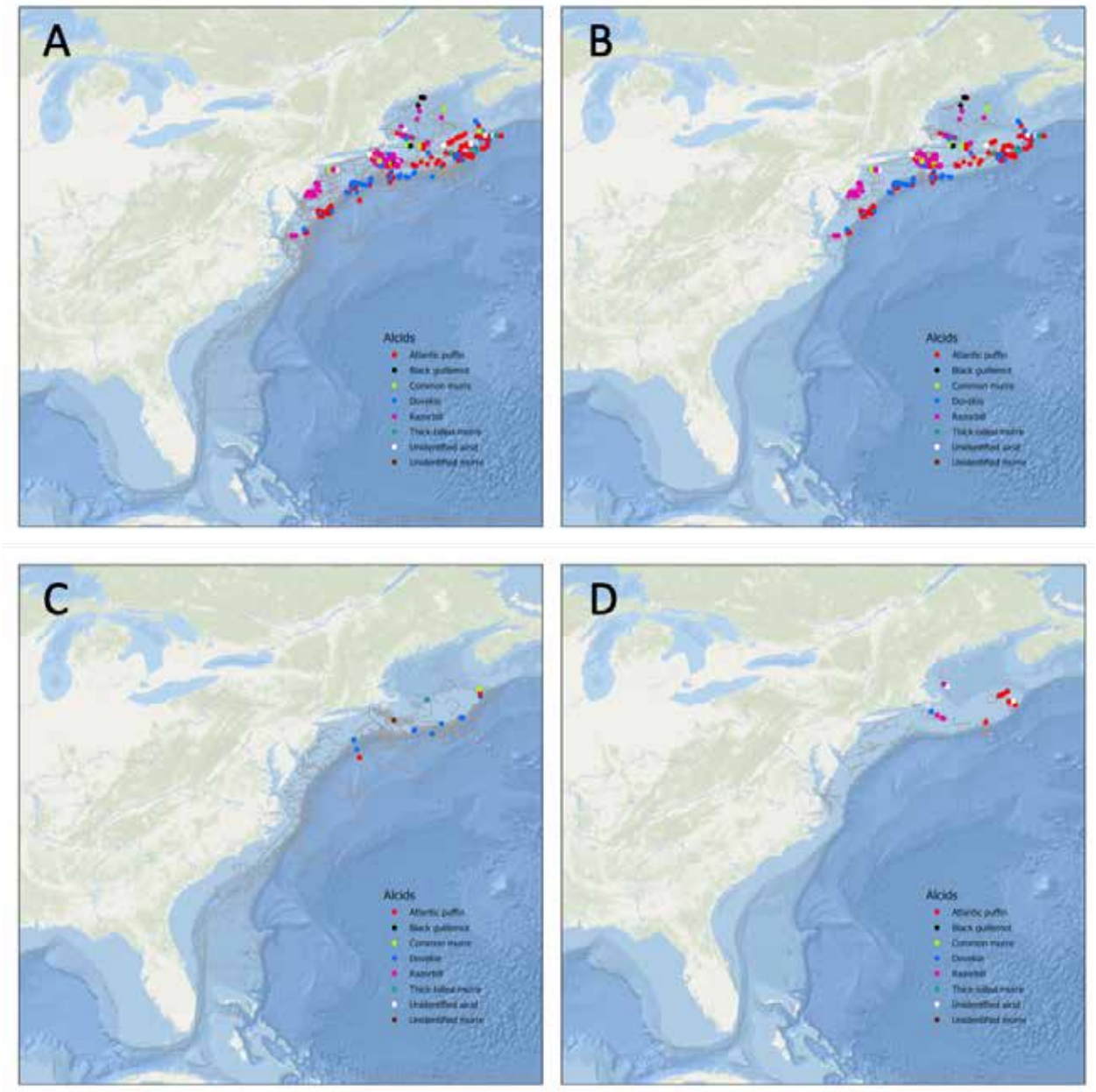

Figure 9-2 Visual track lines and positively identified sightings of Alcids
From NEFSC cruises during 2011 to 2019 for all seasons (A), spring (B), Summer (C), and Fall (D). Spring is 1 March to 31 May; summer is 1 June to 31 August; and fall is 1 September to 30 November.

Table 9-3 Summary of birds at a species level on NEFSC cruises during 2017 to 2019
Percent frequency of occurrence (% FO), and mean relative proportion of total birds counted on all cruises and seasonally (spring, summer, and fall) sorted in alphabetical order of common name.

Common Name	% FO	All	Spring	Summer	Fall
American Golden Plover	6	0.014	0	0	0.048
American Goldfinch	6	0.009	0	0	0.031
American Oystercatcher	6	0.003	0.012	0	0
American Pipit	6	0.001	0	0	0.003
American Redstart	12	0.017	0	0.007	0.048
American Robin	12	0.008	0	0	0.026
Arctic Tern	29	0.155	0.496	0.021	0
Atlantic Puffin	29	0.201	0.500	0	0.183
Audubon's Shearwater	71	2.852	0.107	5.910	1.318
Band-rumped Storm-petrel	41	1.135	0	2.667	0.125
Bank Swallow	6	0.037	0	0	0.125
Barn Swallow	53	0.710	0.065	0.475	1.682
Barolo Shearwater	6	0.003	0	0.007	0
Belted Kingfisher	6	0.001	0	0	0.003
Black Guillemot	12	0.017	0.057	0	0
Black Scoter	18	1.313	0	0	4.463
Black Skimmer	6	0.018	0	0.045	0
Black Tern	18	0.194	0	0.025	0.623
Black-bellied Plover	29	0.121	0.031	0.134	0.192
Black-capped Petrel	59	1.725	0.016	4.025	0.213
Black-legged Kittiwake	29	0.291	0.017	0	0.972
Black-throated Blue Warbler	6	0.001	0	0	0.003
Blackpoll Warbler	12	0.004	0.005	0	0.010
Blue-headed Vireo	6	0.001	0	0	0.003
Bobolink	6	0.128	0	0	0.436
Bonaparte's Gull	29	0.706	0.013	0.004	2.381
Brant	6	0.007	0	0	0.024
Bridled Tern	29	0.980	0	1.667	0.997
Brown Booby	47	0.337	0.131	0.279	0.623
Brown Creeper	6	0.005	0	0	0.016
Brown Noddy	18	0.126	0	0.261	0.062
Brown Pelican	35	0.238	0	0.305	0.382
Brown-headed Cowbird	41	0.090	0.044	0.163	0.032
Cattle Egret	6	0.018	0	0	0.062
Cedar Waxwing	24	0.050	0.026	0	0.144
Chimney Swift	18	0.012	0.009	0.023	0
Chipping Sparrow	6	0.003	0	0	0.010
Cliff Swallow	12	0.030	0	0.072	0
Common Eider	18	0.045	0.024	0	0.130
Common Loon	35	0.434	0.838	0.004	0.633
Common Murre	12	0.005	0.017	0	0
Common Tern	59	1.175	3.180	0.346	0.331
Common Yellowthroat	18	0.017	0.009	0	0.048
Common/Arctic Tern	6	0.010	0	0.023	0
Cory's Shearwater	100	8.251	1.471	16.199	3.905
Dark-eyed Junco	18	0.022	0	0	0.075
Double-crested Cormorant	71	2.746	0.495	0.394	8.289
Dovekie	29	0.046	0.145	0	0.010
Dowitcher	29	0.470	1.207	0.042	0.334
Dunlin	6	0.009	0	0	0.031
Eastern Kingbird	6	0.009	0	0.023	0
Eurasian Hobby	6	0.005	0.016	0	0
European Starling	6	0.003	0	0	0.010
Field Sparrow	6	0.001	0	0	0.003
Forster's Tern	6	0.002	0	0.004	0

Common Name	% FO	All	Spring	Summer	Fall
Franklin's Gull	6	0.004	0.013	0	0
Greater Yellowlegs	6	0.001	0.005	0	0
Golden-crowned Kinglet	12	0.006	0	0	0.019
Gray Catbird	12	0.005	0	0	0.017
Great Black-backed Gull	71	2.340	2.673	1.255	3.527
Great Blue Heron	29	0.074	0.005	0	0.248
Great Cormorant	6	0.001	0	0	0.003
Great Crested Flycatcher	6	0.014	0	0	0.048
Great Egret	6	0.001	0.004	0	0
Great Skua	12	0.006	0	0.004	0.014
Greater Shearwater	100	18.734	19.798	23.292	11.288
Greater Yellowlegs	6	0.013	0	0.030	0
Green Heron	6	0.001	0.005	0	0
Hermit Thrush	6	0.001	0	0	0.003
Herring Gull	76	3.603	3.986	0.984	6.884
Hooded Warbler	6	0.002	0	0.004	0
Laughing Gull	59	1.047	0.493	0.778	1.977
Leach's Storm-petrel	82	4.405	3.299	7.300	1.459
Leach's/Band-rumped storm-petrel	6	0.048	0	0.117	0
Leach's/Harcourt's Storm-petrel	6	0.058	0	0.141	0
Least Sandpiper	18	0.040	0	0.053	0.062
Least Tern	18	0.040	0.043	0.068	0
Lesser Black-backed Gull	35	0.110	0.008	0.054	0.291
Lesser Scaup	6	0.005	0	0	0.016
Lincoln's Sparrow	6	0.001	0	0	0.003
Little Blue Heron	6	0.055	0	0	0.187
Long-tailed Jaeger	35	0.096	0.051	0	0.275
Magnificent Frigatebird	18	0.349	0	0.313	0.748
Magnolia Warbler	12	0.007	0.023	0	0
Manx Shearwater	76	0.721	0.452	0.426	1.403
Marsh Wren	12	0.004	0	0	0.013
Masked Booby	12	0.115	0	0.013	0.374
Mourning Dove	12	0.016	0	0	0.055
Northern Flicker	12	0.029	0	0	0.099
Northern Fulmar	41	2.107	5.762	0	1.403
Northern Gannet	59	4.481	3.019	0.253	11.862
Northern Parula	6	0.001	0.004	0	0
Osprey	35	0.295	0.048	0.007	0.945
Ovenbird	12	0.017	0	0.007	0.048
Palm Warbler	6	0.001	0	0	0.003
Parasitic Jaeger	53	0.188	0.078	0.090	0.435
Pectoral Sandpiper	6	0.013	0	0.030	0
Peregrine Falcon	18	0.018	0.013	0.023	0.017
Pine Siskin	6	0.009	0	0	0.031
Pine Warbler	6	0.001	0	0	0.003
Pomarine Jaeger	76	0.408	0.098	0.296	0.874
Prairie Warbler	12	0.014	0	0.034	0
Prothonotary Warbler	6	0.001	0	0	0.003
Purple Martin	12	0.005	0.008	0.007	0
Razorbill	29	0.042	0.055	0	0.088
Red Knot	6	0.061	0	0.148	0
Red Phalarope	59	4.140	13.263	0.049	0.744
Red-bellied Woodpecker	6	0.004	0.013	0	0
Red-billed Tropicbird	12	0.017	0	0.041	0
Red-breasted Merganser	6	0.005	0	0	0.016
Red-breasted Nuthatch	12	0.019	0	0.023	0.031
Red-necked Phalarope	53	0.387	0.266	0.449	0.422
Red-throated Loon	29	0.079	0.026	0	0.244

Common Name	% FO	All	Spring	Summer	Fall
Red-winged Blackbird	18	0.007	0	0.007	0.013
Ring-billed Gull	24	0.038	0.005	0	0.124
Roseate Spoonbill	6	0.018	0	0	0.062
Roseate Tern	6	0.015	0.050	0	0
Royal Tern	47	1.238	0.040	0.509	3.458
Ruby-crowned Kinglet	12	0.006	0	0	0.019
Ruddy Turnstone	24	0.060	0.100	0.030	0.062
Sabine's Gull	12	0.010	0.004	0.023	0
Sanderling	29	0.072	0.019	0.004	0.220
Sandwich Tern	12	0.057	0	0.004	0.187
Scarlet Tanager	6	0.003	0	0	0.010
Semipalmated Plover	6	0.002	0	0.004	0
Semipalmated Sandpiper	18	0.013	0.004	0.029	0
Short-billed Dowitcher	6	0.013	0	0.030	0
Snow Bunting	6	0.006	0	0	0.020
Snow Goose	6	0.005	0	0	0.016
Snowy Egret	6	0.055	0	0	0.187
Solitary Sandpiper	12	0.034	0	0.084	0
Song Sparrow	12	0.009	0	0	0.031
Sooty / Bridled Tern	18	0.202	0	0.269	0.312
Sooty Shearwater	71	3.063	10.156	0.140	0.061
Sooty Tern	24	1.734	0	3.454	1.059
South Polar Skua	65	0.393	0.625	0.498	0.013
Spotted Sandpiper	6	0.018	0	0	0.062
Stilt Sandpiper	6	0.013	0	0.030	0
Surf Scoter	24	0.181	0	0	0.617
Swamp Sparrow	6	0.003	0	0	0.010
Tennessee Warbler	6	0.018	0	0	0.062
Tree Swallow	12	0.010	0	0.025	0
Trinidad Petrel	12	0.012	0	0.030	0
Unidentified Alcid	18	0.018	0.040	0	0.020
Unidentified Blackbird	6	0.001	0	0	0.003
Unidentified Duck	12	0.084	0	0	0.287
Unidentified Egret	6	0.018	0	0	0.062
Unidentified Grebe	6	0.005	0	0	0.016
Unidentified Jaeger	53	0.102	0.082	0.088	0.143
Unidentified large Alcid	6	0.001	0	0	0.003
Unidentified large Gull	18	0.016	0.051	0	0.003
Unidentified large Shearwater	18	0.590	0.044	1.402	0
Unidentified large Tern	6	0.008	0	0.019	0
Unidentified Loon	6	0.005	0	0	0.016
Unidentified Passerine	41	0.391	0.413	0.011	0.900
Unidentified Petrel	18	0.019	0.013	0.036	0
Unidentified Phalarope	65	0.794	1.570	0.283	0.734
Unidentified Plover	6	0.042	0	0	0.144
Unidentified Puffinus	12	0.013	0	0.031	0
Unidentified Sandpiper	18	0.101	0.103	0	0.240
Unidentified Scoter	18	0.950	2.947	0	0.283
Unidentified Shearwater	41	0.133	0.042	0.244	0.068
Unidentified Shorebird	59	0.179	0.030	0.187	0.316
Unidentified Skua	24	0.012	0.012	0.004	0.024
Unidentified small Gull	6	0.005	0	0	0.016
Unidentified small Shearwater	24	0.028	0.059	0.022	0.003
Unidentified small Shorebird	24	0.722	2.403	0.033	0.003
Unidentified small Tern	12	0.268	0.859	0.037	0
Unidentified Sparrow	6	0.002	0	0	0.007
Unidentified Storm-petrel	82	0.588	0.193	1.144	0.205
Unidentified Sulid	6	0.001	0	0	0.003

Common Name	% FO	All	Spring	Summer	Fall
Unidentified Swallow	12	0.030	0	0.073	0
Unidentified Tern	47	0.502	0.784	0.121	0.753
Unidentified Warbler	12	0.111	0.005	0	0.374
Whimbrel	12	0.028	0	0.067	0
White-faced Storm-petrel	29	0.340	0	0.551	0.384
White-tailed Tropicbird	12	0.028	0	0.069	0
White-throated Sparrow	12	0.007	0	0	0.024
White-winged Scoter	29	0.863	0.049	0	2.886
Willet	6	0.016	0	0.039	0
Wilson's Storm-petrel	88	16.584	16.859	20.958	10.187
Winter Wren	6	0.002	0	0	0.007
Wood Duck	6	0.003	0	0	0.010
Yellow-rumped Warbler	12	0.013	0	0	0.044

9.3.3.2 Gannet and Boobies

Observers detected 7 species in the order Suliformes: 1 frigatebird, 3 boobies, 1 gannet, and 2 cormorants on NEFSC cruises from 2011 to 2019 (Figure 9-3). Northern Gannet, Double-crested Cormorant, Brown Booby, and Masked Booby had the highest relative proportions (Table 9-3). During the spring, Northern Gannet and Double-crested Cormorant were on the NEUS shelf including the Gulf of Maine and along the continental shelf-break of the NEUS Shelf (Figure 9-3B). During the summer, Northern Gannet were over coastal waters of the Southern New England region of the NEUS Shelf and the Gulf of Maine, while, Double-crested Cormorant were widely dispersed (Figure 9-3C). During the fall, Northern Gannet were over NEUS Shelf waters including Georges Bank, while the Double-crested Cormorant was over coastal waters off Chesapeake Bay (Figure 9-3D). During the summer, Masked Booby and Brown Booby were over the Gulf of Mexico, along the shelf-break of both the SEUS and NEUS Shelves, and over deep ocean waters (Figure 9-3C). In contrast during the fall, both species were south of Cape Hatteras along the continental shelf-break of the SEUS Shelf and in the Gulf of Mexico (Figure 9-3D).

9.3.3.3 Gulls

Observers detected 13 species of Gulls on NEFSC cruises from 2011 to 2019 (Figure 9-4). Herring Gull, Great Black-backed Gull, Laughing Gull, Bonaparte's Gull had the highest relative proportion from 2017 to 2019 (Table 9-3). During the spring, Herring Gull, Great Black-backed Gull, and Bonaparte's Gull were over NEUS Shelf waters including in the Gulf of Maine, while Laughing Gulls were more near the coast from Cape Cod south to Cape Hatteras (Figure 9-4B). During the summer, Greater Great Black-backed Gull were over coastal waters of the NEUS Shelf south of Long Island and shelf waters including Georges Bank and the Gulf of Maine, while Herring Gull were mainly on the NEUS Shelf off Long Island and north into the Gulf of Maine (Figure 9-4C). In the summer, Laughing Gulls were primarily over coastal waters of the NEUS Shelf south of Long Island (Figure 9-4C). During the fall, Herring Gull, Great Black-backed Gull, Laughing Gull, Bonaparte's Gull species were over the NEUS Shelf waters including the Gulf of Maine (Figure 9-4D).

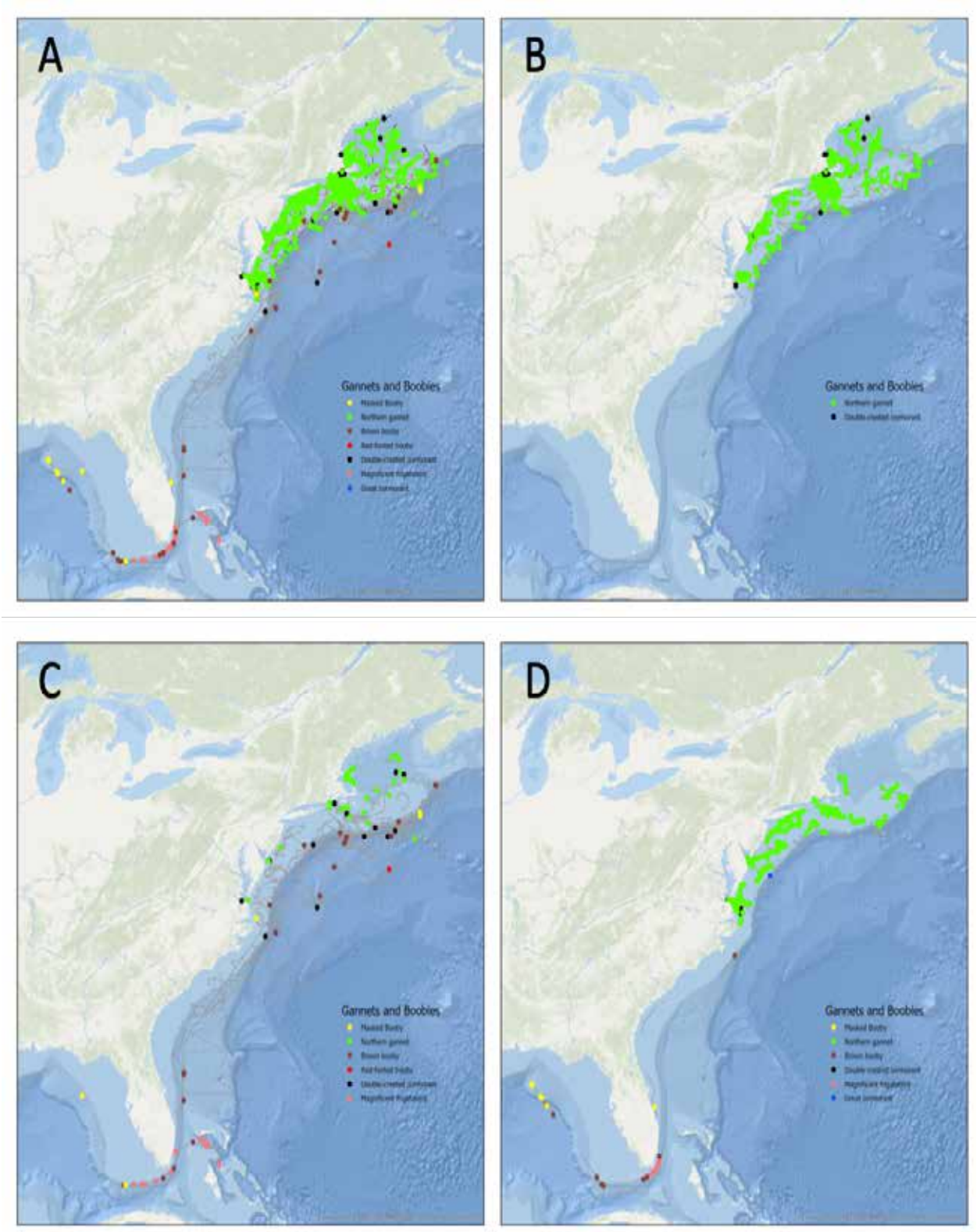

Figure 9-3 Visual track lines and positively identified sightings of Gannets and Boobies
From NEFSC cruises during 2011 to 2019 for all seasons (A), spring (B), summer (C) and fall (D). Spring is 1 March to 31 May; summer is 1 June to 31 August; and fall is 1 September to 30 November.

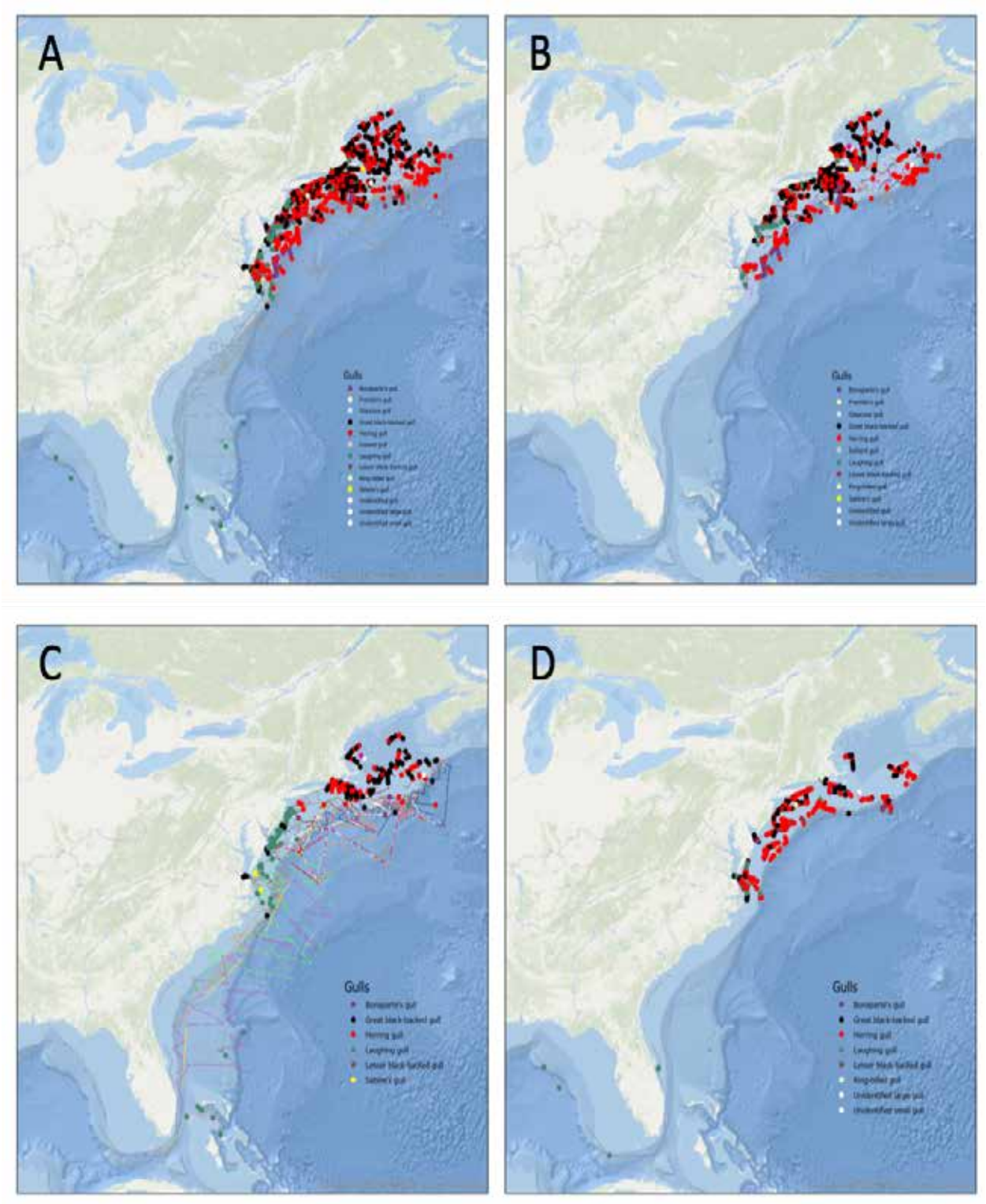

Figure 9-4 Visual track lines and positively identified sightings of Gulls
From NEFSC cruises during 2011 to 2019 for all seasons (A), spring (B), summer (C) and fall (D). Spring is 1 March to 31 May; summer is 1 June to 31 August; and fall is 1 September to 30 November.

9.3.3.4 Loons

Observers detected 3 species of Loons on NEFSC cruises from 2011 to 2019 (Figure 9-5) mostly in the spring and fall. Common Loon and Red-throated Loon were the most abundant from 2017 to 2019 (Table 9-3). During the spring, Loons were over NEUS Shelf waters including the Gulf of Maine (Figure 9-5B). During the fall, Loons are mainly over NEUS Shelf waters between Chesapeake Bay and Cape Cod (Figure 9-5D).

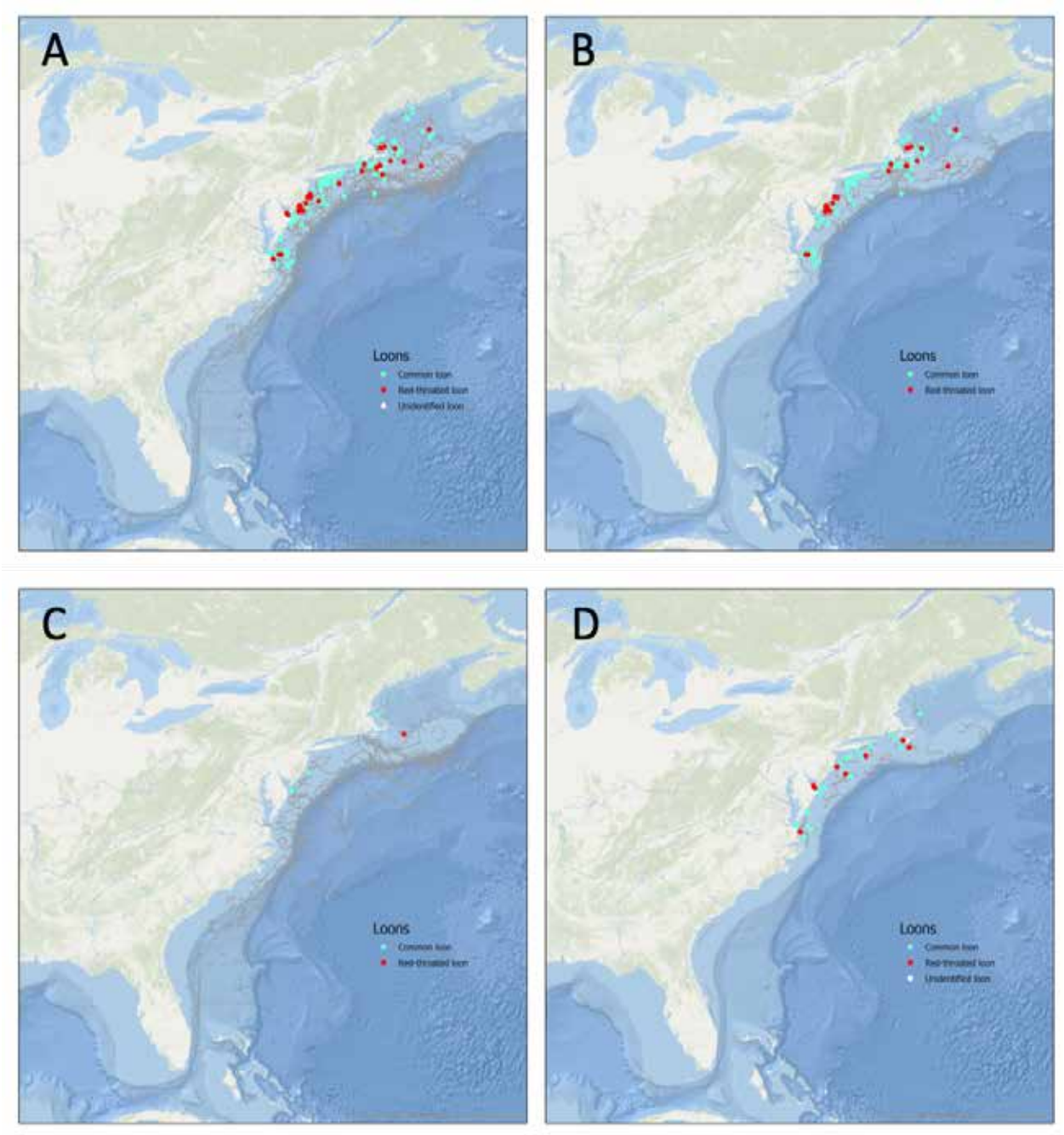

Figure 9-5 Visual track lines and positively identified sightings of Loons
From NEFSC cruises during 2011 to 2019 for all seasons (A), spring (B), summer (C) and fall (D). Spring is 1 March to 31 May; summer is 1 June to 31 August; and fall is 1 September to 30 November.

9.3.3.5 Petrels

Observers detected 5 species of Petrels on NEFSC cruises from 2011 to 2019 (Figure 9-6). Black-capped Petrel, Unidentified Petrel, and Trinidad Petrel had the highest relative proportion from 2017 to 2019 (Table 9-3). During the summer, Petrels were almost exclusively over oceanic waters off the NEUS and SEUS Shelves (Figure 9-6C).

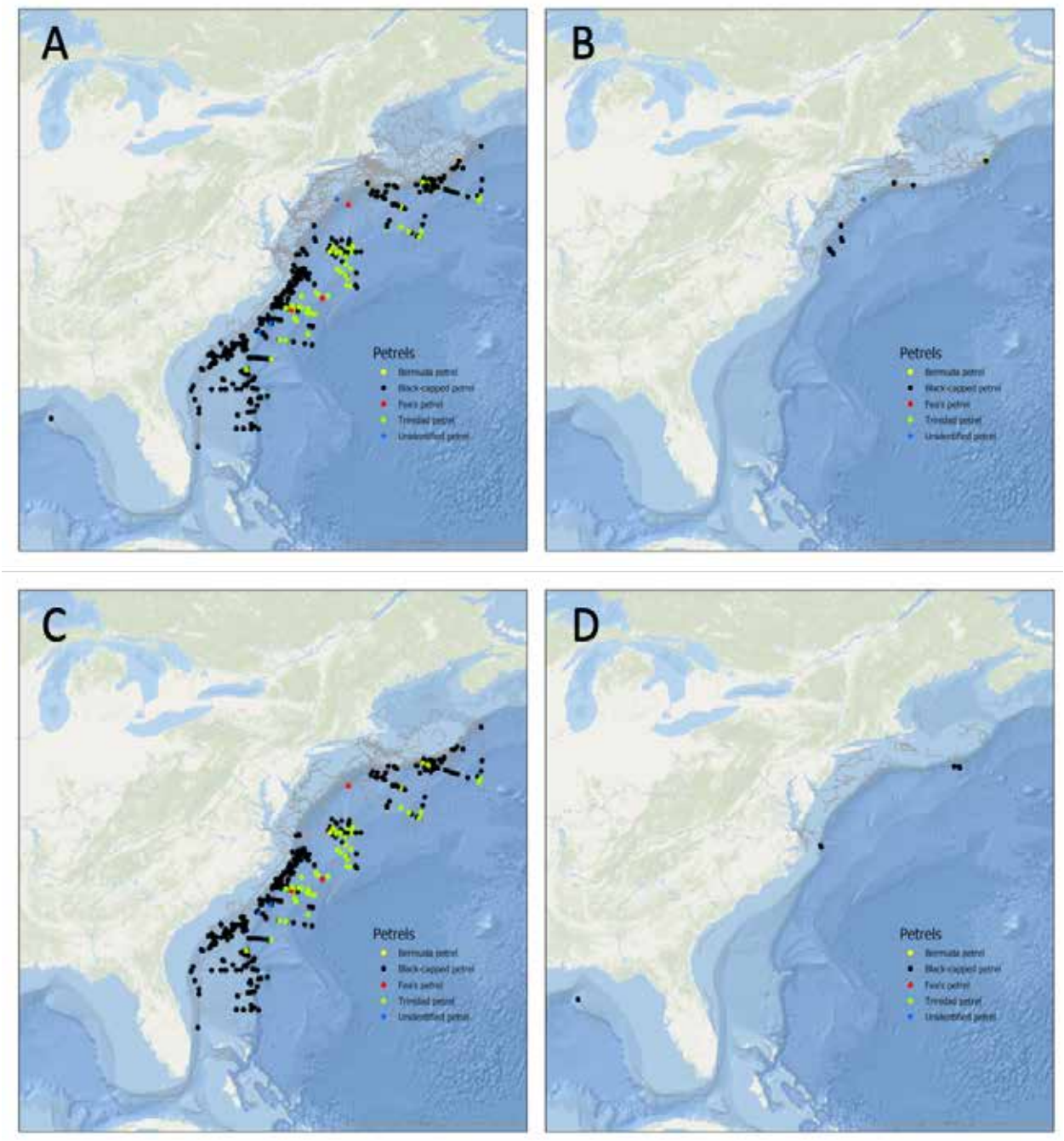

Figure 9-6 Visual track lines and positively identified sightings of Petrels
From NEFSC cruises during 2011 to 2019 for all seasons (A), spring (B), summer (C) and fall (D). Spring is 1 March to 31 May; summer is 1 June to 31 August; and fall is 1 September to 30 November.

9.3.3.6 Shearwaters

Observers detected 10 species of Shearwaters on NEFSC cruises from 2011 to 2019 (Figure 9-7 and Table 9-3). Greater Shearwater, Cory's Shearwater, Sooty Shearwater, Audubon's Shearwater, Manx Shearwater had the highest relative proportion from 2017 to 2019 (Table 9-3). During the spring, Greater Shearwater, Sooty Shearwater, and Cory's Shearwater were over NEUS Shelf waters including the Gulf of Maine, while, Manx Shearwater were along the continental shelf-break of the NEUS Shelf south of Cape Cod and on Georges Bank and in the Gulf of Maine (Figure 9-7B). During the summer, Greater Shearwater and Cory's Shearwater were over the NEUS Shelf and along the continental shelf-breaks and adjacent offshore waters of both the SEUS and NEUS Shelves; Sooty Shearwater were mainly over NEUS Shelf waters north of Delaware Bay; while Audubon's Shearwater and Manx Shearwater were over offshore waters off the SEUS and NEUS Shelves (Figure 9-7C). During the fall, Greater Shearwater and Manx Shearwater were over NEUS Shelf waters, while Cory's Shearwater and Audubon's Shearwater were along the continental shelf-break of the SEUS Shelf and Gulf of Mexico (Figure 9-7D).

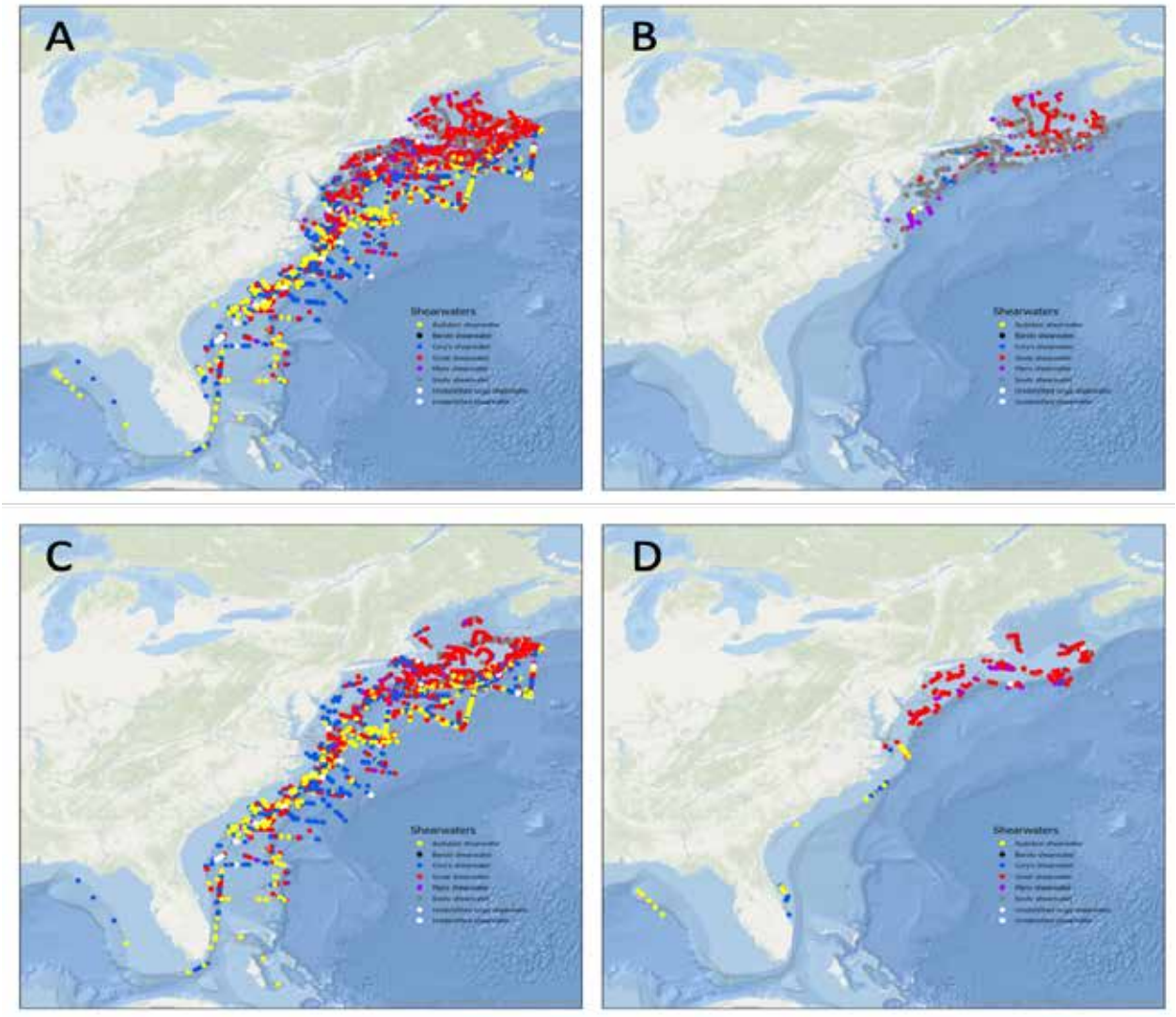

Figure 9-7 Visual track lines and positively identified sightings of Shearwaters
From NEFSC cruises during 2011 to 2019 for all seasons (A), spring (B), summer (C) and fall (D). Spring is 1 March to 31 May; summer is 1 June to 31 August; and fall is 1 September to 30 November.

9.3.3.7 Skuas

Observers detected 7 species of Skuas on NEFSC cruises from 2011 to 2019 (Figure 9-8 and Table 9-3). Pomarine Jaeger, South Polar Skua, and Parasitic Jaeger had the highest relative proportion from 2017 to 2019 (Table 9-3). During the spring, South Polar Skua, Pomarine Jaeger, and Parasitic Jaeger were over the NEUS Shelf and along the continental shelf-break north off Delaware Bay to Georges Bank including the Gulf of Maine (Figure 9-8B). During the summer, Pomarine Jaeger, South Polar Skua, and Parasitic Jaeger were over NEUS Shelf waters from off Massachusetts to Georges Bank and along the continental shelf-break of the SEUS and NEUS Shelves and adjacent offshore waters from the Blake Plateau to off Georges Bank (Figure 9-8C). During the fall, Pomarine Jaeger and Parasitic Jaeger are over NEUS Shelf waters and along the continental shelf-break of the NEUS Shelf (Figure 9-8D).

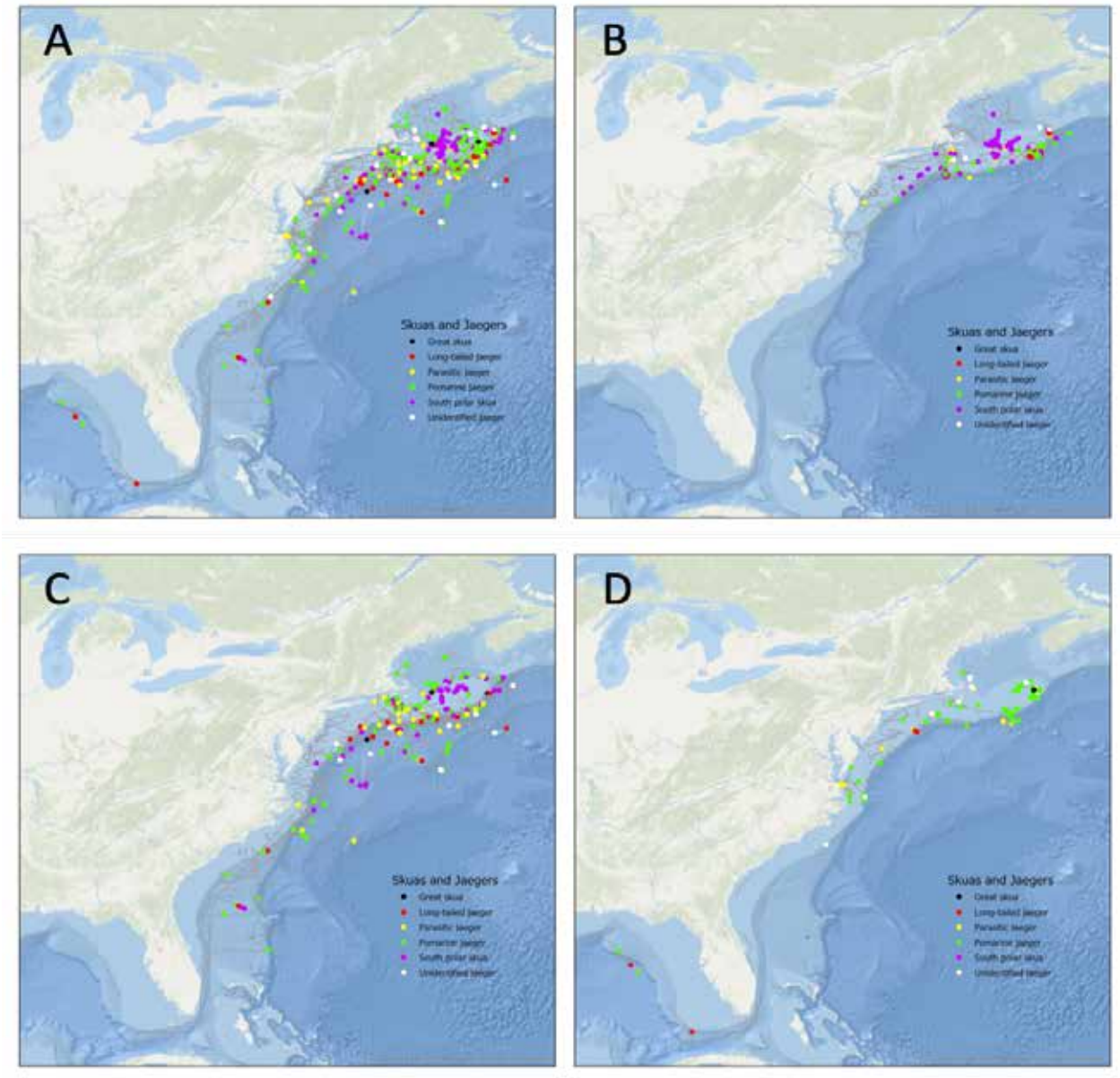

Figure 9-8 Visual track lines and positively identified sightings of Skuas and Jaegers
From NEFSC cruises during 2011 to 2019 for all seasons (A), spring (B), summer (C) and fall (D). Spring is 1 March to 31 May; summer is 1 June to 31 August; and fall is 1 September to 30 November.

9.3.3.8 Storm-petrels

Observers detected 7 species of Storm-petrels on NEFSC cruises from 2011 to 2019 (Figure 9-9 and Table 9-3). Wilson's Storm-petrel, Leach's Storm-petrel, and Band-rumped Storm-petrel had the highest relative proportion from 2017 to 2019 (Table 9-3). During the spring, Wilson's Storm-petrel were over NEUS Shelf waters from off North Carolina into the Gulf of Maine, while Leach's Storm-petrel were in the Gulf of Maine and on Georges Bank (Figure 9-9B). During the summer, Wilson's Storm-petrel were over NEUS Shelf waters and along the continental shelf-break of the SEUS and NEUS Shelves and adjacent offshore waters, while Band-rumped Storm-petrel and Leach's Storm-petrel were mainly along the continental shelf-break of the SEUS and NEUS Shelves and adjacent offshore waters (Figure 9-9C). During the fall, Wilson's Storm-petrel and Leach's Storm-petrel were over the continental shelf-break of the NEUS, primarily near canyons (Figure 9-9D).

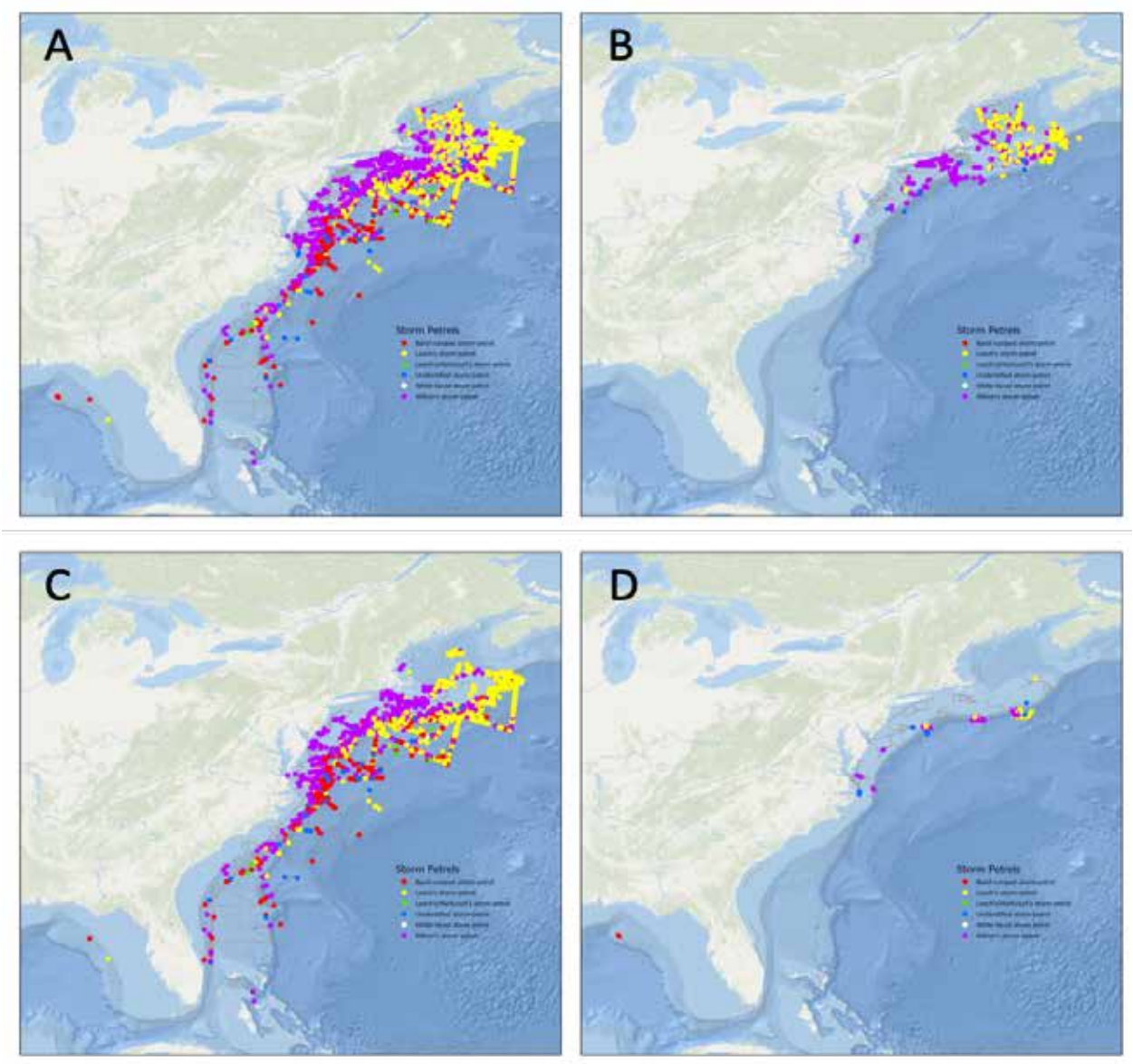

Figure 9-9 Visual track lines and positively identified sightings of Storm-petrels
From NEFSC cruises during 2011 to 2019 for all seasons (A), spring (B), summer (C) and fall (D). Spring is 1 March to 31 May; summer is 1 June to 31 August; and fall is 1 September to 30 November.

9.3.3.9 Terns

Observers detected 15 species of Terns on NEFSC cruises from 2011 to 2019 (Figure 9-10 and Table 9-3). Sooty Tern, Royal Tern, Common Tern, and Bridled Tern had the highest relative proportion from 2017 to 2019 (Table 9-3). During the spring, Common Tern, Roseate Tern, and Arctic Tern were over NEUS Shelf waters including the Gulf of Maine (Figure 9-10B). During the summer, Sooty Tern and Bridled Tern were along the continental shelf-breaks of the Gulf of Mexico, SEUS Shelf, and NEUS Shelf and adjacent offshore waters; while Royal Tern and Common Tern were over SEUS and NEUS Shelf waters and adjacent offshore waters (Figure 9-10C). During the fall, most Terns were over waters from off Chesapeake Bay south to the Gulf of Mexico (Figure 9-10D).

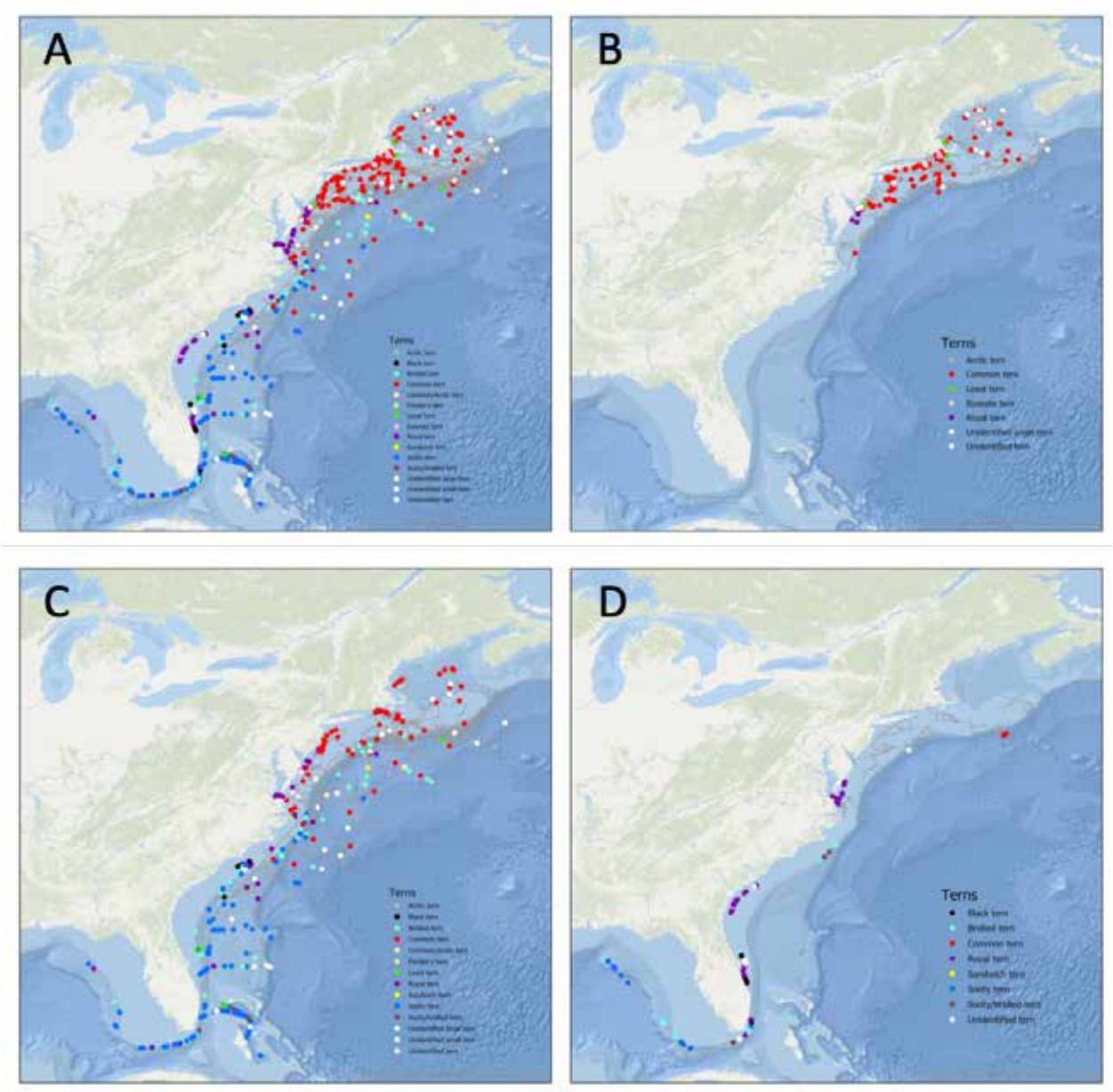

Figure 9-10 Visual track lines and positively identified sightings of Terns
From NEFSC cruises during 2011 to 2019 for all seasons (A), spring (B), summer (C) and fall (D). Spring is 1 March to 31 May; summer is 1 June to 31 August; and fall is 1 September to 30 November.

9.3.4 Species Seasonal and Spatial Sightings

Species composition and abundance varied with seasonal coverage and spatial location (Tables 9-3 and 9-4). Greater Shearwater and Cory's Shearwater were the only 2 species detected on every cruise from 2017 to 2019 (Table 9.3). Greater Shearwater, Wilson's Storm-petrel, Cory's Shearwater, Northern Gannet, and Leach's Storm-petrel accounted for 50% of the relative proportion of sightings (Table 9-3). The addition of Red Phalarope, Herring Gull, Sooty Shearwater, Audubon's Shearwater, Double-crested Cormorant, Great Black-backed Gull, Northern Fulmar, and Sooty Tern increased the total to 75% of sightings (Table 9-3).

Shorebirds dominated the spring sightings across the shelf-break front in Southern New England (SNE) (Table 9-4). Red Phalarope and Unidentified small Shorebirds totalled 50% of the relative proportion of sightings, and Unidentified Phalarope and Common Tern increased the total to 75% of sightings (Table 9-4). Wilson's Storm-petrel, Sooty Shearwater, Greater Shearwater, Northern Fulmar, Herring Gull, and Leach's Storm-petrel accounted for 50% of the relative proportion of sightings on the entire NEUS Shelf during spring cruises, with Unidentified Scoter and Northern Gannet increasing the total to 75% (Table 9-4). No observations were in the oceanic waters off the SEUS or NEUS Shelves (offshore) during the spring.

During the summer, Greater Shearwater accounted for 50% of the sightings across the shelf-break front in the SNE and Wilson's Storm-petrel accounted for another 25% (Table 9-4). Similarly, Greater Shearwater, Wilson's Storm-petrel, and Cory's Shearwater dominated the NEUS Shelf sightings during summer, accounting for 50% of the sightings, and Great Black-backed Gull and Unidentified large Shearwaters increased the total to 75% of sightings (Table 9-4). Wilson's Storm-petrel, Greater Shearwater, and Cory's Shearwater accounted for 50 % of the sightings of offshore waters during the summer (Table 9.4). Leach's Storm-petrel and Audubon's Shearwater added another 25% to sightings in the offshore during summer (Table 9-4).

We did not collect fall observations across the shelf-break front in SNE. However, Northern Gannet, Greater Shearwater, Double-crested Cormorant, and Herring Gull accounted for 50% of the sightings of NEUS Shelf waters during the fall; while Black Scoter, Great Black-backed Gull, White-winged Scoter added another 25% of sightings (Table 9-4). Fifty percent of sightings in offshore waters during the fall were Wilson's Storm-petrel, and Greater Shearwater, while, Leach's Storm-petrel, Manx Shearwater, and Unidentified Passerines accounted for another 25% of the sightings.

9.3.5 Summary of Other Projects that used AMAPPS Seabird Data

The AMAPPS seabird sightings data are available to the public to conduct other types of analyses. We shared the seabird data collected on AMAPPS surveys with NOAA National Center for Coastal Ocean Science Biogeography Branch. They used the AMAPPS survey data, in addition to about 80 other surveys spanning 4 decades to model the Atlantic at-sea density of marine birds (Winship et al. 2018). They used an ensemble machine-learning technique called component wise boosting of hierarchical zero-inflated count models to relate the relative density of each species to multiple spatial and temporal predictor variables while accounting for survey heterogeneity and the aggregated nature of sightings. The formulations of the dynamic spatial environmental predictor variables were long-term climatologies.

White and Veit (2020) integrated AMAPPS and other NMFS data to identify important interactions between diving marine birds, prey, and oceanography on Nantucket Shoals. Through this work, BOEM recognized the importance of Nantucket Shoals and removed potential offshore wind lease blocks from the area to conserve its important habitat and diversity.

Dr. Timothy White and others from BOEM used AMAPPS surveys to identify areas important to sensitive marine mammal, seabird, and turtle communities. BOEM will be publishing some of this work in their upcoming Oil and Gas Leasing Environmental Impact Statement.

Table 9-4 Dominant species by location and season
Species of birds that cumulatively make up 75% of the birds in each 3 regions (SNE = Southern New England, Shelf = entire Northeast Atlantic U.S. Shelf, Offshore = Oceanic waters off the Northeast and Southeast Atlantic U.S. Shelves) averaged over cruises during the spring, summer, and fall of 2017 to 2019. Bolded species accounted for 50% of the observations.

Location	Spring	Summer	Fall
SNE	**Red Phalarope**	**Greater Shearwater**	
	Unidentified small Shorebird	Wilson's Storm-petrel	
	Unidentified Phalarope		
	Common Tern		
Shelf	**Wilson's Storm-petrel** **Sooty Shearwater**	**Greater Shearwater** **Wilson's Storm-petrel**	**Northern Gannet** **Greater Shearwater**
	Greater Shearwater	**Cory's Shearwater**	**Double-crested Cormorant**
	Northern Fulmar	Great Black-backed Gull	**Herring Gull**
	Herring Gull	Unidentified large Shearwater	Black Scoter
	Leach's Storm-petrel		Great Black-backed Gull
	Unidentified Scoter		White-winged Scoter
	Northern Gannet		
Offshore		**Wilson's Storm-petrel**	**Wilson's Storm-petrel**
		Greater Shearwater	Greater Shearwater
		Cory's Shearwater	Leach's Storm-petrel
		Leach's Storm-petrel	Manx Shearwater
		Audubon’s Shearwater	Unidentified Passerine

9.4 Key Findings

Seabirds are an important part of marine ecosystems and our results showed that there were significant spatial and seasonal changes in species composition and abundance on the NEUS Shelf and adjacent offshore waters. For example, across the shelf-break front in Southern New England waters, shorebirds dominated the sightings in the spring surveys, while during the summer, Greater Shearwater accounted for 50% of the sightings and Wilson's Storm-petrel accounted for another 25%.

9.5 Data Gaps and Future Work

There have been modeling efforts to identify hotspots (Veit et al. 2015), and the addition of biotic and abiotic covariates has improved the understanding of the habitat use of seabird species (White and Veit 2020). Thus, the continued support of NEFSC EcoMon, AMAPPS, and similar survey efforts to concurrently monitor seabirds with oceanographic and plankton sampling should aid in the ongoing efforts to understand the spatial-temporal distributions of the seabirds.

9.6 Acknowledgements

We maintain the visual sightings data from each cruise in an Oracle Database at the Northeast Fisheries Science Center and distribute to the Seabird Compendium. We acknowledge the officers and crew of NOAA ships *Ronald H. Brown*, *Henry B. Bigelow* and *Gordon Gunter* and the R/V *Thomas G. Thompson* and R/V *Hugh R. Sharp* for their great ship support. We would also like to thank Dr. Dennis McGillicuddy of Woods Hole Oceanographic Institution for providing a berth for an observer aboard their research cruises. This seabird-monitoring project received funding from the U.S. Department of the

Interior, Bureau of Ocean Energy Management, Environmental Studies Program, Washington, DC, through an Inter-Agency Agreement with the National Marine Fisheries Service as the Atlantic Marine Assessment Program for Protected Species (AMAPPS), and by the Northeast Fisheries Science Center.

9.7 References Cited

Anonymous. 2011. Seabird Survey Instruction Protocol. Seabird distribution and abundance, Summer 2011. NOAA ship *Henry B. Bigelow*. Northeast Fisheries Science Center.

Ballance LT. 2011. Seabird Survey Instruction Manual, PICEAS 2011. Ecosystems Studies Program Southwest Fisheries Science Center, La Jolla, California.

Biodiversity Research Institute (BRI) 2020. Data management: SeaScribe website. (Assessed 5 Oct 2020).

Heinemann D. 1981. A range finder for pelagic bird censusing. J. Wildl. Manag. 45:489-493.

Tasker ML, Hope Jones P, Dixon T, Blake BF. 1984. Counting seabirds at sea from ships; a review of methods employed and a suggestion for a standardized approach. Auk 101:567-577.

Veit RR, Goyert HF, White TP, Martin MC, Manne LL, Gilbert A. 2015. Pelagic Seabirds off the east coast of the United States 2008-2013. US Dept. of the Interior, Bureau of Ocean Energy Management, Office of Renewable Energy Programs, Sterling, VA. OCS Study BOEM 2015-024; 186 pp.

Nantucket Shoals. Ecosphere 11(1):e3002.

Winship AJ, Kinlan BP, White TP, Leirness JB, Christensen J. 2018. Modeling at-sea density of marine birds to support Atlantic marine renewable energy planning: Final report. U.S. Department of the Interior, Bureau of Ocean Energy Management, Office of Renewable Energy Programs, Sterling, VA. OCS Study BOEM 2018-010; x+67 pp.

10 Ecosystem Research

Primary authors: Elisabeth Broughton, Michael Jech, Chris Orphanides, and Harvey Walsh.

10.1 Introduction

One way to gain insight into what influences the patterns of distribution and density of protected species (marine mammals, sea turtles, and sea birds) is to understand what physical and biological characteristics are associated with them (Pendleton et al. 2009; 2020; White and Veit 2020). Such insight could potentially allow the discrimination between changes in cetacean populations that are due to natural environmental variability versus anthropogenic impacts. In addition, such insights could improve population assessments by incorporating ecosystem aspects into single or multiple species population assessments, as has been the trend in fish population assessments (Jurado-Molina et al. 2005; Möllmann et al. 2014). In this chapter, we address aspects of 2 of the 7 AMAPPS objectives (taken from the complete list of objectives in Chapter 3):

5) Identify currently used viable technologies and explore alternative platforms and technologies to improve population assessment studies, if necessary;
6) Assess the population size of surveyed species at regional scales; and develop models and associated tools to translate these survey data into seasonal, spatially explicit density estimates incorporating habitat characteristics.

Protected species studied under AMAPPS inhabit waters over the continental shelf and farther offshore which includes the shelfbreak (to 200 m depth), mesopelagic (to 1000 m) and the bathypelagic (to 4000 m). The continental shelf is where many human activities are, such as, fishing (Amoroso et al. 2018) and development of wind energy areas (BOEM 2020). The continental shelf is also where much of the scientific research occurs (such as research at the federal level (e.g., Northeast Fisheries Science Center (NEFSC)), state level (e.g., Northeast Area Monitoring and Assessment Program), by private organizations (e.g., Woods Hole Oceanographic Institution), and by university (e.g., Rutgers). However, most of the protected species also depend on habitats offshore of continental shelf waters, so we also need information on these off-shelf waters if we are to fully understand the protected species distribution, abundance, and habitat needs. The research cruises conducted under AMAPPS provided an opportunity to discover what is happening in these environments, where we had the opportunity to conduct sampling in canyons, oceanic waters, warm-core rings, and along the shelf/slope front.

In this chapter, we document the hydrographics of the water column and the spatiotemporal distributions of lower trophic level organisms such as mesopelagic fish and plankton collected during the 2015 to 2019 AMAPPS II NEFSC surveys. We can ultimately use these data to compare with distributional patterns of protected species, such as the exploratory study documented in section 6.4. We also highlight several studies conducted by other researchers using data collected during AMAPPS shipboard surveys. Details on the types of data collected during 2010 to 2015 AMAPPS I NEFSC surveys are in Palka et al. (2017).

10.2 Methods

In support of the AMAPPS objectives, we collected active acoustic, oceanographic, and biological (e.g., plankton, fish, and cephalopods) data. We collected active acoustic multi-frequency echosounder data continuously in active and passive modes to provide spatially comprehensive information on the vertical and areal distributions of biomass. We collected oceanographic data using conductivity, temperature, and depth (CTD) casts that were in conjunction with plankton sampling casts along the visual transect lines to provide depth delimited oceanographic conditions in the study area. We sampled plankton and mesopelagic communities using a 61cm bongo net along the visual transect lines daily at dawn, noon, and dusk. During daylight hours the depth of important cetacean food sources that are phototrophic, such as

euphausiids and myctophiids, precludes easy sampling. For this reason, we collected additional biological samples during the night when visual transects could not be conducted but we could sample the mesopelagic species because they migrated closer to the surface. We also deployed larger plankton nets and midwater trawls at night to create a spatially detailed characterization of the plankton and nekton from the surface to 800 m depth. These biological samples helped verify the species composition of the acoustic backscatter data and increased the spatial coverage of the lower trophic level categorization. Since nets can damage delicate gelatinous zooplankton and we cannot sample these plankton types quantitatively in nets, we deployed an imaging system to capture species and distribution information on gelatinous zooplankton, in addition to the nightly net sampling.

10.2.1 EK60 Active Acoustics

We collected acoustic backscatter data using multifrequency (NOAA ship *Henry B. Bigelow*: 18, 38, 70, 120, and 200 kHz; NOAA ship *Gordon Gunter*: 18, 38, 120, and 200 kHz; Figure 10-1) Simrad EK60 echosounders (1 narrowband frequency per echosounder). All transducers were split-beam and mounted on the hull of the vessel “looking” downward. We collected data in “active” mode, where the echosounders are actively transmitting a pulse of sound and then listening for echoes, and in “passive” mode, where the echosounders are not transmitting any sound and only listening for reverberation. We collected acoustic data continuously in active mode during nighttime for all cruises. We collected acoustic data in active mode during daytime on every second day or during periods where visual surveying was not conducted (e.g., transit) and in passive mode otherwise, to assess potential impacts that the sound pulses produced by the echosounders might have had on the visual and passive acoustic monitoring of cetaceans. During periods when we did not collect data in active mode, we typically secured the EK60 so that it was not transmitting or receiving, or it was set to passive mode. The EK60 echosounders were set to transmit at 1 ping per second, which allowed them to ping as fast as they could, given a sample range of 3000 m and signal processing time. In general, the EK60 echosounders transmitted once every 5 to 6 seconds when off the continental shelf. In active mode, each frequency transmitted a 1-ms continuous wave pulse.

We calibrated the EK60 echosounders at the beginning of HB1503 and HB1603 using the standard target method at the Newport Naval Anchorage. We used a 38.1-mm-diameter tungsten carbide with 6% cobalt binder sphere suspended at about 20 m range from the transducers to calibrate all frequencies. We used a wireless calibration system, consisting of 3 remotely controlled downriggers and automated software that positioned the target under the split-beam transducers. The software then automatically moved the sphere throughout the acoustic beams and collected the data. We used the Simrad Lobe program to playback the calibration data for each echosounder individually.

Figure 10-1 EK60 set up on the NOAA ship
Debra Palka (chief scientist; left) and Michael Murphy (survey technician; right) are sitting in front EK60 computer setup during the 2007 marine mammal abundance survey.

10.2.2 Imaging Systems

10.2.2.1 VPR

We conducted tows with a Seascan V-fin mounted, internally recording, black and white Video Plankton Recorder (VPR; Figure 10-2). The VPR was also equipped with a Seabird Fastcat CTD, a WetLabs Fluorometer-Transmissometer, and a Benthos altimeter. The VPR sampled at 16 frames per second with each frame representing a specific water volume determined by the camera setting. We mounted a Seabird Seacat 19+ CTD profiler on the wire < 1 m above the V-fin to provide real time data on gear depth and oceanographic conditions. We conducted all tows at 3 – 4 kts speed through the water to maximize sampling area and to minimize image frame overlap. VPR haul depth was limited to 300 m but the maximum depth of most hauls was less than 100 m to maximize sampling time in the densest biological layers.

All hauls were “tow-yo” hauls towed repetitively from the surface to the maximum sampling depth and back to the surface to quantify plankton vertical distributions in the sampling area. Because high densities of gelatinous zooplankton, which were present in all years of the study, clog up the net samplers (Figure 10-3), we also deployed the VPR to make a quick inspection for high densities of gelatinous zooplankton in a proposed net sampling area before deciding to deploy the larger net samplers.

Upon retrieval of the VPR, when at sea, we downloaded the compressed video data to specialized image processing computers. These computers used Autodeck programming from Seascan to quantitatively extract image frames that contained “Regions of Interest”, that is, potentially contained a planktonic species. We then scanned each Region of Interest image set to remove bad frames, images of air bubbles, and images of duplicate plankton. After the cruise at the NEFSC Woods Hole laboratory, using a modified version of Visual Plankton developed by the Woods Hole Oceanographic Institution (Tang et al. 1998), we re-analyzed the Regions of Interests to classify the planktonic images to general taxonomic categories. We then hand corrected the Region of Interest taxonomic categories to improve accuracy and to extract lower level taxonomic categories of interest. In addition, when at sea, we used the

oceanographic data from tow-yo VPR hauls to create interpolated profiles of temperature, salinity, density, raw chlorophyll and raw turbidity values. These profiles were available in near real time for the protected species visual teams on the ship.

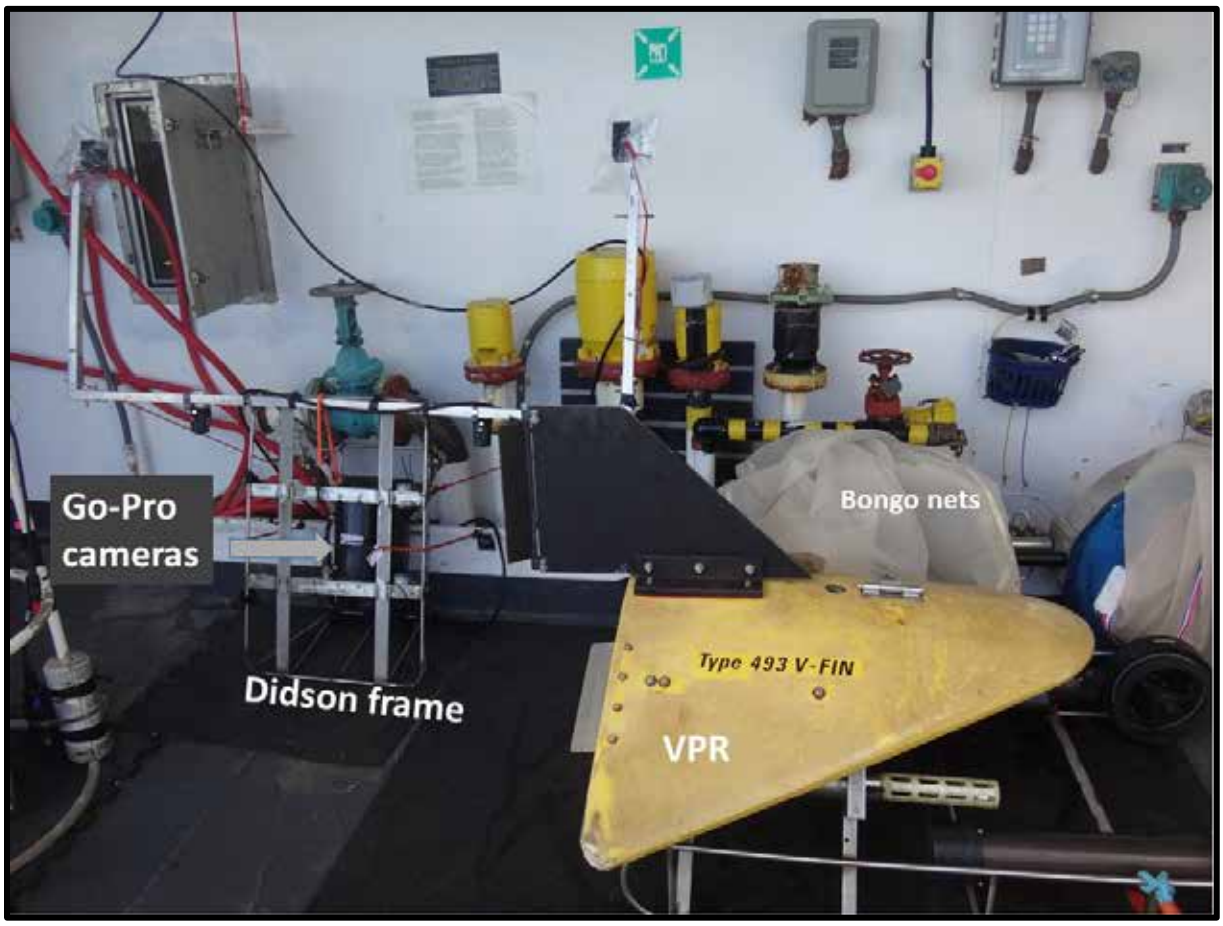

Figure 10-2 VPR, bongo nets, and Didson frame with Go-Pro cameras
Photograph of the side sampling station on the NOAA ship *Henry B. Bigelow*.

Figure 10-3 Photograph of clogging the mesh of the midwater trawl

10.2.2.2 Go-Pro

We used Go-Pro cameras in 2015 and 2017 to collect vertical profile video data. In 2015, we mounted 2 Go-Pros facing each other separated by 148.2 cm and boomed out 70 cm on a rigid frame with the DIDSON (Figure 10-4). With the cameras set to 1080 wide and the refraction of the water, this allowed the overlapping video coverage of the 2 cameras to record images from 1 square meter when lowered and raised vertically though the water column. We attached a Star-Oddi DST–CTD to the platform to record temperature and salinity. During each cast the platform was lowered to 100 meters then slowly brought to the surface pausing for 2 mins at 7 depths (100, 75, 50, 40, 30, 20, and 10 m). In 2017 an improved, 2-camera, 2-light GO-pro system was mounted on the top bar of the frame-net (Figure 10-4). We turned on the cameras and lights just before deployment. We recorded oceanographic data from a Seacat19+ mounted on the wire just above the net. Plankton individuals react strongly to light, where light attracts some species and other species avoid light. To study if the strong continual light needed for the cameras affected capture rates, the illumination was white light for some tows and red light for the rest.

Figure 10-4 Photograph of Go-Pro cameras and lights deployed on the top bar of the frame-net
From the 2017 *NOAA ship Henry B. Bigelow* cruise HB1704.

10.2.2.3 DIDSON

In 2015, we deployed a Sound Metrics DIDSON 300 imaging sonar mounted in a steel cage immediately after deploying the Go-Pro in its frame (Figure 10-2). The DIDSON was set to sample a small area, with a focus of 1.04 m and followed the same sampling profile as the cameras, being lowered to 100 meters then slowly brought to the surface pausing for 2 mins at 7 depths (100, 75, 50, 40, 30, 20, and 10 m).

10.2.3 Net Samplers

10.2.3.1 Bongo Net

We collected samples by making double oblique tows using the 61-cm bongo frame equipped with 2 335 µm nets and a Seabird Seacat 19+ CTD mounted 1 m above the bongo frame with an 80-pound lead weight below the frame (Figure 10-5). We made tows to approximately 5 m above the bottom, or to a maximum depth of 200 m. We conducted all plankton tows at a ship speed of 1.5 to 2.0 kts. We deployed the bongo approximately 3 times a day: once before the daily visual surveying started (about 0500 to 0530), at lunchtime (about 1200 when the ship stopped surveying), and again, after surveying (approximately 1800, depending on weather and timing of sunset). We also deployed bongos at night to fill special sample requests or increase geographical coverage.

We rinsed plankton samples from the nets using the lowest water pressure possible and immediately preserved the plankton. We preserved 1 net in undenatured ethanol that we changed after 24 to 48 hrs. We preserved the other net in 5% formalin and seawater. We shipped the samples in formalin to the Polish Sorting Center for processing. We removed all ichthyoplankton, identified larvae to the lowest taxonomic level possible, enumerated, and measured the standard lengths of a subset. We split the remaining zooplankton to subsample containing a minimum of 500 individuals. We enumerated and identified individual planktons to the lowest possible taxonomic level and life stage. To preserve the genetic integrity of the ichthyoplankton in the sub-set of samples preserved in ethanol, staff in Woods Hole and Narragansett removed, identified, and enumerated all the ichthyoplankton.

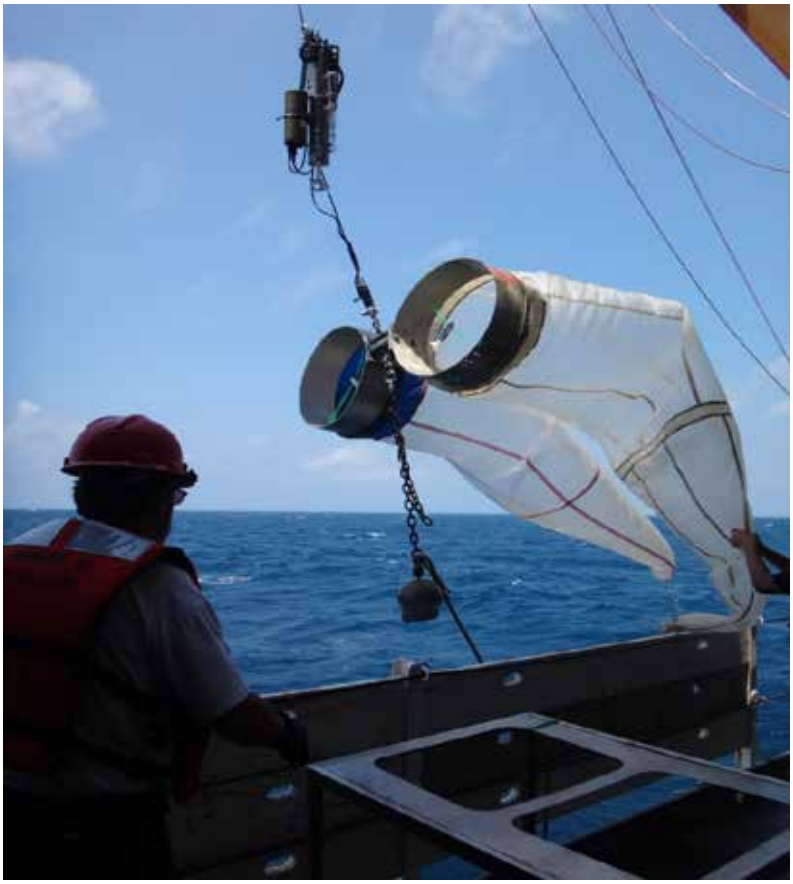

Figure 10-5 Photograph of bongo net being deployed with Seacat CTD on the wire above bongo

10.2.3.2 1 x 2m Frame-net

During 2016 and 2017 we deployed a 1x2 m rectangular frame-net (Figure 10-4) equipped with a 335 µm mesh net and analog flowmeter opportunistically when the oceanographic conditions were within the temperature and salinity parameters to target Atlantic bluefin tuna larvae (*Thunnus thynnus*). We towed the net in a "W" pattern between the surface and 25 m depth. Note, this net set up is similar to a neuston net, but by naming convention, a neuston net is only a surface tow. Each frame-net tow was accompanied by a bongo tow so Atlantic larval bluefin abundances could be compared with standard plankton survey methods used in the Northeast Atlantic, Gulf of Mexico, and Mediterranean Sea. We rinsed the samples from the nets using the lowest water pressure possible and immediately preserved the samples in undenatured ethanol, which we changed after 24 to 48 hrs. Currently we are processing samples to remove all ichthyoplankton and identify the larva to the lowest taxonomic level possible.

10.2.3.3 Midwater Trawl

During 2015 and 2016, we used a modified Marinovich midwater trawl as the primary trawl to sample pelagic fish and macrozooplankton (Figure 10-6). We deployed the midwater trawl with 1.8 m super krub doors, 100 lbs tom weights, 30-fathom bridles, while traveling at about 3 kts. The mouth opening when fishing was approximately 6 x 8 m (horizontal x vertical). The codend liner was ¼" (0.625 cm) knotless nylon. We brought a polytron midwater rope trawl as a backup, but we never deployed it. We monitored the midwater trawl during deployment by a Simrad FS70 trawl sonar mounted on the head rope. The FS70 provided real-time data and recorded the data to a file that we archived at the NEFSC.

We deployed midwater trawls to sample acoustic backscatter observed in the multifrequency acoustic data and decisions on where and when to sample were made on an *ad hoc* basis depending on the observed backscattering patterns. Tow depths and durations were set separately for each trawl and were not consistent among trawl hauls.

Figure 10-6 Marinovich Midwater trawl
We suspended the trawl at the NEFSC net loft facility to provide a better view of its size. Michael Jech is standing in the mouth (i.e., opening) of the net for scale.

10.2.4 Physical Oceanography

10.2.4.1 SeaCAT 19+ CTD

We mounted a Sea-bird SeaCAT 19+ CTD on the wire above the sampling gear on all bongo (Figure 10-5), frame-net, and VPR hauls. The Seabird 19+ provided real time depth and oceanographic data allowing accurate deployments of net and imaging systems. We took water samples twice daily to provide salinity calibration data for the conductivity sensor. We used temperature and salinity data from daily CTD casts to calculate sound speed values for use in instrument calibration by the active and passive acoustic teams.

10.2.4.2 Sea-bird 911 CTD

We deployed a Sea-bird 911 CTD equipped with a 12 Niskin bottle rosette, a Benthos altimeter, a WetLabs Fluorometer-Transmissometer, an oxygen sensor and a Photosynthetically Active Radiation light sensor both opportunistically in addition to immediately after each midwater trawl (Figure 10-7). We deployed the Seabird 911 in a vertical fashion when the ship was holding station.

Figure 10-7 Sea-bird 911 CTD on a 12 Niskin bottle rosette
Also, on the side sampling station of the NOAA ship *Henry B. Bigelow* are the VPR, bongo nets and the Frame-net.

10.3 Results

We summarized the status of data processing in Table 10-1.

Table 10-1 Number of oceanographic and net samples and their processing status
Samples collected from the 2015 to 2019 AMAPPS II cruises. See Chapter 11 for more on each cruise. NA = not applicable.

Equipment	Action	HB1503	HB1603	HB1704	EN1801	GU1803	EN1901	TOTAL
CTD 19+	Number	53	239	56	17	16	17	398
	status	complete	complete	Complete	complete	complete	processing	
CTD 911	Number	10	13	0	4	5	3	35
	Status	complete	complete	NA	complete	complete	processing	
Bongo	Number	26	113	16	5	5	5	170
(333µm)	Status	complete	complete	Complete	complete	complete	processing	
Bongo	Number	26	113	15	5	5	5	169
(150µm)	Status	complete	complete	processing	processing	processing	processing	
VPR	Number	4	0	26	4	0	4	38
(TowYo)	Status	complete	NA	Complete	complete	NA	complete	
Go-Pro	Number	16	0	16	0	0	0	32
	Status	processing	NA	processing	NA	NA	NA	
Frame-Net	Number	0	34	33	0	1	0	68
	Status	NA	processing	processing	NA	processing	NA	
DIDSON	Number	8	0	0	0	0	0	8
	Status	processing	NA	NA	NA	NA	NA	
Midwater	Number	24	35	0	0	0	0	
Trawl	Status	complete	complete	NA	NA	NA	NA	

10.3.1 EK60

We collected narrowband, multifrequency acoustic data throughout the cruises in 2015, 2016, and 2017. We calibrated the EK60 echosounders in 2015 and 2016 immediately prior to each cruise and in September 2017 for the fall bottom trawl survey. We applied these calibration settings to the AMAPPS data collected during HB1704. We have processed all EK60 data collected on the NOAA ship *Henry B. Bigelow* during 2015 to 2017.

Figure 10-8 illustrates a representative echogram from 2016 showing a 24-hr period that depicts the diurnal vertical migrations of mesopelagic animals at dawn and dusk and images of animals that we captured in the midwater net at the same time.

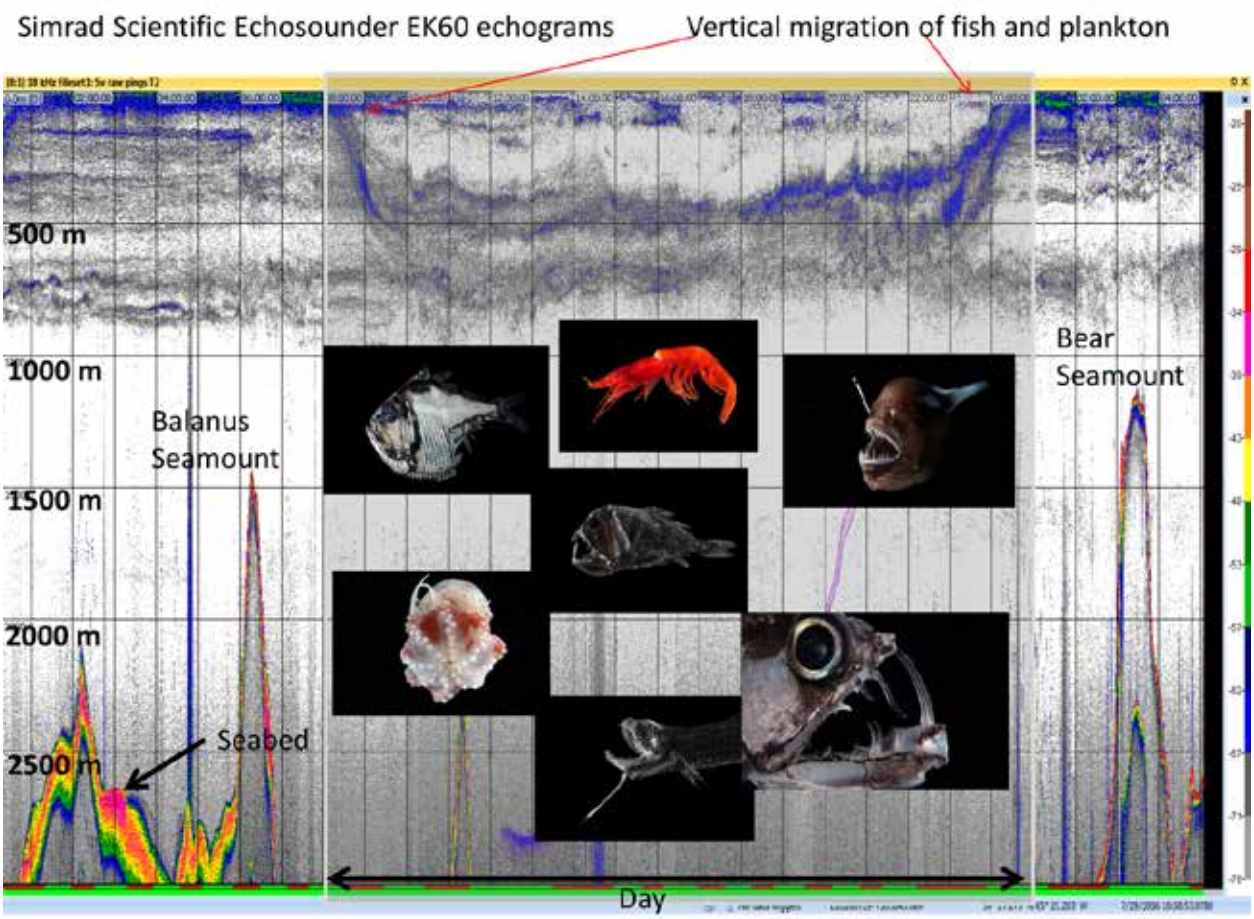

Figure 10-8 Annotated echogram showing 18-kHz EK60 active acoustic data during 2016
The daily migration of mesopelagic organisms is seen during the daytime as the animals migrate from 500 to 800 m depth to near the surface. We have shown a collage of specimens captured in the midwater net including a hatchetfish (*Argyropelicus* spp.), deep-sea shrimp, anglerfish (*Melanocetus* spp.), viperfish (*Chauliodus sloani*), bristlemouth (Gonostomatidae), squid, and ogrefish (*Anoplogaster cornuta*) (spiraling clockwise starting with the upper left image).

10.3.2 Imaging

10.3.2.1 VPR

We conducted 38 tow-yo VPR hauls between 2015 and 2019. We hand corrected all hauls taken during AMAPPS cruises to provide quality control of category identifications and creation of categories for small but important classes of plankton such as ichthyoplankton.

Orphanides et al. (2019) utilized the data from VPR hauls made on the 2018 R/V *Endeavor* cruise, EN1801 to compare the ctenophore (*Mertensia ovum*) area measurements generated by Visual Plankton using pixel brightness to areas calculated using length and width measurements taken by hand. The hand area measurements (mean 161.29 mm/m^3 per frame, standard deviation 292.10 mm/m^3) were generally larger than the Visual Plankton generated measurements (mean 73.02 mm/m^3 per frame, standard deviation 133.41 mm/m^3). Since all images of ctenophores, including *Mertensia*, have large areas of darkness between the brighter areas of the ctenophores (Figure 10-9), it is understandable that the Visual Plankton area measurement method utilizing pixel brightness underestimated total area. This highlights that we need to conduct more analyses to determine the accuracy of the Visual Plankton generated area

data for each taxonomic category before using the Visual Plankton generated area data in future comparisons with the EK60 or protected species data.

The process of matching the hand measured Regions of Interests to the Visual Plankton processed Regions of Interests revealed that Visual Plankton only processed Regions of Intersts smaller than 300K. Consequently, we re-wrote the Visual Plankton sub-programs affecting processing size to take advantage of the capabilities of newer computers to process images up to 1500K in size. We have now reprocessed all VPR haul data conducted during the AMAPPS cruises. In addition, all data were hand corrected to quantify the effects on zooplankton densities. Preliminary analysis between the 2 programs indicated that the older version of Visual Plankton had accurate density calculations for smaller size categories like copepods, hydromedusa, and pteropods; however, the older version under-estimated the density calculations of larger size categories such as ctenophores and crustacea.

Figure 10-9 VPR image of taken on Nantucket Shoals
On the April 2018 *R/V Endeavor* cruise, EN1801 cruise.

10.3.3 Net Samplers

10.3.3.1 Bongo Net

We completed 169 bongo tows during cruises in AMAPPS II (2015 to 2019). Bongo tows from the AMAPPS cruises extended the range of plankton sampling conducted by the NEFSC Oceans and Climate Branch to include the area of the Northwest Atlantic extending from New England to the mid Atlantic Bight between the shelf slope and the Gulf Stream. In addition, the locations of some of the AMAPPS bongo tows provided additional coverage in under sampled areas of the standard NEFSC EcoMon plankton surveys on the shelf.

We archived all processed bongo samples and ichthyoplankton samples at the NEFSC Narragansett Laboratory. We also added the plankton data to the NEFSC plankton Oracle database, which are available upon request from the NEFSC Oceans and Climate Branch. The longer-term goal is to use these plankton data to compare to protected species distribution and density patterns and to include them in environmental field models.

We classified all zooplankton data into taxonomic categories and plotted them to show abundance and sampling coverage over the AMAPPS sampling period from 2011 to 2015. Because we conducted the majority of sampling at night, the diel vertical migrations of some off-shelf species resulted in a variable catch of these species in our nets that sampled from the surface to a maximum of 200 m. A consequence of this is that some of the plotted plankton densities may not be the densities the marine mammals we detected during the day encountered within the top 200 m. Pteropods are very episodic so seasonal plots are not accurate and gelatinous zooplankton densities are currently not quantitative so we did not include these categories in this report.

The all-inclusive zooplankton category plot showed consistently higher zooplankton densities on the continental shelf as compared to farther offshore (Figure 10-10).

The copepod category comprised mainly of copepod species, though small crustaceans (crab zoea, ostracods and barnacle nauplii) were also minor contributors. The copepod category seasonal distribution patterns (Figure 10-11) generally followed patterns previously reported for zooplankton biomass, with lower densities in the fall and higher densities in the spring and summer (Sherman et al. 1998).

Density plots of the number of copepods per 100 m^3 collected from the 2011 to 2015 AMAPPS shipboard bongo tows during the spring (A), summer (B), fall (C) and all seasons (D). This category also included crab zoea, ostracods, and barnacle nauplii. The copepod category comprised mainly of copepod species, though small crustaceans (crab zoea, ostracods and barnacle nauplii) were also minor contributors. The copepod category seasonal distribution patterns (Figure 10-11) generally followed patterns previously reported for zooplankton biomass, with lower densities in the fall and higher densities in the spring and summer (Sherman et al. 1998).

The ichthyoplankton category (Figure 10-12) comprises of larval fish and small mesopelagic fish. On the shelf, this category comprised of mostly larval fish, while off the shelf, it comprised of mostly myctophiids, a small mesopelagic fish. The high densities of ichthyoplankton off Delaware Bay and just south of Nantucket Shoals are important summer nursery areas for many species of larval fish.

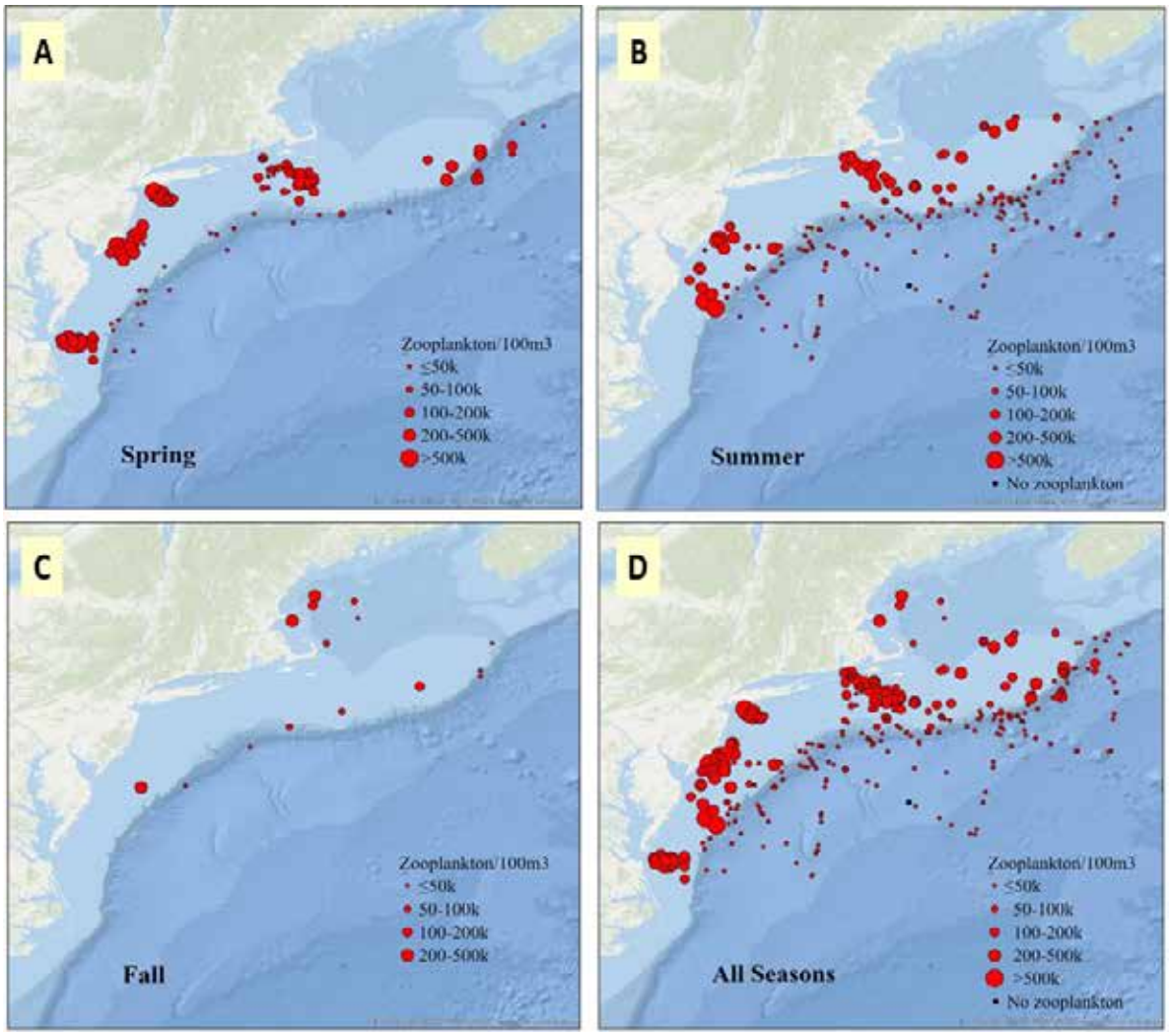

Figure 10-10 Seasonal distribution and density plots of all zooplankton from bongo hauls
Density plots of the number of zooplankton per 100 m^3 collected from the 2011 to 2015 AMAPPS shipboard cruises during the spring (A), summer (B), fall (C) and all seasons (D). Spring is 1 March to 31 May; summer is 1 June to 31 August; and fall is 1 September to 30 November.

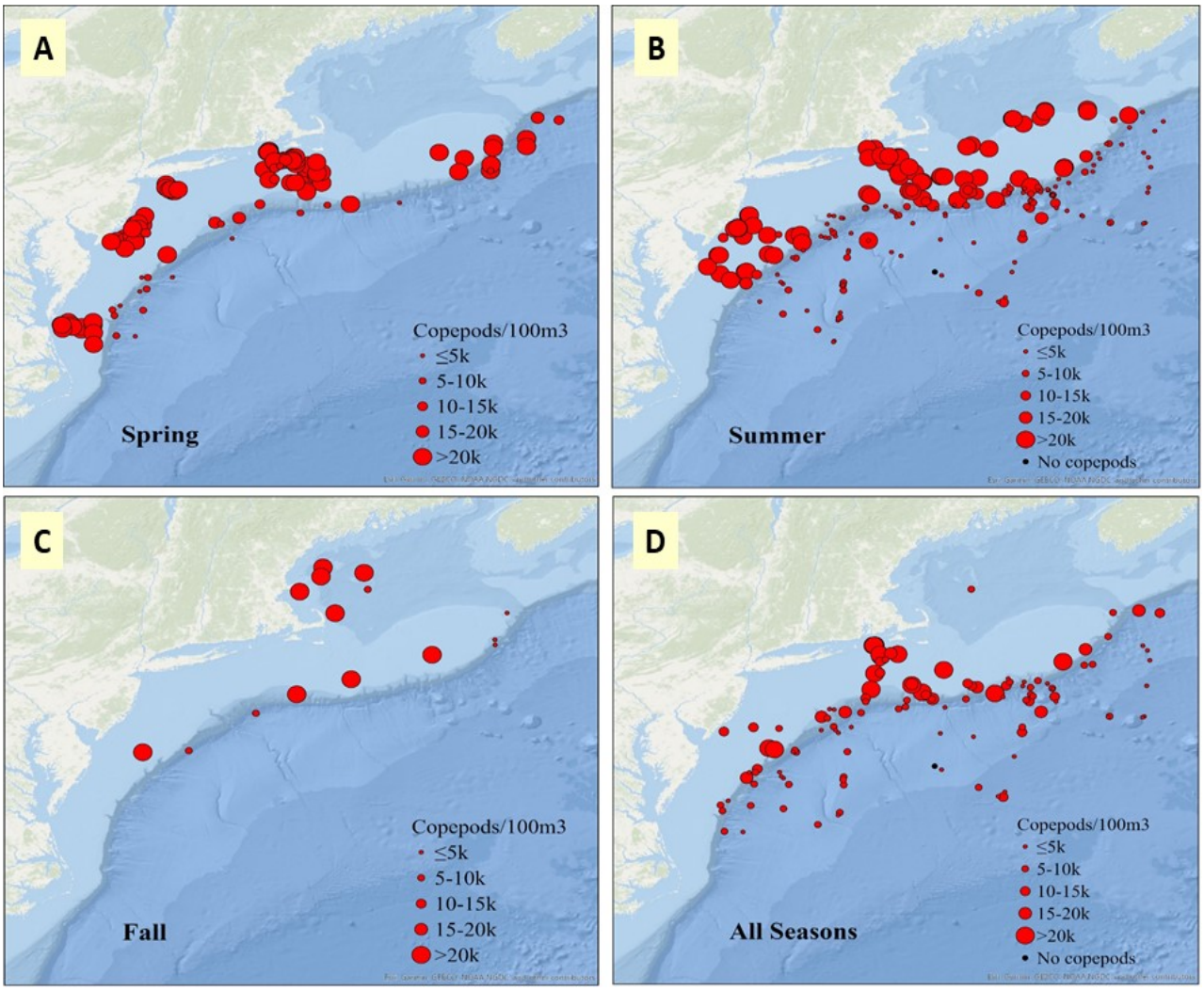

Figure 10-11 Seasonal distribution and density plots of the copepod category
Spring is 1 March to 31 May; summer is 1 June to 31 August; and fall is 1 September to 30 November.

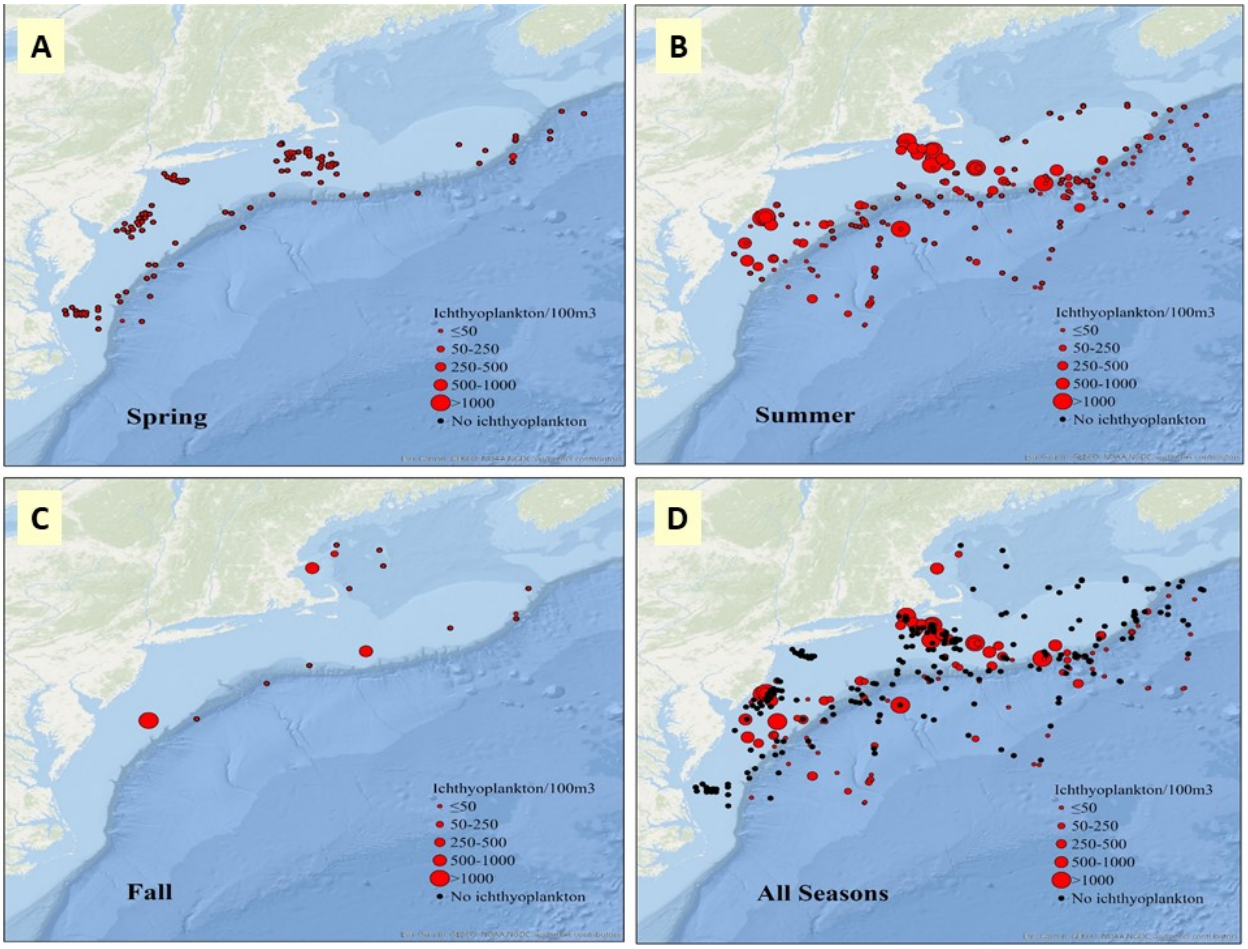

Figure 10-12 Seasonal distribution and density plots of the ichthyoplankton category
Density plots of the number of ichthyoplankton per 100 m^3 collected from the 2011 to 2015 AMAPPS shipboard bongo tows during the spring (A), summer (B), fall (C) and all seasons (D). This category included larval fish and small mesopelagic fish such as Mychophiidae. Spring is 1 March to 31 May; summer is 1 June to 31 August; and fall is 1 September to 30 November.

The crustacea category (Figure 10-13) comprised of large (>1cm) crustaceans: krill, amphipods, shrimp, and mysids. The high densities of crustacean on the shelf were mostly shrimp or mysids, while the higher densities along the shelfbreak and offshore were mostly krill. Sampling sites on the shelf also included Gammarid amphipods, which are common epibenthic swarmers. We found hyperiid amphipods throughout the sampling area associated with gelatinous zooplankton. Because larger crustaceans can avoid bongo nets, and krill and gammarids have strong diel vertical migrations, these crustacea density plots offer an incomplete description of their distribution and relative abundance.

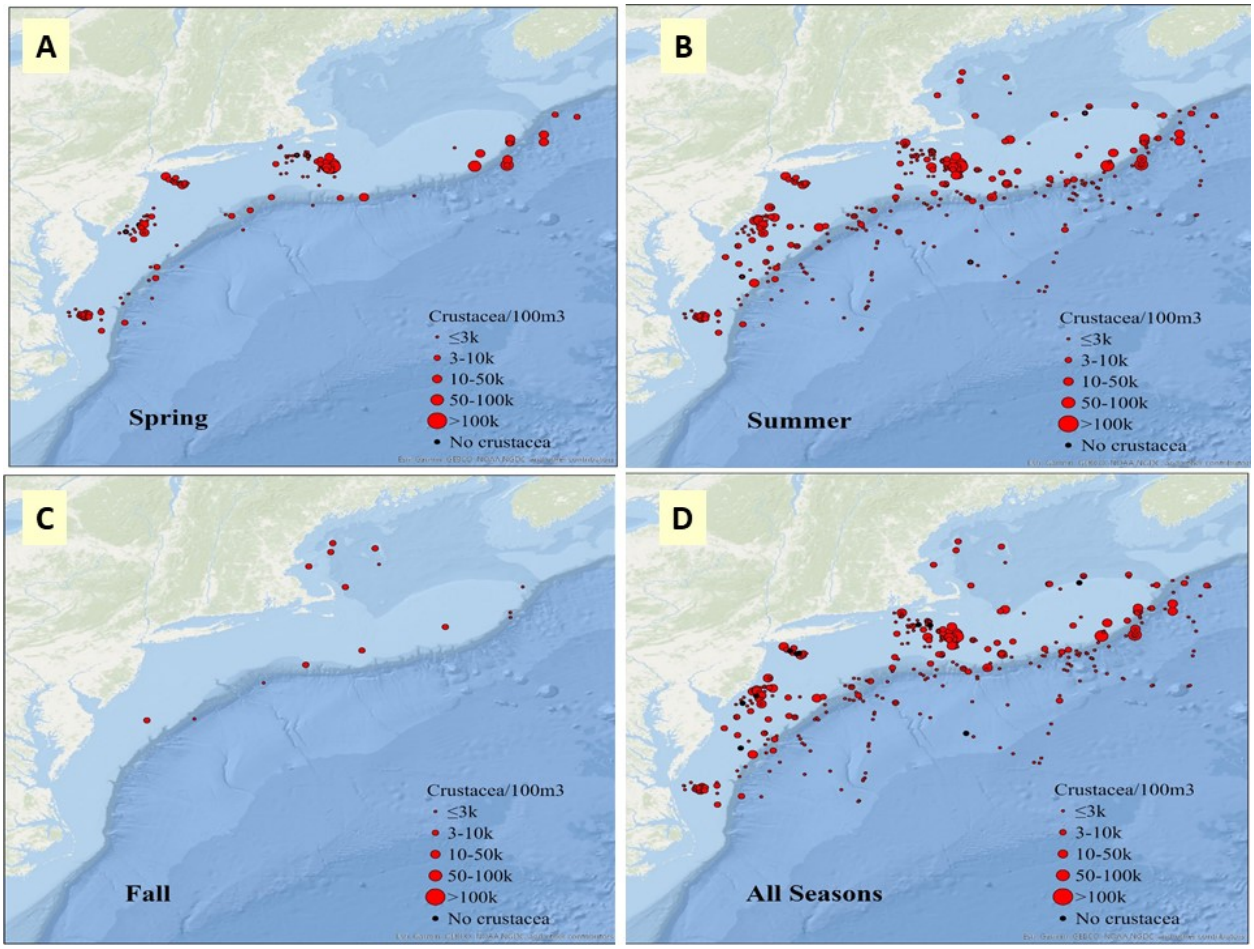

Figure 10-13 Seasonal distribution and density plots of the Crustacea category
Density plots of the number of Crustacea per 100 m^3 collected from the 2011 to 2015 AMAPPS shipboard bongo tows during the spring (A), summer (B), fall (C) and all seasons (D). This category included krill, amphipods, shrimp, and mysids. Spring is 1 March to 31 May; summer is 1 June to 31 August; and fall is 1 September to 30 November.

10.3.3.2 Frame-net

Ocean and Climate branch staff in Narragansett, RI is currently processing frame-net samples. We are removing all ichthyoplankton and cephalopod paralarvae from each sample and identifying them to the lowest taxonomic level possible. We then plan to measure a subset of, and count, each fish larvae. All larval bluefin tuna are being additionally processed (see Special Studies section for details).

10.3.3.3 Midwater Trawl

We conducted midwater trawl sampling only during dark hours as we conducted the sampling opportunistically after the completion of the visual survey component each day. We directed trawl hauls to sample acoustic scattering layers from about 50 m to about 800 m depth, with each tow sampling a consistent depth (Figure 10-14). We sorted catches to the lowest taxonomic level possible (Table 10-2), where we weighted en masse each taxon, and we measured up to about 100 individual lengths. We collected trawl hauls 1 to 16 during HB1503 on the shelf and the remaining trawl hauls in deeper oceanic waters during the 2015 and 2016 cruises.

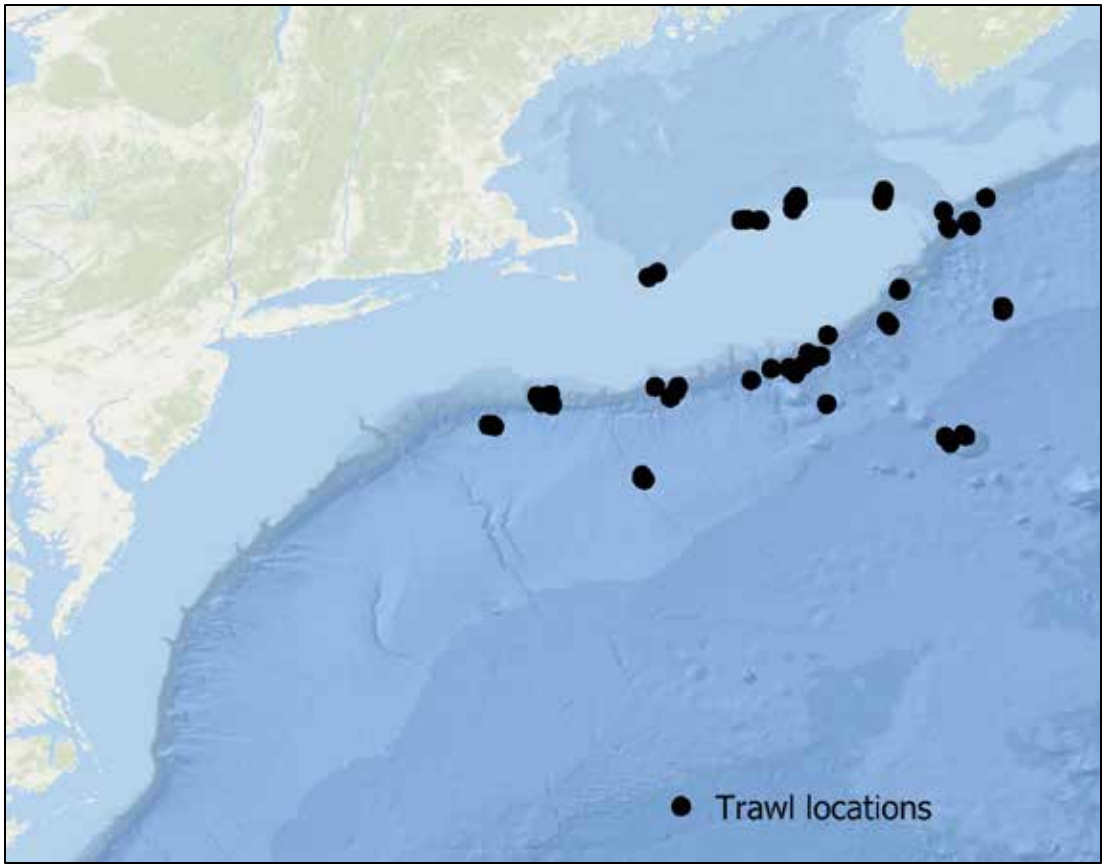

Figure 10-14 Location of trawl sites during AMAPPS II surveys

Table 10-2 List of animals captured during HB1603 in midwater trawl catches

This species list is representative of animals captured during HB1503 as well. The code "UNK" denotes classification not completed to that taxonomic level.

Order	Family	Genus	Species
Amphipoda	Phronimidae	phronima	UNK
Anguilliformes	Anguillidae	Anguilla	UNK
Anguilliformes	Derichthyidae	Derichthys	serpentinus
Anguilliformes	Derichthyidae	Nessorhamphus	ingolfianus
Anguilliformes	Nemichthyidae	Labichthys	carinatus
Anguilliformes	Nemichthyidae	Nemichthys	scolopaceus
Anguilliformes	Serrivomeridae	Serrivomer	beanii
Argentiniformes	Argentinidae	UNK	UNK
Argentiniformes	Bathylagidae	Bathylagus	euryops
Aulopiformes	Alepisauridae	Alepisaurus	brevirostris
Aulopiformes	Anotopteridae	Anotopterus	pharao
Aulopiformes	Evermannellidae	Evermannella	balbo
Aulopiformes	Notosudidae	Scopelosaurus	lepidus
Aulopiformes	Paralepididae	Paralepis	UNK
Beryciformes	Anoplogastridae	Anoplogaster	cornuta
Beryciformes	Holocentridae	UNK	UNK
Cephalopoda	UNK	UNK	UNK
Cetomimiformes	Rondeletiidae	Rondeletia	loricata

Order	Family	Genus	Species
Cnidaria	UNK	UNK	UNK
Decapoda	Acanthephyridae	Acanthephyra	UNK
Decapoda	Pasiphaeidae	UNK	UNK
Decapoda	UNK	UNK	UNK
Decapodiformes	Chtenopterygidae	Chtenopteryx	UNK
Gadiformes	Macrouridae	Coryphaenoides	UNK
Gadiformes	Merlucciidae	UNK	UNK
Lampriformes	Regalecidae	Regalecus	glesne
Lampriformes	Stylephoridae	Stylephorus	UNK
Littorinimorpha	Carinariidae	Carinaria	lamarckii
Lophiiformes	Ceratiidae	Cryptosaras	couesii
Lophiiformes	Melanocetidae	Melanocetus	johnsonii
Myliobatiformes	Dasyatidae	Pteroplatytrygon	violacea
Mytctophiformes	Myctophidae	Benthosema	UNK
Mytctophiformes	Myctophidae	Diaphus	UNK
Mytctophiformes	Myctophidae	Diogenichthys	UNK
Mytctophiformes	Myctophidae	Gonichthys	UNK
Mytctophiformes	Myctophidae	Lampadena	UNK
Mytctophiformes	Myctophidae	Lampanyctus	UNK
Mytctophiformes	Myctophidae	Lepidophanes	UNK
Mytctophiformes	Myctophidae	Loweina	UNK
Mytctophiformes	Myctophidae	Myctophum	UNK
Mytctophiformes	Myctophidae	Notoscopelus	UNK
Mytctophiformes	Myctophidae	Protomyctophum	UNK
Mytctophiformes	Myctophidae	Taaningichthys	UNK
Mytctophiformes	Myctophidae	UNK	UNK
Octopoda	Alloposidae	Haliphron	atlanticus
Octopoda	Amphitretidae	Bolitaena	UNK
Octopoda	Octopodidae	UNK	UNK
Oegopsida	Ancistrocheiridae	UNK	UNK
Oegopsida	Chiroteuthidae	UNK	UNK
Oegopsida	Cranchiidae	UNK	UNK
Oegopsida	Cycloteuthidae	UNK	UNK
Oegopsida	Enoploteuthidae	UNK	UNK
Oegopsida	Histioteuthidae	Histioteuthis	UNK
Oegopsida	Histioteuthidae	UNK	UNK
Oegopsida	Histioteuthidae	UNK	UNK
Oegopsida	Histioteuthidae	UNK	UNK
Oegopsida	Histioteuthidae	UNK	UNK
Oegopsida	Lepidoteuthidae	Lepidoteuthis	UNK
Oegopsida	Octopoteuthidae	Octopoteuthis	UNK
Oegopsida	Ommastrephidae	Illex	illecebrosus
Oegopsida	Ommastrephidae	UNK	UNK
Perciformes	Ariommatidae	Ariomma	bondi
Perciformes	Carangidae	Caranx	crysos
Perciformes	Carangidae	Caranx	hippos
Perciformes	Carangidae	Selene	setapinnis

Order	Family	Genus	Species
Perciformes	Carangidae	UNK	UNK
Perciformes	Gempylidae	Nealotus	tripes
Perciformes	Howellidae	Howella	sherborni
Perciformes	Luvaridae	Luvarus	imperialis
Perciformes	Moronidae	UNK	UNK
Perciformes	Priacanthidae	Heteropriacanthus	cruentatus
Perciformes	Scombridae	Auxis	rochei
Perciformes	Scombridae	Auxis	thazard
Perciformes	Scombrolabracidae	Scombrolabrax	heterolepis
Perciformes	Trichiuridae	Aphanopus	carbo
Perciformes	Trichiuridae	Benthodesmus	simonyi
Perciformes	Trichiuridae	Trichiurus	lepturus
Perciformes	Zoarcidae	Melanostigma	atlanticum
Salpida	Salpidae	Salpa	UNK
Salpida	Salpidae	Thetys	vagina
Scorpaeniformes	Sebastidae	Helicolenus	dactylopterus
Sepiolida	Sepiolidae	UNK	UNK
Stephanoberyciformes	Melamphaidae	Scopelogadus	beanii
Stephanoberyciformes	Melamphaidae	UNK	UNK
Stomiiformes	Gonostomatidae	Bonapartia	pedaliota
Stomiiformes	Gonostomatidae	Sigmops	UNK
Stomiiformes	Gonostomatidae	UNK	UNK
Stomiiformes	Sternoptychidae	Argyropelecus	aculeatus
Stomiiformes	Sternoptychidae	Maurolicus	muelleri
Stomiiformes	Sternoptychidae	Sternoptyx	diaphana
Stomiiformes	Sternoptychidae	UNK	UNK
Stomiiformes	Stomiidae	Aristostomias	tittmanni
Stomiiformes	Stomiidae	Astronesthes	leucopogon
Stomiiformes	Stomiidae	Astronesthes	niger
Stomiiformes	Stomiidae	Chauliodus	sloani
Stomiiformes	Stomiidae	Chirostomias	pliopterus
Stomiiformes	Stomiidae	Echiostoma	barbatum
Stomiiformes	Stomiidae	Idiacanthus	fasciola
Stomiiformes	Stomiidae	Malacosteus	niger
Stomiiformes	Stomiidae	Melanostomias	bartonbeani
Stomiiformes	Stomiidae	Photostomias	guernei
Stomiiformes	Stomiidae	Stomias	boa
Stomiiformes	Stomiidae	Trigonolampa	miriceps
Stomiiformes	Stomiidae	UNK	UNK
Syngnathiformes	Aulostomidae	Aulostomus	maculatus
Syngnathiformes	Fistulariidae	Fistularia	petimba
Teleostei	UNK	UNK	UNK
Tetraodontiformes	Monacanthidae	Aluterus	monoceros
Tetraodontiformes	Monacanthidae	Monacanthus	ciliatus
Tetraodontiformes	Monacanthidae	Stephanolepis	hispidus
Zeiformes	Grammicolepididae	Xenolepidichthys	dalgleishi

10.3.4 Physical Oceanography

We conducted 398 Sea-bird SeaCAT 19+ deployments (Table 10-1). The Sea-bird 19+ provided real time oceanographic and depth data to the shipboard operator conducting bongo, VPR, Niskin, and Frame-net sampling. Deployments were always with a piece of sampling gear so the location of about 80% of the Sea-bird SeaCAT 19+ is in the bongo plots, such as Figure 10-5.

We conducted 35 Sea-bird 911 casts along the shelfbreak mostly immediately after the midwater trawls to about 50m deeper than the net.

The inshore position of the Gulf Stream in 2016 offered a unique opportunity to conduct sampling within the Gulf Stream and in the oceanic waters beyond the Gulf Stream. We conducted opportunistic transects in 2017 that bisected a warm core ring and transected Oceanographer Canyon. Continued oceanographic sampling in the off-shelf area are particularly important to study the increased variability in the Gulf Stream's path (Andres, 2016).

We archived the oceanographic data in the NEFSC Oceans and Climate Branch physical oceanography database and the National Centers for Environmental Information World Ocean Database.

Towing in water with strong turbulent oceanographic features inadvertently creates noisy raw data. Thus, we plan to smooth out the data and remove outliers created by the turbulence during future processing.

10.3.5 Special Studies

The AMAPPS cruises provided a unique opportunity to collect data in under sampled habitats. Thus, we receive requests from other organizations to collect specific species. Below we describe several of these studies.

10.3.5.1 Salps

Dr. Ann Bucklin and her University of Connecticut students and colleagues used samples of salps collected on several AMAPPS cruises (HB1603, GU1702, and HB1704). This research is in collaboration with the Woods Hole Oceanographic Institution (WHOI) Ocean Twilight Zone Project, funded as part of The Audacious Project.

During each AMAPPS cruise, we removed the salps from net and trawl samples, tentatively identified to species, and preserved them in undenatured ethanol for genetic analysis. Several ecologically important, but largely overlooked, salp species were among the samples provided, including *Salpa aspera*, *S. fusiformis*, *Lasis zonaria*, *Thetys vagina*, *Cyclosalpa* spp., and others. Because it is difficult to discriminate the salp species reliably, Bucklin et al. are using the specimens to develop molecular protocols for species identification based on DNA barcodes. These new 'long read' DNA barcodes use Nanopore MinIon and PromethIon sequencing platforms that are available at the University of Connecticut Integrated Systems Genomics facility. They are also using the specimens for molecular analysis of the salp's diet. Salps are among the most important and efficient primary consumers in pelagic zones, but their actual diet and trophic interactions are difficult to analyze. DNA metabarcoding (i.e., high throughput DNA sequencing from complex samples) of salp gut contents is revealing differences between salp species in the taxonomic composition of consumed prey, and is providing new insights into particle and energy transfer in pelagic food webs.

10.3.5.2 Bluefin Tuna

Plankton sampling in 2016 yielded approximately 200 Atlantic bluefin tuna larvae from the Slope Sea (region between the Gulf Stream and the northeast U.S. continental shelf), with processing of samples still

ongoing. Additionally, while not a comprehensive study, a genetic analysis revealed the presence of Atlantic bluefin tuna eggs. Given the water temperatures at the time of collection, the eggs were likely less than 24 hrs old. This sampling confirmed previous work that included AMAPPS I samples that documented the Slope Sea as a spawning area for Atlantic bluefin tuna (Richardson et al. 2016).

We provided larvae from the 2013 sampling Slope Sea sampling to researchers at the AZTI-Tecnalia in Spain that resulted in a 2019 publication on bluefin genetic population structure (Rodríguez-Ezepeleta 2019). They are continuing to work on the population structure issue. This work has facilitated the the tuna that allows for the assignment of catches to their population of origin, which is crucial for ensuring that managers base their actions on biologically meaningful stock units rather than simply on catch location. We sent an additional 40 larvae from the 2016 survey to AZTI-Tecnalia researchers, who are including them in further analyses.

Of the bluefin tuna identified, we have dissected 66 samples to retrieve their otoliths for age and growth analyses. The data from these otoliths indicate an average growth rate of 0.37 mm per day over the first 8 daily increments (Figures 10-15). This growth rate is very similar to that of larvae spawned in the Gulf of Mexico. This project formed a dissertation chapter for C. Hernández (WHOI; Hernández 2021).

In July 2017, during HB1704, we found Atlantic bluefin tuna larvae in an anti-cyclonic eddy immediately east of Georges Bank (Figure 10-16). We released a set of 3 drifters with satellite transmission inside this eddy on 11 July 2017. Two drifters stayed together, possibly caught on 1 another; these 2 drifters made 3 complete revolutions in the eddy, exited to the southwest, and began to move southwestward along the shelfbreak at Georges Bank. One of these drifters then broke apart, and the crew of a fishing vessel recovered the buoy and transponder and brought it into port at New Bedford/Fairhaven, Massachusetts where C. Hernández retrieved it (Hernandez 2021). The second drifter continued to move southward along the shelfbreak, recording until 15 December 2017. The third drifter moved faster as the drifters departed their initial position; it made 4 full revolutions in the eddy and made an additional elliptical revolution to the southeast of the eddy position (Figure 10-16). This drifter continued to move eastward into the Atlantic Ocean and transmitted its position until 13 February 2018. The full tracks and corresponding data are available online through the NOAA drifter program.

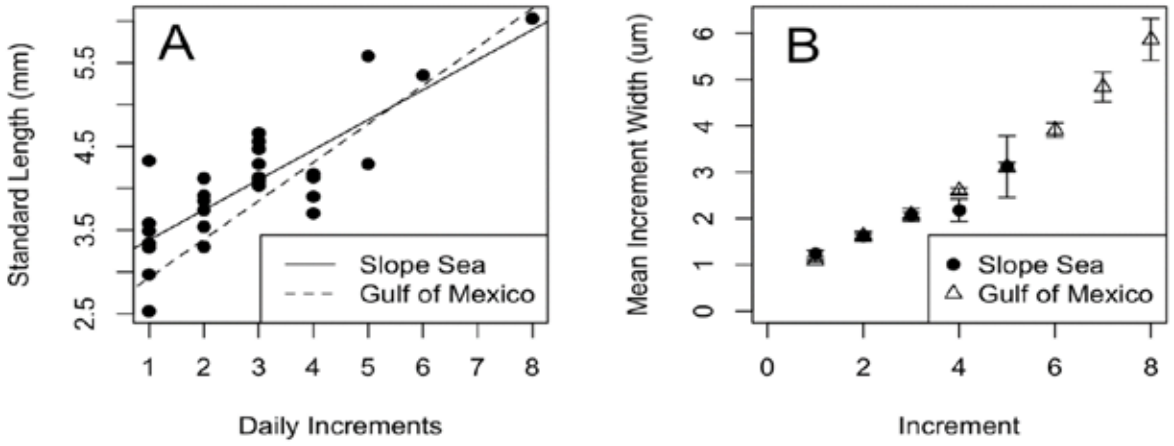

Figure 10-15 Preliminary growth data from North Atlantic bluefin tuna larval otoliths
(A) Plot of length-at-age for Slope Sea larvae (n=30), with the best fitting line in solid (Standard Length = 3.02+0.36·Daily Increments) and the best fitting line for Gulf of Mexico larvae (n=138) up to 8 days plotted as a dashed line (Standard Length = 2.47+0.46*Daily Increment). (B) Plot of daily increment widths for Slope Sea and Gulf of Mexico larvae, where all daily increments with data were from at least 3 larvae.

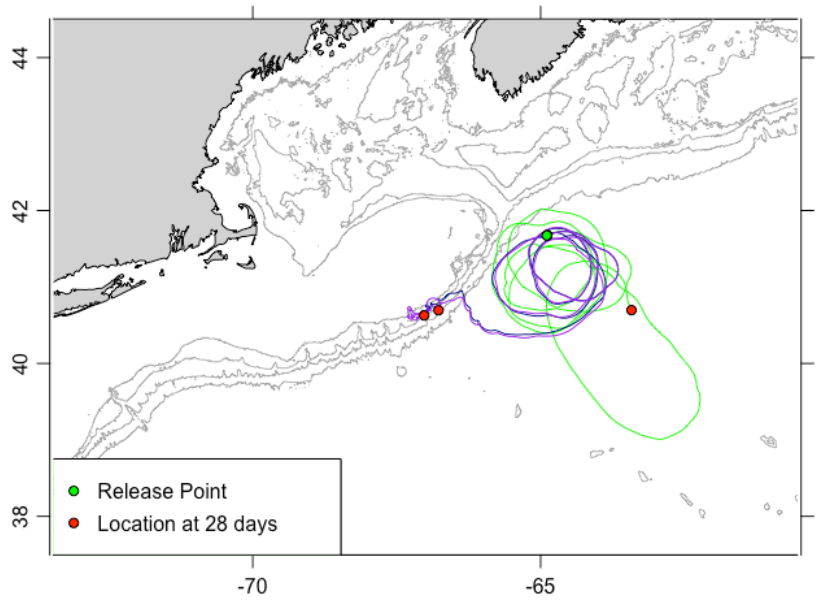

Figure 10-16 Drifter tracks from 11 July to 8 August 2017
We released 3 drifters into an anticyclonic eddy after Atlantic bluefin tuna larvae were in 2 consecutive stations along a cross-eddy transect. The bathymetric contours are 100, 200, 1000, and 2000 m, and are from the GEBCO_2014 Grid, version 20150318.

10.3.5.3 VPR Image Processing

The large VPR image data sets made possible by the AMAPPS opportunistic have highlighted our limitations in data processing. Even with computer advancements and programming upgrades, we are at the upper limits of the math-based matrix-analysis image identification programs that we have been using. We applied for and received a grant from the NOAA High Performance Computing and Communications program to upgrade the VPR cameras to color and to begin to adapt the Video and Image Analytics for a Marine Environment (VIAME) software for Region of Interest identification. VIAME is an open-source system for analysis of underwater video and imagery for fisheries stock assessment developed by Kitware in cooperation with NOAA's Automated Image Analysis Strategic Initiative. Leveraging the capabilities of Machine Learning presents an opportunity to improve the speed, accuracy, and cost of plankton image identification. Improving the Data Analytics associated with plankton image data; especially analytics, data transfer, querying, curating, and sharing, will make fine scale plankton data available for distribution, modeling, and other studies. The project will use VPR data collected during the AMAPPS cruises to evaluate VIAME as a tool to increase the quality and speed up the availability of plankton data by improving processing speed, accuracy of automated identification, and sharing of completed data. We are in the process of prototyping and documenting the adaptation of VIAME machine learning to identify VPR images. We will create programming using open-source code to aggregate data to a relevant format, and store imagery and data in an Oracle database using the NEFSC Plankton Database format. The plan is to share the documentation, processes, image databases, tools, and code so other researchers can use it.

10.3.5.4 Imaging Flow Cytobot

During the 2016 abundance survey on the NOAA ship *Henry B. Bigelow* Robert Olsen and Heidi Sosik of WHOI connected to the ship's flow through seawater system an Imaging Flow Cytobot. This sampled water at 3 m depth and continuously sampled 5 ml aliquots of seawater. For each sample, the Cytobot imaged all phytoplankton in a size range of 10 to 100 . To complement these data, we added a Wetlabs Eco-flur turbidity and fluorescence sensor to the Seabird 19+ CTD. The software associated with the

Cytobot archived all images and allowed images to be visualized in real time. Data and more information are available at the Imaging Flow Cytobot website.

10.3.5.5 Relating echosounding to cetaceans

See section 6.4 that describes an explorative study to test the utility of echosounder-based predictive variables for modeling the spatiotemporal distribution and abundance of marine mammals (Orphanides 2019). We used the multi-frequency echosounder data to quantify the density of 4 organism types (fish with swim bladders, larval fish and phytoplankton, fluid-like zooplankton, and fish with no swim bladder).

10.4 Key Findings

From what we are finding in other parts of this report, the patterns of distribution and abundance of cetaceans, sea birds, and sea turtles are variability, both within the year and between years, and some species appear to be shifting their distribution farther north. To understand these patterns, we need to learn more about the target's species biotic and abiotic environment. This chapter has highlighted the lower trophic level biotic data we collected in the data poor areas of the US Atlantic shelfbreak and offshore regions. Though it takes a long time to process these types of data, we have completed some of it and we are starting to see the pay-off.

Through the samples collected during AMAPPS, we, along with our collaborators, have documented North Atlantic bluefin tuna eggs and larvae in the Slope Sea showing that this area is a spawning area for the bluefin tuna. In addition, the bluefin tuna larvae are growing at rates similar to larvae spawned in the Gulf of Mexico, the previously only known spawning area in US waters.

Another key finding is we showed that the EK60 echosounder data collected during the AMAPPS shipboard surveys quantified the density of 4 organism types (fish with swim bladders, larval fish and phytoplankton, fluid-like zooplankton, and fish with no swim bladder). We were then able to in an exploratory study use these densities as habitat covariates to develop cetacean density-habitat models, where for some species the models fit as well as models using a multitude of proxy habitat covariates. See section 6.4 for more details. We plan to expand this exploratory study.

10.5 Data Gaps and Future Work

Shelfbreak and offshore data are limited due to the lack of research cruises in these waters, despite the fact that many species at all trophic levels utilize these waters. These off-shelf waters serve either as a permanent residence or as part of migratory paths for many species. Enhancing the off-shelf ecosystem descriptions is essential to understanding and accurately describing protected species habitat. Continued plankton and oceanographic sampling in conjunction with the AMAPPS cruises will extend the temporal and geographic coverage of the data set.

With the lower trophic level data recently processed and those data still to be processed, some of the questions that we will address with longer-term data sets include the following:

1) Are the observations about gelatinous zooplankton blooms single events, ongoing processes, or annual occurrences?
2) What is the annual variability in plankton densities and dominant gelatinous zooplankton species along the shelfbreak?
3) What is the annual variability in Atlantic bluefin tuna larvae and egg production?

Answers to these questions should enhance our ability to be able to associate the lower-trophic level species' changes in distribution and density to the changes and/or variability in higher-level trophic level species, such as cetaceans, sea turtles, and sea birds. We are planning to continue to use the plankton and oceanographic sampling data to help understand the oceanographic processes that drive both the shelf and offshore ecosystems. We are planning to expand the exploratory study that linked echosounder data with cetacean abundance and distribution data in species density models by including additional years of data to ensure robust models and by including areas off the shelfbreak to allow for abundance estimations over a wider region. Future research should confirm proper bin sizes for best model fit, assess additional covariates that could provide insights for deep diving animals, and strive to produce better representations of squid densities. See the discussion sections in Chapter 6 for more future work related to species density models. We plan to make the results of these products available to the public.

10.6 Acknowledgements

The Bureau of Ocean Energy Management (BOEM) and the U.S. Navy through 2 Interagency Agreements and the NOAA Fisheries Service funded the data collection. The Oceans and Climate Branch of the Northeast Fisheries Science Center Data funded the processing and analysis of the oceanography, Video Plankton Recorder, and plankton data.

10.7 References Cited

Andres D. 2016. On the recent destabilization of the Gulf Stream path downstream of Cape Hatteras. Geophys. Res. Lett. 43(18):9836-9842.

Amoroso RO, Pitcher CR, Rijnsdorp AD, et al. 2018. Bottom trawl fishing footprints on the world's continental shelves. Proc. Natl. Acad. Sci. U.S.A. 115 (43):E10275-E10282.

Bureau of Ocean Energy Management (BOEM). 2020. Renewable energy fact sheet. (Accessed 08 October 2020).

Hernandez CM. 2021. Distribution, growth, and transport of larval fishes and implications for population dynamics. PhD Dissertation; Woods Hole Oceanographic Institute; Woods Hole, MA.

Jurado-Molina J, Livingston PA, Ianelli JN. 2005. Incorporating predation interactions in a statistical catch-at-age model for a predator-prey system in the eastern Bering Sea. Can. J. Fish. Aquat. Sci. 62(8): 1865-1873.

Möllmann C, Lindegren M, Blenckner T, Bergström L, Casini M, Diekmann R, Flinkman J, Müller-Karulis B, Neuenfeldt S, Schmidt JO, Tomczak M, Voss R, Gårdmark A. 2014. Implementing ecosystem-based fisheries management: from single-species to integrated ecosystem assessment and advice for Baltic Sea fish stocks. ICES J. Mar. Sci. 71(5):1187–1197.

Orphanides, CD. 2019. Relating marine mammal distribution to prey abundance. Ph.D. Dissertation. Graduate School of Oceanography, University of Rhode Island, Kingston, RI

Palka DL, Chavez-Rosales S, Josephson E, Cholewiak D, Haas HL, Garrison L, Jones M, Sigourney D, Waring G (retired), Jech M, Broughton E, Soldevilla M, Davis G, DeAngelis A, Sasso CR, Winton MV, Smolowitz RJ, Fay G, LaBrecque E, Leiness JB, Dettlof M, Warden M, Murray K, Orphanides C. 2017. Atlantic marine assessment program for protected species: 2010- 2014. US Dept. of the

Interior, Bureau of Ocean Energy Management, Atlantic OCS Region, Washington, DC. OCS Study BOEM 2017-071; 211 pp.

Pendleton DE, Pershing AJ, Brown MW, Mayo CA, Kenney RD, Record NR, Cole TVN. 2009. Regional-scale mean copepod concentration indicates relative abundance of North Atlantic right whales. Mar. Ecol. Prog. Ser. 378:211–225.

Pendleton DE, Holmes EE, Redfern J, Ahang J. 2020. Using modelled prey to predict the distribution of a highly mobile marine animal. Divers. Distrib. 26(11):1612-1626.

Richardson DE, Marancik KE, Guyon JR, Lutcavage ME, Galuardi B, Lam CH, Walsh HJ, Wildes S, Yates DA, Hare JA. 2016 Discovery of a spawning ground reveals diverse migration strategies in Atlantic bluefin tuna (*Thunnus thynnus*). Proc.Natl. Acad.Sci. USA. 113:3299-3304.

Rodríguez-Ezpeleta, N, Díaz-Arce N, Walter III JF, Richardson DE, Rooker JR, Nøttestad L, Hanke A, Franks JS, Deguara S, Lauretta MV, Addis ., Varela JL, Fraile I, Goñi N, Abid N, Alemany F, Oray IK, Quattro JM, Sow FN, Itoh T, Karakulak FS, Pascual-Alayón PJ, Santos M., Tsukahara Y, Lutcavage M, Fromentin J-M, Arrizabalaga H. 2019. Determining natal origin for improved management of Atlantic bluefin tuna. Front. Ecol. Environ. 17:439-444.

Sherman K, Solow A, Jossi J, Kane J. 1998. Biodiversity and abundance of the zooplankton of the Northeast Shelf ecosystem. ICES J. Mar. Sci. 55:730-738.

Tang X, Stewart KW, Vincent L, Huang H, Marra M, Gallager SM, Davis CS. 1998. Automatic plankton image recognition. ArtifIntell Rev 12:177-199.

Nantucket Shoals. Ecosphere 11(1):e03002.

11 Databases and Data Sharing

As a multi-year and multi-Agency effort, the projects conducted under Atlantic Marine Assessment Program for Protected Species (AMAPPS) I and AMAPPS II have been responsible for the collection of large amounts of data. All 7 of the AMAPPS objectives (Chapter 3) require collecting, processing, and archiving data. In this chapter, we describe datasets that the Northeast Fisheries Science Center (NEFSC) and Southeast Fisheries Science Center (SEFSC) collected over the course of the AMAPPS program, from 2010 through 2019. Shipboard surveys in particular, provided platforms for round-the-clock collection of a myriad of oceanographic and acoustic information to supplement the visual observations of marine mammal, sea turtles, and seabirds. In addition, we also describe important external datasets we collated to use in data analyses.

Table 11-1 shows the types of data collected on each survey. You can find additional details on each survey in individual cruise reports found in AMAPPS annual reports.

Table 11-1 Overall summary of data collection during AMAPPS I and II

Trip Identifier/Project[1]	Year	Description	Agency and Partners[2]	Visual MM Observation	Visual Seabird	Passive Acoustics	Archival PA Recorder	Sonobuoy Deployment	EK-60	Bongos	CTD/XBT	Trawl	VPR	Tag Deployment	Blood/Tissue Sampling	Photo-Id	UAS deployment	eDNA collection
TONE10SUM	2010	summer aerial survey	NEFSC	X														
TOSE10SUM	2010	summer aerial survey	SEFSC	X														
SEFSC Turtle Tagging	2010	loggerhead capture and tagging	SEFSC											X	X			
NEFSC Turtle Tagging	2010	loggerhead capture and tagging	NEFSC, CFF											X	X			
TONE11SUM	2011	summer aerial survey	NEFSC	X										X	X			
TONE11WIN	2011	winter aerial survey	NEFSC	X														
TOSE11SUM	2011	summer aerial survey	SEFSC	X														
TOSE11WIN	2011	winter aerial survey	SEFSC	X														
HB1103	2011	shipboard abundance survey	NEFSC	X	X	X			X	X	X		X					
GU1102	2011	shipboard abundance survey	SEFSC	X	X	X			X		X				X			
NEFSC Turtle Tagging	2011	loggerhead capture and tagging	NEFSC, CFF											X	X			
Canadian Loggerhead Tagging	2011	Canadian Grand Banks loggerhead tagging	NEFSC, DFO											X				
Harbor Seal Survey	2011	pupping season aerial	NEFSC	X										X	X			

Trip Identifier/Project[1]	Year	Description	Agency and Partners[2]	Visual MM Observation	Visual Seabird	Passive Acoustics	Archival PA Recorder	Sonobuoy Deployment	EK-60	Bongos	CTD/XBT	Trawl	VPR	Tag Deployment	Blood/Tissue Sampling	Photo-Id	UAS deployment	eDNA collection
		survey of Maine coast																
TONE12FAL	2012	fall aerial survey	NEFSC	X														
TONE12SPR	2012	spring aerial survey	NEFSC	X														
Harbor Seal Survey	2012	pupping season aerial survey of Maine coast	NEFSC	X										X	X			
TOSE12FAL	2012	fall aerial survey	SEFSC	X														
TOSE12SPR	2012	spring aerial survey	SEFSC	X														
TOSE13WIN	2013	winter aerial survey	SEFSC	X														
HB1303	2013	shipboard abundance survey	NEFSC	X					X	X	X		X					
GU1304	2013	shipboard abundance survey	SEFSC	X	X	X			X		X				X			
Gray Seal Captures	2013	adult gray seal captures	NEFSC, IFAW, WHOI, Duke, DFO											X	X			
NEFSC Turtle Tagging	2013	loggerhead capture and tagging	NEFSC, CFF					X						X	X			
HB1403	2014	shipboard habitat survey	NEFSC	X	X	X	X		X	X	X	X	X					

Trip Identifier/Project[1]	Year	Description	Agency and Partners[2]	Visual MM Observation	Visual Seabird	Passive Acoustics	Archival PA Recorder	Sonobuoy Deployment	EK-60	Bongos	CTD/XBT	Trawl	VPR	Tag Deployment	Blood/Tissue Sampling	Photo-Id	UAS deployment	eDNA collection
	2014	beaked whale survey	NEFSC	X	X				X	X	X	X						
TOSE14SPR	2014	spring aerial survey	SEFSC	X														
TONE14SPR	2014	spring aerial survey	NEFSC	X														
TONE14WIN	2014	winter aerial survey	NEFSC	X														
HB1503-1	2015	sei whale survey	NEFSC	X	X	X		X	X		X	X				X		
HB1503-2	2015	turtle tagging	NEFSC	X					X	X	X		X	X	X		X	
Gray seal pup captures	2015	gray seal pup capture	NEFSC, MIT, etc.											X	X			
TOSE15WIN	2015	winter aerial survey	SEFSC	X														
TONE16FAL	2016	fall aerial survey	NEFSC	X														
TOSE16FAL	2016	fall aerial survey	SEFSC	X														
TOSE16SUM	2016	summer aerial survey	SEFSC	X														
TONE16SUM	2016	summer aerial survey	NEFSC	X														
HB1603	2016	shipboard abundance survey	NEFSC	X	X				X	X	X	X	X					
GU1605	2016	shipboard abundance survey	SEFSC	X		X		X	X		X				X			
TONE17SPR	2017	spring aerial survey	NEFSC	X														
TONE17WIN	2017	winter aerial survey	NEFSC	X														

Trip Identifier/Project[1]	Year	Description	Agency and Partners[2]	Visual MM Observation	Visual Seabird	Passive Acoustics	Archival PA Recorder	Sonobuoy Deployment	EK-60	Bongos	CTD/XBT	Trawl	VPR	Tag Deployment	Blood/Tissue Sampling	Photo-Id	UAS deployment	eDNA collection
TOSE17FAL	2017	fall aerial survey	SEFSC	X														
TOSE17SPR	2017	spring aerial survey	SEFSC	X														
EN2017	2017	marine mammal distribution	NEFSC	X					X		X							
GU1701	2017	Ecosystem monitoring	NEFSC	X	X				X	X	X							
GU1702	2017	Ecosystem monitoring	NEFSC	X	X				X	X	X							
GU1706	2017	Ecosystem monitoring	NEFSC	X	X				X	X	X							
HB1704	2017	cetacean and turtle survey	NEFSC	X			X		X	X	X		X	X	X			
HRS1701	2017	beaked whale survey	NEFSC	X	X	X												
EN2018	2018	marine mammal distribution	NEFSC	X														
GU1803	2018	shipboard shelfbreak ecology	NEFSC	X														
HB1803	2018	Ecosystem monitoring	NEFSC	X	X				X	X	X							
TONE19SPR	2019	spring aerial survey	NEFSC	X														
TOSE19SPR	2019	spring aerial survey	SEFSC	X														
EN2019	2019	marine mammal distribution	NEFSC	X					X	X	X	X	X					
HRS1910	2019	beaked whale survey	NEFSC	X														

Trip Identifier/Project[1]	Year	Description	Agency and Partners[2]	Visual MM Observation	Visual Seabird	Passive Acoustics	Archival PA Recorder	Sonobuoy Deployment	EK-60	Bongos	CTD/XBT	Trawl	VPR	Tag Deployment	Blood/Tissue Sampling	Photo-Id	UAS deployment	eDNA collection
TONE19FAL	2019	fall aerial survey	NEFSC	X														
TOSE19WIN	2019/ 2020	winter aerial survey	SEFSC	X														

[1] First 2 letters of trip identifier indicated the ship or plane. EN = R/V Endeavor; HB = NOAA ship *Henry B. Bigelow*; GU = NOAA ship *Gordon Gunter*; HRS = R/V *Hugh R. Sharp*; TO = NOAA's Twin Otter aircraft. For the aerial surveys, the 3rd and 4th digits indicates if the lead center: NE = Northeast Fisheries Science Center; SE = Southeast Fisheries Science Center; the 5th and 6th digits indicates the year; and the last 3 digits indicate the season the survey was conducted in: FAL = fall; SPR = spring; SUM = summer; WIN = winter. For the shipboard surveys, the 2nd and 3rd digits indicate the year, and the last 2 digits indicate the cruise number within the year, except for the Endeavor cruises which have the last 4 digits as the year.

[2] CFF = Coonamessett Farm Foundation; DFO = Department of Fisheries and Oceans Canada; Duke = Duke University, NC; IFAW = International Fund for Animal Welfare; MIT = Massachusetts Institute of Technology; NEFSC = Northeast Fisheries Science Center; SEFSC = Southeast Fisheries Science Center; WHOI = Woods Hole Oeanographic Institution.

11.1 Visual Data (Seabirds, Marine Mammals and Sea Turtles)

Primary authors: Elizabeth Josephson, Laura Aichinger Dias, and Debra Palka

11.1.1 Provenance

The NEFSC and the SEFSC conducted shipboard and aerial surveys following standard line-transect survey methods used elsewhere (Hiby and Hammond 1989; Buckland et al. 2004). Surveys used the "independent observer" data collection approach with distance sampling analysis methods to estimate detection probabilities for observed marine mammal groups (Laake and Borchers 2004; Garrison et al. 2011). During the shipboard surveys, 2 teams, each with 2 marine mammal observers using "big-eye" binoculars (25 × 150) positioned on port and starboard sides of the flying bridge and bridge deck, worked isolated from 1 another to avoid cueing each other to the presence of marine mammals. Data recorders maintained independent communication with both teams and recorded data on sightings by each team. Data recorders entered data on a custom-developed program called VisSurvey. Specific data fields collected by the NEFSC and the SEFSC differed slightly but for most sightings they included group size, bearing and distance to the sighting, presence of calves, behavior, and the factor that cued the observer to the sighting (blow, splash, etc.). Time and position were automatically recorded when the sighting was entered. Observers scored environmental conditions such as Beaufort sea state, cloud cover, swell height and direction, visibility, and precipitation at a minimum of every 30 mins or when conditions changed. Observers changed postitions every 30 mins.

Similarly, during aerial surveys 2 independent teams with 2 observers and 1 data recorded each, in addition to 2 pilots, conducted the surveys. All surveys used a DeHavilland Twin Otter DHC-6 flying at 183 m (600 ft) above the water surface at about 200 km/h (100 kts). The forward team consisted of 2 observers stationed in bubble windows on each side (left and right) of the plane and 1 data recorder. The back team (aft) consisted of 2 observers, 1 stationed in a rear right side bubble window and 1 in a belly window (looking straight down), and 1 recorder. The NEFSC collected data using the data entry program VOR and the SEFSC used a similar program to VisSurvey (as described for the ship surveys).

Observer teams on both ships and planes were "on-effort" when actively scanning the water for cetaceans or sea turtles and the ship was steadily cruising on a trackline or the plane flying at survey altitude and speed. Sightings seen by off-duty observers, other crewmembers or during other operations were "off-effort". We conducted the aerial surveys over the continental shelf and shelfbreak out to about the 200 or 2000m depth contour. Shipboard surveys were generally in the deeper offshore waters, deeper than 100 m. The overall density of survey effort by season for all shipboard and aerial surveys conducted under AMAPPS I and II is in Figure 11-1. We surveyed over 220,000 km of track lines in the aerial surveys (Table 11-2).

The marine mammal observers onboard the ship and plane collected data on marine mammals and sea turtles. In addition, dedicated observers stationed on the ship's flying bridge collected data on seabird occurrence to allow analysis of seabird abundance and spatial distribution. Seabird observations operated simultaneously with the marine mammal teams throughout most of the shipboard surveys.

For detailed descriptions of survey methods for each cruise, please refer to cruise reports in the AMAPPS annual reports and Chapters 5 to 10 in this report.

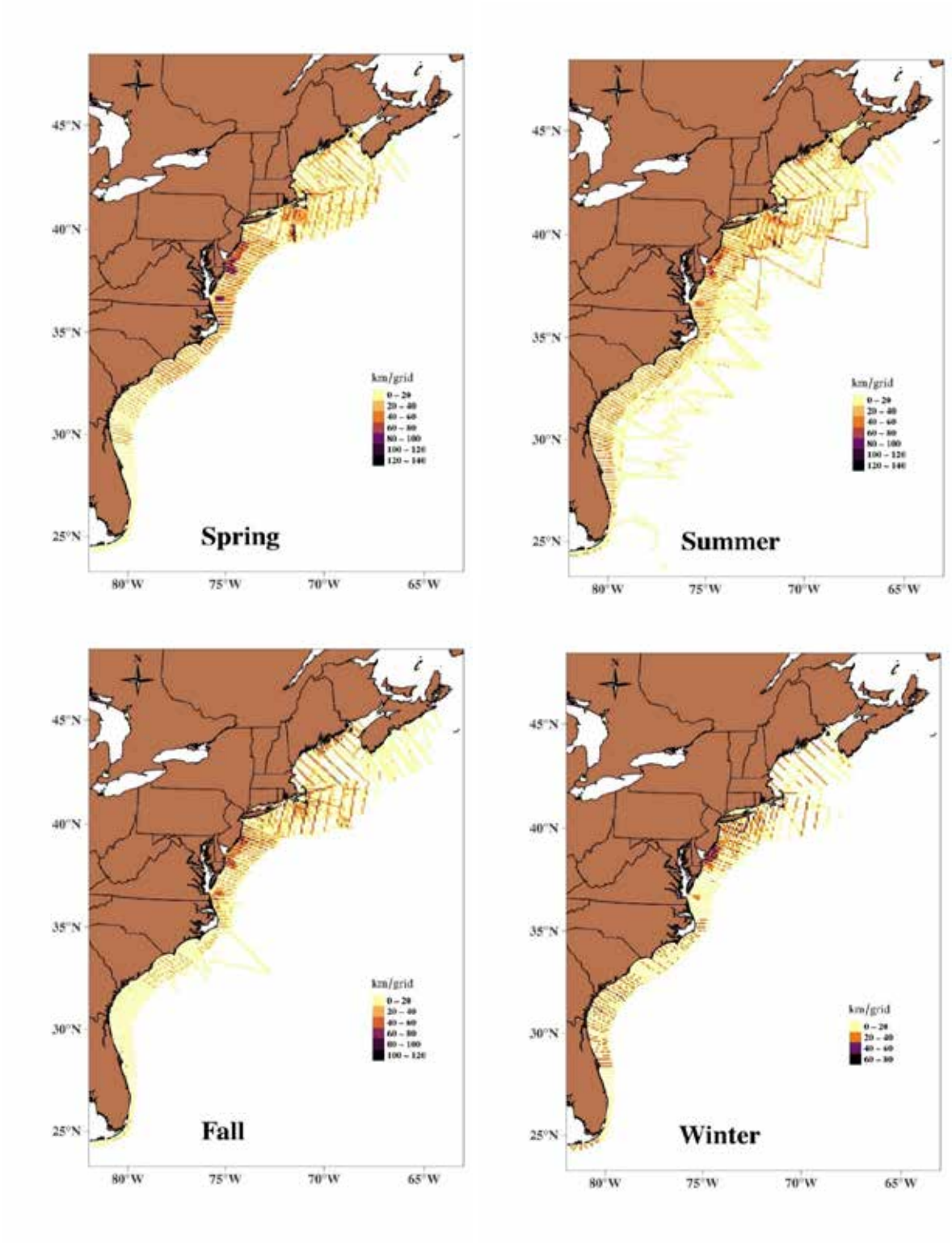

Figure 11-1 Visual effort by grid and season for all AMAPPS I and II surveys
Spring is March to May; summer is June to August; fall is September to November; and winter is December to February. Grid cells are 10 km x 10 km.

Table 11-2 Aerial and shipboard survey effort by season, 2010 to 2019

Season	Aerial On-effort Track line Length (km)	Shipboard On-effort Track line Length (km)
Spring (March - May)	70,470	6,709
Summer (June - August)	55,711	57,084
Fall (September - November)	47,117	5,853
Winter (December - February)	47,113	0
TOTAL	220,411	69,646

11.1.1.1 NEFSC Shipboard Surveys

During 2010 to 2019, the NEFSC completed 21 shipboard surveys that collected line-transect sightings data under the AMAPPS programs (Table 11-3). These included 4 dedicated abundance surveys with 2-independent team data collection. The remaining surveys included some with specific taxa focus or other types of surveys during which a visual observer collected data opportunistically. During AMAPPS II, we conducted 284 survey days, resulting in 31,282 km of on-effort track lines, 7,870 marine mammal, 169 sea turtle and 16,945 sea bird unique sightings seen by 1 or both teams during on- and off-effort times (Table 11-3).

Table 11-3 Summary of NEFSC shipboard surveys conducted during 2010 to 2019
Mammal and turtle sightings may include duplicates and resightings.

Trip Identifier	Year	Purpose	Start Date	End Date	Days with Sighting Effort	Number of Visual Teams	Visual Survey On-Effort (km)	Mammal Sighting Records[1]	Turtle Sighting Records[1]	Bird Sighting Records
HB1103	2011	abundance survey	2-Jun	1-Aug	40	2	4,973	2,543	25	1,135
HB1303	2013	abundance survey	2-Jul	18-Aug	38	2	5,021	2,119	74	2,207
GU1402	2014	abundance survey	12-Mar	27-Apr	33	2	4,014	998	3	2,493
HB1403	2014	beaked whale survey	25-Jul	30-Jul	5	2	740	221	2	336
HB1502	2015	ecosystem monitoring	20-May	2-Jun	14	1	NA[2]	155	4	0
HB1503-1	2015	sei whale survey	10-Jun	19-Jun	8	2	1,228	704	2	937
HB1503-2	2015	turtle tagging	24-Jun	1-Jul	6	1	NA[2]	86	13	0
HB1603	2016	abundance survey	28-Jun	24-Aug	45	2	5,203	5,097	58	2,031
EN2017	2017	marine mammal distribution	14-Apr	19-Apr	6	1	58	61	0	0
GU1701	2017	ecosystem monitoring	16-May	6-Jun	18	1	2,923	91	22	1,773
GU1702	2017	ecosystem monitoring	10-Jun	22-Jun	13	1	1,856	37	2	1,177
GU1706	2017	ecosystem monitoring	31-Oct	9-Nov	10	1	1,083	21	1	861
HB1704	2017	cetacean and turtle survey	7-Jul	18-Jul	12	1	NA[2]	168	10	0
HRS1701	2017	beaked whale survey	8-Sep	17-Sep	10	1	NA[2]	244	0	255
EN2018	2018	marine mammal distribution	3-Apr	8-Apr	4	1	NA[2]	3	0	0

Trip Identifier	Year	Purpose	Start Date	End Date	Days with Sighting Effort	Number of Visual Teams	Visual Survey On-Effort (km)	Mammal Sighting Records[1]	Turtle Sighting Records[1]	Bird Sighting Records
HS1801	2018	ecosystem monitoring	1-Nov	12-Nov	10	1	1,099	16	3	1,282
HB1803	2018	ecosystem monitoring	23-May	4-Jun	13	1	2,214	54	1	1,516
GU18TN	2018	NOAA ship transit	11-Jul	16-Jul	6	1	1,213	10	2	371
GU1803	2018	beaked whale survey	21-Jul	1-Aug	13	1	NA[2]	758	0	522
HB18TN	2018	NOAA ship transit	1-Aug	6-Aug	6	1	1,213	51	0	485
GU1804	2018	ecosystem monitoring	22-Aug	30-Aug	9	1	1,537	28	18	636
GU18TS	2018	NOAA ship transit	2-Sep	9-Sep	8	1	1,216	21	10	327
EN2019	2019	marine mammal distribution	18-Apr	23-Apr	5	1	NA[2]	3	0	0
HB1902	2019	ecosystem monitoring	24-May	5-Jun	13	1	2,614	144	4	1,510
GU1902	2019	ecosystem monitoring	15-Aug	29-Aug	14	1	2,334	50	7	1,364
GU1905	2019	ecosystem monitoring	15-Oct	30-Oct	14	1	1,675	40	11	1,100
HRS1910	2019	beaked whale survey	18-Aug	27-Aug	8	1	580	8	1	441
RB1904	2019	ecosystem monitoring	13-May	24-May	11	1	2,422	20	0	202
TN368	2019	ecosystem monitoring	6-Jul	17-Jul	12	1	814	3	0	155
Subtotal – AMAPPS I	2010 – 2014				116		14,748	5,881	104	6,171
Subtotal – AMAPPS II	2015 – 2019				284		31,282	7,870	169	169,945
GRAND TOTAL	2010 – 2019				400		46,030	13,751	273	23,116

[1] Mammal and turtle sighting counts include duplicates and resightings.

[2] Not applicable (NA) because these cruises did not conduct standardized line transect searching protocols since the goals of these surveys required searching procedures.

11.1.1.2 NEFSC Aerial Surveys

NEFSC completed 13 aerial surveys under the AMAPPS program during 2010 to 2019 (Table 11-4). We completed spring surveys in 2012, 2014, 2017, and 2019, summer surveys in 2010, 2011, and 2016, fall surveys in 2012, 2016, and 2019, and winter surveys in 2011, 2014, and 2017. The 2010 and 2011 NEFSC summer aerial surveys used the single team “circle-back” data collection and analysis methods to estimate perception bias and the probability of detecting a group on the track line (Hiby and Lovell 1989; Hiby 1999). All other surveys used the 2 independent team procedures. During AMAPPS II, on 78 survey days, we flew over 54,000 km of on-effort track lines and detected 5,000 marine mammal and 995 sea turtle unique sightings seen by 1 or both teams during on- and off-effort times (Table 11-4).

Table 11-4 Summary of NEFSC aerial abundance surveys during 2010 to 2019
Spring is March to May; summer is June to August; fall is September to November; and winter is December to February.

Trip Identifier	Year	Description	Start Date	End Date	Days with Sighting Effort	Visual Survey On-Effort (km)	Mammal Sighting Records*	Turtle Sighting Records*
TONE10SUM	2010	summer	17-Aug	26-Sep	16	9,206	449	87
TONE11SUM	2011	summer	8-Aug	26-Aug	11	6,481	386	85
TONE11WIN	2011	winter	28-Jan	15-Mar	8	4,550	303	2
TONE12FAL	2012	fall	17-Oct	19-Nov	11	7,134	354	62
TONE12SPR	2012	spring	28-Mar	3-May	10	6,793	500	0
TONE14SPR	2014	spring	22-Feb	25-Mar	12	4,904	182	0
TONE14WIN	2014	winter	5-Dec	14-Jan	14	5,671	107	3
TONE16FAL	2016	fall	17-Oct	17-Nov	11	6,995	647	23
TONE16SUM	2016	summer	15-Aug	26-Sep	17	11,782	713	676
TONE17SPR	2017	spring	10-Jun	9-Jul	10	9,479	976	270
TONE17WIN	2017	winter	23-Nov	3-Jan	10	7,738	648	11
TONE19FAL	2019	fall	15-Oct	23-Nov	14	7,771	736	13
TONE19SPR	2019	spring	5-Apr	13-May	16	10,392	1,280	2
Subtotal – AMAPPS I	2010 – 2014				82	44,729	2,281	239
Subtotal – AMAPPS II	2015 – 2019				78	54,157	5,000	995
GRAND TOTAL	2010 – 2019				160	98,896	7,281	1,234

* Mammal and turtle sighting counts include duplicates and resightings.

11.1.1.3 SEFSC Shipboard Surveys

During 2010 to 2019, the SEFSC completed 3 shipboard line-transect surveys under the AMAPPS program (Table 11-5). During all surveys, we used the 2 independent team procedures, where observers focused primarily on recording marine mammals, which took precedence over turtles. In the 2016 survey, sea turtles were not systematically recorded and no seabird observers were onboard the ship. We conducted these surveys during summer in 121 survey days, resulting in 17,387 km of on-effort tracklines, 1,436 marine mammal, 197 sea turtle, and 2,509 seabird unique sightings seen by 1 or both teams during on- and off-effort times.

Table 11-5 Summary of SEFSC shipboard surveys during 2010 to 2019

Trip Identifier	Year	Purpose	Start Date	End Date	Days with Sighting Effort	Visual Survey On-Effort (km)	Mammal Sighting Records	Turtle Sighting Records	Bird Sighting Records
GU1102	2011	abundance survey	19-Jun	1-Aug	35	5,210	331	21	1,135
GU1304	2013	abundance survey	16-Jul	15-Sep	42	6,209	561	174	1,374
GU1605	2016	abundance survey	1-Jul	24-Aug	44	5,968	544	2	0*
Subtotal-AMAPPS I	2010 – 2014				77	11,419	892	195	2,509
Subtotal-AMAPPS II	2015 – 2019				44	5,968	544	2	0*
GRAND TOTAL	2010 – 2019				121	17,387	1,436	197	2,509

*no seabird survey conducted

11.1.1.4 SEFSC Aerial Surveys

During 2010 to 2019, the SEFSC completed 14 aerial line-transect surveys under AMAPPS, across all seasons (Table 11-6). During all surveys, we used the 2 independent team procedures. During AMAPPS II, the SEFSC conducted 110 on-effort days resulting in 56,644 km of on-effort track lines, 1,190 marine mammal and 5,375 sea turtle unique sightings seen by 1 or both teams during on- and off-effort times.

11.1.2 Processing

11.1.2.1 Quality control checks

We subject both shipboard and aerial data to rigorous quality control. First, the data entry program has limited data value checking, such as allowing the entry of only a pre-specified range of acceptable values for some variables or using drop down choices for other variables. Observers note mistakes in an Error log and data managers edit the data daily while in the field, as needed. Afterwards, data managers make corrections based on the Error log notes and check the data to identify fields inadvertently left blank or out of range. We also check to make sure the data are internally consistent. Examples include:

at any time each observer is only assigned to 1 position on 1 team and the location of sightings correctly reflect these positions;

the total number of animals in the group should be greater than the number of calves recorded for that group;

the on-effort segments, as defined by the times entered by the record, correspond to straight and uninterrupted segments of track lines, as defined by the GPS file that independently recorded the time and location of the ship or plane, and this should be consistent for both teams;

all sightings not detected on an on-effort track line are categorized as off-effort sightings; and the species identification of a group detected by both teams is the same for both teams.

Table 11-6 Summary of SEFSC aerial abundance surveys during 2010 to 2019
Spring is March to May; summer is June to August; fall is September to November; and winter is December to February.

Trip Identifier	Year	Description	Start Date	End Date	Days with Sighting Effort	Visual Survey On-Effort (km)	Mammal Sighting Records	Turtle Sighting Records
TOSE10SUM	2010	summer	24-Jul	11-Aug	14	8,072	181	1,411
TOSE11SUM	2011	summer	6-Jul	29-Jul	15	8,765	199	1,426
TOSE11WIN	2011	winter	7-Feb	13-Mar	11	4,892	159	793
TOSE12FAL	2012	fall	11-Sep	20-Oct	22	11,818	241	1,722
TOSE12SPR	2012	spring	3-Apr	21-May	22	11,670	290	1,353
TOSE13WIN	2013	winter	15-Feb	23-Mar	16	7,402	197	139
TOSE14SPR	2014	spring	24-Mar	28-Apr	13	7,815	152	495
TOSE15WIN	2015	winter	23-Jan	3-Mar	13	6,314	133	573
TOSE16SUM	2016	summer	23-Nov	31-Dec	10	11,406	183	1,516
TOSE16FAL	2016	fall	3-Jul	9-Aug	21	5,893	114	87
TOSE17FAL	2017	fall	18-Oct	20-Nov	17	7,507	132	561
TOSE17SPR	2017	spring	17-Apr	20-May	17	9,703	241	839
TOSE19SPR	2019	spring	18-May	24-Jun	18	9,713	260	1,304
TOSE19WIN	2019/2020	winter	7-Dec	24-Jan	14	6,108	127	495
Subtotal-AMAPPS I	2010 – 2014				113	60,434	1,419	7,339
Subtotal-AMAPPS II	2015 – 2019				110	56,644	1,190	5,375
GRAND TOTAL	2010 – 2019				223	117,078	2,609	12,714

11.1.2.2 Duplicate Resolution

During 2-team sighting surveys, only 1 team detects some groups of animals, while both teams detect other groups of animals. We determined the groups that were detected by both teams (termed a duplicate sighting) by investigating the times and locations of the sightings. This determination can be done in real-time or during the data quality checking stage.

Since the plane is traveling fast, the amount of time an animal group is available to either team is relatively short. Consequently, most groups that we can confidently define as a duplicate (termed a “definite” duplicate) were recorded within a few seconds of each other (less than about 3 sec), on the same side of the plane, and at about the same angle of declination (less than 10°). We defined the angle of declination as the angle between the line straight down from the plane to the line between the plane and the geometric center of the group. However, due to measurement error in the angle or a slow response to record a group, we defined a “possible” duplicate as a group detected by both teams within 6 secs and within 20° of each other. In the case of larger groups (greater than 5 animals), it is feasible that observers took their angle of declination measurements at different locations within the spatial region covered by the group, thus we used the criteria of a possible duplicate for a definite duplicate of a large group. We took special care when determining duplicates for recorded groups close to the track line (within 5°). This is because it is feasible that an observer sitting on 1 side of the plane can see all or part of a group when viewing through the large bubble windows, where the group is actually on the other side of the plane yet close to the track line.

We used the same concepts to identify duplicates from the shipboard data, but it is more complicated because the ship is traveling slowly and the window of opportunity to detect a group of animals using high-powered binoculars (25 x 150) is more in the range of 10 to 15 min. We have identified duplicates in real-time while on the ship, where an independent person who talks with both teams (while still maintaining no communication between the teams) assimilates all the information and makes a decision. We have also identified duplicates after field data collection, by matching up the tracks of detected groups from both teams using the time, location, and swim direction recorded at the initial location and at subsequent "follow-up" locations of the same group.

During SEFSC ship surveys, we identified duplicate groups in real-time by an independent data recorder who communicates separately with observers in both teams and makes a decision. We based the determination usually on the location of the sighting (usually detections less than 1 nm from each other), animal behavior, and species or taxa group identification. Before approaching the group to identify species and count group sizes (if needed), the data recorder waited until the sighting passed abeam of the ship so that both teams have the chance to see it. Only then did the data recorder ask the captain to deviate from the trackline. Each observer entered group sizes independently without group discussion. During aerial surveys, if only 1 team detected a marine mammal sighting, that team waited until the sighting was aft of the airplane to ask the pilots to depart from the trackline to circle the sightings to verify species and count group sizes. Therefore, for example, if only the forward team detected a sighting, the data recorder marked this group as detected by the forward team and "missed" by the aft team. The recorder entered a common and single group size for sightings seen by both teams. We treated sea turtle sightings differently. We recorded sea turtles independently by each team. We identified duplicate sea turtle sightings after the survey during the data quality checking stage. We based the determination upon time (sightings less than 15 sec of each other), location (same side of the aircraft), position relative to the trackline (angles measured by both teams are ± 15° apart) and number of animals (must be equal).

11.1.2.3 Derived Fields

We store several parameters important for data analysis with the Oracle datasets as derived fields. We calculated some derived fields by using stored Oracle functions and others we calculated externally before data upload. Examples of derived fields include the spatial point geometry field that we calculated from the latitude and longitude entries for each sighting and a spatial line geometry field we added after creating line segments (see below). We converted the shipboard binocular reticle values recorded by observers into linear distances based on the height of the ship's platform and type of binocular. We calculated perpendicular distances from the radial distance and bearing values entered by observers for shipboard sightings, and from the survey altitude and angle of declination of the aerial sightings. In addition, we created some derived fields to accommodate and standardize differences in data collection over the years and between regions.

11.1.2.4 Segmentation

We convert raw effort tables to summarized tables that compress data to short straight-line segments with a start and end position. If there is a speed or course change recorded, change in environmental conditions recorded by observers, rotation of observers, or any break in effort status, we created a new line segment. We considered as off-effort times when maneuvering between tracklines, transits to and from tracklines, circling over sightings during aerial surveys, and closing on sightings during ship surveys.

11.1.2.5 Oracle Upload

We developed R scripts to upload data to Oracle data tables housed on NEFSC servers.

11.1.2.6 Gridding

In preparation for their use in density-habitat models, we associated all sightings and visual survey effort data with a custom-developed 10 km x 10 km grid, in oblique Mercator projection, that encompassed the Atlantic study area. In addition, to facilitate matching to temporally explicit covariates such as satellite-derived ocean color products, we associated all sighting and visual effort data with an 8-day temporal segment.

11.1.2.7 Preparation for Distance Analysis

In preparation for use in analysis using the distance software package (Thomas et al. 2009), we processed the sightings and visual effort data to present the on-effort survey distance for each spatial stratum by 8-day segment. We aggregated the data such that each sighting had a record for each sighting team, with information on whether that team sighted or did not sight that animal group. All grids with effort were associated with environmental sighting conditions as recorded by observers, as well as static and non-static environmental covariates.

11.1.3 Presentation

11.1.3.1 Cruise Reports

Detailed cruise reports are included in AMAPPS annual reports.

11.1.3.2 Submissions to Online Websites

As part of the Ocean Biodiversity Information System (OBIS), a group of investigators from Duke University, built a spatially, temporally interactive online archive for marine megafauna including marine mammals and sea turtles known as OBIS-SEAMAP (Ocean Biodiversity Information System - Spatial Ecological Analysis of Megavertebrate Populations). Contributors from all over the world share their distributional data (Halpin et al. 2009).

We have contributed to OBIS-SEAMAP the data collected during AMAPPS shipboard and aerial surveys. These data include primarily on-effort marine mammal and sea turtle sightings seen by the flying bridge team only (ship survey), the forward team only (aerial survey) or both teams combined (ship and aerial surveys). The on-effort trackline data accompanied the sighting data.

We have submitted the seabird data regularly to managers of the Atlantic Offshore Seabird Dataset Catalog. These data went into the Avian Knowledge Network and iPac tools and contributed to such publications as “Modeling at-sea density of marine birds to support Atlantic marine renewable energy planning” by Winship et al. (2018). We archived the raw data with the National Centers for Environmental Information (e.g. this dataset) and in the Global Biodiversity Information Facility.

We contributed the AMAPPS marine mammal and seabird data to develop a multi-dataset NOAA NCCOS model that is publicly available on the Northeast Regional Ocean Council and MARCO Mid-Atlantic Ocean data portals as maps.

We also archived and documented the NEFSC and SEFSC visual sighting data through the InPort metadata library. NEFSC has the AMAPPS survey data set available as 1 entry and SEFSC has an archive node for vessel surveys and 1 for aerial surveys.

11.1.3.3 Other Reports and Publications

The sightings data and associated abundance estimates and density-habitat models are important components of marine mammal stock assessment reports. A full list of publications produced using these data during AMAPPS I is in Palka et al. (2017) and those produced during AMAPPS II is in Table 1-2.

11.1.3.4 Model Viewer

Outputs from density-habitat models generated by using data collected from AMAPPS I are on the AMAPPS Marine Mammal Model Viewer website. The plan is to update this website with the updated models reported in Chapter 6 and Appendix I.

11.2 Environmental Covariate Data

Primary authors: Kim Hyde, Joshua Hatch, Samuel Chavez-Rosales, and Elizabeth Josephson.

11.2.1 Provenance

We compiled different types of environmental covariate data to use as candidates in density surface models that modeled the relationships between a species density (and number of groups detected) and environmental habitat descriptors, as described in Chapter 6.

11.2.1.1 Static Covariates

Several static covariates were candidates for the density-habitat models, including depth, slope, distance from shore, and distance from various isobaths. We obtained bathymetric depth from the ETOPO 11 Arc-Minute Global Relief Model (Amante and Eakin 2009; NOAA NGDC 2009). We obtained the nearest distance from the coastline to the center point of each grid from the National Aeronautics and Space Administration (NASA) 0.04° OceanColorWeb dataset.

11.2.1.2 Satellite-derived Covariates

We obtained high resolution (1 km) remotely sensed ocean color and sea surface temperature (SST) data from the Moderate Resolution Imaging Spectroradiometer (MODIS) (NASA Ocean Biology Processing Group 2017) on the Aqua and Terra (SST only) satellites from the NASA Ocean Biology Processing Group. We used the MODIS-Terra and Aqua 1-km resolution SST data for the SST-frontal gradient analysis (NASA Ocean Biology Processing Group 2018). We acquired additional SST data from the Group for High Resolution Sea Surface Temperature Multiscale Ultrahigh Resolution (MUR, version 4.1) Level 4 (Project JPL MUR MEaSUREs 2015; Chin et al. 2017) data.

11.2.1.3 Ocean Data Assimilation Covariates

Ocean data assimilation products that we used included bottom temperature, mixed layer depth, salinity, and sea surface height. These products were the result of integrated output from ocean modeling, *in situ* observations, and remotely sensed images of environmental variables.

One reason for using products from ocean data assimilations is that they overcome limitations of ocean models in terms of resolution and ability to accurately reflect phenomena of surface and subsurface flows (Chassignet et al. 2009). Ocean data assimilations incorporate modeling and data assimilation techniques to produce high resolution near real-time global ocean prediction systems. One such system is the U.S. Navy nowcast/forecast system that uses the 1/12 HYbrid Coordinate Ocean Model (HYCOM) and the 3-demensional multivariate optimum interpolation Navy Coupled Ocean Data Assimilation technique.

Distributions of hindcasts from the global U.S. Navy HYCOM + Navy Coupled Ocean Data Assimilation ocean prediction system are available through the HYCOM consortium at hycom.org. To date, they provide 11 fields that include surface water flux, mixed layer depth, mixed layer thickness, surface heat flux, sea surface height, surface salinity trend, surface temperature trend, salinity, potential temperature, u-velocity, and v-velocity.

The HYCOM Consortium provided access to near real-time global ocean predictions based on the HYCOM and Navy Coupled Ocean Data Assimilation technique. Outputs from the near real-time global ocean prediction system were converted to a native Mercator-curvilinear HYCOM horizontal grid with a 1/12 equatorial resolution, which consisted of a Mercator projection from 78°S to 47°N and a bipolar patch north of 47°N. The HYCOM Data Service provided access to modeled outputs using NetCDF files through a subsetting service, allowing for a user-specified bounding box.

11.2.1.4 Distance from the Gulf Stream

We calculated the distances between the centers of the spatiotemporal strata to the north and south Gulf Stream wall locations on a corresponding date by using ArcGis. The Gulf Stream location data are available from the Naval Oceanographic Office's website. The location of the Gulf Stream is based on the maximum surface temperature change over 10 nm from detailed analyses of Infra-Red satellites, bathythermographs, and drifting buoy data. The reported positions are accurate to within 11 nm.

11.2.1.5 North Atlantic Oscillation Index

The NOAA Climate Prediction Center provided the North Atlantic Oscillation (NAO) daily index. The daily NAO index corresponds to the NAO patterns, which vary from 1 month to the next. We standardized each daily value by the standard deviation of the monthly NAO index from 1950 to 2020 interpolated to the day in question. We based the procedure used to calculate the daily NAO teleconnection index on the Rotated Principal Component Analysis used by Barnston and Livezey (1987). This procedure isolates the primary teleconnection patterns for all months and allows constructing a time series of the patterns. The use of the Rotated Principal Component Analysis allowed the monthly mean standardization of 500-mb height anomalies obtained from the Climate Data Assimilation System in the analysis region 20°N to 90°N between January 1950 and December 2000.

11.2.2 Processing

11.2.2.1 Static Covariates

We computed slope from the depth raster using the R ‘terrain’ package. We then resampled the depth, slope, and distance from shore rasters using bilinear or nearest neighbor methods with the R function “spatial_sync_raster” from the spatial.tools R package to align to the extent, projection, and resolution of the AMAPPS study grid.

11.2.2.2 Satellite-derived Covariates

We processed the MODIS Level 1A ocean color files and level 2 SST data from the “Terra” and “Aqua” satellites using the NASA Ocean Biology Processing Group SeaDAS software version 7.4, with all data files spatially subset to the AMAPPS study area (SW longitude=-82°, SW latitude=23°, NE longitude=-52°, NE latitude=52°) using L1AEXTRACT_MODIS. We used SeaDAS’s L2GEN program to generate Level 2 (L2) files with the default settings and optimal ancillary files, and the L2BIN program to spatially and temporally aggregate the ocean color and sea surface temperature to create daily Level 3 binned files. We aggregated the daily files at 2 km resolution then stored them in a global, nearly equal-area,

integerized sinusoidal grid, with the default L2 ocean color flag masks. We created running 8-day means from the daily files, and then projected into the AMAPPS oblique Mercator 10 km x 10 km grid.

The L2 ocean color products include chlorophyll *a*, particulate inorganic carbon, particulate organic carbon, photosynthetic available radiation, remote sensing reflectance, and several inherent optical property products. The chlorophyll *a* product combined 2 algorithms, the O'Reilly band ratio algorithm (O'Reilly et al. 1998) and the Hu color index algorithm (Hu et al. 2012). We calculated particulate organic carbon by using an empirical power law algorithm derived from *in situ* measurements of particulate organic carbon and blue-to-green band ratios of remote sensing reflectance. We calculated particulate inorganic carbon by using observed *in situ* relationships between water-leaving radiances, spectral backscattering coefficients, and concentrations of particulate inorganic carbon (i.e., calcium carbonate or calcite). The satellite particulate inorganic carbon algorithm was a hybrid of 2 independent approaches, defined here as the 2-band primary algorithm (Balch et al. 2005) and 3-band (Gordon et al. 2001), which we used in case of 2-band failure.

We calculated the detections of oceanic fronts for SST and the natural log of the chlorophyll *a* (due to the log-normal distribution of chlorophyll) using the Belkin and O'Reilly (2009) algorithm, and a contextual median filter to isolate noise while preserving edges in the daily Level 3 binned files. We computed the gradient vector using IDL's CONVOL function using 2 3 x 3 convolution kernels. We used the width and height of each pixel to compute the gradient magnitude per km in the X (G_x) and Y (G_y) directions. We calculated the gradient magnitude by using the equation, .

We estimated net primary production as a function of chlorophyll a, photosynthetically available radiation and the photosynthetic efficiency by using a variation of the Vertically Generalized Production - Eppley Model (Behrenfeld and Falkowski 1997). Prior to being input into the Vertically Generalized Production - Eppley Model, we temporally interpolated and smoothed the daily chlorophyll *a* data to increase the data coverage and better match data collected from different sensors and different times. Because cloud cover did not affect the daily photosynthetic available radiation data and the MUR SST data was a blended/gap free data product, we did not interpolate these products.

We extracted the daily data at each pixel location covering the entire date range to create a pixel time series ($D_{x,y}$) that was linearly-interpolated based on days in the time series using interpx.pro. Prior to interpolation, we log-transformed the chlorophyll *a* data to account for the lognormal distribution of the data (Campbell 1995). Interpolating the entire times series required a large amount of processing time so we processed the series 1 year at a time. Each yearly series included 60 days from the previous year and 60 days from the following year to improve the interpolation at the beginning and end of the year. Following interpolation, we smoothed the data with a tri-cube filter (width = 7) using IDL's CONVOL function. To avoid over interpolating data when there were several days of missing data in the time series, we removed and replaced the interpolated data with blank data if the window of interpolation spanned more than 7 days. After we processed all $D_{x,y}$ pixels, we converted the one-dimensional pixel time series back to 2-dimensional daily files.

In the Vertically Generalized Production - Eppley Model version, we replaced the original temperature-dependent function to estimate the chlorophyll-specific photosynthetic efficiency with the exponential "Eppley" function as modified by Morel (1991). For more details, see NEFSC (2020).

For chlorophyll *a*, particulate inorganic carbon, particulate organic carbon, photosynthetic available radiation, and gradient magnitude, we calculated statistics, including the arithmetic mean, geometric mean, standard deviation, and coefficient of variation at daily (8-day running means) intervals.

If values of an environmental variable within the AMAPPS study area were missing, we used a hierarchical spatial-temporal interpolation approach to replace missing values. This approach first filled in a missing value using the calculated mean from the nearest-neighbor cells from the same time that contained non-missing data. Then, if that was not sufficient, the missing value was calculated from the mean value for the spatial stratum of interest for the 8-day time period before and after. This process provided enough information of the seasonal tendency, without compromising the overall quality of the data.

11.2.2.3 Ocean Data Assimilation Covariates

The AMAPPS prediction grid extends beyond 47°N and continues into the HYCOM bipolar patch. This makes it difficult to synchronize HYCOM data to the AMAPPS projection north of 47°N, and as such, we used 47°N as an upper bound to retrieve HYCOM data. To date, no AMAPPS survey effort extended beyond 47°N, which suggests that this is a reasonable cutoff. We spatially synchronized HYCOM data to the AMAPPS prediction grid by using the following process:

1) We downloaded HYCOM data for each day from 2010 to 2019 using a bounding box defined by North = 47°N; South = 22°N; East = 320°E; and West = 277°E.
2) We spatially synchronized the HYCOM data to the AMAPPS grid by re-projecting into the AMAPPS projection, and then re-sampling to the AMAPPS resolution using bilinear interpolation.
3) We created 8-day composites from the synced HYCOM data.
4) We wrote rasters to CDF files.

The variables we downloaded included: ocean mixed layer depth (m), ocean mixed layer thickness, bottom temperature (°C) and surface salinity (psu).

The mixed layer depth is the depth (in m) at which the density changes from the surface by 0.03 kg/m^3. We defined the bottom temperature as the temperature (in °C) of the deepest HYCOM z-level.

11.2.3 Presentation

We used these covariates as candidate predictor variables in the density surfacing models described in Chapter 6. They are downloadable from the NEFSC Inport metadata library.

11.3 Telemetry Data

Primary authors: Heather Haas and Christopher Sasso

11.3.1 Provenance

During 2010 to 2019, NMFS worked collaboratively with many partners to deploy hundreds of animal-borne data loggers and transmitters on loggerhead turtles (*Caretta caretta*) and leatherback turtles (*Dermochelys coriacea*). The types of tags deployed vary by taxa. Across the full suite of tags, we collected information on animal location and behavior, wet/dry status, depth, and water temperature (Table 11-7). Chapter 7 of this report provides further information on the beaked whale tag, while Chapter 8 provides further information on the turtle tagged animal tracking and data collection.

Table 11-7 Summary of data associated with animal-borne tags
Note these tags and data fields are only those that relate to AMAPPS and are available to NEFSC/SEFSC in collaboration with other research groups. We deployed most tags as part of a collaboration, where AMAPPS did not financially support many of the tags.

Type of tags and information recorded	Loggerhead Turtles	Leatherback Turtles
Number of long term satellite tags applied	214	31
- Non-interpolated Argos and GPS records	634,970	25,145
- Number of wet/dry records	132,279	1,260
- Number of animal depth records	257,673	7,385
- Number of temperature records	42,645	696
Number of short term high resolution tags applied	0	24

11.3.2 Processing

For animal behavior data coming from the Sea Mammal Research Unit satellite-relay data loggers, the manufacturer's website routinely uploaded all data into an NEFSC-maintained Oracle database. We then merged these telemetry-based behavior data with deployment data into Oracle Views where some basic quality control filtering also occurred. For selected research topics, additional data processing (including interpolation) also occurred. During AMAPPS III, we plan to incorporate data from Wildlife Computer Tags into the Oracle database system, and we plan to improve database organization and documentation.

11.3.3 Presentation

Results from the sea turtle telemetry data are available publicly via publications and datasets (Table 11-8).

Table 11-8 Summary of publications and publicly available databases in relation to data types
Location = latitude and longitude locations; Bio=Biological data from physical samples.

Publications and Publically Available Datasets	Location	Depth	Water Temperature	Video	Biological Data
Yang et al. (2019)	x		x		x
Winton et al. (2018)	x				
Patel et al. (2018)	x	x	x		
Patel et al. (2016)		x	x	x	
Ceriani et al. (2014)	x				x
Estimated monthly distributions of tagged loggerheads: shape files and Northeast Ocean Data Portal interactive map	x				
Temperature and depth data from tagged loggerheads: CSV file	x	x	x		

11.4 Passive Acoustic Data

Primary authors: Danielle Cholewiak, Annamaria DeAngelis, Genevieve Davis, Nicole Pegg, Liam Mueller-Brennan, Elizabeth Josephson, and Melissa Soldevilla

11.4.1 Provenance

11.4.1.1 NEFSC Towed Hydrophone Array Data

During 2010 to 2019, the NEFSC AMAPPS program completed 10 shipboard surveys that collected data from towed hydrophone arrays. These included 4 dedicated abundance surveys; the remaining surveys focused on studies of specific taxa. During AMAPPS II, these surveys collected acoustic data on 91 days during about 15,000 km of track lines (Table 11-9).

The passive acoustic team deployed a towed hydrophone array approximately 300 m behind the vessel, in water depths greater than 100 m. The array configuration and specifications varied over the years and between surveys. The primary array contained 1 or 2 oil-filled sections with multiple hydrophones (manufactured by HTI, APC, and/or Reson) and a depth sensor (Keller America, PA7FLE). We typically collected hydrophone array data for 12 to 24h/day on the abundance surveys and focal taxa surveys, depending on survey needs and design. The passive acoustic team recorded data and monitored the array using a variety of acoustical software packages including PAMGUARD, Ishmael, WhalTrack, RainbowClick, Logger, and Raven. Ishmael is acoustic localization and digital recording software, developed by Dave Mellinger, Oregon State University Pacific Marine Environmental Laboratory, Newport, Oregon (Mellinger et al. 2018). Whaltrak is a data logging and mapping program, developed by Jay Barlow, NOAA Fisheries Southwest Fisheries Science Center, La Jolla, California, and designed to interface with Ishmael. PAMGUARD is an open-source software program for real-time acoustic monitoring and post-processing applications, developed by Doug Gillespie (Gillespie et al. 2008). RainbowClick is a program designed for the detection and analysis of sounds made by sperm whales and other odontocetes, developed by The International Fund for Animal Welfare. Logger is an automatic field

data logging program that automatically collects data from GPS and other ships instruments and stores it in an Access database, developed by The International Fund for Animal Welfare. Raven is a program for the acquisition, visualization, measurement, and analysis of sounds, developed by The Cornell University's Center for Conservation Biology.

Table 11-9 Summary of towed hydrophone array data from NEFSC shipboard surveys
Acoustic survey effort often differed from visual survey effort because the acoustic monitoring can continue during night and inclement weather.

Trip Identifier	Year	Purpose	Start Date	End Date	Days with Acoustic Effort	Acoustic Survey Effort (km)
HB1103	2011	abundance survey	2-Jun	1-Aug	40	~ 5,580
HB1303	2013	abundance survey	2-Jul	18-Aug	33	~ 5,940
GU1402	2014	abundance survey	12-Mar	27-Apr	16	~ 2,610
HB1403	2014	beaked whale survey	25-Jul	30-Jul	4	~ 800
HB1503-1	2015	sei whale survey	10-Jun	19-Jun	7	~ 540
HB1503-2	2015	turtle tagging	24-Jun	1-Jul	3	332
HB1603	2016	abundance survey	28-Jun	24-Aug	40	5,354
HRS1701	2017	beaked whale survey	8-Sep	17-Sep	9	2,053
GU1803	2018	beaked whale survey	21-Jul	1-Aug	23	4,470
HRS1910	2019	beaked whale survey	17-Aug	28-Aug	9	1,050
Subtotal-AMAPPS I	2010 – 2014				93	~ 14,930
Subtotal-AMAPPS II	2015 – 2019				91	~ 13,799
GRAND TOTAL	2010 – 2019				184	~ 28,729

11.4.1.2 SEFSC Towed Hydrophone Array Data

During 2010 to 2019, the SEFSC AMAPPS program completed 3 shipboard abundance surveys that collected data from towed hydrophone arrays. During AMAPPS II, these surveys collected acoustic data on 39 days during over 5,000 km of track lines (Table 11-10).

Table 11-10 Summary of towed hydrophone array data from SEFSC shipboard surveys
Acoustic survey effort often differed from visual survey effort because the acoustic monitoring can continue during night and inclement weather.

Cruise/Project	Year	Purpose	Start Date	End Date	Days with acoustic effort	Acoustic Survey Effort (Km)
GU1102	2011	abundance survey	21-Jun	2-Aug	33	4,275
GU1304	2013	abundance survey	16-Jul	15-Sep	37	1,900
GU1605	2016	abundance survey	1-Jul	24-Aug	39	5,381
Subtotal-AMAPPS I	2010 – 2014				70	6,175
Subtotal-AMAPPS II	2015 – 2019				39	5,381
GRAND TOTAL	2010 – 2019				109	11,556

11.4.1.3 Bottom-mounted Recorder Data

During 2015 to 2019, the NEFSC worked with collaborators at Scripps Institution of Oceanography and Cornell University to deploy bottom-mounted archival acoustic recorders along the continental shelf and on the shelfbreak (Table 11-11). We collected continuous passive acoustic recordings (10 Hz to 100 kHz) from High-Frequency Acoustic Recording Packages (HARPs; Wiggins and Hildebrand 2007) at 8 sites along the North American east coast during April 2015 to June 2019. These sites were at varying depths, ranging from about 800 m to 1100 m. HARPs recorded continuously at a sampling rate of 200 kHz and lasted typically for up to a year. In contrast, we deployed multiple marine autonomous recording units (MARUs, Clark et al. 2010) in 5 lines spanning the continental shelf, from south of Nantucket, MA to Brunswick, GA. MARUs recorded continuously at a sampling rate of 2 kHz for up to 6 months. We recovered and redeployed recording units multiple times, with the goal of maintaining continuous sampling for 3 yrs.

Table 11-11 Summary of bottom-mounted recorders deployed under AMAPPS
HARP deployments involved a single recorder at a single site. MARU deployments involved multiple recorders (numbers in parentheses) spanning the continental shelf; thus, we provided a representative latitude, longitude, and date range. Note, individual recording units may have recorded for less than the date range specified.

Recorder Type	Site Name; Location	Recording Date Range	Latitude (N)	Longitude (W)
HARP	WAT_HZ; Heezen Canyon	Jun 2015–Mar 2016 Apr 2016–Jun 2017 Jul 2017–Jan 2018 Jun 2018–May 2019	41.0619	-66.3515
HARP	WAT_OC; Oceanographer Canyon	Apr 2015–Feb 2016 Apr 2016–May 2017 Jul 2017–May 2019	40.2633	-67.9862
HARP	WAT_NC; Nantucket Canyon	Apr 2015–Sep 2015 Apr 2016–May 2017 Jul 2017–Apr 2018 Jun 2018–Jun 2019	39.8325	-69.9821
HARP	WAT_BC; Babylon Canyon	Apr 2016 - May 2019	39.1911	-72.2287
HARP	WAT_WC; Wilmington Canyon	Apr 2016 - May 2019	38.3742	-73.3707
HARP	WAT_GS; Gulf Stream	Apr 2016 - Jun 2019	33.6656	-76.0014
HARP	WAT_BP; Blake Plateau	Apr 2016 - May 2019	32.1060	-77.0943
HARP	WAT_BS; Blake Spur	Apr 2016 - Jun 2019	30.5838	-77.3907
Deep-HARP	WAT_BR	Jul 2018–Aug 2018	40.0328	-67.9884
MARU (4-7 recorders)	Nantucket, MA	Dec 2015–Feb 2018 Dec 2018–Jun 2019	41.2499	-70.3895
MARU (1-5 recorders)	Cape Hatteras, NC	Oct 2015–Jul 2018	35.4012	-75.4010
MARU (1-5 recorders)	Cape Fear, NC	Nov 2015–Feb 2018 Nov 2018–Jun 2019	34.3674	-77.4878
MARU (1-7 recorders)	Charleston, SC	Nov 2015–Jan 2018	32.8781	-79.4803
MARU (3-8 recorders)	Brunswick, GA	Oct 2015–Aug 2018 Oct 2018–May 2019	31.0079	-81.1553

11.4.1.4 Other Passive Acoustic Data (Drifting Recorders, DTAG)

During 2010 to 2019, the NEFSC and SEFSC also collected passive acoustic data during shipboard surveys from drifting platforms (Table 11-12). These included sonobuoys, provided by the U.S. Navy, and drifting autonomous spar buoy recorders (DASBRs), constructed by the NEFSC in collaboration with the Southwest Fisheries Science Center. Both of these platforms provided the opportunity to collect

passive acoustic monitoring data from a drifting recorder that was distant from the vessel and so did not have vessel noise interference. Sonobuoys transmitted acoustic data directly to the ship, while we had to recover the DASBRs to download their data. In addition, the NEFSC deployed a digital acoustic recording tag (DTAG) on a True's beaked whale (*Mesoplodon mirus*) to collect environmental acoustic detections, as well as dive profile information.

Table 11-12 Summary of passive acoustic data collected using mobile or drifting platforms

Platform Type	Trip Identifier	Number of Deployments	Approximate Total Duration (hh:mm)
Sonobuoys	HB1503-1	14 (11 successful; 3 failed)	?
Sonobuoys	HB1603	30 (22 successful; 8 failed)	62:26
Sonobuoys	GU1605	30	?
DASBR	GU1803	5	155:58
DTAG	GU1803	1	?

11.4.2 Processing

11.4.2.1 Towed Hydrophone Array Data

The acoustic team used a suite of software packages to collect and monitor the data, including PAMGUARD, Ishmael, WhalTrack, RainbowClick, Logger, and Raven. Real-time data processing varied depending on the goals and needs of the individual survey. Analysts recorded information such as species identification, bearing, GPS location, and correspondence with visual sightings for target species groups. We also conducted detailed post-processing data analyses, focused on addressing targeted questions for each survey. Details of these analyses are in the AMAPPS annual reports and in the manuscripts listed below.

11.4.2.2 Bottom-mounted Recorder Data

The primary goals of the bottom-mounted data collection were to document baleen whale occurrence and migratory movements along the continental shelf, with a focus on North Atlantic right whales (MARUs), document cetacean species occurrence and diversity along the shelfbreak (HARPs), and determine the impacts of anthropogenic noise on cetacean vocal activity at specific shelf-break sites (HARPs). For all datasets, we used a combination of manual review and automated acoustic detectors/classifiers to determine the occurrence of target species groups. In addition, we quantified the daily presence of anthropogenic activities such as airguns, echosounders, sonar, and vessel noise at each of the HARP sites. Analyses are still ongoing. For many of the ongoing analyses we are working closely with collaborators at the Woods Hole Oceanographic Institution and Scripps Institution of Oceanography.

11.4.2.3 Drifting Recorder Data

We use sonobuoys during shipboard surveys to conduct acoustic point sampling for baleen whales because the towed hydrophone array used during shipboard surveys could not sufficiently capture baleen whale vocalizations. Sonobuoys transmit audio data in real-time, and we used the software packages Raven and PAMGUARD to record and analyze these data. DASBRs archive audio recordings, and are

equipped with satellite GPS transmitters for real-time tracking. We used a combination of manual review and automated acoustic detectors and classifiers to determine the occurrence of target species groups.

11.4.2.4 DTAG Data

We used custom-built MATLAB scripts to identify times of the clicks made by the tagged True's beaked whale, as well as those made by members of its group. We also analyzed the accelerometer data to provide a dive profile over the course of the tag duration, complete with vocal periods. We also analyzed the other types of sounds recorded by the DTAG using the software Raven.

11.4.3 Presentation

The daily presence results for the 5 baleen whale species processed (North Atlantic right whale, humpback, blue, sei, and fin whales), beaked whales, pygmy/dwarf sperm whales, and sperm whales are currently displayed on a Passive Acoustic Cetacean Map that will be available online soon. This website allows the exploration of acoustic presence for each of these species from these datasets, as well as all other passive acoustic monitoring detection datasets available in the western North Atlantic Ocean. The metadata for these datasets are in the NEFSC Oracle database and we will send them to the National Centers for Environmental Information in the upcoming years.

A full list of publications and presentations produced using these data during AMAPPS I is in Palka et al. (2017) and those produced during AMAPPS II is in Table 1-2.

11.5 Oceanographic data

Primary authors: Laura Aichinger Dias, Elizabeth Josephson, and Harvey Walsh

11.5.1 Provenance

11.5.1.1 Scientific Computer System Data

Shipboard sensors connected to the ship's Scientific Computer System collect constant records of *in-situ* environmental parameters including water temperature, salinity, and weather conditions (e.g., wind speed and wind direction). Table 11-13 is an example of the suite of parameters collected on a survey.

11.5.1.2 CTD/XBT

We deployed Conductivity, Temperature, and Depth (CTD) casts at least once a day on most shipboard surveys (Figure 11-2). On some surveys, we deployed expendable bathythermographs (XBT) at regular intervals along the trackline at stations typically spaced 15 to 20 km apart.

Table 11-13 Information collected from ship Scientific Computer System recording systems

Sensor/Parameter (units)	Sensor/Parameter (units)
Date (MM/DD/YYYY)	Time (hh:mm:ss)
TSG-Conductivity (s/m)	EK60-38kHz-Depth (m)
TSG-External-Temp (ºC)	EK60-18kHz-Depth (m)
TSG-InternalTemp (ºC)	ADCP-Depth (m)
TSG-Salinity (PSU)	ME70-Depth (m)
TSG-Sound-Velocity (m/s)	ES60-50kHz-Depth (m)
MX420-Time (GMT)	Doppler-Depth (m)
MX420-COG (º)	Air-Temp (ºC)
MX420-SOG (Kts)	Barometer-2 (mbar)
MX420-Lat (DDMM.MM)	YOUNG-TWIND-Direction (º)
MX420-Lon (DDMM.MM)	YOUNG-TWIND-Speed (Kts)
Doppler-F/A-BottomSpeed (Kts)	Rel-Humidity (%)
Doppler-F/A-WaterSpeed (Kts)	Rad-Case-Temp (ºC)
Doppler-P/S-BottomSpeed (Kts)	Rad-Dome-Temp (ºC)
Doppler-P/S-WaterSpeed (Kts)	Rad-Long-Wave-Flux (W/m2)
High-Sea Temp (ºC)	Rad-Short-Wave-Flux (W/m2)
POSMV – Time (hhmmss)	ADCP-F/A – GroundSpeed (Kts)
POSMV – Elevation (m)	ADCP-F/A – WaterSpeed (Kts)
POSMV – Heading (º)	ADCP-P/S – GroundSpeed (Kts)
POSMV – COG (Kts)	ADCP-P/S – WaterSpeed (Kts)
POSMV – SOG (Kts)	Gyro (º)
POSMV – Latitude (DDMM.MM)	POSMV – Quality (1=std)
POSMV – Longitude (DDMM.MM)	POSMV – Sats (none)
POSMV – hdops (none)	

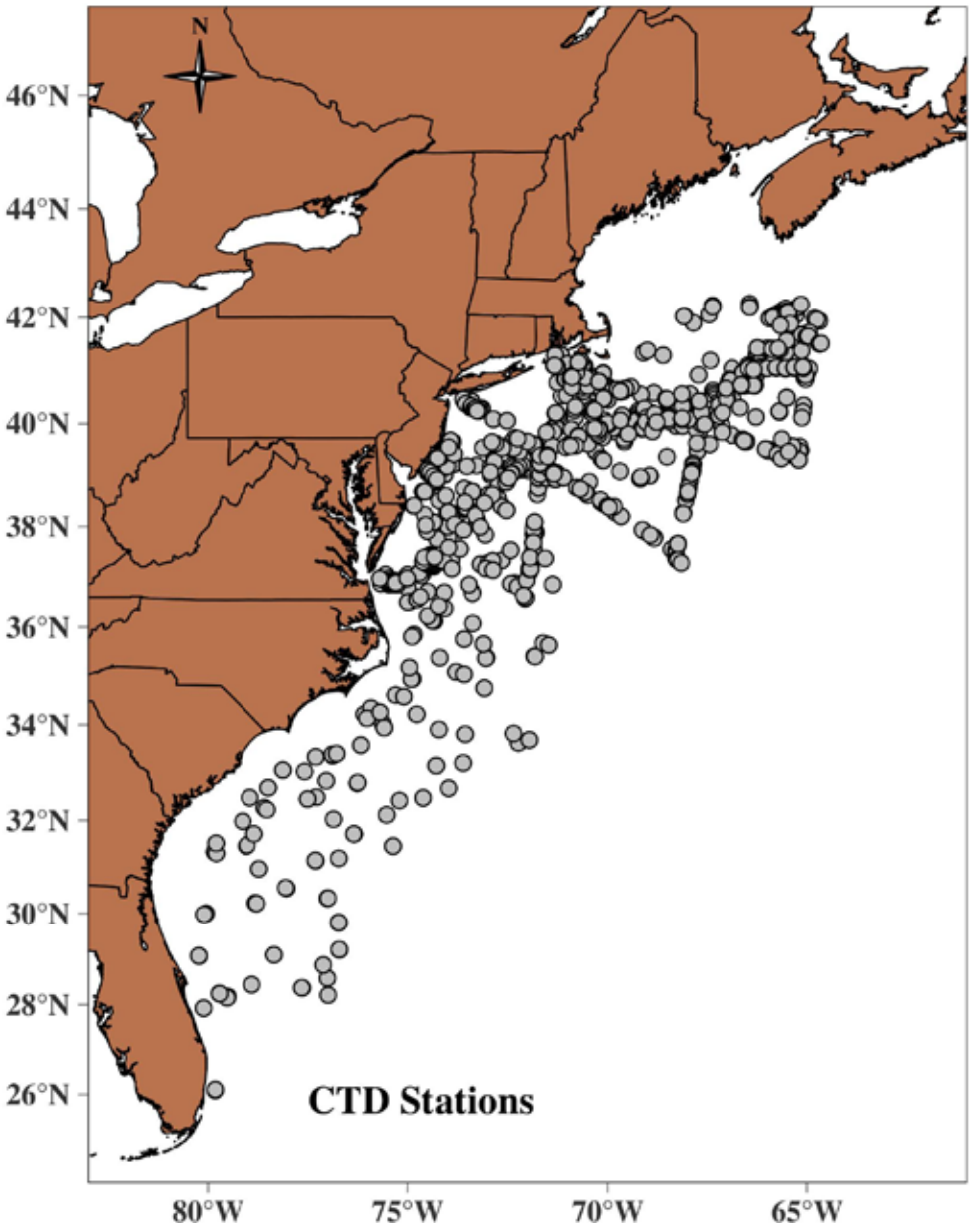

Figure 11-2 Locations of CTD sampling stations during 2010 to 2019

11.5.2 Processing

Technicians perform basic quality check procedures on SSC and CTD/XBT data.

11.5.3 Presentation

We upload the NEFSC CTD data to the Oceanography Database system maintained on NEFSC servers. We store oceanographic data from the SEFSC cruises within each survey's dataset in a central Windows 2016 server and a Netgear storage device. The backup system is a combination of Dell server and Qualstar LTO-6 tape library. Incremental backups occur to disk nightly. Off-site backups go to tape, which go off site every 2 months. Scientific Computer System data from NOAA ships are accessible through the National Centers for Environmental Information website.

11.6 Biological Sampling

Primary authors for this section: Danielle Cholewiak, Elizabeth Josephson, Laura Aichinger Dias, Chris Orphanides, Michael Jech, Elisabeth Broughton

11.6.1 Provenance

11.6.1.1 Mesopelagic and Benthic Sampling

We conducted mesopelagic and benthic sampling on AMAPPS shipboard surveys using sampling techniques including imaging (e.g. towed Visual Plankton Recorder, GoPro, and Sonar), acoustic (e.g. echosounder), and direct sampling (e.g. bongo net, mid-water trawl, and bottom grabs). We describe these sampling techniques, locations of sampling, and summaries of the numbers of samples with processing status in Chapter 10.

11.6.1.2 eDNA Sampling

Environmental DNA (eDNA) sampling refers to genetic signatures from the environment of the animal, rather than directly sampling animal tissue. With advances in DNA magnification and sequencing techniques, it is now possible to detect and identify species from samples with very low densities of genetic material (Ficetola et al. 2008). In 2017 and 2018, NEFSC conducted pilot studies where we collected eDNA samples on 2 shipboard surveys dedicated to study the ecology of deep-diving cetaceans in offshore habitats (Table 11-14; Figure 11-3). Scientists recorded data for each eDNA sample that included GPS location, time, date, target species, and sample location relative to animal location (when applicable). The reasons why we collected eDNA data were to:

1) determine whether eDNA sampling can be used to confirm species identification of cryptic species, such as beaked whales;
2) determine whether eDNA samples can be used to provide data related to stock structure; and
3) test the efficacy of eDNA sampling under various conditions (i.e. within the flukeprint of an animal upon a dive, at a distance or depth from an aggregation of animals, etc.).

Table 11-14 Summary of the numbers of eDNA samples per target species

Trip Identifier	Year	Species	Number of Samples
HRS1701	2017	*Mesoplodon mirus*	9
HRS1701	2017	*Ziphius cavirostris*	5
GU1803	2018	*Mesoplodon mirus*	12
GU1803	2018	*Ziphius cavirostris*	2
GU1803	2018	*Stenella coeruleoalba*	1
GU1803	2018	Deep water CTD	3
TOTAL			32

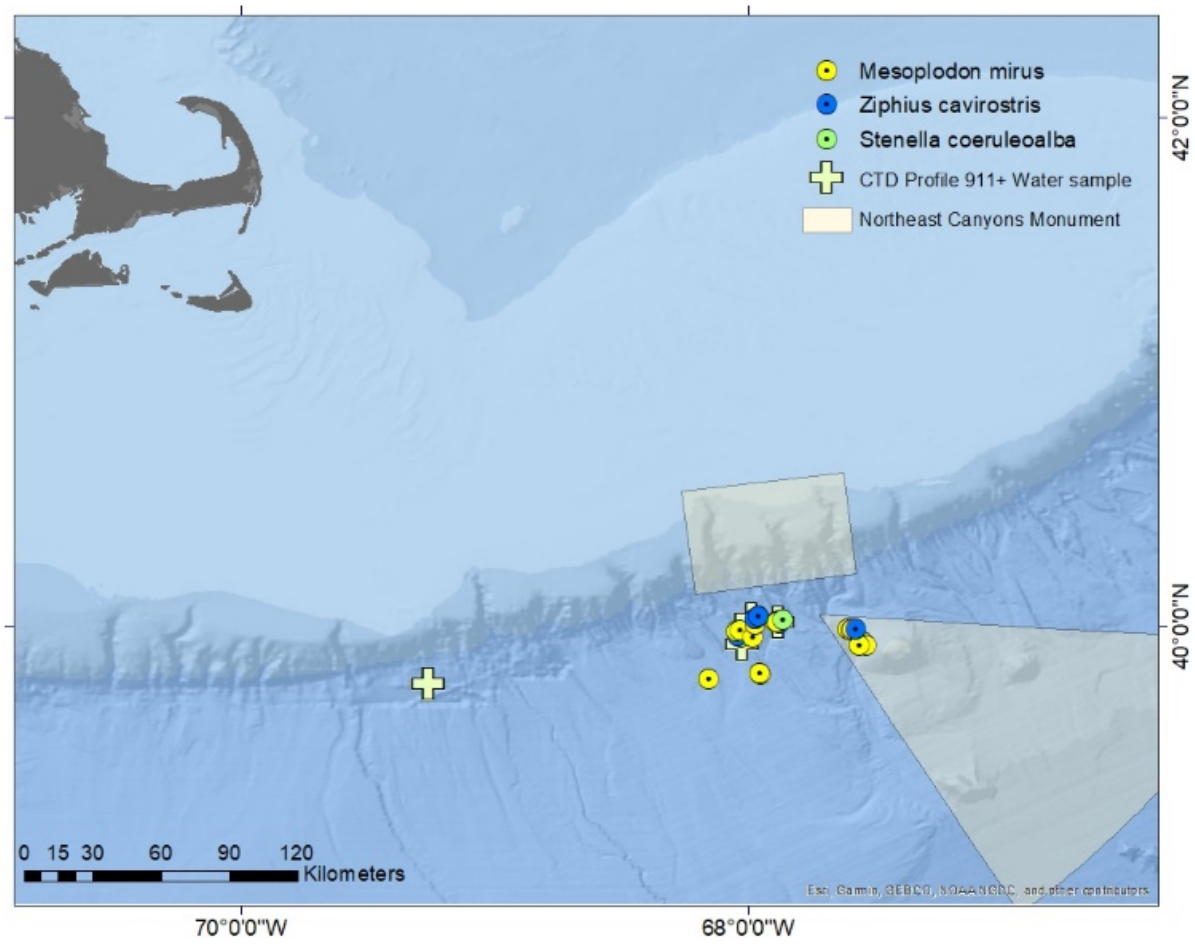

Figure 11-3 Location of eDNA samples collected in 2017 and 2018 by species

11.6.1.3 Biopsy Sampling

Whenever possible, scientists onboard the SEFSC and NEFSC shipboard surveys collected biopsy samples from marine mammals (Figure 11-4). Only personnel trained and authorized under marine mammal research permits conducted the biopsy sampling. From the bow of the ship, scientists used a modified 0.22 caliber dart rifle fitted with a tethered dart and custom designed biopsy heads to sample bow-riding delphinids. We also used a rigid-hulled inflatable boat deployed from the survey ship to sample larger cetaceans, like sperm whales (*Physeter macrocephalus*), baleen whales, and pilot whales (*Globicephala* spp.). We collected biopsies of the larger cetaceans by using a crossbow fitted with custom designed biopsy heads.

The biopsy heads on both sampling tools extract a small plug of tissue from the animals, usually including skin and blubber. We usually subsample the cetacean tissues to use for various analyses (Table 11-15). We have used the skin for stable isotopes analyses to investigate diet, and for genetic analyses to identify the species and determine population structure. We have subsampled the blubber for contaminant and hormone analyses. Scientists recorded data on each biopsy attempt that included GPS location, time, date, sampler and recorder name, species, body location struck, behavioral reaction, and whether or not we obtained a sample. Samples located in the Gulf of Mexico were collected during transit to/from port.

We combined turtle biopsy sampling with other biological sampling procedures for turtles, such as morphometrics and blood draw, when we brought a captured turtle on board the vessel. Chapter 8 of this report provides more information on the numbers and locations of sampled turtles, and the sampling protocols we used.

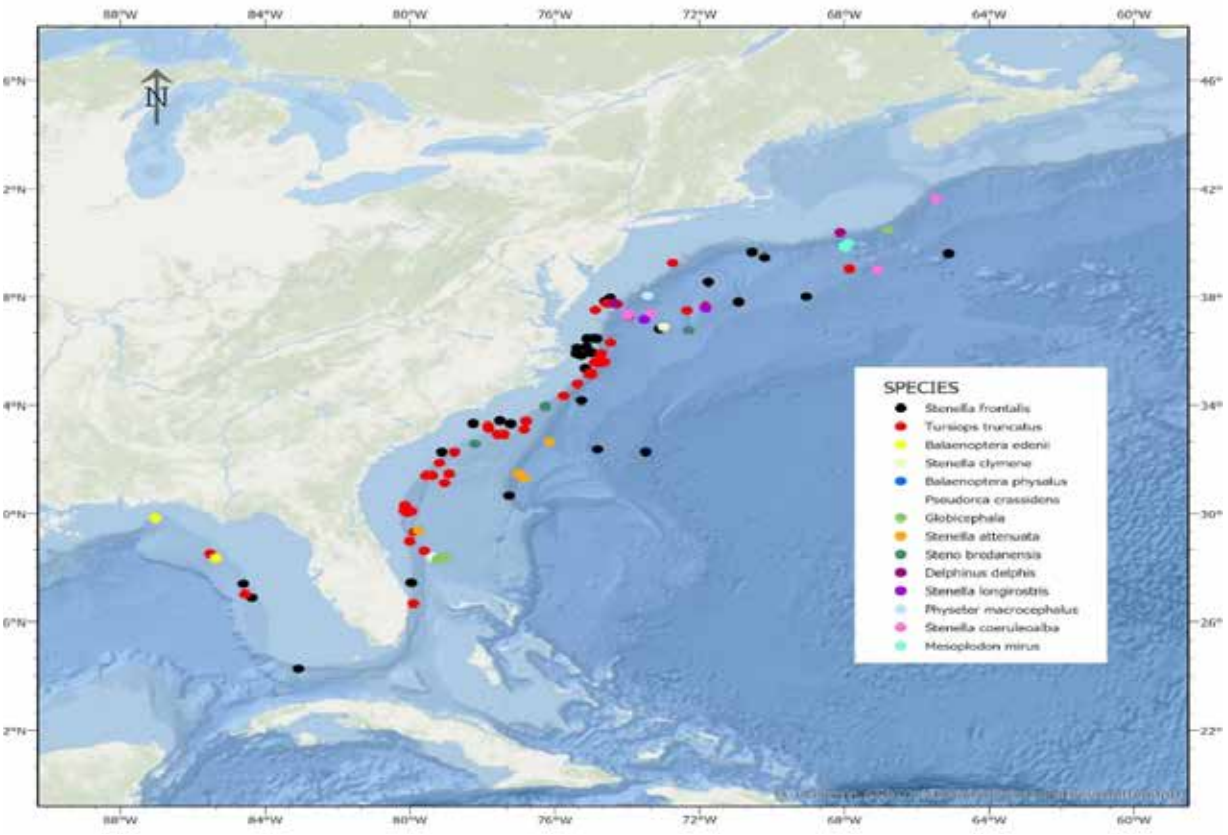

Figure 11-4 Location of biopsy-sampled marine mammals by species
We collected samples located in Gulf of Mexico during transit to and from port.

Table 11-15 Numbers of cetacean biopsy subsamples by analysis types

	Animals Sampled	Skin-DMSO[1] or Ethanol (Genetics)	Skin-Frozen (Stable Isotope)	Blubber-Frozen (Contaminants, Hormones)	Blubber (RNA[2] genetics)	Other	Total Subsamples
Balaenoptera edeni	4	4	0	0	0	0	4
Balaenoptera physalus	1	2	0	0	0	0	2
Delphinus delphis	3	5	0	0	0	0	5
Globicephala spp.	6	8	4	6	0	0	18
Mesoplodon mirus	3	4	0	0	0	0	4
Physeter macrocephalus	1	2	1	2	0	4	9
Pseudorca crassidens	1	1	0	0	0	0	1
Stenella attenuata	5	5	5	6	0	0	16
Stenella clymene	1	1	1	0	1	0	3
Stenella coeruleoalba	7	7	0	0	0	0	7
Stenella frontalis	40	40	20	21	7	1	89
Stenella longirostris	3	5	1	2	0	0	8
Steno bredanensis	3	3	1	0	1	0	5
Tursiops truncatus	57	59	22	24	8	0	113
TOTAL	135	146	55	61	17	5	284

[1] DMSO = Dimethyl sulfoxide
[2] RNA = Ribonucleic acid

11.6.2 Processing

11.6.2.1 Mesopelagic and Benthic Sample Processing

Chapter 10 of this report details the processing and data handling for mesopelagic and benthic samples from a variety of sampling techniques.

11.6.2.2 eDNA Sample Processing

During daytime small boat operations in 2017 and 2018, we collected paired water samples for eDNA testing using 1L bottles from either side of the small boat, and in the flukeprint of an animal upon a dive. We maintained water samples in a cooler with frozen ice packs, and transferred them back to the ship for

refrigerator storage at either midday or end of day. We also collected several water samples concurrent with deep-CTD casts. We performed the initial processing of the eDNA samples on board the vessel according to standard protocols. We filtered samples through 0.4 µM filters, and we stored them in Longmire's buffer for subsequent analyses. Qualified laboratories are conducting DNA extraction and analyses (Baker et al. 2018).

11.6.2.3 Biopsy Sample Processing

Researchers process the subsamples from the biopsy tissues in various ways according to study goals (Table 11-15). Onboard the ships, researchers only conduct limited subsampling, preservation and storage of the samples. Qualified laboratories conducted DNA extraction and other analyses. We did not list samples associated with stranded or bycaught animals. This tally included some samples that we have now consumed in analyses and so are not available for further analyses. Although we collected the samples on an AMAPPS supported field study, collaborators conducted and funded most of the analyses of the tissue samples.

11.6.3 Presentation

We archived the mesopelagic and benthic sampling data from trawls, including deployment date, time, duration, latitude, longitude, tow depth-time profile, catch weight and numbers by taxa, and individual lengths by taxa, locally in the NEFSC trawl database and they are available publicly through the InPort portal.

All active acoustic data (EK60 and other echosounder data) are accessible through the NOAA National Centers for Environmental Information water column sonar data portal.

The Oceans and Climate Branch at the NEFSC in Woods Hole, MA maintains all hydrographic, plankton and VPR data. Hydrographic data are accessible through the Branch website and the NCEI World Ocean Database. After researchers identify and enumerate the plankton samples, the plankton data are in the Plankton Archive. VPR oceanographic data and images are currently available by request only.

Woods Hole Oceanographic Institution maintained all Imaging Flow Cytobot data. Metadata and images are available through the Imaging Flow Cytobot website.

We incorporated information from biopsy sampling into several research publications and maintain an extensive archive of tissue samples for later analyses or sharing in an NEFSC Oracle database.

The genetic samples that the SEFSC collected during the cruises in 2011, 2013 and 2016 are stored at the Marine Mammal Molecular Genetics laboratory in Lafayette, LA. Scientists at this lab extracted DNA from some biopsies for ongoing studies; publications are forthcoming. All other samples are stored either at the Miami facility in FL or at the Pascagoula laboratory in MS.

Similarly, we are incorporating data from the eDNA sampling into several research publications (in preparation). We will archive new genetic information in GenBank, as appropriate.

11.7 References Cited

Amante C, Eakins BW. 2009. ETOPO1 1 Arc-Minute Global Relief Model: Procedures, data sources and analysis. NOAA Tech Memo NESDIS NGDC-24; 25 pp.

Baker CS, Steel D, Nieukirk S, Klinck H. 2018. Environmental DNA (eDNA) from the wake of the whales: droplet digital PCR for detection and species identification. Front. Mar. Sci. 5:133.

Balch WM, Gordon HR, Bowler BC, Drapeau DT, Booth ES. 2005. Calcium carbonate measurements in the surface global ocean based on Moderate-Resolution Imaging Spectroradiometer data. J. Geophys. Res. 110:C07001.

Barnston AG, Livezey RE. 1987. Classification, seasonality and persistence of low-frequency atmospheric circulation patterns. Mon. Wea. Rev. 115:1083-1126.

Behrenfeld MJ, Falkowski PG. 1997. Photosynthetic rates derived from satellite-based chlorophyll concentration. Limnol. Oceanogr. 42 (1):1-20.

Belkin IM, O'Reilly JE. 2009. An algorithm for oceanic front detection in chlorophyll and SST satellite imagery. J. Mar. Syst. 78:319-326.

Buckland ST, Anderson DR, Burnham KP, Laake JL, Borchers DL, Thomas L (eds). 2004. Advanced Distance Sampling. Oxford University Press, Oxford.

Campbell JW. 1995. The lognormal distribution as a model for bio-optical variability in the sea. J. Geophys. Res. Oceans 100 (C7):13237-13254.

Ceriani SA, Roth JD, Sasso CR, McClellan CM, James MC, Haas HL, Smolowitz RJ, Evans DR, Addison DS, Bagley DA, Ehrhart LM, Weishampel JF. 2014. Modeling and mapping isotopic patterns in the Northwest Atlantic derived from loggerhead sea turtles. Ecosphere 5(9):122.

Chassignet EP, Hurlburt HE, Metzger EJ, Smedstad OM, Cummings JA, Halliwell GR, Bleck R, Baraille R, Wallcraft AJ, Lozano C, Tolman HL, Srinivasan A, Hankin S, Cornillon P, Weisberg R, Barth A, He R, Werner F, Wilkin J. 2009. US GODAE: Global ocean prediction with the HYbrid Coordinate Ocean Model (HYCOM). Oceanography 22(2): 64–75.

Chin TM, Vazquez-Cuervo J, Armstrong EM. 2017. A Multi-Scale High-Resolution Analysis of Global Sea Surface Temperature. Remote Sens. Environ. 200: 154–69.

Clark CW, Brown MW, Corkeron P. 2010. Visual and acoustic surveys for North Atlantic right whales, *Eubalaena glacialis*, in Cape Cod Bay, Massachusetts, 2001–2005: Management implications. Mar. Mammal Sci. 26(4):837-854.

Ficetola GF, Miaud C, Pompanon F, Taberlet P. 2008. Species detection using environmental DNA from water samples. Biol. Lett. 2008:423-425.

Garrison LP, Martinez AM, Foley KM. 2011. Habitat and abundance of marine mammals in continental slope waters of the southeastern U.S. Atlantic. J. Cetacean Res. Manag. 11:267-277.

Gillespie DM, Gordon J, McHugh R, McLaren D, Mellinger D, Redmond P, Thode A. 2008. "PAMGUARD: Semiautomated, open source software for real-time acoustic detection and localisation of cetaceans." Proc.Instit. Acoust. 30, Part 5.

Gordon HR, Boynton GC, Balch WM, Groom SB, Harbour DS, Smyth TJ. 2001. Retrieval of coccolithophore calcite concentration from SeaWiFS imagery. Geophys. Res. Lett. 28(8): 1587-1590.

Hiby AR, Hammond PS. 1989. Survey techniques for estimating the abundance of cetaceans. Reports of the International Whaling Commission, pp. 47-80.

Hiby AR, Lovell P. 1998. Using aircraft in tandem formation to estimate abundance of harbor porpoise. Biometrics 54:1280-1289.

Hiby AR. 1999. The objective identification of duplicate sightings in aerial survey for porpoise. In. Garner GW, Amstrup SC, Laake JL, Manly BFJ, McDonall LL, Robertson DG, editors. Marine mammal survey and assessment methods. Rotterdam (Netherlands): AA Balkema. Pg 179-189.

Hu C, Lee Z, Franz B. 2012. Chlorophyll a algorithms for Oligotrophic Oceans: A novel approach based on three-band reflectance difference. J.Geophys. Res. 117 (C1):C01011.

Halpin PN, Read AJ, Fujioka E, Best BD, Donnelly B, Hazen LJ, Kot C, Urian K, LaBrecque E, Dimatteo A, Cleary J, Good C, Crowder LB, Hyrenbach KD. 2009. OBIS-SEAMAP: The world data center for marine mammal, seabird and sea turtle distributions. Oceanography 22(2):104-115.

Laake JL, Borchers DL. 2004. Methods for incomplete detection at distance zero. *In:* Advanced distance sampling., by D.R. Andersen, K.P. Burnham, J.L. Laake and L. Thomas (eds.) S.T. Buckland, 108-189. Oxford University Press, New York.

Mellinger DK, Nieukirk SL, Heimlich SL. 2018. ISHMAEL 3.0 User Guide.

Morel A. 1991. Light and marine photosynthesis: A spectral model with geochemical and climatological implications. Prog. Oceanogr. 26 (3): 263–306.

NASA Ocean Biology Processing Group. 2017. MODIS-Aqua level-3 binned Garver, Siegel, Maritorena Model (GSM) data Version R2018.0. NASA Ocean Biology DAAC GSM 2018.

NASA Ocean Biology Processing Group. 2018. SEAWIFS-ORBVIEW-2 level 3 mapped chlorophyll data Version R2018.0. NASA Ocean Biology DAAC SEAWIFS CHL.

NOAA National Geophysical Data Center [NGDC]. 2009: ETOPO1 1 arc-minute Global Relief Model. NOAA National Centers for Environmental Information.

Northeast Fisheries Science Center [NEFSC]. 2020. Technical Documentation, State of the Ecocystem.

O'Reilly JE, Maritorena S, Mitchell BG, Siegel DA, Carder KL, Garver SA, Kahru M, McClain C. 1998. Ocean color chlorophyll algorithms for Seawifs. J. Geophys. Res. Oceans 103(C11):24937-53.

Palka DL, Chavez-Rosales S, Josephson E, Cholewiak D, Haas HL, Garrison L, Jones M, Sigourney D, Waring G (retired), Jech M, Broughton E, Soldevilla M, Davis G, DeAngelis A, Sasso CR, Winton MV, Smolowitz RJ, Fay G, LaBrecque E, Leiness JB, Dettlof M, Warden M, Murray K, Orphanides C. 2017. Atlantic marine assessment program for protected species: 2010- 2014. US Dept. of the Interior, Bureau of Ocean Energy Management, Atlantic OCS Region, Washington, DC. OCS Study BOEM 2017-071; 211 pp.

Patel SH, Dodge KL, Haas HL, Smolowitz RJ. 2016. Videography reveals in-water behavior of loggerhead turtles (*Caretta caretta*) at a foraging ground. Front. Mar. Sci. 3:254.

Patel SH, Barco SG, Crowe LM, Manning JP, Matzen E, Smolowitz RJ, Haas HL. 2018. Loggerhead turtles are good ocean-observers in stratified mid-latitude regions. Estuar. Coast Shelf Sci. 213:128-136.

Project JPL MUR MEaSUREs. 2015. Group for High Resolution Sea Surface Temperature (GHRSST) level 4 Mur global foundation sea surface temperature analysis (V4.1). CA, USA. NASA PO.DAAC/GHGMR-4FJ04.

Saha K, Zhao X, Zhang H, Casey KS, Zhang D, Baker-Yeboah S, Kilpatrick KA, Evans RH, Ryan T, Relph JM. 2018. AVHRR Pathfinder version 5.3 level 3 collated (L3C) global 4km sea surface temperature for 1981-present. NOAA National Centers for Environmental Information/V52J68XX. Accessed in 2016 and 2018.

Thomas L, Laake JL, Rexstad E, Strindberg S, Marques FFC, Buckland ST, Borchers DL, Anderson DR, Burnham KP, Burt ML, Hedley SL, Pollard JH, Bishop JRB, Marques TA. 2009. Distance 6.0. Release 229 2. [Internet]. University of St. Andrews.

Wiggins SM, Hildebrand JA. 2007. High-frequency acoustic recording package (HARP) for broad-band, long-term marine mammal monitoring, International Symposium on Underwater Technology 2007 and International Workshop on Scientific Use of Submarine Cables and Related Technologies 2007. Institute of Electrical and Electronics Engineers, Tokyo, Japan. 551-557.

Winship AJ, Kinlan BP, White TP, Leirness JB, Christensen J. 2018. Modeling at-sea density of marine birds to support Atlantic marine renewable energy planning: Final report. U.S. Department of the Interior, Bureau of Ocean Energy Management, Office of Renewable Energy Programs, Sterling, VA. OCS Study BOEM 2018-010. x+67 pp.

Winton M, Fay G, Haas HL, Arendt M, Barco S, James MC, Sasso C, Smolowitz R. 2018. Estimating the distribution and relative density of satellite-tagged loggerhead sea turtles in the western North Atlantic using geostatistical mixed effects models. Mar. Ecol. Prog. Ser. 586:217-232.

Yang T, Haas HL, Patel SH, Smolowitz R, James MC, Williard A. 2019. Blood biochemistry and hematology of migrating loggerhead turtles (*Caretta caretta*) in the Northwest Atlantic: reference intervals and intrapopulation comparisons. Conserv. Physiol. 7(1):coy079.

Department of the Interior (DOI)

The Department of the Interior protects and manages the Nation's natural resources and cultural heritage; provides scientific and other information about those resources; and honors the Nation’s trust responsibilities or special commitments to American Indians, Alaska Natives, and affiliated island communities.

Bureau of Ocean Energy Management (BOEM)

The mission of the Bureau of Ocean Energy Management is to manage development of U.S. Outer Continental Shelf energy and mineral resources in an environmentally and economically responsible way.

BOEM Environmental Studies Program

The mission of the Environmental Studies Program is to provide the information needed to predict, assess, and manage impacts from offshore energy and marine mineral exploration, development, and production activities on human, marine, and coastal environments. The proposal, selection, research, review, collaboration, production, and dissemination of each of BOEM’s Environmental Studies follows the DOI Code of Scientific and Scholarly Conduct, in support of a culture of scientific and professional integrity, as set out in the DOI Departmental Manual (305 DM 3).